Biochemistry

EIGHTH EDITION

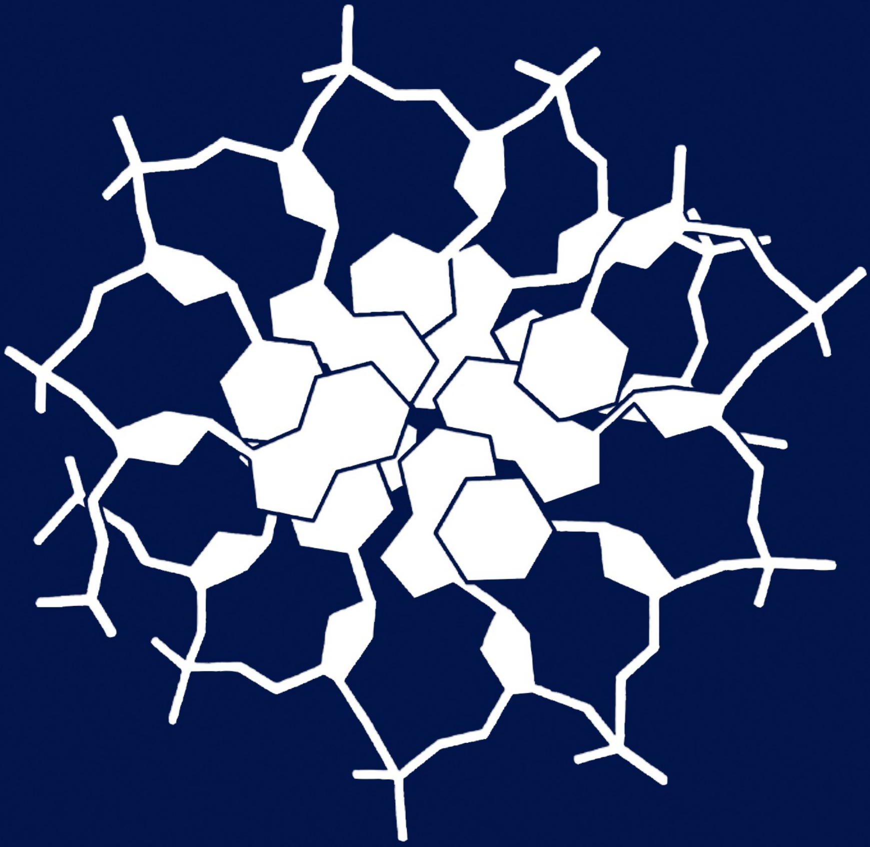

Jeremy M. Berg
John L. Tymoczko
Gregory J. Gatto, Jr
Lubert Stryer

Biochemistry

EIGHTH EDITION

Jeremy M. Berg
John L. Tymoczko
Gregory J. Gatto, Jr.
Lubert Stryer

Publisher: Kate Ahr Parker
Senior Acquisitions Editor: Lauren Schultz
Developmental Editor: Irene Pech
Editorial Assistants: Shannon Moloney and Nandini Ahuja
Senior Project Editor: Denise Showers with Sherrill Redd
Manuscript Editors: Irene Vartanoff and Mercy Heston
Cover and Interior Design: Vicki Tomaselli
Illustrations: Jeremy Berg with Network Graphics, Gregory J. Gatto, Jr.
Illustration Coordinator: Janice Donnola
Photo Editor: Christine Buese
Photo Researcher: Jacquelyn Wong
Production Coordinator: Paul Rohloff
Executive Media Editor: Amanda Dunning
Media Editor: Donna Brodman
Executive Marketing Manager: Sandy Lindelof
Composition:Aptara®, Inc.
Printing and Binding: RR Donnelley

Library of Congress Control Number: 2014950359

Gregory J. Gatto, Jr., is an employee of GlaxoSmithKline (GSK), which has not supported or funded this work in any way. Any views expressed herein do not necessarily represent the views of GSK.

ISBN-13: 978-1-4641-2610-9
ISBN-10: 1-4641-2610-0

©2015, 2012, 2007, 2002 by W. H. Freeman and Company; © 1995, 1988, 1981, 1975 by Lubert Stryer

All rights reserved

Printed in the United States of America

First printing

W. H. Freeman and Company
41 Madison Avenue
New York, NY 10010

www.whfreeman.com

To our teachers and our students

ABOUT THE AUTHORS

JEREMY M. BERG received his B.S. and M.S. degrees in Chemistry from Stanford (where he did research with Keith Hodgson and Lubert Stryer) and his Ph.D. in Chemistry from Harvard with Richard Holm. He then completed a postdoctoral fellowship with Carl Pabo in Biophysics at Johns Hopkins University School of Medicine. He was an Assistant Professor in the Department of Chemistry at Johns Hopkins from 1986 to 1990. He then moved to Johns Hopkins University School of Medicine as Professor and Director of the Department of Biophysics and Biophysical Chemistry, where he remained until 2003. He then became Director of the National Institute of General Medical Sciences at the National Institutes of Health. In 2011, he moved to the University of Pittsburgh where he is now Professor of Computational and Systems Biology and Pittsburgh Foundation Professor and Director of the Institute for Personalized Medicine. He served as President of the American Society for Biochemistry and Molecular Biology from 2011…2013. He is a Fellow of the American Association for the Advancement of Science and a member of the Institute of Medicine of the National Academy of Sciences. He received the American Chemical Society Award in Pure Chemistry (1994) and the Eli Lilly Award for Fundamental Research in Biological Chemistry (1995), was named Maryland Outstanding Young Scientist of the Year (1995), received the Harrison Howe Award (1997), and received public service awards from the Biophysical Society, the American Society for Biochemistry and Molecular Biology, the American Chemical Society, and the American Society for Cell Biology. He also received numerous teaching awards, including the W. Barry Wood Teaching Award (selected by medical students), the Graduate Student Teaching Award, and the Professor•s Teaching Award for the Preclinical Sciences. He is coauthor, with Stephen J. Lippard, of the textbook Principles of Bioinorganic Chemistry.

JOHN L. TYMOCZKO is Towsley Professor of Biology at Carleton College, where he has taught since 1976. He currently teaches Biochemistry, Biochemistry Laboratory, Oncogenes and the Molecular Biology of Cancer, and Exercise Biochemistry and coteaches an introductory course, Energy Flow in Biological Systems. Professor Tymoczko received his B.A. from the University of Chicago in 1970 and his Ph.D. in Biochemistry from the University of Chicago with Shutsung Liao at the Ben May Institute for Cancer Research. He then had a postdoctoral position with Hewson Swift of the Department of Biology at the University of Chicago. The focus of his research has been on steroid receptors, ribonucleoprotein particles, and proteolytic processing enzymes.

GREGORY J. GATTO, JR., received his A.B. degree in Chemistry from Princeton University, where he worked with Martin F. Semmelhack and was awarded the Everett S. Wallis Prize in Organic Chemistry. In 2003, he received his M.D. and Ph.D. degrees from the Johns Hopkins University School of Medicine, where he studied the structural biology of peroxisomal targeting signal recognition with Jeremy M. Berg and received the Michael A. Shanoff Young Investigator Research Award. He completed a postdoctoral fellowship in 2006 with Christopher T. Walsh at Harvard Medical School, where he studied the biosynthesis of the macrolide immunosuppressants. He is currently a Senior Scientific Investigator in the Heart Failure Discovery Performance Unit at GlaxoSmithKline.

LUBERT STRYER is Winzer Professor of Cell Biology, Emeritus, in the School of Medicine and Professor of Neurobiology, Emeritus, at Stanford University, where he has been on the faculty since 1976. He received his M.D. from Harvard Medical School. Professor Stryer has received many awards for his research on the interplay of light and life, including the Eli Lilly Award for Fundamental Research in Biological Chemistry, the Distinguished Inventors Award of the Intellectual Property Owners• Association, and election to the National Academy of Sciences and the American Philosophical Society. He was awarded the National Medal of Science in 2006. The publication of his first edition of Biochemistry in 1975 transformed the teaching of biochemistry.

PREFACE

For several generations of students and teachers, Biochemistry has been an invaluable resource, presenting the concepts and details of molecular structure, metabolism, and laboratory techniques in a streamlined and engaging way. Biochemistry•s success in helping students learn the subject for the first time is built on a number of hallmark features:

€ Clear writing and simple illustrations. The language of biochemistry is made as accessible as possible for students learning the subject for the first time. To complement the straightforward language and organization of concepts in the text, figures illustrate a single concept at a time to help students see main points without the distraction of excess detail.

€ Physiological relevance. It has always been our goal to help students connect biochemistry to their own lives on a variety of scales. Pathways and processes are presented in a physiological context so students can see how biochemistry works in the body and under different conditions, and Clinical Application sections in every chapter show students how the concepts they are studying impact human health. The eighth edition includes a number of new Clinical Application sections based on recent discoveries in biochemistry and health. (For a full list, see p. xi)

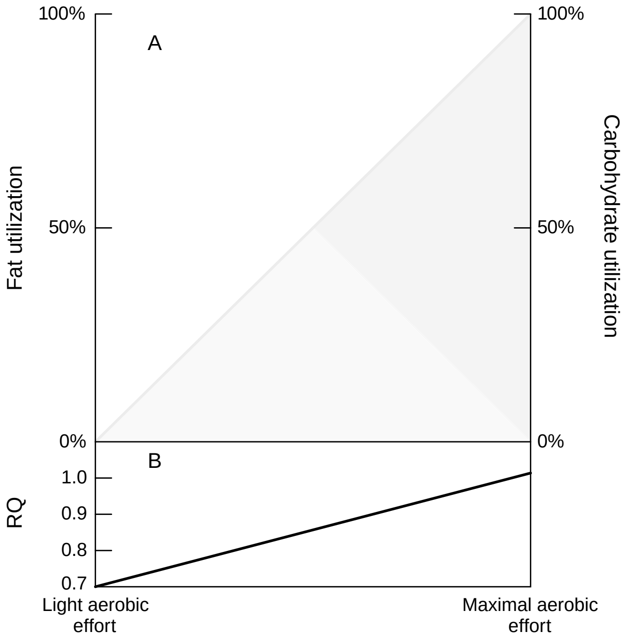

Figure 27.12 An idealized representation of fuels use as a function of aerobic exercise intensity. (A) With increased exercise intensity, the use of fats as fuels falls as the utilization of glucose increases. (B) The respiratory quotient (RQ) measures the alteration in fuel use.

€ Evolutionary perspective. Discussions of evolution are woven into the narrative of the text, just as evolution shapes every pathway and molecular structure described in the text. Molecular Evolution sections highlight important milestones in the evolution of life as a way to provide context for the processes and molecules being discussed. (For a full list, see p. x)

€ Problem-solving practice. Every chapter of Biochemistry provides numerous opportunities for students to practice problem-solving skills and apply the concepts described in the text. End-of-chapter problems are divided into three categories to address different problem-solving skills: Mechanism problems ask students to suggest or describe a chemical mechanism; Data interpretation problems ask students to draw conclusions from data taken from real research papers; and chapter integration problems require students to connect concepts from across chapters. Further problem-solving practice is provided online, on the Biochemistry LaunchPad. (For more details on LaunchPad resources, see p. viii)

€ A variety of molecular structures. All molecular structures in the book, with few exceptions, have been selected and rendered by Jeremy Berg and Gregory Gatto to emphasize the aspect of structure most important to the topic at hand. Students are introduced to realistic renderings of molecules through a molecular model •primerŽ in the appendices to Chapters 1 and 2 so they are well-equipped to recognize and interpret the structures throughout the book. Figure legends direct students explicitly to the key features of a model, and often include PDB numbers so the reader can access the file used in generating the structure from the Protein Data Bank website (www.pdb.org). Students

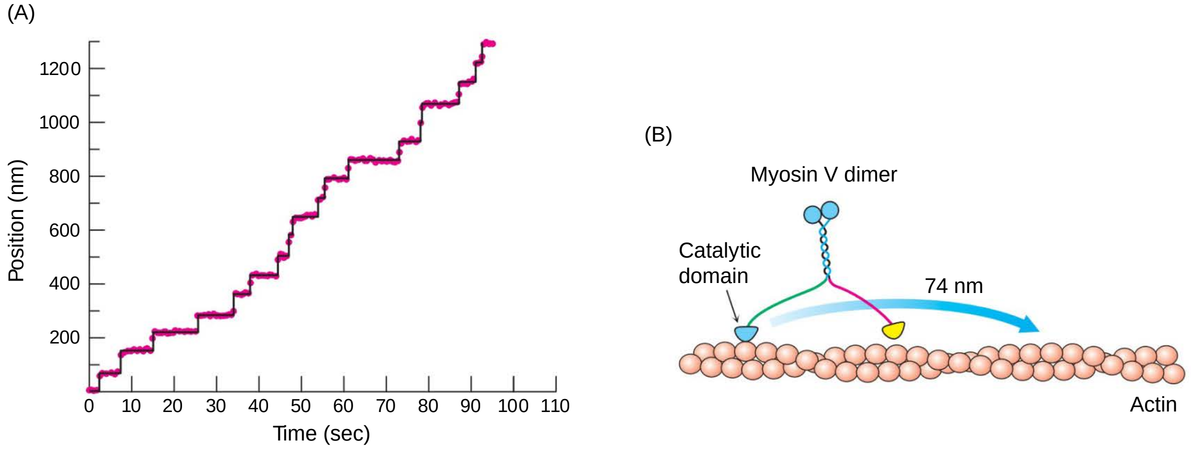

Figure 9.48 Single molecule motion. (A) A trace of the position of a single dimeric myosin V molecule as it moves across a surface coated with actin filaments. (B) A model of how the dimeric molecule moves in discrete steps with an average size of 74 6 5 nm. [Data from A. Yildiz et al., Science 300(5628)2061–2065, 2003.]

can explore molecular structures further online through the Living Figures, in which they can rotate 3D models of molecules and view alternative renderings.

In this revision of Biochemistry, we focused on building on the strengths of the previous editions to present biochemistry in an even more clear and streamlined manner, as well as incorporating exciting new advances from the field. Throughout the book, we have updated explanations of basic concepts and bolstered them with examples from new research. Some new topics that we present in the eighth edition include:

- Environmental factors that influence human biochemistry (Chapter 1)
- Genome editing (Chapter 5)
- Horizontal gene transfer events that may explain unexpected branches of the evolutionary tree (Chapter 6)
- Penicillin irreversibly inactivating a key enzyme in bacterial cell-wall synthesis (Chapter 8)
- Scientists watching single molecules of myosin move (Chapter 9)
- Glycosylation functions in nutrient sensing (Chapter 11)
- The structure of a SNARE complex (Chapter 12)
- The mechanism of ABC transporters (Chapter 13)
- The structure of the gap junction (Chapter 13)
- The structural basis for activation of the b-adrenergic receptor (Chapter 14)
- Excessive fructose consumption can lead to pathological conditions (Chapter 16)
- Alterations in the glycolytic pathway by cancer cells (Chapter 16)
- Regulation of mitochondrial ATP synthase (Chapter 18)
- Control of chloroplast ATP synthase (Chapter 19)
- Activation of rubisco by rubisco activase (Chapter 20)

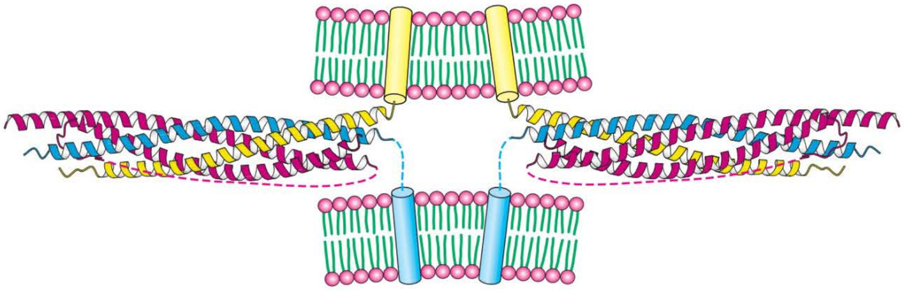

Figure 12.39 SNARE complexes initiate membrane fusion. The SNARE protein synaptobrevin (yellow) from one membrane forms a tight four-helical bundle with the corresponding SNARE proteins syntaxin-1 (blue) and SNAP25 (red) from a second membrane. The complex brings the membranes close together, initiating the fusion event. [Drawn from 1SFC.pdb.]

- The role of the pentose phosphate pathway in rapid cell growth (Chapter 20)
- Biochemical characteristics of muscle fiber types (Chapter 21)
- Alteration of fatty acid metabolism in tumor cells (Chapter 22)
- Biochemical basis of neurological symptoms of phenylketonuria (Chapter 24)
- Ribonucleotide reductase as a chemotherapeutic target (Chapter 25)
- The role of excess choline in the development of heart disease (Chapter 26)
- Cycling of the LDL receptor is regulated (Chapter 26)
- The role of ceramide metabolism in stimulating tumor growth (Chapter 26)
- The extraordinary power of DNA repair systems illustrated by Deinococcus radiodurans (Chapter 28)
- The structural details of ligand binding by TLRs (Chapter 34)

LaunchPad

All of the new media resources for Biochemistry will be available in our new system.

www.macmillanhighered.com/launchpad/berg8e

LaunchPad is a dynamic, fully integrated learning environment that brings together all of our teaching and learning resources in one place. It also contains the fully interactive e-Book and other newly updated resources for students and instructors, including the following:

- NEW Case Studies are a series of biochemistry case studies you can integrate into your course. Each case study gives students practice in working with data, developing critical thinking skills, connecting topics, and applying knowledge to real scenarios. We also provide instructional guidance with each case study (with suggestions on how to use the case in the classroom) and aligned assessment questions for quizzes and exams.

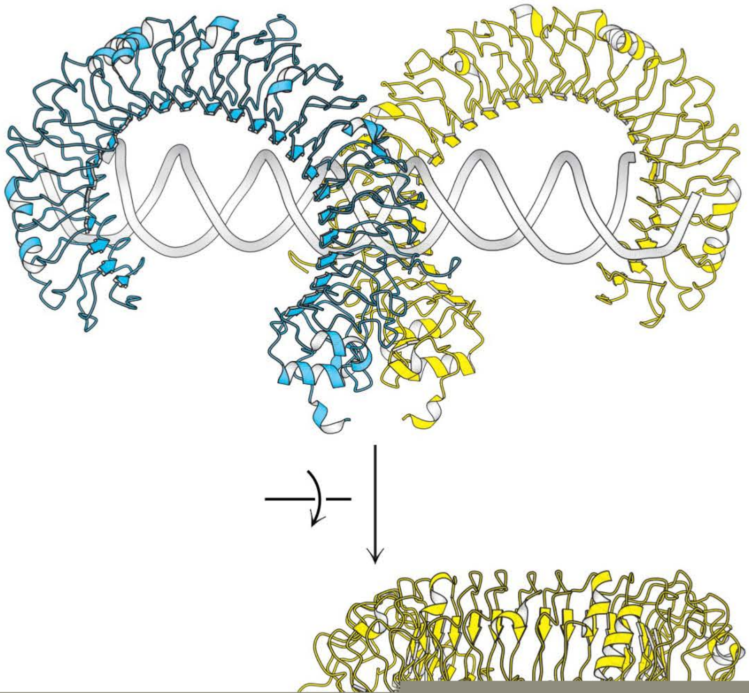

Figure 34.3 Recognition of a PAMP by a Toll-like receptor. The structure of TLR3 bound to its PAMP, a fragment of double-stranded RNA, as seen from the side (top) and from above (bottom). Notice that the PAMP induces receptor dimerization by binding the surfaces on the side of each of the extracellular domains. [Drawn from 3CIY.pdb].

- Newly Updated Clicker Questions allow instructors to integrate active learning in the classroom and to assess students' understanding of key concepts during lectures. Available in Microsoft Word and PowerPoint (PPT).
- Newly Updated Lecture PowerPoints have been developed to minimize preparation time for new users of the book. These files offer suggested lectures including key illustrations and summaries that instructors can adapt to their teaching styles.
- Updated Layered PPTs deconstruct key concepts, sequences, and processes from the textbook images, allowing instructors to present complex ideas step-by-step.
- Updated Textbook Images and Tables are offered as high-resolution JPEG files. Each image has been fully optimized to increase type sizes and adjust color saturation. These images have been tested in a large lecture hall to ensure maximum clarity and visibility.
- The Clinical Companion, by Gregory Raner, The University of North Carolina at Greensboro and Douglas Root, University of North Texas, applies concepts that students have learned in the book to novel medical situations. Students read clinical case studies and use basic biochemistry concepts to solve the medical mysteries, applying and reinforcing what they learn in lecture and from the book.
- Hundreds of self-graded practice problems allow students to test their understanding of concepts explained in the text, with immediate feedback.
- The Metabolic Map helps students understand the principles and applications of the core metabolic pathways. Students can work through guided tutorials with embedded assessment questions, or explore the Metabolic Map on their own using the dragging and zooming functionality of the map.
- Jmol tutorials by Jeffrey Cohlberg, California State University at Long Beach, teach students

How does a protein end up at the correct destination? A newly synthesized protein will float inside the ER lumen until it binds to an integral membrane protein called a *cargo receptor*. This binding sequesters the cargo protein into a small region of the membrane that can subsequently form a membrane bud. The bud will carry the protein to a specific destination—plasma membrane, lysosome, or cell exterior. The key to ensuring that the protein reaches the proper destination is that the protein must bind to a receptor in the ER region associated with the protein's destination. To ensure the proper match of protein with ER region, cargo receptors recognize various characteristics of the cargo protein, such as a particular amino acid sequence or an added carbohydrate.

The formation of buds is facilitated by the binding of *coat proteins* (COPs) to the cytoplasmic side of the bud. The coat proteins associate with one another to pinch off the vesicle. After the transport vesicle has formed and is released, the coat proteins are shed to reveal another integral protein called *v-SNARE* ("v" for *v*esicle). v-SNARE will bind to a particular *t-SNARE* ("t" for *t*arget) in the target membrane. This binding leads to the fusion of the transport vesicle to the target membrane, and the cargo is delivered. Thus, the assignment of identical v-SNARE proteins to the same region of the ER membrane causes an ER region to be associated with a particular destination.

SUMMARY

30.1 Protein Synthesis Requires the Translation of Nucleotide Sequences into Amino Acid Sequences

Protein synthesis is called translation because information present as a nucleic acid sequence is translated into a different language, the sequence of amino acids in a protein. This complex process is mediated by the coordinated interplay of more than a hundred macromolecules, including mRNA, rRNAs, tRNAs, aminoacyl-tRNA synthetases, and protein factors. Given that a protein typically comprises from 100 to 1000 amino acids, the frequency at which an incorrect amino acid is incorporated in the course of protein synthesis must be less than 10^{-4}. Transfer RNAs are the adaptors that make the link between a nucleic acid and an amino acid. These molecules, single chains of about 80 nucleotides, have an L-shaped structure.

30.2 Aminoacyl Transfer RNA Synthetases Read the Genetic Code

Each amino acid is activated and linked to a specific transfer RNA by an enzyme called an aminoacyl-tRNA synthetase. The synthetase links the carboxyl group of an amino acid to the $2'$- or $3'$-hydroxyl group of the adenosine unit of a CCA sequence at the $3'$ end of the tRNA by an ester linkage. There is at least one specific aminoacyl-tRNA synthetase and at least one specific tRNA for each amino acid. A synthetase utilizes both the functional groups and the shape of its cognate amino acid to prevent the attachment of an incorrect amino acid to a tRNA. Some synthetases have a separate active site at which incorrectly linked amino acids are removed by hydrolysis. A synthetase recognizes the anticodon, the acceptor stem, and sometimes other parts of its tRNA substrate. By specifically recognizing both amino acids and tRNAs, aminoacyl-tRNA synthetases implement the instructions of the genetic code.

The codons of messenger RNA recognize the anticodons of transfer RNAs rather than the amino acids attached to the tRNAs. A codon on mRNA forms base pairs with the anticodon of the tRNA. Some tRNAs are recognized by more than one codon because pairing of the third base of a codon is less crucial than that of the other two (the wobble mechanism). There are two evolutionary distinct classes of synthetases, each recognizing 10 amino acids. The two classes recognize opposite faces of tRNA molecules.

30.3 The Ribosome Is the Site of Protein Synthesis

Protein synthesis takes place on ribosomes—ribonucleoprotein particles (about two-thirds RNA and one-third protein) consisting of large and small subunits. In *E. coli,* the 70S ribosome (2500 kDa) is made up of 30S and 50S subunits. The 30S subunit consists of 16S ribosomal RNA and 21 different proteins; the 50S subunit consists of 23S and 5S rRNA and 34 different proteins. The ribosome includes three sites for tRNA binding called the A (aminoacyl) site, the P (peptidyl) site, and the E (exit) site.

Protein synthesis takes place in three phases: initiation, elongation, and termination. In bacteria, mRNA, formylmethionyl-tRNA$_f$ (the special initiator tRNA that recognizes AUG), and a 30S ribosomal subunit come together with the assistance of initiation factors to form a 30S initiation complex. A 50S ribosomal subunit then joins this complex to form a 70S initiation complex, in which fMet-tRNA$_f$ occupies the P site of the ribosome.

Elongation factor Tu delivers the appropriate aminoacyl-tRNA to the ribosome's A site as an EF-Tu–aminoacyl-tRNA–GTP ternary complex. EF-Tu serves both to protect the aminoacyl-tRNA from premature cleavage and to increase the fidelity of protein synthesis by ensuring that the correct anticodon–codon pairing has taken place before hydrolyzing GTP and releasing aminoacyl-tRNA into the A site. A peptide bond is formed when the amino group of the aminoacyl-tRNA nucleophilically attacks the ester linkage of the peptidyl-tRNA. On peptide-bond formation, the tRNAs and mRNA are translocated for the next cycle to begin. The deacylated tRNA moves to the E site and then leaves the ribosome, and the peptidyl-tRNA moves from the A site into the P site. Elongation factor G uses the free energy of GTP hydrolysis to drive translocation. Protein synthesis is terminated by release factors, which recognize the termination codons UAA, UGA, and UAG and cause the hydrolysis of the ester bond between the polypeptide and tRNA.

30.4 Eukaryotic Protein Synthesis Differs from Bacterial Protein Synthesis Primarily in Translation Initiation

The basic plan of protein synthesis in eukaryotes is similar to that in bacteria, but there are some significant differences between them. Eukaryotic ribosomes (80S) consist of a 40S small subunit and a 60S large subunit. The initiating amino acid is again methionine, but it is not formylated. The initiation of protein synthesis is more complex in eukaryotes than in bacteria. In eukaryotes, the AUG closest to the 5′ end of mRNA is nearly always the start site. The 40S ribosome finds this site by binding to the 5′ cap and then scanning the RNA until AUG is reached. The regulation of translation in eukaryotes provides a means for regulating gene expression.

30.5 A Variety of Antibiotics and Toxins Can Inhibit Protein Synthesis

Many clinically important antibiotics function by inhibiting protein synthesis. All steps of protein synthesis are susceptible to inhibition by one antibiotic or another. Diphtheria toxin inhibits protein synthesis by covalently modifying an elongation factor, thereby preventing elongation. Ricin, a toxin from castor beans, inhibits elongation by removing a crucial adenine residue from rRNA.

30.6 Ribosomes Bound to the Endoplasmic Reticulum Manufacture Secretory and Membrane Proteins

Proteins contain signals that determine their ultimate destination. The synthesis of all proteins begins on free ribosomes in the cytoplasm. In eukaryotes, protein synthesis continues in the cytoplasm unless the nascent chain contains a signal sequence that directs the ribosome to the endoplasmic reticulum. Amino-terminal signal sequences consist of a hydrophobic segment of 9 to 12 residues preceded by a positively charged amino acid. The signal-recognition particle, a ribonucleoprotein assembly, recognizes signal sequences and brings ribosomes bearing them to the ER. A GTP–GDP cycle releases the signal sequence from SRP and then detaches SRP from its receptor. The nascent chain is then translocated across the ER membrane. Proteins are transported throughout the cell in transport vesicles.

KEY TERMS

translation (p. 893)
ribosome (p. 893)
aminoacyl-tRNA synthetase (p. 894)
codon (p. 895)
transfer RNA (tRNA) (p. 895)
anticodon (p. 895)
wobble hypothesis (p. 897)
30S subunit (p. 902)
50S subunit (p. 902)
Shine–Dalgarno sequence (p. 906)
initiation factor (p. 907)
elongation factor Tu (EF-Tu) (p. 907)
accommodation (p. 907)
elongation factor Ts (EF-Ts) (p. 907)
peptidyl transferase center (p. 908)
elongation factor G (EF-G) (translocase) (p. 909)
polysome (p. 910)
release factor (RF) (p. 910)
signal sequence (p. 916)
signal peptidase (p. 916)
signal-recognition particle (SRP) (p. 916)
SRP receptor (SR) (p. 917)
translocon (p. 917)
transport vesicle (p. 918)
coat proteins (p. 919)
v-SNARE (p. 919)
t-SNARE (p. 919)

PROBLEMS

1. *Babel fish.* Why is protein synthesis also called translation?

2. *Careful, but not too careful.* Why is it crucial that protein synthesis has an error frequency of 10^{-4}?

3. *Commonalities.* What features are common to all tRNA molecules?

4. *The ol' two step.* What two reaction steps are required for the formation of an aminoacyl-tRNA?

5. *The same but different.* Why must tRNA molecules have both unique structural features and common structural features?

6. *Charge it.* In the context of protein synthesis, what is meant by an activated amino acid?

7. *Synthetase mechanism.* The formation of isoleucyl-tRNA proceeds through the reversible formation of an enzyme-bound Ile-AMP intermediate. Predict whether ^{32}P-labeled ATP is formed from $^{32}PP_i$ when each of the following sets of components is incubated with the specific activating enzyme:

(a) ATP and $^{32}PP_i$

(b) tRNA, ATP, and $^{32}PP_i$

(c) Isoleucine, ATP, and $^{32}PP_i$

8. *1 = 2, for sufficiently large values of 1.* The energetic equivalent of two molecules of ATP is used to activate an amino acid, yet only one molecule of ATP is used. Explain.

9. *Sieves.* Using threonyl-tRNA synthetase as an example, account for the specificity of threonyl-tRNA formation.

10. *Use all available information.* Suggest a reason why there are two classes of aminoacyl-tRNA synthetases, with each class recognizing a different face of the tRNA.

11. *Going wobbly.* Explain how it is possible that some tRNA molecules recognize more than one codon.

12. *Light and heavy ribosomes.* Ribosomes were isolated from bacteria grown in a "heavy" medium (^{13}C and ^{15}N) and from bacteria grown in a "light" medium (^{12}C and ^{14}N). These 60S ribosomes were added to an in vitro system engaged in protein synthesis. An aliquot removed several hours later was analyzed by density-gradient centrifugation. How many bands of 70S ribosomes would you expect to see in the density gradient?

13. *The price of protein synthesis.* What is the smallest number of molecules of ATP and GTP consumed in the synthesis of a 200-residue protein, starting from amino acids? Assume that the hydrolysis of PP_i is equivalent to the hydrolysis of ATP for this calculation.

14. *Correct phasing.* What is meant by the phrase *reading frame?*

15. *Suppressing frameshifts.* The insertion of a base in a coding sequence leads to a shift in the reading frame, which in

most cases produces a nonfunctional protein. Propose a mutation in a tRNA that might suppress frameshifting.

16. *Tagging a ribosomal site.* Design an affinity-labeling reagent for one of the tRNA-binding sites in *E. coli* ribosomes.

17. *Viral mutation.* An mRNA transcript of a T7 phage gene contains the base sequence

↓
5′–AACUGCACGAGGUAACACAAGAUGGCU–3′

Predict the effect of a mutation that changes the red G to A.

18. *A new translation.* A transfer RNA with a UGU anticodon is enzymatically conjugated to ^{14}C-labeled cysteine. The cysteine unit is then chemically modified to alanine. The altered aminoacyl-tRNA is added to a protein-synthesizing system containing normal components except for this tRNA. The mRNA added to this mixture contains the following sequence:

5′–UUUUGCCAUGUUUGUGCU–3′

What is the sequence of the corresponding radiolabeled peptide?

19. *Two synthetic modes.* Compare and contrast protein synthesis by ribosomes with protein synthesis by the solid-phase method (Section 3.4).

20. *Triggered GTP hydrolysis.* Ribosomes markedly accelerate the hydrolysis of GTP bound to the complex of EF-Tu and aminoacyl-tRNA. What is the biological significance of this enhancement of GTPase activity by ribosomes?

21. *Blocking translation.* Devise an experimental strategy for switching off the expression of a specific mRNA without changing the gene encoding the protein or the gene's control elements.

22. *Directional problem.* Suppose that you have a protein-synthesis system that is synthesizing a protein designated A. Furthermore, you know that protein A has four trypsin-sensitive sites, equally spaced in the protein, that, on digestion with trypsin, yield the peptides A_1, A_2, A_3, A_4, and A_5. Peptide A_1 is the amino-terminal peptide, and A_5 is the carboxyl-terminal peptide. Finally, you know that your system requires 4 minutes to synthesize a complete protein A. At $t = 0$, you add all 20 amino acids, each carrying a ^{14}C label.

(a) At $t = 1$ minute, you isolate intact protein A from the system, cleave it with trypsin, and isolate the five peptides. Which peptide is most heavily labeled?

(b) At $t = 3$ minutes, what will be the order of the labeling of peptides from greatest to least?

(c) What does this experiment tell you about the direction of protein synthesis?

23. *Translator.* Aminoacyl-tRNA synthetases are the only component of gene expression that decodes the genetic code. Explain.

24. *A timing device.* EF-Tu, a member of the G-protein family, plays a crucial role in the elongation process of translation. Suppose that a slowly hydrolyzable analog of GTP were added to an elongating system. What would be the effect on the rate of protein synthesis?

25. *Not just RNA.* What are the roles of the protein factors required for protein synthesis?

26. *Membrane transport.* What four components are required for the translocation of proteins across the endoplasmic reticulum membrane?

27. *Push. Don't pull.* What is the energy source that powers the cotranslational movement of proteins across the endoplasmic reticulum?

28. *You have to know where to look.* Bacterial messenger RNAs usually contain many AUG codons. How does the ribosome identify the AUG specifying initiation?

29. *Fundamentally the same, yet …* List the differences between bacterial and eukaryotic protein synthesis.

30. *Like a border collie.* What is the role of the signal-recognition particle in protein translocation?

31. *An assembly line.* Why is the fact that protein synthesis takes place on polysomes advantageous?

32. *Match 'em*

(a) Initiation ______
(b) Elongation ______
(c) Termination ______

1. GTP
2. AUG
3. f Met
4. RRF
5. IF2
6. Shine–Dalgarno
7. EF-Tu
8. Peptidyl transferase
9. UGA
10. Transformylase

33. *Wasted effort?* Transfer RNA molecules are quite large, given that the anticodon consists of only three nucleotides. What is the purpose of the rest of the tRNA molecule?

Mechanism Problems

34. *Evolutionary amino acid choice.* Ornithine is structurally similar to lysine except ornithine's side chain is one methylene group shorter than that of lysine. Attempts

to chemically synthesize and isolate ornithinyl-tRNA proved unsuccessful. Propose a mechanistic explanation. (Hint: Six-membered rings are more stable than seven-membered rings.)

Chapter Integration Problems

35. *Contrasting modes of elongation.* The two basic mechanisms for the elongation of biomolecules are represented in the adjoining illustration. In type 1, the activating group (X) is released from the growing chain. In type 2, the activating group is released from the incoming unit as it is added to the growing chain. Indicate whether each of the following biosyntheses is by means of a type 1 or a type 2 mechanism:

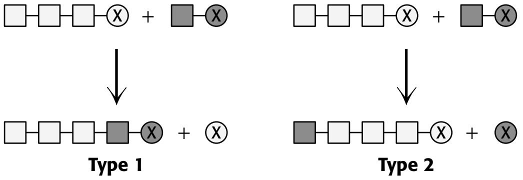

(a) Glycogen synthesis

(b) Fatty acid synthesis

(c) $C_5 \rightarrow C_{10} \rightarrow C_{15}$ in cholesterol synthesis

(d) DNA synthesis

(e) RNA synthesis

(f) Protein synthesis

36. *Enhancing fidelity.* Compare the accuracy of DNA replication, RNA synthesis, and protein synthesis. Which mechanisms are used to ensure the fidelity of each of these processes?

37. *Déjà vu.* Which protein in G-protein cascades plays a role similar to that of elongation factor Ts?

38. *Family resemblance.* Eukaryotic elongation factor 2 is inhibited by ADP ribosylation catalyzed by diphtheria toxin. What other G proteins are sensitive to this mode of inhibition?

39. *The exceptional E. coli.* In contrast with *E. coli,* most bacteria do not have a full complement of aminoacyl-tRNA synthetases. For instance, *Helicobacter pylori,* the cause of stomach ulcers, has tRNA^{Gln}, but no Gln-tRNA synthetase. However, glutamine is a common amino acid in *H. pylori* proteins. Suggest a means by which glutamine can be incorporated into proteins in *H. pylori.* (Hint: Glu-tRNA synthetase can misacylate tRNA^{Gln}.)

40. *The final step.* What aspect of primary structure allows the transfer of linear nucleic acid information into the functional three-dimensional structure of proteins?

Data Interpretation Problems

41. *Helicase helper.* The initiation factor eIF-4 displays ATP-dependent RNA helicase activity. Another initiation factor, eIF-4H, has been proposed to assist the action of eIF-4. Graph A shows some of the experimental results from an assay that can measure the activity of eIF-4 helicase in the presence of eIF-4H.

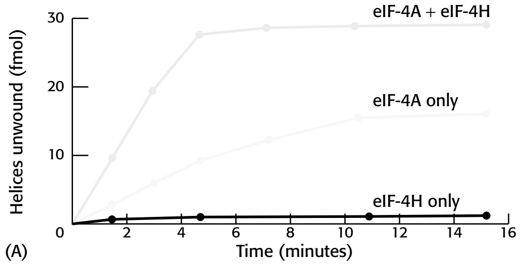

(a) What are the effects on eIF-4 helicase activity in the presence of eIF-4H?

(b) Why did measuring the helicase activity of eIF-4H alone serve as an important control?

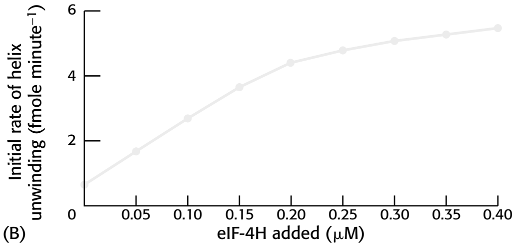

(c) The initial rate of helicase activity of 0.2 μM of eIF-4 was then measured with varying amounts of eIF-4H (graph B). What ratio of eIF-4H to eIF-4 yielded optimal activity?

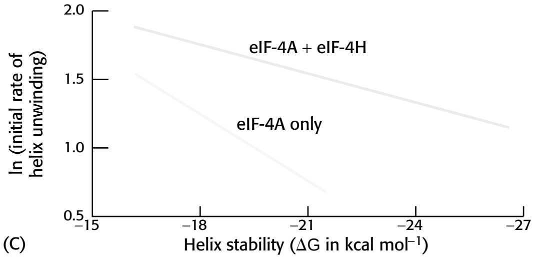

[Data from N. J. Richter, G. W. Rodgers, Jr., J. O. Hensold, and W. C. Merrick. Further biochemical and kinetic characterization of human eukaryotic initiation factor 4H., *J. Biol. Chem.* 274:35415–35424, 1999.]

(d) Next, the effect of RNA–RNA helix stability on the initial rate of unwinding in the presence and absence of eIF-4H was tested (graph C). How does the effect of eIF-4H vary with helix stability?

(e) How might eIF-4H affect the helicase activity of eIF-4A?

42. *Size separation*. The protein-synthesizing machinery was isolated from eukaryotic cells and briefly treated with a low concentration of RNase. The sample was then subjected to sucrose gradient centrifugation. The gradient was fractionated and the absorbance, or optical density (OD), at 254 nm was recorded for each fraction. The following plot was obtained.

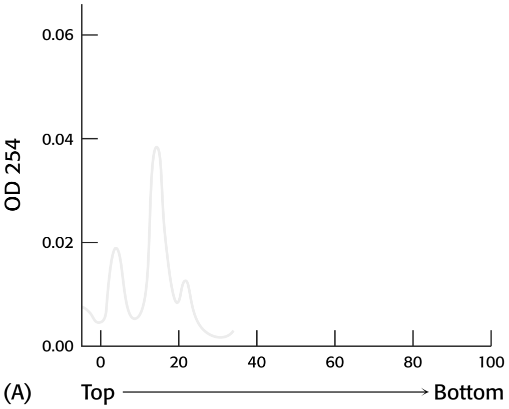

(a) What do the three peaks of absorbance in graph A represent?

The experiment was repeated except that, this time, the RNase treatment was omitted.

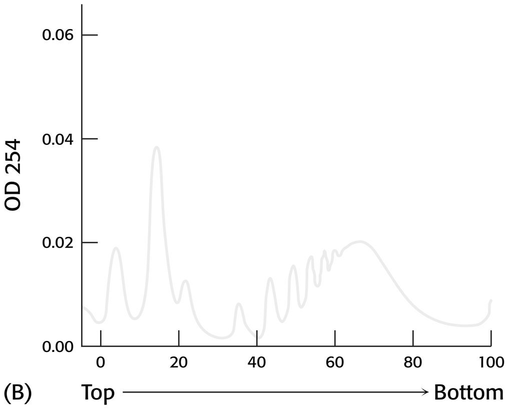

(b) Why is the centrifugation pattern in graph B more complex? What do the series of peaks near the bottom of the centrifuge tube represent?

Before the isolation of the protein-synthesizing machinery, the cells were grown in low concentrations of oxygen (hypoxic conditions). Again the experiment was repeated without RNase treatment (graph C).

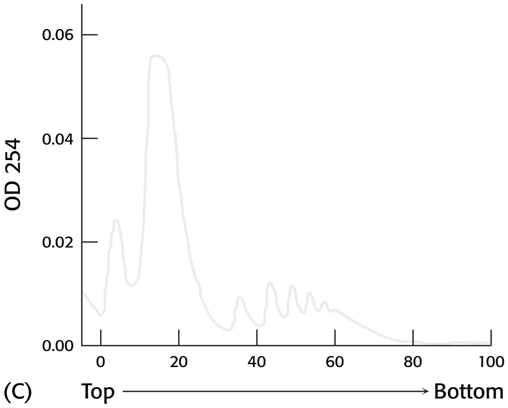

[Data from M. Koritzinsky et al., *EMBO J.* 25:1114–1125, 2006.]

(c) What is the effect of growing cells under hypoxic conditions?

CHAPTER

31

The Control of Gene Expression in Prokaryotes

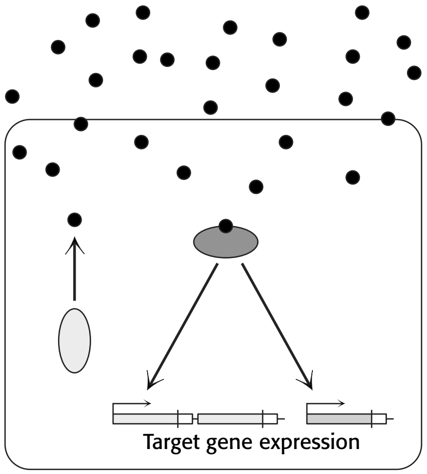

Bacteria respond to changes in their environments. A micrograph of the light organ of a newly hatched squid (*Euprymna scolopes*) is shown on the left. The light spots are due to colonies of the bacteria *Vibrio fischeri* that live symbiotically within these organs. These bacteria become luminescent when they reach an appropriately high density. The density is sensed by the circuit shown on the right in which each bacterium releases a small molecule into the environment. The molecule is subsequently taken up by other bacterial cells, which start a signaling cascade that stimulates the expression of specific genes. [Spencer V. Nyholm, Eric V. Stabb, Edward G. Ruby, and Margaret J. McFall-Ngai, “Establishment of an animal–bacterial association: Recruiting symbiotic vibrios from the environment.” *PNAS* 97(2000): 10231-10235. Copyright 2000 National Academy of Sciences.]

Even simple prokaryotic cells must respond to changes in their metabolism or in their environments. Much of this response takes place through changes in gene expression. A gene is *expressed* when it is transcribed into RNA and, for most genes, translated into proteins. Genomes comprise thousands of genes. Some of these genes are expressed all the time. These genes are subject to *constitutive expression.* Many other genes are expressed only under some circumstances—that is, under a particular set of physiological conditions. These genes are subject to *regulated expression.* For example, the level of expression of some genes in bacteria may vary more than a 1000-fold in response to the supply of nutrients or to environmental challenges.

In this chapter, we will examine gene-regulation mechanisms in prokaryotes, particularly *E. coli,* because many of these processes were first discovered in this organism. In Chapter 32, we will turn to gene-regulation mechanisms in eukaryotes. We shall see both substantial similarities and fundamental differences in comparing gene-regulatory mechanisms of the two types of organisms.

How is gene expression controlled? *Gene activity is controlled first and foremost at the level of transcription.* Whether a gene is transcribed is determined

OUTLINE

31.1 Many DNA-Binding Proteins Recognize Specific DNA Sequences

31.2 Prokaryotic DNA-Binding Proteins Bind Specifically to Regulatory Sites in Operons

31.3 Regulatory Circuits Can Result in Switching Between Patterns of Gene Expression

31.4 Gene Expression Can Be Controlled at Posttranscriptional Levels

largely by the interplay between specific DNA sequences and certain proteins that bind to these sequences. Most often, these proteins repress the expression of specific genes by blocking the access of RNA polymerase to their promoters. In some cases, however, the proteins can activate the expression of specific genes. We shall learn about several different strategies that allow the coordinated regulation of sets of genes. Some genes are also controlled at stages beyond the level of transcription and we shall examine several mechanisms at these stages. Finally, we will examine several important examples of how gene expression is regulated in response to changes in the concentrations of specific molecules in the environment of prokaryotic cells.

31.1 Many DNA-Binding Proteins Recognize Specific DNA Sequences

How do regulatory systems distinguish the genes that need to be activated or repressed from genes that are constitutive? After all, the DNA sequences of genes themselves do not have any distinguishing features that would allow regulatory systems to recognize them. Instead, gene regulation depends on other sequences in the genome. In prokaryotes, these regulatory sites are close to the region of the DNA that is transcribed. Regulatory sites are usually binding sites for specific DNA-binding proteins, which can stimulate or repress gene expression. These regulatory sites were first identified in *E. coli* in studies of changes in gene expression. In the presence of the sugar lactose, the bacterium starts to express a gene encoding β-galactosidase, an enzyme that can process lactose for use as a carbon and energy source. The sequence of the regulatory site for this gene is shown in Figure 31.1. The nucleotide sequence of this site shows a nearly perfect inverted repeat, indicating that the DNA in this region has an approximate twofold axis of symmetry. Recall that cleavage sites for restriction enzymes such as EcoRV have similar symmetry properties (Section 9.3). Symmetry in such regulatory sites usually corresponds to symmetry in the protein that binds the site. *Symmetry matching is a recurring theme in protein–DNA interactions.*

5′-...TGTGTGGAATTGTGAGCGGATAACAATTTCACACA...3′
3′-...ACACACCTTAACACTCGCCTATTGTTAAAGTGTGT...5′

FIGURE 31.1 Sequence of the *lac* regulatory site. The nucleotide sequence of this regulatory site shows a nearly perfect inverted repeat, corresponding to twofold rotational symmetry in the DNA. Parts of the sequences that are related by this symmetry are shown in the same color.

To understand these protein–DNA interactions in detail, scientists examined the structure of the complex between an oligonucleotide that includes this site and the DNA-binding unit that recognizes it (Figure 31.2).

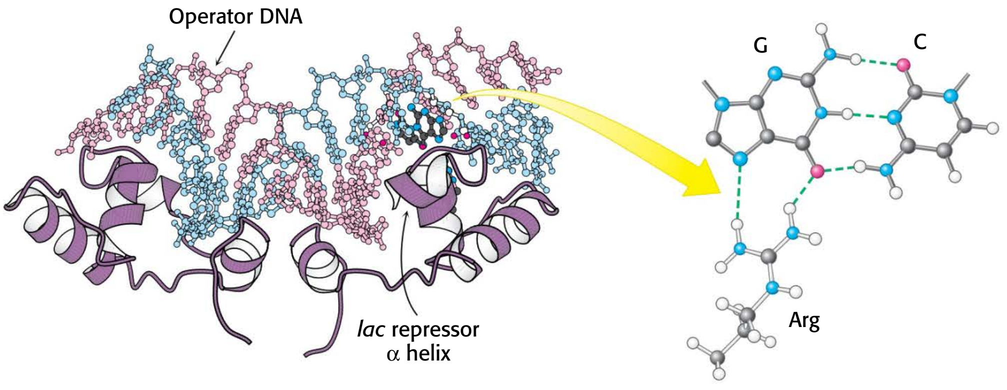

FIGURE 31.2 The *lac* repressor–DNA complex. The DNA-binding domain from a gene-regulatory protein, the *lac* repressor, binds to a DNA fragment containing its preferred binding site (referred to as operator DNA) by inserting an α helix into the major groove of operator DNA. *Notice* that a specific contact forms between an arginine residue of the repressor and a G–C base pair in the binding site. [Drawn from 1EFA.pdb.]

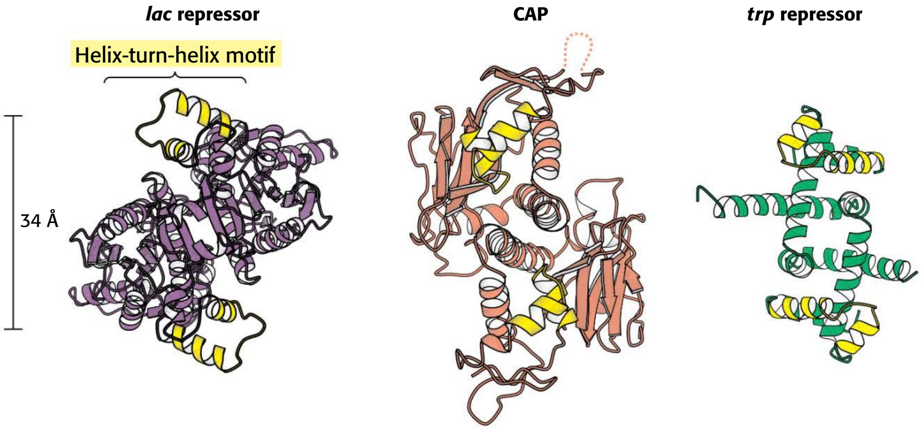

FIGURE 31.3 Helix-turn-helix motif. These structures show three sequence-specific DNA-binding proteins that interact with DNA through a helix-turn-helix motif (highlighted in yellow). *Notice* that, in each case, the helix-turn-helix units within a protein dimer are approximately 34 Å apart, corresponding to one full turn of DNA. [Drawn from 1EFA, 1RUN, and 1TRO.pdb.]

The DNA-binding unit comes from a protein called the *lac repressor,* which represses the expression of the lactose-processing gene. As expected, this DNA-binding unit binds as a dimer, and the twofold axis of symmetry of the dimer matches the symmetry of the DNA. An α helix from each monomer of the protein is inserted into the major groove of the DNA, where amino acid side chains make specific contacts with exposed edges of the base pairs. For example, the side chain of an arginine residue of the protein forms a pair of hydrogen bonds with a guanine residue of the DNA, which would not be possible with any other base. This interaction and similar ones allow the *lac* repressor to bind more tightly to this site than to the wide range of other sites present in the *E. coli* genome.

The helix-turn-helix motif is common to many prokaryotic DNA-binding proteins

Are similar strategies utilized by other prokaryotic DNA-binding proteins? The structures of many such proteins have now been determined, and amino acid sequences are known for many more. Strikingly, the DNA-binding surfaces of many, but not all, of these proteins consist of a pair of α helices separated by a tight turn (Figure 31.3). In complexes with DNA, the second of these two helices (often called the *recognition helix*) lies in the major groove, where amino acid side chains make contact with the edges of base pairs. In contrast, residues of the first helix participate primarily in contacts with the DNA backbone. *Helix-turn-helix motifs* are present on many proteins that bind DNA as dimers, and thus two of the units will be present, one on each monomer.

Although the helix-turn-helix motif is the most commonly observed DNA-binding unit in prokaryotes, not all regulatory proteins bind DNA through such units. A striking example is provided by the *E. coli* methionine repressor (Figure 31.4). This protein binds DNA through the insertion of a pair of β strands into the major groove.

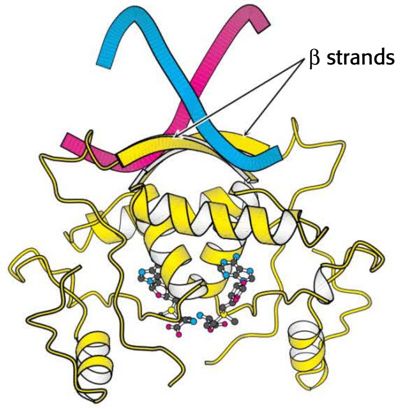

FIGURE 31.4 DNA recognition through β strands. A methionine repressor is shown bound to DNA. *Notice* that residues in β strands, rather than in α helices, participate in the crucial interactions between the protein and the DNA. [Drawn from 1CMA.pdb.]

31.2 Prokaryotic DNA-Binding Proteins Bind Specifically to Regulatory Sites in Operons

A historically important example reveals many common principles of gene regulation by DNA-binding proteins. Bacteria such as *E. coli* usually rely on glucose as their source of carbon and energy, even when other sugars are available. However, when glucose is scarce, *E. coli* can use lactose as their carbon source, even though this disaccharide does not lie on any major metabolic pathways. An essential enzyme in the metabolism of lactose is

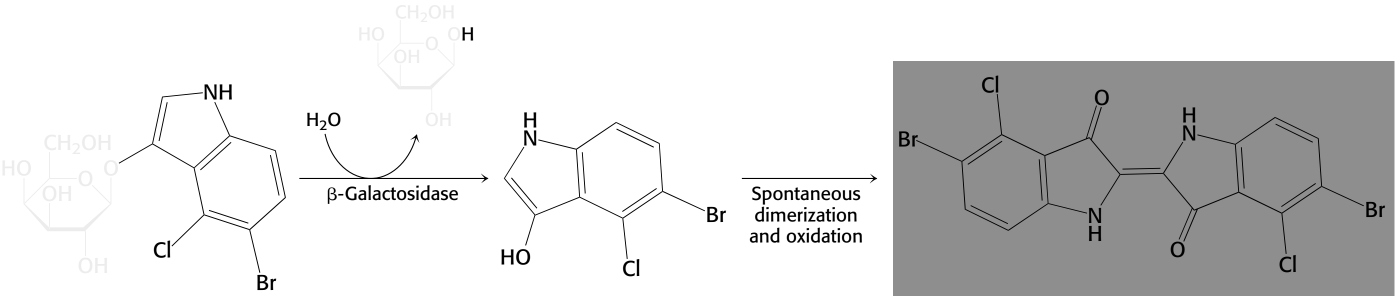

X-Gal

5,5 -Dibromo-4,4 -dichloro-indigo

FIGURE 31.5 **Monitoring the β-galactosidase reaction.** The galactoside substrate X-Gal produces a colored product on cleavage by β-galactosidase. The appearance of this colored product provides a convenient means for monitoring the amount of the enzyme both in vitro and in vivo.

-*galactosidase,* which hydrolyzes lactose into galactose and glucose. These products are then metabolized by pathways discussed in Chapter 16.

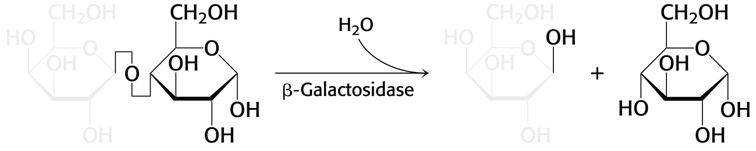

Lactose **Galactose** **Glucose**

This reaction can be conveniently followed in the laboratory through the use of alternative galactoside substrates that form colored products such as X-Gal (Figure 31.5). An *E. coli* cell growing on a carbon source such as glucose or glycerol contains fewer than 10 molecules of β-galactosidase. In contrast, the same cell will contain several thousand molecules of the enzyme when grown on lactose (Figure 31.6). The presence of lactose in the culture medium induces a large increase in the amount of β-galactosidase by eliciting the synthesis of new enzyme molecules rather than by activating a preexisting but inactive precursor.

A crucial clue to the mechanism of gene regulation was the observation that two other proteins are synthesized in concert with β-galactosidase—namely, *galactoside permease* and *thiogalactoside transacetylase.* The permease is required for the transport of lactose across the bacterial cell membrane (Section 13.3). The transacetylase is not essential for lactose metabolism but appears to play a role in the detoxification of compounds that also may be transported by the permease. Thus, *the expression levels of a set of enzymes that all contribute to the adaptation to a given change in the environment change together.* Such a coordinated unit of gene expression is called an *operon.*

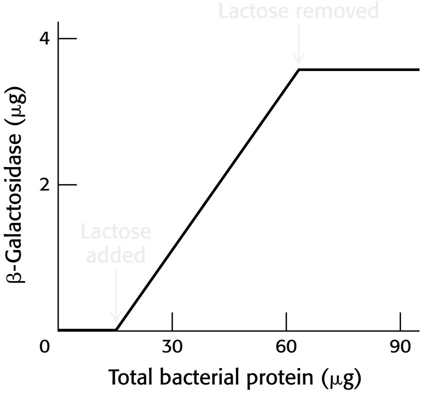

FIGURE 31.6 **β-Galactosidase induction.** The addition of lactose to an *E. coli* culture causes the production of β-galactosidase to increase from very low amounts to much larger amounts. The increase in the amount of enzyme parallels the increase in the number of cells in the growing culture. β-Galactosidase constitutes 6.6% of the total protein synthesized in the presence of lactose.

An operon consists of regulatory elements and protein-encoding genes

The parallel regulation of β-galactosidase, the permease, and the transacetylase suggested that the expression of genes encoding these enzymes is controlled by a common mechanism. François Jacob and Jacques Monod proposed the *operon model* to account for this parallel regulation as well as the results of other genetic experiments. The genetic elements of the model are a *regulator gene* that encodes a regulatory protein, a regulatory DNA sequence called *an operator site,* and a *set of structural genes* (Figure 31.7).

The regulator gene encodes a *repressor* protein that binds to the operator site. The binding of the repressor to the operator prevents transcription of the structural genes. The operator and its associated structural genes constitute

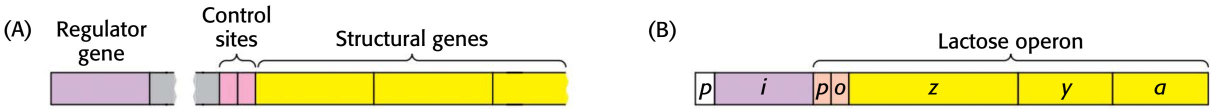

FIGURE 31.7 Operons. (A) The general structure of an operon as conceived by Jacob and Monod. (B) The structure of the lactose operon. In addition to the promoter, *p,* in the operon, a second promoter is present in front of the regulator gene, *i,* to drive the synthesis of the regulator.

the operon. For the *lactose (lac) operon,* the *i* gene encodes the repressor, *o* is the operator site, and the *z, y,* and *a* genes are the structural genes for β-galactosidase, the permease, and the transacetylase, respectively. The operon also contains a promoter site (denoted by *p*), which directs the RNA polymerase to the correct transcription initiation site. The *z, y,* and *a* genes are transcribed to give a single mRNA molecule that encodes all three proteins. An mRNA molecule encoding more than one protein is known as a *polygenic* or *polycistronic* transcript.

The *lac* repressor protein in the absence of lactose binds to the operator and blocks transcription

In the absence of lactose, the lactose operon is repressed. How does the *lac* repressor mediate this repression? The *lac repressor* exists as a tetramer of 37-kDa subunits with two pairs of subunits coming together to form the DNA-binding unit previously discussed. In the absence of lactose, the repressor binds very tightly and rapidly to the operator. When the *lac* repressor is bound to DNA, the repressor prevents RNA polymerase from transcribing the protein-coding genes inasmuch as the operator site is directly adjacent to and downstream of the promoter site where the repressor would block the progress of RNA polymerase.

How does the *lac* repressor locate the operator site in the *E. coli* chromosome? The *lac* repressor binds 4×10^6 times as strongly to operator DNA as it does to random sites in the genome. This high degree of selectivity allows the repressor to find the operator efficiently even with a large excess (4.6×10^6) of other sites within the *E. coli* genome. The dissociation constant for the repressor–operator complex is approximately 0.1 pM (10^{-13} M). The rate constant for association ($\approx 10^{10}\ \mathrm{M}^{-1}\ \mathrm{s}^{-1}$) is strikingly high, indicating that the repressor finds the operator primarily by diffusing along a DNA molecule (a one-dimensional search) rather than encountering it from the aqueous medium (a three-dimensional search). This diffusion has been confirmed by studies that monitored the behavior of fluorescently labeled single molecules of *lac* repressor inside living *E. coli* cells.

Inspection of the complete *E. coli* genome sequence reveals two sites within 500 bp of the primary operator site that approximate the sequence of the operator. When one dimeric DNA-binding unit binds to the operator site, the other DNA-binding unit of the *lac* repressor tetramer can bind to one of these sites with similar sequences. The DNA between the two bound sites forms a loop. No other sites that closely match the sequence of the *lac operator* site are present in the rest of the *E. coli* genome sequence. Thus, *the DNA-binding specificity of the* lac *repressor is sufficient to specify a nearly unique site within the* E. coli *genome.*

The three-dimensional structure of the *lac* repressor has been determined in various forms. Each monomer consists of a small amino-terminal domain that binds DNA and a larger domain that mediates the formation of the dimeric DNA-binding unit and the tetramer (Figure 31.8). A pair of the amino-terminal domains come together to form the functional DNA-binding unit. Each monomer has a helix-turn-helix unit that interacts with the major groove of the bound DNA.

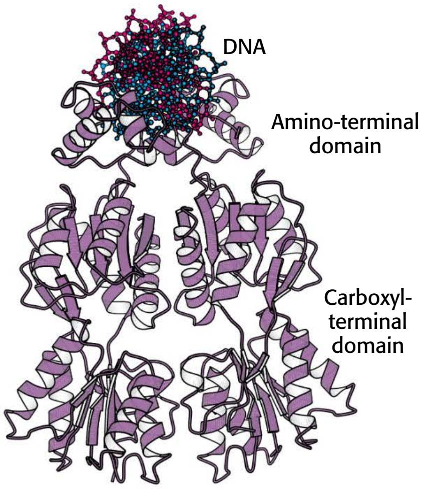

FIGURE 31.8 Structure of the *lac* repressor. A *lac* repressor dimer is shown bound to DNA. *Notice* that the amino-terminal domain binds to DNA, whereas the carboxyl-terminal domain forms a separate structure. A part of the structure that mediates the formation of *lac* repressor tetramers is not shown. [Drawn from 1EFA.pdb.]

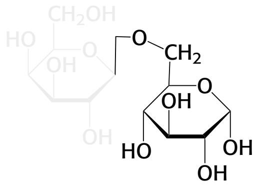

1,6-Allolactose

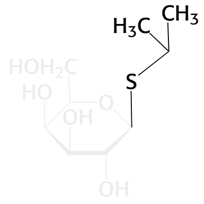

Isopropylthiogalactoside (IPTG)

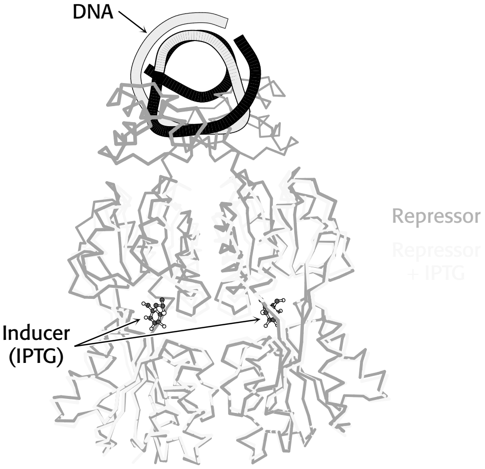

FIGURE 31.9 Effects of IPTG on *lac* repressor structure. The structure of the *lac* repressor bound to the inducer isopropylthiogalactoside (IPTG), shown in orange, is superimposed on the structure of the *lac* repressor bound to DNA, shown in purple. *Notice* that the binding of IPTG induces structural changes that alter the relation between the two DNA-binding domains so that they cannot interact effectively with DNA. The DNA-binding domains of the *lac* repressor bound to IPTG are not shown, because these regions are not well ordered in the crystals studied.

Ligand binding can induce structural changes in regulatory proteins

In the situation just described, glucose is present and lactose is absent, and the *lac* operon is repressed. How does the presence of lactose trigger the relief of this repression and, hence, the expression of the *lac* operon? Interestingly, lactose itself does not have this effect; rather, *allolactose,* a combination of galactose and glucose with an α-1,6 rather than an α-1,4 linkage, does. Allolactose is thus referred to as the *inducer* of the *lac* operon. Allolactose is a side product of the β-galactosidase reaction and is produced at low levels by the few molecules of β-galactosidase that are present before induction. Some other β-galactosides such as *isopropylthiogalactoside* (IPTG) are potent inducers of β-galactosidase expression, although they are not substrates of the enzyme. IPTG is useful in the laboratory as a tool for inducing gene expression in engineered bacterial strains.

The inducer triggers gene expression by preventing the *lac* repressor from binding the operator. *The inducer binds to the* lac *repressor and thereby greatly reduces the repressor's affinity for operator DNA.* An inducer molecule binds in the center of the large domain within each monomer. This binding leads to conformational changes that modify the relation between the two small DNA-binding domains (Figure 31.9). These domains can no longer easily contact DNA simultaneously, leading to a dramatic reduction in DNA-binding affinity.

Let us recapitulate the processes that regulate gene expression in the lactose operon (Figure 31.10). In the absence of inducer, the *lac* repressor is bound to DNA in a manner that blocks RNA polymerase from transcribing the *z, y,* and *a* genes. Thus, very little β-galactosidase, permease, or transacetylase are produced. The addition of lactose to the environment leads to the formation of allolactose. This inducer binds to the *lac* repressor, leading to conformational changes and the release of DNA by the *lac* repressor. With the operator site unoccupied, RNA polymerase can then transcribe the other *lac* genes and the bacterium will produce the proteins necessary for the efficient use of lactose.

The structure of the large domain of the *lac* repressor is similar to those of a large class of proteins that are present in *E. coli* and other bacteria. This family of homologous proteins binds ligands such as sugars and amino acids at their centers. Remarkably, domains of this family are utilized by eukaryotes in taste proteins and in neurotransmitter receptors, as will be discussed in Chapter 33.

The operon is a common regulatory unit in prokaryotes

Many other gene-regulatory networks function in ways analogous to those of the *lac* operon. For example, genes taking part in purine and, to a lesser degree, pyrimidine biosynthesis are repressed by the

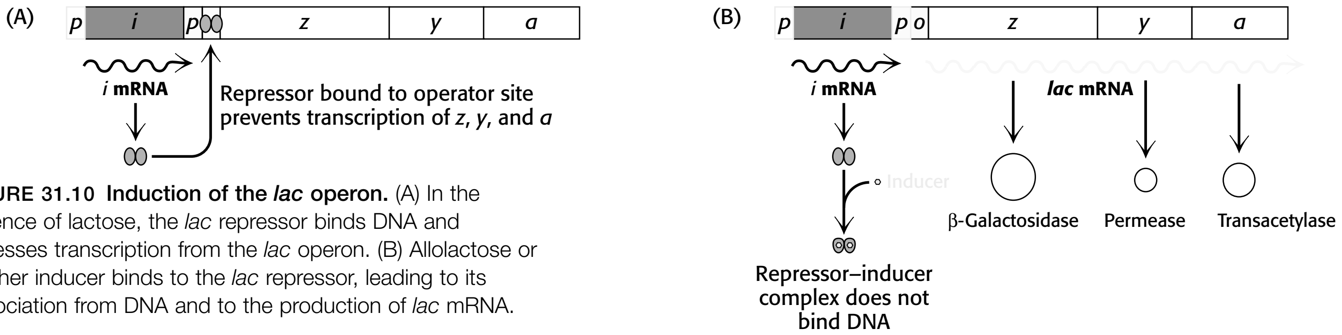
(A)
p
i
p
z
y
a
i mRNA
Repressor bound to operator site prevents transcription of z, y, and a
(B)
p
i
p
o
z
y
a
i mRNA
lac mRNA
inducer
β-Galactosidase
Permease
Transacetylase
Repressor–inducer complex does not bind DNA

FIGURE 31.10 Induction of the *lac* operon. (A) In the absence of lactose, the *lac* repressor binds DNA and represses transcription from the *lac* operon. (B) Allolactose or another inducer binds to the *lac* repressor, leading to its dissociation from DNA and to the production of *lac* mRNA.

pur repressor. This dimeric protein is 31% identical in sequence with the *lac* repressor and has a similar three-dimensional structure. However, the behavior of the *pur* repressor is opposite that of the *lac* repressor: whereas the *lac* repressor is *released* from DNA by binding to a small molecule, *the* pur *repressor binds DNA specifically, blocking transcription, only when bound to a small molecule.* Such a small molecule is called a *corepressor.* For the *pur* repressor, the corepressor can be either guanine or hypoxanthine. The dimeric *pur* repressor binds to inverted-repeat DNA sites of the form 5′-AN**G**C**AA**N**CG**N**TT**N**C**N**T**-3′, in which the bases shown in boldface type are particularly important. Examination of the *E. coli* genome sequence reveals the presence of more than 20 such sites, regulating 19 operons and including more than 25 genes (Figure 31.11).

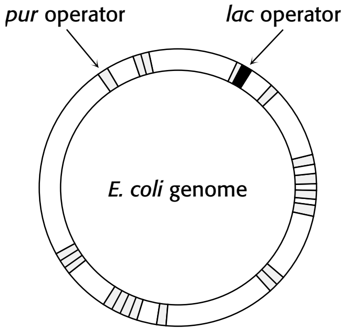

FIGURE 31.11 Binding-site distributions. The *E. coli* genome contains only a single region that closely matches the sequence of the *lac* operator (shown in blue). In contrast, 20 sites match the sequence of the *pur* operator (shown in red). Thus, the *pur* repressor regulates the expression of many more genes than does the *lac* repressor.

Because the DNA-binding sites for these regulatory proteins are short, it is likely that they evolved independently and are not related by divergence from an ancestral regulatory site. Once a ligand-regulated DNA-binding protein is present in a cell, binding sites for the protein may arise by mutation adjacent to additional genes. Binding sites for the *pur* repressor have evolved in the regulatory regions of a wide range of genes taking part in nucleotide biosynthesis. All such genes can then be regulated in a concerted manner.

The organization of prokaryotic genes into operons is useful for the analysis of completed genome sequences. Sometimes a gene of unknown function is discovered to be part of an operon containing well-characterized genes. Such associations can provide powerful clues to the biochemical and physiological functions of the uncharacterized gene.

Transcription can be stimulated by proteins that contact RNA polymerase

All the DNA-binding proteins discussed thus far function by inhibiting transcription until some environmental condition, such as the presence of lactose, is met. There are also DNA-binding proteins that stimulate transcription. One particularly well studied example is a protein in *E. coli* that stimulates the expression of catabolic enzymes.

E. coli grown on glucose, a preferred energy source, have very low levels of catabolic enzymes for metabolizing other sugars. Clearly, the synthesis of these enzymes when glucose is abundant would be wasteful. Glucose has an inhibitory effect on the genes encoding these enzymes, an effect called *catabolite repression.* It is due to the fact that glucose lowers the concentration of cyclic AMP in *E. coli.* When the cAMP concentration is high, it stimulates the concerted transcription of many catabolic enzymes by acting through a protein called the *catabolite activator protein* (CAP), which is also known as the cAMP receptor protein (CRP).

When bound to cAMP, CAP stimulates the transcription of lactose- and arabinose-catabolizing genes. CAP is a sequence-specific DNA-binding protein. Within the *lac* operon, CAP binds to an inverted repeat that is centered near position −61 relative to the start site for transcription (Figure 31.12). This site is approximately 70 base pairs from the operator site. As expected from the symmetry of the binding site, CAP functions as a dimer of identical subunits.

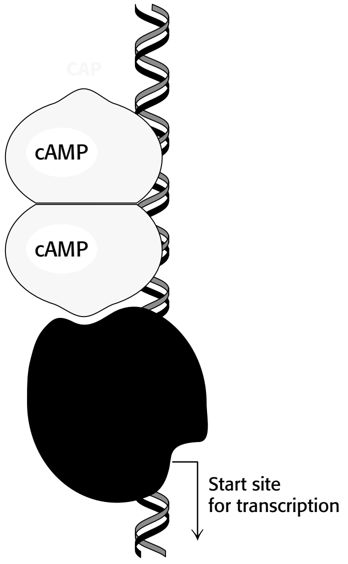

FIGURE 31.12 Binding site for catabolite activator protein (CAP). This protein binds as a dimer to an inverted repeat that is at the position −61 relative to the start site of transcription. The CAP-binding site on DNA is adjacent to the position at which RNA polymerase binds.

The CAP–cAMP complex stimulates the initiation of transcription by approximately a factor of 50. Energetically favorable contacts between CAP and RNA polymerase increase the likelihood that transcription will be initiated at sites to which the CAP–cAMP complex is bound (Figure 31.13). Thus, in regard to the *lac* operon, gene expression is maximal when the

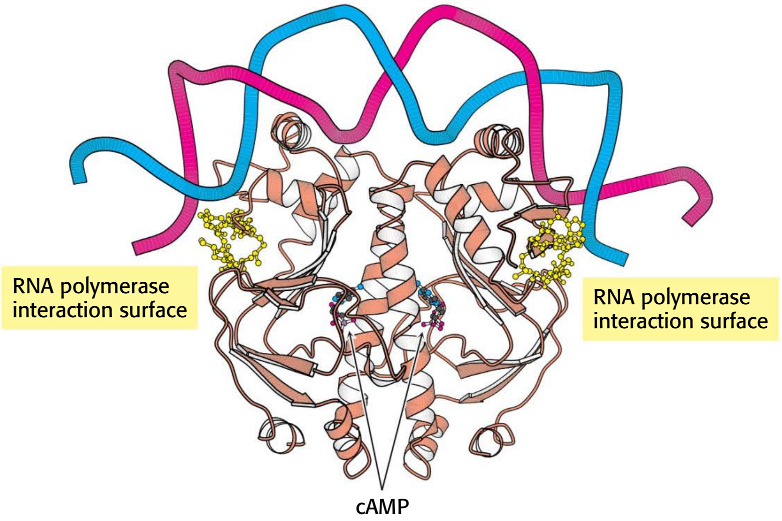
RNA polymerase interaction surface
RNA polymerase interaction surface
cAMP

FIGURE 31.13 Structure of a dimer of CAP bound to DNA. The residues shown in yellow in each CAP monomer have been implicated in direct interactions with RNA polymerase. [Drawn from 1RUN.pdb.]

binding of allolactose relieves the inhibition by the *lac* repressor and the CAP–cAMP complex stimulates the binding of RNA polymerase.

The *E. coli* genome contains many CAP-binding sites in positions appropriate for interactions with RNA polymerase. Thus, an increase in the cAMP level inside an *E. coli* bacterium results in the formation of CAP–cAMP complexes that bind to many promoters and stimulate the transcription of genes encoding a variety of catabolic enzymes.

31.3 Regulatory Circuits Can Result in Switching Between Patterns of Gene Expression

The study of viruses that infect bacteria has led to significant advances in our understanding of the processes that control gene expression. Again, sequence-specific DNA-binding proteins play key roles in these processes. Investigations of bacteriophage λ have been particularly revealing. We examined the alternative infection modes of λ phage in Chapter 5. In the lytic pathway, most of the genes in the viral genome are transcribed, initiating the production of many virus particles and leading to the eventual lysis of the bacterial cell with the concomitant release of approximately 100 virus particles. In the lysogenic pathway, the viral genome is incorporated into the bacterial DNA where most of the viral genes remain unexpressed, allowing the viral genome to be carried along as the bacteria replicate. Two key proteins and a set of regulatory sequences in the viral genome are responsible for the switch that determines which of these two pathways is followed.

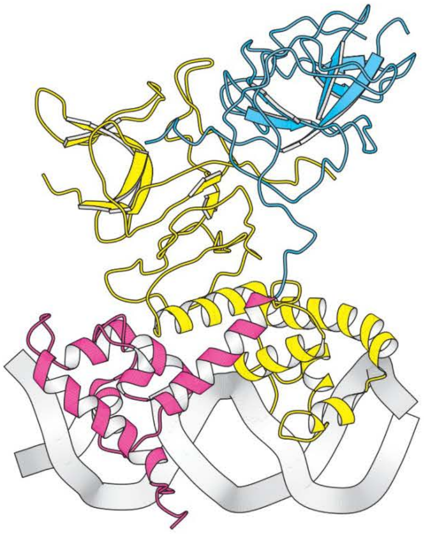

FIGURE 31.14 Structure of the λ repressor bound to DNA. The λ repressor binds to DNA as a dimer. The amino-terminal domain of one subunit is shown in red and the carboxyl-terminal domain is shown in blue. In the other subunit, both domains are shown in yellow. *Notice* how α helices on the amino-terminal domains fit into the major groove of the DNA. [Drawn from 3DBN.pdb.]

The λ repressor regulates its own expression

The first protein that we shall consider is the *repressor*, sometimes known as the λ cI protein. This protein is key because it blocks, either directly or indirectly, the transcription of almost all genes encoded by the virus. The one exception is the gene that encodes the λ repressor itself. The λ repressor consists of an amino-terminal DNA-binding domain and a carboxyl-terminal domain that participates in protein oligomerization (Figure 31.14). This protein binds to a number of key sites in the λ phage genome. The sites of greatest interest for our present discussion are in the so-called right operator (Figure 31.15). This region includes three binding sites for the λ repressor dimer, as well as two promoters within a region of approximately 80 base pairs. One promoter drives the expression of the gene for the λ repressor itself, whereas the other drives the expression of a number of other viral genes.

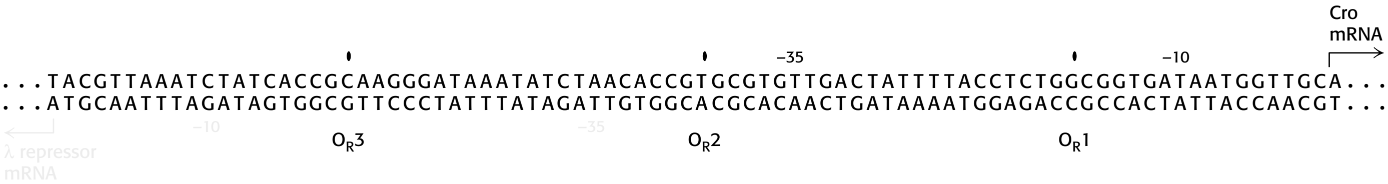
Cro
mRNA
−35
−10
. . . TACGTTAAATCTATCACCGCAAGGGATAAATATCTAACACCGTGCGTGTTGACTATTTTACCTCTGGCGGTGATAATGGTTGCA . . .
. . . ATGCAATTTAGATAGTGGCGTTCCCTATTTATAGATTGTGGCACGCACAACTGATAAAATGGAGACCGCCACTATTACCAACGT . . .
−10
−35
λ repressor
mRNA
O_R3
O_R2
O_R1

FIGURE 31.15 Sequence of the λ right operator. The three operator sites (O_R1, O_R2, and O_R3) are shaded yellow with their centers indicated. The start sites for the λ repressor mRNA and the Cro mRNA are indicated, as are their −10 and −35 sequences.

The λ repressor does not have the same affinity for the three sites; it binds the site O_R1 with the highest affinity. In addition, the binding to adjacent sites is cooperative so that, after a λ repressor dimer has bound at O_R1, the likelihood that a protein will bind to the adjacent site O_R2 increases by approximately 25-fold. Thus, when λ repressor is present in the cell at moderate concentrations, the most likely configuration has λ repressor bound at O_R1 and O_R2, but not at O_R3. In this configuration, the λ repressor dimer bound at O_R1 blocks access to the promoter on the right side of the operator sites, repressing transcription of the adjacent gene, which encodes a protein termed Cro (*c*ontroller of *r*epressor and *o*thers), while the repressor dimer at O_R2 can be in contact with RNA polymerase and stimulate transcription of the promoter that controls the transcription of the gene that encodes the λ repressor itself.

Thus, the λ repressor stimulates its own production. As the concentration of the λ repressor increases further, an additional repressor dimer can bind to the O_R3 site, blocking the other promoter and repressing the production of additional repressor. Thus, the right operator serves to maintain the λ repressor in a narrow, stable concentration range (Figure 31.16). The λ repressor also blocks other promoters in the λ phage genome so that the repressor is the only phage protein produced, which corresponds to the lysogenic state.

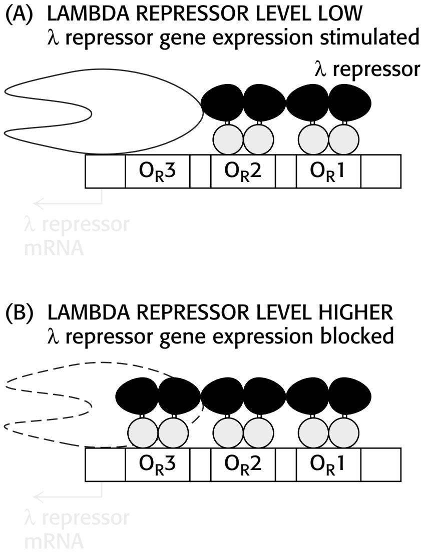
(A) LAMBDA REPRESSOR LEVEL LOW
λ repressor gene expression stimulated
λ repressor
O_R3
O_R2
O_R1
λ repressor
mRNA
(B) LAMBDA REPRESSOR LEVEL HIGHER
λ repressor gene expression blocked
O_R3
O_R2
O_R1
λ repressor
mRNA

FIGURE 31.16 The λ repressor controls its own synthesis. (A) When λ repressor levels are relatively low, the repressor binds to sites O_R1 and O_R2 and stimulates the transcription of the gene that encodes the λ repressor itself. (B) When λ repressor levels are higher, the repressor also binds to site O_R3, blocking access to its promoter and repressing transcription from this gene.

A circuit based on the λ repressor and Cro forms a genetic switch

What stimulates the switch to the lytic pathway? Changes such as DNA damage initiate the cleavage of the λ repressor at a specific bond between the DNA-binding and oligomerization domains. This process is mediated by the *E. coli* RecA protein (Section 28.5). After this cleavage has taken place, the affinity of the λ repressor for DNA is reduced. After the λ repressor is no longer bound to the O_R1 site, the Cro gene can be transcribed. *Cro* is a small protein that binds to the same sites as the λ repressor does, but with a different order of affinity for the three sites in the right operator. In particular, Cro has the highest affinity for O_R3. Cro bound in this site blocks the production of new repressor. The absence of repressor leads to the production of other phage genes, leading to the production of virus particles and the eventual lysis of the host cells. Thus, this genetic circuit acts as a switch with two stable states: (1) repressor high, Cro low, corresponding to the lysogenic state, and (2) Cro high, repressor low, corresponding to the lytic state (Figure 31.17). Regulatory circuits with different DNA-binding proteins controlling the expression of each other's genes constitute a common motif for controlling gene expression.

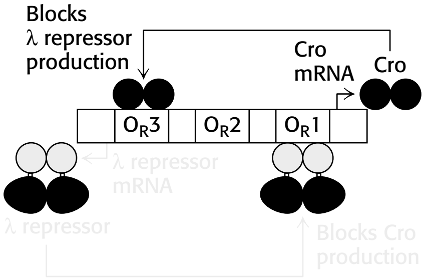
Blocks
λ repressor
production
Cro
mRNA
Cro
O_R3
O_R2
O_R1
λ repressor
mRNA
λ repressor
Blocks Cro
production

FIGURE 31.17 The λ repressor and Cro form a genetic circuit. The λ repressor blocks the production of Cro by binding most favorably to site O_R1 whereas Cro blocks the production of the λ repressor by binding most favorably to site O_R3. This circuit forms a switch that determines whether the lysogenic or the lytic pathway is followed.

Many prokaryotic cells release chemical signals that regulate gene expression in other cells

Prokaryotic cells have been traditionally viewed as solitary single cells. However, it is becoming increasingly clear that, in many circumstances, prokaryotic cells live in complex communities, interacting with other cells

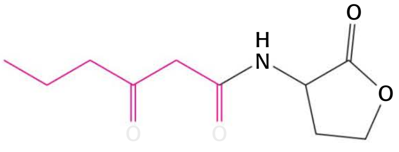

Acyl-homoserine lactone (AHL)

FIGURE 31.18 Autoinducer structure. The structure of the acyl-homoserine lactone *N*-3-oxo-hexanoyl homoserine lactone, the autoinducer from *V. fischeri*. The autoinducers from other bacterial species can have different acyl groups (shown in red).

of their own and different species. *These social interactions change the patterns of gene expression within the cells.*

An important type of interaction is called *quorum sensing*. This phenomenon was discovered in the bacteria *Vibrio fischeri,* a species of bacterium that can live inside a specialized light organ in the bobtail squid. In this symbiotic relation, the bacteria produce luciferase and bioluminesce, providing protection for the squid (by preventing being backlit by moonlight) in exchange for a safer place to live and reproduce. When these bacteria are grown in culture at low density, they are not bioluminescent. However, when the cell density reaches a critical level, the gene for luciferase is expressed and the cells bioluminesce. A key observation was that, when *V. fischeri* cells were transferred to a sterile medium in which other *V. fischeri* cells had been grown to high density, the cells became bioluminescent even at low cell density. This experiment revealed that a chemical, subsequently shown to be *N*-3-oxo-hexanoyl homoserine lactone (hereafter AHL for acyl-homoserine lactone), had been released into the medium where it triggered the development of the bioluminescence (Figure 31.18). This compound and other compounds that play similar roles are termed *autoinducers*.

Cells of *V. fischeri* release the autoinducer into their environment and other *V. fischeri* cells take up the chemical. *V. fischeri* cells express a DNA-binding protein LuxR that serves as the receptor for the autoinducer. LuxR comprises two domains, one of which binds AHL and the other of which binds DNA through a helix-turn-helix motif (Figure 31.19). After the AHL concentration inside the cell has increased to an appropriate level, a substantial fraction of the LuxR molecules bind AHL. When bound to AHL, LuxR dimers bind to specific sites on DNA and increase the rate of transcription initiation at specific genes. The target genes include an operon that contains LuxA and LuxB, which together encode the luciferase enzyme, and LuxI, which produces an enzyme that catalyzes the formation of more AHL.

Because each cell produces only a small amount of the autoinducer, this regulatory system allows each *V. fischeri* cell to determine the density of the *V. fischeri* population in its environment—hence the term *quorum sensing* for this process. Studies of other prokaryotic cells are revealing an elaborate chemical language of different autoinducers (as well as autorepressors that repress specific genes). The "words" in this language include other acyl-homoserine lactone molecules with different acyl chain lengths and functionalities, as well as other distinct classes of molecules.

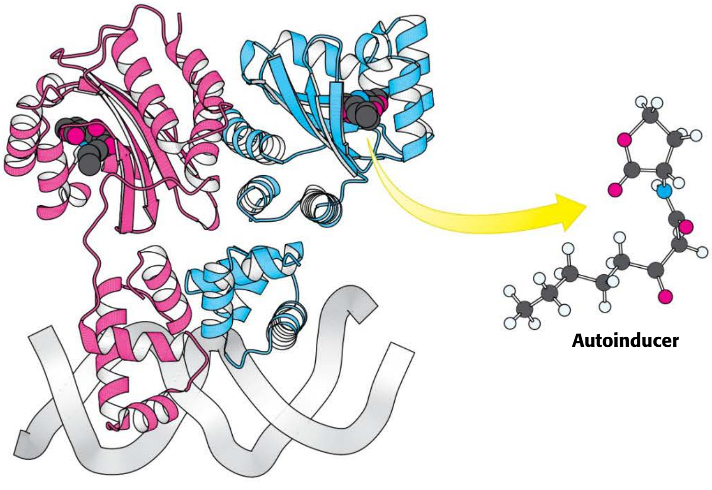

FIGURE 31.19 Quorum-sensing gene regulator. The structure of a homolog of LuxR (TraR from the bacterium *Agrobacterium tumefaciens*) is shown. *Notice* that the dimeric protein binds to DNA through an α-helical domain, whereas the autoinducer binds to a separate domain.

Biofilms are complex communities of prokaryotes

Many species of prokaryotes can be found in specialized structures termed *biofilms* that can form on surfaces. Biofilms are of considerable medical importance because organisms within them are often quite resistant to the immune response of the host as well as to antibiotics. Quorum sensing appears to play a major role in the formation of biofilms, in that cells are able to sense other cells in their environments and to promote the formation of communities with particular compositions. Some genes controlled by quorum-sensing mechanisms promote the formation of specific molecules that serve as scaffolds for the biofilm. An intriguing recent discovery is that many of the organisms that are present in biofilms on or in our bodies (perhaps 95% or more) have not been grown in culture. Through DNA-sequencing methods, we are developing a better census of our microbiome and are working toward understanding the gene-regulatory mechanisms that support these complex communities.

31.4 Gene Expression Can Be Controlled at Posttranscriptional Levels

The modulation of the rate of transcription initiation is the most common mechanism of gene regulation. However, other stages of transcription also can be targets for regulation. In addition, the process of translation provides other points of intervention for regulating the level of a protein produced in a cell. In Chapter 29, we considered riboswitches that control transcription termination (Section 29.1). Other riboswitches control gene expression by other mechanisms such as the formation of structures that inhibit translation. Additional mechanisms for posttranscriptional gene regulation have been discovered, one of which will be described here.

Attenuation is a prokaryotic mechanism for regulating transcription through the modulation of nascent RNA secondary structure

A means for regulating transcription in bacteria was discovered by Charles Yanofsky and his colleagues as a result of their studies of the tryptophan operon. This operon encodes five enzymes that convert chorismate into tryptophan. Analysis of the 5′ end of *trp* mRNA revealed the presence of a *leader sequence* of 162 nucleotides before the initiation codon of the first enzyme. The next striking observation was that bacteria produced a transcript consisting of only the first 130 nucleotides when the tryptophan level was high, but they produced a 7000-nucleotide *trp* mRNA, including the entire leader sequence, when tryptophan was scarce. Thus, when tryptophan is plentiful and the biosynthetic enzymes are not needed, transcription is abruptly broken off before any mRNA coding for the enzymes is produced. The site of termination is called the attenuator, and this mode of regulation is called *attenuation*.

Attenuation depends on features at the 5′ end of the mRNA product (Figure 31.20). The first part of the leader sequence encodes a 14-amino-acid leader peptide. Following the open reading frame for the peptide is the

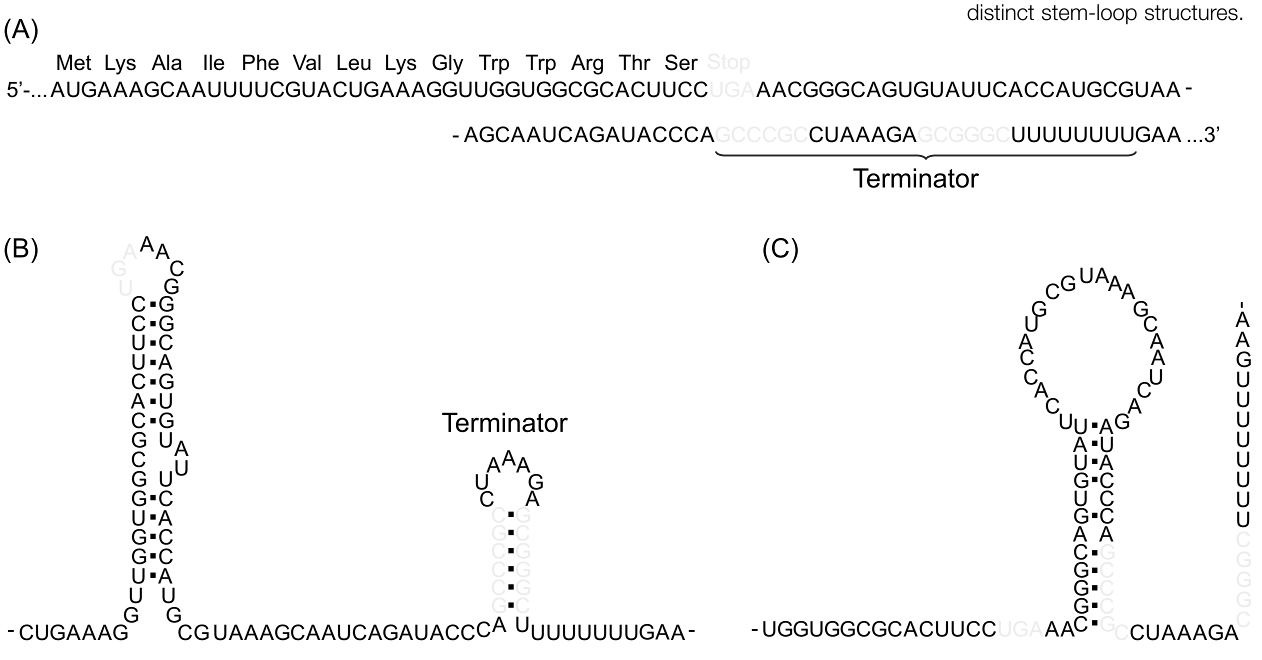
(A)
Met Lys Ala Ile Phe Val Leu Lys Gly Trp Trp Arg Thr Ser Stop
5'-...AUGAAAGCAAUUUUCGUACUGAAAGGUUGGUGGCGCACUUCCUGAAACGGGCAGUGUAUUCACCAUGCGUAA-
-AGCAAUCAGAUACCCAGCCCGCCUAAAGAGCGGGCUUUUUUUUGAA ...3'
Terminator
(B)
Terminator
-CUGAAAG
CGUAAAGCAAUCAGAUACCC
UUUUUUUUGAA-
(C)
-UGGUGGCGCACUUCCUGAAAC
CUAAAGA

FIGURE 31.20 Leader region of *trp* mRNA. (A) The nucleotide sequence of the 5′ end of *trp* mRNA includes a short open reading frame that encodes a peptide comprising 14 amino acids; the leader encodes two tryptophan residues and has an untranslated attenuator region that includes a region that can form a terminator structure (red and blue). (B and C) The attenuator region can adopt either of two distinct stem-loop structures.

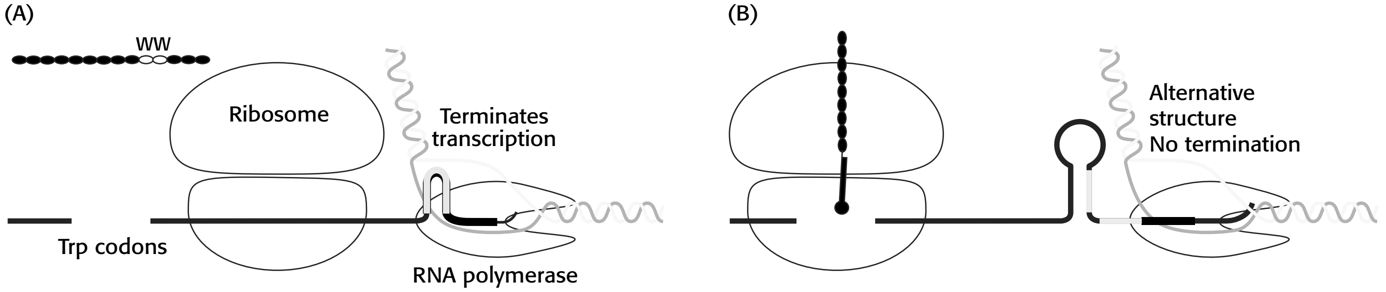

FIGURE 31.21 **Attenuation.** (A) In the presence of adequate concentrations of tryptophan (and, hence, Trp-tRNA), translation proceeds rapidly and an RNA structure forms that terminates transcription. (B) At low concentrations of tryptophan, translation stalls while awaiting Trp-tRNA, giving time for an alternative RNA structure to form that prevents the formation of the terminator and transcription can proceed.

attenuator, a region of RNA that is capable of forming several alternative structures. Recall that transcription and translation are tightly coupled in bacteria. Thus, the translation of the *trp* mRNA begins soon after the ribosome-binding site has been synthesized.

How does the level of tryptophan alter transcription of the *trp* operon? An important clue was the finding that the 14-amino-acid leader peptide includes two adjacent tryptophan residues. A ribosome is able to translate the leader region of the mRNA product only in the presence of adequate concentrations of tryptophan. When enough tryptophan is present, a stem-loop structure forms in the attenuator region, which leads to the release of RNA polymerase from the DNA (Figure 31.21). However, when tryptophan is scarce, transcription is terminated less frequently. Little tryptophanyl-tRNA is present, and so the ribosome stalls at the tandem UGG codons encoding tryptophan. This delay leaves the adjacent region of the mRNA exposed as transcription continues. An alternative RNA structure that does not function as a terminator is formed, and transcription continues into and through the coding regions for the enzymes. Thus, attenuation provides an elegant means of sensing the supply of tryptophan required for protein synthesis.

Several other operons for the biosynthesis of amino acids in *E. coli* also are regulated by attenuator sites. The leader peptide of each contains an abundance of the amino acid residues of the type synthesized by the operon (Figure 31.22). For example, the leader peptide for the phenylalanine operon includes 7 phenylalanine residues among 15 residues. The threonine operon encodes enzymes required for the synthesis of both threonine and isoleucine; the leader peptide contains 8 threonine and 4 isoleucine residues in a 16-residue sequence. The leader peptide for the histidine operon includes

(A)

Met - Lys - Arg - Ile - Ser - Thr - Thr - Ile - Thr - Thr - Thr - Ile - Thr - Ile - Thr - Thr -

5 AUG AAA CGC AUU AGC ACC ACC AUU ACC ACC ACC AUC ACC AUU ACC ACA 3

(B)

Met - Lys - His - Ile - Pro - Phe - Phe - Phe - Ala - Phe - Phe - Phe - Thr - Phe - Pro - Stop

5 AUG AAA CAC AUA CCG UUU UUC UUC GCA UUC UUU UUU ACC UUC CCC UGA 3

(C)

Met - Thr - Arg - Val - Gln - Phe - Lys - His - His - His - His - His - His - His - Pro - Asp -

5 AUG ACA CGC GUU CAA UUU AAA CAC CAC CAU CAU CAC CAU CAU CCU GAC 3

FIGURE 31.22 **Leader peptide sequences.** Amino acid sequences and the corresponding mRNA nucleotide sequences of the (A) threonine operon, (B) phenylalanine operon, and (C) histidine operon. In each case, an abundance of one amino acid in the leader peptide sequence leads to attenuation.

7 histidine residues in a row. In each case, low levels of the corresponding charged tRNA cause the ribosome to stall, trapping the nascent mRNA in a state that can form a structure that allows RNA polymerase to read through the attenuator site. Evolution has apparently converged on this strategy repeatedly as a mechanism for controlling amino acid biosynthesis.

The examples of prokaryotic gene regulation that we have been describing come from bacteria, as opposed to archaea. The transcriptional apparatus present in archaea shares many features with that found in eukaryotes. This commonality is frequently interpreted to suggest that eukaryotes evolved after a cell fusion event in which a bacterial cell was engulfed by an archaeal cell. Nonetheless, the key principles of gene regulation such as the occurrence of operons and the roles of DNA-binding proteins in directly blocking or stimulating RNA polymerase are the same in bacteria and archaea, perhaps because of similar genome sizes. As we shall see in the next chapter, eukaryotic cells with larger genomes and, often, many distinct cell types, utilize quite different strategies.

SUMMARY

31.1 Many DNA-Binding Proteins Recognize Specific DNA Sequences

The regulation of gene expression depends on the interplay between specific sequences within the genome and proteins that bind specifically to these sites. Specific DNA-binding proteins recognize regulatory sites that usually lie adjacent to the genes whose transcription is regulated by these proteins. The proteins of the largest family contain a helix-turn-helix motif. The first helix of this motif inserts into the major groove of DNA and makes specific hydrogen-bonding and other contacts with the edges of the base pairs.

31.2 Prokaryotic DNA-Binding Proteins Bind Specifically to Regulatory Sites in Operons

In prokaryotes, many genes are clustered into operons, which are units of coordinated genetic expression. An operon consists of control sites (an operator and a promoter) and a set of structural genes. In addition, regulator genes encode proteins that interact with the operator and promoter sites to stimulate or inhibit transcription. The treatment of *E. coli* with lactose induces an increase in the production of β-galactosidase and two additional proteins that are encoded in the lactose operon. In the absence of lactose or a similar galactoside inducer, the *lac* repressor protein binds to an operator site on the DNA and blocks transcription. The binding of allolactose, a derivative of lactose, to the *lac* repressor induces a conformational change that leads to dissociation from DNA. RNA polymerase can then move through the operator to transcribe the *lac* operon.

Some proteins activate transcription by directly contacting RNA polymerase. For example, cyclic AMP stimulates the transcription of many catabolic operons by binding to the catabolite activator protein. The binding of the cAMP–CAP complex to a specific site in the promoter region of an inducible catabolic operon enhances the binding of RNA polymerase and the initiation of transcription.

31.3 Regulatory Circuits Can Result in Switching Between Patterns of Gene Expression

The study of bacterial viruses, particularly bacteriophage λ, has revealed key aspects of gene-regulatory networks. Bacteriophage λ can develop by either a lytic or a lysogenic pathway. A key regulatory protein, the λ repressor, regulates its own expression, promoting transcription of the gene that encodes the repressor when repressor levels are low and blocking transcription of the gene when levels are high. This behavior depends on the λ right operator, which includes three sites to which λ repressor dimers can bind. Cooperative binding of the λ repressor to two of the sites stabilizes the state in which two λ repressor dimers are bound. The Cro protein binds to the same sites as does the λ repressor, but with reversed affinities. When Cro is present at sufficient concentrations, it blocks the transcription of the gene for the λ repressor while allowing the transcription of its own gene. Thus, these two proteins and the operator form a genetic switch that can exist in either of two states.

Some prokaryotic species participate in quorum sensing. This process includes the release of chemicals called autoinducers into the medium surrounding the cells. These autoinducers are often, but not always, acyl homoserine lactones. Autoinducers are taken up by surrounding cells. When the autoinducer concentration reaches an appropriate level, it is bound by receptor proteins that activate the expression of genes, including those that promote the synthesis of more autoinducer. These chemically mediated social interactions allow these prokaryotes to change their gene-expression patterns in response to the number of other cells in their environments. Biofilms are complex communities of prokaryotes that are promoted by quorum-sensing mechanisms.

31.4 Gene Expression Can Be Controlled at Posttranscriptional Levels

Gene expression can also be regulated at the level of translation. In prokaryotes, many operons important in amino acid biosynthesis are regulated by attenuation, a process that depends on the formation of alternative structures in mRNA, one of which favors the termination of transcription. Attenuation is mediated by the translation of a leader region of mRNA. A ribosome stalled by the absence of an aminoacyl-tRNA needed to translate the leader mRNA alters the structure of mRNA, allowing RNA polymerase to transcribe the operon beyond the attenuator site.

KEY TERMS

helix-turn-helix motif (p. 927)
β-galactosidase (p. 928)
operon model (p. 928)
operator site (p. 928)
repressor (p. 928)
lac repressor (p. 929)
lac operator (p. 929)
inducer (p. 930)
isopropylthiogalactoside (IPTG) (p. 930)
pur repressor (p. 931)
corepressor (p. 931)
catabolite repression (p. 931)
catabolite activator protein (CAP) (p. 931)
λ repressor (p. 932)
CRO (p. 933)
quorum sensing (p. 934)
autoinducer (p. 934)
biofilm (p. 934)
attenuation (p. 935)

PROBLEMS

1. *Missing genes.* Predict the effects of deleting the following regions of DNA:

(a) The gene encoding *lac* repressor

(b) The *lac* operator

(c) The gene encoding CAP

2. *Minimal concentration.* Calculate the concentration of *lac* repressor, assuming that one molecule is present per cell. Assume that each *E. coli* cell has a volume of 10^{-12} cm^3. Would you expect the single molecule to be free or bound to DNA?

3. *Counting sites.* Calculate the expected number of times that a given 8-base-pair DNA site should be present in the *E. coli* genome. Assume that all four bases are equally probable. Repeat for a 10-base-pair site and a 12-base-pair site.

4. *The same but not the same.* The *lac* repressor and the *pur* repressor are homologous proteins with very similar three-dimensional structures, yet they have different effects on gene expression. Describe two important ways in which the gene-regulatory properties of these proteins differ.

5. *The opposite direction.* Some compounds called anti-inducers bind to repressors such as the *lac* repressor and inhibit the action of inducers; that is, transcription is repressed and higher concentrations of inducer are required to induce transcription. Propose a mechanism of action for anti-inducers.

6. *Inverted repeats.* Suppose that a nearly perfect 20-base-pair inverted repeat is observed in a DNA sequence. Provide two possible explanations.

7. *Broken operators.* Consider a hypothetical mutation in O_R2 that blocks both λ repressor and Cro binding. How would this mutation affect the likelihood of bacteriophage λ entering the lytic phase?

8. *Promoters*. Compare the −10 and −35 sequences for the λ repressor and Cro genes in the right operator. How many differences are there between these sequences?

9. *Positive and negative feedback*. What is the effect of an increased Cro concentration on the expression of the gene for the λ repressor? Of an increased concentration of λ repressor on the expression of the Cro gene? Of an increased concentration of λ repressor on the expression of the λ repressor gene?

10. *Leaderless*. The mRNA for the λ repressor begins with 5′-AUG-3′, which encodes the methionine residue that begins the protein. What is unusual about this beginning? Would it cause the mRNA to translate efficiently or not?

11. *Quorum count*. Suppose you have a series of compounds that you wish to test for the autoinducer activity in *Vibrio fischeri*. Propose a simple assay, assuming that you can grow *V. fischeri* cultures at low cell densities.

12. *Codon utilization*. There are four codons that encode threonine. Consider the leader sequence in Figure 31.22A. What codons are used and with what frequency?

Mechanism Problem

13. *Follow the stereochemistry*. The hydrolysis of lactose is catalyzed by β-galactosidase. Does the overall reaction proceed with retention or inversion of configuration? Given that each step likely proceeds with inversion of configuration, what does the overall change in stereochemistry suggest about the mechanism? A key residue in the reaction has been identified to be Glu 537. Propose an overall mechanism for the hydrolysis of lactose.

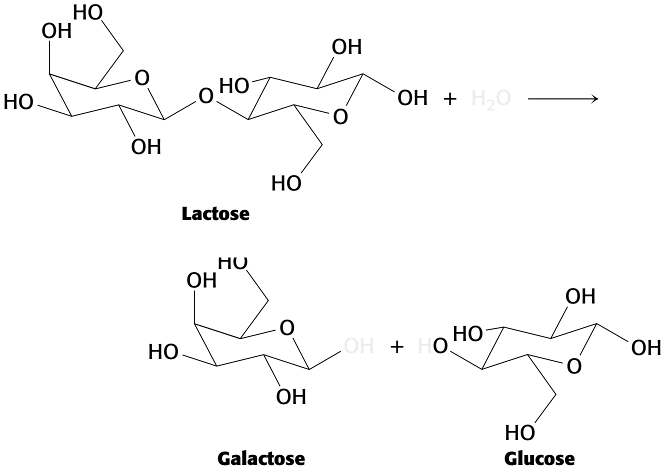

Data Interpretation Problem

14. *Leaving tracks*. A powerful method for examining protein–DNA interactions is called DNA footprinting. In this method, a DNA fragment containing a potential binding site is radiolabeled on one end. The labeled DNA is then treated with a DNA-cleaving agent such as DNase I such that each DNA molecule within the population is cut only once. The same cleavage process is carried out in the presence of the DNA-binding protein. The bound protein protects some sites within the DNA from cleavage. The patterns of DNA fragments in the cleaved pool of DNA molecules are then examined by electrophoresis followed by autoradiography (a).

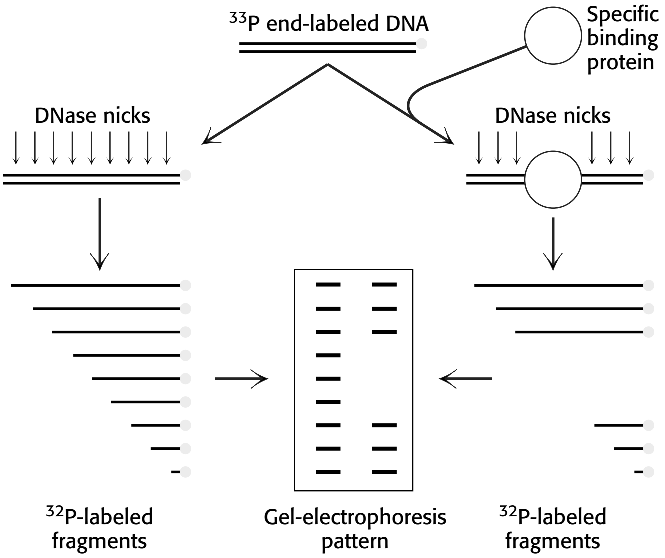

This method is applied to a DNA fragment containing a single binding site for the λ repressor in the presence of different concentrations of the λ repressor. The results are shown below (b):

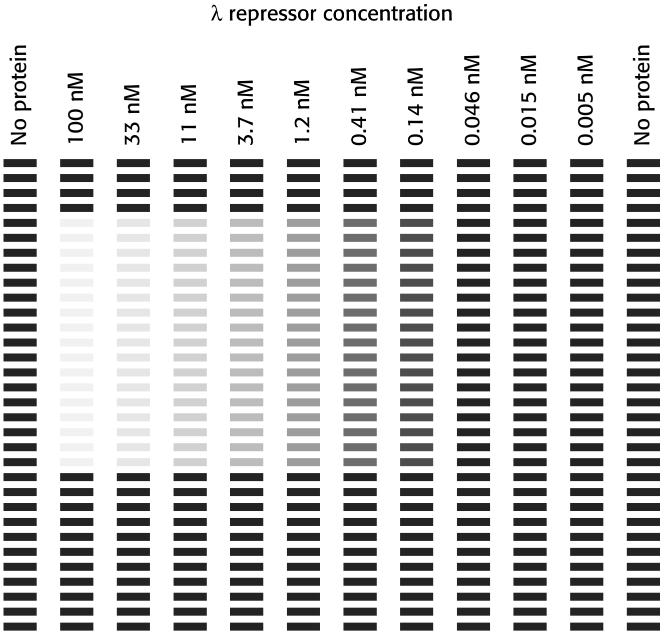
λ repressor concentration
No protein
100 nM
33 nM
11 nM
3.7 nM
1.2 nM
0.41 nM
0.14 nM
0.046 nM
0.015 nM
0.005 nM
No protein

Estimate the dissociation constant for the λ repressor–DNA complex and the standard free energy of binding.

CHAPTER

32

The Control of Gene Expression in Eukaryotes

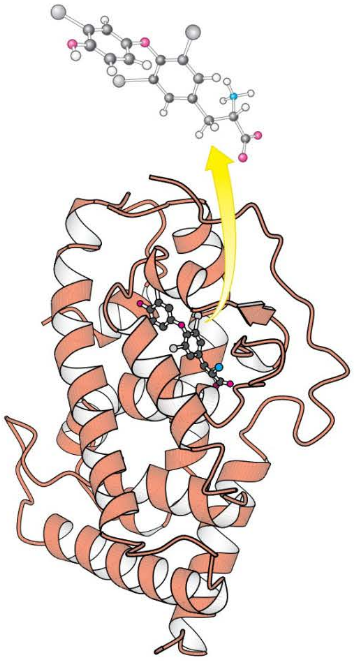

Complex biological processes often require coordinated control of the expression of many genes. The maturation of a tadpole into a frog is largely controlled by thyroid hormone. This hormone regulates gene expression by binding to a protein, the thyroid-hormone receptor, as shown at the right. In response to the hormone's binding, this protein binds to specific DNA sites in the genome and modulates the expression of nearby genes. [(Left) Gary Meszaros/Getty Images.]

Many of the most important and intriguing features in modern biology and medicine, such as the pathways crucial for the development of multicellular organisms, the changes that distinguish normal cells and cancer cells, and the evolutionary changes leading to new species, entail networks of gene-regulatory pathways. Gene regulation in eukaryotes is significantly more complex than in prokaryotes in several ways. First, the genomes being regulated are significantly larger. The *E. coli* genome consists of a single, circular chromosome containing 4.6 megabases (Mb). This genome encodes approximately 2000 proteins. In comparison, one of the simplest eukaryotes, *Saccharomyces cerevisiae* (baker's yeast), contains 16 chromosomes ranging in size from 0.2 to 2.2 Mb (Figure 32.1). The yeast genome totals 12 Mb and encodes approximately 6000 proteins. The genome within a human cell contains 23 pairs of chromosomes ranging in size from 50 to 250 Mb. Approximately 21,000 genes are present within the 3000 Mb of human DNA.

Second, whereas prokaryotic genomic DNA is relatively accessible, eukaryotic DNA is packaged into chromatin, a complex between the DNA and a special set of proteins (Figure 32.2). Although the principles for the construction of chromatin are relatively simple, the chromatin structure for a complete genome is quite complex. Importantly, in a given eukaryotic cell, some genes and their associated regulatory regions are relatively accessible

OUTLINE

32.1 Eukaryotic DNA Is Organized into Chromatin

32.2 Transcription Factors Bind DNA and Regulate Transcription Initiation

32.3 The Control of Gene Expression Can Require Chromatin Remodeling

32.4 Eukaryotic Gene Expression Can Be Controlled at Posttranscriptional Levels

Megabase

A length of DNA consisting of 10^6 base pairs (if double stranded) or 10^6 bases (if single stranded).

1 Mb = 10^3 kb = 10^6 bases

for transcription and regulation, whereas other genes are tightly packaged and are thus rendered inactive. Eukaryotic gene regulation frequently requires the manipulation of chromatin structure.

A manifestation of this complexity is the presence of many different *cell types* in most eukaryotes. A liver cell, a pancreatic cell, and an embryonic stem cell contain the same DNA sequences, yet the subset of genes highly expressed in cells from the pancreas, which secretes digestive enzymes, differs markedly from the subset highly expressed in the liver, the site of lipid transport and energy transduction. Embryonic stem cells do not express any subset of genes at high levels; the most highly expressed genes are "housekeeping" genes involved in the cytoskeleton and processes such as translation (Table 32.1). The existence of stable cell types is due to differences in the *epigenome,* differences in chromatin structure, and covalent modifications of the DNA, not in the DNA sequence itself. Thus, different cell types share the same genome (DNA sequence) but differ in their epigenomes, the packaging and modification of this genome.

In addition, eukaryotic genes are not generally organized into operons. Instead, genes that encode proteins for steps within a given pathway are often spread widely across the genome. This characteristic requires that other mechanisms function to regulate genes in a coordinated way.

Despite these differences, some aspects of gene regulation in eukaryotes are quite similar to those in prokaryotes. In particular, activator and repressor proteins that recognize specific DNA sequences are central to many gene-regulatory processes. In this chapter, we will focus first on chromatin structure. We will then turn to transcription factors—DNA-binding proteins similar in many ways to the prokaryotic proteins that we encountered in the preceding chapter. Eukaryotic transcription factors can act directly by interacting with the transcriptional machinery or indirectly by influencing chromatin structure. Finally, we examine selected

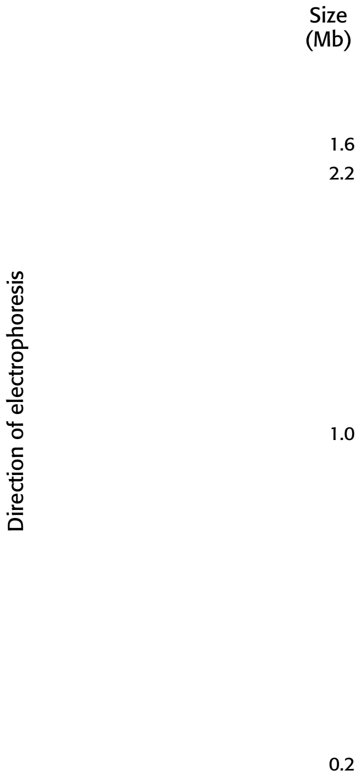

FIGURE 32.1 Yeast chromosomes. Pulsed-field electrophoresis allows the separation of 16 yeast chromosomes. [From G. Chu, D. Vollrath, and R. W. Davis, *Science* 234:1582–1585, 1986.]

FIGURE 32.2 Chromatin structure. An electron micrograph of chromatin showing its "beads on a string" character. The beads correspond to DNA complexes with specific proteins. [Don W. Fawcett/Science Source.]

TABLE 32.1 Highly expressed protein-encoding genes of the pancreas, liver, and embryonic stem cells (as percentage of total mRNA pool)

Rank	Proteins expressed in pancreas	%	Proteins expressed in liver	%	Proteins expressed in stem cells	%
1	Procarboxypeptidase A1	7.6	Albumin	3.5	Glyceraldehyde-3-phosphate dehydrogenase	0.7
2	Pancreatic trypsinogen 2	5.5	Apolipoprotein A-I	2.8	Translation elongation factor 1 α1	0.6
3	Chymotrypsinogen	4.4	Apolipoprotein C-I	2.5	Tubulin α	0.5
4	Pancreatic trypsin 1	3.7	Apolipoprotein C-III	2.1	Translationally controlled tumor protein	0.5
5	Elastase IIIB	2.4	ATPase 6/8	1.5	Cyclophilin A	0.4
6	Protease E	1.9	Cytochrome oxidase 3	1.1	Cofilin	0.4
7	Pancreatic lipase	1.9	Cytochrome oxidase 2	1.1	Nucleophosmin	0.3
8	Procarboxypeptidase B	1.7	α_1-Antitrypsin	1.0	Connexin 43	0.3
9	Pancreatic amylase	1.7	Cytochrome oxidase 1	0.9	Phosphoglycerate mutase	0.2
10	Bile-salt-stimulated lipase	1.4	Apolipoprotein E	0.9	Translation elongation factor 1 β2	0.2

Sources: Data for pancreas from V. E. Velculescu, L. Zhang, B. Vogelstein, and K. W. Kinzler, *Science* 270:484–487, 1995. Data for liver from T. Yamashita, S. Hashimoto, S. Kaneko, S. Nagai, N. Toyoda, T. Suzuki, K. Kobayashi, and K. Matsushima, *Biochem. Biophys. Res. Commun.* 269:110–116, 2000. Data for stem cells from M. Richards, S. P. Tan, J. H. Tan, W. K. Chan, and A. Bongso, *Stem Cells* 22:51–64, 2004.

posttranscriptional gene-regulatory mechanisms, including those based on microRNAs, an important class of gene-regulatory molecules discovered in recent years.

32.1 Eukaryotic DNA Is Organized into Chromatin

Eukaryotic DNA is tightly bound to a group of small basic proteins called *histones*. In fact, histones constitute half the mass of a eukaryotic chromosome. The entire complex of a cell's DNA and associated protein is called *chromatin*. Chromatin compacts and organizes eukaryotic DNA and its presence has dramatic consequences for gene regulation.

Nucleosomes are complexes of DNA and histones

Chromatin is made up of repeating units, each containing 200 bp of DNA and two copies each of four histone proteins H2A, H2B, H3, and H4. Histones have strikingly basic properties because a quarter of the residues in each histone are either arginine or lysine, positively charged amino acids that strongly interact with the negatively charged DNA. The protein complex is called the *histone octamer*. The repeating units of the histone octamer and the associated DNA are known as *nucleosomes*. Chromatin viewed with the electron microscope has the appearance of beads on a string (Figure 32.2); each bead has a diameter of approximately 100 Å. Partial digestion of chromatin with DNase yields the isolated beads. These particles consist of fragments of DNA about 200 bp in length bound to the histone octamer. More-extensive digestion yields a shorter DNA fragment of 145 bp bound to the octamer. The smaller complex formed by the histone octamer and the 145-bp DNA fragment is the *nucleosome core particle*. The DNA connecting core particles in undigested chromatin is called linker DNA. Histone H1 binds, in part, to the linker DNA.

DNA wraps around histone octamers to form nucleosomes

The overall structure of the nucleosome was revealed through electron microscopic and x-ray crystallographic studies pioneered by Aaron Klug and his colleagues. More recently, the three-dimensional structure of a reconstituted nucleosome core particle (Figure 32.3) was determined to

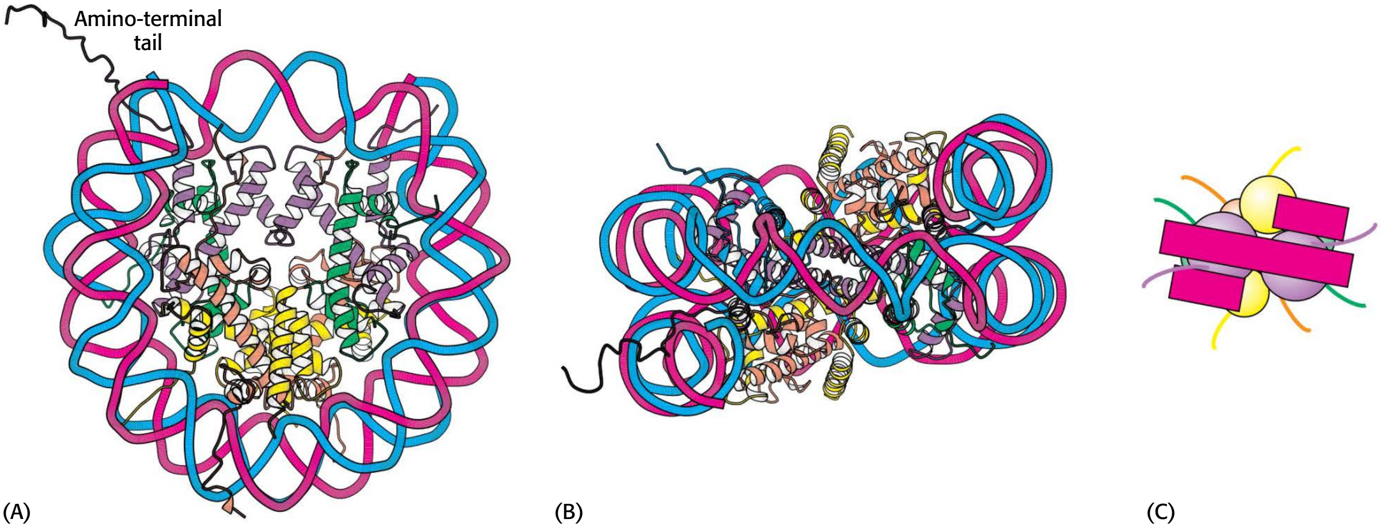

FIGURE 32.3 Nucleosome core particle. The structure consists of a core of eight histone proteins surrounded by DNA. (A) A view showing the DNA wrapping around the histone core. (B) A 90-degree rotation of the view in part (A). *Notice* that the DNA forms a left-handed superhelix as it wraps around the core. (C) A schematic view. [Drawn from 1AOI.pdb.]

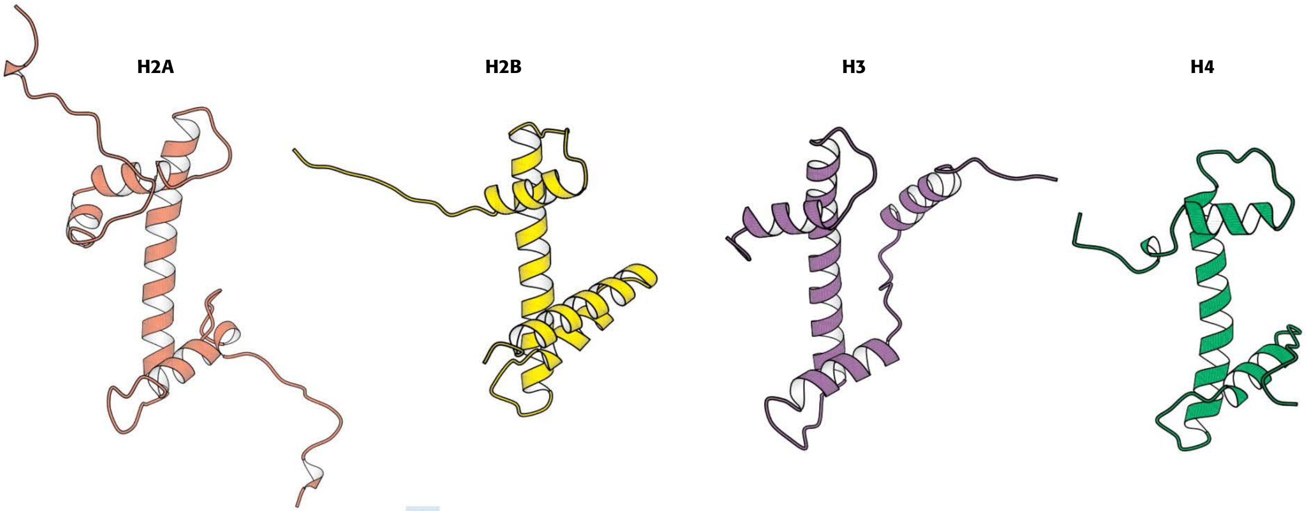

FIGURE 32.4 Homologous histones. Histones H2A, H2B, H3, and H4 adopt a similar three-dimensional structure as a consequence of common ancestry. Some parts of the tails at the termini of the proteins are not shown. [Drawn from 1AOI.pdb.]

higher resolution by x-ray diffraction methods. The four types of histone that make up the protein core are homologous and similar in structure (Figure 32.4). The eight histones in the core are arranged into a $(H3)_2(H4)_2$ tetramer and a pair of H2A–H2B dimers. The tetramer and dimers come together to form a left-handed superhelical ramp around which the DNA wraps. In addition, each histone has an amino-terminal tail that extends out from the core structure. These tails are flexible and contain a number of lysine and arginine residues. As we shall see, *covalent modifications of these tails play an essential role in regulating gene expression.*

The DNA forms a left-handed superhelix as it wraps around the outside of the histone octamer. The protein core forms contacts with the inner surface of the DNA superhelix at many points, particularly along the phosphodiester backbone and the minor groove. Nucleosomes will form on almost all DNA sites, although some sequences are preferred because the dinucleotide steps are properly spaced to favor bending around the histone core. A histone with a different structure from that of the others, called histone H1, seals off the nucleosome at the location at which the linker DNA enters and leaves. The amino acid sequences of histones, including their amino-terminal tails, are remarkably conserved from yeast to human beings.

The winding of DNA around the nucleosome core contributes to the packing of DNA by decreasing its linear extent. An extended 200-bp stretch of DNA would have a length of about 680 Å. Wrapping this DNA around the histone octamer reduces the length to approximately 100 Å along the long dimension of the nucleosome. Thus the DNA is compacted by a factor of 7. However, human chromosomes in metaphase, which are highly condensed, are compacted by a factor of 10^4. Clearly, the nucleosome is just the first step in DNA compaction. What is the next step? The nucleosomes themselves are arranged in a helical array approximately 360 Å across, forming a series of stacked layers approximately 110 Å apart (Figure 32.5). The folding of these fibers of nucleosomes into loops further compacts DNA.

The wrapping of DNA around the histone octamer as a left-handed helix also stores negative supercoils; if the DNA in a nucleosome is straightened out, the DNA will be underwound. This underwinding is exactly what is needed to separate the two DNA strands during replication and transcription.

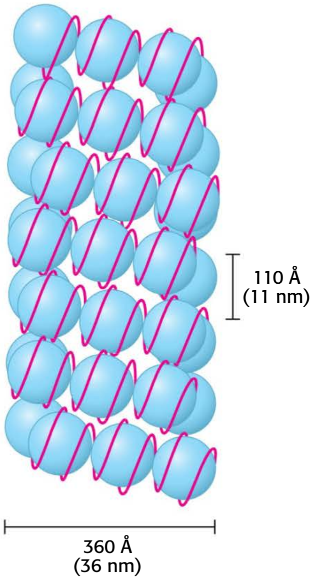

FIGURE 32.5 Higher-order chromatin structure. A proposed model for chromatin arranged in a helical array consisting of six nucleosomes per turn of helix. The DNA double helix (shown in red) is wound around each histone octamer (shown in blue). The actual structure in cells is likely more heterogeneous and dynamic than suggested by this model. [Information from J. T. Finch and A. Klug, *Proc. Natl. Acad. Sci. U. S. A.* 73:1897–1901, 1976.]

32.2 Transcription Factors Bind DNA and Regulate Transcription Initiation

DNA-binding *transcription factors* are key to gene regulation in eukaryotes, just as they are in prokaryotes. However, the roles of eukaryotic transcription factors are different in several ways. First, whereas the DNA-binding sites crucial for the control of gene expression in prokaryotes are usually quite close to promoters, those in eukaryotes can be farther away from promoters and can exert their action at a distance. Second, most prokaryotic genes are regulated by single transcription factors, and multiple genes in a pathway are expressed in a coordinated fashion because such genes are often transcribed as part of a polycistronic mRNA. In eukaryotes, the expression of each gene is typically controlled by multiple transcription factors, and the coordinated expression of different genes depends on having similar transcription-factor-binding sites in each gene in the set. Third, in prokaryotes, transcription factors usually interact directly with RNA polymerase. In eukaryotes, while some transcription factors interact directly with RNA polymerase, many others act more indirectly, interacting with other proteins associated with RNA polymerase or modifying chromatin structure. Let us now examine eukaryotic transcription factors in more detail.

Eukaryotic transcription factors usually consist of several domains. The *DNA-binding domain* binds to regulatory sequences that can either be adjacent to the promoter or at some distance from it. Most commonly, transcription factors include additional domains that help activate transcription. When a transcription factor is bound to the DNA, its *activation domain* promotes transcription by interacting with RNA polymerase II, by interacting with other associated proteins, or by modifying the local structure of chromatin.

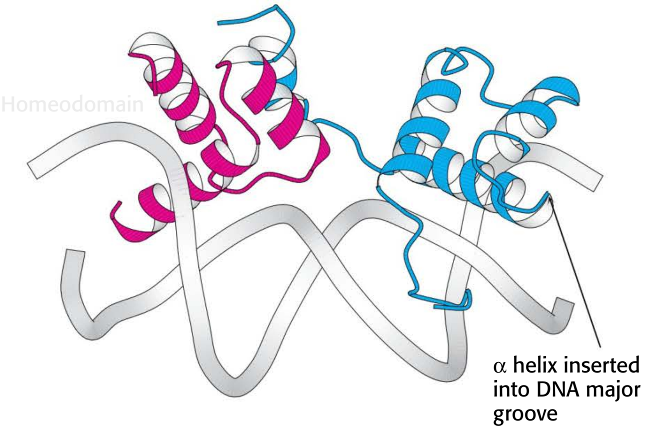

FIGURE 32.6 Homeodomain structure. The structure of a heterodimer formed from two different DNA-binding domains, each based on a homeodomain. *Notice* that each homeodomain has a helix-turn-helix motif with one helix inserted into the major groove of DNA. [Drawn from 1AKH.pdb.]

A range of DNA-binding structures are employed by eukaryotic DNA-binding proteins

The structures of many eukaryotic DNA-binding proteins have been determined and a range of structural motifs have been observed, but we will focus on three that reveal the common features and the diversity of these motifs. The first class of eukaryotic DNA-binding unit that we will consider is the *homeodomain* (Figure 32.6). The structure of the homeodomain and its mode of recognition of DNA are very similar to those of the prokaryotic helix-turn-helix proteins. In eukaryotes, homeodomain proteins often form heterodimeric structures, sometimes with other homeodomain proteins, that recognize asymmetric DNA sequences.

The second class of eukaryotic DNA-binding unit comprises the *basic-leucine zipper* (bZip) *proteins* (Figure 32.7). This DNA-binding unit consists of a pair of long α helices. The first part of each α helix is a basic region that lies in the major groove of the DNA and makes contacts responsible for DNA-site recognition. The second part of each α helix forms a coiled-coil structure with its partner. Because these units are often stabilized by appropriately spaced leucine residues, these structures are often referred to as *leucine zippers*.

The final class of eukaryotic DNA-binding units that we will consider here are the *Cys$_2$His$_2$ zinc-finger domains* (Figure 32.8). A DNA-binding unit of this class comprises tandem sets of small domains, each of which binds a zinc ion through conserved sets of two cysteine and two histidine residues. These structures, often called *zinc-finger domains,* form a string that follows the major

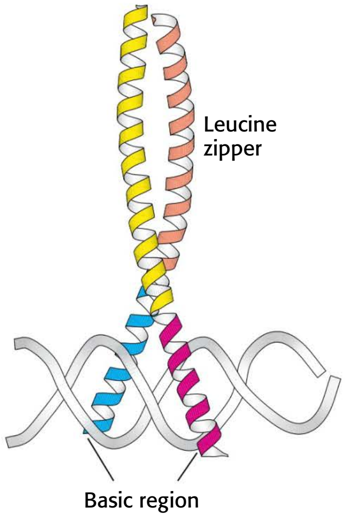

FIGURE 32.7 Basic-leucine zipper. This heterodimer comprises two basic-leucine zipper proteins. *Notice* that the basic region lies in the major groove of DNA. The leucine-zipper part stabilizes the protein dimer. [Drawn from 1FOS.pdb.]

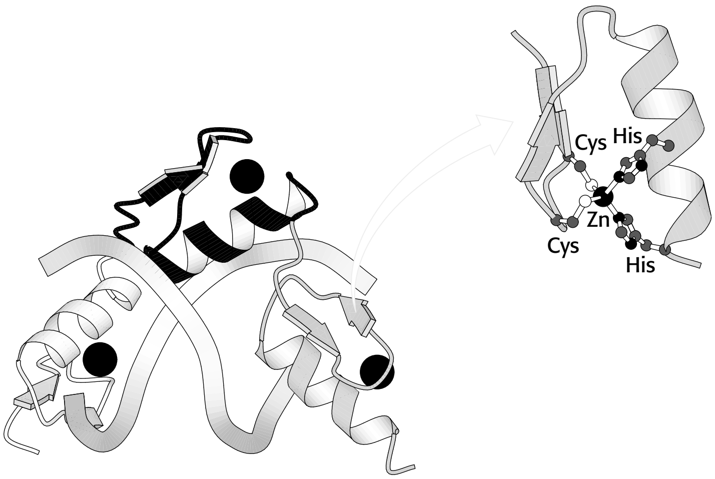

FIGURE 32.8 Zinc-finger domains. A DNA-binding domain comprising three Cys_2His_2 zinc-finger domains (shown in yellow, blue, and red) is shown in a complex with DNA. Each zinc-finger domain is stabilized by a bound zinc ion (shown in green) through interactions with two cysteine residues and two histidine residues. *Notice* how the protein wraps around the DNA in the major groove. [Drawn from 1AAY.pdb.]

groove of DNA. An α helix from each domain makes specific contact with the edges of base pairs within the groove. Some proteins contain arrays of 10 or more zinc-finger domains, potentially enabling them to contact long stretches of DNA. The human genome encodes several hundred proteins that contain zinc-finger domains of this class. We will encounter another class of zinc-based DNA-binding domain when we consider nuclear hormone receptors in Section 32.3.

Activation domains interact with other proteins

The activation domains of transcription factors generally recruit other proteins that promote transcription. In some cases, these activation domains interact directly with RNA polymerase II or closely associated proteins. The activation domains act through intermediary proteins that bridge between the transcription factors and the polymerase. An important target of activators is *mediator,* a complex of 25 to 30 subunits conserved from yeast to human beings, that acts as a bridge between transcription factors and promoter-bound RNA polymerase II (Figure 32.9).

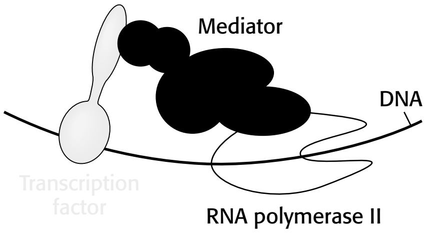

FIGURE 32.9 Mediator. Mediator, a large complex of protein subunits, acts as a bridge between transcription factors bearing activation domains and RNA polymerase II. These interactions help recruit and stabilize RNA polymerase II near specific genes that are then transcribed.

Activation domains are less conserved than DNA-binding domains. In fact, very little sequence similarity has been found. For example, they may be acidic, hydrophobic, glutamine rich, or proline rich. However, they have certain features in common. First, they are often *redundant;* that is, a part of the activation domain can be deleted without loss of function. Second, they are *modular* and can activate transcription when paired with a variety of DNA-binding domains. Third, they can act *synergistically:* two activation domains acting together create a stronger effect than either acting separately.

We have been considering the case in which gene control increases the expression level of a gene. In many cases, the expression of a gene must be decreased by blocking transcription. The agents in such cases are *transcriptional repressors*. Like activators, transcriptional repressors act in many cases by altering chromatin structure.

Multiple transcription factors interact with eukaryotic regulatory regions

The basal transcription complex described in Chapter 29 initiates transcription at a low frequency. Recall that several general transcription factors join with RNA polymerase II to form the basal transcription complex. Additional transcription factors must bind to other sites that can be near the promoter or quite distant for a gene to achieve a higher rate of mRNA synthesis. In contrast with the regulators of prokaryotic transcription, few eukaryotic transcription factors have any effect on their own. Instead, each factor recruits other proteins to build up large complexes that interact with the transcriptional machinery to activate transcription.

A major advantage of this mode of regulation is that a given regulatory protein can have different effects, depending on what other proteins are present in the same cell. This phenomenon, called *combinatorial control,* is crucial to multicellular organisms that have many different cell types. Even in unicellular eukaryotes such as yeast, combinatorial control allows the generation of distinct cell types.

Enhancers can stimulate transcription in specific cell types

Transcription factors can often act even if their binding sites lie at a considerable distance from the promoter. These distant regulatory sites are called *enhancers* (Chapter 29). Enhancers function by serving as binding sites for specific transcription factors. An enhancer is effective only in the specific cell types in which appropriate regulatory proteins are expressed. In many cases, these DNA-binding proteins influence transcription initiation by perturbing the local chromatin structure to expose a gene or its regulatory sites rather than by direct interactions with RNA polymerase. This mechanism accounts for the ability of enhancers to act at a distance.

The properties of enhancers are illustrated by studies of the enhancer controlling the muscle isoform of creatine kinase (Figure 32.10). The results of mutagenesis and other studies revealed the presence of an enhancer located between 1350 and 1050 base pairs upstream of the start site of the gene for this enzyme. Experimentally inserting this enhancer near a gene not normally expressed in muscle cells is sufficient to cause the gene to be expressed at high levels in muscle cells but not in other cells (Figure 32.11).

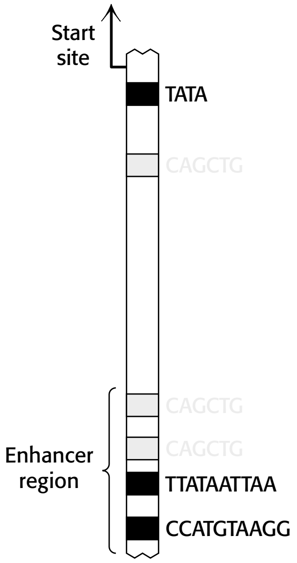

FIGURE 32.10 Enhancer binding sites. A schematic structure for the region 1 kb upstream of the start site for the muscle creatine kinase gene. One binding site of the form 5′-CAGCTG-3′ is present near the TATA box. The enhancer region farther upstream contains two binding sites for the same protein and two additional binding sites for other proteins.

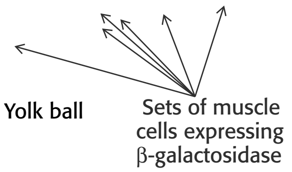

FIGURE 32.11 An experimental demonstration of enhancer function. A promoter for muscle creatine kinase artificially drives the transcription of β-galactosidase in a zebrafish embryo. Only specific sets of muscle cells produce β-galactosidase, as visualized by the formation of the blue product on treatment of the embryo with X-Gal. [From F. Müller, D. W. Williamson, J. Kobolák, L. Gauvry, G. Goldspink, L. Orbán, and N. MacLean, *Mol. Reprod. Dev.* 47:404–412, 1997.]

Induced pluripotent stem cells can be generated by introducing four transcription factors into differentiated cells

An important application illustrating the power of transcription factors is the development of *induced pluripotent stem* (iPS) *cells.* Pluripotent stem cells have the ability to differentiate into many different cell types on appropriate treatment. Previously isolated cells derived from embryos show a very high degree of pluripotency. Over time, researchers identified dozens of genes in embryonic stem cells that contributed to this pluripotency when expressed. In a remarkable experiment reported for mouse cells in 2006 and human cells in 2007, Shinya Yamanaka demonstrated that just four genes out of this entire set could induce pluripotency in already-differentiated skin cells. Yamanaka introduced genes encoding four transcription factors into skin cells called fibroblasts. The fibroblasts de-differentiated into cells that appeared to have characteristics very nearly identical with those of embryonic stem cells (Figure 32.12).

These iPS cells represent powerful research tools and, potentially, a new class of therapeutic agents. The proposed concept is that a sample of a patient's fibroblasts could be readily isolated and converted into iPS cells. These iPS cells could be treated to differentiate into a desired cell type that could then be transplanted into the patient. For example, such an approach might be used to restore a particular class of nerve cells that had been depleted by a neurodegenerative disease. Although the field of iPS cell research is still evolving, it holds great promise as a possible approach to treat any common and difficult-to-treat diseases.

FIGURE 32.12 Induced pluripotent stem cells. A micrograph of human induced pluripotent stem cells stained green for a transcription factor that is characteristic of pluripotent cells. [From K. Takahashi et al., *Cell* 131:861–872, 2007; with permission from Elsevier, courtesy of Shinya Yamanaka, Kyoto University.]

32.3 The Control of Gene Expression Can Require Chromatin Remodeling

Early observations suggested that chromatin structure plays a major role in controlling eukaryotic gene expression. DNA that is densely packaged into chromatin is less susceptible to cleavage by the nonspecific DNA-cleaving enzyme DNase I. Regions adjacent to genes that are being transcribed are more sensitive to cleavage by DNase I than are other sites in the genome, suggesting that the DNA in these regions is less compacted than it is elsewhere and more accessible to proteins. In addition, some sites, usually within 1 kb of the start site of an active gene, are exquisitely sensitive to DNase I and other nucleases. These *hypersensitive sites* correspond to regions that have few nucleosomes or contain nucleosomes in an altered conformation *Hypersensitive sites are cell-type specific and developmentally regulated*. For example, globin genes in the precursors of erythroid cells from 20-hour-old chicken embryos are insensitive to DNase I. However, when hemoglobin synthesis begins at 35 hours, regions adjacent to these genes become highly susceptible to digestion. In tissues such as the brain that produce no hemoglobin, the globin genes remain resistant to DNase I throughout development and into adulthood. These studies suggest that a prerequisite for gene expression is a relaxing of the chromatin structure.

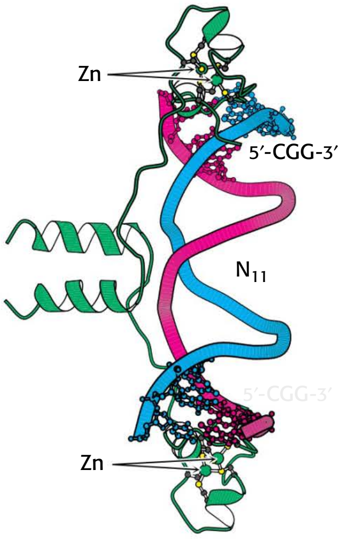

FIGURE 32.13 GAL4 binding sites. The yeast transcription factor GAL4 binds to DNA sequences of the form 5′-CGG(N)$_{11}$CCG-3′. Two zinc-based domains are present in the DNA-binding region of this protein. *Notice* that these domains contact the 5′-CGG-3′ sequences, leaving the center of the site uncontacted. [Drawn from 1D66.pdb.]

Recent experiments even more clearly revealed the role of chromatin structure in regulating access to DNA-binding sites. Genes required for galactose utilization in yeast are activated by a transcription factor called GAL4, which recognizes DNA-binding sites with two 5′-CGG-3′ sequences on complementary strands separated by 11 base pairs (Figure 32.13). Approximately 4000 potential GAL4 binding sites of the form 5′-CGG(N)$_{11}$CCG-3′ are present in the yeast genome, but only 10 of them regulate genes necessary for galactose metabolism. How is GAL4 targeted to only a small fraction of the potential binding sites? This question is addressed through the use of a technique called *chromatin immunoprecipitation* (ChIP; Figure 32.14). GAL4 is first cross-linked to its DNA-binding sites in chromatin. The DNA is then fragmented into small pieces, and antibodies to GAL4 are used to isolate the chromatin fragments containing GAL4. The cross-linking is reversed, and the DNA is isolated and characterized. The results of these studies reveal that only approximately 10 of the 4000 potential GAL4 sites are occupied by GAL4 when the cells are growing on galactose; more than 99% of the sites appear to be blocked, presumably by the local chromatin structure. Thus, whereas in prokaryotes all sites appear to be equally accessible, chromatin structure

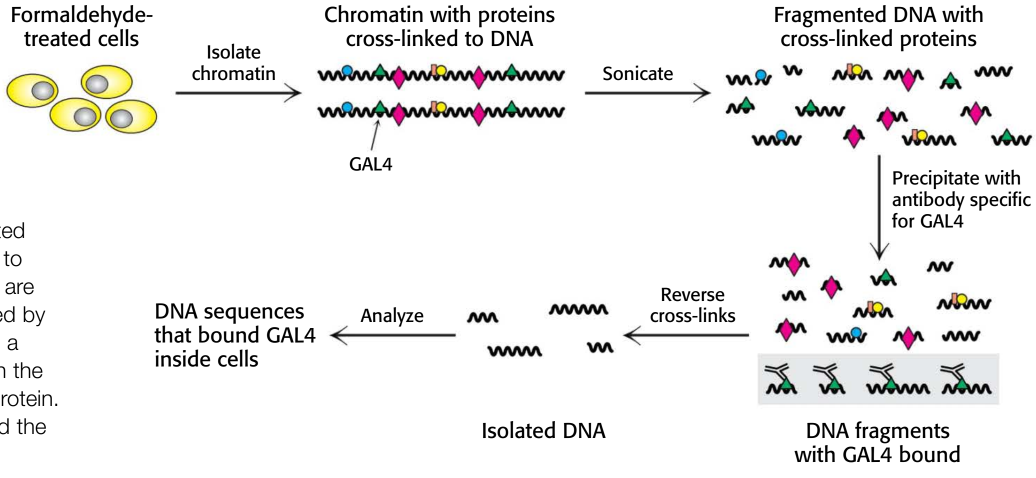
Formaldehyde-treated cells
Isolate chromatin
Chromatin with proteins cross-linked to DNA
GAL4
Sonicate
Fragmented DNA with cross-linked proteins
Precipitate with antibody specific for GAL4
DNA fragments with GAL4 bound
Reverse cross-links
Isolated DNA
Analyze
DNA sequences that bound GAL4 inside cells

FIGURE 32.14 Chromatin immunoprecipitation. Cells or isolated nuclei are treated with formaldehyde to cross-link proteins to DNA. The cells are then lysed and the DNA is fragmented by sonication. DNA fragments bound to a particular protein are isolated through the use of an antibody specific for that protein. The cross-links are then reversed and the DNA fragments are characterized.

shields a large number of the potential binding sites in eukaryotic cells. GAL4 is thereby prevented from binding to sites that are unimportant in galactose metabolism. These lines of evidence and others reveal that chromatin structure is altered in active genes compared with inactive ones.

The methylation of DNA can alter patterns of gene expression

The degree of methylation of DNA provides another mechanism, in addition to packaging with histones, for inhibiting gene expression inappropriate to a specific cell type. Carbon 5 of cytosine can be methylated by specific methyltransferases. About 70% of the 5′-CpG-3′ sequences (where "p" represents the phosphate residue in the DNA backbone) in mammalian genomes are methylated. However, the distribution of these methylated cytosines varies, depending on the cell type. Consider the β-globin gene. In cells that are actively expressing hemoglobin, the region from approximately 1 kb upstream of the start site to approximately 100 bp downstream of the start site is less methylated than the corresponding region in cells that do not express this gene. The relative absence of 5-methylcytosines near the start site is referred to as *hypomethylation.* The methyl group of 5-methylcytosine protrudes into the major groove where it could easily interfere with the binding of proteins that stimulate transcription.

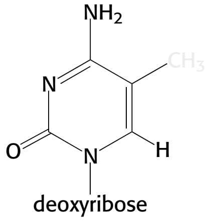

5-Methylcytosine

The distribution of CpG sequences in mammalian genomes is not uniform. Many CpG sequences have been converted into TpG through mutation by the deamination of 5-methylcytosine to thymine. However, sites near the 5′ ends of genes have been maintained because of their role in gene expression. Thus, most genes are found in *CpG islands,* regions of the genome that contain approximately four times as many CpG sequences as does the remainder of the genome.

Steroids and related hydrophobic molecules pass through membranes and bind to DNA-binding receptors

We next look at an example that illustrates how transcription factors can stimulate changes in chromatin structure that affect transcription. We will consider in some detail the system that detects and responds to estrogens. Synthesized and released by the ovaries, *estrogens,* such as estradiol, are cholesterol-derived steroid hormones (Section 26.4). They are required for the development of female secondary sex characteristics and, along with progesterone, participate in the ovarian cycle.

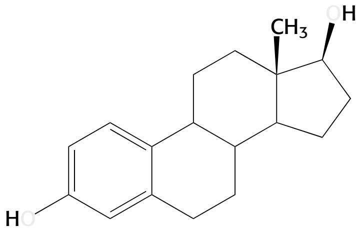

Estradiol
(an estrogen)

Because they are hydrophobic molecules, estrogens easily diffuse across cell membranes. When inside a cell, estrogens bind to highly specific, soluble receptor proteins. Estrogen receptors are members of a large family of proteins that act as receptors for a wide range of hydrophobic molecules, including other steroid hormones, thyroid hormones, and retinoids.

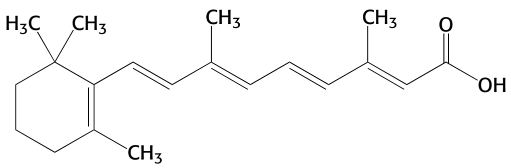

All-*trans*-retinoic acid
(a retinoid)

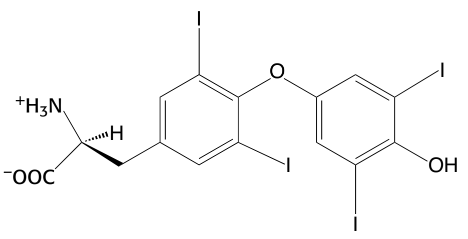

Thyroxine
(L-3,5,3′,5′-Tetraiodothyronine)
(a thyroid hormone)

The human genome encodes approximately 50 members of this family, often referred to as *nuclear hormone receptors.* The genomes of other

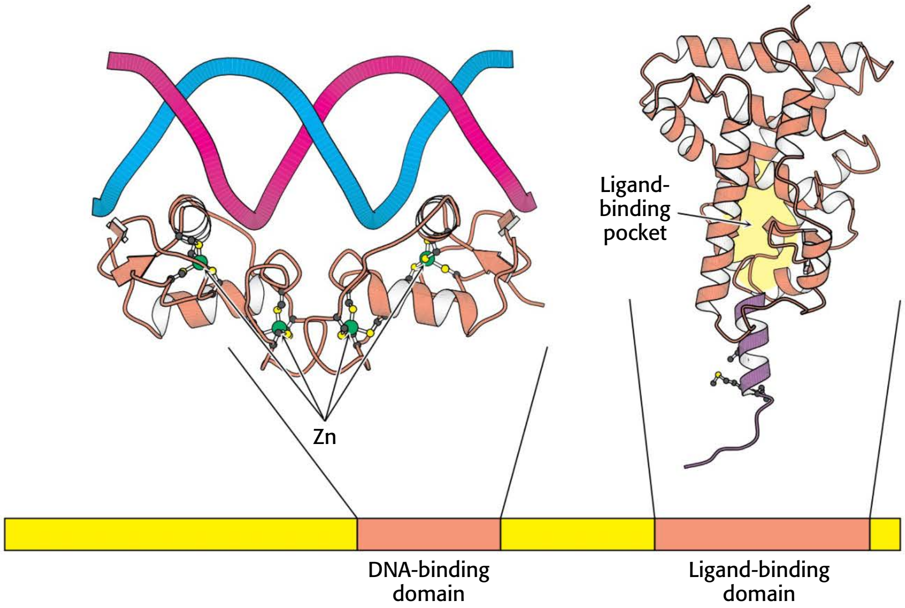

FIGURE 32.15 Structure of two nuclear hormone-receptor domains. Nuclear hormone receptors contain two crucial conserved domains: (1) a DNA-binding domain toward the center of the sequence and (2) a ligand-binding domain toward the carboxyl terminus. The structure of a dimer of the DNA-binding domain bound to DNA is shown, as is one monomer of the normally dimeric ligand-binding domain. [Drawn from 1HCQ and 1LBD.pdb.]

multicellular eukaryotes encode similar numbers of nuclear hormone receptors, although they are absent in yeast.

All these receptors have a similar mode of action. On binding of the signal molecule (called, generically, a *ligand*), the ligand–receptor complex modifies the expression of specific genes by binding to control elements in the DNA. Estrogen receptors bind to specific DNA sites (referred to as *estrogen response elements* or EREs) that contain the consensus sequence 5′-**AGGTCA**NNN**TGACCT**-3′. As expected from the symmetry of this sequence, an estrogen receptor binds to such sites as a dimer.

A comparison of the amino acid sequences of members of this family reveals two highly conserved domains: a DNA-binding domain and a ligand-binding domain (Figure 32.15). The DNA-binding domain lies toward the center of the molecule and consists of a set of zinc-based domains different from the Cys_2His_2 zinc-finger proteins introduced in Section 32.2. These zinc-based domains bind to specific DNA sequences by virtue of an α helix that lies in the major groove in the specific DNA complexes formed by estrogen receptors.

Nuclear hormone receptors regulate transcription by recruiting coactivators to the transcription complex

The second highly conserved domain of the nuclear receptor proteins lies near the carboxyl terminus and is the ligand-binding site. This domain folds into a structure that consists almost entirely of α helices, arranged in three layers. The ligand binds in a hydrophobic pocket that lies in the center of this array of helices (Figure 32.16). This domain changes conformation when it binds its ligand, estrogen. How does ligand binding lead to changes in gene expression? The simplest model would have the binding of ligand alter the DNA-binding properties of the receptor, analogously to the *lac* repressor in prokaryotes. However, experiments with purified nuclear hormone receptors revealed that ligand binding does *not* significantly alter DNA-binding affinity and specificity. Another mechanism is operative.

Investigators sought to determine whether specific proteins might bind to the nuclear hormone receptors only in the presence of ligand. Such searches led to the identification of several related proteins called *coactivators,* such as SRC-1 (*s*teroid *r*eceptor *c*oactivator-1), GRIP-1 (glucocorticoid *r*eceptor *i*nteracting *p*rotein-1), and NcoA-1 (*n*uclear hormone receptor

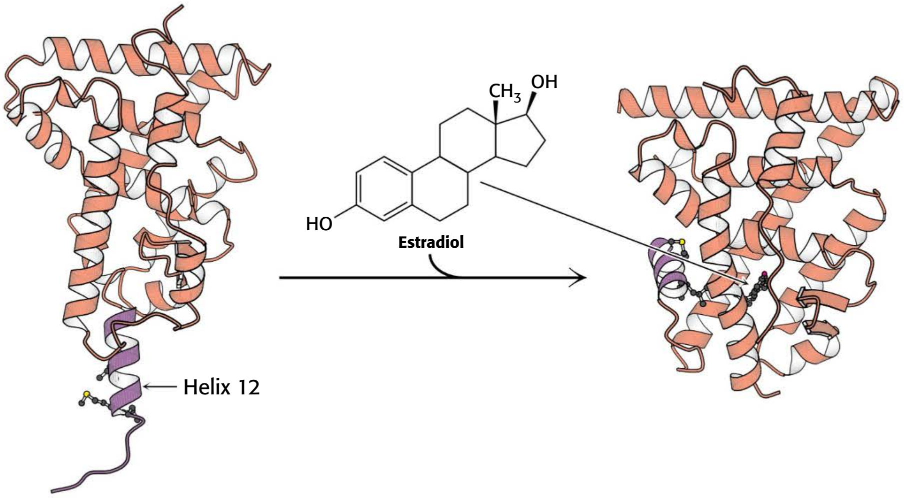

FIGURE 32.16 Ligand binding to nuclear hormone receptor. The ligand lies completely surrounded within a pocket in the ligand-binding domain. *Notice* that the last α helix, helix 12 (shown in purple), folds into a groove on the side of the structure on ligand binding. [Drawn from 1LDB and 1ERE.pdb.]

*coa*ctivator-1). These coactivators are referred to as the p160 family because of their size. The binding of ligand to the receptor induces a conformational change that allows the recruitment of a coactivator (Figure 32.17). In many cases, these coactivators are enzymes that catalyze reactions that lead to the modification of chromatin structure.

Steroid-hormone receptors are targets for drugs

Molecules such as estradiol that bind to a receptor and trigger signaling pathways are called *agonists.* Athletes sometimes take natural and synthetic agonists of the androgen receptor, a member of the family of nuclear hormone receptors, because their binding to the androgen receptor stimulates the expression of genes that enhance the development of lean muscle mass.

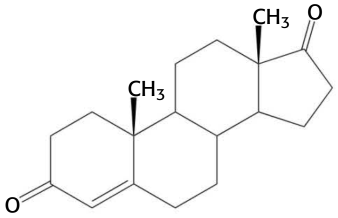

Androstendione
(a natural androgen)

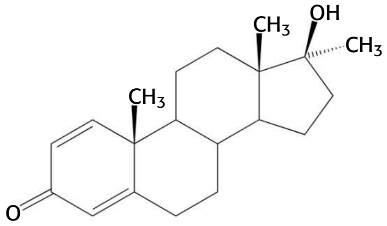

Dianabol
(methandrostenolone)
(a synthetic androgen)

Referred to as *anabolic steroids,* such compounds used in excess are not without side effects. In men, excessive use leads to a decrease in the secretion of testosterone, to testicular atrophy, and sometimes to breast enlargement

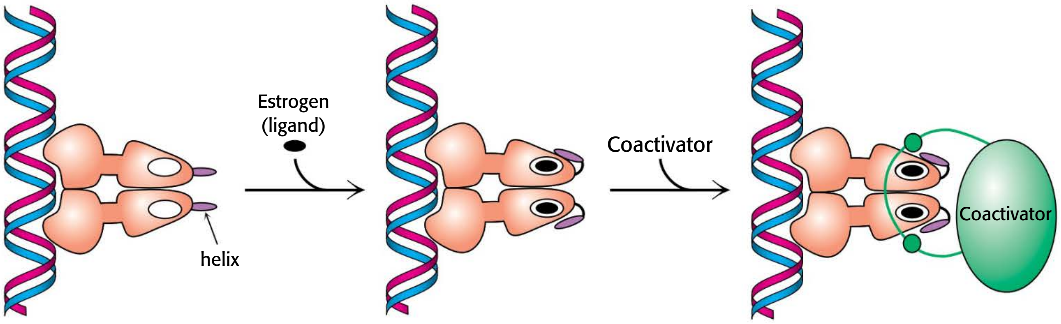

FIGURE 32.17 Coactivator recruitment. The binding of ligand to a nuclear hormone receptor induces a conformational change in the ligand-binding domain. This change in conformation generates favorable sites for the binding of a coactivator.

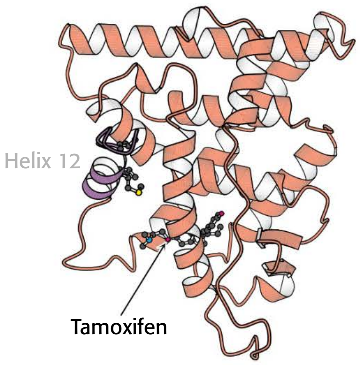

FIGURE 32.18 Estrogen receptor—tamoxifen complex. Tamoxifen binds in the pocket normally occupied by estrogen. However, *notice* that part of the tamoxifen structure extends from this pocket, and so helix 12 cannot pack in its usual position. Instead, this helix blocks the coactivator-binding site. [Drawn from 3ERT.pdb.]

(gynecomastia) if some of the excess androgen is converted into estrogen. In women, excess testosterone causes a decrease in ovulation and estrogen secretion; it also causes breast regression and growth of facial hair.

Other molecules bind to nuclear hormone receptors but do not effectively trigger signaling pathways. Such compounds are called *antagonists* and are, in many ways, like competitive inhibitors of enzymes. Some important drugs are antagonists that target the estrogen receptor. For example, *tamoxifen* and *raloxifene* are used in the treatment and prevention of breast cancer, because some breast tumors rely on estrogen-mediated pathways for growth. Because some of these compounds have distinct effects on different forms of the estrogen receptor, they are referred to as *selective estrogen receptor modulators* (SERMs).

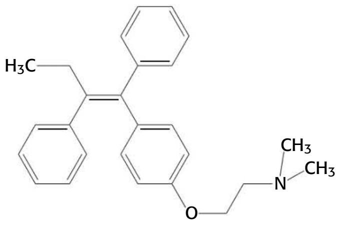

Tamoxifen

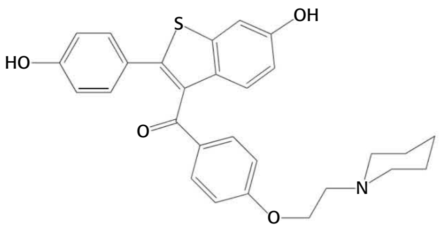

Raloxifene

The determination of the structures of complexes between the estrogen receptor and these drugs revealed the basis for their antagonist effect (Figure 32.18). Tamoxifen binds to the same site as estradiol does. However, tamoxifen has a group that extends out of the normal ligand-binding pocket, as do other antagonists. These groups block the normal conformational changes induced by estrogen. Tamoxifen blocks the binding of coactivators and thus inhibits the activation of gene expression.

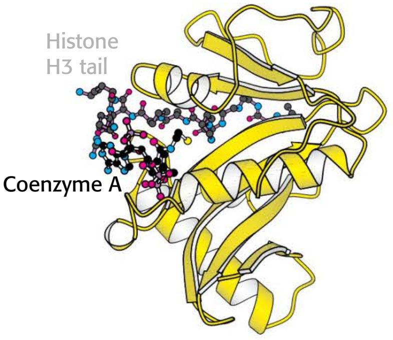

FIGURE 32.19 Structure of histone acetyltransferase. The amino-terminal tail of histone H3 extends into a pocket in which a lysine side chain can accept an acetyl group from acetyl Coenzyme A bound in an adjacent site. [Drawn from 1QSN.pdb.]

Chromatin structure is modulated through covalent modifications of histone tails

We have seen that nuclear receptors respond to signal molecules by recruiting coactivators. Now we can ask, How do coactivators modulate transcriptional activity? *These proteins act to loosen the histone complex from the DNA, exposing additional DNA regions to the transcription machinery.*

Much of the effectiveness of coactivators appears to result from their ability to covalently modify the amino-terminal tails of histones as well as regions on other proteins. Some of the p160 coactivators and the proteins that they recruit catalyze the transfer of acetyl groups from acetyl CoA to specific lysine residues in these amino-terminal tails.

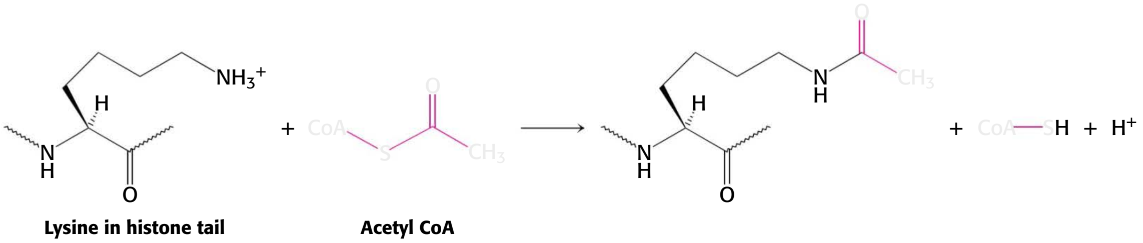

Enzymes that catalyze such reactions are called *histone acetyltransferases* (HATs). The histone tails are readily extended; so they can fit into the HAT active site and become acetylated (Figure 32.19).

What are the consequences of histone acetylation? Lysine bears a positively charged ammonium group at neutral pH. The addition of an acetyl group generates an uncharged amide group. This change dramatically reduces the affinity of the tail for DNA and modestly decreases the affinity of the entire histone complex for DNA, loosening the histone complex from the DNA.

In addition, the acetylated lysine residues interact with a specific *acetyllysine-binding domain* that is present in many proteins that regulate eukaryotic transcription. This domain, termed a *bromodomain,* comprises approximately 110 amino acids that form a four-helix bundle containing a peptide-binding site at one end (Figure 32.20).

Bromodomain-containing proteins are components of two large complexes essential for transcription. One is a complex of more than 10 polypeptides that binds to the *TATA-box-binding protein.* Recall that the TATA-box-binding protein is an essential transcription factor for many genes (Section 29.2). Proteins that bind to the TATA-box-binding protein are called *TAFs* (for *T*ATA-box-binding protein *a*ssociated *f*actors). In particular, TAF1 contains a pair of bromodomains near its carboxyl terminus. The two domains are oriented such that each can bind one of two acetyllysine residues at positions 5 and 12 in the histone H4 tail. Thus, *acetylation of the histone tails provides a mechanism for recruiting other components of the transcriptional machinery.*

Bromodomains are also present in some components of large complexes known as *chromatin-remodeling complexes* or *chromatin-remodeling engines.* These complexes, which also contain domains homologous to those of helicases, utilize the free energy of ATP hydrolysis to shift the positions of nucleosomes along the DNA and to induce other conformational changes in chromatin (Figure 32.21). Histone acetylation can lead to a reorganization of the chromatin structure, potentially exposing binding sites for other factors. *Thus, histone acetylation can activate transcription through a combination of three mechanisms: by reducing the affinity of the histones for DNA, by recruiting other components of the transcriptional machinery, and by initiating the remodeling of the chromatin structure.*

Nuclear hormone receptors also include regions that interact with components of the mediator complex. Thus, two mechanisms of gene regulation can work in concert. Modification of histones and chromatin remodeling can open up regions of chromatin into which the transcription complex can be recruited through protein–protein interactions.

Histone deacetylases contribute to transcriptional repression

Just as in prokaryotes, some changes in a cell's environment lead to the repression of genes that had been active. The modification of histone tails

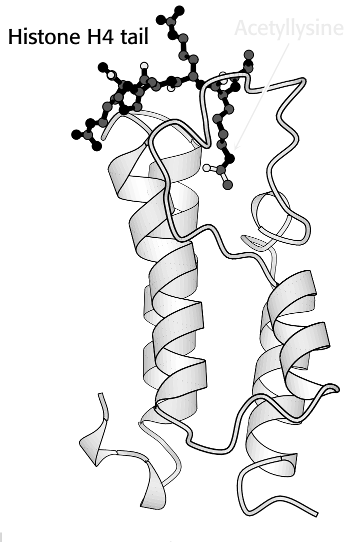

FIGURE 32.20 Structure of a bromodomain. This four-helix-bundle domain binds peptides containing acetyllysine. *Notice* that an acetylated peptide from histone H4 is bound in the structure. [Drawn from 1EGI.pdb.]

FIGURE 32.21 Chromatin remodeling. Eukaryotic gene regulation begins with an activated transcription factor bound to a specific site on DNA. One scheme for the initiation of transcription by RNA polymerase II requires five steps: (1) recruitment of a coactivator, (2) acetylation of lysine residues in the histone tails, (3) binding of a remodeling-engine complex to the acetylated lysine residues, (4) ATP-dependent remodeling of the chromatin structure to expose a binding site for RNA polymerase II or for other factors, and (5) recruitment of RNA polymerase II. Only two subunits are shown for each complex, although the actual complexes are much larger. Other schemes are possible.

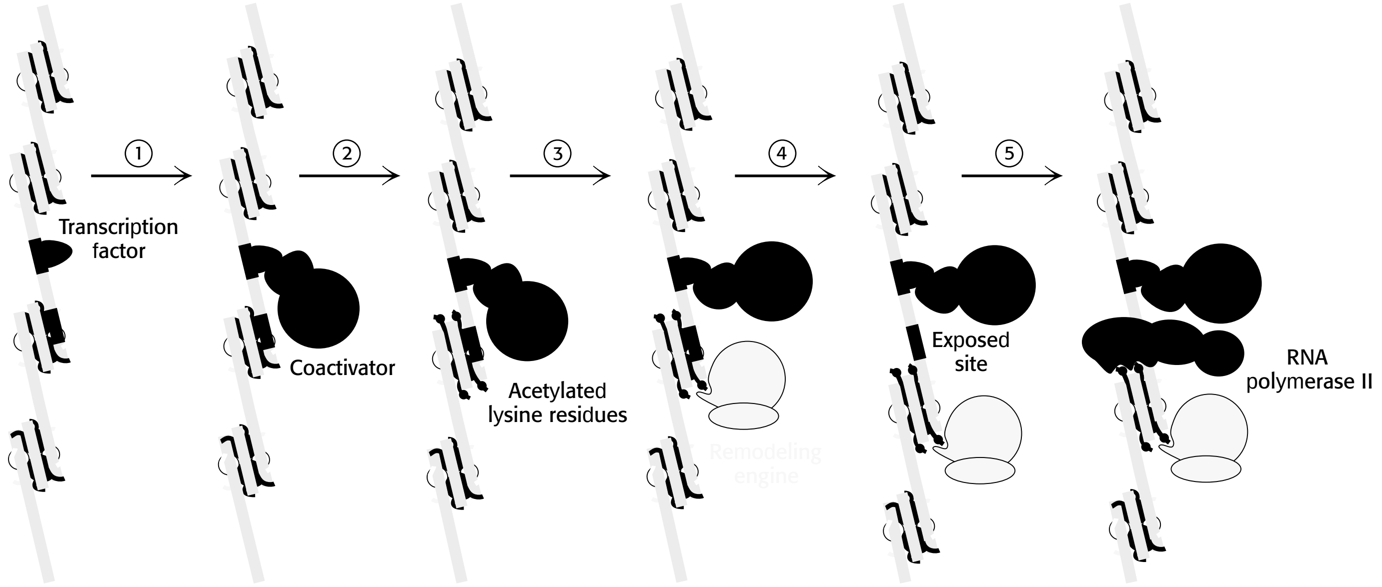

TABLE 32.2 Selected histone modifications

Modification	Associated with
H4 K8 acetylation	Activation
H3 K14 acetylation	Activation
H3 K27 monomethylation	Activation
H3 K27 trimethylation	Repression
H3 R17 methylation	Activation
H2B S14 phosphorylation	DNA repair
H2B K120 ubiquitination	Activation

again plays an important role. However, in repression, a key reaction appears to be the deacetylation of acetylated lysine, catalyzed by specific *histone deacetylase* enzymes.

In many ways, the acetylation and deacetylation of lysine residues in histone tails (and, likely, in other proteins) is analogous to the phosphorylation and dephosphorylation of serine, threonine, and tyrosine residues in other stages of signaling processes. Like the addition of phosphoryl groups, the addition of acetyl groups can induce conformational changes and generate novel binding sites. Without a means of removal of these groups, however, these signaling switches will become stuck in one position and lose their effectiveness. Like phosphatases, deacetylases help reset the switches.

Acetylation is not the only modification of histones and other proteins in gene-regulation processes. The methylation of specific lysine and arginine residues also can be important. Some of the more common modifications are shown in Table 32.2.

The elucidation of the roles of these modifications is a very active area of research at present. The relation between various histone modifications and their roles in controlling gene expression is sometimes referred to as "the histone code." Although important generalizations have been discovered, this code clearly is subtle and complicated rather than being a set of hard and fast rules. Nonetheless, the development and application of methods that allow probing of histone modifications on a genome-wide scale in a range of cell types has provided large data sets that can be examined to test and refine models.

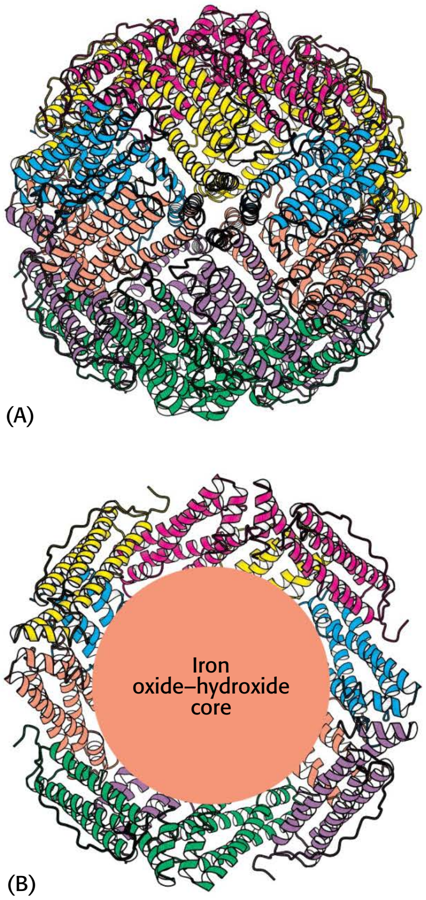

FIGURE 32.22 Structure of ferritin. (A) Twenty-four ferritin polypeptides form a nearly spherical shell. (B) A cutaway view reveals the core that stores iron as an iron oxide–hydroxide complex [Drawn from 1IES.pdb.]

32.4 Eukaryotic Gene Expression Can Be Controlled at Posttranscriptional Levels

Just as in prokaryotes, gene expression in eukaryotes can be regulated subsequent to transcription. We shall consider two examples. The first is the regulation of genes taking part in iron metabolism through key features in RNA secondary structure, similar in many ways to prokaryotic posttranscriptional regulation (Section 31.4). The second entails an entirely new mechanism, first glimpsed with the discovery of RNA interference (p. 162). Certain small regulatory RNA molecules allow the regulation of gene expression through interaction with a range of mRNA molecules. Remarkably, this mechanism, discovered only recently, affects the expression of approximately 60% of all human genes.

Genes associated with iron metabolism are translationally regulated in animals

RNA secondary structure plays a role in the regulation of iron metabolism in eukaryotes. Iron is an essential nutrient, required for the synthesis of hemoglobin, cytochromes, and many other proteins. However, excess iron can be quite harmful because, untamed by a suitable protein environment, iron can initiate a range of free-radical reactions that damage proteins, lipids, and nucleic acids. Animals have evolved sophisticated systems for the accumulation of iron in times of scarcity and for the safe storage of excess iron for later use. Key proteins include *transferrin,* a transport protein that carries iron in the serum, *transferrin receptor,* a membrane protein that binds iron-loaded transferrin and initiates its entry into cells, and *ferritin,* an impressively efficient iron-storage protein found primarily in the liver and kidneys. Twenty-four ferritin polypeptides form a nearly spherical shell that encloses as many as 2400 iron atoms, a ratio of one iron atom per amino acid (Figure 32.22).

Ferritin and transferrin-receptor expression levels are reciprocally related in their responses to changes in iron levels. When iron is scarce, the amount of

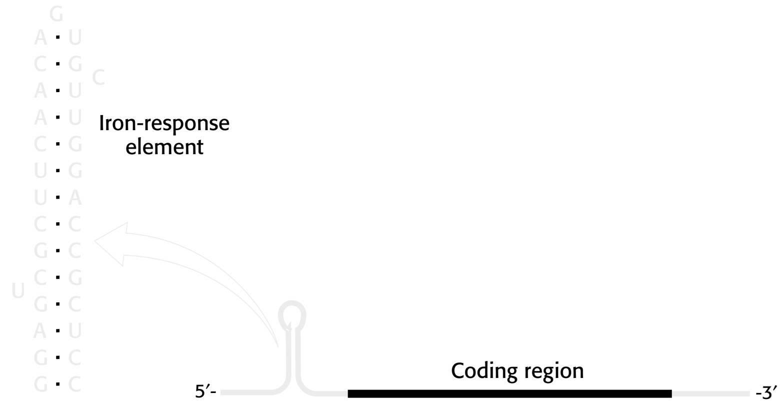

FIGURE 32.23 Iron-response element. Ferritin mRNA includes a stem-loop structure, termed an iron-response element (IRE), in its 5′ untranslated region. The IRE binds a specific protein that blocks the translation of this mRNA under low iron conditions.

transferrin receptor increases and little or no new ferritin is synthesized. Interestingly, the extent of mRNA synthesis for these proteins does not change correspondingly. Instead, regulation takes place at the level of translation.

Consider ferritin first. Ferritin mRNA includes a stem-loop structure termed an *iron-response element* (IRE) in its 5′ untranslated region (Figure 32.23). This stem-loop binds a 90-kDa protein, called an *IRE-binding protein* (IRP), that blocks the initiation of translation as the IRE binds on the 5′ side of the coding region. When the iron level increases, the IRP binds iron as a 4Fe-4S cluster. The IRP bound to iron cannot bind RNA, because the binding sites for iron and RNA substantially overlap. Thus, in the presence of iron, ferritin mRNA is released from the IRP and translated to produce ferritin, which sequesters the excess iron.

An examination of the nucleotide sequence of transferrin-receptor mRNA reveals the presence of several IRE-like regions. However, these regions are located in the 3′ untranslated region rather than in the 5′ untranslated region (Figure 32.24). Under low-iron conditions, IRP binds to these IREs. However, given the location of these binding sites, the transferrin-receptor mRNA can still be translated. What happens when the iron level increases and the IRP no longer binds transferrin-receptor mRNA? Freed from the IRP, transferrin-receptor mRNA is rapidly degraded. Thus, an increase in the cellular iron level leads to the destruction of transferrin-receptor mRNA and, hence, a reduction in the production of transferrin-receptor protein.

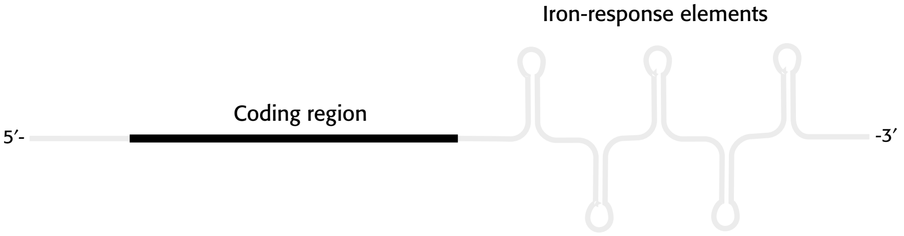

FIGURE 32.24 Transferrin-receptor mRNA. This mRNA has a set of iron-response elements (IREs) in its 3′ untranslated region. The binding of the IRE-binding protein to these elements stabilizes the mRNA but does not interfere with translation.

The purification of the IRP and the cloning of its cDNA were sources of truly remarkable insight into evolution. The IRP was found to be approximately 30% identical in amino acid sequence with the citric acid cycle enzyme aconitase from mitochondria. Further analysis revealed that the IRP is, in fact, an active aconitase enzyme; it is a cytoplasmic aconitase that had been known for a long time, but its function was not well understood (Figure 32.25). The iron–sulfur center at the active site of the IRP is rather unstable, and loss

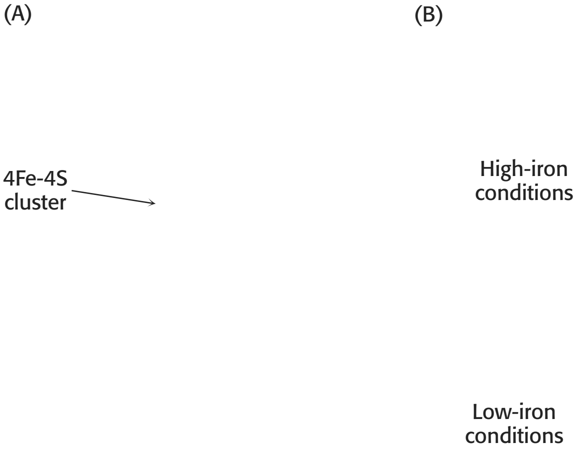

FIGURE 32.25 The IRP is an aconitase. (A) Aconitase contains an unstable 4Fe-4S cluster at its center. (B) Under conditions of low iron, the 4Fe-4S cluster dissociates and appropriate RNA molecules can bind in its place. [Drawn from 1C96.pdb.]

of the iron triggers significant changes in protein conformation. Thus, this protein can serve as an iron-sensing factor.

Other mRNAs, including those taking part in heme synthesis, have been found to contain IREs. Thus, genes encoding proteins required for iron metabolism acquired sequences that, when transcribed, provided binding sites for the iron-sensing protein. An environmental signal—the concentration of iron—controls the translation of proteins required for the metabolism of this metal. Thus, mutations in the untranslated region of mRNAs have been selected for beneficial regulation by iron levels.

Small RNAs regulate the expression of many eukaryotic genes

Genetic studies of development in *C. elegans* revealed that a gene called *lin-4* encodes an RNA molecule 61 nucleotides long that can regulate the expression of certain other genes. The 61-nucleotide *lin-4* RNA does not encode a protein, but rather is cleaved into a 22-nucleotide RNA that possesses the regulatory activity. This discovery was the first view of a large class of regulatory RNA molecules that are now called *microRNAs* or *miRNAs*. The key to the activity of microRNAs and their specificity for particular genes is their ability to form Watson–Crick base-pair-stabilized complexes with the mRNAs of those genes.

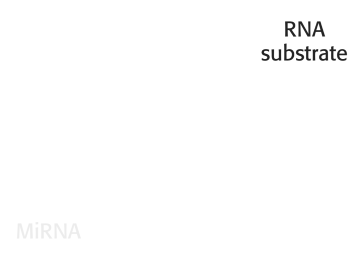

FIGURE 32.26 MicroRNA–Argonaute complex. The miRNA (shown in red) is bound by the Argonaute protein. *Notice* that the miRNA serves as a guide that binds the RNA substrate (shown in gray) through the formation of a double helix. Two magnesium ions are shown in green. [Drawn from 3HK2.pdb.]

These miRNAs do not function on their own. Instead, the miRNAs bind to members of a class of proteins called the *Argonaute* family (Figure 32.26). These Argonaute–miRNA complexes can then bind mRNAs that have sequences that are substantially complementary to the miRNAs. Once bound, such an mRNA can be cleaved by the Argonaute–miRNA complex through the action of a magnesium-based active site. Thus, *the miRNAs serve as guide RNAs that determine the specificity of the Argonaute complex* (Figure 32.27). Cleavage of mRNA by the Argonaute–miRNA complex is similar to the mechanism of RNA interference (p. 162). The small RNA molecules participating in RNAi, however, come from a different source. In RNAi, double-stranded RNAs are cleaved into 21-nucleotide fragments, single-stranded components of which are bound by members of the Argonaute family to form an RNA-induced silencing complex (RISC) that cleaves complementary mRNAs. For miRNAs, the single-stranded RNAs are generated from larger genetically encoded precursors, as described in Chapter 29.

The occurrence of gene regulation by miRNAs was originally thought to be limited to a relatively small number of species. However, subsequent studies have revealed that this mode of gene regulation is nearly ubiquitous in eukaryotes. Indeed, more than 700 miRNAs encoded by the human genome have been identified. Each miRNA can regulate many different genes because many different target sequences are present in each mRNA. An estimated 60% of all human genes are regulated by one or more miRNAs. As one example, consider the human miRNA called miR-206. This miRNA down-regulates the expression of one isoform of the estrogen receptor. In addition, it appears to down-regulate the expression of several different coactivators that interact with the estrogen receptor. Thus, this

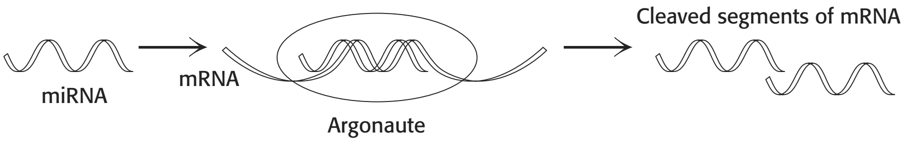

FIGURE 32.27 MicroRNA action. MicroRNAs bind to members of the Argonaute family where they target specific mRNA molecules for cleavage.

miRNA can mute the influence of estrogen by blocking the estrogen-initiated signaling pathway at several different steps.

The microRNA pathway has tremendous implications for the evolution of gene-regulatory pathways. Most of the target sites for miRNAs are present in the $3'$-untranslated regions of mRNAs. These sequences are quite free to mutate because they do not encode proteins and are not required to fold into any specific structures. Thus, in the context of a set of expressed miRNAs, mutations in this region of any particular gene could, in principle, increase or decrease the affinity for one or more miRNAs and, hence, alter the regulation of the gene.

SUMMARY

32.1 Eukaryotic DNA Is Organized into Chromatin

Eukaryotic DNA is tightly bound to basic proteins called histones; the combination is called chromatin. DNA wraps twice around an octamer of core histones to form a nucleosome. The four core histones are homologous and fold into similar structures. Each core histone has an amino-terminal tail rich in lysine and arginine residues. Nucleosomes are the first stage of compaction of eukaryotic DNA. Chromatin blocks access to many potential DNA-binding sites. Changes in chromatin structure play a major role in regulating gene expression.

32.2 Transcription Factors Bind DNA and Regulate Transcription Initiation

Most eukaryotic genes are not expressed unless they are activated by the binding of specific proteins, called transcription factors, to sites on the DNA. These specific DNA-binding proteins interact directly or indirectly with RNA polymerases or their associated proteins. Eukaryotic transcription factors are modular: they consist of separate DNA-binding and activation domains. Important classes of DNA-binding proteins include the homeodomains, the basic-leucine zipper proteins, and Cys_2His_2 zinc-finger proteins. Each of these classes of proteins uses an α helix to make specific contacts with DNA. Activation domains interact with RNA polymerases or their associated factors or with other protein complexes such as mediator. Enhancers are DNA elements that can modulate gene expression from more than 1000 bp away from the start site of transcription. Enhancers are often specific for certain cell types, depending on which DNA-binding proteins are present. The introduction of genes for a specific set of four transcription factors into fibroblasts can cause these cells to dedifferentiate into induced pluripotent stem cells.

32.3 The Control of Gene Expression Can Require Chromatin Remodeling

Chromatin structure is crucial to the control of gene expression; it is more open near the transcription start sites of actively transcribed genes. Steroids such as estrogens bind to eukaryotic transcription factors called nuclear hormone receptors. These proteins are capable of binding DNA whether or not ligands are bound. The binding of ligands induces a conformational change that allows the recruitment of additional proteins called coactivators. Among the most important functions of coactivators is to catalyze the addition of acetyl groups to lysine residues in the tails of histone proteins. Histone acetylation decreases the affinity of the histones for DNA, making additional genes accessible for transcription. In addition, acetylated histones are targets for proteins containing specific binding units called bromodomains. Bromodomains are components of two classes of large complexes: (1) chromatin-remodeling engines and (2) factors associated with RNA polymerase II. These complexes open up sites on chromatin and initiate transcription.

32.4 Eukaryotic Gene Expression Can Be Controlled at Posttranscriptional Levels

Genes encoding proteins that transport and store iron are regulated at the translational level. Iron-response elements, structures that are present in certain mRNAs, are bound by an IRE-binding protein when this protein is not binding iron. Whether the expression of a gene is stimulated or inhibited in response to changes in the iron status of a cell depends on the location of the IRE within the mRNA. The IRE-binding protein is a cytoplasmic aconitase that loses its iron–sulfur center under low-iron conditions. MicroRNAs are specialized RNA molecules encoded as parts of larger RNA precursors. They bind to proteins of the Argonaute family; the bound miRNAs function as guides that help bind specific mRNA molecules that are then cleaved.

KEY TERMS

cell type (p. 942)
histone (p. 943)
chromatin (p. 943)
nucleosome (p. 943)
nucleosome core particle (p. 943)
transcription factor (p. 945)
homeodomain (p. 945)
basic-leucine zipper (bZip) protein (p. 945)
Cys$_2$His$_2$ zinc-finger domain (p. 945)
mediator (p. 946)
combinatorial control (p. 946)
enhancer (p.947)
induced pluripotent stem (iPS) cell (p. 947)
hypersensitive site (p. 948)
chromatin immunoprecipitation (ChIP) (p. 948)
hypomethylation (p. 949)
CpG island (p. 949)
nuclear hormone receptor (p. 949)
estrogen response element (ERE) (p. 950)
coactivator (p. 950)
agonist (p. 951)
anabolic steroid (p. 951)
antagonist (p. 952)
selective estrogen receptor modulator (SERM) (p. 952)
histone acetyltransferase (HAT) (p. 952)
acetyllysine-binding domain (p. 953)
bromodomain (p. 953)
TATA-box-binding protein associated factor (TAF) (p. 953)
chromatin-remodeling complex (p. 953)
histone deacetylase (p. 954)
transferrin (p. 954)
transferrin receptor (p. 954)
ferritin (p. 954)
iron-response element (IRE) (p. 955)
IRE-binding protein (IRP) (p. 955)
microRNA (miRNA) (p. 956)
Argonaute family proteins (p. 956)

PROBLEMS

1. *Charge neutralization.* Given the histone amino acid sequences illustrated below, estimate the charge of a histone octamer at pH 7. Assume that histidine residues are uncharged at this pH. How does this charge compare with the charge on 150 base pairs of DNA?

Histone H2A

MSGRGKQGGKARAKAKTRSSRAGLQFPVGRVHRLLRKGNYSERVGAGAPVYLAAVLEYLTAEILELAGNA

ARDNKKTRIIPRHLQLAIRNDEELNKLLGRVTIAQGGVLPNIQAVLLPKKTESHHKAKGK

Histone H2B

MPEPAKSAPAPKKGSKKAVTKAQKKDGKKRKRSRKESYSVYVYKVLKQVHPDTGISSKAMGIMNSFVNDI

FERIAGEASRLAHYNKRSTITSREIQTAVRLLLPGELAKHAVSEGTKAVTKYTSSK

Histone H3

MARTKQTARKSTGGKAPRKQLATKAARKSAPSTGGVKKPHRYRPGTVALREIRRYQKSTELLIRKLPFQR

LVREIAQDFKTDLRFQSAAIGALQEASEAYLVGLFEDTNLCAIHAKRVTIMPKDIQLARRIRGERA

Histone H4

MSGRGKGGKGLGKGGAKRHRKVLRDNIQGITKPAIRRLARRGGVKRISGLIYEETRGVLKVFLENVIRDA

VTYTEHAKRKTVTAMDVVYALKRQGRTLYGFGG

2. *Chromatin immunoprecipitation.* You have used the technique of chromatin immunoprecipitation to isolate DNA fragments containing a DNA-binding protein of interest. Suppose that you wish to know whether a particular known DNA fragment is present in the isolated mixture. How might you detect its presence?

3. *Around we go.* Assuming that 145 base pairs of DNA wrap around the histone octamer 1.75 times, estimate the radius of the histone octamer. Assume 3.4 Å per base pair and simplify the calculation by assuming that the wrapping is in two rather than three dimensions and neglecting the thickness of the DNA.

4. *Nitrogen substitution.* Growth of mammalian cells in the presence of 5-azacytidine results in the activation of some normally inactive genes. Propose an explanation.

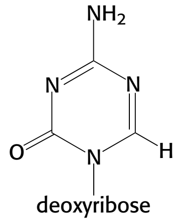

5-Azacytidine

5. *A new domain*. A protein domain that recognizes 5-methylcytosine in the context of double-stranded DNA has been characterized. What role might proteins containing such a domain play in regulating gene expression? Where on a double-stranded DNA molecule would you expect such a domain to bind?

6. *Hybrid receptor*. Through recombinant DNA methods, a modified steroid hormone receptor was prepared that consists of an estrogen receptor with its ligand-binding domain replaced by the ligand-binding domain from the progesterone receptor. Predict the expected responsiveness of gene expression for cells treated with estrogen or with progesterone.

7. *Different modifications*. What is the effect of acetylation of a lysine residue on the charge of a histone protein? Of lysine methylation?

8. *Transformer*. The following amino acid sequence of one of the four transcription factors is used to generate iPS cells:

HTCDYAGCGKTYTKSSHLKAHLRTHTGEKPYHCDWDGCGWKFARSDELTRHYRKHTGHRPFQCQKCD
RAFSRSDHLALHMKRHF

This transcription factor belongs to one of the three structural classes discussed in Section 32.2. Identify the class.

9. *Coverage*. What percentage of the DNA sites in yeast are accessible, assuming that the fraction of sites observed for GAL4 is typical? To how many base pairs of the 12-Mb yeast genome does this percentage correspond?

10. *Count the methyl groups*. Examination of the histone modifications of a gene reveals an abundance of histone H3 with lysine 27 modified with a single methyl group. Does this suggest that this gene is activated or repressed? How would your answer change if many lysine 27 residues were modified with three methyl groups each?

11. *Iron regulation*. What effect would you expect from the addition of an IRE to the 5′ end of a gene that is not normally regulated by iron levels? To the 3′ end?

12. *Predicting microRNA regulation*. Suppose that you have identified an miRNA that has the sequence 5′-GCCUAGCCUUAGCAUUGAUUGG-3′. Propose a strategy for identifying mRNA that might be regulated by this miRNA, given the sequences of all mRNAs encoded by the human genome.

Mechanism Problem

13. *Acetyltransferases*. Propose a mechanism for the transfer of an acetyl group from acetyl CoA to the amino group of lysine.

Data Interpretation Problem

14. *Limited restriction*. The restriction enzyme HpaII is a powerful tool for analyzing DNA methylation. This enzyme cleaves sites of the form 5′-CCGG-3′ but will not cleave such sites if the DNA is methylated on any of the cytosine residues. Genomic DNA from different organisms is treated with HpaII and the results are analyzed by gel electrophoresis (see the adjoining patterns). Provide an explanation for the observed patterns.

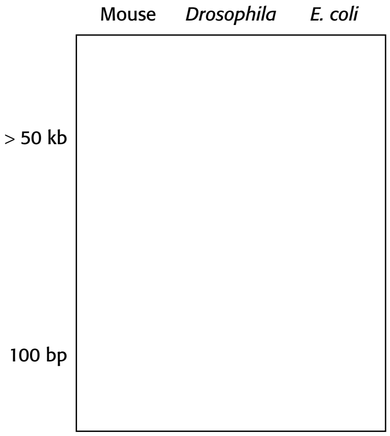

CHAPTER

33

Sensory Systems

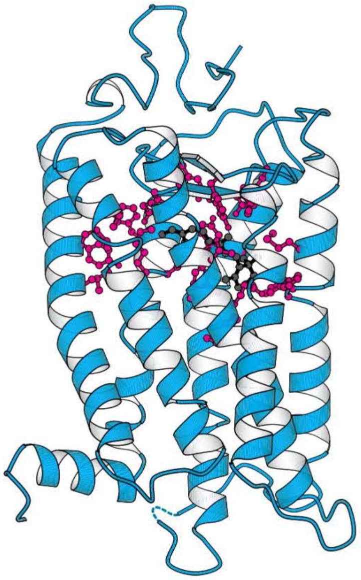

Color perception requires specific photoreceptors. The photoreceptor rhodopsin (right), which absorbs light in the process of vision, consists of the protein opsin and a bound vitamin A derivative, retinal. The amino acids (shown in red) that surround the retinal determine the color of light that is most efficiently absorbed. A person lacking a light-absorbing photoreceptor for the color green will see a bowl of fruits of many colors (left) as similar shades of yellow-green (middle). [From Africa Studio/Shutterstock (left), modified by Jeremy Berg using Coblis (www.color-blindness.com/coblis-color-blindness-simulator/) (middle).]

Our senses provide us with means for detecting a diverse set of external signals, often with incredible sensitivity and specificity. For example, when fully adapted to a darkened room, our eyes allow us to sense very low levels of light, down to a limit of less than 10 photons. With more light, we are able to distinguish millions of colors. Through our senses of smell and taste, we are able to detect thousands of chemicals in our environment and sort them into categories: pleasant or unpleasant? healthful or toxic? Finally, we can perceive mechanical stimuli in the air and around us through our senses of hearing and touch.

How do our sensory systems work? How are the initial stimuli detected? How are these initial biochemical events transformed into perceptions and experiences? We have already encountered systems that sense and respond to chemical signals—namely, receptors that bind to growth factors and hormones. Our knowledge of these receptors and their associated signal-transduction pathways provides us with concepts and tools for unraveling some of the workings of sensory systems. For example, 7TM receptors (seven-transmembrane receptors; Section 14.1) play key roles in olfaction, taste, and vision. Ion channels that are sensitive to mechanical stress are essential for hearing and touch.

In this chapter, we focus on the five major sensory systems found in human beings and other mammals: olfaction (the sense of smell—i.e., the detection of small molecules in the air), taste, or gustation (the detection of selected organic compounds and ions by the tongue), vision (the detection

OUTLINE

33.1 A Wide Variety of Organic Compounds Are Detected by Olfaction

33.2 Taste Is a Combination of Senses That Function by Different Mechanisms

33.3 Photoreceptor Molecules in the Eye Detect Visible Light

33.4 Hearing Depends on the Speedy Detection of Mechanical Stimuli

33.5 Touch Includes the Sensing of Pressure, Temperature, and Other Factors

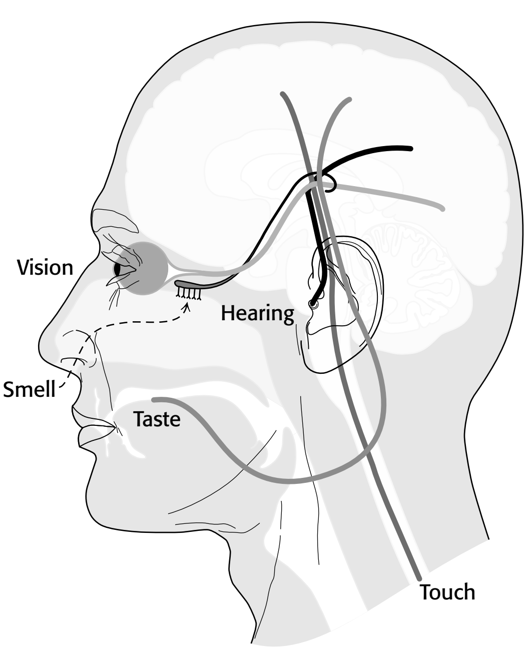

FIGURE 33.1 Sensory connections to the brain. Sensory nerves connect sensory organs to the brain and spinal cord.

of light), hearing (the detection of sound, or pressure waves in the air), and touch (the detection of changes in pressure, temperature, and other factors by the skin). Each of these primary sensory systems contains specialized sensory neurons that transmit nerve impulses to the central nervous system (Figure 33.1). In the central nervous system, these signals are processed and combined with other information to yield a perception that may trigger a change in behavior. By these means, our senses allow us to detect changes in our environments and to adjust our behavior appropriately.

33.1 A Wide Variety of Organic Compounds Are Detected by Olfaction

Human beings can detect and distinguish thousands of different compounds by smell, often with considerable sensitivity and specificity. Most odorants are small organic compounds with sufficient volatility that they can be carried as vapors into the nose. For example, a major component responsible for the odor of almonds is the simple aromatic compound benzaldehyde, whereas the sulfhydryl compound 3-methylbutane-1-thiol is a major component of the odor of skunks.

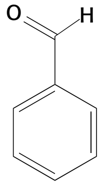

Benzaldehyde (Almond)

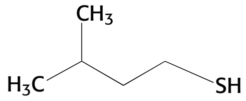

3-Methylbutane-1-thiol (Skunk)

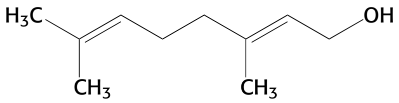

Geraniol (Rose)

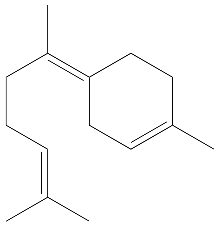

Zingiberene (Ginger)

What properties of these molecules are responsible for their odors? First, *the shape of the molecule rather than its other physical properties is crucial.* We can most clearly see the importance of shape by comparing molecules such as those responsible for the odors of spearmint and caraway.

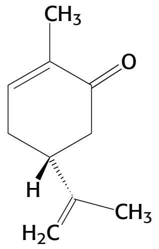

***R*-Carvone (Spearmint)**

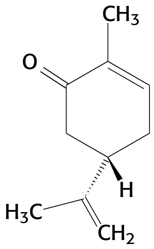

***S*-Carvone (Caraway)**

These compounds are identical in essentially all physical properties such as hydrophobicity because they are exact mirror images of one another. Thus, the odor produced by an odorant depends not on a physical property but on the compound's interaction with a specific binding surface, most likely a protein receptor. Second, some human beings (and other animals) suffer from *specific anosmias;* that is, they are incapable of smelling specific compounds even though their olfactory systems are otherwise normal. Such anosmias are often inherited. These observations suggest that mutations in individual receptor genes lead to the loss of the ability to detect a small subset of compounds.

Olfaction is mediated by an enormous family of seven-transmembrane-helix receptors

Odorants are detected in a specific region of the nose, called the *main olfactory epithelium,* that lies at the top of the nasal cavity (Figure 33.2). Approximately 1 million sensory neurons line the surface of this region. Cilia containing the odorant-binding protein receptors project from these neurons into the mucous lining of the nasal cavity.

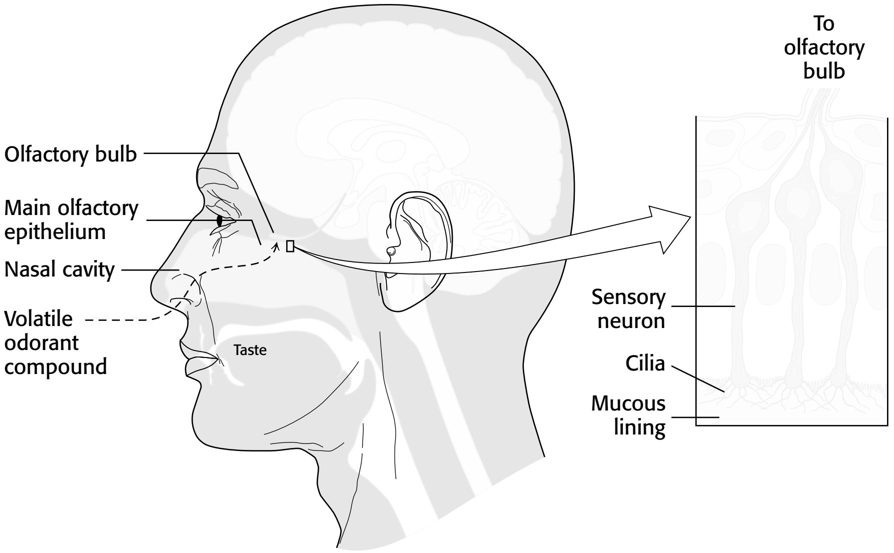

FIGURE 33.2 The main nasal epithelium. This region of the nose, which lies at the top of the nasal cavity, contains approximately 1 million sensory neurons. Nerve impulses generated by odorant molecules binding to receptors on the cilia travel from the sensory neurons to the olfactory bulb.

Biochemical studies in the late 1980s examined isolated cilia from rat olfactory epithelia that had been treated with odorants. Exposure to the odorants increased the cellular level of cyclic AMP, and this increase was observed only in the presence of GTP. On the basis of what was known about signal-transduction systems, *the participation of cAMP and GTP strongly suggested the involvement of a G protein and, hence, 7TM receptors.* Indeed, Randall Reed purified and cloned a G-protein α subunit, termed $G_{(olf)}$, which is uniquely expressed in olfactory cilia. The involvement of 7TM receptors suggested a strategy for identifying the olfactory receptors themselves. Complementary DNAs were sought that (1) were expressed primarily in the sensory neurons lining the nasal epithelium, (2) encoded members of the 7TM-receptor family, and (3) were present as a large and diverse family to account for the range of odorants. Through the use of these criteria, cDNAs for odorant receptors from rats were identified in 1991 by Richard Axel and Linda Buck.

The *odorant receptor* (hereafter, OR) family is even larger than expected: *more than 1000 OR genes are present in the mouse and the rat, whereas the human genome encodes approximately 350 ORs*. In addition, the human genome includes approximately 500 OR pseudogenes containing mutations that prevent the generation of a full-length, proper odorant receptor. The OR family is thus one of the largest gene families in human beings. Further analysis of primate OR genes reveals that the fraction of pseudogenes is greater in species more closely related to human beings (Figure 33.3). Thus, we may have a glimpse at the evolutionary loss of acuity in the sense of smell as higher mammals presumably became less dependent on this sense for survival. For rodents that are highly dependent on their sense of smell, essentially all OR genes encode functional proteins.

The OR proteins are typically 20% identical in sequence with the β-adrenergic receptor (Section 14.1) and from 30% to 60% identical with one another. Several specific sequence features are present in most or all OR family members (Figure 33.4). The central region,

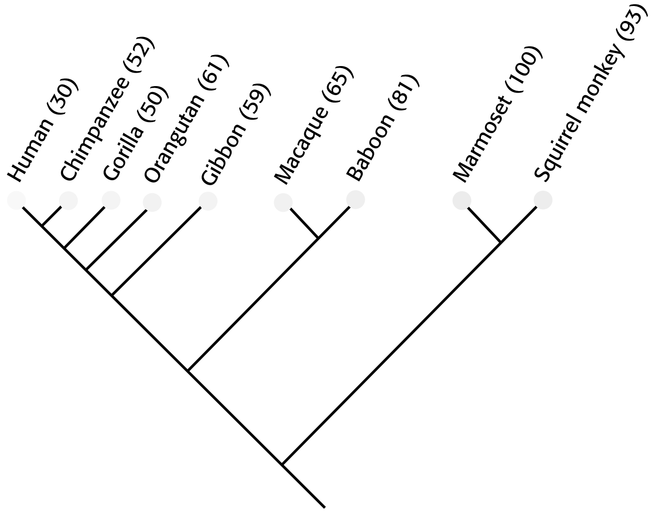

FIGURE 33.3 Evolution of odorant receptors. Odorant receptors appear to have lost function through conversion into pseudogenes in the course of primate evolution. The percentage of OR genes that appear to be functional for each species is given in parentheses.

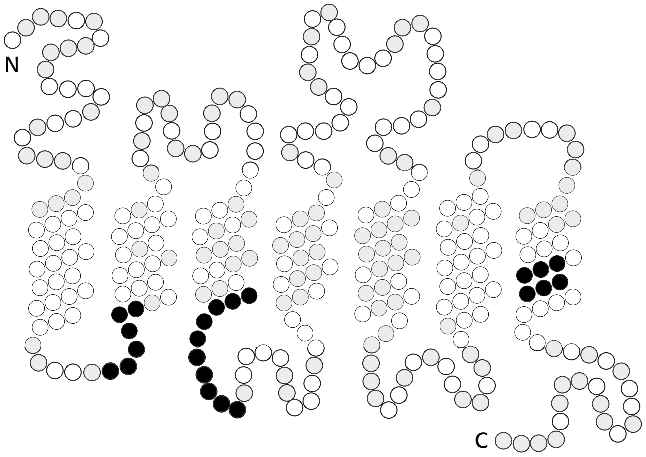

FIGURE 33.4 Conserved and variant regions in odorant receptors. Odorant receptors are members of the 7TM-receptor family. The green cylinders represent the seven presumed transmembrane helices. Strongly conserved residues characteristic of this protein family are shown in blue, whereas highly variable residues are shown in red.

particularly transmembrane helices 4 and 5, is highly variable, suggesting that this region is the site of odorant binding. That site must be different in odorant receptors that bind distinct odorant molecules.

What is the relation between OR gene expression and the individual neuron? Interestingly, *each olfactory neuron expresses only a single OR gene,* among hundreds available. Apparently, the precise OR gene expressed is determined largely at random. After one OR gene is expressed and a functional OR protein is produced, the expression of all other OR genes is suppressed by a feedback mechanism that remains to be fully elucidated.

The binding of an odorant to an OR on the neuronal surface initiates a signal-transduction cascade that results in an action potential (Figure 33.5). The ligand-bound OR activates $G_{(olf)}$, the specific G protein mentioned earlier. $G_{(olf)}$ is initially in its GDP-bound form. When activated, it releases GDP, binds GTP, and releases its associated βγ subunits. The α subunit then activates a specific adenylate cyclase, increasing the intracellular concentration of cAMP. The rise in the intracellular concentration of cAMP activates a nonspecific cation channel that allows calcium and other cations into the cell. The flow of cations through the channel depolarizes the neuronal membrane and initiates an action potential. This action potential, combined with those from other olfactory neurons, leads to the perception of a specific odor.

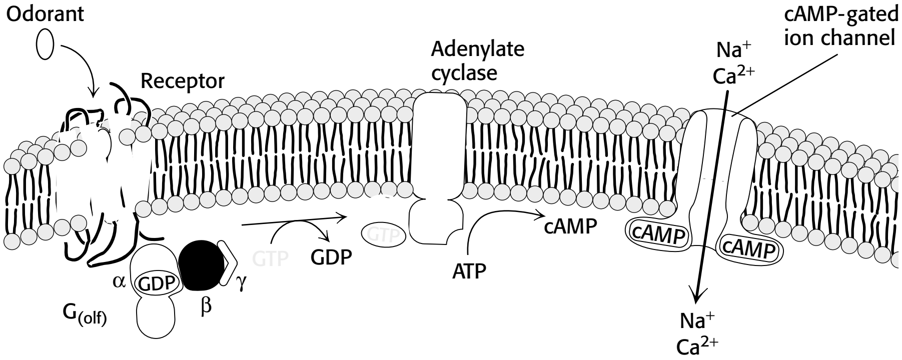

FIGURE 33.5 The olfactory signal-transduction cascade. The binding of odorant to the olfactory receptor activates a signaling pathway similar to those initiated in response to the binding of some hormones to their receptors. The final result is the opening of cAMP-gated ion channels and the initiation of an action potential.

Odorants are decoded by a combinatorial mechanism

An obvious challenge presented to an investigator by the large size of the OR family is to match each OR with the one or more odorant molecules to which it binds. Exciting progress has been made in this regard. Initially, an OR was matched with odorants by overexpressing a single, specific OR gene in rats. This OR responded to straight-chain aldehydes, most favorably to *n*-octanal and less strongly to *n*-heptanal and *n*-hexanal. More-dramatic progress was made by taking advantage of our knowledge of the OR signal-transduction pathway and the power of the polymerase chain reaction (PCR). A section of nasal epithelium from a mouse was loaded with the calcium-sensitive dye Fura-2 (Section 14.1). The tissue was then treated with different odorants, one at a time, at a specific concentration. If the

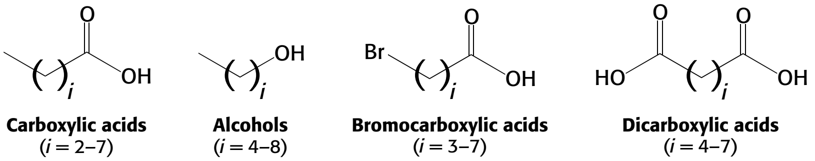

FIGURE 33.6 Four series of odorants tested for olfactory-receptor activation.

odorant had bound to an OR and activated it, that neuron could be detected under a microscope by the change in fluorescence caused by the influx of calcium that takes place as part of the signal-transduction process. To determine which OR was responsible for the response, cDNA was generated from mRNA that had been isolated from single identified neurons. The cDNA was then subjected to PCR with the use of primers that are effective in amplifying most or all OR genes. The sequence of the PCR product from each neuron was then determined and analyzed.

Using this approach, investigators analyzed the responses of neurons to a series of compounds having varying chain lengths and terminal functional groups (Figure 33.6). The results of these experiments appear surprising at first glance (Figure 33.7). Importantly, there is not a simple 1:1 correspondence between odorants and receptors. *Almost every odorant activates a number of receptors* (usually to different extents) and *almost every receptor is activated by more than one odorant*. Note, however, that each odorant activates a unique combination of receptors. In principle, this combinatorial mechanism allows even a small array of receptors to distinguish a vast number of odorants.

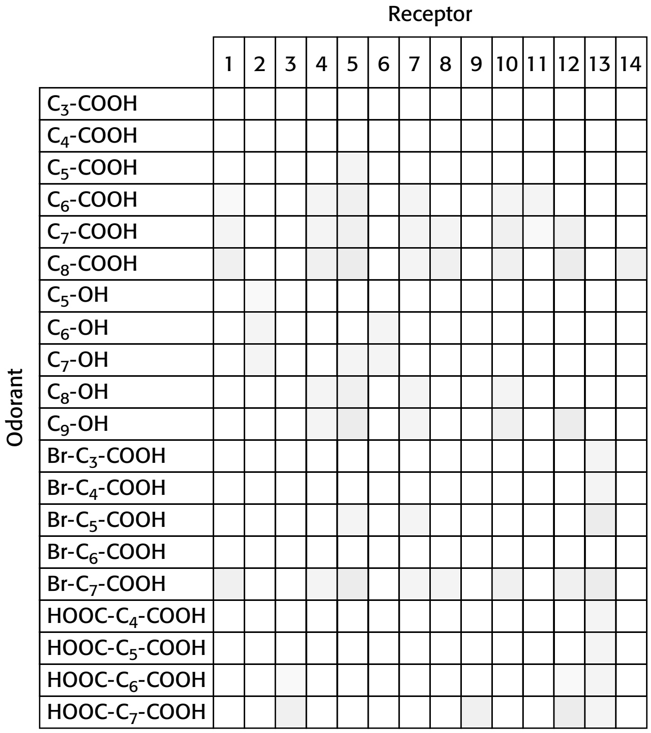

Odorant \ Receptor	1	2	3	4	5	6	7	8	9	10	11	12	13	14
C_3-COOH														
C_4-COOH														
C_5-COOH					▨									
C_6-COOH	▨			▨	▨		▨			▨	▨			
C_7-COOH	▨			▨	▨		▨	▨		▨	▨	▨		
C_8-COOH	▨			▨	▨		▨	▨		▨		▨		▨
C_5-OH		▨												
C_6-OH		▨				▨								
C_7-OH		▨			▨	▨								
C_8-OH				▨	▨		▨			▨				
C_9-OH				▨	▨		▨			▨		▨		
Br-C_3-COOH													▨	
Br-C_4-COOH													▨	
Br-C_5-COOH					▨		▨						▨	
Br-C_6-COOH														
Br-C_7-COOH	▨			▨	▨		▨	▨		▨		▨	▨	
HOOC-C_4-COOH													▨	
HOOC-C_5-COOH													▨	
HOOC-C_6-COOH			▨									▨	▨	
HOOC-C_7-COOH			▨						▨			▨	▨	

FIGURE 33.7 Patterns of olfactory-receptor activation. Fourteen different receptors were tested for responsiveness to the compounds shown in Figure 33.6. A colored box indicates that the receptor at the top responded to the compound at the left. Darker colors indicate that the receptor was activated at a lower concentration of odorant.

How is the information about which receptors have been activated transmitted to the brain? Recall that each neuron expresses only one OR and that the pattern of expression appears to be largely random. A substantial clue to the connections between receptors and the brain has been provided by the creation of mice that express a gene for an easily detectable colored marker in conjunction with a specific OR gene. Olfactory neurons that express the OR–marker-protein combination were traced to their destination in the brain, a structure called the olfactory bulb (Figure 33.8). The processes from neurons that express the same OR gene were found to connect to the same location in the olfactory bulb. Moreover, this pattern of neuronal connection was found to be identical in all mice examined. Thus, *neurons that express specific ORs are linked to specific sites in the brain*. This property creates a spatial map of odorant-responsive neuronal activity within the olfactory bulb.

Can such a combinatorial mechanism truly distinguish many different odorants? An electronic "nose" that functions by the same principles

FIGURE 33.8 Converging olfactory neurons. This section of the nasal cavity is stained to reveal processes from sensory neurons expressing the same olfactory receptor. The processes converge to a single location in the olfactory bulb. [Reprinted from *Cell*, 87, P. Mombaerts, F. Wang, C. Dulac, S. K. Chao, A. Nemes, M. Mendelsohn, J. Edmondson, & R. Axel, Visualizing an Olfactory Sensory Map, p. 675–689, Copyright 1996, with permission from Elsevier.]

provides compelling evidence that it can (Figure 33.9). The receptors for the electronic nose are polymers that bind a range of small molecules. Each polymer binds every odorant, but to varying degrees. Importantly, the electrical properties of these polymers change on odorant binding. A set of 32 of these polymer sensors, wired together so that the pattern of responses can be evaluated, is capable of distinguishing individual compounds such as *n*-pentane and *n*-hexane as well as complex mixtures such as the odors of fresh and spoiled fruit.

FIGURE 33.9 The Cyranose 320. The electronic nose may find uses in the food industry, animal husbandry, law enforcement, and medicine. [Courtesy of Smiths Medical.]

33.2 Taste Is a Combination of Senses That Function by Different Mechanisms

The inability to taste food is a common complaint when nasal congestion reduces the sense of smell. Thus, smell greatly augments our sense of taste (also known as *gustation*), and taste is, in many ways, the sister sense to olfaction. Nevertheless, the two senses differ from each other in several important ways. First, we are able to sense several classes of compounds by taste that we are unable to detect by smell; salt and sugar have very little odor, yet they are primary stimuli of the gustatory system. Second, whereas we are able to discriminate thousands of odorants, discrimination by taste is much more modest. Five primary tastes are perceived: *bitter, sweet, sour, salty,* and *umami* (the taste of glutamate and aspartate from the Japanese word for "deliciousness"). These five tastes serve to classify compounds into potentially nutritive and beneficial (sweet, salty, umami) or potentially harmful or toxic (bitter, sour). Tastants (the molecules sensed by taste) are quite distinct for the different groups (Figure 33.10).

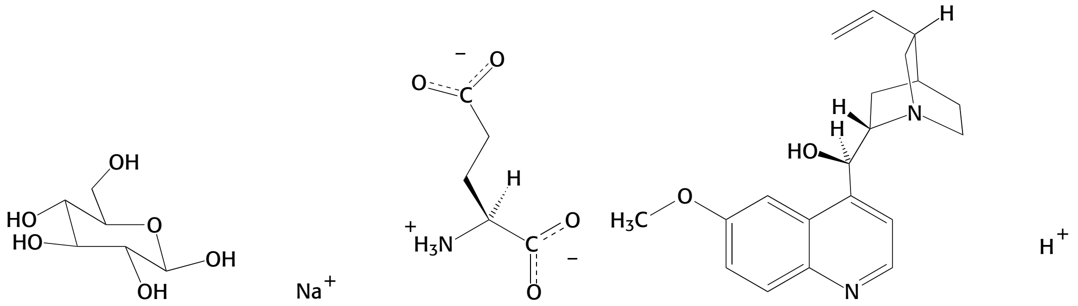

Glucose (sweet)

Sodium ion (salty)

Glutamate (umami)

Quinine (bitter)

Hydrogen ion (sour)

FIGURE 33.10 Examples of tastant molecules. Tastants fall into five groups: sweet, salty, umami, bitter, and sour.

The simplest tastant, the hydrogen ion, is perceived as sour. Other simple ions, particularly sodium ion, are perceived as salty. The taste called umami is evoked by the amino acids glutamate and aspartate, the former often encountered as the flavor enhancer monosodium glutamate (MSG). In contrast, *tastants perceived as sweet and, particularly, bitter are extremely diverse*. Many bitter compounds are alkaloids or other plant products, many of which are toxic. However, they do not have any common structural elements or other common properties. Carbohydrates such as glucose and sucrose are perceived as sweet, as are other compounds including some simple peptide derivatives, such as aspartame, and even some proteins.

These differences in specificity among the five tastes are due to differences in their underlying biochemical mechanisms. The sense of taste is, in fact, a number of independent senses all utilizing the same organ, the tongue, for their expression.

Tastants are detected by specialized structures called *taste buds,* which contain approximately 150 cells, including sensory neurons (Figure 33.11). Fingerlike projections called *microvilli,* which are rich in taste receptors, project from one end of each sensory neuron to the surface of the tongue. Nerve fibers at the opposite end of each neuron carry electrical impulses to the brain in response to stimulation by tastants. Structures called *taste papillae* contain numerous taste buds.

FIGURE 33.11 A taste bud. Each taste bud contains sensory neurons that extend microvilli to the surface of the tongue, where they interact with tastants.

Sequencing of the human genome led to the discovery of a large family of 7TM bitter receptors

Just as in olfaction, a number of clues pointed to the involvement of G proteins and, hence, 7TM receptors in the detection of bitter and sweet tastes. The evidence included the isolation of a specific G-protein α subunit termed *gustducin,* which is expressed primarily in taste buds (Figure 33.12). How could the 7TM receptors be identified? The ability to detect some compounds depends on specific genetic loci in both human beings and mice. For instance, the ability to taste the bitter compound 6-*n*-propyl-2-thiouracil (PROP) was mapped to a region on human chromosome 5 by comparing DNA markers of persons who vary in sensitivity to this compound.

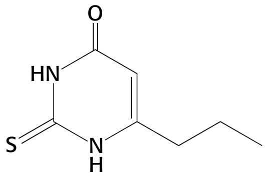

6-*n*-Propyl-2-thiouracil (PROP)

This observation suggested that this region might encode a 7TM receptor that responded to PROP. Approximately 450 kilobases in this region had been sequenced early in the human genome project. This sequence was searched by computer for potential 7TM-receptor genes, and, indeed, one was detected and named T2R1. Additional database searches detected approximately 30 sequences similar to T2R1 in the human genome. The encoded proteins are between 30 and 70% identical with T2R1 (Figure 33.13).

Are these proteins, in fact, bitter receptors? Several lines of evidence suggest that they are. First, their genes are expressed in taste-sensitive cells—in fact, in many of the same cells that express gustducin. Second, cells that express individual members of this family respond to specific bitter compounds. For example, cells that express a specific mouse receptor (mT2R5) responded when exposed specifically to cycloheximide. Third, mice that had been found unresponsive to cycloheximide were found to have point mutations in the gene encoding mT2R5. Finally, cycloheximide

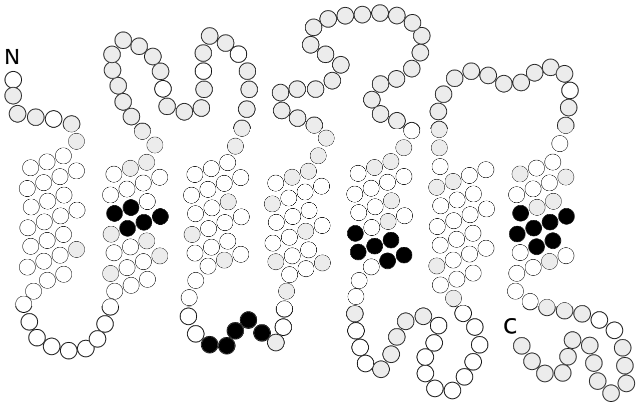

FIGURE 33.13 Conserved and variant regions in bitter receptors. The bitter receptors are members of the 7TM-receptor family. Strongly conserved residues characteristic of this protein family are shown in blue, and highly variable residues are shown in red.

(A)

(B)

FIGURE 33.12 Expression of gustducin in the tongue. (A) A section of tongue stained with a fluorescent antibody reveals the position of the taste buds. (B) The same region stained with an antibody directed against gustducin reveals that this G protein is expressed in taste buds. [Courtesy of Dr. Charles S. Zuker.]

specifically stimulates the binding of GTP analogs to gustducin in the presence of the mT2R5 protein (Figure 33.14).

Importantly, each taste-receptor cell expresses many different members of the T2R family. This pattern of expression stands in sharp contrast to the pattern of one receptor type per cell that characterizes the olfactory system (Figure 33.15). The difference in expression patterns accounts for the much greater specificity of our perceptions of odors compared with tastes. *We are able to distinguish among subtly different odors because each odorant stimulates a unique pattern of neurons. In contrast, many tastants stimulate the same neurons*. Thus, we perceive only "bitter" without the ability to discriminate cycloheximide from quinine.

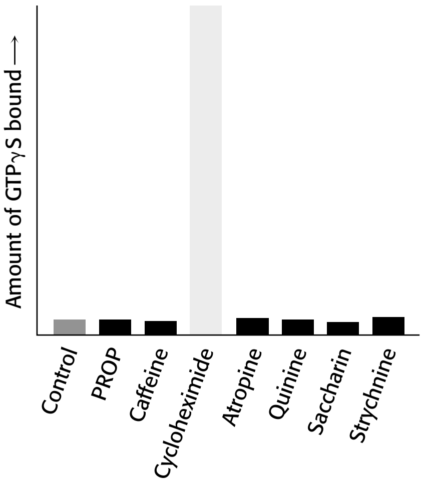

FIGURE 33.14 Evidence that T2R proteins are bitter taste receptors. Cycloheximide uniquely stimulates the binding of the GTP analog GTPγS to gustducin in the presence of the mT2R protein. [Information from J. Chandrashekar et al., *Cell* 100:703–711, 2000.]

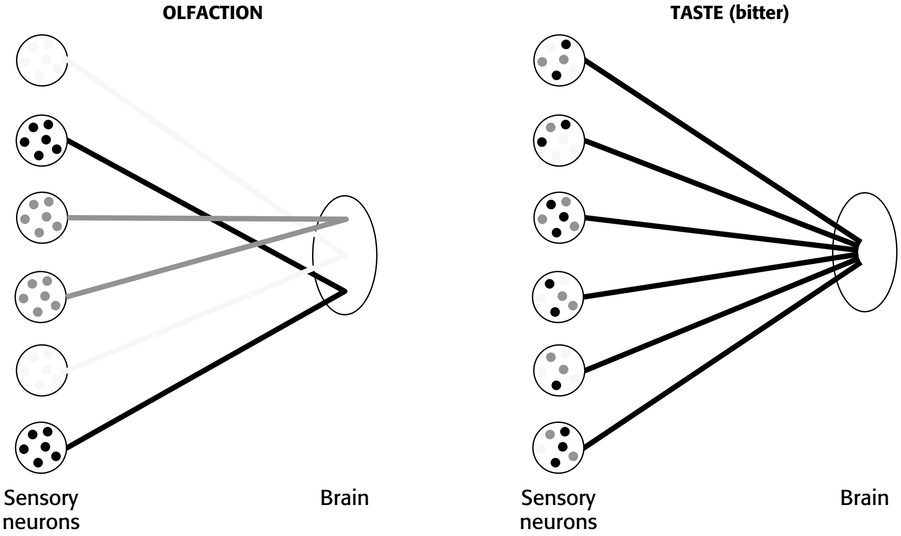

FIGURE 33.15 Differing gene-expression and connection patterns in olfactory and bitter taste receptors. In olfaction, each neuron expresses a single OR gene, and the neurons expressing the same OR converge to specific sites in the brain, enabling specific perception of different odorants. In gustation, each neuron expresses many bitter receptor genes, and so the identity of the tastant is lost in transmission.

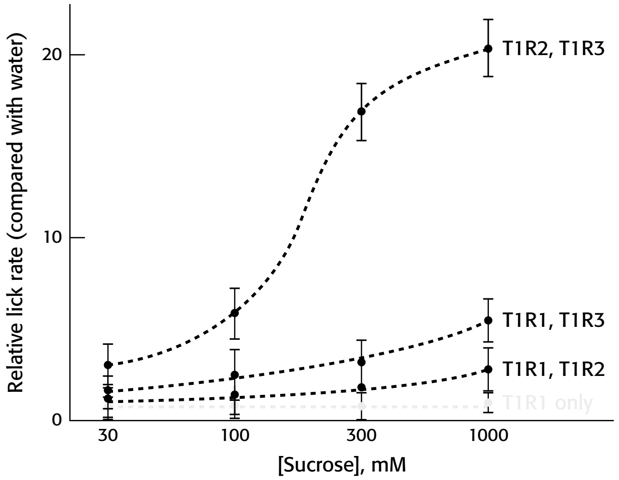

FIGURE 33.16 Evidence for a heterodimeric sweet receptor. The sensitivity to sweetness of mice with genes for T1R1 only, both T1R1 and T1R2, both T1R1 and T1R3, or both T1R2 and T1R3 was determined by observing the relative rates at which they licked solutions containing various amounts of sucrose. These studies revealed that both T1R2 and T1R3 were required for a full response to sucrose. [Data from G. Q. Zhao et al., *Cell* 115:255–266, 2003.]

A heterodimeric 7TM receptor responds to sweet compounds

Most sweet compounds are carbohydrates, energy rich and easily digestible. Some noncarbohydrate compounds such as saccharin and aspartame also taste sweet. Members of a second family of 7TM receptors are expressed in taste-receptor cells sensitive to sweetness. The three members of this family, referred to as T1R1, T1R2, and T1R3, are distinguished by their large extracellular domains compared with those of the bitter receptors. Studies in knockout mice have revealed that T1R2 and T1R3 are expressed simultaneously in mice able to taste carbohydrates (Figure 33.16). Thus, T1R2 and T1R3 appear to form a specific heterodimeric receptor responsible for mediating the response to sugars. This heterodimeric receptor also responds to artificial sweeteners and to sweet-tasting proteins and therefore appears to be the receptor responsible for responses to all sweet tastants. Note that T1R2 and T1R3 do respond to sweet tastants individually but only at very high concentrations of tastant.

The requirement for an *oligomeric* 7TM receptor for a fully functional response is surprising, considering our previous understanding of 7TM receptors. This discovery has at least two possible explanations. First, the sweet receptor could be a member of a small subset of the 7TM-receptor family that functions well only as oligomers. Alternatively, many 7TM receptors may function as oligomers, but this notion is not clear, because these oligomers contain only one type of 7TM-receptor subunit. Further studies will be required to determine which of these explanations is correct.

Umami, the taste of glutamate and aspartate, is mediated by a heterodimeric receptor related to the sweet receptor

The family of receptors responsible for detecting sweetness is also responsible for detecting amino acids. In human beings, only glutamate and aspartate elicit a taste response. Studies similar to those for the sweet receptor revealed that the umami receptor consists of T1R1 and T1R3. Thus, this receptor has one subunit (T1R3) in common with the sweet receptor but has an additional subunit (T1R1) that does not participate in the sweet response. This conclusion is supported by the observation that mice in which the gene for T1R1 is disrupted do not respond to aspartate but do respond normally to sweet tastants; mice having disrupted genes for both T1R1 and T1R3 respond poorly to both umami and sweet tastants.

Salty tastes are detected primarily by the passage of sodium ions through channels

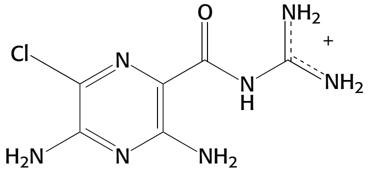

Amiloride

Salty tastants are not detected by 7TM receptors. Rather, they are detected directly by their passage through ion channels expressed on the surface of cells in the tongue. Evidence for the role of these ion channels comes from examining known properties of Na^+ channels characterized in other biological contexts. One class of channels, characterized first for its role in salt reabsorption, is thought to be important in the detection of salty tastes because these channels are sensitive to the compound *amiloride,* which mutes the taste of salt and significantly lowers sensory-neuron activation in response to sodium.

An *amiloride-sensitive* Na^+ *channel* comprises four subunits that may be either identical or distinct but in any case are homologous. An individual subunit ranges in length from 500 to 1000 amino acids and includes two presumed membrane-spanning helices as well as a large extracellular domain in between them (Figure 33.17). The extracellular region includes two (or, sometimes, three) distinct regions rich in cysteine residues (and, presumably, disulfide bonds). A region just ahead of the second membrane-spanning helix appears to form part of the pore in a manner analogous to that of the structurally characterized potassium channel. The members of the amiloride-sensitive Na^+ -channel family are numerous and diverse in their biological roles. We shall encounter them again in the context of the sense of touch.

Sodium ions passing through these channels produce a significant transmembrane current. Amiloride blocks this current, accounting for its effect on taste. However, about 20% of the response to sodium remains even in the presence of amiloride, suggesting that other ion channels also contribute to salt detection.

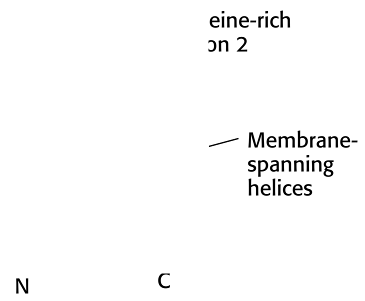

FIGURE 33.17 Schematic structure of the amiloride-sensitive sodium channel. Only one of the four subunits that constitute the functional channel is illustrated. The amiloride-sensitive sodium channel belongs to a superfamily having common structural features, including two hydrophobic membrane-spanning regions, intracellular amino and carboxyl termini, and a large, extracellular region with conserved cysteine-rich domains.

Sour tastes arise from the effects of hydrogen ions (acids) on channels

Like salty tastes, *sour tastes are detected by direct interactions with ion channels,* but the incoming ions are hydrogen ions (in high concentrations) rather than sodium ions. For example, in the absence of high concentrations of sodium, hydrogen ion flow can induce substantial transmembrane currents through amiloride-sensitive Na^+ channels. However, hydrogen ions are also sensed by mechanisms other than their direct passage through membranes. Binding by hydrogen ions blocks some potassium ion channels and activates other types of channels. Together, these mechanisms lead to changes in membrane polarization in sensory neurons that produce the sensation of sour taste. We shall consider an additional receptor related to taste, one responsible for the "hot" taste of spicy food, when we examine mechanisms of touch perception.

33.3 Photoreceptor Molecules in the Eye Detect Visible Light

Vision is based on the absorption of light by photoreceptor cells in the eye. These cells are sensitive to light in a narrow region of the electromagnetic spectrum, the region with wavelengths between 390 and 750 nm (Figure 33.18). Vertebrates have two kinds of photoreceptor cells, called *rods* and *cones* because of their distinctive shapes. Cones function in bright light and are responsible for color vision, whereas rods function in dim light but do not perceive color. A human retina contains about 3 million cones and 100 million rods. Remarkably, a rod cell can respond to a single photon, and the brain requires fewer than 10 such responses to register the sensation of a flash of light.

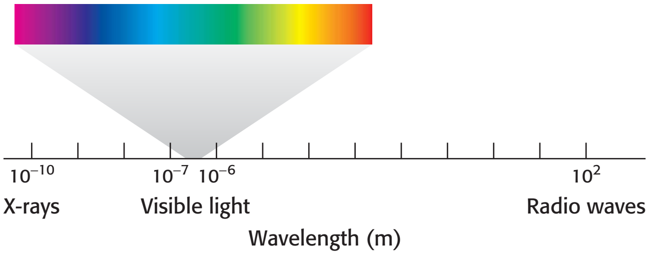

FIGURE 33.18 The electromagnetic spectrum. Visible light has wavelengths between 390 and 750 nm.

Rhodopsin, a specialized 7TM receptor, absorbs visible light

Rods are slender, elongated structures; the outer segment is specialized for photoreception (Figure 33.19). It contains a stack of about 1000 discs, which are membrane-enclosed sacs densely packed with photoreceptor molecules. The photosensitive molecule is often called a *visual pigment* because it is highly colored owing to its ability to absorb light. The photoreceptor molecule in rods is *rhodopsin* (Section 14.1), which consists of the protein *opsin* linked to 11-cis-*retinal*, a prosthetic group.

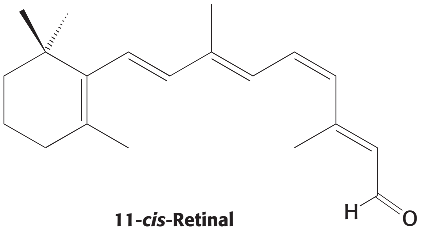

11-*cis*-Retinal

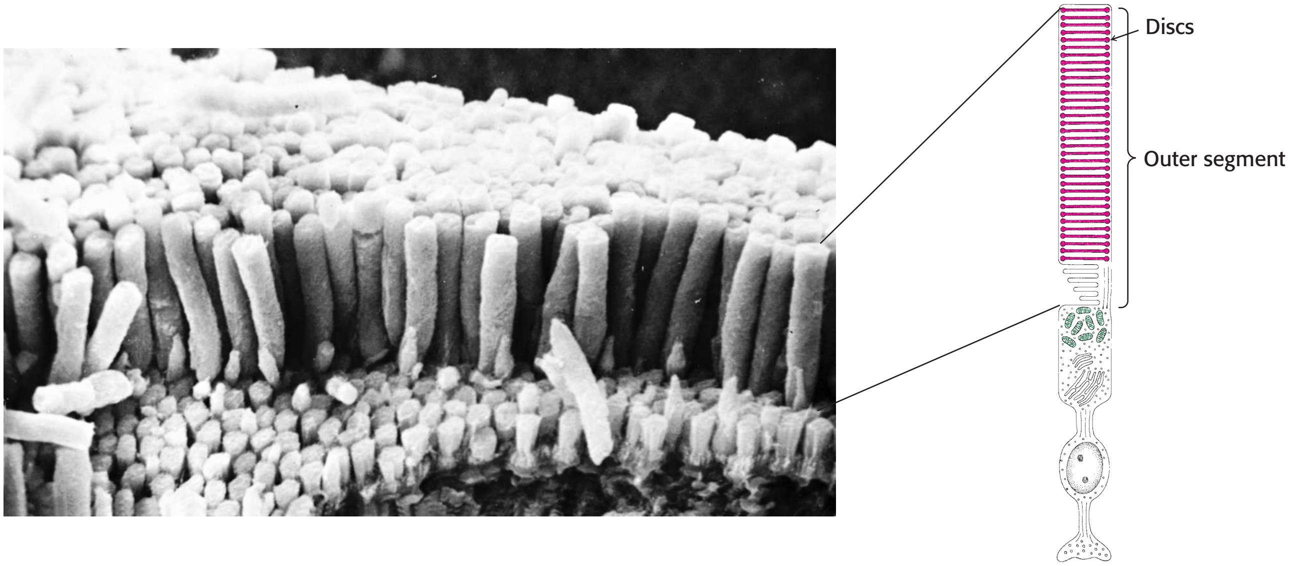

FIGURE 33.19 The rod cell. (Left) Scanning electron micrograph of retinal rod cells. (Right) Schematic representation of a rod cell. [Photograph courtesy of Dr. Deric Bownds.]

Rhodopsin absorbs light very efficiently in the middle of the visible spectrum, its absorption being centered on 500 nm, which nicely matches the solar output (Figure 33.20). A rhodopsin molecule will absorb a high percentage of the photons of the correct wavelength that strike it, as indicated by the extinction coefficient of 40,000 $M^{-1}cm^{-1}$ at 500 nm. The extinction coefficient for rhodopsin is more than an order of magnitude greater than that for tryptophan, the most efficient absorber in proteins that lack prosthetic groups.

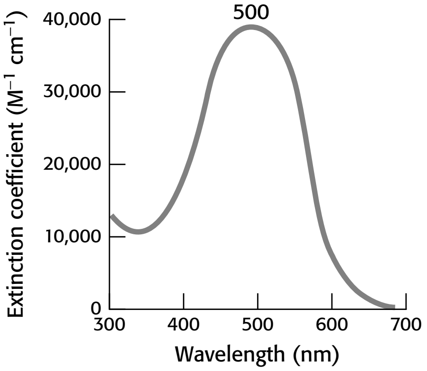

FIGURE 33.20 Rhodopsin absorption spectrum. Almost all photons with wavelengths near 500 nm that strike a rhodopsin molecule are absorbed.

Opsin, the protein component of rhodopsin, is a member of the 7TM-receptor family. Indeed, rhodopsin was the first member of this family to be purified, its gene was the first to be cloned and sequenced, and its three-dimensional structure was the first to be determined. The color of rhodopsin and its responsiveness to light depend on the presence of the light-absorbing group *(chromophore)* 11-*cis*-retinal. This compound is a powerful absorber of light because it is a polyene; its six alternating single and double bonds constitute a long, unsaturated electron network. Recall that alternating single and double bonds account for the chromophoric properties of chlorophyll (Section 19.2). The aldehyde group of 11-*cis*-retinal forms a Schiff base (Figure 33.21) with the ε-amino group of lysine residue 296, which lies in the center of the seventh transmembrane helix. Free retinal absorbs maximally at 370 nm, and its unprotonated Schiff-base adduct absorbs at 380 nm, whereas the protonated Schiff base absorbs at 440 nm or longer wavelengths. Thus, *the 500-nm absorption maximum for rhodopsin strongly suggests that the Schiff base is protonated;* additional interactions with opsin shift the absorption maximum farther toward the red. The positive charge of the protonated Schiff base is compensated by the negative charge of glutamate 113 located in helix 2; the glutamate residue closely approaches the lysine–retinal linkage in the three-dimensional structure of rhodopsin.

FIGURE 33.21 Retinal–lysine linkage. Retinal is linked to lysine 296 in opsin by a Schiff-base linkage. In the resting state of rhodopsin, this Schiff base is protonated.

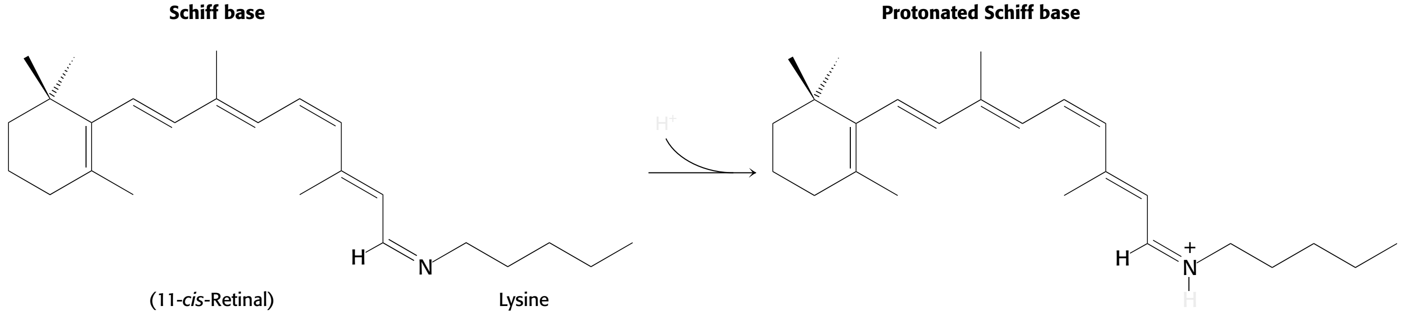

Light absorption induces a specific isomerization of bound 11-*cis*-retinal

How does the absorption of light by the retinal Schiff base generate a signal? George Wald and his coworkers discovered that *light absorption results in the isomerization of the 11-*cis*-retinal group of rhodopsin to its all-*trans* form* (Figure 33.22). This isomerization causes the Schiff-base nitrogen atom to move approximately 5 Å, assuming that the cyclohexane ring of the retinal group remains fixed. In essence, *the light energy of a photon is converted into atomic motion*. The change in atomic positions, like the binding of a ligand to other 7TM receptors, sets in train a series of events that lead to the closing of ion channels and the generation of a nerve impulse.

The isomerization of the retinal Schiff base takes place within a few picoseconds of a photon being absorbed. The initial product, termed *bathorhodopsin,* contains a strained all-*trans*-retinal group. Within approximately

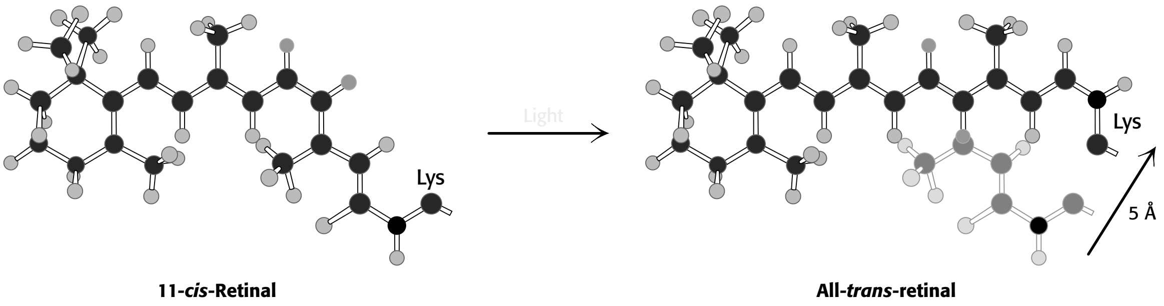

FIGURE 33.22 Atomic motion in retinal. The Schiff-base nitrogen atom moves 5 Å as a consequence of the light-induced isomerization of 11-*cis*-retinal to all-*trans*-retinal by rotation about the bond shown in red.

1 ms, this intermediate is converted through several additional intermediates into *metarhodopsin II*. In metarhodopsin II, the Schiff base is deprotonated and the opsin protein has undergone significant reorganization.

Metarhodopsin II (also referred to as R*) is analogous to the ligand-bound state of 7TM receptors such as the β_2-adrenergic receptor (Section 14.1) and the odorant and tastant receptors discussed previously (Figure 33.23). Like these receptors, this form of rhodopsin activates a heterotrimeric G protein that propagates the signal. The G protein associated with rhodopsin is called *transducin*. Metarhodopsin II triggers the exchange of GDP for GTP by the α subunit of transducin (Figure 33.24). On the binding of GTP, the βγ subunits of transducin are released and the α subunit switches on a *cGMP phosphodiesterase* by binding to an inhibitory subunit and removing it. The activated phosphodiesterase is a potent enzyme that rapidly hydrolyzes cGMP to GMP. The reduction in cGMP concentration causes *cGMP-gated ion channels* to close, leading to the hyperpolarization of the membrane and neuronal signaling. *At each step in this process, the initial signal—the absorption of a single photon—is amplified so that it leads to sufficient membrane hyperpolarization to result in signaling.*

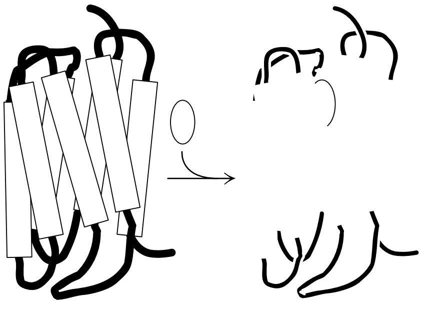
Ligand-bound
7TM receptor

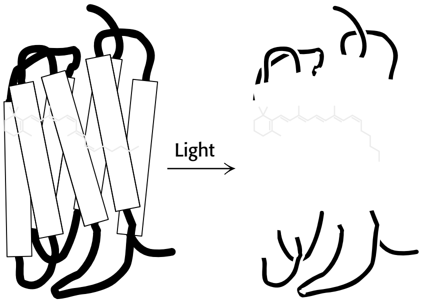

Metarhodopsin II

FIGURE 33.23 Analogous 7TM receptors. The conversion of rhodopsin into metarhodopsin II activates a signal-transduction pathway analogously to the activation induced by the binding of other 7TM receptors to appropriate ligands.

Light-induced lowering of the calcium level coordinates recovery

As we have seen, the visual system responds to changes in light and color within a few milliseconds, quickly enough that we are able to perceive continuous motion at nearly 1000 frames per second. To achieve a rapid response, the signal must also be terminated rapidly and the system must be returned to its initial state. First, activated rhodopsin must be blocked from continuing to activate transducin. *Rhodopsin kinase* catalyzes the phosphorylation of the carboxyl terminus of R* at multiple serine and threonine residues. *Arrestin,* an inhibitory protein then binds phosphorylated R* and prevents additional interaction with transducin.

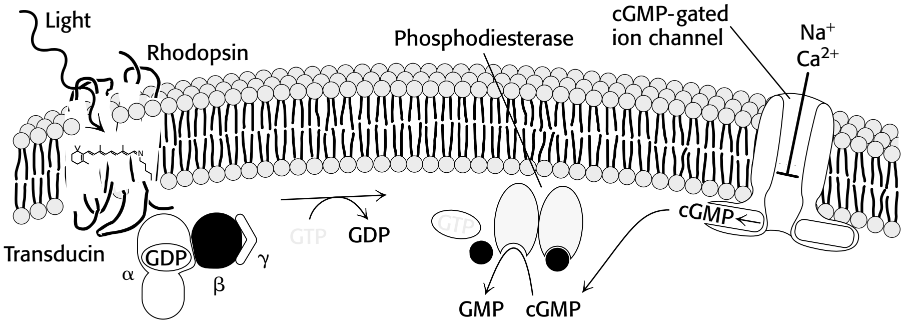

FIGURE 33.24 Visual signal transduction. The light-induced activation of rhodopsin leads to the hydrolysis of cGMP, which in turn leads to ion-channel closing and the initiation of an action potential.

Second, the α subunit of transducin must be returned to its inactive state to prevent further signaling. Like other G proteins, the α subunit possesses built-in GTPase activity that hydrolyzes bound GTP to GDP. Hydrolysis takes place in less than a second when transducin is bound to the phosphodiesterase. The GDP form of transducin then leaves the phosphodiesterase and reassociates with the βγ subunits, and the phosphodiesterase returns to its inactive state. Third, the level of cGMP must be raised to reopen the cGMP-gated ion channels. *The action of guanylate cyclase accomplishes this third step by synthesizing cGMP from GTP.*

Calcium ion plays an essential role in controlling guanylate cyclase because it markedly inhibits the activity of the enzyme. In the dark, Ca^{2+} as well as Na^+ enter the rod outer segment through the cGMP-gated channels. Calcium ion influx is balanced by its efflux through an exchanger, a transport system that uses the thermodynamically favorable flow of four Na^+ ions into the cell and one K^+ ion out of the cell to extrude one Ca^{2+} ion. After illumination, the entry of Ca^{2+} through the cGMP-gated channels stops, but its export through the exchanger continues. Thus, the cytoplasmic Ca^{2+} level drops from 500 nM to 50 nM after illumination. This drop markedly stimulates guanylate cyclase, rapidly restoring the concentration of cGMP to reopen the cGMP-gated channels.

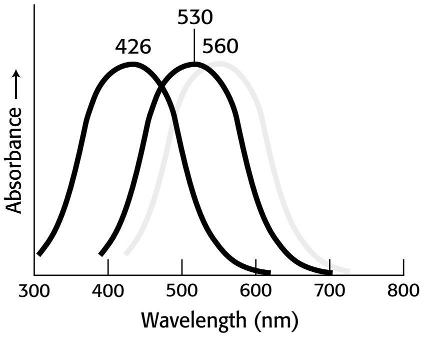

FIGURE 33.25 Cone-pigment absorption spectra. The absorption spectra of the cone visual pigment responsible for color vision.

$$\begin{array}{lllll} \underline{\text{Activation}} & & \underline{\text{Recovery}} & & \end{array}$$

$$[\text{cGMP}]\downarrow \longrightarrow \begin{array}{c}\text{Ion}\\ \text{channels}\\ \text{closed}\end{array} \longrightarrow [\text{Ca}^{2+}]\downarrow \longrightarrow \begin{array}{c}\text{Guanylate}\\ \text{cyclase}\\ \text{activity}\\ \text{increased}\end{array} \longrightarrow [\text{cGMP}]\uparrow$$

By controlling the rate of cGMP synthesis, Ca^{2+} levels govern the speed with which the system is restored to its initial state.

Color vision is mediated by three cone receptors that are homologs of rhodopsin

Cone cells, like rod cells, contain visual pigments. Like rhodopsin, these photoreceptor proteins are members of the 7TM-receptor family and use 11-*cis*-retinal as their chromophore. In human cone cells, there are three distinct photoreceptor proteins with absorption maxima at 426, 530, and ~560 nm (Figure 33.25). *These absorbances correspond to the blue, green, and yellow-green regions of the spectrum.* Recall that the absorption maximum for rhodopsin is 500 nm. The photoreceptor protein with its absorption maximum near 560 nm absorbs red light (with wavelength >620 nm) whereas the other two photoreceptors do not. For simplicity, we shall refer to the three proteins as the blue, green, and red photoreceptors.

The amino acid sequences of the cone photoreceptors have been compared with one another and with rhodopsin. The result is striking. Each of the cone photoreceptors is approximately 40% identical in sequence with rhodopsin. Similarly, the blue photoreceptor is 40% identical with each of the green and red photoreceptors. The green and red photoreceptors, however, are >95% identical with each other, differing in only 15 of 364 positions (Figure 33.26).

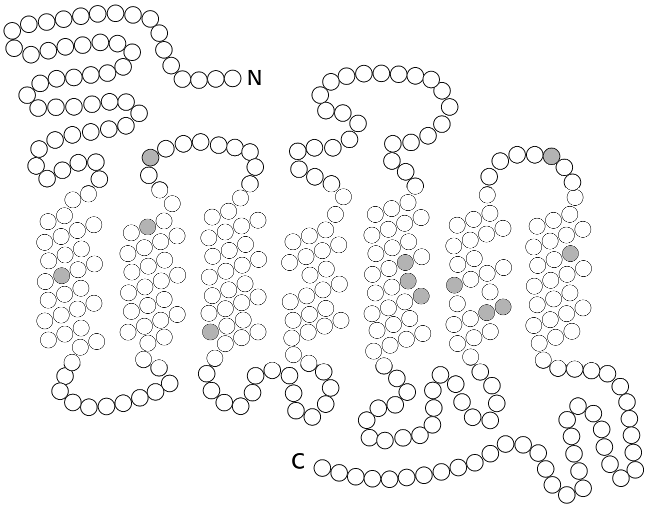

FIGURE 33.26 Comparison of the amino acid sequences of the green and red photoreceptors. Open circles correspond to identical residues, whereas colored circles mark residues that are different. The differences in the three black positions are responsible for most of the difference in their absorption spectra.

These observations are sources of insight into photoreceptor evolution. First, the green and red

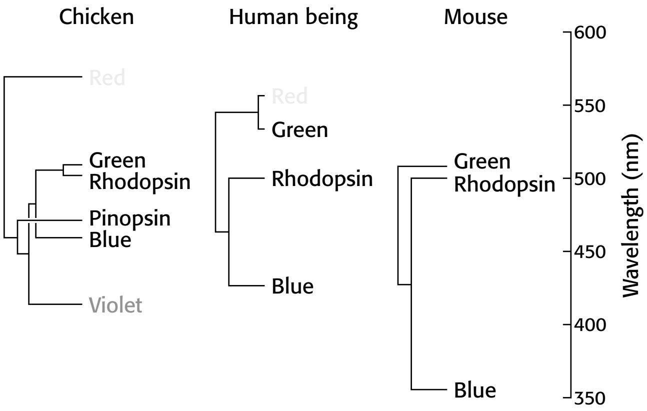

FIGURE 33.27 Evolutionary relationships among visual pigments. Visual pigments have evolved by gene duplication along different branches of the animal evolutionary tree. The branch lengths of the "trees" correspond to the percentage of amino acid divergence. [Information from J. Nathans, *Neuron* 24:299–312, 1999; by permission of Cell Press.]

photoreceptors are clearly products of a recent evolutionary event (Figure 33.27). The green and red pigments appear to have diverged in the primate lineage approximately 35 million years ago. Mammals, such as dogs and mice, that diverged from primates earlier have only two cone photoreceptors, blue and green. They are not sensitive to light as far toward the infrared region as we are, and they do not discriminate colors as well. In contrast, birds such as chickens have a total of six pigments: rhodopsin, four cone pigments, and a pineal visual pigment called *pinopsin*. Birds have highly acute color perception.

Second, the high level of similarity between the green and the red pigments has made the identification of the specific amino acid residues responsible for spectral tuning possible. Three residues (at positions 180, 277, and 285) are responsible for most of the difference between the green and the red pigments. In the green pigment, these residues are alanine, phenylalanine, and alanine, respectively; in the red pigment, they are serine, tyrosine, and threonine. A hydroxyl group has been added to each amino acid in the red pigment. The hydroxyl groups can interact with the photoexcited state of retinal and lower its energy, leading to a shift toward the lower-energy (red) region of the spectrum.

Homologous recombination
The exchange of DNA segments with substantial sequence similarity at equivalent positions between chromosomes.

Rearrangements in the genes for the green and red pigments lead to "color blindness"

The genes for the green and red pigments lie adjacent to each other on the human X chromosome. These genes are more than 98% identical in nucleotide sequence, including introns and untranslated regions as well as the protein-coding region. Regions with such high similarity are very susceptible to unequal homologous recombination.

FIGURE 33.28 Recombination pathways leading to color blindness. Rearrangements in the course of DNA replication may lead to (A) the loss of visual pigment genes or (B) the formation of hybrid pigment genes that encode photoreceptors with anomalous absorption spectra. Because the amino acids most important for determining absorption spectra are in the carboxyl-terminal half of each photoreceptor protein, the part of the gene that encodes this region most strongly affects the absorption characteristics of hybrid receptors. [Information from J. Nathans, *Neuron* 24:299–312, 1999; by permission of Cell Press.]

Recombination can take place either between or within transcribed regions of the gene (Figure 33.28). If recombination takes place between transcribed regions, the product chromosomes will differ in the number of pigment genes that they carry. One chromosome will lose a gene and thus may lack the gene for, say, the green pigment; the other chromosome will gain a gene. Consistent with this scenario, approximately 2% of human X chromosomes carry only a single color-pigment gene, approximately 20% carry two, 50% carry three, 20% carry four, and 5% carry five or more. A person lacking the gene for the green pigment will have trouble distinguishing red and green color, characteristic of the most common form of color blindness. Approximately 5% of males have this form of color blindness. Recombination can also take place within the

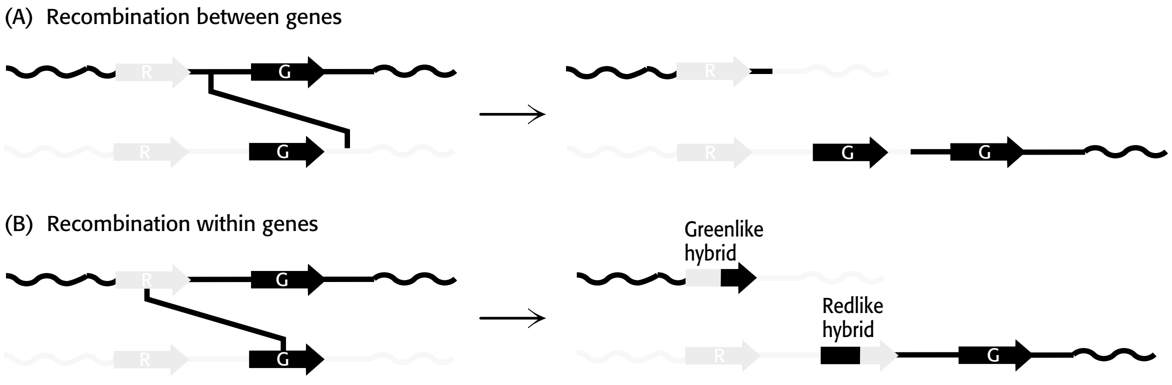
(A) Recombination between genes

(B) Recombination within genes

transcription units, resulting in genes that encode hybrids of the green and red photoreceptors. The absorption maximum of such a hybrid lies between that of the red and green pigments. A person with such hybrid genes who also lacks either a functional red- or green-pigment gene does not discriminate color well.

33.4 Hearing Depends on the Speedy Detection of Mechanical Stimuli

Hearing and touch are based on the detection of mechanical stimuli. Although the proteins of these senses have not been as well characterized as those of the senses already discussed, anatomical, physiological, and biophysical studies have elucidated the fundamental processes. *A major clue to the mechanism of hearing is its speed.* We hear frequencies ranging from 200 to 20,000 Hz (cycles per second), corresponding to times of 5 to 0.05 ms. Furthermore, our ability to locate sound sources, one of the most important functions of hearing, depends on the ability to detect the time delay between the arrival of a sound at one ear and its arrival at the other. Given the separation of our ears and the speed of sound, we must be able to accurately sense time differences of 0.7 ms. In fact, human beings can locate sound sources associated with temporal delays as short as 0.02 ms. This high time resolution implies that hearing must employ direct transduction mechanisms that do not depend on second messengers. Recall that, in vision, for which speed also is important, the signal-transduction processes take place in milliseconds.

Stereocilia

Hair cell

FIGURE 33.29 Hair cells, the sensory neurons crucial for hearing. These specialized neurons are capped with hairlike projections called stereocilia that are responsible for detecting very subtle vibrations. [Information from A. J. Hudspeth, *Nature* 341:397–404, 1989.]

Hair cells use a connected bundle of stereocilia to detect tiny motions

Sound waves are detected inside the cochlea of the inner ear. The *cochlea* is a fluid-filled, membranous sac that is coiled like a snail shell. The primary detection is accomplished by specialized neurons inside the cochlea called *hair cells* (Figure 33.29). Each cochlea contains approximately 16,000 hair cells, and each hair cell contains a hexagonally shaped bundle of 20 to 300 hairlike projections called *stereocilia* (Figure 33.30). These stereocilia are graded in length across the bundle. Mechanical deflection of the hair bundle, as takes place when a sound wave arrives at the ear, creates a change in the membrane potential of the hair cell.

Micromanipulation experiments have directly probed the connection between mechanical stimulation and membrane potential. Displacement toward the direction of the tallest part of the hair bundle results in the depolarization of the hair cell, whereas displacement in the opposite direction results in its hyperpolarization (Figure 33.31). Motion perpendicular to the hair-length gradient does not produce any change in resting potential.

FIGURE 33.30 An electron micrograph of a hair bundle. [Courtesy of Dr. A. Jacobs and Dr. A. J. Hudspeth.]

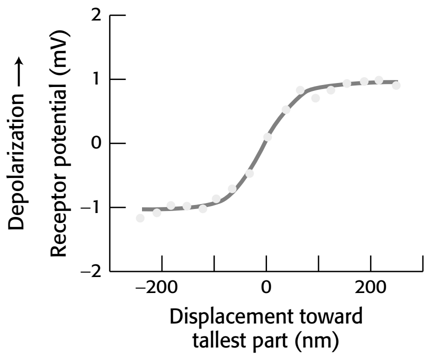

FIGURE 33.31 Micromanipulation of a hair cell. Movement toward the tallest part of the bundle depolarizes the cell as measured by the microelectrode. Movement toward the shortest part hyperpolarizes the cell. Lateral movement has no effect. [After A. J. Hudspeth, *Nature* 341:397–404, 1989.]

Remarkably, *displacement of the hair bundle by as little as 3 Å (0.3 nm) results in a measurable (and functionally important) change in membrane potential*. This motion of 0.001 degree corresponds to a 0.3 inch movement of the top of the Empire State Building.

How does the motion of the hair bundle create a change in membrane potential? The rapid response, within microseconds, suggests that the movement of the hair bundle acts on ion channels directly. An important observation is that adjacent stereocilia are linked by individual filaments called *tip links* (Figure 33.32).

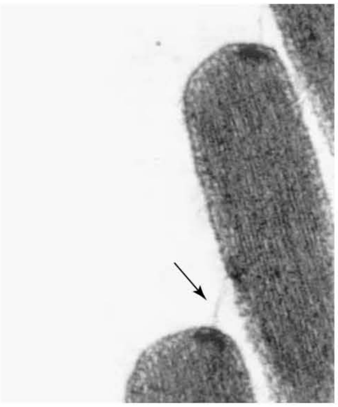

FIGURE 33.32 Electron micrograph of tip links. The tip link between two hair fibers is marked by an arrow. [Courtesy of Dr. A. Jacobs and Dr. A. J. Hudspeth.]

The presence of these tip links suggests a simple mechanical model for transduction by hair cells (Figure 33.33). The tip links are coupled to ion channels in the membranes of the stereocilia that are gated by mechanical stress. In the absence of a stimulus, approximately 15% of these channels are open. When the hair bundle is displaced toward its tallest part, the stereocilia slide across one another and the tension on the tip links increases, causing additional channels to open. The flow of ions through the newly opened channels depolarizes the membrane. Conversely, if the displacement is in the opposite direction, the tension on the tip links decreases, the open channels close, and the membrane hyperpolarizes. *Thus, the mechanical motion of the hair bundle is directly converted into current flow across the hair-cell membrane*.

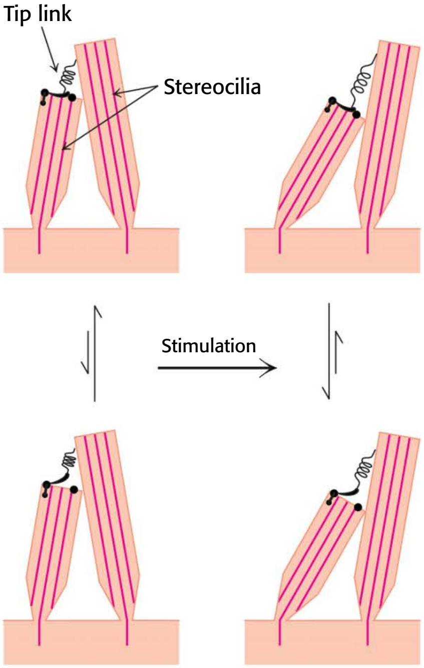

FIGURE 33.33 Model for hair-cell transduction. When the hair bundle is tipped toward the tallest part, the tip link pulls on an ion channel and opens it. Movement in the opposite direction relaxes the tension in the tip link, increasing the probability that any open channels will close. [Information from A. J. Hudspeth, *Nature* 341:397–404, 1989.]

Mechanosensory channels have been identified in *Drosophila* and vertebrates

The search for ion channels that respond to mechanical impulses has been pursued in a variety of organisms. *Drosophila* have sensory bristles used for detecting small air currents. These bristles respond to mechanical displacement in ways similar to those of hair cells; displacement of a bristle in one direction leads to substantial transmembrane current. Strains of mutant fruit flies that show uncoordinated motion and clumsiness have been examined for their electrophysiological responses to displacement of the sensory bristles. In one set of strains, transmembrane currents were dramatically reduced. The mutated gene in these strains was found to encode a protein of 1619 amino acids, called NompC for *no* *me*chanoreceptor *p*otential.

The carboxyl-terminal 469 amino acids of NompC resemble a class of ion-channel proteins called TRP (*t*ransient *r*eceptor *p*otential) channels. This region includes six putative transmembrane helices with a pore-like region between the fifth and the sixth helices. The amino-terminal 1150 amino acids consist almost exclusively of 29 *ankyrin repeats* (Figure 33.34).

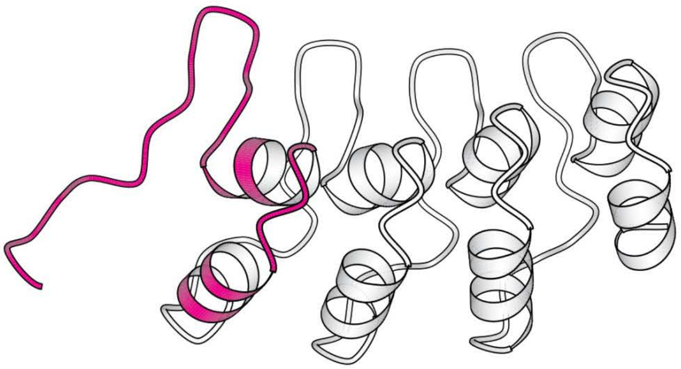

FIGURE 33.34 Ankyrin repeat structure. One ankyrin domain is shown in red in this series of four ankyrin repeats. *Notice* the hairpin loop followed by a helix-turn-helix motif in the red-colored ankyrin unit. Ankyrin domains interact with other proteins, primarily through their loops. [Drawn from 1AWC.pdb.]

Ankyrin repeats are structural motifs consisting of a hairpin loop followed by a helix-turn-helix. Importantly, in other proteins, regions with tandem arrays of these motifs mediate protein–protein interactions, suggesting that these arrays couple the motions of other proteins to the activity of the NompC channel.

A candidate for at least one component of the mechanosensory channel taking part in hearing has been identified. The protein, TRPA1, is a member of the TRP channel family. The sequence of TRPA1 also includes 17 ankyrin repeats. TRPA1 is expressed in hair cells, particularly near their tips. Further studies are under way to test and extend the exciting hypothesis that this protein is a component of the sought-after channel.

33.5 Touch Includes the Sensing of Pressure, Temperature, and Other Factors

Like taste, touch is a combination of sensory systems that are expressed in a common organ—in this case, the skin. The detection of pressure and the detection of temperature are two key components. Amiloride-sensitive Na^+ channels, homologous to those of taste, appear to play a role. Other systems are responsible for detecting painful stimuli such as high temperature, acid, or certain specific chemicals. Although our understanding of this sensory system is not as advanced as that of the others, recent work has revealed a fascinating relation between pain and taste sensation, a relation well known to anyone who has eaten "spicy" food.

Studies of capsaicin reveal a receptor for sensing high temperatures and other painful stimuli

Our sense of touch is intimately connected with the sensation of pain. Specialized neurons, termed *nociceptors,* transmit signals from skin to pain-processing centers in the spinal cord and brain in response to the onset of tissue damage. What is the molecular basis for the sensation of pain? An intriguing clue came from the realization that *capsaicin,* the chemical responsible for the "hot" taste of spicy food, activates nociceptors.

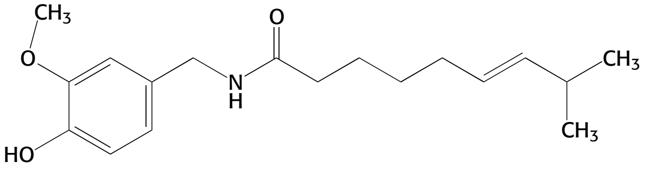

Capsaicin

Early research suggested that capsaicin would act by opening ion channels that are expressed in nociceptors. Thus, a cell that expresses the *capsaicin receptor* should take up calcium on treatment with the molecule. This insight led to the isolation of the capsaicin receptor with the use of cDNA from cells expressing this receptor. Such cells had been detected by their fluorescence when loaded with the calcium-sensitive compound Fura-2 and then treated with capsaicin or related molecules. Cells expressing the capsaicin receptor, which is called VR1 (for *v*anilloid *r*eceptor 1), respond to capsaicin below a concentration of 1 μM. The deduced 838-residue sequence of VR1 revealed it to be a member of the TRP channel family (Figure 33.35). The amino-terminal region of VR1 includes three ankyrin repeats.

C

FIGURE 33.35 The membrane topology deduced for VR1, the capsaicin receptor. The proposed site of the membrane pore is indicated in red, and the three ankyrin (A) repeats are shown in orange. The active receptor comprises four of these subunits. [Information from M. J. Caterina et al., *Nature* 389:816–824, 1997.]

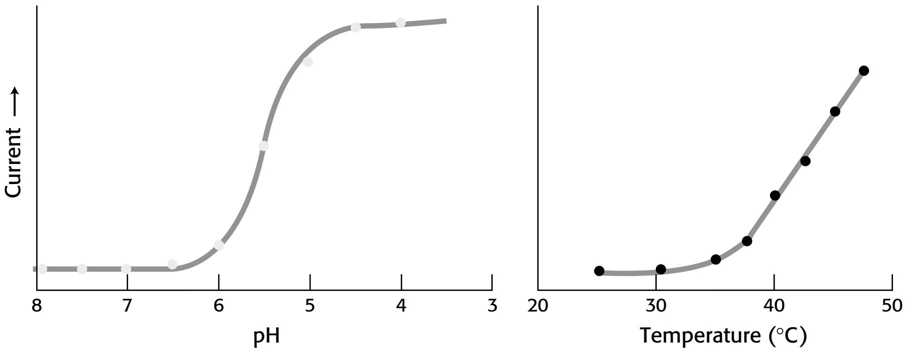

FIGURE 33.36 Response of the capsaicin receptor to pH and temperature. The ability of this receptor to respond to acid and to increased temperature helps detect potentially noxious situations. [Data from M. Tominaga et al., *Neuron* 21:531–543, 1998.]

Currents through VR1 are also induced by temperatures above 40°C and by exposure to dilute acid, with a midpoint for activation at pH 5.4 (Figure 33.36). Temperatures and acidity in these ranges are associated with infection and cell injury. The responses to capsaicin, temperature, and acidity are not independent. The response to heat is greater at lower pH, for example. Thus, *VR1 acts to integrate several noxious stimuli*. We feel these responses as pain and act to prevent the potentially destructive conditions that cause the unpleasant sensation. Studies of mice that do not express VR1 suggest that this is the case; such mice do not mind food containing high concentrations of capsaicin and are, indeed, less responsive than control mice to normally noxious heat. Plants such as chili peppers presumably gained the ability to synthesize capsaicin and other "hot" compounds to protect themselves from being consumed by mammals. Birds, which play the beneficial role of spreading pepper seeds into new territory, do not appear to respond to capsaicin.

Because of its ability to simulate VR1, capsaicin is used in pain management for arthritis, neuralgia, and other neuropathies. How can a compound that induces pain assist in its alleviation? Chronic exposure to capsaicin overstimulates pain-transmitting neurons, leading to their desensitization.

SUMMARY

Smell, taste, vision, hearing, and touch are based on signal-transduction pathways activated by signals from the environment. These sensory systems function similarly to the signal-transduction pathways for many hormones. These intercellular signaling pathways appear to have been appropriated and modified to process environmental information.

33.1 A Wide Variety of Organic Compounds Are Detected by Olfaction

The sense of smell, or olfaction, is remarkable in its specificity; it can, for example, discern stereoisomers of small organic compounds as distinct aromas. The 7TM receptors that detect these odorants operate in conjunction with $G_{(\text{olf})}$, a G protein that activates a cAMP cascade resulting in the opening of an ion channel and the generation of a nerve impulse. An outstanding feature of the olfactory system is its ability to detect a vast array of odorants. Each olfactory neuron expresses only one type of receptor and connects to a particular region of the olfactory bulb. Odors are decoded by a combinatorial mechanism: each odorant activates a number of receptors, each to a different extent, and most receptors are activated by more than one odorant.

33.2 Taste Is a Combination of Senses That Function by Different Mechanisms

We can detect only five tastes: bitter, sweet, salt, sour, and umami. The transduction pathways that detect taste are, however, diverse. Bitter, sweet, and umami tastants are experienced through 7TM receptors acting through a special G protein called gustducin. Salty and sour tastants act directly through membrane channels. Salty tastants are detected by passage though Na^+ channels, whereas sour taste results from the effects of hydrogen ions on a number of types of channels. The end point is the same in all cases—membrane polarization that results in the transmission of a nerve impulse.

33.3 Photoreceptor Molecules in the Eye Detect Visible Light

Vision is perhaps the best understood of the senses. Two classes of photoreceptor cells exist: cones, which respond to bright lights and colors, and rods, which respond only to dim light. The photoreceptor in rods is rhodopsin, a 7TM receptor that is a complex of the protein opsin and the chromophore 11-*cis*-retinal. The absorption of light by 11-*cis*-retinal changes its structure into that of all-*trans*-retinal, setting in motion a signal-transduction pathway that leads to the breakdown of cGMP, to membrane hyperpolarization, and to a subsequent nerve impulse. Color vision is mediated by three distinct 7TM photoreceptors that employ 11-*cis*-retinal as a chromophore and absorb light in the blue, green, and red parts of the spectrum.

33.4 Hearing Depends on the Speedy Detection of Mechanical Stimuli

The immediate receptors for hearing are found in the hair cells of the cochleae, which contain bundles of stereocilia. When the stereocilia move in response to sound waves, cation channels will open or close, depending on the direction of movement. The mechanical motion of the cilia is converted into current flow and then into a nerve impulse.

33.5 Touch Includes the Sensing of Pressure, Temperature, and Other Factors

Touch, detected by the skin, senses pressure, temperature, and pain. Specialized nerve cells called nociceptors transmit signals that are interpreted in the brain as pain. A receptor responsible for the perception of pain has been isolated on the basis of its ability to bind capsaicin, the molecule responsible for the hot taste of spicy food. The capsaicin receptor, also called VR1, functions as a cation channel that initiates a nerve impulse.

KEY TERMS

main olfactory epithelium (p. 962)
$G_{(\text{olf})}$ (p. 963)
odorant receptor (p. 963)
bitter (p. 966)
sweet (p. 966)
sour (p. 966)
salty (p. 966)
umami (p. 966)
gustducin (p. 967)
amiloride-sensitive Na^+ channel (p. 969)
rod (p. 970)
cone (p. 970)
rhodopsin (p. 970)
opsin (p. 970)
retinal (p. 970)
chromophore (p. 971)
transducin (p. 972)
cGMP phosphodiesterase (p. 972)
cGMP-gated ion channel (p. 972)
rhodopsin kinase (p. 972)
arrestin (p. 972)
guanylate cyclase (p. 973)
hair cell (p. 975)
stereocilia (p. 975)
tip link (p. 976)
nociceptor (p. 977)
capsaicin receptor (VR1) (p. 977)

PROBLEMS

1. *Olfaction in worms*. Unlike the olfactory neurons in the mammalian systems discussed herein, olfactory neurons in the nematode *C. elegans* express multiple olfactory receptors. In particular, one neuron (called AWA) expresses receptors for compounds to which the nematode is attracted, whereas a different neuron (called AWB) expresses receptors for compounds that the nematode avoids. Suppose that a transgenic nematode is generated such that one of the receptors for an attractant is expressed in AWB rather than AWA. What behavior would you expect in the presence of the corresponding attractant?

2. *Odorant matching*. A mixture of two of the compounds illustrated in Figure 33.6 is applied to a section of olfactory epithelium. Only receptors 3, 5, 9, 12, and 13 are activated, according to Figure 33.7. Identify the likely compounds in the mixture.

3. *Timing*. Compare the aspects of taste (bitter, sweet, salty, sour) in regard to their potential for rapid time resolution.

4. *Two ears*. Our ability to determine the direction from which a sound is coming is partly based on the difference in time at which our two ears detect the sound. Given the speed of sound (350 m s^{-1}) and the separation between our ears (0.15 m), what difference is expected in the times at which a sound arrives at our two ears? How does this difference compare with the time resolution of the human hearing system? Would a sensory system that utilized 7TM receptors and G proteins be capable of adequate time resolution?

5. *It's better to be bitter*. Some nontoxic plants taste very bitter to us. Suggest one or more explanations.

6. *Of mice and men*. In human beings, the umami taste is triggered only by glutamate and aspartate. In contrast, mice respond to many more amino acids. Design an experiment to test which of the subunits (T1R1 or T1R3) determines the specificity of this response. Assume that all desired mouse strains can be readily produced.

7. *It's not easy being green*. Would you expect light with wavelength 530 nm to be absorbed only by the "green" photoreceptor?

8. *Color discrimination*. Some women who have had male children who display color blindness have been demonstrated to distinguish between colors that are not readily distinguished by other people. Propose an explanation.

9. *Combinatorial power*. How many different odorants could a person distinguish if each odorant is bound by a single type of receptor and each receptor binds only a single odorant? How many if each odorant binds to two different odorant receptors? Three odorant receptors?

10. *Light action*. Describe the effect of light absorption on 11-*cis*-retinal bound within rhodopsin.

11. *Mirror, mirror*. Compounds A and B typically evoke different odors, with compound A described as smelling like tropical fruit and compound B smelling oniony.

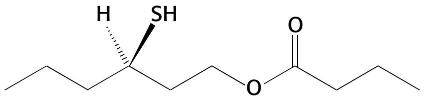

A

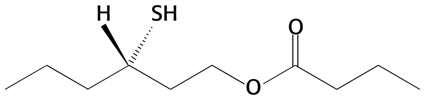

B

Explain how two such similar compounds can smell so different.

12. *Channeling*. Provide an example of an ion channel in vision, taste, and hearing.

Chapter Integration Problem

13. *Energy and information*. The transmission of sensory information requires the input of free energy. For each sensory system (olfaction, gustation, vision, hearing, and touch), identify mechanisms for the input of free energy that allow the transmission of sensory information.

Mechanism Problem

14. *Schiff-base formation*. Propose a mechanism for the reaction between opsin and 11-*cis*-retinal.

CHAPTER

34

The Immune System

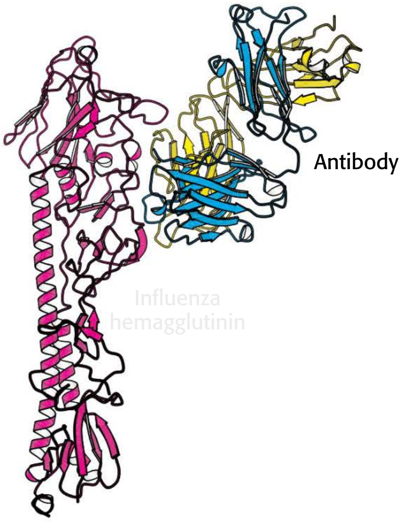

Just as medieval fortresses, such as the Dover Castle, used walls and fortifications to defend their territory, the immune system constantly battles against foreign invaders such as viruses, bacteria, and parasites to defend the organism. Antibody molecules provide a key element in the immune system's defensive arsenal. For example, specific antibodies can bind to molecules on the surfaces of viruses and prevent the viruses from infecting cells. Above right, an antibody binds to one subunit on hemagglutinin from the surface of influenza virus. [Skyscan Photolibrary/Alamy.]

We are constantly exposed to an incredible diversity of bacteria, viruses, and parasites, many of which would flourish in our cells or extracellular fluids were it not for our immune system. How does the immune system protect us? The human body has two lines of defense: an *innate immune system* that responds rapidly to features present in many pathogens, and an *adaptive immune system* that responds to specific features present only in a given pathogen. *Both the innate and the adaptive immune systems first identify features on disease-causing organisms and then work to eliminate or neutralize those organisms.* While a thorough description of the immune system is certainly beyond the scope of this book, this chapter will focus on how biochemical concepts such as protein structure, receptor-ligand interactions, and signal transduction are applied to the identification of pathogens.

The immune system must meet two tremendous challenges in the identification of pathogens: (1) to produce a system of receptors diverse enough to recognize a wide array of potential pathogens and (2) to distinguish invaders and their disease-causing products from the organism's own products (i.e., self- versus nonself-recognition). To meet these challenges, the innate immune system evolved the ability to recognize structural elements,

OUTLINE

34.1 Antibodies Possess Distinct Antigen-Binding and Effector Units

34.2 Antibodies Bind Specific Molecules Through Hypervariable Loops

34.3 Diversity Is Generated by Gene Rearrangements

34.4 Major-Histocompatibility-Complex Proteins Present Peptide Antigens on Cell Surfaces for Recognition by T-Cell Receptors

34.5 The Immune System Contributes to the Prevention and the Development of Human Diseases

such as specific glycolipids or forms of nucleic acid, that are well conserved in pathogens but absent in the host organism. The repertoire of such elements is limited, however, and so some pathogens have strategies to escape detection. The adaptive immune system has the remarkable ability to produce more than 10^8 distinct proteins, called antibodies, that can recognize different foreign molecules, and more than 10^{12} receptors on immune cells, called T-cell receptors (TCRs), each of which presents a different surface with the potential to specifically bind a structure from a foreign organism. In producing this vast range of defensive molecules, however, the adaptive immune system has the potential to create antibodies and T-cells that recognize and attack cells or molecules normally present in our bodies—a situation that can result in autoimmune diseases.

This chapter will examine these challenges, focusing first on the structures of proteins that recognize foreign organisms and then on the mechanisms for protecting us from a specific pathogen once it has been recognized. The chapter will closely examine the modular construction of the proteins of the immune system—identifying structural motifs and considering how spectacular diversity can arise from modular construction.

Innate immunity is an evolutionarily ancient defense system

Innate immunity is an evolutionarily ancient defense system found, at least in some form, in all multicellular plants and animals. The innate immune system represents the first line of defense against foreign pathogens, relying on common features of invading organisms to identify and eliminate these threats. Components of the innate immune system include the epithelial lining that surrounds host cells and the specialized cells, called *phagocytes*, that can ingest and destroy pathogens without the aid of the adaptive immune system.

The innate immune system also includes a family of receptors that can recognize specific features present in most pathogens and yet not respond to materials normally present in the host. The best-understood of these receptors are the *Toll-like receptors* (TLRs). The name "toll-like" is derived from a receptor known as Toll encoded in the *Drosophila* genome; Toll was first identified in a screen for genes important for *Drosophila* development and was subsequently shown to play a key role in the innate immune system. The TLRs have a common structure (Figure 34.1). Each receptor consists of a large extracellular domain built primarily from repeated amino acid sequences termed leucine-rich repeats (LRRs). Each LRR typically contains 20–30 residues, including 6 that are usually leucine. The human TLRs have from 18 to 27 LRR repeats that are capped by a cysteine-rich domain and followed by a sequence forming a single transmembrane helix and an intracellular signaling domain. This signaling domain is not a protein kinase but acts as a docking site for other proteins. Most TLRs are expressed in the cell membrane for the detection of extracellular pathogens such as fungi and bacteria. Other TLRs are located in the membranes of internal compartments for the detection of intracellular pathogens such as viruses and some bacteria.

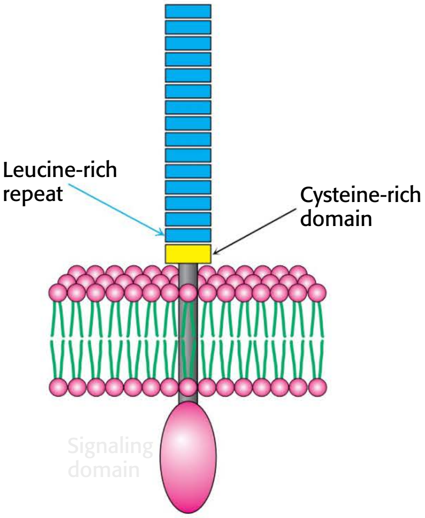

FIGURE 34.1 Toll-like receptor. Each receptor is made up of a set of 18 or more leucine-rich repeat sequences, followed by a cysteine-rich domain, a single transmembrane helix, and an intracellular domain that functions in signal transduction.

Each TLR targets a specific molecular characteristic, often called a *pathogen-associated molecular pattern* (PAMP), found primarily on invading organisms (Table 34.1). Typically, a PAMP is a critical component of the pathogen's function: mutations in these targets cannot easily block recognition by the TLR without compromising the activity of the pathogen. One particularly important PAMP is lipopolysaccharide (LPS), also referred to as *endotoxin*, a specific class of glycolipid found in the cell walls of Gram-negative bacteria such as *E. coli*. LPS is recognized by TLR4. The response

TABLE 34.1 Pathogen-associated molecular patterns (PAMPs) recognized by human TLRs

Receptor	PAMP	Source of PAMP
TLR1 (with TLR2)	Triacyl lipoprotein	Bacteria
TLR2	Lipoprotein	Bacteria, viruses, parasites
TLR3	Double-stranded RNA (dsRNA)	Viruses
TLR4	Lipopolysaccharide (LPS)	Bacteria, viruses
TLR5	Flagellin	Bacteria
TLR6 (with TLR2)	Diacyl lipoprotein	Bacteria, viruses
TLR7	Single-stranded RNA (ssRNA)	Viruses, bacteria
TLR8	Single-stranded RNA (ssRNA)	Viruses, bacteria
TLR9	CpG-DNA motifs	Viruses, bacteria, protozoa
TLR10	Unknown	Unknown

Data from: O. Takeuchi and S. Akira, *Cell* 140:805–820, 2010.

of the innate immune system to LPS can be easily demonstrated. Injection of less than 1 mg of LPS into a human being produces a fever and other signs of inflammation even though no living organisms are introduced.

How do TLRs recognize PAMPs? The extracellular domain from human TLR3 has a remarkable structure that is representative of many other TLRs (Figure 34.2). Each LRR contributes a single β strand to a large parallel β sheet that lines the inside of a concave, hooklike structure. In most cases, the PAMP is recognized by the surface formed between two receptors. The PAMP for TLR3, double-stranded RNA, fits in the groove between two monomers, colored blue and yellow in Figure 34.3. Ligand-induced dimerization of the receptor enables the initiation of a signaling cascade within the cell. We encountered similar examples of signal transduction across a membrane through receptor dimerization in Chapter 14.

Because the TLRs and other components of the innate immune system are always expressed, they provide the host organism with a rapid response to resist attack by pathogens. However, a number of pathogens have evolved the ability to escape detection by the innate immune system. For protection against such pathogens, the host relies on the adaptive immune system, which is able to target specific pathogens, even those that it has never encountered in the course of evolution.

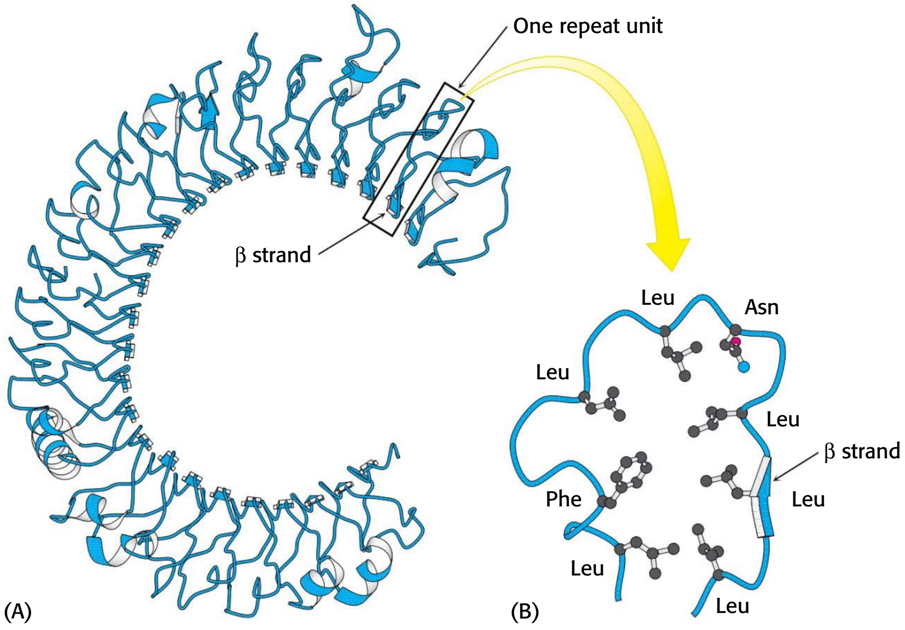

FIGURE 34.2 Extracellular domain of the Toll-like receptor. (A) The structure of the leucine-rich repeat (LRR) domain from human TLR3. *Notice* that the LRR units come together to form a central parallel β sheet that curls to form a concave structure. (B) The structure of a single LRR showing the positions of the residues that are generally approximately conserved. *Notice* that the leucine residues come together to form a hydrophobic core with the single β strand on one side. [Drawn from 1ZIW.pdb].

The adaptive immune system responds by using the principles of evolution

The adaptive immune system comprises two parallel but interrelated systems: humoral and cellular immune responses. In the *humoral immune response,* soluble proteins called *antibodies (immunoglobulins)* function as recognition elements that bind to foreign molecules and serve as markers signaling foreign invasion. Antibodies are secreted by *plasma cells,* which are derived from *B lymphocytes (B cells)* (Figure 34.4). A foreign macromolecule that binds selectively to an antibody is called an *antigen.* In a physiological context, if the binding of the foreign molecule stimulates an immune response, that molecule is called an *immunogen*. The specific affinity of an antibody is not for the entire macromolecular antigen but for a particular site on the antigen called the *epitope* or *antigenic determinant.* Each B cell produces just one type of antibody that can recognize a single epitope.

In the *cellular immune response*, cells called *cytotoxic T lymphocytes* (also commonly called *killer T cells*) destroy cells that have been invaded by a pathogen. Because intracellular pathogens do not leave markings on the exteriors of infected cells, vertebrates have evolved a mechanism to mark the exterior of cells with a sample of the interior contents, both self and foreign. Some of the internal proteins are broken into peptides, which are then bound to a complex of integral membrane proteins encoded by the *major histocompatibility complex* (MHC). T cells continually scan the bound peptides to find and kill cells that display foreign motifs on their surfaces. Another class of T cells called *helper T lymphocytes (helper T cells)* contributes to both the humoral and the cellular immune responses by stimulating the differentiation and proliferation of appropriate B cells and cytotoxic T cells. The cellular immune response is mediated by specific receptors that are expressed on the surfaces of the T cells.

The remarkable ability of the immune system to adapt to an essentially limitless set of potential pathogens requires a powerful system for transforming the immune cells and molecules in response to the presence of pathogens. *This adaptive system operates through the principles of evolution, including reproduction with variation followed by selection of the most well suited members of a population.*

If the human genome contains, by the latest estimates, only 21,000 genes, how can the immune system generate more than 10^8 different antibody proteins and 10^{12} T-cell receptors? The answer is found in a novel mechanism for generating a highly diverse set of genes from a limited set of genetic building blocks. Linking different sets of DNA regions in a combinatorial manner produces many distinct protein-encoding genes that are not present in the genome. A rigorous selection process then leaves for proliferation only cells that synthesize proteins determined to be useful in the immune response. The subsequent reproduction of these cells without additional recombination enriches the cell population with members expressing particular protein species.

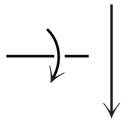

FIGURE 34.3 Recognition of a PAMP by a Toll-like receptor. The structure of TLR3 bound to its PAMP, a fragment of double-stranded RNA, as seen from the side (top) and from above (bottom). *Notice* that the PAMP induces receptor dimerization by binding the surfaces on the side of each of the extracellular domains. [Drawn from 3CIY.pdb].

FIGURE 34.4 Immunoglobulin production. An electron micrograph of a plasma cell shows the highly developed rough endoplasmic reticulum necessary for antibody secretion. [Courtesy of Lynne Mercer.]

Critical to the development of the immune response is the selection process, which determines which immune cells will reproduce. The process comprises several stages. In the early stages of immune cell development, cells expressing molecules that bind tightly to self-molecules are destroyed or silenced, whereas cells expressing molecules that do not bind strongly to self-molecules and that have the potential for binding strongly to foreign molecules are preserved. The appearance of an immunogenic invader at a later time will stimulate the reproduction of cells expressing antibodies or T-cell receptors that bind specifically to elements of that pathogen—in evolutionary terms, such cells are positively selected. Thus, the immune response is based on the selection of cells expressing molecules that are specifically effective against a particular invader; the response evolves from a population with wide-ranging specificities to a more-focused collection of cells and molecules that are well suited to defend the host when confronted with that particular challenge.

Not only are antibodies and T-cell receptors a result of genetic diversity and recombination, but antibodies have highly diverse structures as well. Antibodies require many different structural solutions for binding many different antigens, each of which has a different form. T-cell receptors, in contrast, are not structurally diverse, because they have coevolved with the MHC. The docking mode of a T-cell receptor to the peptide bound to MHC is similar for all structures. As a consequence of this coevolution, every T-cell receptor has an inherent reactivity with every MHC. The coevolution ensures that all T-cell receptors can scan all peptide–MHC complexes on all tissues. The genetic diversity of the 10^{12} different T-cell receptors is concentrated in a highly diverse set of residues in the center of the MHC groove. This localized diversity allows the T-cell receptor to recognize the many different foreign peptides bound to the MHC. T-cell receptors must survey many different MHC–peptide complexes with rapid turnover. Therefore, the binding affinities between T-cell receptors and the MHC are weaker than those between antibody and antigen.

34.1 Antibodies Possess Distinct Antigen-Binding and Effector Units

Antibodies are central molecular players in the immune response. In Chapter 3, we discussed the application of antibodies as tools to study proteins; let us now consider the native structures and functions of these remarkable molecules. In 1959, Rodney Porter showed that *immunoglobulin G* (IgG), the major antibody in serum, can be cleaved into three 50-kDa fragments by the limited proteolytic action of papain. Two of these fragments bind antigen. They are called F_{ab} (*F* stands for *f*ragment, *ab* for *a*ntigen *b*inding). The other fragment, called F_c because it crystallizes readily, does not bind antigen, but it has other important biological activities, including the mediation of responses termed *effector functions*. These functions include the initiation of the *complement cascade,* a process that leads to the lysis of target cells. Although such effector functions are crucial to the functioning of the immune system, they will not be considered further here.

How do these fragments relate to the three-dimensional structure of whole IgG molecules? Immunoglobulin G consists of two kinds of polypeptide chains, a 25-kDa *light* (L) *chain* and a 50-kDa *heavy* (H) *chain*

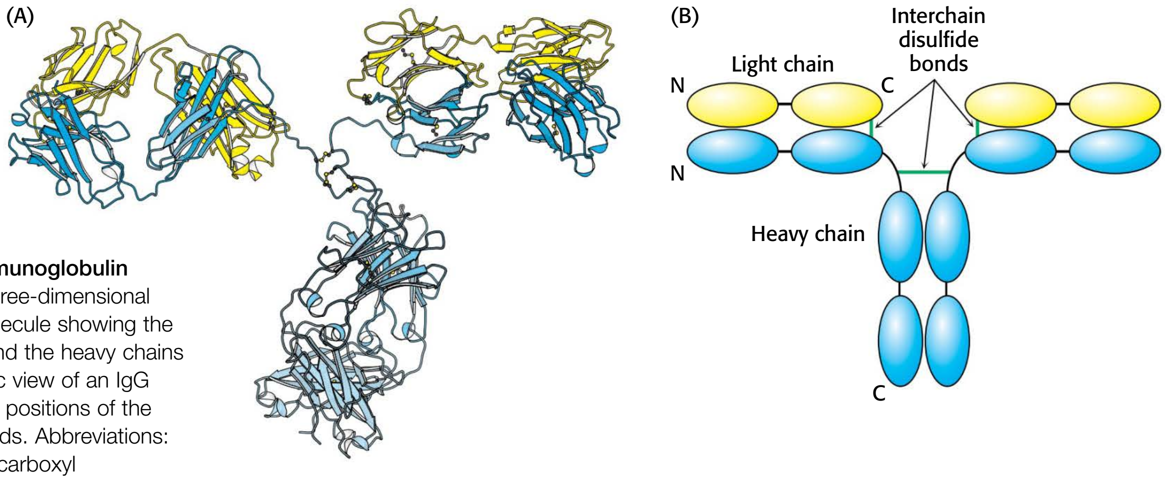

FIGURE 34.5 Immunoglobulin G structure. (A) The three-dimensional structure of an IgG molecule showing the light chains in yellow and the heavy chains in blue. (B) A schematic view of an IgG molecule indicating the positions of the interchain disulfide bonds. Abbreviations: N, amino terminus; C, carboxyl terminus. [Drawn from 1IGT.pdb.]

(Figure 34.5). The subunit composition is L_2H_2. Each L chain is linked to an H chain by a disulfide bond, and the H chains are linked to each other by at least one disulfide bond. Examination of the amino acid sequences and three-dimensional structures of IgG molecules reveals that each L chain comprises two homologous domains, termed *immunoglobulin domains,* to be described in detail in Section 34.2. Each H chain has four immunoglobulin domains. Overall, the molecule adopts a conformation that resembles the letter Y. The stem of this Y, corresponding to the F_c fragment obtained by cleavage with papain, consists of the two carboxyl-terminal immunoglobulin domains of each H chain. The two arms of the Y, corresponding to the two F_{ab} fragments, are formed by the two amino-terminal domains of each H chain and the two domains of each L chain. The linkers between the stem and the two arms consist of extended polypeptide regions within the H chains and are quite flexible.

Papain cleaves the H chains on the carboxyl-terminal side of the disulfide bond that links each L and H chain (Figure 34.6). Thus, each F_{ab} consists of an entire L chain and the amino-terminal half of an H chain, whereas F_c consists of the carboxyl-terminal halves of both H chains. Each F_{ab} contains a single antigen-binding site. Because an intact IgG molecule contains two F_{ab} components and therefore has two binding sites, it can cross-link multiple antigens (Figure 34.7). Furthermore, the F_c and the two F_{ab} units of the intact IgG are joined by flexible polypeptide regions that allow

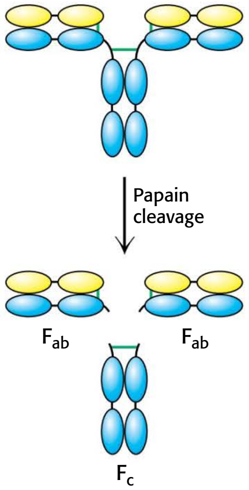

FIGURE 34.6 Immunoglobulin G cleavage. Treatment of intact IgG molecules with the protease papain results in the formation of three large fragments: two F_{ab} fragments that retain antigen-binding capability and one F_c fragment that does not.

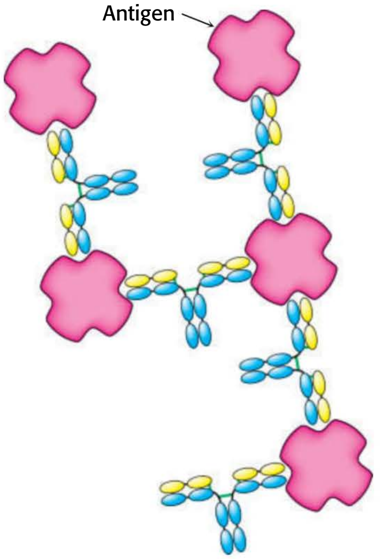

FIGURE 34.7 Antigen cross-linking. Because IgG molecules include two antigen-binding sites, antibodies can cross-link multivalent antigens such as viral surfaces.

TABLE 34.2 Properties of immunoglobulin classes

Class	Serum concentration (mg ml^{-1})	Mass (kDa)	Light chains	Heavy chains	Chain structure
IgG	12	150	κ or λ	γ	$\kappa_2\gamma_2$ or $\lambda_2\gamma_2$
IgA	3	180–500	κ or λ	α	$(\kappa_2\alpha_2)_n$ or $(\lambda_2\alpha_2)_n$
IgM	1	950	κ or λ	μ	$(\kappa_2\mu_2)_5$ or $(\lambda_2\mu_2)_5$
IgD	0.1	175	κ or λ	δ	$\kappa_2\delta_2$ or $\lambda_2\delta_2$
IgE	0.001	200	κ or λ	ε	$\kappa_2\varepsilon_2$ or $\lambda_2\varepsilon_2$

Note: $n = 1, 2,$ or 3. IgM and oligomers of IgA also contain J chains that connect immunoglobulin molecules. IgA in secretions has an additional component.

facile variation in the angle between the F_{ab} units through a wide range (Figure 34.8). This kind of mobility, called *segmental flexibility,* can enhance the formation of an antibody–antigen complex by enabling both recognition sites on an antibody to bind an antigen that possesses multiple binding sites, such as a viral coat composed of repeating identical monomers. The sites at the tips of the F_{ab} units simply move to match the distance between specific determinants on the antigen.

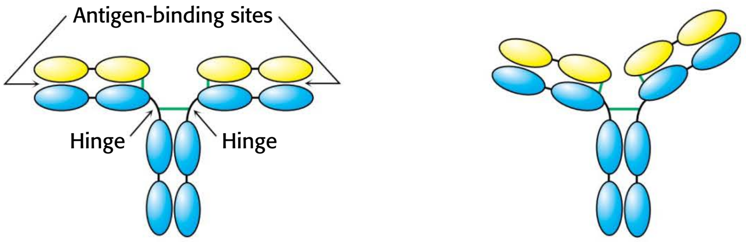

FIGURE 34.8 Segmental flexibility. The linkages between the F_{ab} and the F_c regions of an IgG molecule are flexible, allowing the two antigen-binding sites to adopt a range of orientations with respect to each other. This flexibility allows effective interactions with a multivalent antigen without requiring that the epitopes on the target be a precise distance apart.

Immunoglobulin G is the antibody present in highest concentration in the serum, but other classes of immunoglobulin also are present (Table 34.2). Each class includes an L chain (either κ or λ) and a distinct H chain (Figure 34.9). The heavy chains in IgG are called γ chains, whereas those in immunoglobulins A, M, D, and E are called α, μ, δ, and ε, respectively. *Immunoglobulin M* (IgM) is the first class of antibody to appear in the serum after exposure to an antigen. The presence of 10 antigen recognition sites enables IgM to bind especially tightly to antigens containing multiple identical epitopes. The strength of an interaction comprising multiple independent binding interactions between partners is termed *avidity* rather than affinity, which denotes the binding strength of a single binding site.

Immunoglobulin A (IgA) is the major class of antibody in external secretions, such as saliva, tears, bronchial mucus, and intestinal mucus. Thus, IgA serves as a first line of defense against bacterial and viral antigens. The role of *immunoglobulin D* (IgD) has long been a mystery, but recent studies suggest IgD plays a role in the activation of basophils, white blood cells that have antiparasitic functions. *Immunoglobulin E* (IgE) is important in conferring

FIGURE 34.9 Classes of immunoglobulin. Each of five classes of immunoglobulin has the same light chain (shown in yellow) combined with a different heavy chain (γ, α, μ, δ, or ε). Disulfide bonds are indicated by green lines. The IgA dimer and the IgM pentamer have a small polypeptide chain in addition to the light and heavy chains.

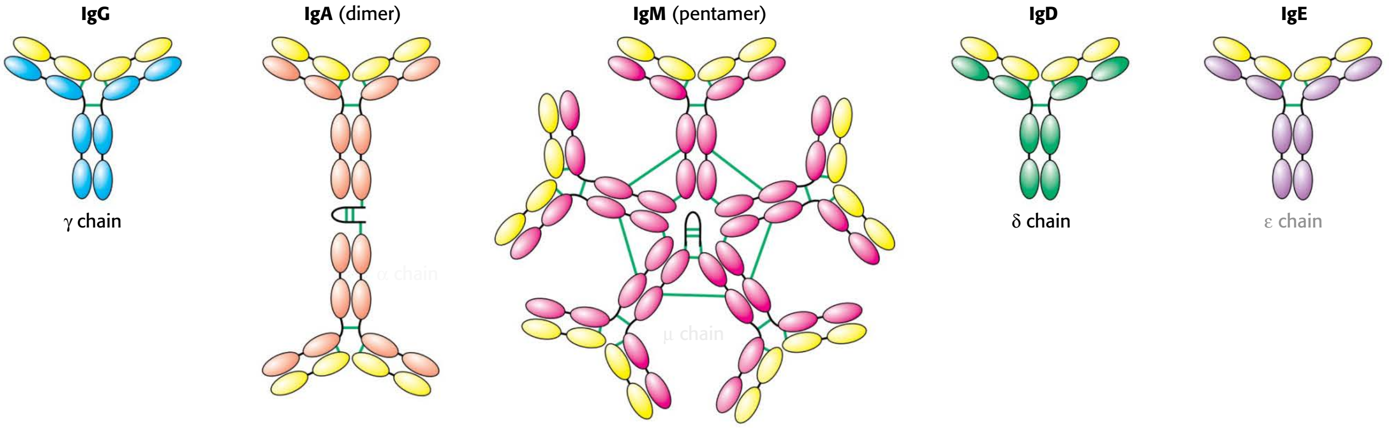

protection against parasites, but IgE also participates in allergic reactions. IgE–antigen complexes form cross-links with receptors on the surfaces of mast cells to trigger a cascade that leads to the release of granules containing pharmacologically active molecules. Histamine, one of the agents released, induces smooth-muscle contraction and stimulates the secretion of mucus.

34.2 Antibodies Bind Specific Molecules Through Hypervariable Loops

A comparison of the amino acid sequences of different IgG antibodies from human beings or mice shows that the carboxyl-terminal half of the L chains and the carboxyl-terminal three-quarters of the H chains are very similar in all of the antibodies. Importantly, the amino-terminal domain of each chain is more variable, including three stretches of approximately 7 to 12 amino acids within each chain that are hypervariable, as shown for the H chain in Figure 34.10. The amino-terminal immunoglobulin domain of each chain is thus referred to as the *variable region,* whereas the remaining immunoglobulin domains are much more similar in all antibodies and are referred to as *constant regions* (Figure 34.11).

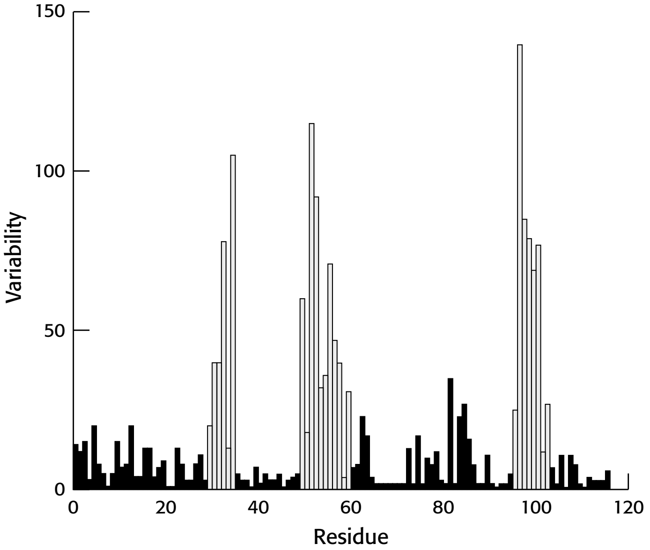

FIGURE 34.10 Immunoglobulin sequence diversity. A plot of sequence variability as a function of position along the sequence of the amino-terminal immunoglobulin domain of the H chain of human IgG molecules. Three regions (in red) show remarkably high levels of variability. These hypervariable regions correspond to three loops in the immunoglobulin domain structure. [Data from R. A. Goldsby, T. J. Kindt, and B. A. Osborne, *Kuby Immunology*, 4th ed. (W. H. Freeman and Company, 2000), p. 91.]

The immunoglobulin fold consists of a beta-sandwich framework with hypervariable loops

An IgG molecule consists of a total of 12 immunoglobulin domains. These domains have many sequence features in common and adopt a common structure, the *immunoglobulin fold* (Figure 34.12). Remarkably, this same structural domain is found in many other proteins that play key roles in both immune and nonimmune functions.

The immunoglobulin fold consists of a pair of β sheets, each built of antiparallel β strands, that surround a central hydrophobic core. A single disulfide bond bridges the two sheets. Two aspects of this structure are particularly important for its function. First, three loops present at one end of the structure form a potential binding surface. These loops contain the hypervariable sequences present in antibodies and in T-cell receptors. Variation of the amino acid sequences of these loops provides the major mechanism for the generation of the vastly diverse set of antibodies and T-cell receptors expressed by the immune system. These loops are referred to as *hypervariable loops* or *complementarity-determining regions* (CDRs). Second, the amino terminus and the carboxyl terminus are at opposite ends of the structure, which allows structural domains to be strung together to form chains, as in the L and H chains of antibodies. Such chains are present in several other key molecules in the immune system.

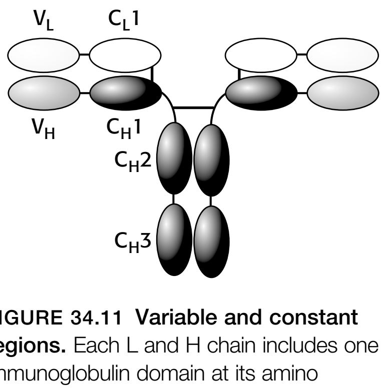

FIGURE 34.11 Variable and constant regions. Each L and H chain includes one immunoglobulin domain at its amino terminus that is quite variable from one antibody to another. These domains are referred to as V_L and V_H. The remaining domains are more constant from one antibody to another and are referred to as constant domains (C_L1, C_H1, C_H2, and C_H3).

The immunoglobulin fold is one of the most prevalent domains encoded by the human genome: more than 750 genes encode proteins with at least one immunoglobulin fold recognizable at the level of amino acid sequence. Such domains are also common in other multicellular animals such as flies and nematodes. However, from inspection of amino acid sequence alone, immunoglobulin-fold domains do not appear to be present in yeast or plants, although these organisms possess other structurally similar domains, including the key photosynthetic electron-transport protein plastocyanin in plants (Section 19.3). Thus, the immunoglobulin-fold family appears to have expanded greatly along evolutionary branches leading to animals—particularly, vertebrates.

X-ray analyses have revealed how antibodies bind antigens

For each class of antibody, the variable domains at the amino-terminal ends of the L and H chains (designated V_L and V_H) come together to form a binding surface. The positions of the CDRs are striking. These hypervariable sequences, present in three loops of each domain, come together so that all six loops form a single surface at the end of each arm (Figure 34.13). Because virtually any V_L can pair with any V_H, *a very large number of different binding sites can be constructed by their combinatorial association*.

The results of x-ray crystallographic studies of several hundred large and small antigens bound to F_{ab} molecules have been sources of much insight into the structural basis of antibody specificity. The binding of antigens to antibodies is governed by the same principles that govern the binding of substrates to enzymes. The interaction between complementary shapes results in numerous contacts between amino acids at the binding surfaces of both molecules. Many hydrogen bonds, electrostatic interactions, and van der Waals interactions, reinforced by hydrophobic interactions, combine to give specific and strong binding.

A few aspects of antibody binding merit specific attention, inasmuch as they relate directly to the structure of immunoglobulins. The binding site on the antibody incorporates some or all of the CDRs in the variable domains of the antibody. Small molecules are likely to make contact with fewer CDRs, with perhaps 15 residues of the antibody participating in the binding interaction. Macromolecules often make more extensive contact, sometimes interacting with all six CDRs and 20 or more residues of the antibody. Small molecules often bind in a cleft of the antigen-binding region. Macromolecules, such as globular proteins, tend to interact across larger, fairly flat apposed surfaces bearing complementary protrusions and depressions.

A well-studied case of small-molecule binding is seen in an example of phosphorylcholine bound to F_{ab}. Crystallographic analysis revealed phosphorylcholine bound to a cavity lined by residues from five CDRs—two from the L chain and three from the H chain (Figure 34.14). The positively charged trimethylammonium group of phosphorylcholine is buried inside the wedge-shaped cavity, where it interacts electrostatically with two negatively charged residues, a glutamate and an aspartate. The negatively charged phosphoryl group of phosphorylcholine binds to the positively charged guanidinium group of an arginine residue at the mouth of the crevice and is hydrogen bonded to the side chain of a nearby tyrosine residue.

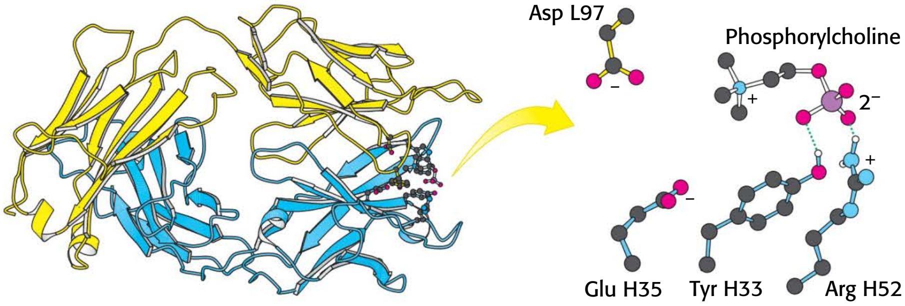

FIGURE 34.14 Binding of a small antigen. The structure of a complex between an F_{ab} fragment of an antibody (blue and yellow) and its target—in this case, phosphorylcholine. *Notice* that residues from the antibody interact with phosphorylcholine through hydrogen bonding and electrostatic interactions. [Drawn from 2MCP.pdb.]

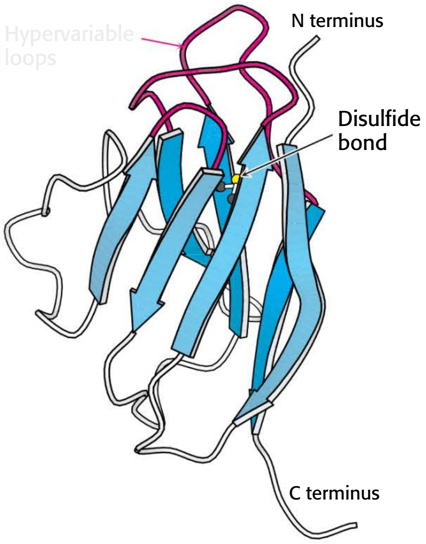

FIGURE 34.12 Immunoglobulin fold. An immunoglobulin domain consists of a pair of β sheets linked by a disulfide bond and hydrophobic interactions. *Notice* that three hypervariable loops lie at one end of the structure. [Drawn from 1DQJ.pdb.]

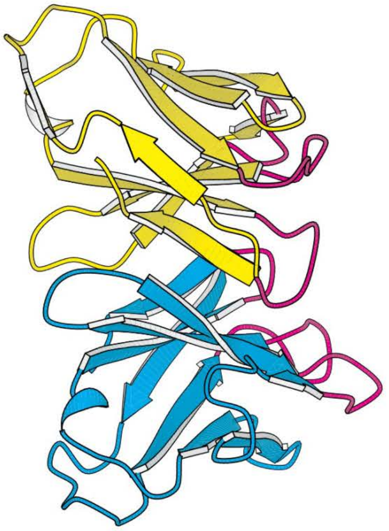

FIGURE 34.13 Variable domains. A side view of the variable domains of the L chain (yellow) and the H chain (blue); the complementarity-determining regions (CDRs) are shown in red. *Notice* that the six CDRs come together to form a binding surface. The specificity of the surface is determined by the sequences and structures of the CDRs. [Drawn from 1DQJ.pdb.]

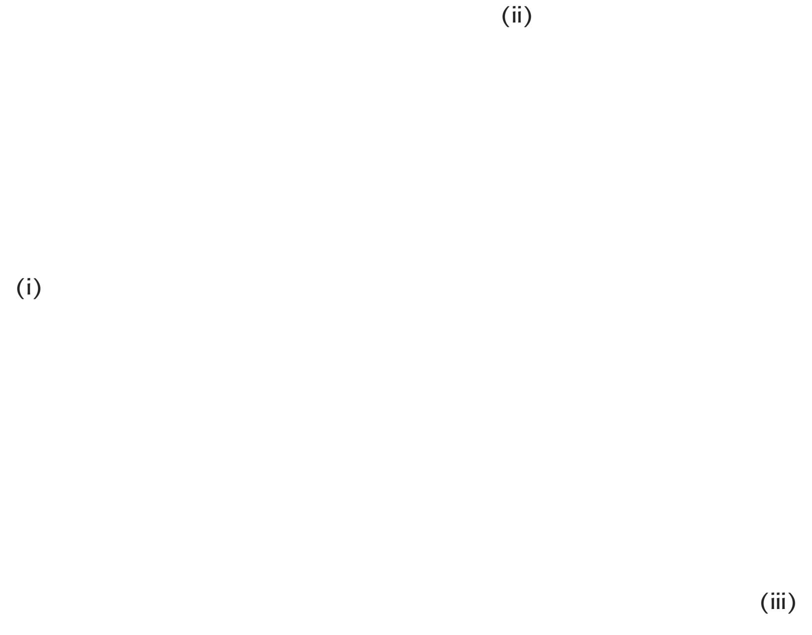

FIGURE 34.15 Antibodies against lysozyme. The structures of three complexes (i, ii, iii) between F_{ab} fragments (blue and yellow) and hen egg-white lysozyme (red) shown with lysozyme in the same orientation in each case. *Notice* that the three antibodies recognize completely different epitopes on the lysozyme molecule. [Drawn from 3HFL, 1DQJ, and 1FDL.pdb.]

Numerous van der Waals interactions, such as those made by a tryptophan side chain, also stabilize this complex.

Residues from five CDRs participate in the binding of phosphorylcholine to human F_{ab}. This binding does not significantly change the structure of the antibody, yet induced fit plays a role in the formation of many antibody–antigen complexes. A malleable binding site can accommodate many more kinds of ligands than can a rigid one. Thus, induced fit increases the repertoire of antibody specificities.

Large antigens bind antibodies with numerous interactions

How do large antigens interact with antibodies? A large collection of antibodies against hen egg-white lysozyme has been structurally characterized in great detail (Figure 34.15). Each different antibody binds to a distinct surface of lysozyme. Let us examine the interactions in one of these complexes (complex ii in Figure 34.15) in detail. This antibody binds two polypeptide segments of lysozyme that are widely separated in the primary structure (Figure 34.16).

All six CDRs of the antibody make contact with this epitope. The region of contact is quite extensive (about 30 × 20 Å). The apposed surfaces are rather flat. The only exception is the side chain of glutamine 121 of lysozyme, which penetrates deeply into the antibody's binding site, where it forms a hydrogen bond with a main-chain carbonyl oxygen atom and is surrounded by three aromatic side chains. The formation of 12 hydrogen bonds and numerous van der Waals interactions contributes to the high affinity ($K_d = 20$ nM) of this antibody–antigen interaction. Examination of the F_{ab} molecule without bound protein reveals that the structures of the V_L and V_H domains change little on binding, although they slide 1 Å apart to allow more intimate contact with lysozyme.

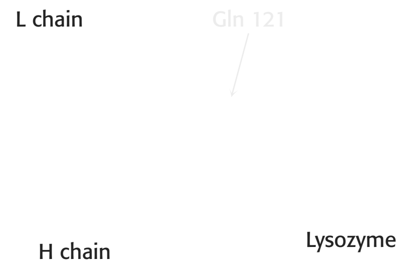

FIGURE 34.16 Antibody–protein interactions. *Notice* that a single residue of lysozyme, glutamine 121, penetrates more deeply into the antibody binding site. [Drawn from 1FDL.pdb.]

34.3 Diversity Is Generated by Gene Rearrangements

A mammal such as a mouse or a human being can synthesize large amounts of specific antibody against virtually any foreign determinant within a matter of days after exposure. We have seen that antibody specificity is determined by the amino acid sequences of the variable regions of both light and heavy chains, which brings us to the key question: How are different variable-region sequences generated?

The discovery of distinct variable and constant regions in the L and H chains raised the possibility that the genes that encode immunoglobulins have an unusual architecture that facilitates the generation of a diverse set of polypeptide products. In 1965, William Dreyer and Claude Bennett proposed that multiple *V (variable) genes* are separate from a single *C (constant) gene* in embryonic (germ-line) DNA. According to their model, one of these V genes becomes joined to the C gene in the course of differentiation of the antibody-producing cell. A critical test of this novel hypothesis had to await the isolation of pure immunoglobulin mRNA and the development of techniques for analyzing mammalian genomes. Twenty years later, Susumu Tonegawa found that V and C genes are indeed far apart in embryonic DNA but are closely associated in the DNA of antibody-producing cells. Thus, immunoglobulin genes are rearranged in the differentiation of lymphocytes.

J (joining) genes and D (diversity) genes increase antibody diversity

Sequencing studies carried out by Susumu Tonegawa, Philip Leder, and Leroy Hood revealed that V genes in embryonic cells do not encode the entire variable region of L and H chains. Consider, for example, the region that encodes the κ light-chain family. A tandem array of 40 segments, each of which encodes approximately the first 97 residues of the variable domain of the L chain, is present on human chromosome 2 (Figure 34.17).

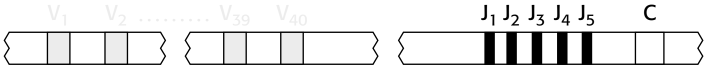

FIGURE 34.17 The κ light-chain locus. This part of human chromosome 2 includes an array of 40 segments that encode the variable (V) region (approximately residues 1–97) of the light chain, an array of 5 segments that encode the joining (J) region (residues 98–110), and a single region that encodes the constant (C) region.

However, the variable region of the L chain contains 110 residues. Where is the DNA that encodes the last 13 residues of the variable domain? For L chains in undifferentiated cells, this stretch of DNA is located in an unexpected place: near the C gene. It is called the *J gene* because it *j*oins the V and C gene segments in a differentiated cell. In fact, a tandem array of five J gene segments is located near the C gene in embryonic cells. In the differentiation of an antibody-producing cell, a V gene segment is joined to a J gene segment to form a complete gene for the variable region (Figure 34.18). RNA splicing (Section 29.3) generates an mRNA molecule for the complete

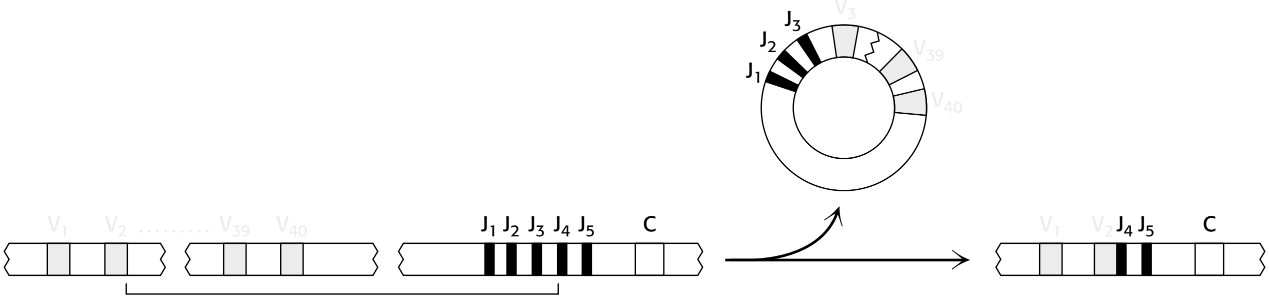

FIGURE 34.18 VJ recombination. A single V gene (in this case, V_2) is linked to a J gene (here, J_4) to form an intact VJ region. The intervening DNA is released in a circular form. Because the V and J regions are selected at random and the joint between them is not always in exactly the same place, many VJ combinations can be generated by this process.

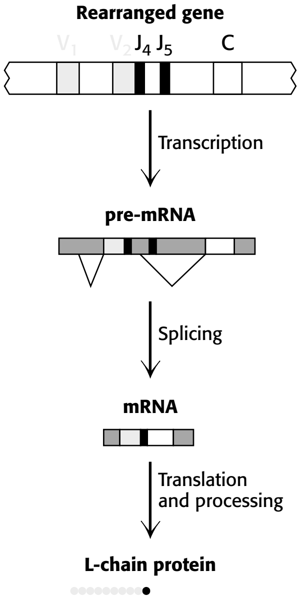

FIGURE 34.19 Light-chain expression. The light-chain protein is expressed by the transcription of the rearranged gene to produce a pre-RNA molecule with the VJ and C regions separated. RNA splicing removes the intervening sequences to produce an mRNA molecule with the VJ and C regions linked. Translation of the mRNA and processing of the initial protein product produce the light chain.

L chain by linking the coding regions for the rearranged VJ unit with that for the C unit (Figure 34.19).

J gene segments are important contributors to antibody diversity because they encode part of the last hypervariable segment (CDR3). In forming a continuous variable-region gene, any of the 40 V gene segments can become linked to any of 5 J gene segments. Thus, somatic recombination of these gene segments amplifies the diversity already present in the germ line. The linkage between V and J is not precisely controlled. Recombination between these genes can take place at one of several bases near the codon for residue 95, generating additional diversity. A similar array of V and J gene segments encoding the λ light chain is present on human chromosome 22. This region includes 30 Vλ gene segments and four Jλ gene segments. In addition, this region includes four distinct C genes, in contrast with the single C gene in the κ locus.

In humans, the genes encoding the heavy chain are present on chromosome 14. Remarkably, the variable domain of heavy chains is assembled from *three* rather than two segments. In addition to V_H gene segments that encode residues 1 through 94 and J_H gene segments that encode residues 98 through 113, this chromosomal region includes a distinct set of segments that encode residues 95 through 97 (Figure 34.20). These gene segments are called D (for *d*iversity). Some 27 D gene segments lie between 51 V_H and 6 J_H gene segments. The recombination process first joins a D gene segment to a J_H gene segment; a V_H gene segment is then joined to DJ_H. A greater variety of antigen-binding patches and clefts can be formed by the H chain than by the L chain because the H chain is encoded by three rather than two gene segments. Moreover, CDR3 of the H chain is diversified by the action of terminal deoxyribonucleotidyl transferase, a special DNA polymerase that requires no template. This enzyme inserts extra nucleotides between V_H and D. The *V(D)J recombination* of both the L and the H chains is executed by specific enzymes present in immune cells. These proteins, called *RAG-1* and *RAG-2*, recognize specific DNA sequences called *recombination signal sequences* (RSSs) adjacent to the V, D, and J gene segments and facilitate the cleavage and religation of the DNA segments.

More than 10^8 antibodies can be formed by combinatorial association and somatic mutation

Let us recapitulate the sources of antibody diversity. The germ line contains a rather large repertoire of variable-region genes. For κ light chains, there are about 40 V-segment genes and 5 J-segment genes. Hence, a total of 40 × 5 = 200 kinds of complete V_κ genes can be formed by the combinations of V and J. A similar analysis suggests that at least 120 different λ light chains can be generated. A larger number of heavy-chain genes can be formed because of the role of the D segments. For 51 V, 27 D, and 6 J gene segments, the number of complete V_H genes that can be formed is 8262. The association of 320 kinds of L chains with 8262 kinds of H chains would yield 2.6×10^6

FIGURE 34.20 V(D)J recombination. The heavy-chain locus includes an array of 51 V segments, 27 D segments, and 6 J segments. Gene rearrangement begins with D–J joining, followed by further rearrangement to link the V segment to the DJ segment.

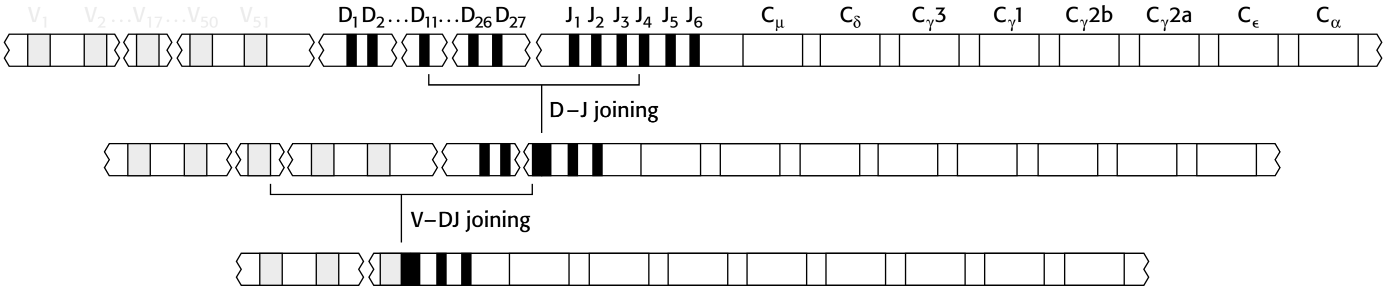

different antibodies. Variability in the exact points of segment joining and other mechanisms increases this value by at least two orders of magnitude.

Even more diversity is introduced into antibody chains by *somatic mutation*—that is, by the introduction of mutations into the recombined genes. In fact, a 1000-fold increase in binding affinity is seen in the course of a typical humoral immune response, arising from somatic mutation, a process called *affinity maturation*. The generation of an expanded repertoire leads to the selection of antibodies that more precisely fit the antigen. Thus, nature draws on each of three sources of diversity—a germ-line repertoire, somatic recombination, and somatic mutation—to form the rich variety of antibodies that protect an organism from foreign incursions.

The oligomerization of antibodies expressed on the surfaces of immature B cells triggers antibody secretion

The processes heretofore described generate a highly diverse set of antibody molecules—a key first step in the generation of an immune response. The next stage is the selection of a particular set of antibodies directed against a specific invader. How is this selection accomplished? Each immature B cell, produced in the bone marrow, expresses a specific monomeric form of IgM attached to its surface (Figure 34.21). Each cell expresses approximately 10^5 IgM molecules, but *all of these molecules are identical in amino acid sequence and, hence, in antigen-binding specificity*. Thus, the selection of a particular immature B cell for growth will lead to the amplification of an antibody with a unique specificity. The selection process begins with the binding of an antigen to the membrane-bound antibody.

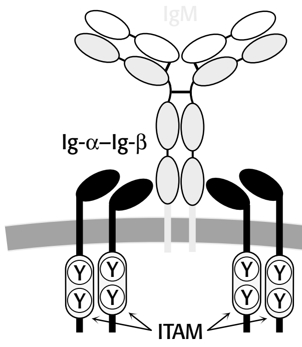

FIGURE 34.21 B-cell receptor. This complex consists of a membrane-bound IgM molecule noncovalently bound to two Ig-α–Ig-β heterodimers. The intracellular domains of each of the Ig-α and Ig-β chains include an immunoreceptor tyrosine-based activation motif (ITAM).

Associated with each membrane-linked IgM molecule are two molecules of a heterodimeric membrane protein called Ig-α–Ig-β (Figure 34.21). Examination of the amino acid sequences of Ig-α and Ig-β is highly instructive. The amino terminus of each protein lies outside the cell and corresponds to a single immunoglobulin fold, and the carboxyl terminus, which lies inside the cell, includes a sequence of 18 amino acids called an *immunoreceptor tyrosine-based activation motif* (ITAM; Figure 34.21). As its name suggests, each ITAM includes key tyrosine residues, which are subject to phosphorylation by particular protein kinases present in immune-system cells.

A fundamental observation linking the binding of antigen to membrane-bound antibody with the subsequent initiation of an immune response is that *oligomerization, or clustering, of the antibody molecules is required* (Figure 34.22). The requirement for oligomerization is reminiscent of the dimerization of receptors triggered by epidermal growth factor and insulin encountered in Section 14.3; indeed, the associated signaling mechanisms appear to be quite similar. The oligomerization of the membrane-bound antibodies results in the phosphorylation of the tyrosine residues within the ITAMs by protein tyrosine kinases including Lyn, a homolog of Src (Section 14.5). The phosphorylated ITAMs serve as docking sites for a protein kinase termed *s*pleen *t*yrosine *k*inase (Syk), which has two SH2 domains that interact with the pair of phosphorylated tyrosine residues in each ITAM. Docked Syk adopts an active confirmation, which then phosphorylates other signal-transduction proteins, including an inhibitory subunit of the transcription factor NF-κB and

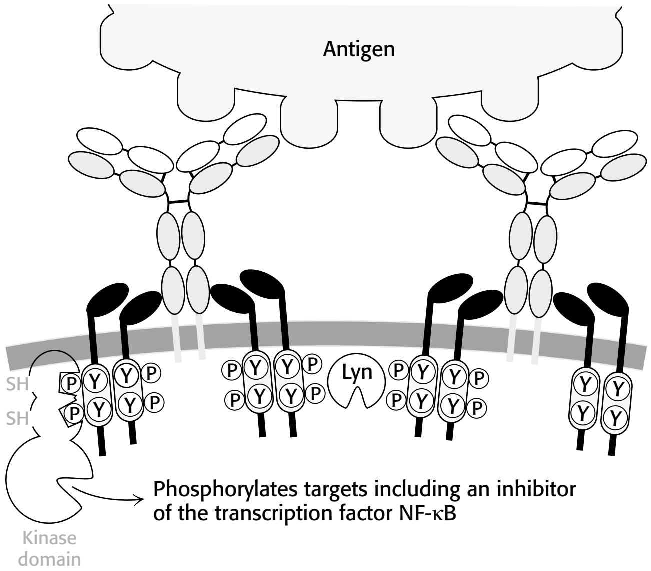
Antigen
SH
SH
P
Y
Lyn
Phosphorylates targets including an inhibitor of the transcription factor NF-κB
Kinase domain

FIGURE 34.22 B-cell activation. The binding of a multivalent antigen such as a bacterial or viral surface links membrane-bound IgM molecules. This oligomerization triggers the phosphorylation of tyrosine residues in the ITAM sequences by protein tyrosine kinases such as Lyn. After phosphorylation, the ITAMs serve as docking sites for Syk, a protein kinase that phosphorylates a number of targets, including transcription factors.

an isoform of phospholipase C. The signaling processes continue downstream to activate gene expression, leading to the stimulation of cell growth and initiating further B-cell differentiation.

Drugs that modulate the immune system have served as sources of insight into immune-system signaling pathways. For example, *cyclosporin,* a powerful suppressor of the immune system, inhibits *calcineurin,* a phosphatase which normally activates a transcription factor called NF-AT by dephosphorylating it.

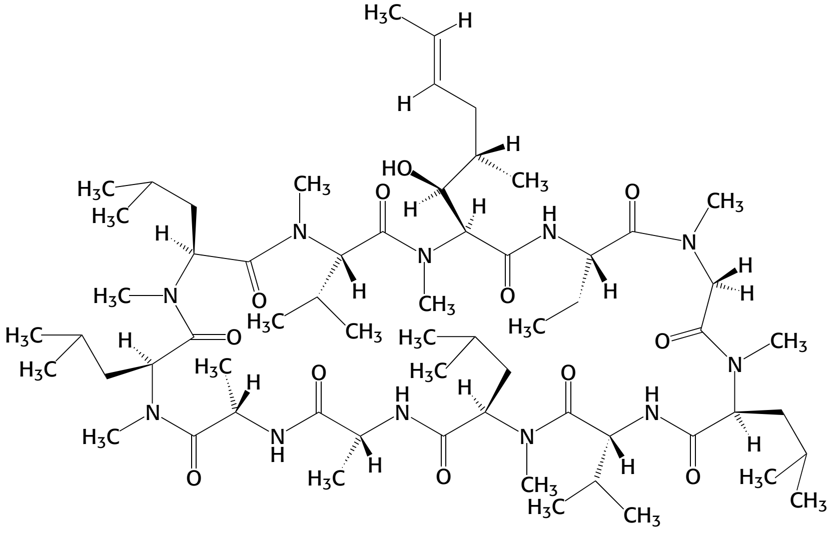

Cyclosporin A

The potent inhibition of the immune system, or *immunosuppression*, induced by cyclosporin reveals how crucial the activity of NF-AT is to the development of an immune response. Without such drugs, organ transplantation would be extremely difficult because transplanted tissue expresses a wide range of foreign antigens, causing the host immune system to reject the new tissue.

The role of oligomerization in the B-cell signaling pathway is illuminated when we consider the nature of many antigens presented by pathogens. The surfaces of many viruses, bacteria, and parasites are characterized by arrays of identical membrane proteins or membrane-linked carbohydrates. Thus, most pathogens present multiple binding surfaces that will naturally cause membrane-associated antibodies to oligomerize as they bind adjacent epitopes. In addition, the mechanism accounts for the observation that most small molecules do not induce an immune response; however, coupling multiple copies of a small molecule to a large oligomeric protein such as keyhole limpet hemocyanin (KLH), which has a molecular mass of 1 million daltons or more, promotes antibody oligomerization and, hence, the production of antibodies against the small-molecule epitope. The large protein is called the *carrier* of the attached chemical group, which is called a *haptenic determinant*. The small foreign molecule by itself is called a *hapten*. Antibodies elicited by attached haptens will bind unattached haptens as well.

Different classes of antibodies are formed by the hopping of V_H genes

The development of an effective antibody-based immune response depends on the secretion into the blood of antibodies that have appropriate effector functions. At the beginning of this response, an alternative mRNA-splicing pathway is activated so that the production of membrane-linked IgM is

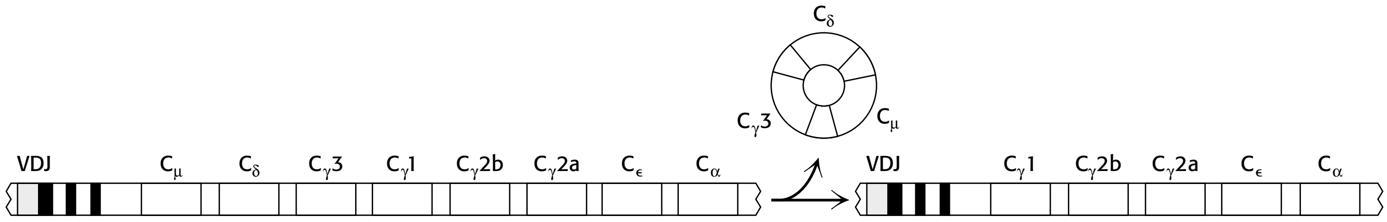

FIGURE 34.23 Class switching. Further rearrangement of the heavy-chain locus results in the generation of genes for antibody classes other than IgM. In the case shown, rearrangement places the VDJ region next to the Cγ1 region, resulting in the production of IgG1. Note that no further rearrangement of the VDJ region takes place, and so the specificity of the antibody is not affected.

supplanted by the synthesis of secreted IgM. As noted in Section 34.1, secreted IgM is pentameric and has a high avidity for antigens containing multiple identical epitopes. Later, the antibody-producing cell makes either IgG, IgA, IgD, or IgE of the same specificity as that of the initially secreted IgM. In this switch, the light chain and the variable region of the heavy chain are unchanged. Only the constant region of the heavy chain changes. This step in the differentiation of an antibody-producing cell is called *class switching* (Figure 34.23). In undifferentiated cells, the genes for the constant region of each class of heavy chain, called C_μ, C_δ, C_γ, C_ε, and C_α, are next to one another. There are eight in all, including four genes for the constant regions of γ chains. A complete transcript for the heavy chain of an IgM antibody is formed by the translocation of a V_H gene segment to a DJ_H gene segment within the genomic DNA (Figure 34.20), followed by RNA splicing of the V_HDJ_H segment to the C_μ segment, analogous to what is shown in Figure 34.19.

How are other heavy chains formed? Class switching is mediated by a gene-rearrangement process that moves a VDJ gene from a site near one C gene to a site near another C gene. Importantly, *the antigen-binding specificity is conserved in class switching because the entire V_HDJ_H gene is translocated in an intact form*. For example, the antigen-combining specificity of IgA produced by a particular cell is the same as that of IgM synthesized at an earlier stage of its development. The biological significance of C_H switching is that a whole recognition domain (the variable domain) is shifted from the early constant region (C_μ) to one of several other constant regions that mediate different effector functions.

34.4 Major-Histocompatibility-Complex Proteins Present Peptide Antigens on Cell Surfaces for Recognition by T-Cell Receptors

Soluble antibodies are highly effective against extracellular pathogens, but they confer little protection against microorganisms that are predominantly intracellular, such as some viruses and mycobacteria (which cause tuberculosis and leprosy). These pathogens are shielded from antibodies by the host-cell membrane (Figure 34.24). A different and more subtle strategy, *cell-mediated immunity*, evolved to cope with intracellular pathogens. *T cells* continually scan the surfaces of all cells and kill those that exhibit foreign markings. The task is not simple; intracellular microorganisms are not so obliging as to intentionally leave telltale traces on the surface of their host. Quite the contrary, successful pathogens are masters of the art of camouflage. Vertebrates have evolved an ingenious mechanism—cut and display—to reveal the presence of stealthy intruders. Nearly all vertebrate cells exhibit on their surfaces a sample of peptides derived from the digestion of proteins in their cytoplasm. These peptides are

FIGURE 34.24 Intracellular pathogen. An electron micrograph showing mycobacteria (arrows) inside an infected macrophage. [Courtesy of Dr. Stanley Falkow.]

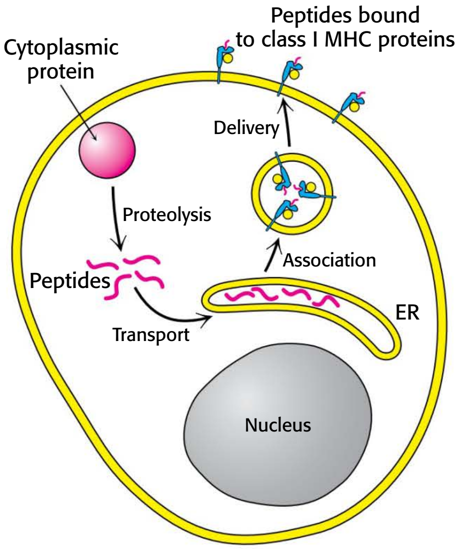

FIGURE 34.25 Presentation of peptides from cytoplasmic proteins. Class I MHC proteins on the surfaces of most cells display peptides that are derived from cytoplasmic proteins by proteolysis.

displayed by integral membrane proteins that are encoded by the *major histocompatibility complex* (MHC). Specifically, peptides derived from cytoplasmic proteins are bound to and displayed by *class I MHC proteins*. The dendritic cells of the innate immune system that subject pathogens to phagocytosis migrate to lymphatic tissue, where they use an MHC-like mechanism to present foreign peptides or lipid components to T cells—thus linking the innate and adaptive immune responses to pathogens.

How are these peptides generated and delivered to the plasma membrane? The process starts in the cytoplasm with the degradation of proteins—self-proteins as well as those of pathogens (Figure 34.25). Digestion is carried out by proteasomes (Section 23.2). The resulting peptide fragments are transported from the cytoplasm into the lumen of the endoplasmic reticulum by the *TAP protein* (for *t*ransporter associated with *a*ntigen *p*rocessing), a member of the ABC transporter family of ATP-driven pumps (Section 13.2). In the ER, peptides combine with nascent class I MHC proteins; these complexes are then targeted to the plasma membrane.

MHC proteins embedded in the plasma membrane tenaciously grip their bound peptides so that they can be touched and scrutinized by T-cell receptors on the surface of a killer cell. Foreign peptides bound to class I MHC proteins signal that a cell is infected and mark it for destruction by cytotoxic T cells. An assembly consisting of the foreign peptide—MHC complex, the T-cell receptor, and numerous accessory proteins—triggers a cascade that induces apoptosis in the infected cell. Strictly speaking, infected cells are not killed but, instead, are triggered to commit suicide to benefit the host.

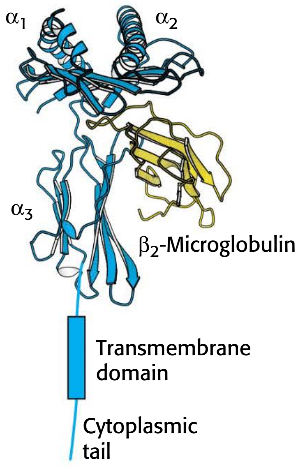

FIGURE 34.26 Class I MHC protein. A protein of this class consists of two chains. *Notice* that the α chain begins with two domains (α_1, α_2) that include α helices and continues with an immunoglobulin domain (α_3), a transmembrane domain, and a cytoplasmic tail. The second chain, β_2-microglobulin, adopts an immunoglobulin fold. [Drawn from 1HHK.pdb.]

Peptides presented by MHC proteins occupy a deep groove flanked by alpha helices

The three-dimensional structure of a large extracellular fragment of a human MHC class I protein, *human leukocyte antigen A2* (HLA-A2), was solved in 1987 by Don Wiley and Pamela Bjorkman. Class I MHC proteins consist of a 44-kDa α chain noncovalently bound to a 12-kDa polypeptide called $_2$-*microglobulin*. The α chain has three extracellular domains (α_1, α_2, and α_3), a transmembrane segment, and a tail that extends into the cytoplasm (Figure 34.26). The β_2-microglobulin and the α_3 domains have immunoglobulin folds, although the pairing of the two domains differs

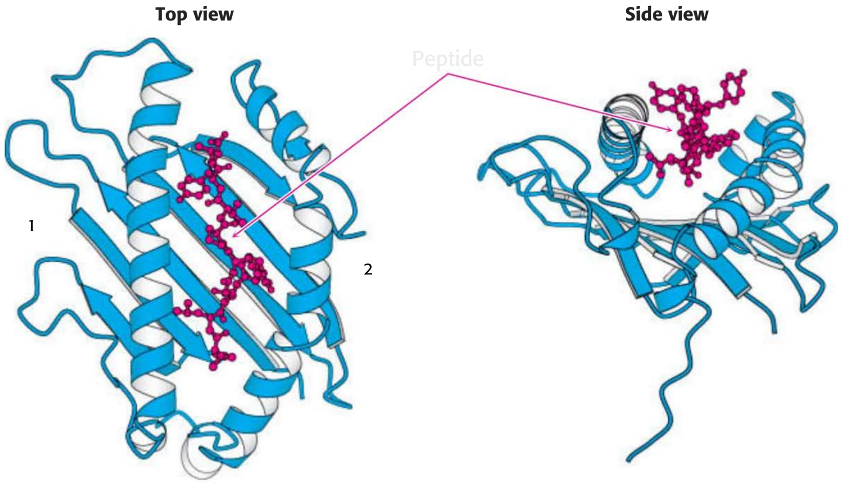

FIGURE 34.27 Class I MHC peptide-binding site. The α_1 and α_2 domains come together to form a groove in which peptides are displayed. *Notice* that that the peptide is surrounded on three sides by a β sheet and two α helices, but it is accessible from the top of the structure. [Drawn from 1HHK.pdb.]

from that in antibodies. The α_1 and α_2 domains exhibit a novel and remarkable architecture. They associate intimately to form a deep groove that serves as the peptide-binding site (Figure 34.27). The floor of the groove, which is about 25 Å long and 10 Å wide, is formed by eight β strands, four from each domain. A long helix contributed by the α_1 domain forms one side, and a helix contributed by the α_2 domain forms the other side. *This groove is the binding site for the presentation of peptides*.

The groove can be filled by a peptide from 8 to 10 residues long in an extended conformation. As we shall see (p. 1002), MHC proteins are remarkably diverse in the human population; each person expresses as many as six distinct class I MHC proteins, and many different forms are present in different people. The first structure determined, HLA-A2, binds peptides that almost always have leucine in the second position and valine in the last position (Figure 34.28). Side chains from the MHC molecule interact with the amino and carboxyl termini and with the side chains in these two key positions. These two residues are often referred to as the *anchor residues*. The other residues are highly variable. Thus, many millions of different peptides can be presented by this particular class I MHC protein; the

FIGURE 34.28 Anchor residues. (A) The amino acid sequences of three peptides that bind to the class I MHC protein HLA-A2 are shown. Each of these peptides has leucine in the second position and valine in the carboxyl-terminal position. (B) Comparison of the structures of these peptides reveals that the amino and carboxyl termini, as well as the side chains of the leucine and valine residues, are in essentially the same positions in each peptide, whereas the remainder of the structures are quite different.

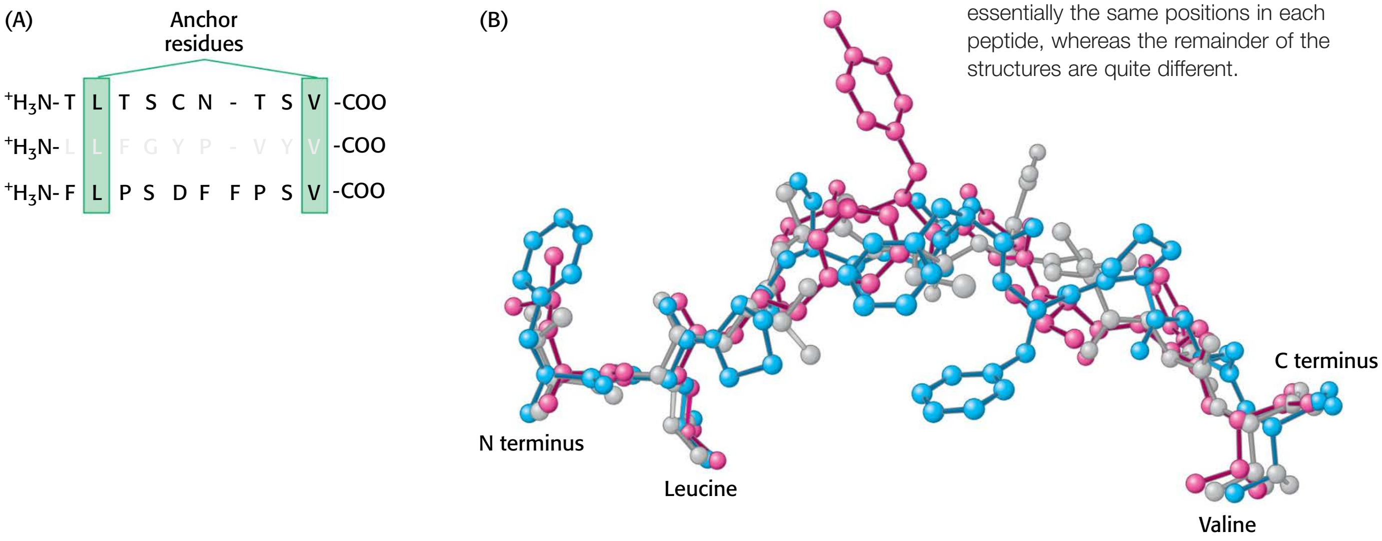
(A)
Anchor residues
+H3N- T L T S C N - T S V -COO
+H3N- L L F G Y P - V Y V -COO
+H3N- F L P S D F F P S V -COO
(B)
N terminus
Leucine
C terminus
Valine

identities of only two of the nine residues are crucial for binding. Each class of MHC molecules requires a unique set of anchor residues. Thus, a tremendous range of peptides can be presented by these molecules. Note that *one face of the bound peptide is exposed to solution, where it can be examined by other molecules, particularly T-cell receptors*. An additional remarkable feature of MHC–peptide complexes is their kinetic stability; once bound, a peptide is not released, even after a period of days.

T-cell receptors are antibody-like proteins containing variable and constant regions

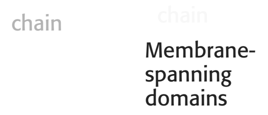

FIGURE 34.29 T-cell receptor. This protein consists of an α chain and a β chain, linked by a disulfide bond. *Notice* that each chain consists of two immunoglobulin domains on the cell surface, a membrane-spanning domain, and a short cytoplasmic tail. [Drawn from 1BD2.pdb.]

We are now ready to consider the receptor that recognizes peptides displayed by MHC proteins on target cells. The *T-cell receptor* consists of a 43-kDa α chain joined by a disulfide bond to a 43-kDa β chain (Figure 34.29). Each chain spans the plasma membrane and has a short carboxyl-terminal region on the cytoplasmic side. A small proportion of T cells express a receptor consisting of γ and δ chains in place of α and β. The α and β chains of the T-cell receptor, like immunoglobulin L and H chains, consist of *variable* and *constant* regions. Indeed, *these domains of the T-cell receptor are homologous to the V and C domains of immunoglobulins*. Furthermore, hypervariable sequences present in the V regions of the α and β chains of the T-cell receptor form the binding site for the epitope.

The genetic architecture of these proteins is similar to that of immunoglobulins, though the antibody genetic diversity is distributed over all the CDR loops, whereas T-cell-receptor genetic diversity is concentrated in the CDR3 loop that interacts with the peptide bound to the MHC. The variable region of the T-cell receptor α chain is encoded by about 50 V gene segments and 70 J gene segments. The T-cell receptor β chain is encoded by two D gene segments in addition to 57 V gene segments and 13 J gene segments. Again, the diversity of gene segments and the use of slightly imprecise modes of joining them increase the number of distinct proteins formed. *At least 10^{12} different specificities could arise from combinations of this repertoire of genes*. Thus, T-cell receptors, like immunoglobulins, can recognize a very large number of different epitopes. All the receptors on a particular T cell have the same specificity.

How do T cells recognize their targets? The variable regions of the α and β chains of the T-cell receptor form a binding site that recognizes a combined epitope–foreign peptide bound to an MHC protein (Figure 34.30). Neither the foreign peptide alone nor the MHC protein alone forms a complex with the T-cell receptor. Thus, fragments of an intracellular pathogen are presented in a context that allows their detection, leading to the initiation of an appropriate response.

T-cell receptor
MHC class I

FIGURE 34.30 T-cell receptor–class I MHC complex. The T-cell receptor binds to a class I MHC protein containing a bound peptide (red). *Notice* that the T-cell receptor contacts both the MHC protein and the peptide. [Drawn from 1BD2.pdb.]

CD8 on cytotoxic T cells acts in concert with T-cell receptors

The T-cell receptor does not act alone in recognizing and mediating the fate of target cells. Cytotoxic T cells also express a protein termed *CD8* on their surfaces that is crucial for the recognition of the class I MHC–peptide complex. The abbreviation CD stands for *cluster of differentiation,* referring to a cell-surface marker that is used to identify a lineage or stage of differentiation. Antibodies specific for particular CD proteins have been invaluable in following the development of leukocytes and in discovering new interactions between specific cell types.

Each chain in the CD8 dimer contains a domain that resembles an immunoglobulin variable domain (Figure 34.31). CD8 interacts primarily with the constant α_3 domain of class I MHC proteins. This interaction further stabilizes the interactions between the T cell and its target.

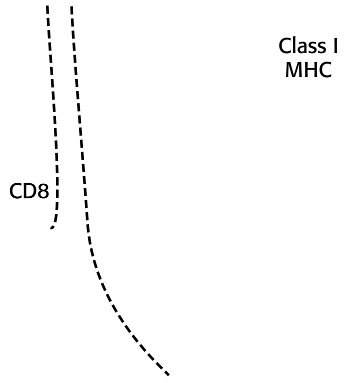

FIGURE 34.31 The coreceptor CD8. This dimeric protein extends from the surface of a cytotoxic T cell and binds to class I MHC molecules that are expressed on the surface of the cell that is bound to the T cell. The dashed lines represent extended polypeptide chains that link the immunoglobulin domains of CD8 to the membrane. *Notice* that the coreceptor interacts primarily with the constant α_3 domain of the class I MHC domain. [Drawn from 1AKJ.pdb.]

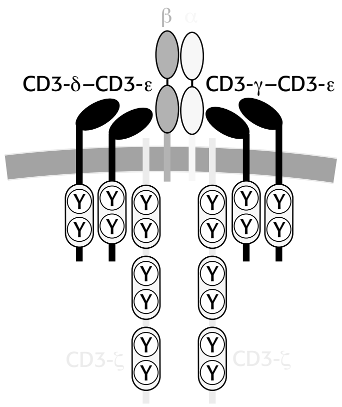

FIGURE 34.32 T-cell receptor complex. The T-cell receptor is associated with six CD3 molecules: a CD3-γ–CD3-ε heterodimer, a CD3-δ–CD3-ε heterodimer, and two chains of CD3-ζ. Single ITAM sequences are present in the cytoplasmic domains of CD3-γ, CD3-δ, and CD3-ε, whereas three such sequences are found in each CD3-ζ chain.

The cytoplasmic tail of CD8 contains a docking site for Lck, a cytoplasmic tyrosine kinase akin to Src. The T-cell receptor itself is associated with six polypeptides that form the CD3 complex (Figure 34.32). The γ, δ, and ε chains of CD3 are homologous to Ig-α and Ig-β associated with the B-cell receptor (Figure 34.21); each chain consists of an extracellular immunoglobulin domain and an intracellular ITAM region. These chains associate into CD3-γε and CD3-δε heterodimers. An additional component, the CD3-ζ chain, has only a small extracellular domain and a larger intracellular domain containing three ITAM sequences.

On the basis of these components, a model for T-cell activation can be envisaged that is closely parallel to the pathway for B-cell activation (Section 34.3; Figure 34.33). The binding of the T-cell receptor to the class I MHC–peptide complex and the concomitant binding of CD8 from the T cell to the MHC molecule link the kinase Lck to the ITAM substrates of the components of the CD3 complex. The phosphorylation of the tyrosine residues in the ITAM sequences generates docking sites for a protein kinase called ZAP-70 (for 70-kDa *z*eta-*a*ssociated *p*rotein) that is homologous to Syk in B cells. Docked by its two SH2 domains, ZAP-70 phosphorylates

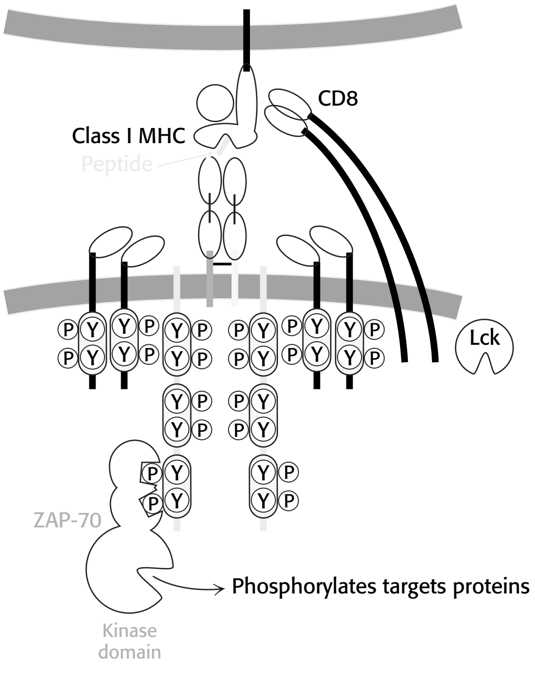

FIGURE 34.33 T-cell activation. The interaction between the T-cell receptor and a class I MHC–peptide complex results in the binding of CD8 to the MHC protein, the recruitment of the protein tyrosine kinase Lck, and the phosphorylation of tyrosine residues in the ITAM sequences of the CD3 chains. After phosphorylation, the ITAM regions serve as docking sites for the protein kinase ZAP-70, which phosphorylates protein targets to transmit the signal.

downstream targets in the signaling cascade. Additional molecules, including a membrane-bound protein phosphatase called CD45 and a cell-surface protein called CD28, play ancillary roles in this process.

T-cell activation has two important consequences. First, the activation of cytotoxic T cells results in the secretion of several proteins, including *perforin* and *granzymes*. Perforin is a 70-kDa protein that destabilizes the plasma membrane of the target cell, enabling the entry of *granzymes* into the cytoplasm of the target cell. Granzymes are serine proteases (Section 9.1) that initiate the pathway of apoptosis, leading to the death of the target cell and the fragmentation of its DNA, including any viral DNA that may be present. Second, after it has stimulated its target cell to commit suicide, the activated T cell disengages and is stimulated to reproduce. Thus, additional T cells that express the same T-cell receptor are generated to continue the battle against the invader after these T cells have been identified as a suitable weapon.

Helper T cells stimulate cells that display foreign peptides bound to class II MHC proteins

Not all T cells are cytotoxic. *Helper T cells* stimulate the proliferation of specific B lymphocytes and cytotoxic T cells and thereby serve as partners in determining the immune responses that are produced. The importance of helper T cells is graphically revealed by the devastation wrought by AIDS, a condition that destroys these cells. Helper T cells, like cytotoxic T cells, detect foreign peptides that are presented on cell surfaces by MHC proteins. However, the source of the peptides, the MHC proteins that bind them, and the transport pathway are different.

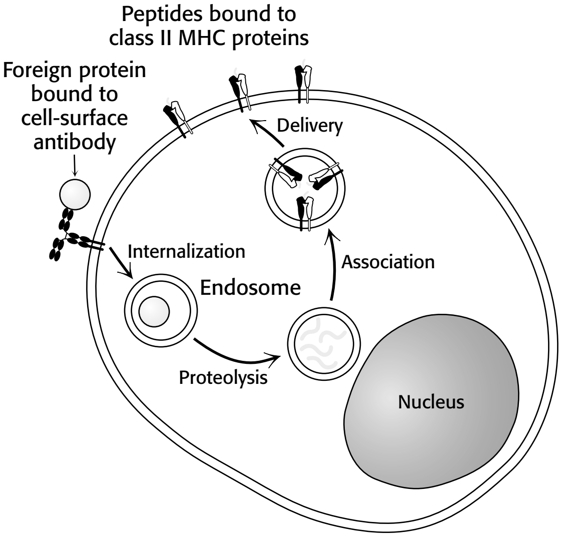
Peptides bound to class II MHC proteins
Foreign protein bound to cell-surface antibody
Delivery
Internalization
Association
Endosome
Proteolysis
Nucleus

FIGURE 34.34 Presentation of peptides from internalized proteins. Antigen-presenting cells bind and internalize foreign proteins and display peptides that are formed from the digestion of these proteins in class II MHC proteins.

Helper T cells recognize peptides bound to MHC molecules referred to as class II. Their helping action is focused on B cells, macrophages, and dendritic cells. *Class II MHC proteins are expressed only by these antigen-presenting cells*, unlike class I MHC proteins, which are expressed on nearly all cells. The peptides presented by class II MHC proteins do not come from the cytoplasm. Rather, *they arise from the degradation of proteins that have been internalized by endocytosis*. Consider, for example, a virus particle that is captured by membrane-bound immunoglobulins on the surface of a B cell (Figure 34.34). This complex is delivered to an endosome, a membrane-enclosed acidic compartment, where it is digested. The resulting peptides become associated with class II MHC proteins, which move to the cell surface. Peptides from the cytoplasm cannot reach class II proteins, whereas peptides from endosomal compartments cannot reach class I proteins. This segregation of displayed peptides is biologically critical. The association of a foreign peptide with a class II MHC protein signals that a cell has *encountered* a pathogen and serves as a call for *help*. In contrast, association with a class I MHC protein signals that a cell has *succumbed* to a pathogen and is a call for *destruction*.

Helper T cells rely on the T-cell receptor and CD4 to recognize foreign peptides on antigen-presenting cells

The overall structure of a class II MHC molecule is remarkably similar to that of a class I molecule. Class II molecules consist of a 33-kDa α chain and a noncovalently bound 30-kDa β chain (Figure 34.35). Each contains two extracellular domains, a transmembrane segment, and a short cytoplasmic tail. The peptide-binding site is formed by the α_1 and β_1 domains, each of

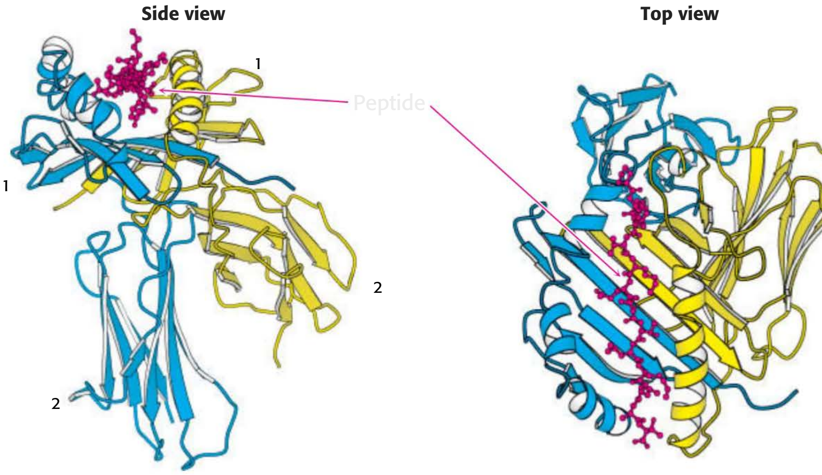

FIGURE 34.35 Class II MHC protein. A class II MHC protein consists of homologous α and β chains, each of which has an amino-terminal domain that constitutes half of the peptide-binding structure, as well as a carboxyl-terminal immunoglobulin domain. *Notice* the trough-like peptide-binding site, which is similar to that in class I MHC proteins except that it is open at both ends, allowing class II MHC proteins to bind longer peptides than those bound by class I. [Drawn from 1DLH.pdb.]

which contributes a long helix and part of a β sheet. Thus, the same structural elements are present in class I and class II MHC molecules, but they are combined into polypeptide chains in different ways. The peptide-binding site of a class II molecule is open at both ends, and so this groove can accommodate longer peptides than can be bound by class I molecules; typically, peptides between 13 and 18 residues long are bound. The peptide-binding specificity of each class II molecule depends on binding pockets that recognize particular amino acids, also known as anchor residues, in specific positions along the sequence.

Helper T cells express T-cell receptors that are produced from the same genes as those on cytotoxic T cells. These T-cell receptors interact with class II MHC molecules in a manner that is analogous to T-cell-receptor interaction with class I MHC molecules. Nonetheless, helper T cells and cytotoxic T cells are distinguished by other proteins that they express on their surfaces. In particular, helper T cells express a protein called *CD4* instead of expressing CD8. CD4 consists of four immunoglobulin domains that extend from the T-cell surface, as well as a small cytoplasmic region (Figure 34.36). The amino-terminal immunoglobulin domains of CD4 interact with the base on the class II MHC molecule. Thus, helper T cells bind cells expressing class II MHC specifically because of the interactions with CD4 (Figure 34.37).

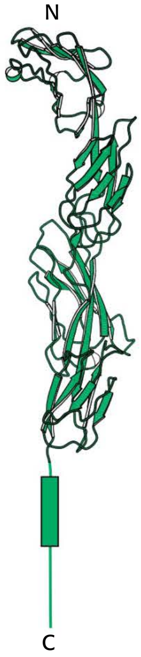

FIGURE 34.36 Coreceptor CD4. This protein comprises four tandem immunoglobulin domains that extend from the surface of a helper T cell. [Drawn from 1WIO.pdb.]

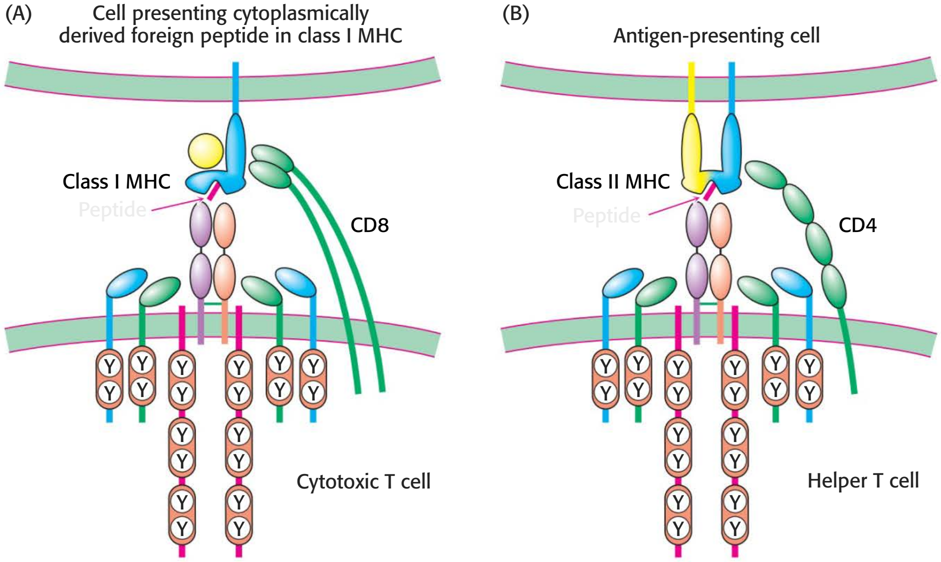

FIGURE 34.37 Variations on a theme. (A) Cytotoxic T cells recognize foreign peptides presented in class I MHC proteins with the aid of the coreceptor CD8. (B) Helper T cells recognize peptides presented in class II MHC proteins by specialized antigen-presenting cells with the aid of the coreceptor CD4.

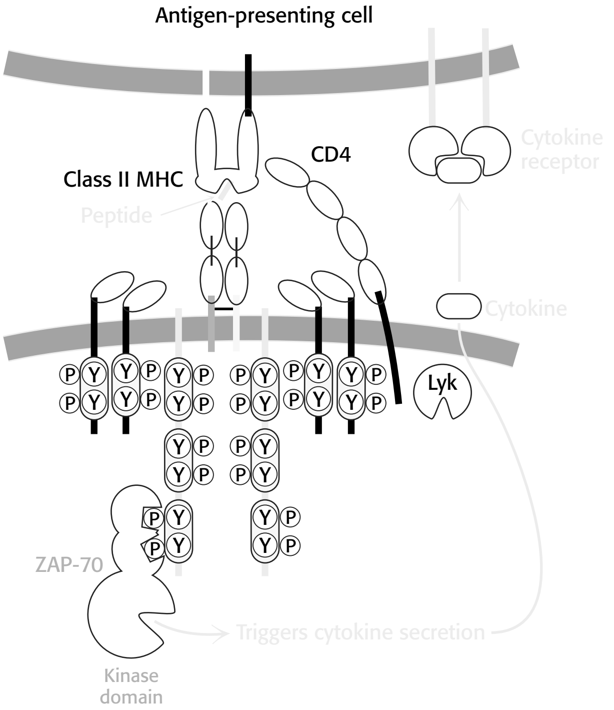

FIGURE 34.38 Helper-T-cell action. The engagement of the T-cell receptor in helper T cells results in the secretion of cytokines. These cytokines bind to cytokine receptors expressed on the surface of the antigen-presenting cell, stimulating cell growth, differentiation, and, in regard to a B cell, antibody secretion.

When a helper T cell binds to an antigen-presenting cell expressing an appropriate class II MHC–peptide complex, signaling pathways analogous to those in cytotoxic T cells are initiated by the action of the kinase Lck on ITAMs in the CD3 molecules associated with the T-cell receptor. However, rather than triggering events leading to the death of the attached cell, *these signaling pathways result in the secretion of cytokines from the helper cell*. Cytokines are a family of molecules that include, among others, interleukin-2 and interferon-γ. Cytokines bind to specific receptors on the antigen-presenting cell and stimulate its growth and differentiation (Figure 34.38). For example, these cytokines stimulate the differentiation of B cells into *plasma cells*, which specialize in the production of large amounts of antibody. Thus, the internalization and presentation of parts of a foreign pathogen help to generate a local environment in which cells taking part in the defense against this pathogen can flourish through the action of helper T cells.

MHC proteins are highly diverse

MHC class I and II proteins, the presenters of peptides to T cells, were discovered because of their role in *transplantation rejection.* A tissue transplanted from one person to another or from one mouse to another is usually rejected by the immune system. In contrast, tissues transplanted from one identical twin to another or between mice of an inbred strain are accepted. Genetic analyses revealed that rejection occurs when tissues are transplanted between individual organisms having different genes in the major histocompatibility complex, a cluster of more than 75 genes playing key roles in immunity. The 3500-kb span of the MHC is nearly the length of the entire *E. coli* chromosome. The MHC encodes class I proteins (presenters to cytotoxic T cells) and class II proteins (presenters to helper T cells), as well as class III proteins (components of the complement cascade) and many other proteins that play key roles in immunity.

Human beings express six different class I genes (three from each parent) and six different class II genes. The three loci for class I genes are called HLA-A, -B, and -C; those for class II genes are called HLA-DP, -DQ, and -DR. These loci are *highly polymorphic:* many alleles of each are present in the population. For example, more than 50 each of HLA-A, -B, and -C alleles are known; the numbers discovered increase each year. Hence, the likelihood that two unrelated persons have identical class I and II proteins is very small ($<10^{-4}$), accounting for transplantation rejection unless the genotypes of donor and acceptor are closely matched in advance.

Differences between class I proteins are located mainly in the α_1 and α_2 domains, which form the peptide-binding site (Figure 34.39). The α_3 domain, which interacts with a constant β_2-microglobulin, is largely conserved. Similarly, the differences between class II proteins cluster near the peptide-binding groove. Why are MHC proteins so highly variable? *Their diversity makes the presentation of a very wide range of peptides to T cells possible*. A *particular* class I or class II molecule may not be able to bind any of the peptide fragments of a viral protein. The likelihood of a fit is markedly increased by having several kinds (usually six) of each class of presenters in each individual organism. If all members of a species had identical class I or class II molecules, the population would be much more vulnerable to devastation by a pathogen that had mutated and thereby evaded presentation. The evolution of the diverse human MHC repertoire has been driven by the selection for individual members of the species who resist infections to which other members of the population may be susceptible.

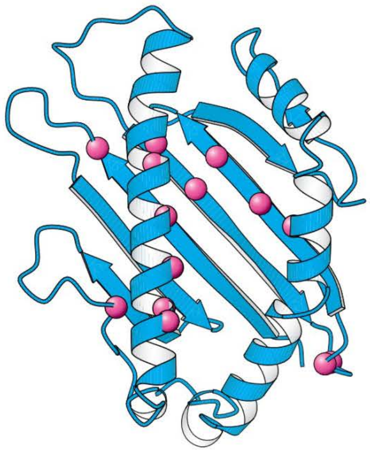

FIGURE 34.39 Polymorphism in class I MHC proteins. *Notice* that the positions of sites with a high degree of polymorphism in the human population are displayed as red spheres on the structure of the amino-terminal part of a class I MHC protein. [Drawn from 1HHK.pdb.]

Human immunodeficiency viruses subvert the immune system by destroying helper T cells

In 1981, the first cases of a new disease now called *acquired immune deficiency syndrome* (AIDS) were recognized. The victims died of rare infections because their immune systems were crippled. The cause was identified 2 years later by Luc Montagnier and coworkers. AIDS is produced by *human immunodeficiency virus* (HIV), of which two major classes are known: HIV-1 and the much less common HIV-2. Like other *retroviruses,* HIV contains a single-stranded RNA genome that is replicated through a double-stranded DNA intermediate. This viral DNA becomes integrated into the genome of the host cell. In fact, viral genes are transcribed only when they are integrated into the host DNA.

The HIV virion is enveloped by a lipid-bilayer membrane containing two glycoproteins: gp41 spans the membrane and is associated with gp120, which is located on the external face (Figure 34.40). The core of the virus contains two copies of the RNA genome and associated transfer RNAs, as well as several molecules of reverse transcriptase. They are surrounded by many copies of two proteins called p17 and p24. *The host cell for HIV is the helper T cell*. The gp120 molecules on the membrane of HIV bind to CD4 molecules on the surface of the helper T cell (Figure 34.41). This interaction allows the associated viral gp41 to insert its amino-terminal head into the host-cell membrane. The viral membrane and the helper-T-cell membrane fuse, and the viral core is released directly into the cytoplasm. Infection by

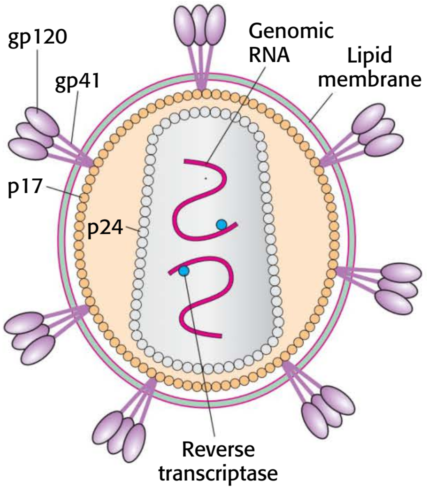

FIGURE 34.40 Human immunodeficiency virus. A schematic representation of HIV reveals its proteins and nucleic acid components. [Information from G. B. Karlsson Hedestam et al., *Nat. Rev. Microbiol.* 6:143–155, 2008, Fig. 2a.]

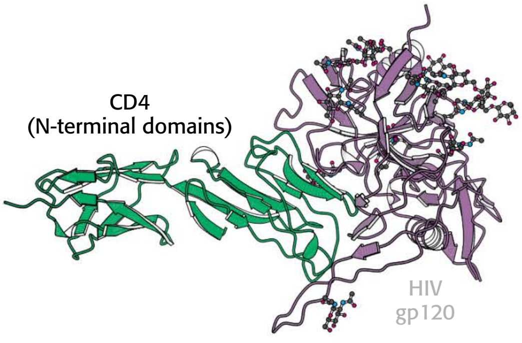

FIGURE 34.41 HIV receptor. A complex between a modified form of the envelope glycoprotein gp120 from HIV and a peptide corresponding to the two amino-terminal domains from the helper-T-cell protein CD4 reveals how viral infection of helper T cells is initiated. [Drawn from 1GC1.pdb.]

HIV leads to the destruction of helper T cells because the permeability of the host plasma membrane is markedly increased by the insertion of viral glycoproteins and the budding of virus particles. The influx of ions and water disrupts the ionic balance, causing osmotic lysis.

34.5 The Immune System Contributes to the Prevention and the Development of Human Diseases

The primary function of the immune system is to protect the host from invasion by foreign organisms. But how does the immune system prevent itself from mounting attacks against its host? In other words, how does the immune system distinguish between self and nonself? Clearly, proteins from the organism itself do not bear some special tag identifying them. Instead, selection processes early in the developmental pathways for immune cells kill or suppress those immune cells that react strongly with self-antigens. The evolutionary paradigm still applies; immune cells that recognize self-antigens are generated, but selective mechanisms eliminate such cells in the course of development.

T cells are subjected to positive and negative selection in the thymus

T cells derive their name from the location of their production—the thymus, a small organ situated just above the heart. Examination of the developmental pathways leading to the production of mature cytotoxic and helper T cells reveals the selection mechanisms that are crucial for distinguishing self from nonself. These selection criteria are quite stringent; approximately 98% of the thymocytes, the precursors of T cells, die before the completion of the maturation process.

Thymocytes produced in the bone marrow do not express the T-cell receptor complex, CD4, or CD8. On relocation to the thymus and rearrangement of the T-cell-receptor genes, the immature thymocyte expresses all of these molecules. These cells are first subjected to *positive selection* (Figure 34.42). Cells for which the T-cell receptor can bind with reasonable affinity to either class I or class II MHC molecules survive this selection; those for which the T-cell receptor does not participate in such an interaction undergo apoptosis and die. *The role of the positive selection step is to prevent the production of T cells that will not bind to any MHC complex present, regardless of the peptide bound.*

The cell population that survives positive selection is subjected to a second step, *negative selection.* Here, T cells that bind with high affinity to MHC complexes bound to self-peptides expressed on the surfaces of

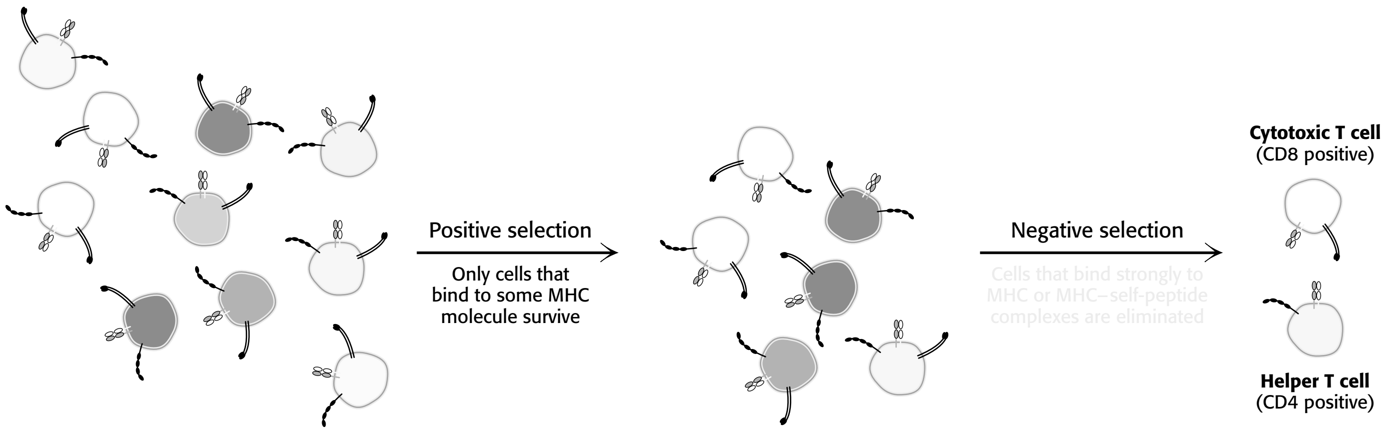
Positive selection
Only cells that bind to some MHC molecule survive
Negative selection
Cells that bind strongly to MHC or MHC–self-peptide complexes are eliminated
Cytotoxic T cell
(CD8 positive)
Helper T cell
(CD4 positive)

FIGURE 34.42 T cell selection. A population of thymocytes is subjected first to positive selection to remove cells that express T-cell receptors that will not bind to MHC proteins expressed by the individual organism. The surviving cells are then subjected to negative selection to remove cells that bind strongly to MHC complexes bound to self-peptides.

(A) (B)

FIGURE 34.43 Consequences of autoimmunity. Photomicrographs of an islet of Langerhans (A) in the pancreas of a normal mouse and (B) in the pancreas of a mouse with an immune response against pancreatic β cells, which results in a disease resembling insulin-dependent diabetes mellitus in human beings. *Notice* that the relatively pale cellular area in the center of part A is populated with the dark nuclei of inflammatory cells in part B. [From M. A. Atkinson and N. K. Maclaren. What causes diabetes? Scientific American, 1990. Courtesy Mark Atkinson.]

antigen-presenting cells in the thymus undergo apoptosis or are otherwise suppressed. Those that do not bind too avidly to any such MHC complex complete development and become mature cytotoxic T cells (which express only CD8) or helper T cells (which express only CD4). The negative selection step leads to *self-tolerance;* cells that bind an MHC–self-peptide complex are removed from the T-cell population. Similar mechanisms apply to developing B cells: maturing B cells that express antibodies that interact strongly with self-antigens are suppressed.

Autoimmune diseases result from the generation of immune responses against self-antigens

Although thymic selection is remarkably efficient in suppressing the immune response to self-antigens, failures do occur. Such failures result in *autoimmune diseases.* These diseases include common illnesses such as insulin-dependent diabetes mellitus, multiple sclerosis, and rheumatoid arthritis. In these illnesses, immune responses against self-antigens result in damage to selective tissues that express the antigen (Figure 34.43).

In many cases, the cause of the generation of self-reactive antibodies or T cells is unclear. However, in other cases, infectious organisms such as bacteria or viruses may play a role. Infection leads to the generation of antibodies and T cells that react with many different epitopes from the infectious organism. If one of these antigens closely resembles a self-antigen, an autoimmune response can result. For example, *Streptococcus* infections sometimes lead to rheumatic fever owing to the production of antibodies to streptococcal antigens that cross-react with exposed epitopes in heart muscle.

The immune system plays a role in cancer prevention

The development of immune responses against proteins encoded by our own genomes can be beneficial in some circumstances. Cancer cells have undergone significant changes that often result in the production of proteins that are not normally expressed. For example, the mutation of genes can generate proteins that do not correspond in amino acid sequence to any normal protein. Such proteins may be recognized as foreign, and an immune response will be generated specifically against the cancer cell. Alternatively, cancer cells often produce proteins that are expressed during embryonic development but are not expressed or are expressed at very low levels after birth. For example, a membrane glycoprotein called *carcinoembryonic antigen* (CEA) appears in the gastrointestinal cells of developing fetuses but is not normally expressed at significant levels after birth. More than 50% of patients with colorectal cancer have elevated serum levels of CEA. Immune cells recognizing epitopes from such proteins will not be subjected to negative selection and, hence, will be present in the adult immune repertoire. These cells may play a cancer surveillance role, killing cells that overexpress antigens such as CEA and preventing genetically damaged cells from developing into tumors.

Vaccines are a powerful means to prevent and eradicate disease

The discovery and utilization of *vaccines*, biological preparations that stimulate immunity to a particular pathogen or disease, represents a significant milestone in modern medical history. The pioneering work of Edward Jenner and Louis Pasteur in the eighteenth and nineteenth centuries revealed that inoculation with inactivated forms of a pathogen could protect against subsequent infection with the active pathogen. Treatment of a person with a vaccine, or *immunization*, leads to the development of *immunological memory*, the ability of the immune system to respond more rapidly and effectively to pathogens that have been encountered previously. At the cellular level, memory arises because positively selected B cells and T cells that have a high affinity for their target persist within the organism as *memory B cells* and *memory T cells*.

In order for a vaccine to be effective, it must generate a sustained protective response appropriate for the targeted pathogen. For example, pathogens such as *Clostridium tetani*, the causative agent of tetanus, cause disease by the release of destructive proteins called *toxins*. Hence, an effective tetanus vaccine should generate a strong B-cell-mediated response. In contrast, a vaccine designed to prevent disease caused by an intracellular pathogen should generate a strong T-cell-mediated response. The active component of a vaccine that is responsible for stimulating this immune response can take many forms:

Killed or *inactivated vaccines* contain pathogens that have been rendered harmless by treatment with chemicals or high heat.

Live attenuated vaccines contain live pathogens that have accumulated mutations so that they are no longer virulent to human cells. These vaccines are most commonly generated by repeated infection of the pathogen in cultured cells until its virulence is lost.

Subunit vaccines contain a purified protein component of the pathogen. Such proteins can be either isolated from infected material (such as blood from chronically infected patients) or generated by recombinant methods.

Toxoid vaccines are used against pathogens that employ an extracellular toxin to cause disease. These vaccines contain a form of the toxin that has been inactivated by treatment with chemicals or high heat.

The effectiveness of immunization efforts has made the global eradication of certain diseases possible. In 1966, 20 million cases of smallpox were reported worldwide. Just 14 years later, after coordinated vaccination efforts in regions of endemic disease, the World Health Assembly declared that smallpox had been eradicated. Nevertheless, despite the success of vaccines in the prevention of many devastating diseases, several pathogens have posed a significant challenge to vaccine development. For example, the development of an effective HIV vaccine has been complicated by the antigenic diversity of HIV strains. Because its mechanism for replication is prone to error, a population of HIV presents an ever-changing array of coat proteins. Indeed, the mutation rate of HIV is more than 65 times higher than that of influenza virus. Nevertheless, the identification of protective antibodies in individuals resistant to HIV and advancements in vaccine design suggest that the development of an effective HIV vaccine remains a real possibility.

SUMMARY

Two lines of defense against pathogens are the innate immune system and the adaptive immune system. The innate immune system targets features common to many different pathogens but misses those pathogens lacking these features. The adaptive immune system is both more specific and wide-reaching. To respond effectively to a vast array of pathogens, this type of immune system must be tremendously flexible. The adaptive immune system follows the principles of evolution: an enormously diverse set of potentially useful proteins is generated; these proteins are then subjected to intense selection so that only cells that express useful proteins flourish and continue development, until an effective immune response to a specific invader is generated.

34.1 Antibodies Possess Distinct Antigen-Binding and Effector Units

The major immunoglobulin in the serum is immunoglobulin G. An IgG protein is a heterotetramer with two heavy chains and two light chains. Treatment of IgG molecules with proteases such as papain produces three fragments: two F_{ab} fragments that retain antigen-binding activity and an F_c fragment that retains the ability to activate effector functions such as the initiation of the complement cascade. The F_{ab} fragments include the L chain and the amino-terminal half of the H chain; the F_c domain is a dimer consisting of the carboxyl-terminal halves of two H chains. Five different classes of antibody—IgG, IgM, IgA, IgD, and IgE—differ in their heavy chains and, hence, in their effector functions.

34.2 Antibodies Bind Specific Molecules Through Hypervariable Loops

One particular protein fold is found in many of the key proteins of the immune system. The immunoglobulin fold consists of a pair of β sheets that pack against each other, linked by a single disulfide bond. Loops projecting from one end of the structure form a binding surface that can be varied by changing the amino acid sequences within the loops. Domains with immunoglobulin folds are linked to form antibodies and other classes of proteins in the immune system, including T-cell receptors. Two chains come together to form the binding surface of an antibody. Three loops from each domain, the complementarity-determining regions, form an essentially continuous surface that can vary tremendously in shape, charge, and other characteristics to allow particular antibodies to bind to molecules ranging from small molecules to large protein surfaces.

34.3 Diversity Is Generated by Gene Rearrangements

The tremendous diversity of the amino acid sequences of antibodies is generated by segmental rearrangements of genes. For antibody κ light chains, 1 of 40 variable regions is linked to 1 of 5 joining regions. The combined VJ unit is then linked to the constant region. Thousands of different genes can be generated in this manner. Similar arrays are rearranged to form the genes for the heavy chains, but an additional region called the diversity region lies between the V and the J regions. The combination of L and H chains, each obtained through such rearranged genes, can produce more than 10^8 distinct antibodies. Different classes of antibodies are also generated by gene rearrangements that lead to class switching. Oligomerization of membrane-bound antibody molecules initiates a signal-transduction cascade inside B cells. Key steps in this signaling process include the phosphorylation of specific tyrosine residues in sequences termed immunoreceptor tyrosine-based activation motifs, present in proteins that associate with the membrane-bound antibodies.

34.4 Major-Histocompatibility-Complex Proteins Present Peptide Antigens on Cell Surfaces for Recognition by T-Cell Receptors

Intracellular pathogens such as viruses and mycobacteria cannot be easily detected. Intracellular proteins are constantly being cut into small peptides by proteasomes and displayed in class I major-histocompatibility-complex proteins on cell surfaces. Such peptides lie in a groove defined by two helices in the class I MHC proteins. The combination of MHC protein and peptide can be bound by an appropriate T-cell receptor. T-cell receptors resemble the antigen-binding domains of antibodies in structure, and diversity in T-cell-receptor sequence is generated by V(D)J gene rearrangements. The T-cell receptor recognizes features of both the peptide and the MHC molecule that presents it.

Cytotoxic T cells initiate apoptosis in cells to which they bind through interactions between T-cell receptors and class I MHC–peptide complexes aided by interactions with the coreceptor molecule CD8. Helper T cells recognize peptides presented in class II MHC proteins, a distinct type of MHC protein expressed only on antigen-presenting cells, such as B cells and macrophages. Helper T cells express the coreceptor CD4 rather than CD8. CD4 interacts with class II MHC proteins present on antigen-presenting cells. Signaling pathways, analogous to those in B cells, are initiated by interactions between MHC–peptide complexes and T-cell receptors and the CD8 and CD4 coreceptors. Human immunodeficiency virus damages the immune system by infecting and killing cells that express CD4, such as helper T cells.

34.5 The Immune System Contributes to the Prevention and the Development of Human Diseases

In principle, the immune system is capable of generating antibodies and T-cell receptors that bind to self-molecules—that is, molecules that are normally present in a healthy and uninfected individual organism. Selection mechanisms prevent such self-directed molecules from being expressed at high levels. The selection process includes both positive selection, to enrich the population of cells that express molecules that have the potential to bind foreign antigens in an appropriate context, and negative selection, which eliminates cells that express molecules with too high an affinity for self-antigens. Autoimmune diseases such as insulin-dependent diabetes mellitus can result from the amplification of a response against a self-antigen. Vaccines stimulate immunological memory so as to prevent, and even eradicate, disease.

KEY TERMS

innate immune system (p. 981)
adaptive immune system (p. 981)
phagocyte (p. 982)
Toll-like receptor (TLR) (p. 982)
pathogen-associated molecular pattern (PAMP) (p. 982)
endotoxin (p. 982)
humoral immune response (p. 984)
B lymphocyte (B cell) (p. 984)

antigen (p. 984)
antigenic determinant (epitope) (p. 984)
cellular immune response (p. 984)
cytotoxic T lymphocyte (killer T cell) (p. 984)
helper T lymphocyte (helper T cell) (p. 984)
immunoglobulin G (IgG) (p. 985)
F_{ab} (p. 985)
F_c (p. 985)
light (L) chain (p. 985)
heavy (H) chain (p. 985)
segmental flexibility (p. 987)
immunoglobulin M (IgM) (p. 987)
immunoglobulin A (IgA) (p. 987)
immunoglobulin D (IgD) (p. 987)
immunoglobulin E (IgE) (p. 987)
variable region (p. 988)
constant region (p. 988)
immunoglobulin fold (p. 988)
hypervariable loop (p. 988)
complementarity-determining region (CDR) (p. 988)
V(D)J recombination (p. 992)
immunoreceptor tyrosine-based activation motif (ITAM) (p. 993)
cyclosporin (p. 994)
hapten (p. 994)
class switching (p. 995)
major histocompatibility complex (MHC)(p. 996)
class I MHC protein (p. 996)
TAP (transporter associated with antigen processing) protein (p. 996)
human leukocyte antigen (HLA) (p. 996)
β_2-microglobulin (p. 996)
T-cell receptor (p. 998)
CD8 (p. 998)
perforin (p. 1000)
granzyme (p. 1000)
class II MHC protein (p. 1000)
CD4 (p. 1001)
plasma cell (p. 1002)
human immunodeficiency virus (HIV) (p. 1003)
positive selection (p. 1004)
negative selection (p. 1004)
autoimmune disease (p. 1005)
carcinoembryonic antigen (CEA) (p. 1006)
vaccine (p. 1006)
immunological memory (p. 1006)
killed, or inactivated, vaccines (p. 1006)
live attenuated vaccines (p. 1006)
subunit vaccines (p. 1006)
toxoid vaccines (p. 1006)

PROBLEMS

1. *First things first.* Distinguish between the innate and adaptive immune systems.

2. *Antibody diversity.* What are the mechanisms used by B cells to generate antibody diversity?

3. *Hang in there.* Explain the difference between *affinity* and *avidity.* For which immunoglobulin class might avidity be particularly important in antigen recognition?

4. *Innate abilities.* A strain of mice has been identified that does not respond to LPS. This lack of response is due to a single amino acid change in the intracellular domain of mouse TLR4. Propose an explanation for the lack of response.

5. *TLR ligands.* The PAMP recognized by TLR3 is double-stranded RNA (dsRNA). Against which pathogens would TLR3 be an effective immune receptor?

6. *Energetics and kinetics*. Suppose that the dissociation constant of an F_{ab}–hapten complex is 3×10^{-7} M at 25°C.

(a) What is the standard free energy of binding?

(b) Immunologists often speak of affinity (K_a), the reciprocal of the dissociation constant, in comparing antibodies. What is the affinity of this F_{ab}?

(c) The rate constant for the release of hapten from the complex is $120\ \text{s}^{-1}$. What is the rate constant for association? What does the magnitude of this value imply about the extent of structural change in the antibody on binding hapten?

7. *A brilliant emitter*. Certain naphthalene derivatives, such as the dansyl group, exhibit a weak yellow fluorescence when they are in a highly polar environment (such as water) and an intense blue fluorescence when they are in a markedly nonpolar environment (such as hexane). The binding of ε-dansyl-lysine to specific antibody is accompanied by a marked increase in its fluorescence intensity and a shift in color from yellow to blue. What does this finding reveal about the hapten–antibody complex?

8. *Miniantibody*. The F_{ab} fragment of an antibody molecule has essentially the same affinity for a monovalent hapten as does intact IgG.

(a) What is the smallest unit of an antibody that can retain the specificity and binding affinity of the whole protein?

(b) Design a compact single-chain protein that is likely to specifically bind antigen with high affinity.

9. *Turning on B cells*. B lymphocytes, the precursors of plasma cells, are triggered to proliferate by the binding of multivalent antigens to receptors on their surfaces. The cell-surface receptors are transmembrane immunoglobulins. Univalent antigens, in contrast, do not activate B cells.

(a) What do these findings reveal about the mechanism of B-cell activation?

(b) How might antibodies be used to activate B cells?

10. *An ingenious cloning strategy*. In the cloning of the gene for the α chain of the T-cell receptor, T-cell cDNAs were

hybridized with B-cell mRNAs. What was the purpose of this hybridization step? Can the principle be applied generally?

11. *Pathogen susceptibility.* Patients carrying specific mutations in the gene encoding the TLR4 protein are susceptible to infections from Gram-negative bacteria. Why are these patients vulnerable to this particular type of pathogen?

12. *Matchmaker, matchmaker.* Why is it important to match HLA alleles between donor and recipient in organ transplantation?

13. *Instruction.* Before the mechanism for generating antibody diversity had been established, a mechanism based on protein folding around an antigen was proposed, primarily by Linus Pauling. In this model, antibodies that had different specificities had the same amino acid sequence but were folded in different ways. Propose a test of this model.

14. *Dealing with nonsense.* Cells, including immune cells, degrade mRNA molecules in which no long open reading frame is present. The process is called nonsense-mediated RNA decay. Suggest a role for this process in immune cells.

15. *Down, but not out.* To understand the genes responsible for growth and infectivity in a disease-causing bacterial strain, you perform chemical mutagenesis on a culture of these bacteria. In the course of your investigation into the properties of the resulting mutants, you identify a set of mutant bacteria that is still viable but their virulence is significantly impaired. How might these mutants be useful for vaccine development?

16. *Presentation.* The amino acid sequence of a small protein is

MSRLASKNLIRSDHAGGLLQATYSAVSSIKNTMSFGAWSNAALNDSRDA

Predict the most likely peptide to be presented by the class I MHC molecule HLA-A2.

Mechanism Problem

17. *Catalytic antibody.* Antibody is generated against a transition state for the hydrolysis of the following ester.

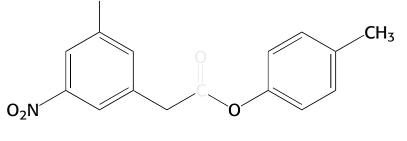

Ester

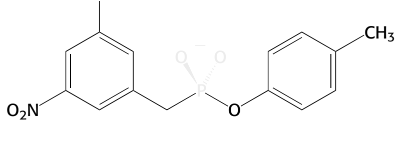

Transition-state analog

Some of these antibodies catalyze the hydrolysis of the ester. What amino acid residue might you expect to find in the binding site on the antibody?

Chapter Integration Problem

18. *Signaling.* Protein tyrosine phosphatases, such as the molecule CD45 expressed in both B cells and T cells, play important roles in activating such protein tyrosine kinases as Fyn and Lck, which are quite similar to Src. Suggest a mechanism for the activation of such protein kinases by the removal of a phosphoryl group from a phosphotyrosine residue.

Data Interpretation Problem

19. *Affinity maturation.* A mouse is immunized with an oligomeric human protein. Shortly after immunization, a cell line that expresses a single type of antibody molecule (antibody A) is derived. The ability of antibody A to bind the human protein is assayed, with the results shown in the graph below.

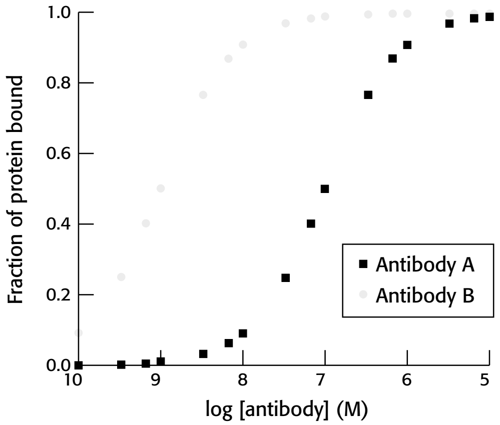

After repeated immunizations with the same protein, another cell line is derived that expresses a different antibody (antibody B). The results of analyzing the binding of antibody B to the protein also are shown. From these data, estimate

(a) the dissociation constant (K_d) for the complex between the protein and antibody A.

(b) the dissociation constant for the complex between the protein and antibody B.

Comparison of the amino acid sequences of antibody A and antibody B reveals them to be identical except for a single amino acid. What does this finding suggest about the mechanism by which the gene encoding antibody B was generated?

CHAPTER

35

Molecular Motors

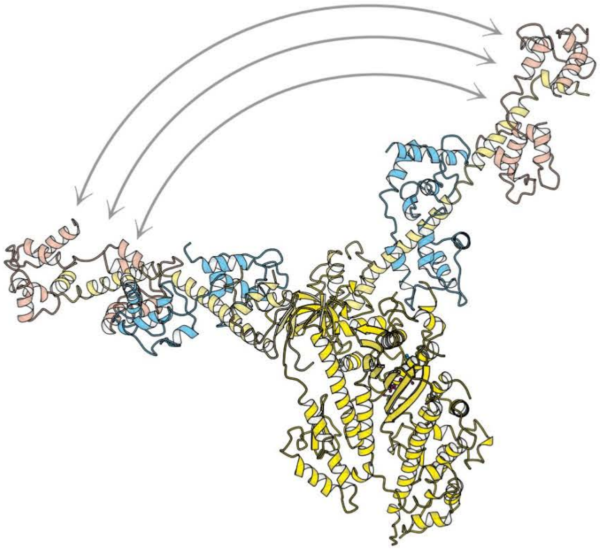

The impressive muscles of the horse, like the muscles of all animals, are powered by the molecular-motor protein myosin. A part of myosin moves dramatically (as shown above) in response to ATP binding, hydrolysis, and product release, propelling myosin along an actin filament. This molecular movement is translated into movement of the entire animal, vividly depicted in da Vinci's rearing horse. [(Left) The Royal Collection © 2014 Her Majesty Queen Elizabeth II/Bridgeman Images.]

OUTLINE

35.1 Most Molecular-Motor Proteins Are Members of the P-Loop NTPase Superfamily

35.2 Myosins Move Along Actin Filaments

35.3 Kinesin and Dynein Move Along Microtubules

35.4 A Rotary Motor Drives Bacterial Motion

Organisms, from human beings to bacteria, move to adapt to changes in their environments, navigating toward food and away from danger. Cells themselves are not static but are bustling assemblies of moving proteins, nucleic acids, and organelles. This motion is enabled by two elements: molecular-motor proteins and complex networks of filamentous proteins termed the *cytoskeleton* (Figure 35.1). The dynamic networks that determine the shape and mobility of calls are among the most active areas of investigation in modern cell biology. Remarkably, the fundamental biochemical mechanisms that produce contractions in our muscles are the same as those that propel organelles along the cytoskeleton. In fact, many of the proteins that play key roles in converting chemical energy into kinetic energy are members of the same protein family, the P-loop NTPases, the hugely important group of proteins that we first examined in Chapter 9. These molecular motors are homologous to proteins that we have encountered in other contexts, including the G proteins in protein synthesis, signaling, and other processes. Once again, we see the economy of evolution in adapting existing proteins to perform new functions.

Molecular motors operate by small increments, converting changes in protein conformation into directed motion. Orderly motion across distances requires a track that steers the motion of the motor assembly. Indeed, we have already encountered a class of molecular motors that utilize mechanisms that we will examine here—namely, the helicases that move along DNA during DNA replication (Section 28.1). The proteins on which we will focus in this chapter move along actin and microtubules—protein filaments composed of repeating subunits. The motor proteins cycle between forms having high or low affinity for the filament tracks in response to ATP binding and hydrolysis, enabling a bind, pull, and release mechanism that generates motion.

We will also consider a completely different strategy for generating motion, one used by bacteria such as *E. coli*. A set of flagella act as propellers, rotated by a motor in the bacterial cell membrane. This rotary motor is driven by a proton gradient across the membrane, rather than by ATP hydrolysis. The mechanism for coupling the proton gradient to rotatory motion is analogous to that used by the F_0 subunit of ATP synthase. Thus, both of the major modes for storing biochemical energy—namely, ATP and ion gradients—have been harnessed by evolution to drive organized molecular motion.

FIGURE 35.1 Motion within cells. This high-voltage electron micrograph shows the mitotic apparatus in a metaphase mammalian cell. The large cylindrical objects are chromosomes, and the threadlike structures stretched across the center are microtubules, key components of the skeleton. Microtubules serve as tracks for the molecular motors that move chromosomes. Many processes, including chromosome segregation in mitosis, depend on the action of molecular-motor proteins. [Courtesy of Dr. J. R. McIntosh.]

35.1 Most Molecular-Motor Proteins Are Members of the P-Loop NTPase Superfamily

Eukaryotic cells contain three major families of motor proteins: myosins, kinesins, and dyneins. Members of each of these classes move along components of the cytoskeleton, but, at first glance, these protein families appear to be quite different from one another. *Myosin*, first characterized on the basis of its role in muscle, moves along filaments of the protein actin. Each molecule of muscle myosin consists of two copies each of a *heavy chain* with a molecular mass of 220 kDa, an *essential light chain*, and a *regulatory light chain*. The human genome encodes more than 40 distinct myosins; some function in muscle contraction, and others participate in a variety of other processes. *Kinesins,* which have roles in protein, mRNA, and vesicle transport as well as construction of the mitotic spindle and chromosome segregation, are generally dimers of two polypeptides. The human genome encodes more than 40 kinesins. *Dyneins* power the motion of cilia and flagella, and a general cytoplasmic dynein contributes to a variety of motions in all cells, including vesicle transport and various transport events in mitosis. Dyneins are enormous, with heavy chains of molecular mass greater than 500 kDa. The human genome encodes approximately 10 dyneins.

Initially, comparison of the amino acid sequences of myosins, kinesins, and dyneins did not reveal significant relationships between these protein families but, after their three-dimensional structures were determined, members of the myosin and kinesin families were found to have remarkable similarities. In particular, both myosin and kinesin contain P-loop NTPase cores homologous to those found in G proteins. Sequence analysis of the dynein heavy chain reveals it to be a member of the AAA subfamily of P-loop NTPases that we encountered in the context of the 19S proteasome (Section 23.2). Dynein has six sequences encoding such P-loop NTPase domains arrayed along its length, although only four actually appear to bind nucleotides. Thus, we expect similarities in the mechanisms of action, and we can draw on our knowledge of P-loop NTPases in general as we analyze the mechanisms of action of these motor proteins.

Molecular motors are generally oligomeric proteins with an ATPase core and an extended structure

Let us first consider the structure of myosin, which we examined briefly in Chapter 9. The results of electron microscopic studies of skeletal-muscle

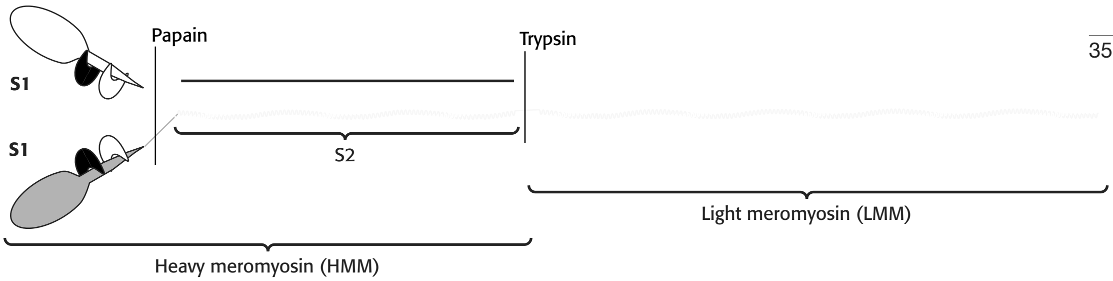
Papain
Trypsin
S1
S1
S2
Light meromyosin (LMM)
Heavy meromyosin (HMM)

FIGURE 35.2 Myosin dissection. Treatment of muscle myosin with proteases forms stable fragments, including subfragments S1 and S2 and light meromyosin. Each S1 fragment includes a head (shown in yellow or purple) from the heavy chain and one copy of each light chain (shown in blue and orange).

myosin show it to be a two-headed structure linked to a long stalk (Figure 9.42). The treatment of myosin with trypsin and papain results in the formation of four fragments: two S1 fragments; heavy meromyosin (HMM) which consists of the S1 fragments and an additional region termed S2; and a fragment called light meromyosin (LMM; Figure 35.2). Each *S1 fragment* corresponds to one of the heads of the intact structure and includes 850 amino-terminal amino acids from one of the two heavy chains as well as one copy of each of the light chains. Examination of the structure of an S1 fragment at high resolution reveals the presence of the P-loop NTPase-domain core that is the site of ATP binding and hydrolysis (Figure 35.3). We examined the structure and mechanism of action of this motor domain in Chapter 9.

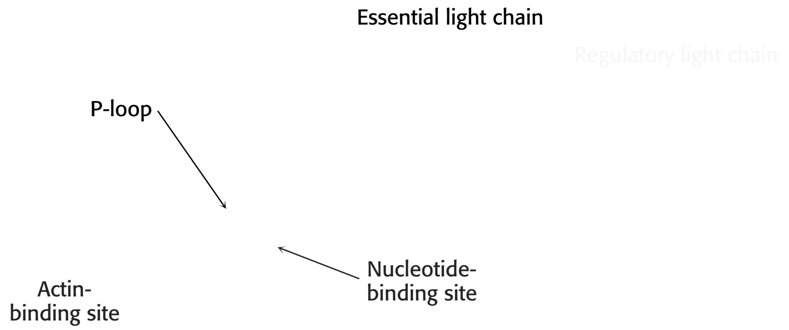
Essential light chain
Regulatory light chain
P-loop
Nucleotide-binding site
Actin-binding site

FIGURE 35.3 Myosin structure at high resolution. The structure of the S1 fragment from muscle myosin reveals the presence of a P-loop NTPase domain (shaded in purple). Notice that an α helix extending from this domain is the binding site for the two light chains. [Drawn from 1DFL.pdb.]

Extending away from this structure is a long α helix from the heavy chain. This helix is the binding site for the two light chains. The light chains are members of the EF-hand family, similar to calmodulin (Figure 14.17), although most of the EF hands in light chains do not bind metal ions (Figure 35.4). Like calmodulin, these proteins wrap around an α helix, serving to thicken and

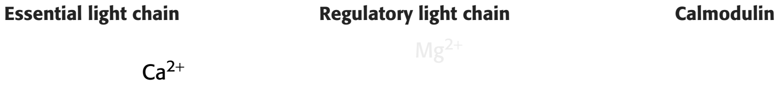
Essential light chain
Regulatory light chain
Calmodulin
Mg2+
Ca2+

FIGURE 35.4 Myosin light chains. The structures of the essential and regulatory light chains of muscle myosin are compared with the structure of calmodulin. Notice the similarities in the structures that allow each of these homologous proteins to bind an α helix (not shown) by wrapping around it. [Drawn from 1DFL.pdb and 1CM1.pdb.]

stiffen it. The remaining fragments of myosin—S2 and light meromyosin—are largely α helical, forming two-stranded coiled coils created by the remaining lengths of the two heavy chains wrapping around each other (Figure 35.5). These structures, together extending approximately 1700 Å, link the myosin heads to other structures. In muscle myosin, several LMM domains come together to form higher-order bundles.

Conventional kinesin (kinesin 1), the first kinesin discovered, has several structural features in common with myosin. The dimeric protein has two heads connected by an extended structure (Figure 35.6). The size of the head domain is approximately one-third that of myosin. Determination of the three-dimensional structure of a kinesin fragment revealed that the head domain also is built around a P-loop NTPase core (Figure 35.7). The myosin domain is so much larger than that of kinesin because of two large insertions in the myosin domain that bind to actin filaments. For conventional kinesin, a region of approximately 500 amino acids extends from the head domain. Like the corresponding region in myosin, the extended part of kinesin forms an α-helical coiled coil. Conventional kinesin also has light chains, but, unlike those of myosin, these light chains bind near the carboxyl terminus of the heavy chain and are thought to link the motor to intracellular cargo.

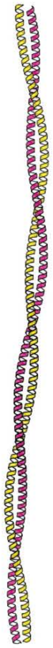

FIGURE 35.5 Myosin two-stranded coiled coil. The two α helices form left-handed supercoiled structures that spiral around each other. Such structures are stabilized by hydrophobic residues at the contact points between the two helices. [Drawn from 2TMA.pdb.]

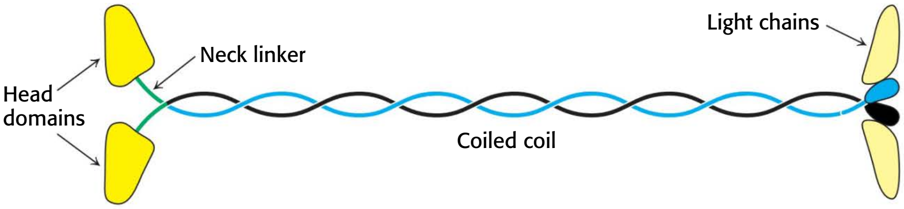

FIGURE 35.6 Structure of kinesin. The elongated structure has the head domains at one end and the cargo-binding domains at the other, linked by a long coiled-coil region.

Dynein has a significantly different structure than myosin or kinesin. As noted earlier, the dynein heavy chain includes six regions that are homologous to the AAA subfamily of ATPase domains. A model for the structure of the motor domain of dynein was generated based on the structures of other AAA ATPases. This model has been confirmed and extended by more recent structure determinations of dynein itself (Figure 35.8). The head domain is appended to a region of approximately 1300 amino acids that forms an extended structure that links dynein units together to form oligomers and interacts with other proteins.

Although the structures of these three classes of molecular motors have significant differences, some common features emerge. Almost all structures are dimeric with two head domains, have regions of extended but quite rigid structures, and have regions for interacting with other proteins. As we shall see, these structures are suitable for actions that resemble climbing a rope, hand over hand. The regions for interacting with other proteins represent the grasping hands, the extended structures represent the arms that act as levers to promote larger-scale motion, and the head domains are the engines that provide the necessary mechanical energy.

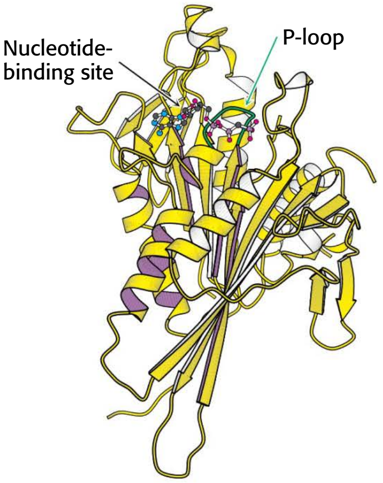

FIGURE 35.7 Structure of head domain of kinesin at high resolution. *Notice* that the head domain of kinesin has the structure of a P-loop NTPase core (indicated by purple shading). [Drawn from 1I6I.pdb.]

ATP binding and hydrolysis induce changes in the conformation and binding affinity of motor proteins

In Chapter 9, we examined the conformational changes that take place in the myosin ATPase domain from the slime mold *Dictyostelium*. The structures

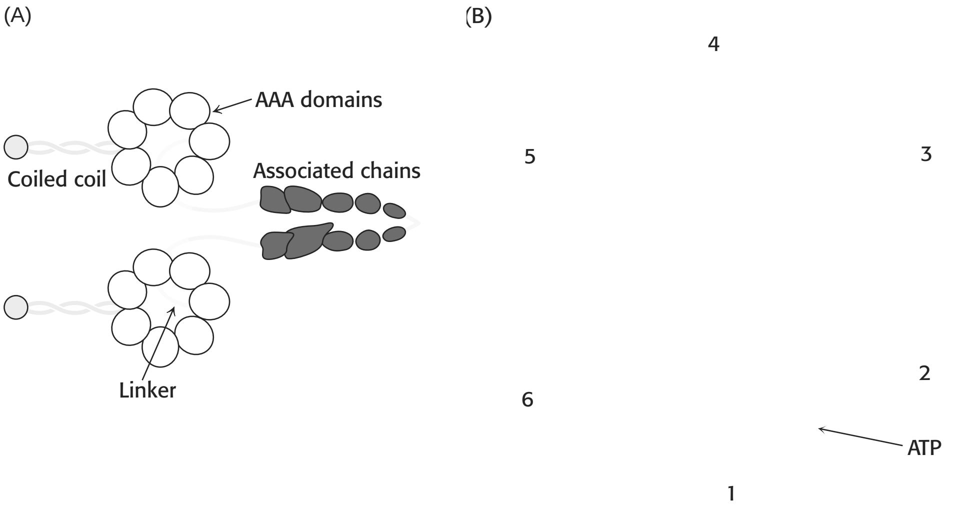

FIGURE 35.8 Dynein structure. (A) The overall structure of dynein. (B) A model of the motor domain of dynein. **Notice** the six P-loop NTPase domains, some of which bind to and hydrolyze ATP. [Drawn from 1HN5.pdb.]

of myosin ATP domains from other sources have been elucidated in a variety of forms as well. The S1 fragment of myosin from scallop muscle provides a striking example of the changes observed (Figure 35.9). The structure of this S1 fragment has been determined in a number of forms including that without bound nucleotide and that bound to a complex formed of ADP and vanadate (VO_4^{3-}), which, as mentioned in Chapter 9, is an analog of the ATP-hydrolysis transition state. The long helix that binds the light chains (hereafter referred to as the *lever arm*) protrudes outward from the head domain. Comparison of the structures reveals that the lever arm has rotated by nearly 90 degrees in the ADP–VO_4^{3-} complex compared with its position in the nucleotide-free form. How does the species in the nucleotide-binding site cause this dramatic transition? Two regions around the nucleotide-binding site (termed *switch I* and *switch II*) tightly conform to the shape of the γ-phosphoryl group of the ATP analog and adopt a looser

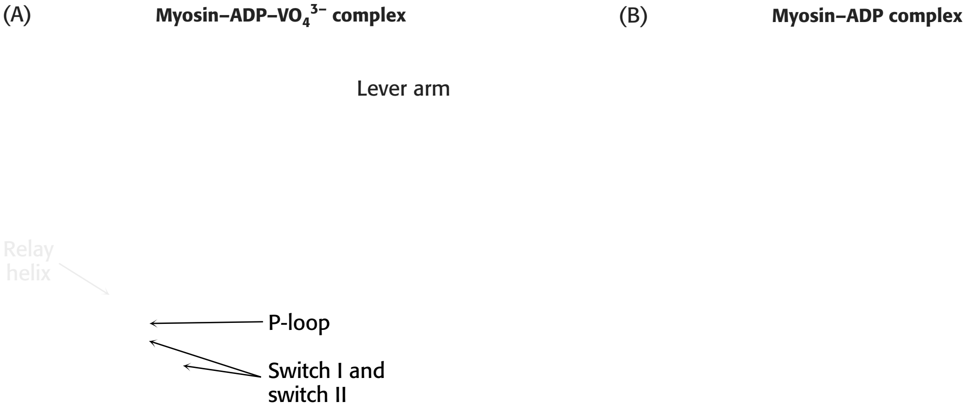

FIGURE 35.9 Lever-arm motion. Two forms of the S1 fragment of scallop-muscle myosin. **Notice** the dramatic conformational changes when the identity of the bound nucleotide changes from the ADP–VO_4^{3-} complex (A) to the nucleotide-free form (B) or vice versa, including a nearly 90-degree reorientation of the lever arm. [Drawn from 1DFL.pdb and 1SR6.pdb.]

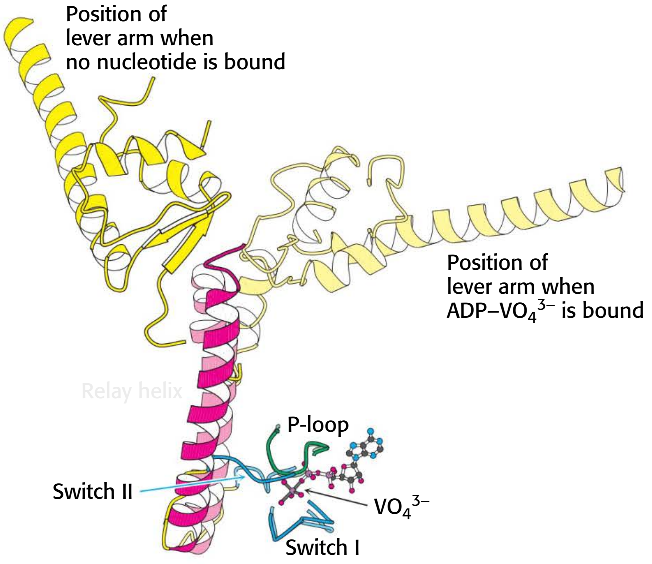

FIGURE 35.10 Relay helix. A superposition of key elements in two forms of scallop myosin reveals the structural changes that are transmitted by the relay helix from the switch I and switch II loops to the base of the lever arm. *Notice* that the switch I and switch II loops interact with VO_4^{3-} in the position that would be occupied by the γ-phosphoryl group of ATP. The structure of the myosin–ADP–VO_4^{3-} complex is shown in lighter colors. [Drawn from 1DFL.pdb and 1SR6.pdb.]

conformation when the γ-phosphoryl group is absent (Figure 35.10). This conformational change allows a long α helix (termed the *relay helix*) to adjust its position. The carboxyl-terminal end of the relay helix interacts with structures at the base of the lever arm, and so a change in the position of the relay helix leads to a reorientation of the lever arm.

Analogous conformational changes take place in kinesin. The kinesins also have a relay helix that can adopt different configurations when kinesin binds different nucleotides. Kinesin lacks an α-helical lever arm, however. Instead, a relatively short segment termed the *neck linker* changes conformation in response to nucleotide binding (Figure 35.11). The neck linker binds to the head domain of kinesin when ATP is bound but is released when the nucleotide-binding site is vacant or occupied by ADP.

35.2 Myosins Move Along Actin Filaments

Myosins, kinesins, and dyneins move by cycling between states with different affinities for the long, polymeric macromolecules that serve as tracks along which they move. For myosin, the molecular track is a polymeric form of *actin,* a 42-kDa protein that is among the most abundant in cells, typically accounting for as much as 10% of the protein in eukaryotic cells. We begin with a general discussion of the polymeric structure of actin and its assembly. We then examine the interactions between myosin and actin, including both structure and the dynamic interactions between these two proteins. Finally, we turn to the structure of muscle and the roles of myosin and actin in muscle contraction.

Actin is a polar, self-assembling, dynamic polymer

The structure of the actin monomer has been determined to atomic resolution by x-ray crystallography and has been used to interpret the structure of actin filaments, already somewhat understood through electron microscopy studies at lower resolution. Each actin monomer comprises four domains

FIGURE 35.11 Neck linker. A comparison of the structures of a kinesin bound to ADP and bound to an ATP analog. *Notice* that the neck linker (orange), which connects the head domain to the remainder of the kinesin molecule, is bound to the head domain in the presence of the ATP analog but is free in the presence of ADP only. [Drawn from 1I6I.pdb and 1I5S.pdb.]

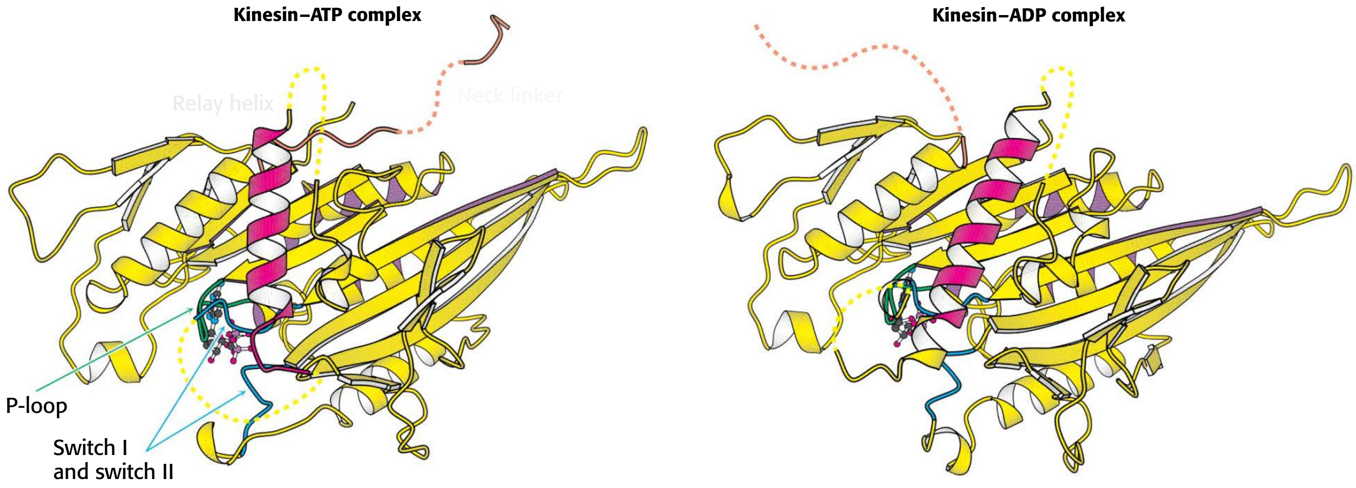

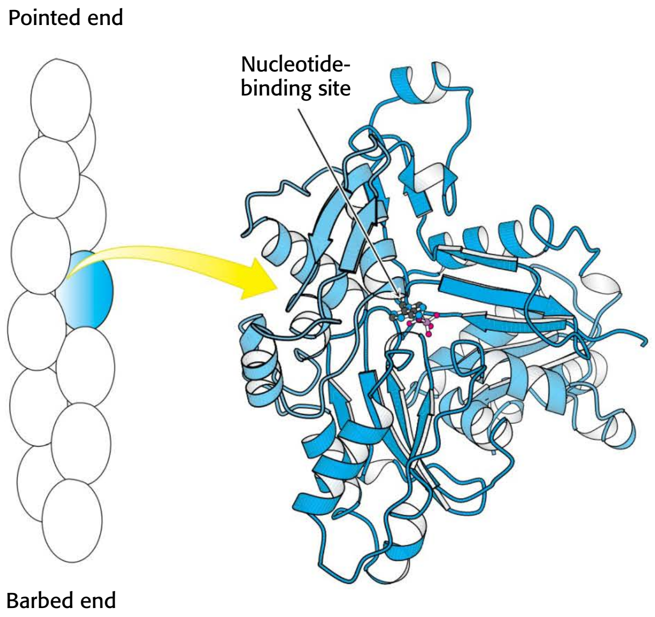

FIGURE 35.12 Actin structure. (Left) Schematic view of actin monomers (one in blue) of an actin filament. (Right) The domains in the four-domain structure of an actin monomer are identified by different shades of blue. *Notice* the nucleotide-binding site at the center of the structure. [Drawn from 1J6Z.pdb.]

(Figure 35.12). These domains come together to surround a bound nucleotide, either ATP or ADP. The ATP form can be converted into the ADP form by hydrolysis.

Actin monomers (often called *G-actin* for globular) come together to form actin filaments (often called *F-actin;* see Figure 35.12). F-actin has a helical structure; each monomer is related to the preceding one by a translation of 27.5 Å and a rotation of 166 degrees around the helical axis. Because the rotation is nearly 180 degrees, F-actin resembles a two-stranded cable. Note that each actin monomer is oriented in the same direction along the F-actin filament, and so the structure is polar, with discernibly different ends. One end is called the barbed (plus) end, and the other is called the pointed (minus) end. The names "barbed" and "pointed" refer to the appearance of an actin filament when myosin S1 fragments are bound to it.

How are actin filaments formed? Like many biological structures, actin filaments self-assemble; that is, under appropriate conditions, actin monomers will come together to form well-structured, polar filaments. The aggregation of the first two or three monomers to form a filament is highly unfavorable. Thus, specialized protein complexes, including one called Arp2/3, serve as nuclei for actin assembly in cells. Once such a filament nucleus exists, the addition of subunits is more favorable. Let us consider the polymerization reaction in more detail. We designate an actin filament with n subunits A_n. This filament can bind an additional actin monomer, A, to form A_{n+1}.

$$K_d = \frac{[A_n][A]}{[A_{n+1}]}$$

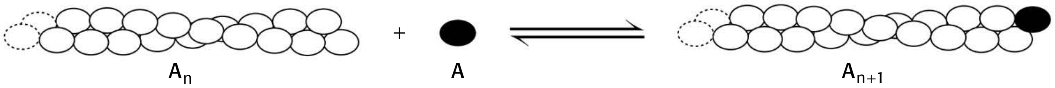

The dissociation constant, K_d, for this reaction, defines the monomer concentrations at which the polymerization reaction will take place, because the concentration of polymers of length $n + 1$ will be essentially equal to that for polymers of length n. Thus,

$$[A_n] \sim [A_{n+1}] \qquad \text{and} \qquad K_d = \frac{[A_n][A]}{[A_{n+1}]} \sim [A]$$

In other words, the polymerization reaction will proceed until the monomer concentration is reduced to the value of K_d. If the monomer concentration is below the value of K_d, the polymerization reaction will not proceed at all; indeed, existing filaments will depolymerize until the monomer concentration reaches the value of K_d. Because of these phenomena, K_d is referred to as the *critical concentration* for the polymer. Recall that actin contains a nucleotide-binding site that can contain either ATP or ADP. The critical concentration for the actin–ATP complex is approximately 20-fold lower than that for the actin–ADP complex; actin–ATP polymerizes more readily than does actin–ADP.

Actin filaments inside cells are highly dynamic structures that are continually gaining and losing monomers. Nucleation by complexes such as Arp2/3 can initiate the polymerization of actin–ATP. In contrast, the hydrolysis of bound ATP to ADP favors actin *d*epolymerization. This reaction acts as a timer to make actin filaments kinetically unstable as ATP hydrolyzes over time, making the filaments more unstable. Proteins that bind actin monomers or promote the severing of actin filaments also play roles. Polymerization reactions can exert force, pushing or pulling on cell membranes. *Regulated actin polymerization is central to the changes in cell shape associated with cell motility in amebae as well as in human cells such as macrophages.*

Myosin head domains bind to actin filaments

It has not been possible to determine the in vivo structure of a complex between actin and myosin at sufficiently high resolution to discern molecular details. However, treatment of actin filaments with myosin S1 fragments in the absence of ATP results in a complex referred to as *decorated actin* for which the structure has been determined by cryoelectron microscopy to a resolution of 13 Å. Although a structure at this resolution alone would not be adequate to observe molecular details, superimposition of the high-resolution structures of actin monomers and the myosin S1 fragment on the structure of decorated actin can be a source of insight into the details of its structure (Figure 35.13). The myosin head domain is in a conformation close to that observed for the nucleotide-free form. This structure also reveals the interaction surfaces between myosin and actin. The modeling suggests that the myosin head-domain conformation changes somewhat to increase its interaction with the actin filament. These conformational changes result in a slight opening of the nucleotide-binding site in myosin. This observation has implications for the mechanism by which myosin moves along actin filaments.

Motions of single motor proteins can be directly observed

Now that we understand the conformational changes behind myosin's action, we can explore how myosin "walks" along its actin track. Studies of *single myosin molecules* moving relative to actin filaments have been sources of deep insight into the mechanisms underlying muscle contraction and

(A)

(B)

FIGURE 35.13 The structure of myosin bound to actin. (A) The gray surface represents the structure observed by cryoelectron microscopy, with the green space-filling model representing one actin subunit. The ribbon diagram shows the structure of the S1 fragment of myosin docked into the cryoelectron microscopic structure. *Notice* that some of the myosin structure lies outside the gray surface. (B) The structure after the myosin S1 fragment has been allowed to adjust to more closely match the structure observed by cryoelectron microscopy. *Notice* that the myosin structure now more closely matches the gray surface. [M. Lorenz and K. Holmes. *PNAS* 2010 (107) 12529–12534. Copyright 2010 National Academy of Sciences.]

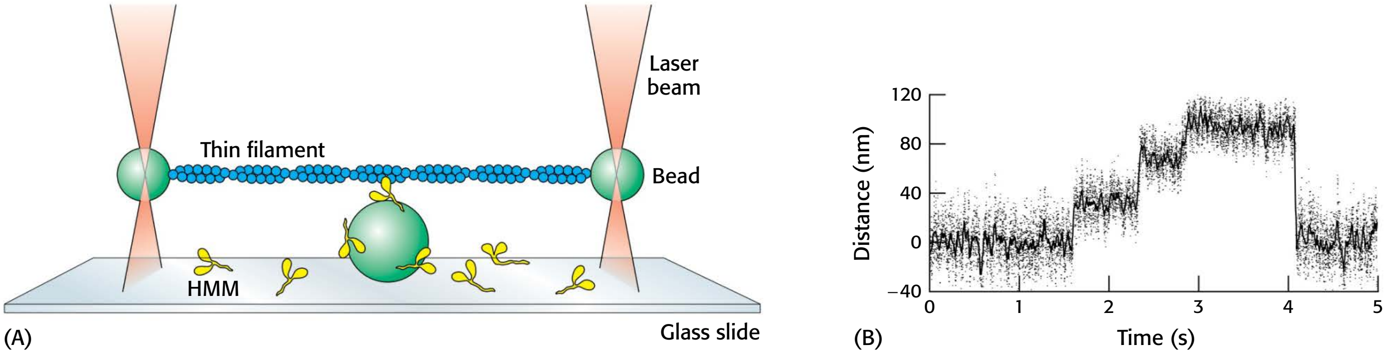

FIGURE 35.14 Watching a single motor protein in action. (A) An actin filament (blue) is placed above a heavy meromyosin (HMM) fragment (yellow) that projects from a bead on a glass slide. A bead attached to each end of the actin filament is held in an optical trap produced by a focused, intense infrared laser beam (orange). The position of these beads can be measured with nanometer precision. (B) Recording of the displacement of an actin filament due to a myosin derivative attached to a bead, influenced by the addition of ATP. Note the fairly uniform step sizes that are observed. [(A) Information from J. T. Finer, R. M. Simmons, and J. A. Spudich, *Nature* 368:113–119, 1994. (B) Data from R. S. Rock, M. Rief, A. D. Metra, and J. A. Spudich, *Methods* 22:378–381, 2000.]

other complex processes. A powerful tool for these studies, called an *optical trap,* relies on highly focused laser beams (Figure 35.14). Small beads can be caught in these traps and held in place in solution.

The position of the beads can be monitored with nanometer precision. James Spudich and his coworkers designed an experimental arrangement consisting of an actin filament that had a bead attached to each end. Each bead could be caught in an optical trap (one at each end of the filament) and the actin filament could be pulled taut over a microscope slide containing other beads that had been coated with fragments of myosin such as the heavy meromyosin fragment (Figure 35.14). On the addition of ATP, transient displacements of the actin filament were observed along its long axis. The size of the displacement steps was fairly uniform with an average size of 11 nm (110 Å).

The results of these studies, performed in the presence of varying concentrations of ATP, are interpreted as showing that individual myosin heads bind the actin filament and undergo a conformational change (the *power stroke*) that pulls the actin filament, leading to the displacement of the beads. After a period of time, the myosin head releases the actin, which then snaps back into place.

Phosphate release triggers the myosin power stroke

How does ATP hydrolysis drive the power stroke? A key observation is that the addition of ATP to a complex of myosin and actin results in the dissociation of the complex. Thus, ATP binding and hydrolysis cannot be directly responsible for the power stroke. We can combine this fact with the structural observations described earlier to construct a mechanism for the motion of myosin along actin (Figure 35.15). Let us begin with nucleotide-free myosin bound to actin. The binding of ATP to actin results in the dissociation of myosin from actin. With ATP bound and free of actin, the myosin domain can undergo the conformational change associated with the formation of the transition state for ATP hydrolysis. This conformational change results in the reorientation of the lever arm. In this form, the myosin head can dock onto the actin filament; phosphate is released with concomitant motion of the lever arm. *This conformational change represents the power stroke and moves the body of the myosin molecule relative to the actin filament by approximately 110* Å. The release of ADP completes the cycle.

Muscle is a complex of myosin and actin

The mechanism of moving a single myosin molecule relative to an actin filament explains how muscles contract. Vertebrate muscle that is under voluntary control, such as the biceps and triceps in your upper arm, has a banded (striated) appearance when examined under a light microscope. It consists of multinucleated cells that are bounded by an electrically excitable plasma

FIGURE 35.15 Myosin motion along actin. A myosin head (yellow) in the apo form is bound to an actin filament (blue). The binding of ATP (1) results in the release of myosin from actin. The reversible hydrolysis of ATP bound to myosin (2) can result in the reorientation of the lever arm. With ATP hydrolyzed but still bound to actin, myosin can bind actin (3). The release of P_i (4) results in the reorientation of the lever arm and the concomitant motion of actin relative to myosin. The release of ADP (5) completes the cycle.

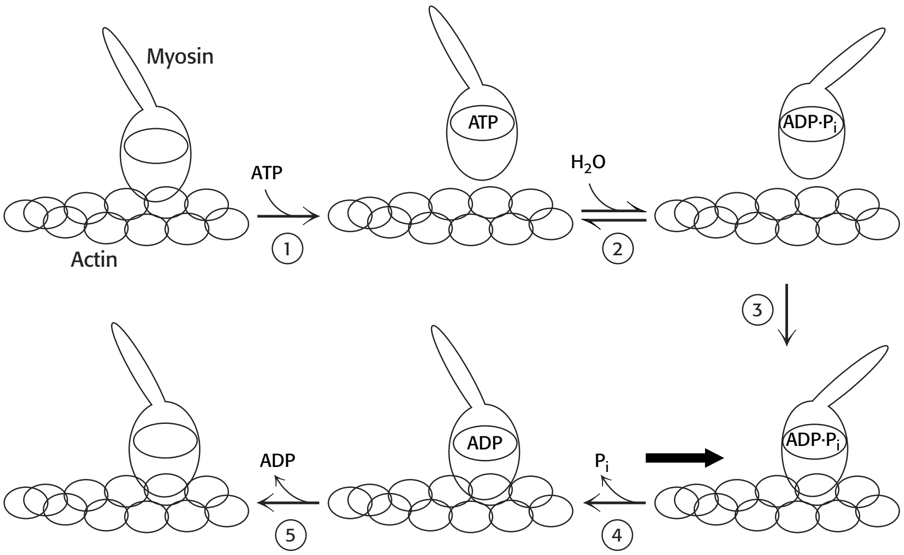

membrane. A muscle cell contains many parallel *myofibrils,* each about 1 μm in diameter. The functional unit, called a *sarcomere,* typically repeats every 2.3 μm (23,000 Å) along the fibril axis in relaxed muscle (Figure 35.16). A dark *A band* and a light *I band* alternate regularly. The central region of the A band, termed the *H zone,* is less dense than the rest of the band. The I band is bisected by a very dense, narrow *Z line*.

The underlying molecular plan of a sarcomere is revealed by cross sections of a myofibril. These cross sections show the presence of two kinds of interacting protein filaments. The *thick filaments* have diameters of about 15 nm (150 Å) and consist primarily of myosin. The *thin filaments* have diameters of approximately 8 nm (80 Å) and consist of actin as well as *tropomyosin* and the *troponin complex*. Muscle contraction is achieved through the sliding of the thin filaments along the length of the thick filaments, driven by the hydrolysis of ATP (Figure 35.17).

To form the thick filaments, myosin molecules self-assemble into thick bipolar structures, with the myosin heads protruding at both ends of a bare region in the center (Figure 35.18A). Approximately 500 head domains line the surface of each thick filament. Each head-rich region associates with two actin filaments, one on each side of the myosin molecules (Figure 35.18B). The interaction of individual myosin heads with actin units creates the sliding force that gives rise to muscle contraction.

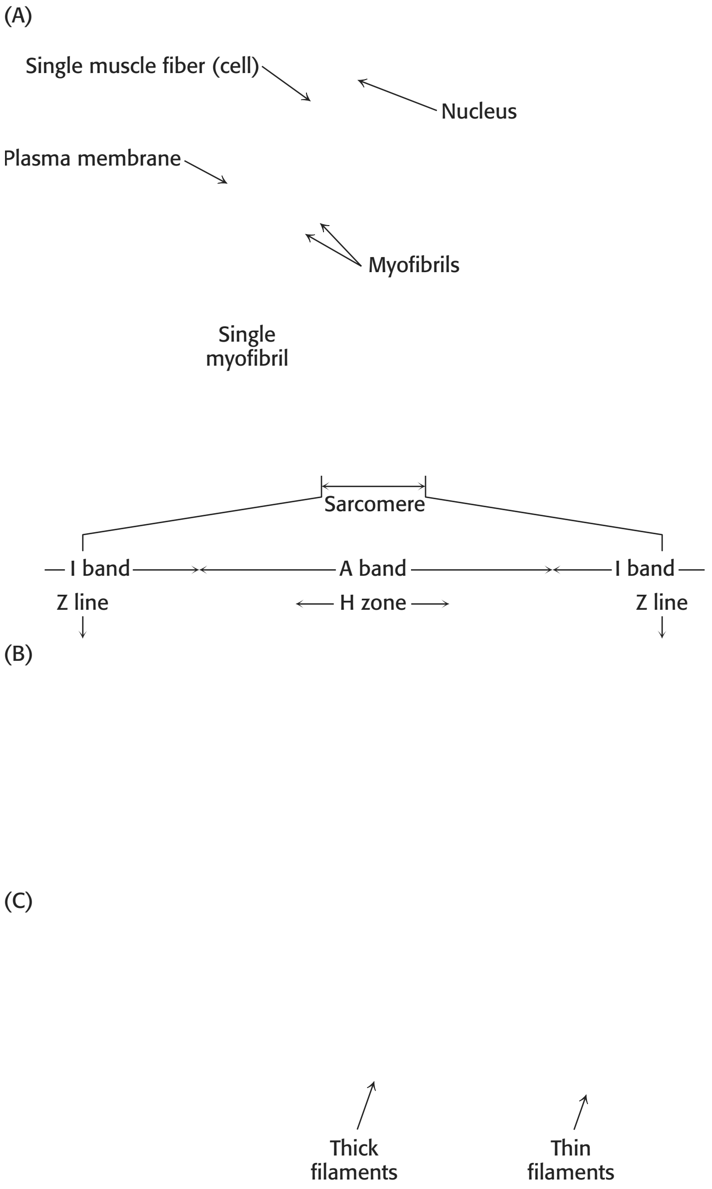

FIGURE 35.16 Sarcomere. (A) Structure of muscle cell and myofibril containing sarcomeres. (B) Electron micrograph of a longitudinal section of a skeletal-muscle myofibril showing a single sarcomere. (C) Schematic representation of the sarcomere corresponding to the regions in the micrograph. [(B) Courtesy of Dr. Hugh Huxley.]

Tropomyosin and the troponin complex regulate this sliding in response to nerve impulses. Under resting conditions, tropomyosin blocks the intimate interaction between myosin and actin. A nerve impulse leads to an increase in calcium ion concentration within the muscle cell. A component of the troponin complex senses the increase in Ca^{2+} and, in response, relieves the inhibition of myosin–actin interactions by tropomyosin.

How does the myosin reaction cycle apply to muscle contraction? Recall that hundreds of head domains project from the ends of each thick filament. The head domains are paired in myosin dimers, but the two heads within each dimer act independently. Actin filaments associate with each head-rich region, with the barbed ends of actin toward the Z line. In the presence of normal levels of ATP, most of the myosin heads are detached from actin. Each head can independently hydrolyze ATP, bind to actin, release P_i, and undergo its power stroke. Because few other heads are attached, the actin filament is relatively free to slide. Each head cycles approximately five times per second with a movement of 110 Å per cycle. However, when hundreds of heads are interacting with the same actin filament, the overall rate of movement of myosin relative to the actin filament may reach 80,000 Å per second, allowing a sarcomere to contract from its fully relaxed to its fully contracted form rapidly. Having many myosin heads briefly and independently attaching and moving an actin filament allows for much greater speed than could be achieved by a single motor protein.

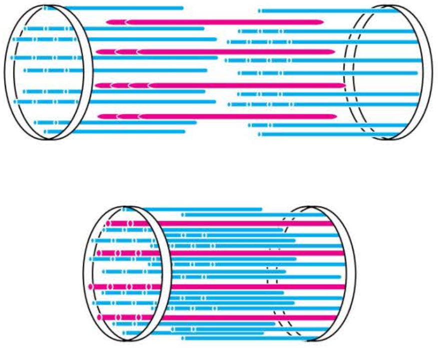

FIGURE 35.17 Sliding-filament model. Muscle contraction depends on the motion of thin filaments (blue) relative to thick filaments (red). [Information from H. E. Huxley. The mechanism of muscular contraction. Copyright © 1965 by Scientific American, Inc. All rights reserved.]

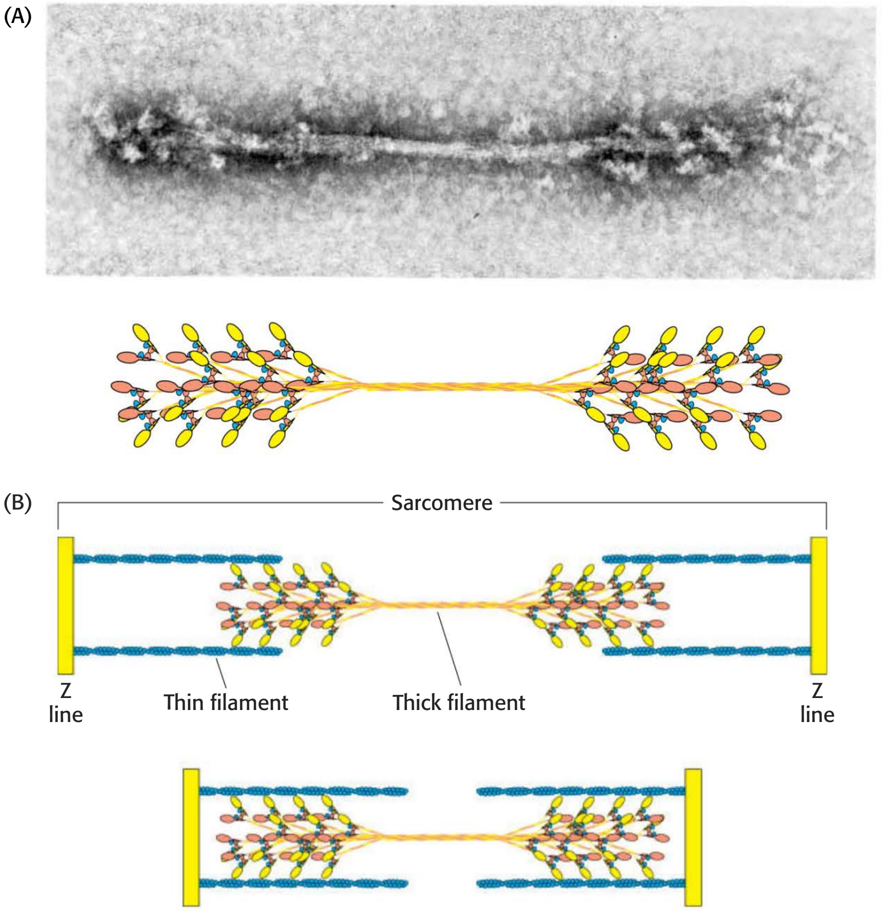

FIGURE 35.18 Thick filament. (A) An electron micrograph of a reconstituted thick filament reveals the presence of myosin head domains at each end and a relatively narrow central region. A schematic view below shows how myosin molecules come together to form the thick filament. (B) A diagram showing the interaction of thick and thin filaments in skeletal-muscle contraction. [(A, top) Courtesy of Dr. Hugh Huxley.]

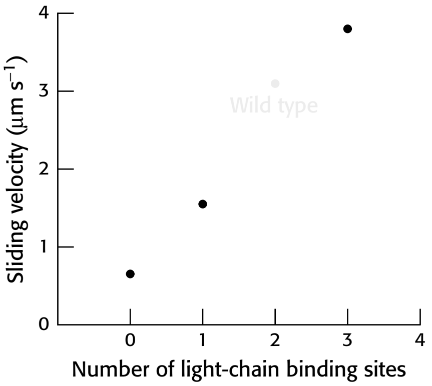

FIGURE 35.19 Myosin lever-arm length. Examination of the rates of actin movement supported by a set of myosin mutants with different numbers of light-chain binding sites revealed a linear relation; the greater the number of light-chain binding sites (and, hence, the longer the lever arm), the faster the sliding velocity. [Data from T. Q. P. Uyeda, P. D. Abramson, and J. A. Spudich, *Proc. Natl. Acad. Sci. U. S. A.* 93:4459–4464, 1996.]

The length of the lever arm determines motor velocity

A key feature of myosin motors is the role of the lever arm as an amplifier. The lever arm amplifies small structural changes at the nucleotide-binding site to achieve the 110-Å movement along the actin filament that takes place in each ATP hydrolysis cycle. A strong prediction of the mechanism proposed for the movement of myosin along actin is that the length traveled per cycle should depend on the length of this lever arm. Thus, the length of the lever arm should influence the overall rate at which actin moves relative to a collection of myosin heads.

This prediction was tested with the use of mutated forms of myosin with lever arms of different lengths. The lever arm in muscle myosin includes binding sites for two light chains (Section 35.1). Thus, investigators shortened the lever arm by deleting the sequences that correspond to one or both of these binding sites. They then examined the rates at which actin filaments were transported along collections of these mutated myosins (Figure 35.19). As predicted, the rate decreased as the lever arm was shortened. A mutated form of myosin with an unusually long lever arm was generated by inserting 23 amino acids corresponding to the binding site for an additional regulatory light chain. Remarkably, this form was found to support actin movement that was *faster than that of the wild-type protein*. These results strongly support the proposed role of the lever arm in contributing to myosin motor activity.

35.3 Kinesin and Dynein Move Along Microtubules

In addition to actin, the cytoskeleton includes other components, notably intermediate filaments and microtubules. Microtubules serve as tracks for two classes of motor proteins—namely, kinesins and dyneins. Kinesins moving along microtubules usually carry cargo such as organelles and vesicles from the center of a cell to its periphery. Dyneins are important in sliding microtubules relative to one another during the beating of cilia and flagella on the surfaces of some eukaryotic cells. Additionally, dynein carries cargo from the cell periphery to the cell center.

Some members of the kinesin family are crucial to the transport of organelles and other cargo to nerve endings at the peripheries of neurons. It is not surprising, then, that mutations in these kinesins can lead to nervous system disorders. For example, mutations in a kinesin called KIF1β can lead to the most common peripheral neuropathy (weakness and pain in the hands and feet), Charcot-Marie-Tooth disease, which affects 1 in 2500 people. A glutamine-to-leucine mutation in the P-loop of the motor domain of this kinesin has been found in some affected persons. Knockout mice with a disruption of the orthologous gene have been generated. Mice heterozygous for the disruption show symptoms similar to those observed in human beings; homozygotes die shortly after birth. Mutations in other kinesin genes have been linked to human spastic paraplegia. In these disorders, defects in kinesin-linked transport may impair nerve function directly, and the decrease in the activity of specific neurons may lead to other degenerative processes.

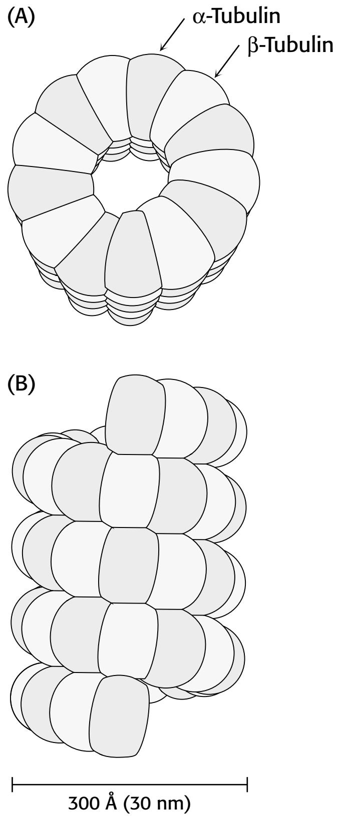

FIGURE 35.20 Microtubule structure. Schematic views of the helical structure of a microtubule. α-Tubulin is shown in dark red and β-tubulin in light red. (A) Top view. (B) Side view.

Microtubules are hollow cylindrical polymers

Microtubules are a major component of the cytoskeleton. They are built from two kinds of homologous 50-kDa subunits, α- and β-tubulin, which assemble in a helical array of alternating tubulin types to form the wall of a hollow cylinder (Figure 35.20). Alternatively, a microtubule can be regarded as 13 protofilaments that run parallel to its long axis. The outer diameter of a microtubule is 30 nm, much larger than that of actin (8 nm). Like actin, microtubules are polar structures. The minus end of a microtubule is anchored near the center of a cell, whereas the plus end extends toward the cell surface.

Microtubules are also key components of cilia and flagella present on some eukaryotic cells. For example, sperm propel themselves through the motion of flagella containing microtubules. The microtubules present in these structures adopt a common architecture (Figure 35.21). A bundle of microtubules called an *axoneme* is surrounded by a membrane contiguous with the plasma membrane. The axoneme is composed of a peripheral group of nine microtubule pairs surrounding two singlet microtubules. This recurring motif is often called a *9 + 2 array.* Dynein drives the motion of one member of each outer pair relative to the other, causing the overall structure to bend.

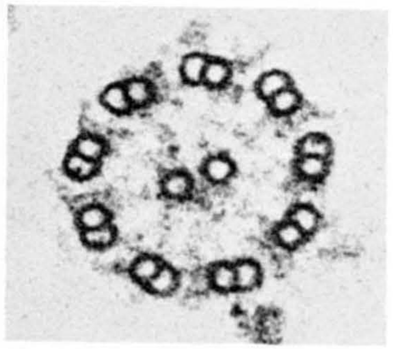

FIGURE 35.21 Microtubule arrangement. Electron micrograph of a cross section of a flagellar axoneme shows nine microtubule doublets surrounding two singlets. [Courtesy of Dr. Joel Rosenbaum.]

Microtubules are important in determining the shapes of cells and in separating daughter chromosomes in mitosis. They are highly dynamic structures that grow through the addition of α- and β-tubulin to the ends of existing structures. Like actin, *tubulins* bind and hydrolyze nucleoside triphosphates, although, for tubulin, the nucleotide is GTP rather than ATP. The critical concentration for the polymerization of the GTP forms of tubulin is lower than that for the GDP forms. Thus, a newly formed microtubule consists primarily of GTP-tubulins. Through time, the GTP is hydrolyzed to GDP. The GDP-tubulin subunits in the interior length of a microtubule remain stably polymerized, whereas GDP subunits exposed at an end have a strong tendency to dissociate. Marc Kirschner and Tim Mitchison found that some microtubules in a population lengthen while others simultaneously shorten. This property, called *dynamic instability,* arises from random fluctuations in the number of GTP- or GDP-tubulin subunits at the plus end of the polymer. The dynamic character of microtubules is crucial for processes such as mitosis, which require the assembly and disassembly of elaborate microtubule-based structures such as spindle fibers.

The structure of a tubulin dimer was determined at high resolution by electron crystallographic methods (Figure 35.22). As expected from their 40% sequence identity, α- and β-tubulin have very similar three- dimensional structures. Further analysis revealed that the tubulins are members of the P-loop NTPase family and contain a nucleotide-binding site adjacent to the P-loop. Tubulins are present only in eukaryotes, although a prokaryotic homolog has been found. Sequence analysis identified a prokaryotic protein called FtsZ (for *f*ilamentous temperature-sensitive mutant *Z*) that is quite similar to the tubulins. The homology was confirmed when the structure was determined by x-ray crystallography. Interestingly, this protein participates in bacterial cell division, forming ring-shaped structures at the constriction that arises when a cell divides. These observations suggest that tubulins may have evolved from an ancient cell-division protein.

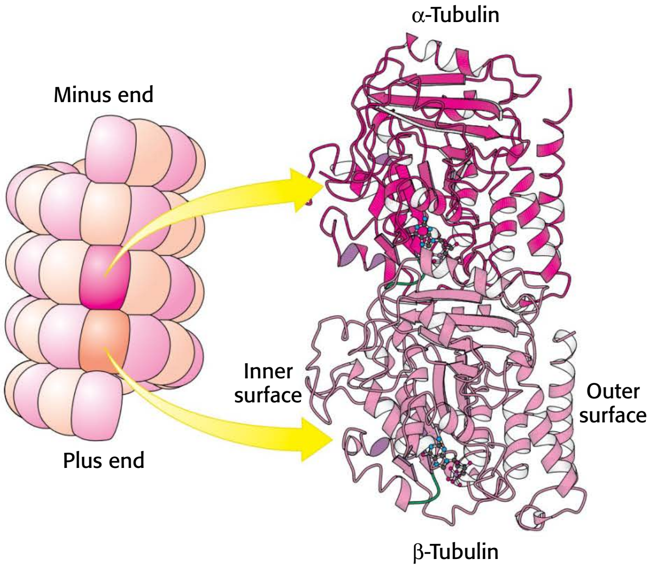

FIGURE 35.22 Tubulin. Microtubules can be viewed as an assembly of α-tubulin–β-tubulin dimers. The structures of α-tubulin and β-tubulin are quite similar. *Notice* that each includes a P-loop NTPase domain (shown in purple) and a bound guanine nucleotide. [Drawn from 1JFF.pdb.]

The continual lengthening and shortening of microtubules is essential to their role in cell division. *Taxol,* a compound isolated from the bark of the Pacific yew tree, was discovered through its ability to interfere with cell proliferation.

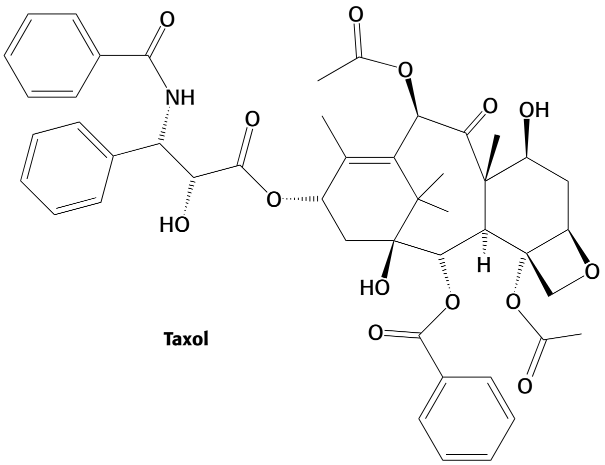

Taxol

Taxol binds to microtubules and stabilizes the polymerized form. Taxol and its derivatives have been developed as anticancer agents because they preferentially affect rapidly dividing cells, such as those in tumors.

Kinesin motion is highly processive

Kinesins are motor proteins that move along microtubules. We have seen that muscle myosin moves along actin filaments by a process in which actin is released in each cycle; a myosin head group acting independently dissociates from actin after every power stroke. In contrast, when a kinesin molecule moves along a microtubule, the two head groups of the kinesin molecule operate in tandem: one binds, and then the next one does. A kinesin molecule may take many steps before both head groups are dissociated at the same time. In other words, the motion of kinesin is highly processive. Single-molecule measurements allow processive motion to be observed (Figure 35.23). A single kinesin molecule will typically take 100 or more steps toward the plus end of a microtubule in a period of seconds before the molecule becomes detached from the microtubule. These measurements also revealed that the average step size is approximately 80 Å, a value that corresponds to the distance between consecutive α- or β-tubulin subunits along each protofilament.

An additional fact is crucial to the development of a mechanism for kinesin motion—namely, that the addition of ATP strongly *increases* the affinity of kinesin for microtubules. This behavior stands in contrast with the behavior of myosin; ATP binding to myosin promotes its *dissociation* from actin. Do these differences imply that kinesin and myosin operate by completely different mechanisms? Indeed not. Kinesin-generated movement

FIGURE 35.23 Monitoring movements mediated by kinesin. (A) The movement of beads or vesicles, carried by individual kinesin dimers along a microtubule, can be directly observed. (B) A trace shows the displacement of a bead carried by a kinesin molecule. Multiple steps are taken in the 6-s interval. The average step size is about 8 nm (80 Å). [(B) Data from K. Svoboda et al., *Nature* 365:721–727, 1993.]

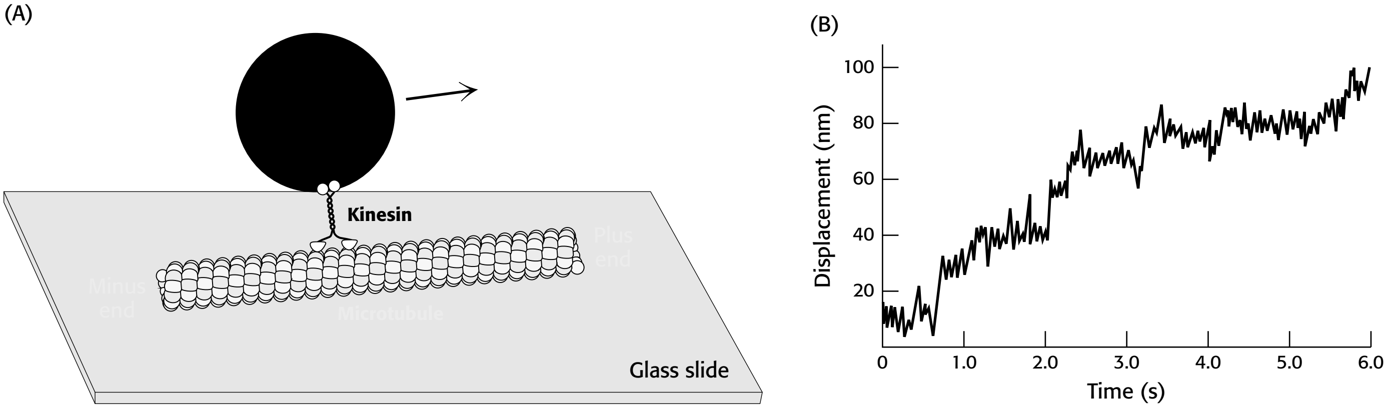

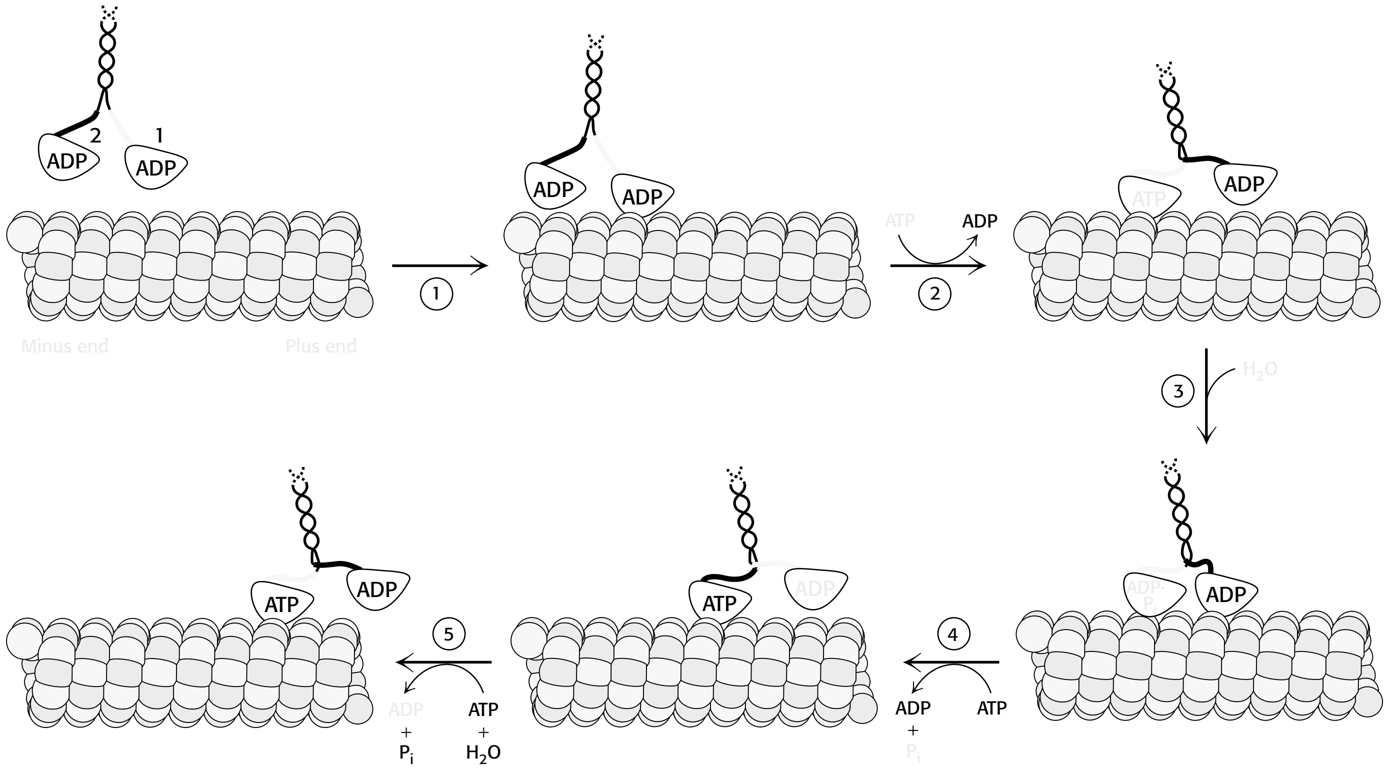

FIGURE 35.24 Kinesin moving along a microtubule. (1) One head of a two-headed kinesin molecule, initially with both heads in the ADP form, binds to a microtubule. (2) The release of ADP and the binding of ATP results in a conformational change that locks the head to the microtubule and pulls the neck linker (orange) to the head domain, throwing the second domain toward the plus end of the microtubule. (3) ATP undergoes hydrolysis while the second head interacts with the microtubule. (4) The exchange of ATP for ADP in the second head pulls the first head off the microtubule, releasing P_i and moving the first domain along the microtubule. (5) The cycle repeats, moving the kinesin dimer farther down the microtubule.

appears to proceed by a mechanism that is quite similar to that used by myosin (Figure 35.24). Let us begin with a two-headed kinesin molecule in its ADP form, dissociated from a microtubule. Recall that the neck linker binds the head domain when ATP is bound and is released when ADP is bound. The initial interaction of one of the head domains with a tubulin dimer on a microtubule stimulates the release of ADP from this head domain and the subsequent binding of ATP. The binding of ATP triggers a conformational change in the head domain that leads to two important events. First, the affinity of the head domain for the microtubule increases, essentially locking this head domain in place. Second, the neck linker binds to the head domain. This change, transmitted through the coiled-coil domain that connects the two kinesin monomers, repositions the other head domain. In its new position, the second head domain is close to a second tubulin dimer, 80 Å along the microtubule in the direction of the plus end. Meanwhile, the intrinsic ATPase activity of the first head domain hydrolyzes the ATP to ADP and P_i. When the second head domain binds to the microtubule, the first head releases ADP and binds ATP. Again, ATP binding favors a conformational change that pulls the first domain forward. This process can continue for many cycles until, by chance, both head domains are in the ADP form simultaneously and kinesin dissociates from the microtubule. Because of the relative rates of the component reactions, a simultaneous dissociation takes place approximately every 100 cycles. Thus, kinesin "walks" hand over hand along the microtubule for approximately 100 steps before both "hands" simultaneously let go. Although recent studies have led to a structural model for the dynein power stroke, the mechanism by which it works is unknown and an interesting research frontier.

Kinesin hydrolyzes ATP at a rate of approximately 80 molecules per second. Thus, given the step size of 80 Å per molecule of ATP, kinesin moves along a microtubule at a speed of 6400 Å per second. This rate is considerably lower than the maximum rate for myosin, which moves relative to actin at

80,000 Å per second. Recall, however, that myosin movement depends on the independent action of hundreds of different head domains working along the same actin filament, whereas the movement of kinesin is driven by the processive action of kinesin head groups working in pairs. Muscle myosin evolved to maximize the speed of the motion, whereas kinesin functions to achieve steady, but slower, transport in one direction along a filament.

35.4 A Rotary Motor Drives Bacterial Motion

In 1 s, a motile bacterium can move approximately 25 μm, or about 10 body lengths. A human being sprinting at a proportional rate would complete the 100-meter dash in slightly more than 5 s. The motors that power this impressive motion are strikingly different from the eukaryotic motors that we have seen so far. In the bacterial motor, an element spins around a central axis rather than moving along a polymeric track. The direction of rotation can change rapidly, a feature that is central to chemotaxis, the process by which bacteria swim preferentially toward an increasing concentration of certain useful compounds and away from potentially harmful ones. One type of flagellar motor, powered by a Na^+ gradient, turns at a rate of 200,000 revolutions per minute.

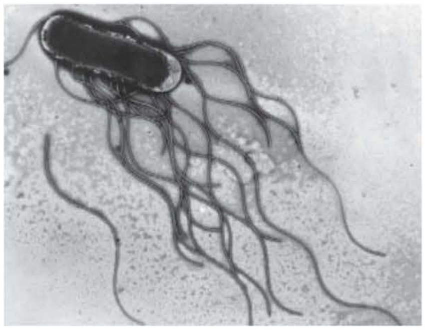

FIGURE 35.25 Bacterial flagella. Electron micrograph of *Salmonella typhimurium* shows flagella directed backwards, where they can form a bundle under appropriate circumstances. [Science Source.]

Bacteria swim by rotating their flagella

Bacteria such as *Escherichia coli* and *Salmonella typhimurium* swim by rotating flagella that lie on their surfaces (Figure 35.25). When the flagella rotate in a counterclockwise direction (viewed from outside a bacterium), the separate flagella form a bundle that very efficiently propels the bacterium through solution.

Bacterial flagella are polymers approximately 15 nm in diameter and as much as 15 μm in length, composed of 53-kDa subunits of a protein called *flagellin* (Figure 35.26). These subunits associate into a helical structure that has 5.5 subunits per turn, giving the appearance of 11 protofilaments. Each flagellum has a hollow core. Remarkably, flagella form not by growing at the base adjacent to the cell body but, instead, by the addition of new subunits that pass through the hollow core and add to the free end. Each flagellum is intrinsically twisted in a left-handed sense. At its base, each flagellum has a rotory motor.

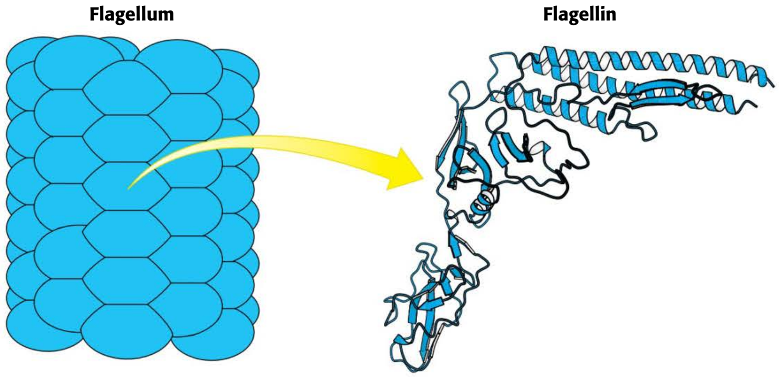

FIGURE 35.26 Structure of flagellin. A bacterial flagellum is a helical polymer of the protein flagellin. *Notice* that each subunit corresponds to a bent structure with a relatively flat surface facing the hollow core of the flagellum. [Drawn from 1IO1.pdb.]

Proton flow drives bacterial flagellar rotation

Early experiments by Julius Adler demonstrated that ATP is *not* required for flagellar motion. What powers these rotary motors? The necessary free energy is derived from the proton gradient that exists across the plasma membrane. The flagellar motor is quite complex, containing as many as 40 distinct proteins (Figure 35.27). Five components particularly crucial to motor function have been identified through genetic studies. MotA is a membrane protein that appears to have four transmembrane helices as well as a cytoplasmic domain. MotB is another membrane protein with a single trans-membrane helix and a large periplasmic domain. Approximately 11 *MotA–MotB pairs* form a ring around the base of the flagellum. The proteins *FliG*, *FliM*, and *FliN* are part of a disc-like structure called the MS (membrane and supramembrane) ring, with approximately 30 FliG subunits coming together to form the ring. The three-dimensional structure of the carboxyl-terminal half of FliG reveals a wedge-shaped domain with a set of charged amino acids, conserved among many species, lying along the thick edge of the wedge (Figure 35.28).

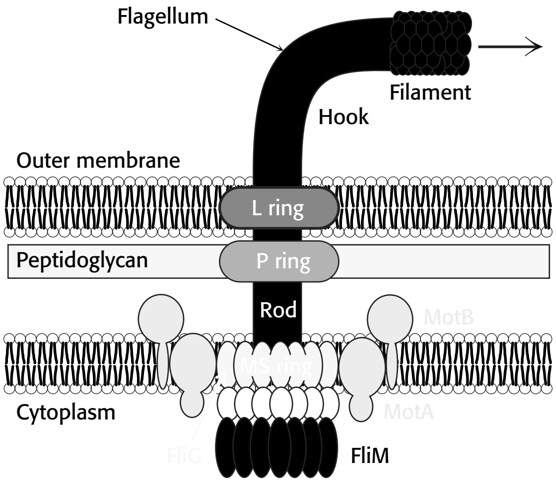

FIGURE 35.27 Flagellar motor. A schematic view of the flagellar motor, a complex structure containing as many as 40 distinct types of protein. The approximate positions of the proteins MotA and MotB (red), FliG (orange), FliN (yellow), and FliM (green) are shown.

The MotA–MotB pair and FliG combine to create a proton channel that drives the rotation of the flagellum. How can proton flow across a membrane drive mechanical rotation? We have seen such a process earlier in regard to ATP synthase (Section 18.4). Recall that the key to driving the rotation of the γ subunit of ATP synthase is the **a** subunit of the F_0 fragment. This subunit appears to have two half-channels; protons can move across the membrane only by moving into the half-channel from the side of the membrane with the higher local proton concentration, binding to a disc-like structure formed by the **c** subunits, riding on this structure as it rotates to the opening of the other half-channel, and exiting to the side with the lower local proton concentration. Could a similar mechanism apply to flagellar rotation? Indeed, such a mechanism was first proposed by Howard Berg to explain flagellar rotation before the rotary mechanism of ATP synthase was elucidated. Each MotA–MotB pair is conjectured to form a structure that has two half-channels; FliG serves as the rotating proton carrier, perhaps with the participation of some of the charged residues identified in crystallographic studies (Figure 35.29). In this scenario, a proton from the periplasmic space passes into the outer half-channel and is transferred to an FliG subunit. The MS ring rotates, rotating the flagellum with it and allowing the proton to pass into the inner half-channel and into the cell. Ongoing structural and mutagenesis studies are testing and refining this hypothesis.

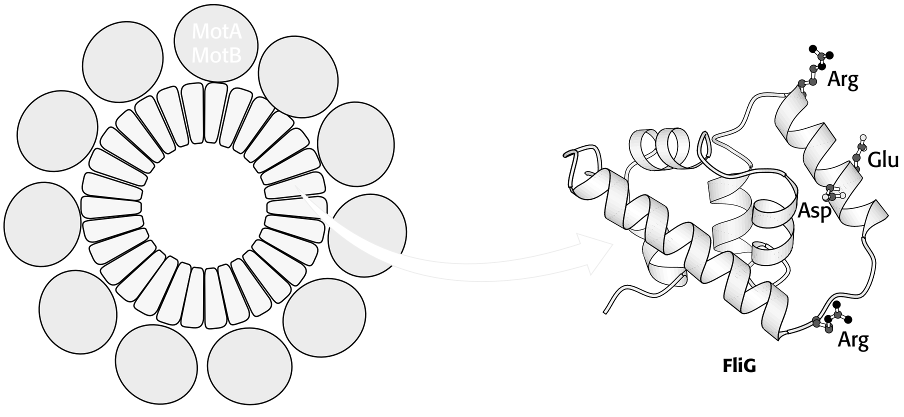

FIGURE 35.28 Flagellar motor components. Approximately 30 subunits of FliG assemble to form part of the MS ring. The ring is surrounded by approximately 11 structures consisting of MotA and MotB. *Notice* that the carboxyl-terminal domain of FliG includes a ridge lined with charged residues that may participate in proton transport. [Drawn from 1QC7.pdb.]

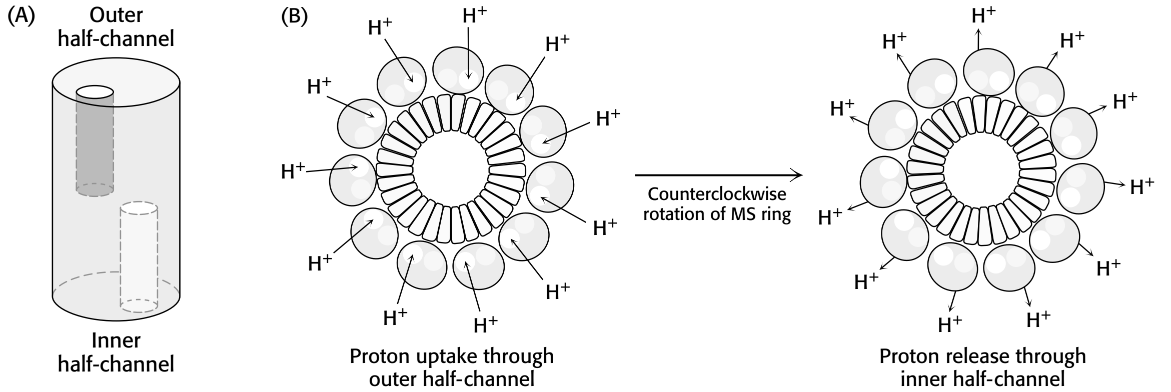
(A)
Outer half-channel
Inner half-channel
(B)
H+
Counterclockwise rotation of MS ring
Proton uptake through outer half-channel
Proton release through inner half-channel

FIGURE 35.29 Proton-transport-coupled rotation of the flagellum. (A) MotA–MotB may form a structure having two half-channels. (B) One model for the mechanism of coupling rotation to a proton gradient requires protons to be taken up into the outer half-channel and transferred to the MS ring. The MS ring rotates in a counterclockwise direction, and the protons are released into the inner half-channel. The flagellum is linked to the MS ring and so the flagellum rotates as well.

Bacterial chemotaxis depends on reversal of the direction of flagellar rotation

Many species of bacteria respond to changes in their environments by adjusting their swimming behavior. Examination of the paths taken is highly revealing (Figure 35.30). The bacteria swim in one direction for some length of time (typically about a second), tumble briefly, and then set off in a new direction. The tumbling is caused by a brief reversal in the direction of the flagellar motor. When the flagella rotate counterclockwise, the helical filaments form a coherent bundle favored by the intrinsic shape of each filament, and the bacterium swims smoothly. When the rotation reverses, the bundle flies apart because the screw sense of the helical flagella does not match the direction of rotation. Each flagellum then pulls in a different direction and the cell tumbles.

In the presence of a gradient of certain substances such as glucose, bacteria swim preferentially toward the direction of the higher concentration of the substance. Such compounds are referred to as *chemoattractants*. Bacteria also swim preferentially away from potentially harmful compounds such as phenol, a *chemorepellant*. The process of moving in specific directions in response to environmental cues is called *chemotaxis*. In the presence of a gradient of a chemoattractant, bacteria swim for longer periods of time without tumbling when moving toward higher concentrations of the chemoattractant. In contrast, they tumble more frequently when moving toward lower concentrations of the chemoattractant. This behavior is reversed for chemorepellants. The result of these actions is a *biased random walk* that facilitates net motion toward conditions more favorable to the bacterium.

Chemotaxis depends on a signaling pathway that terminates at the flagellar motor. The signaling pathway begins with the binding of molecules to receptors in the plasma membrane (Figure 35.31). In their *unoccupied* forms, these receptors initiate a pathway leading eventually to the phosphorylation of a specific aspartate residue on a soluble protein called *CheY*. In its phosphorylated form, CheY binds to the base on the flagellar motor. When bound to phosphorylated CheY, the flagellar motor rotates in a clockwise rather than a counterclockwise direction, causing tumbling.

The binding of a chemoattractant to a surface receptor blocks the signaling pathway leading to CheY phosphorylation. Phosphorylated CheY spontaneously hydrolyzes and releases its phosphoryl group in a process accelerated by another protein, CheZ. The concentration of phosphorylated CheY drops, and the flagella are less likely to rotate in a clockwise direction. Under these conditions, bacteria swim smoothly without tumbling. Thus, the reversible rotary flagellar motor and a phosphorylation-based signaling pathway work together to generate an effective means for responding to environmental conditions.

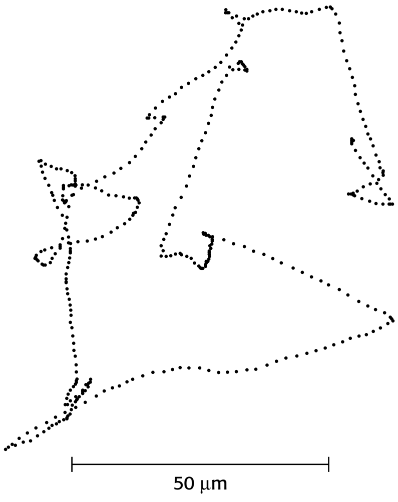

FIGURE 35.30 Charting a course. This projection of the track of an *E. coli* bacterium was obtained with a microscope that automatically follows bacterial motion in three dimensions. The points show the locations of the bacterium at 80-ms intervals. [Information from H. C. Berg, *Nature* 254:389–392, 1975.]

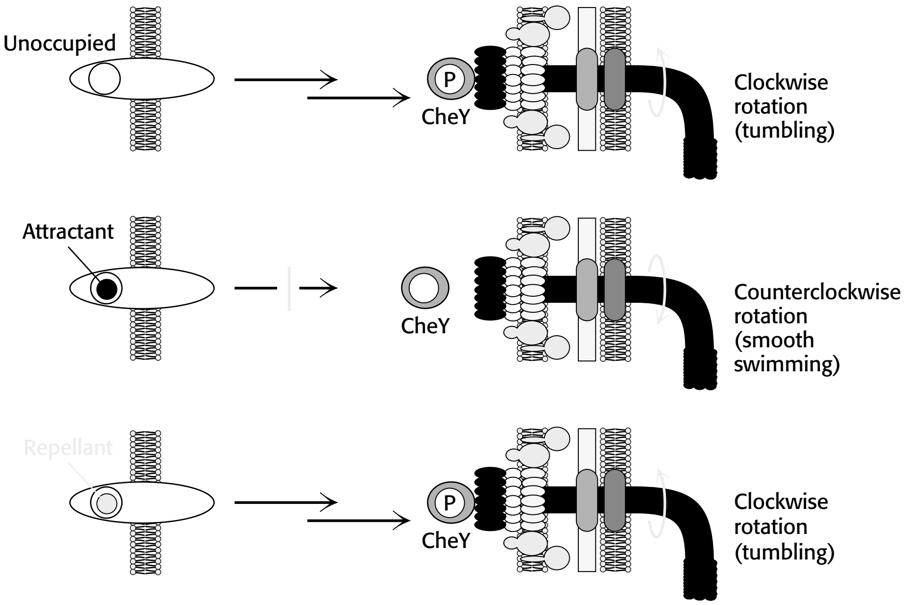

FIGURE 35.31 Chemotaxis signaling pathway. Receptors in the plasma membrane initiate a signaling pathway leading to the phosphorylation of the CheY protein. Phosphorylated CheY binds to the flagellar motor and favors clockwise rotation. When an attractant binds to the receptor, this pathway is blocked, and counterclockwise flagellar rotation and, hence, smooth swimming result. When a repellant binds, the pathway is stimulated, leading to an increased concentration of phosphorylated CheY and, hence, more-frequent clockwise rotation and tumbling.

Bacteria sense spatial gradients of chemoattractants by measurements separated in time. A bacterium sets off in a random direction and, if the concentration of the chemoattractant has increased after the bacterium has been swimming for a period of time, the likelihood of tumbling decreases and the bacterium continues in roughly the same direction. If the concentration has decreased, the tumbling frequency increases and the bacterium tests other random directions. The success of this mechanism once again reveals the power of evolutionary problem solving: many possible solutions are tried at random, and those that are beneficial are selected and exploited.

SUMMARY

35.1 Most Molecular-Motor Proteins Are Members of the P-Loop NTPase Superfamily

Eukaryotic cells contain three families of molecular-motor proteins: myosins, kinesins, and dyneins. These proteins move along tracks defined by the actin and microtubule cytoskeletons of eukaryotic cells, contributing to cell and organismal movement and to the intracellular transport of proteins, vesicles, and organelles. Despite considerable differences in size and a lack of similarity detectable at the level of amino acid sequence, these proteins are homologous, containing core structures of the P-loop NTPase family. The ability of these core structures to change conformations in response to nucleoside triphosphate binding and hydrolysis is key to molecular-motor function. Motor proteins consist of motor domains attached to extended structures that serve to amplify the conformational changes in the core domains and to link the core domains to one another or to other structures.

35.2 Myosins Move Along Actin Filaments

The motile structure of muscle consists of a complex of myosin and actin, along with accessory proteins. Actin, a highly abundant 42-kDa protein, polymerizes to form long filaments. Each actin monomer can bind either ATP or ADP. A myosin motor domain moves along actin filaments in a cyclic manner, beginning with myosin free of bound nucleotides bound to actin: (1) ATP binds to myosin and the myosin is released from actin; (2) a reversible conformational change associated with the hydrolysis of ATP while still bound to myosin leads to a large motion of a lever arm that extends from the motor domain; (3) myosin with bound ADP and P_i binds to actin; (4) P_i is released from myosin, resulting in resetting the position of the lever arm and moving actin relative to myosin; and (5) the release of ADP returns the motor domain to its initial state. The length of the lever arm determines the size of the step taken along actin in each cycle. The ability to monitor single molecular-motor proteins has provided key tests for hypotheses concerning motor function. Muscle contraction entails the rapid sliding of thin filaments, composed of actin, relative to thick filaments, composed of myosin. The thick filaments consist of multiple myosin molecules bound together. Each myosin molecule has two heads that can bind to actin and move it relative to myosin, driven by the hydrolysis of ATP by myosin. Muscle contraction is regulated by tropomyosin and the troponin complex. These proteins prevent actin and myosin from productively interacting until an increase in calcium concentration associated with a nerve impulse results in calcium-induced changes in troponin and tropomyosin.

35.3 Kinesin and Dynein Move Along Microtubules

Kinesin and dynein move along microtubules rather than actin. Microtubules are polymeric structures composed of α- and β-tubulin, two very similar guanine-nucleotide-binding proteins. Each microtubule comprises 13 protofilaments with alternating α- and β-tubulin subunits. Kinesins move along microtubules by a mechanism quite similar to that used by myosin to move along actin but with several important differences. First, ATP binding to kinesin favors motor-domain binding rather than dissociation. Second, the power stroke is triggered by the binding of ATP rather than the release of P_i. Finally, kinesin motion is processive. The two heads of a kinesin dimer work together, taking turns binding and releasing the microtubule, and many steps are taken along a microtubule before both heads dissociate. Most kinesins move toward the plus end of microtubules.

35.4 A Rotary Motor Drives Bacterial Motion

Many motile bacteria use rotating flagella to propel themselves. When rotating counterclockwise, multiple flagella on the surface of a bacterium come together to form a bundle that effectively propels the bacterium through solution. A proton gradient across the plasma membrane, rather than ATP hydrolysis, powers the flagellar motor. The mechanism for coupling transmembrane proton transport to macromolecular rotation appears to be similar to that used by ATP synthase. When rotating clockwise, the flagella fly apart and the bacterium tumbles. Bacteria swim preferentially toward chemoattractants in a process called chemotaxis. When bacteria are swimming in the direction of an increasing concentration of a chemoattractant, clockwise flagellar motion predominates and tumbling is suppressed, leading to a biased random walk in the direction of increasing chemoattractant concentration.

KEY TERMS

cytoskeleton (p. 1011)
myosin (p. 1012)
kinesin (p. 1012)
dynein (p. 1012)
S1 fragment (p. 1013)
conventional kinesin (p. 1014)
lever arm (p. 1015)
relay helix (p. 1016)
neck linker (p. 1016)
actin (p. 1016)
G-actin (p. 1017)
F-actin (p. 1017)

critical concentration (p. 1018)
optical trap (p. 1019)
power stroke (p. 1019)
myofibril (p. 1020)
sarcomere (p. 1020)
thick filaments (p. 1020)
thin filaments (p. 1020)
tropomyosin (p. 1020)
troponin complex (p. 1020)
microtubule (p. 1022)
axoneme (p. 1023)
tubulin (p. 1023)
dynamic instability (p. 1023)
flagellin (p. 1026)
MotA–MotB pair (p. 1027)
FliG (p. 1027)
chemoattractant (p. 1028)
chemorepellant (p. 1028)
chemotaxis (p. 1028)
CheY (p. 1028)

PROBLEMS

1. *Diverse motors.* Skeletal muscle, eukaryotic cilia, and bacterial flagella use different strategies for the conversion of free energy into coherent motion. Compare and contrast these motility systems with respect to (a) the free-energy source and (b) the number of essential components and their identity.

2. *You call that slow?* At maximum speed, a kinesin molecule moves at a rate of 6400 Å per second. Given the dimensions of the motor region of a kinesin dimer of approximately 80 Å, calculate its speed in "body lengths" per second. To what speed does this body-length speed correspond for an automobile 10 feet long?

3. *Heavy lifting.* A single myosin motor domain can generate a force of approximately 4 piconewtons (4 pN). How many times its "body weight" can a myosin motor domain lift? Note that 1 newton = 0.22 pounds (100 g). Assume a molecular mass of 100 kDa for the motor domain.

4. *Compare and contrast.* Describe two similarities and two differences between actin filaments and microtubules.

5. *Lighten up.* What is the primary role of the light chains in myosin? In kinesin?

6. *Rigor mortis.* Propose an explanation for the fact that the body stiffens after death.

7. *Now you see it, now you don't.* Under certain stable concentration conditions, actin monomers in their ATP form will polymerize to form filaments that disperse again into free actin monomers over time. Explain.

8. *Helicases as motors.* Helicases can use single-stranded DNA as tracks. Consider a helicase that moves one base in the $3' \rightarrow 5'$ direction in each cycle. Assuming that the helicase can hydrolyze ATP at a rate of 50 molecules per second in the presence of a single-stranded DNA template, calculate the velocity of the helicase in micrometers per second. How does this velocity compare with that of kinesin?

9. *New moves.* When bacteria such as *E. coli* are starved to a sufficient extent, they become nonmotile. However, when such bacteria are placed in an acidic solution, they resume swimming. Explain.

10. *Going straight.* Suppose you measure the mean distance that an *E. coli* bacterium moves along a straight path before it tumbles over a period of time. Would you expect this distance to change in the presence of a gradient of a chemoattractant? Would it be longer or shorter?

11. *Hauling a load.* Consider the action of a single kinesin molecule in moving a vesicle along a microtubule track. The force required to drag a spherical particle of radius a at a velocity v in a medium having a viscosity η *is*

$$F = 6\pi\eta a v$$

Suppose that a 2-μm-diameter bead is carried at a velocity of 0.6 $\mu\text{m s}^{-1}$ in an aqueous medium ($\eta = 0.01$ poise $= 0.01\ \text{g cm}^{-1}\ \text{s}^{-1}$).

(a) What is the magnitude of the force exerted by the kinesin molecule? Express the value in dynes ($1\ \text{dyne} = 1\ \text{g cm s}^{-2}$).

(b) How much work is performed in 1 s? Express the value in ergs (1 erg = 1 dyne cm).

(c) A kinesin motor hydrolyzes approximately 80 molecules of ATP per second. What is the energy associated with the hydrolysis of this much ATP in ergs? Compare this value with the actual work performed.

12. *Unusual strides.* A publication describes a kinesin molecule that is claimed to move along microtubules with a step size of 6 nm. You are skeptical. Why?

13. *The sound of one hand clapping.* KIF1A is a motor protein that moves toward the plus end of microtubules *as a monomer.* KIF1A has only a single motor domain. What additional structural elements would you expect to find in the KIF1A structure?

14. *Building blocks.* Actin filaments, microtubules, and bacterial flagella are all built from small subunits. Describe three advantages of assembling long filamentous structures from subunits rather than from single, long proteins.

Mechanism Problem

15. *Backward rotation.* On the basis of the proposed structure in Figure 35.29 for the bacterial flagellar motor, suggest

a pathway for transmembrane proton flow when the flagellar motor is rotating clockwise rather than counterclockwise.

Chapter Integration Problem

16. *Smooth muscle.* Smooth muscle, in contrast with skeletal muscle, is not regulated by a tropomyosin–troponin mechanism. Instead, vertebrate smooth-muscle contraction is controlled by the degree of phosphorylation of its light chains. Phosphorylation induces contraction, and dephosphorylation leads to relaxation. Like that of skeletal muscle, smooth-muscle contraction is triggered by an increase in the cytoplasmic calcium ion level. Propose a mechanism for this action of calcium ion on the basis of your knowledge of other signal-transduction processes.

Data Interpretation Problem

17. *Myosin V.* An abundant myosin-family member, myosin V is isolated from brain tissue. This myosin has a number of unusual properties. First, on the basis of its amino acid sequence, each heavy chain has six tandem binding sites for calmodulin-like light chains. Second, it forms dimers but not higher-order oligomers. Finally, unlike almost all other myosin-family members, myosin V is highly processive.

The rate of ATP hydrolysis by myosin has been examined as a function of ATP concentration, as shown in graph A.

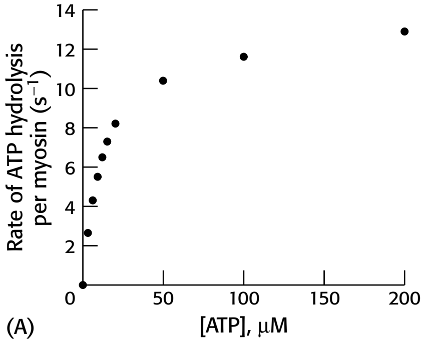

(a) Estimate the values of k_{cat} and K_M for ATP.

With the use of optical-trap measurements, the motion of single myosin V dimers could be followed, as shown in graph B.

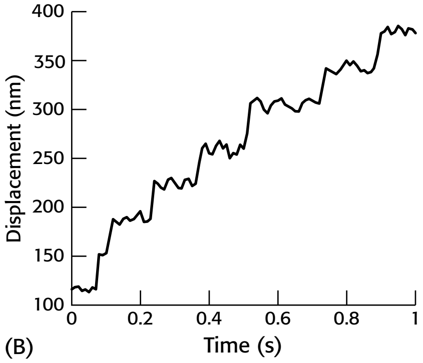

[Based on M. Rief et al., *Proc. Natl. Acad. Sci. U. S. A.* 97:9482–9486, 2000.]

(b) Estimate the step size for myosin V.

The rate of ADP release from myosin V is found to be approximately 13 molecules per second.

(c) Combine the observations about the amino acid sequence of myosin, the observed step size, and the kinetics results to propose a mechanism for the processive motion of myosin V.

CHAPTER

36

Drug Development

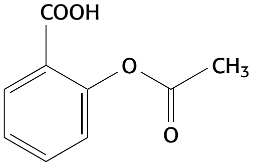

Many drugs are based on natural products. Aspirin (above) is a molecule related to a compound isolated from willow bark (near left). Extracts of willow bark had long been known to have medicinal properties. The active compound was isolated, modified, and, beginning in 1899, packaged for consumers (far left). [(Far left) AP Images/Bayer. (Near left) H. Mark Weidman Photography/Alamy.]

OUTLINE

36.1 The Development of Drugs Presents Huge Challenges

36.2 Drug Candidates Can Be Discovered by Serendipity, Screening, or Design

36.3 Analyses of Genomes Hold Great Promise for Drug Discovery

36.4 The Clinical Development of Drugs Proceeds Through Several Phases

The development of drugs is among the most important interfaces between biochemistry and medicine. Throughout the previous chapters in this book, we have encountered a number of types of proteins—enzymes, receptors, and transporters—that serve as targets for a majority of the drugs in clinical use (Figure 36.1). In most cases, drugs act by binding to these proteins and inhibiting or otherwise modulating their activities. Thus, knowledge of these molecules and the pathways in which they participate is crucial to drug development. An effective drug is much more than a potent modulator of its target, however. Drugs must be readily administered to patients, preferably as small tablets taken orally, and must survive within the body long enough to reach their targets. Furthermore, to prevent unwanted physiological effects, drugs must not modulate the properties of biomolecules other than the intended targets. These requirements tremendously limit the number of compounds that have the potential to be clinically useful drugs.

Drugs have been discovered by two fundamentally distinct approaches (Figure 36.2). The first approach identifies a substance that has a desirable physiological consequence when administered to a human being, to an appropriate animal, or to cells. Such substances can be discovered by serendipity, by the fractionation of plants or other materials known to have

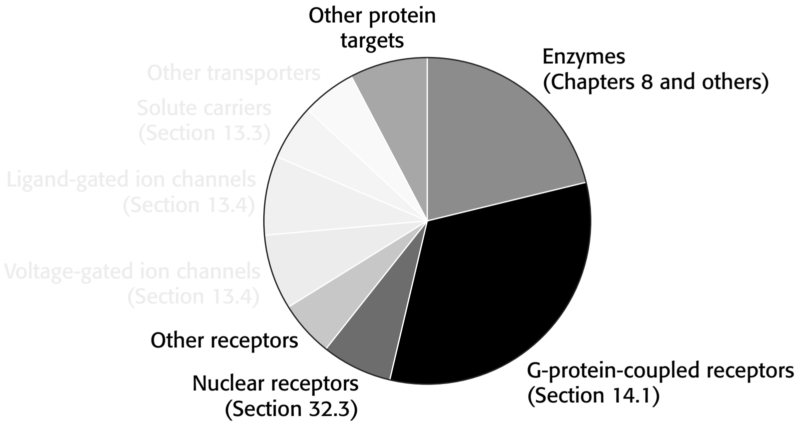

FIGURE 36.1 The targets of drugs in current use. In this pie chart, currently-used drugs that modulate human proteins are sorted by target type: enzymes in green, receptors in blue, transporters in red, and other targets in gray. [Data from M. Rask-Andersen et al., *Nat. Rev. Drug Discov.* 10:579–590, 2011]

medicinal properties, or by screening natural products or other "libraries" of compounds. In this approach, a biological effect is known before the molecular target is identified. The mode of action of the substance is only later identified after substantial additional work. The second approach begins with a known molecular target. Compounds are sought, either by screening or by designing molecules with desired properties, that bind to the target molecule and modulate its properties. After such compounds are available, scientists can explore their effects on appropriate cells or organisms. Many unexpected results may be encountered in this process as the complexity of biological systems reveals itself.

Pharmacology
The science that deals with the discovery, chemistry, composition, identification, biological and physiological effects, uses, and manufacture of drugs.

In this chapter, we explore the science of pharmacology. We examine a number of case histories that illustrate drug development—including many of its concepts, methods, and challenges. We then see how the concepts and tools from genomics are influencing approaches to drug discovery. The chapter ends with a summary of the clinical trial phases required for drug development.

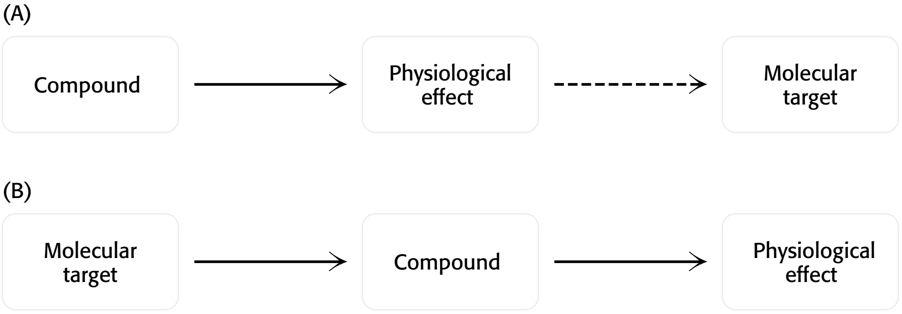

FIGURE 36.2 Two paths to drug discovery. (A) A compound is discovered to have a desirable physiological effect. The molecular target can be identified in a separate step as needed. (B) A molecular target is selected first. Drug candidates that bind to the target are identified and then examined for their physiological effects.

36.1 The Development of Drugs Presents Huge Challenges

Many compounds have significant effects when taken into the body, but only a very small fraction of them have the potential to be useful drugs. A foreign compound, not adapted to its role in the cell through long evolution, must have a range of special properties to function effectively without causing serious harm. Let us consider some of the challenges faced by drug developers.

Drug candidates must be potent and selective modulators of their targets

Most drugs bind to specific proteins, usually receptors or enzymes, within the body. To be effective, a drug should bind a sufficient number of its target proteins when taken at a reasonable dose. One factor in determining drug effectiveness is the strength of the interaction between the drug and its target. A molecule that binds to some target protein is often referred to as a *ligand.* A ligand-binding curve is shown in Figure 36.3. Ligand molecules occupy progressively more target binding sites as ligand concentration increases until essentially all of the available sites are occupied. The tendency of a ligand to bind to its target is measured by the *dissociation constant*, K_d, defined by the expression

$$K_d = [R][L]/[RL]$$

where [R] is the concentration of the free receptor, [L] is the concentration of the free ligand, and [RL] is the concentration of the receptor–ligand complex. The dissociation constant is a measure of the strength of the interaction between the drug candidate and the target; the lower the value, the stronger the interaction. The concentration of free ligand at which one-half of the binding sites are occupied equals the dissociation constant, as long as the concentration of binding sites is substantially less than the dissociation constant.

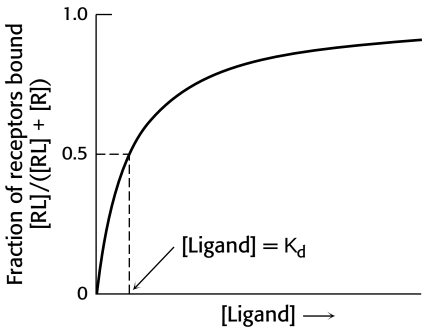

FIGURE 36.3 Ligand binding. The titration of a receptor, R, with a ligand, L, results in the formation of the complex RL. In uncomplicated cases, the binding reaction follows a simple saturation curve. Half of the receptors are bound to ligand when the ligand concentration equals the dissociation constant, K_d, for the RL complex.

In many cases, biological assays using living cells or tissues (rather than direct enzyme or binding assays) are employed to examine the potency of drug candidates. For example, the fraction of bacteria killed by a drug might indicate the potency of a potential antibiotic. In these cases, values such as EC_{50} are used. EC_{50} is the concentration of the drug candidate required to elicit 50% of the maximal biological response (Figure 36.4). Similarly, EC_{90} is the concentration required to achieve 90% of the maximal response. In the example of an antibiotic, EC_{90} would be the concentration required to kill 90% of bacteria exposed to the drug. For drug candidates that are inhibitors, the corresponding terms IC_{50} and IC_{90} are often used to describe the concentrations of the inhibitor required to reduce a response by 50% or 90%, relative to its value in the absence of inhibitor, respectively.

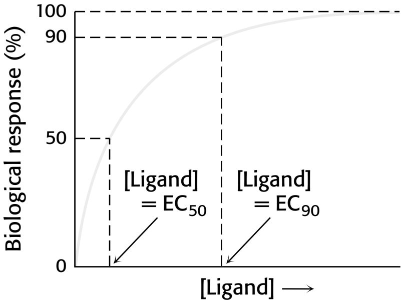

FIGURE 36.4 Effective concentrations. The concentration of a ligand required to elicit a biological response can be quantified in terms of EC_{50}, the concentration required to give 50% of the maximum response, and EC_{90}, the concentration required to give 90% of the maximum response.

Values such as the IC_{50} and EC_{50} are measures of the *potency* of a drug candidate in modulating the activity of the desired biological target. To prevent unwanted effects, often called *side effects,* ideal drug candidates should also be *selective*. That is, they should not bind biomolecules other than the target to any significant extent. Developing such a drug can be quite challenging, particularly if the drug target is a member of a large family of evolutionarily related proteins. The degree of selectivity can be described in terms of the ratio of the K_d values for the binding of the drug candidate to any other molecules to the K_d value for the binding of the drug candidate to the desired target.

Under physiological conditions, achieving sufficient binding of a target site by a drug can be quite challenging. Most drug targets also bind ligands normally present in tissues; often, the drug and these ligands will compete for binding sites on the target. We encountered this scenario when we considered competitive inhibitors in Chapter 8. Suppose that the drug target is an enzyme and the drug candidate is competitive with respect to the enzyme's natural substrate. The concentration of the drug candidate necessary to inhibit the enzyme will depend on the physiological concentration of the normal substrate (Figure 36.5). Biochemists Yung-Chi Cheng and William Prusoff

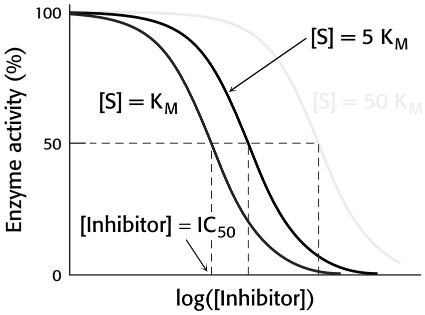

FIGURE 36.5 Inhibitors compete with substrates for enzyme active sites. The measured IC_{50} of a competitive inhibitor to its target enzyme depends on the concentration of substrate present.

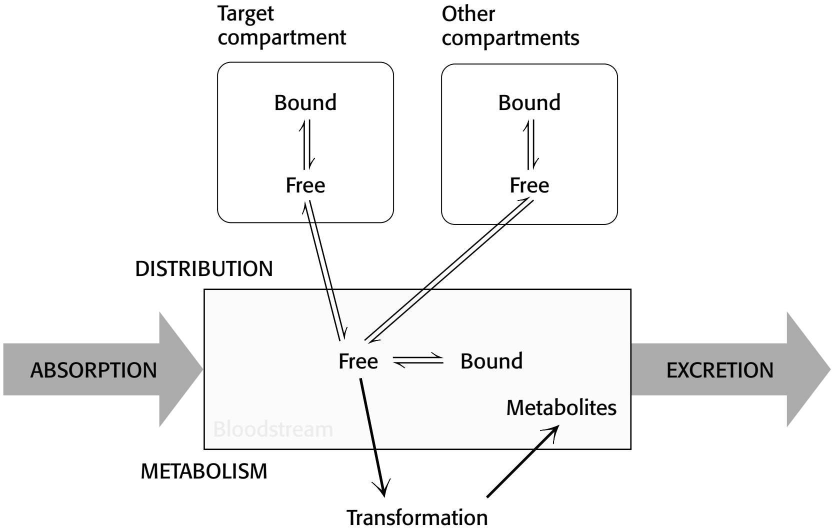

FIGURE 36.6 Absorption, distribution, metabolism, and excretion (ADME). The concentration of a compound at its target site (yellow) is affected by the extents and rates of absorption, distribution, metabolism, and excretion.

described the relation between the IC_{50} of an enzyme inhibitor and its *inhibition constant* K_i (analogous to the dissociation constant, K_d, of a ligand):

$$IC_{50} = K_i(1 + [S]/K_M)$$

This relation, referred to as the *Cheng–Prusoff equation,* demonstrates that the IC_{50} of a competitive inhibitor will depend on the concentration and the Michaelis constant (K_M) for the substrate S. The higher the concentration of the natural substrate, the higher the concentration of drug needed to inhibit the enzyme.

Drugs must have suitable properties to reach their targets

Thus far, we have focused on the ability of molecules to act on specific target molecules. However, an effective drug must also have other characteristics. It must be easily administered and must reach its target at sufficient concentration to be effective. After a drug molecule has entered the body, it is acted upon by several processes—absorption, distribution, metabolism, and excretion—that will determine the effective concentration of this molecule over time (Figure 36.6). A drug's response to these processes is referred to as its *ADME* (pronounced "add-me") properties.

Administration and absorption. Ideally, a drug can be taken orally as a small tablet. An orally administered active compound must be able to survive the acidic conditions in the gut and then be absorbed through the intestinal epithelium. Thus, the compound must be able to pass through cell membranes at a significant rate. Larger molecules such as proteins cannot be administered orally, because they often cannot survive the acidic conditions in the stomach and, if they do, are not readily absorbed. Even many small molecules are not absorbed well; they may be too polar and not pass through cell membranes easily, for example. The ability to be absorbed is often quantified in terms of the *oral bioavailability.* This quantity is defined as the ratio of the peak concentration of a compound given orally to the peak concentration of the same dose injected directly into the bloodstream. Bioavailability can vary considerably from species to species, and so results from animal studies may be difficult to apply to human beings. Despite this variability, some useful generalizations have been made. One powerful set consists of *Lipinski's rules.*

Lipinski's rules tell us that poor absorption is likely when

1. the molecular weight is greater than 500.
2. the number of hydrogen-bond donors is greater than 5.

3. the number of hydrogen-bond acceptors is greater than 10.
4. the partition coefficient [measured as log(P)] is greater than 5.

The partition coefficient is a way to measure the tendency of a molecule to dissolve in membranes, which correlates with its ability to dissolve in organic solvents. It is determined by allowing a compound to equilibrate between water and an organic phase, n-octanol. The log(P) value is defined as $\log_{10}$ of the ratio of the concentration of a compound in n-octanol to the concentration of the compound in water. For example, if the concentration of the compound in the n-octanol phase is 100 times that in the aqueous phase, then log(P) is 2. Although the ability of a drug to partition in organic solvents is ideal, because it implies that the compound can penetrate membranes, a log(P) value that is too high suggests that the molecule may be poorly soluble in an aqueous environment.

Morphine, for example, satisfies all of Lipinski's rules and has moderate bioavailability (Figure 36.7). A drug that violates one or more of these rules may still have satisfactory bioavailability. Nonetheless, these rules serve as guiding principles for evaluating new drug candidates.

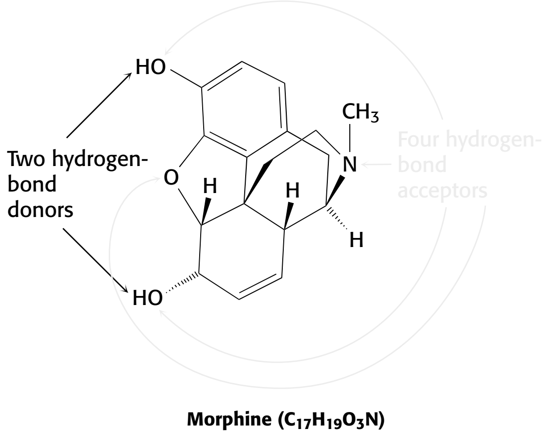

FIGURE 36.7 Lipinski's rules applied to morphine. Morphine satisfies all of Lipinski's rules and has an oral bioavailability in human beings of 33%.

Distribution. Compounds taken up by intestinal epithelial cells can pass into the bloodstream. However, hydrophobic compounds and many others do not freely dissolve in the bloodstream. These compounds bind to proteins, such as albumin (Figure 36.8), that are abundant in the blood serum and by this means are carried throughout the circulatory system.

When a compound has reached the bloodstream, it is distributed to different fluids and tissues, which are often referred to as *compartments.* Some compounds are highly concentrated in their target compartments, either by binding to the target molecules themselves or by other mechanisms. Other compounds are distributed more widely (Figure 36.9). An effective drug will reach the target compartment in sufficient quantity; the concentration of the compound in the target compartment is reduced whenever the compound is distributed into other compartments.

Some target compartments are particularly hard to reach. Many compounds are excluded from the central nervous system by the *blood–brain barrier,* the tight junctions between endothelial cells that line blood vessels within the brain and spinal cord.

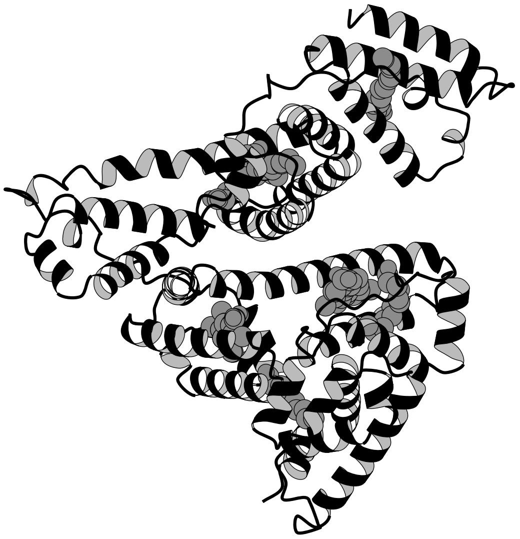

FIGURE 36.8 Structure of the drug carrier human serum albumin. Seven hydrophobic molecules (in red) are shown bound to the molecule. [Drawn from 1BKE.pdb.]

Metabolism. A final challenge to a potential drug molecule is to evade the body's defenses against foreign compounds. Many such compounds (called *xenobiotic compounds*) are released from the body in the urine or stool, often after having been metabolized to aid in excretion. This *drug metabolism* poses a considerable threat to drug effectiveness because the concentration of the desired compound decreases as it is metabolized. Thus, a rapidly metabolized compound must be administered more frequently or at higher doses.

Two of the most common pathways in xenobiotic metabolism are *oxidation* and *conjugation.* Oxidation reactions can aid excretion in at least two ways: by increasing water solubility, and thus ease of transport, and by introducing functional groups that participate in subsequent metabolic steps. These reactions are often promoted by cytochrome P450 enzymes in the liver (Section 26.4). The human genome encodes more than 50 different P450 isozymes, many of which participate in xenobiotic metabolism.

FIGURE 36.9 Distribution of the drug fluconazole. After having been taken in, compounds distribute themselves to various organs within the body. The distribution of the antifungal agent fluconazole has been monitored through the use of positron emission tomography (PET) scanning. These images were taken of a healthy human volunteer 90 minutes after injection of a dose of 5 mg kg^{-1} of fluconazole containing trace amounts of fluconazole labeled with the positron-emitting isotope ^{18}F. [Reprinted by permission from Macmillan Publishers Ltd: Nature Reviews Drug Discovery, Rudin, M., and Weissleder, R., "Molecular imaging in drug discovery and development," 2: 2, p. 123–131, Copyright 2003.]

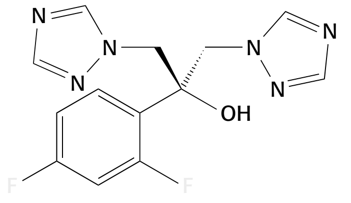

Fluconazole

A typical reaction catalyzed by a P450 isozyme is the hydroxylation of ibuprofen (Figure 36.10).

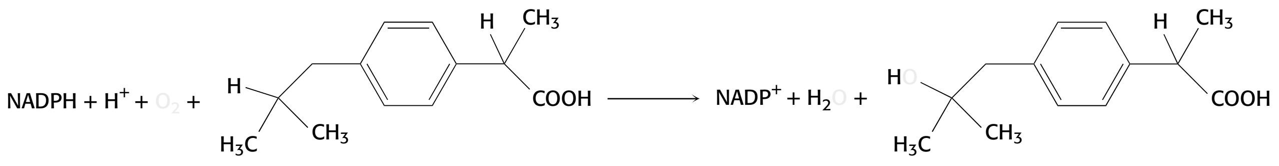

Ibuprofen

FIGURE 36.10 P450 conversion of ibuprofen. Cytochrome P450 isozymes, primarily in the liver, catalyze xenobiotic metabolic reactions such as hydroxylation. The reaction introduces an oxygen atom derived from molecular oxygen.

Conjugation is the addition of particular groups to the xenobiotic compound. Common groups added are glutathione (Section 20.5), glucuronic acid, and sulfate (Figure 36.11). These additions often increase water solubility and provide labels that can be recognized to target excretion. Examples of conjugation include the addition of glutathione to the anticancer drug cyclophosphamide, the addition of glucuronidate to the analgesic morphine, and the addition of a sulfate group to the hair-growth stimulator minoxidil.

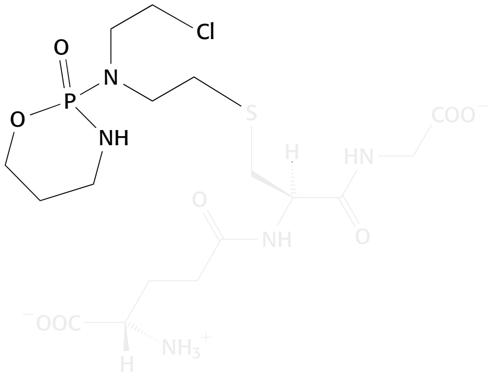

Cyclophosphamide-glutathione conjugate

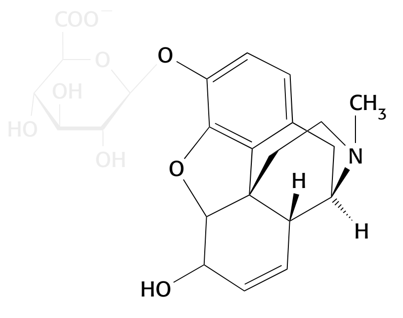

Morphine glucuronidate

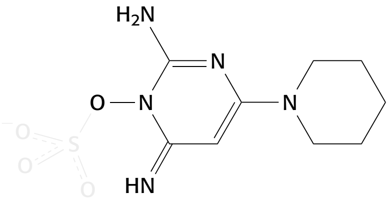

Minoxidil sulfate

Interestingly, the sulfation of minoxidil produces a compound that is more active in stimulating hair growth than is the unmodified compound. Thus, the metabolic products of a drug, though usually less active than the drug, can sometimes be more active.

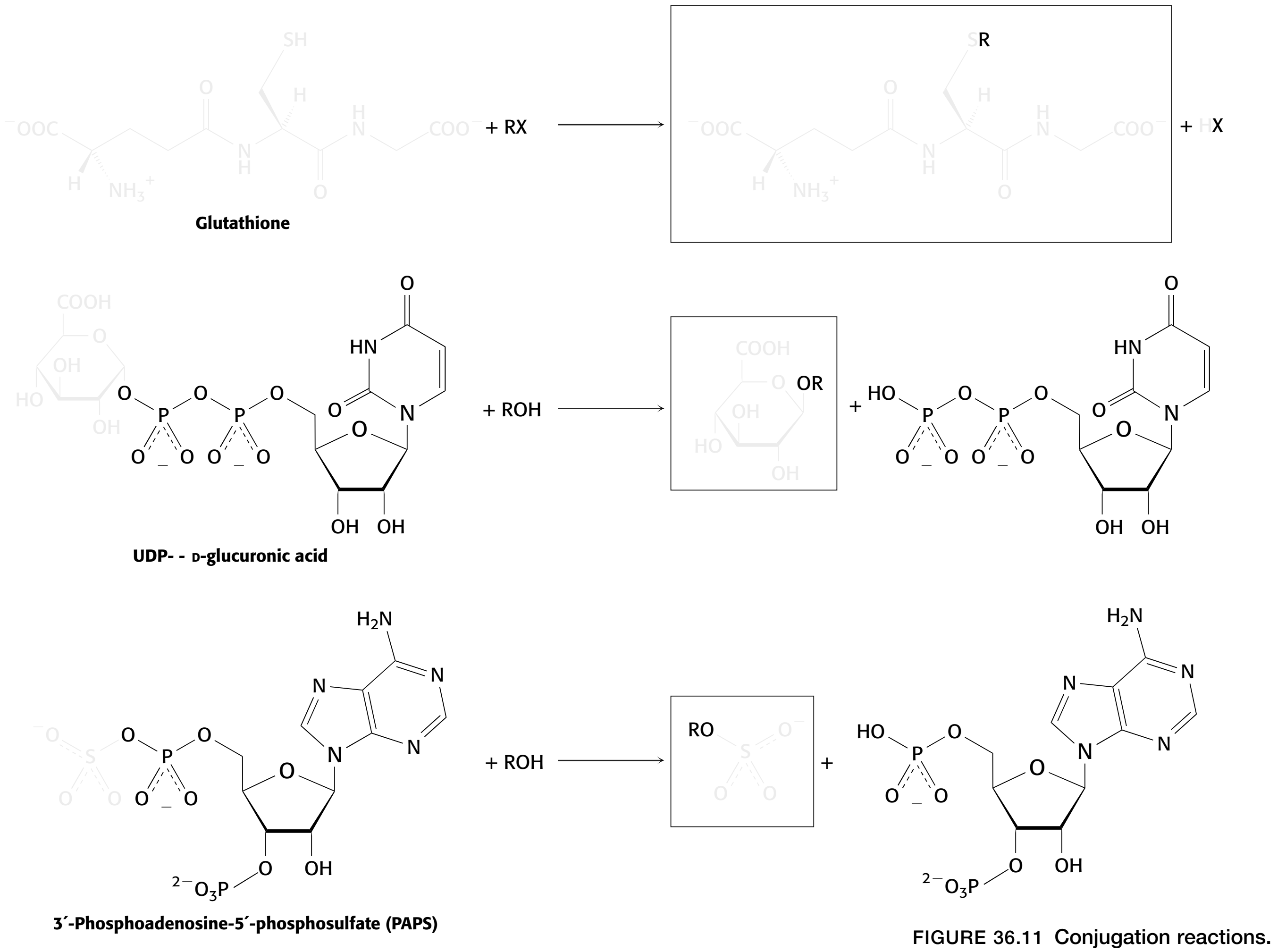

FIGURE 36.11 Conjugation reactions. Compounds that have appropriate groups are often modified by conjugation reactions. Such reactions include the addition of glutathione (top), glucuronic acid (middle), or sulfate (bottom). The conjugated product is shown boxed.

Note that an oxidation reaction often precedes conjugation because the oxidation reaction can generate modifications, such as the hydroxyl group, to which groups such as glucuronic acid can be attached. The oxidation reactions of xenobiotic compounds are often referred to as *phase I transformations,* and the conjugation reactions are referred to as *phase II transformations.* These reactions take place primarily in the liver. Because blood flows from the intestine directly to the liver through the portal vein, xenobiotic metabolism often alters drug compounds before they ever reach full circulation. This *first-pass metabolism* can substantially limit the availability of compounds taken orally.

Excretion. After compounds have entered the bloodstream, they can be removed from circulation and excreted from the body by two primary pathways. First, they can be absorbed through the kidneys and excreted in the urine. In this process, the blood passes through *glomeruli,* networks of fine capillaries in the kidney that act as filters. Compounds with molecular weights less than approximately 60,000 pass though the glomeruli. Many of the water molecules, glucose molecules, nucleotides, and other low-molecular-weight compounds that pass through the glomeruli are reabsorbed into the bloodstream, either by transporters that have broad specificities or by the passive transfer of hydrophobic molecules through membranes. Drugs and metabolites that pass through the first filtration step and are not reabsorbed are excreted.

Second, compounds can be actively transported into bile, a process that takes place in the liver. After concentration in the gall bladder, bile flows into the intestine. In the intestine, the drugs and metabolites can be excreted through the stool, reabsorbed into the bloodstream, or further degraded by

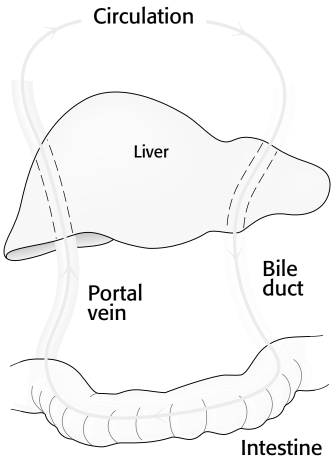

FIGURE 36.12 Enterohepatic cycling. Some drugs can move from the blood circulation to the liver, into the bile, into the intestine, to the liver, and back into circulation. This cycling decreases the rate of drug excretion.

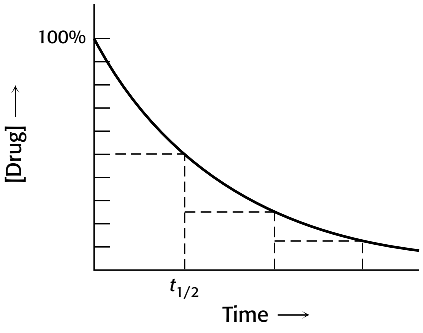

FIGURE 36.13 Half-life of drug excretion. In the case shown, the concentration of a drug in the bloodstream decreases to one-half of its value in a period of time, $t_{1/2}$, referred to as its half-life.

digestive enzymes. Sometimes, compounds are recycled from the bloodstream into the intestine and back into the bloodstream, a process referred to as *enterohepatic cycling* (Figure 36.12). This process can significantly decrease the rate of excretion of some compounds because they escape from an excretory pathway and reenter the circulation.

The kinetics of compound excretion is often complex. In some cases, a fixed percentage of the remaining compound is excreted over a given period of time (Figure 36.13). This pattern of excretion results in exponential loss of the compound from the bloodstream that can be characterized by a half-life ($t_{1/2}$). The half-life is the fixed period of time required to eliminate 50% of the remaining compound. It is a measure of how long an effective concentration of the compound remains in the system after administration. As such, the half-life is a major factor in determining how often a drug must be taken. A drug with a long half-life might need to be taken only once per day, whereas a drug with a short half-life might need to be taken three or four times per day.

Toxicity can limit drug effectiveness

An effective drug must not be so toxic that it seriously harms the person who takes it. A drug may be toxic for any of several reasons. First, it may modulate the target molecule itself *too* effectively. For example, the presence of too much of the anticoagulant drug coumadin can result in dangerous, uncontrolled bleeding and death. Second, the compound may modulate the properties of proteins that are distinct from, but related to, the target molecule itself. Compounds that are directed to one member of a family of enzymes or receptors often bind to other family members. For example, an antiviral drug directed against viral proteases may be toxic if it also inhibits proteases normally present in the body such as those that regulate blood pressure.

A compound may also be toxic if it modulates the activity of a protein unrelated to its intended target. For example, many compounds block ion channels such as the potassium channel hERG (Section 13.4), causing potentially life-threatening disturbances of cardiac rhythm. To prevent cardiac side effects, many compounds are screened for their ability to block such channels.

Finally, even if a compound is not itself toxic, its metabolic by-products may be. Phase I metabolic processes can generate damaging reactive groups in products. An important example is liver toxicity observed with large doses of the common pain reliever acetaminophen (Figure 36.14). A particular cytochrome

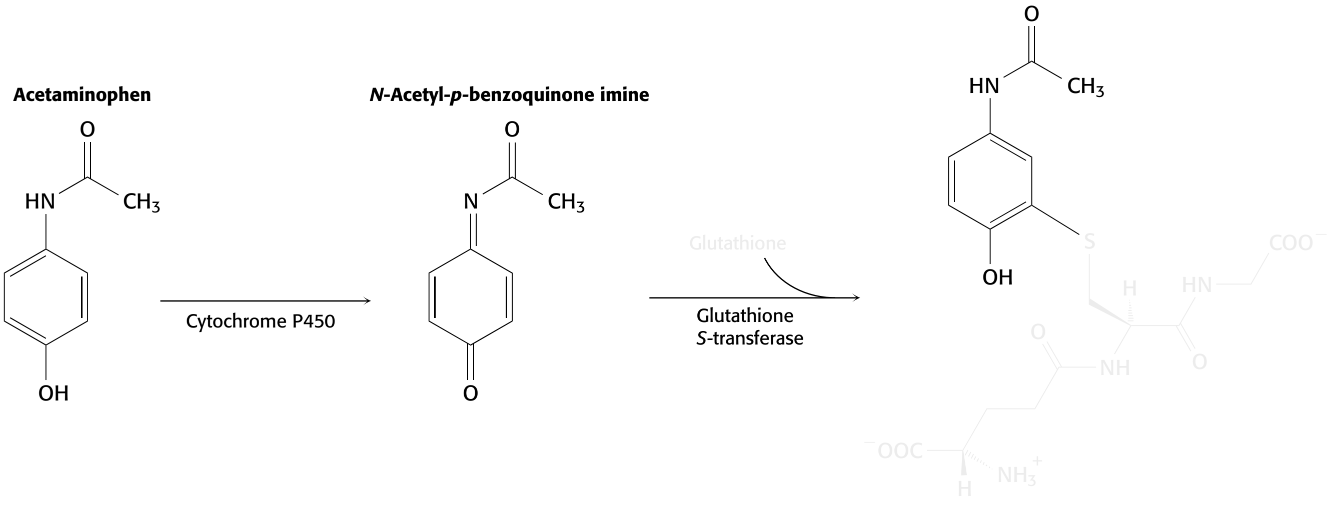

FIGURE 36.14 Acetaminophen toxicity. A minor metabolic product of acetaminophen is *N*-acetyl-*p*-benzoquinone imine. This metabolite is conjugated to glutathione. Large doses of acetaminophen can deplete liver glutathione stores.

P450 isozyme oxidizes acetaminophen to *N*-acetyl-*p*-benzoquinone imine. The resulting compound is conjugated to glutathione. With large doses, however, the liver concentration of glutathione drops dramatically, and the liver is no longer able to protect itself from this reactive compound and others. Initial symptoms of excessive acetaminophen include nausea and vomiting. Within 24 to 48 hours, symptoms of liver failure may appear. Acetaminophen poisoning accounts for about 35% of cases of severe liver failure in the United States. A liver transplant is often the only effective treatment.

The toxicity of a drug candidate can be described in terms of the *therapeutic index*. This measure of toxicity is determined through animal tests, usually with mice or rats. The therapeutic index is defined as the ratio of the dose of a compound that is required to kill one-half of the animals (referred to as the LD_{50} for "lethal dose") to a comparable measure of the effective dose, usually the EC_{50}. Thus, if the therapeutic index is 1000, then lethality is significant only when 1000 times the effective dose is administered. Analogous indices can provide measures of toxicity less severe than lethality.

Many compounds have favorable properties in vitro, yet fail when administered to a living organism because of difficulties with ADME and toxicity. Expensive and time-consuming animal studies are required to verify that a drug candidate is not toxic, yet differences between animal species in their response can confound decisions about moving forward with a compound toward human studies. One hope is that, with more understanding of the biochemistry of these processes, scientists can develop computer-based models to replace or augment animal tests. Such models would need to accurately predict the fate of a compound inside a living organism from its molecular structure or other properties that are easily measured in the laboratory without the use of animals.

36.2 Drug Candidates Can Be Discovered by Serendipity, Screening, or Design

Traditionally, many drugs were discovered by serendipity, or chance observation. More recently, drugs have been discovered by screening collections of natural products or other compounds for molecules that have desired medicinal properties. Alternatively, scientists have designed specific drug candidates by using their knowledge about a preselected molecular target. We will examine several examples of each of these pathways to reveal common principles.

Serendipitous observations can drive drug development

Perhaps the most well-known observation in the history of drug development is Alexander Fleming's chance observation in 1928 that colonies of the bacterium *Staphylococcus aureus* died when they were adjacent to colonies of the mold *Penicillium notatum*. Spores of the mold had landed accidentally on plates growing the bacteria. Fleming soon realized that the mold produced a substance that could kill disease-causing bacteria. This discovery led to a fundamentally new approach to the treatment of bacterial infections. Howard Florey and Ernest Chain developed a powdered form of the substance, termed penicillin, that became a widely used antibiotic in the 1940s. When the structure of penicillin was elucidated in 1945, it was found to contain a four-membered β-lactam ring. This unusual feature is key to the antibacterial function of penicillin, as noted earlier (Section 8.5).

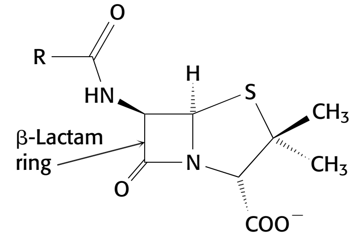

Penicillin

Three steps were crucial to fully capitalize on Fleming's discovery. First, an industrial process was developed for the production of penicillin from *Penicillium* mold on a large scale. Second, penicillin and its derivatives were chemically

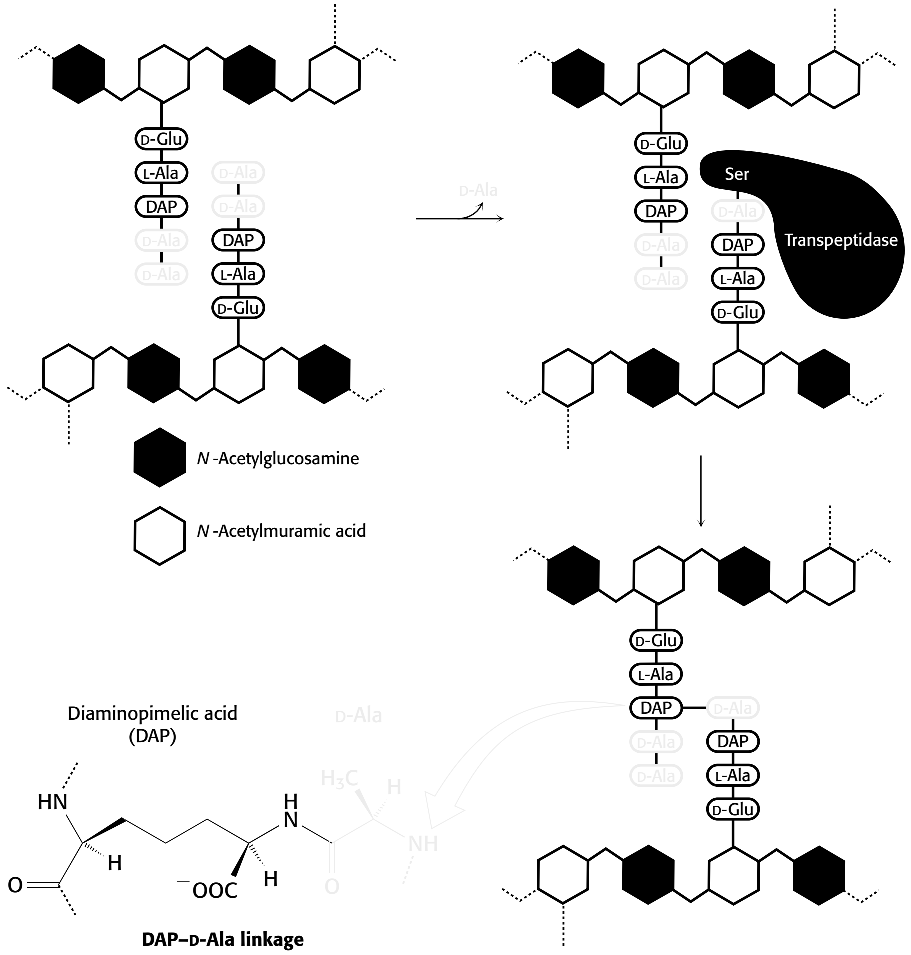

FIGURE 36.15 Mechanism of cell-wall biosynthesis disrupted by penicillin. A transpeptidase enzyme catalyzes the formation of cross-links between peptidoglycan groups. In the case shown, the transpeptidase catalyzes the linkage of D-alanine at the end of one peptide chain to the amino acid diaminopimelic acid (DAP) on another peptide chain. The diaminopimelic acid linkage (bottom left) is found in Gram-negative bacteria such as *E. coli.* Linkages of glycine-rich peptides are found in Gram-positive bacteria. Penicillin inhibits the action of the transpeptidase; so bacteria exposed to the drug have weak cell walls that are susceptible to lysis.

synthesized. The availability of synthetic penicillin derivatives opened the way for scientists to explore the relations between structure and function. Many such penicillin derivatives have found widespread use in medicine. Finally, in 1965, Jack Strominger and James Park independently determined that penicillin exerts its antibiotic activity by blocking a critical transpeptidase reaction in bacterial cell-wall biosynthesis (Figure 36.15), as introduced in Section 8.5.

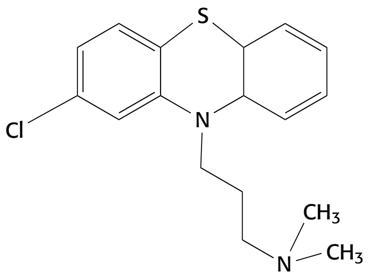

Chlorpromazine

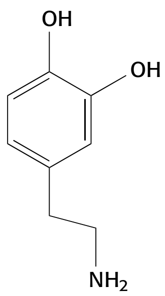

Dopamine

Many other drugs have been discovered by serendipitous observations. Chlorpromazine (Thorazine), a drug used to treat psychosis, was discovered in the course of investigations directed toward the treatment of shock in surgical patients. In 1952, French surgeon Henri Laborit noticed that, after taking the compound, his patients were remarkably calm. This observation suggested that chlorpromazine could benefit psychiatric patients, and, indeed, the drug has been used for many years to treat patients with schizophrenia and bipolar disorder. The drug does have significant side effects, and its use has been largely superseded by more recently developed drugs.

Chlorpromazine acts by binding to receptors for the neurotransmitter dopamine and blocking them. Dopamine D2 receptors are the targets of many other psychoactive drugs. In the search for drugs with more-limited side effects, studies have been performed to correlate drug effects with biochemical parameters such as dissociation constants and binding and release rate constants.

A more recent example of a drug discovered by chance observation is sildenafil (Viagra). This compound was developed as an inhibitor of phosphodiesterase 5 (PDE5), an enzyme that catalyzes the hydrolysis of cGMP to GMP (Figure 36.16). The compound was intended as a treatment for hypertension and angina because cGMP plays a central role in the relaxation of

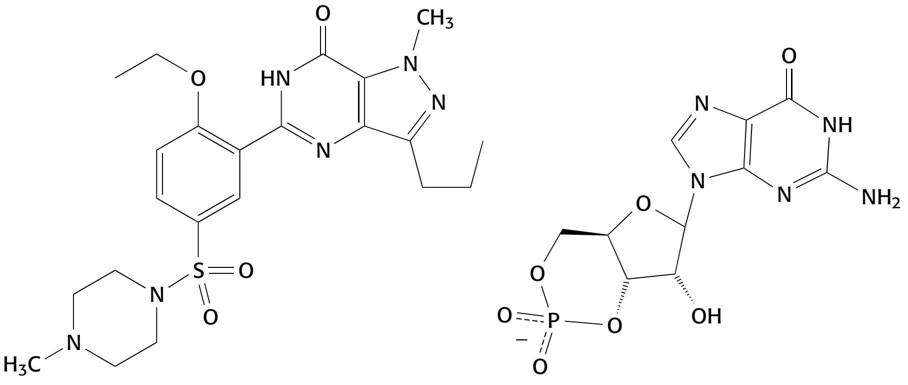

Sildenafil **cGMP**

FIGURE 36.16 Sildenafil, a mimic of cGMP. Sildenafil was designed to resemble cGMP, the substrate of phosphodiesterase 5 (PDE5).

smooth-muscle cells in blood vessels (Figure 36.17). The inhibition of PDE5 was expected to increase the concentration of cGMP by blocking the pathway for its degradation. In the course of early clinical trials in Wales, some men reported unusual penile erections. Whether this chance observation by a few men was due to the compound or to other effects was unclear. However, the observation made some biochemical sense because smooth-muscle relaxation due to increased cGMP levels had been discovered to play a role in penile erection. Subsequent clinical trials directed toward the evaluation of sildenafil for erectile dysfunction were successful. This account testifies to the importance of collecting comprehensive information from clinical-trial participants. In this case, incidental observations led to a new treatment for erectile dysfunction and a multibillion-dollar-per-year drug market.

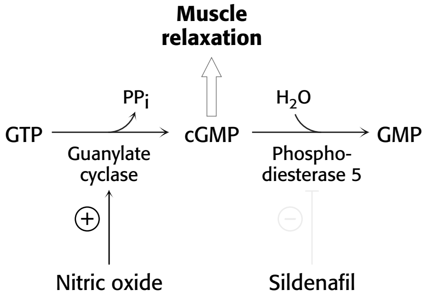

FIGURE 36.17 Muscle-relaxation pathway. Increases in nitric oxide levels stimulate guanylate cyclase, which produces cGMP. The increased cGMP concentration promotes smooth-muscle relaxation. PDE5 hydrolyzes cGMP, which lowers the cGMP concentration. The inhibition of PDE5 by sildenafil maintains elevated levels of cGMP.

Natural products are a valuable source of drugs and drug leads

No drug is as widely used as aspirin. Observers at least as far back as Hippocrates (~400 B.C.) have noted the use of extracts from the bark and leaves of the willow tree for pain relief. In 1829, a mixture called *salicin* was isolated from willow bark. Subsequent analysis identified salicylic acid as the active component of this mixture. Salicylic acid was formerly used to treat pain, but this compound often irritated the stomach. Several investigators attempted to find a means to neutralize salicylic acid. Felix Hoffmann, a chemist working at the German company Bayer, developed a less-irritating derivative by treating salicylic acid with a base and acetyl chloride. This derivative, acetylsalicylic acid, was named *aspirin* from "a" for acetyl chloride, "spir" for *Spiraea ulmaria* (meadowsweet, a flowering plant that also contains salicylic acid), and "in" (a common ending for drugs). Each year, approximately 35,000 tons of aspirin are taken worldwide, nearly the weight of the *Titanic.*

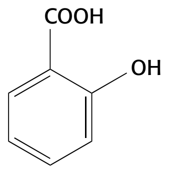

Salicylic acid

As discussed in Chapter 12, the acetyl group in aspirin is transferred to the side chain of a serine residue that lies along the path to the active site of the cyclooxygenase component of prostaglandin H_2 synthase (Figure 12.24). In this position, the acetyl group blocks access to the active site. Thus, even though aspirin binds in the same pocket on the enzyme as salicylic acid, the acetyl group of aspirin dramatically increases its effectiveness as a drug. This account illustrates the value of screening extracts from plants and other materials that are believed to have medicinal properties for active compounds. The large number of herbal and folk medicines are a treasure trove of new drug leads.

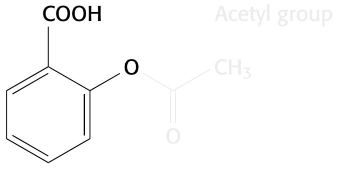

Aspirin (acetylsalicylic acid)

Let us consider another example, which has also had a significant impact on the clinical management of individuals with cardiovascular disease. More than 100 years ago, a fatty, yellowish material was discovered on the arterial walls of patients who had died of vascular disease. The presence of the material was termed *atheroma* from the Greek word for porridge. This material proved to be cholesterol. The Framingham heart study, initiated in 1948, documented a correlation between high blood-cholesterol levels and high mortality rates from heart disease. This observation led to the notion that blocking cholesterol synthesis might lower blood-cholesterol levels and, in turn, lower the risk of heart disease. Initial attempts at blocking cholesterol synthesis focused on steps near the end of the pathway. However, these efforts were abandoned because the accumulation of the insoluble substrate for the inhibited enzyme led to the development of cataracts and other side effects. Investigators eventually identified a more-favorable target—namely, the enzyme HMG-CoA reductase (Section 26.2). This enzyme acts on a substrate, HMG-CoA (3-hydroxy-3-methylglutaryl coenzyme A), that does not accumulate, because it is water-soluble and can be utilized by other pathways.

A promising natural product, compactin, was discovered in a screen of compounds from a fermentation broth from *Penicillium citrinum* in a search for antibacterial agents. In some, but not all, animal studies, compactin was found to inhibit HMG-CoA reductase and to lower serum cholesterol levels. In 1982, a new HMG-CoA reductase inhibitor was discovered in a fermentation broth from *Aspergillus cereus.* This compound, now called lovastatin, was found to be structurally very similar to compactin, bearing one additional methyl group.

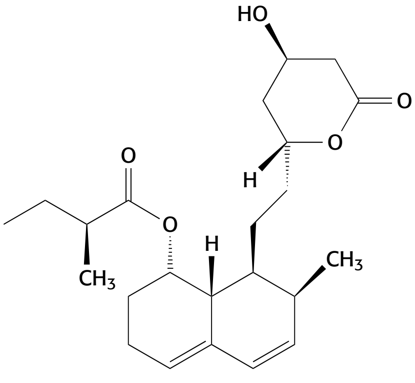

Compactin

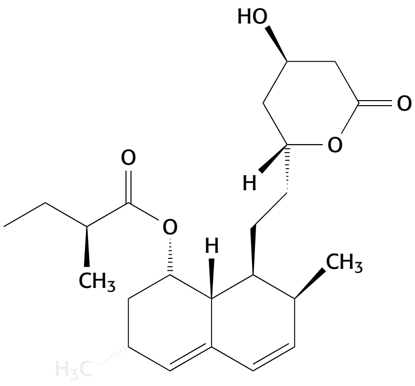

Lovastatin

In clinical trials, lovastatin significantly reduced serum cholesterol levels with few side effects. Most side effects could be prevented by treatment with mevalonate (the product of HMG-CoA reductase), indicating that the side effects were likely due to the highly effective blocking of HMG-CoA reductase. One notable side effect is muscle pain or weakness (termed *myopathy*), although its cause remains to be fully established. After many studies, the Food and Drug Administration (FDA) approved lovastatin for treating high serum cholesterol levels.

A structurally related HMG-CoA reductase inhibitor was later shown to cause a statistically significant decrease in deaths due to coronary heart disease. This result validated the benefits of lowering serum cholesterol levels. Further mechanistic analysis revealed that the HMG-CoA reductase inhibitor acts not only by lowering the rate of cholesterol biosynthesis, but also by inducing the expression of the low-density-lipoprotein (LDL) receptor (Section 26.3). Cells with such receptors remove LDL particles from the bloodstream, and so these particles cannot contribute to atheroma.

Screening libraries of synthetic compounds expands the opportunity for identification of drug leads

Lovastatin and its relatives are either natural products or readily derived from natural products. After the discovery of these compounds, totally synthetic molecules were developed that are more-potent inhibitors of HMG-CoA reductase (Figure 36.18). These compounds were found to be effective

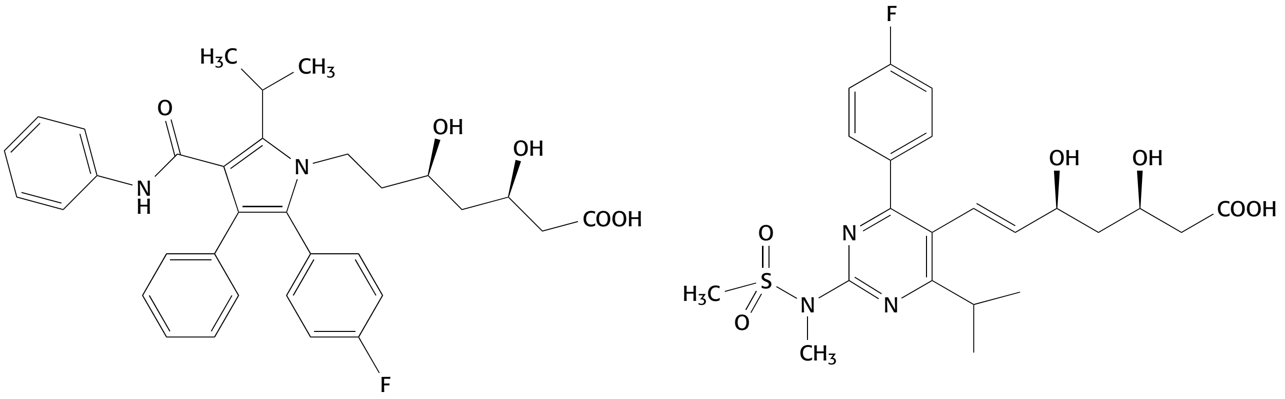

Atorvastatin **Rosuvastatin**

FIGURE 36.18 Synthetic statins. Atorvastatin (Lipitor) and rosuvastatin (Crestor) are completely synthetic drugs that inhibit HMG-CoA reductase.

at lower dose levels, reducing side effects. The original HMG-CoA reductase inhibitors or their precursors were found by screening libraries of natural products. More recently, drug developers have tried screening large libraries of both natural products and purely synthetic compounds prepared in the course of many drug-development programs. Under favorable circumstances, hundreds of thousands or even millions of compounds can be tested in this process, termed *high-throughput screening.* Compounds in these libraries can be synthesized one at a time for testing. An alternative approach is to synthesize a large number of structurally related compounds that differ from one another at only one or a few positions all at once. This approach is often termed *combinatorial chemistry.* Here, compounds are synthesized with the use of the same chemical reactions but a variable set of reactants. Suppose that a molecular scaffold is constructed with two reactive sites and that 20 reactants can be used in the first site and 40 reactants can be used in the second site. A total of 20 × 40 = 800 possible compounds can be produced.

A key method in combinatorial chemistry is *split-pool synthesis* (Figure 36.19). The method depends on solid-phase synthetic methods, first developed for the synthesis of peptides (Section 3.5). Compounds are synthesized on small beads. Beads containing an appropriate starting *scaffold* are produced and divided (split) into *n* sets, with *n* corresponding to the number of building blocks to be used at one site. Reactions adding the reactants at the

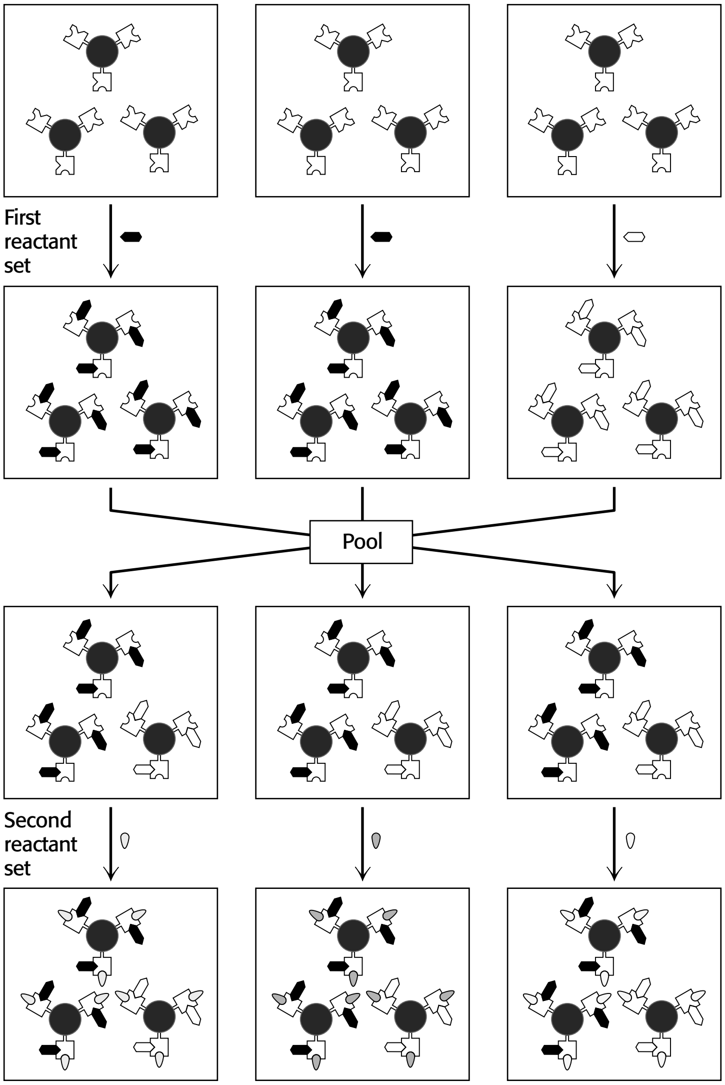

FIGURE 36.19 Split-pool synthesis. Reactions are performed on beads. Each of the reactions with the first set of reactants is performed on a separate set of beads. The beads are then pooled, mixed, and split into sets. The second set of reactants is then added. Many different compounds will be produced, but all of the compounds on a single bead will be identical.

first site are run, and the beads are isolated by filtration. The n sets of beads are then combined (pooled), mixed, and split again into m sets, with m corresponding to the number of reactants to be used at the second site. Reactions adding these m reactants are run, and the beads are again isolated. The important result is that each bead contains only one compound, even though the entire library of beads contains many. Furthermore, although only $n + m$ reactions were run, $n \times m$ compounds are produced. With the preceding values for n and m, $20 + 40 = 60$ reactions produce $20 \times 40 = 800$ compounds. In some cases, assays can be performed directly with the compounds still attached to the bead to find compounds with desired properties (Figure 36.20). Alternatively, each bead can be isolated and the compound can be cleaved from the bead to produce free compounds for analysis. After an interesting compound has been identified, analytical methods of various types must be used to identify which of the $n \times m$ compounds is present.

FIGURE 36.20 Screening a library of synthesized carbohydrates. A small combinatorial library of carbohydrates synthesized on the surface of 130-mm beads is screened for carbohydrates that are bound tightly by a lectin from peanuts. Beads that have such carbohydrates are darkly stained through the action of an enzyme linked to the lectin. [From Figure 3 in Liang et al., "Polyvalent binding to carbohydrates immobilized on an insoluble resin," Proceedings of the National Academy of Sciences, USA, vol. 94, pp. 10554–10559, September 1997. Copyright 2004 National Academy of Sciences, USA.]

Note that the "universe" of druglike compounds is vast. More than an estimated 10^{40} compounds are possible with molecular weights less than 750. Thus, even with "large" libraries of millions of compounds, only a tiny fraction of the chemical possibilities are present for study.

Drugs can be designed on the basis of three-dimensional structural information about their targets

Many drugs bind to their targets in a manner reminiscent of Emil Fischer's lock and key (Figure 8.8). Therefore, we should be able to design a key, given enough knowledge about the shape and chemical composition of the lock. In the idealized case, we would like to design a small molecule that is complementary in shape and electronic structure to a target protein so that it binds effectively to the targeted site. Despite our ability to determine three-dimensional structures rapidly, the achievement of this goal remains in the future. Designing stable compounds *from scratch* that have the correct shape and other properties to fit precisely into a binding site is difficult because predicting the structure that will best fit into a binding site is difficult. Prediction of binding affinity requires a detailed understanding of the interactions between a compound and its binding partner *and* of the interactions between the compound and the solvent when the compound is free in solution.

Nonetheless, *structure-based drug design* has proved to be a powerful tool in drug development. Among its most prominent successes has been the development of drugs that inhibit the protease from the human immunodeficiency virus (HIV; Section 34.4). Consider the development of the protease inhibitor indinavir (Crixivan; Figure 9.19). Two sets of promising inhibitors that had high potency but poor solubility and bioavailability were discovered. X-ray crystallographic analysis and molecular-modeling findings suggested that a hybrid of these two inhibitor sets might have both high potency and improved bioavailability (Figure 36.21). The synthesized hybrid compound did show improvements but required further optimization. The structural data suggested one point where modifications could be tolerated. A series of compounds were prepared and tested for their ability to inhibit the protease (Figure 36.22). These data are a demonstration of a *structure–activity relationship (SAR)*; they provide an opportunity to correlate structure with function and guide design of further molecules. The most-active compound showed poor bioavailability, but one of the other compounds (highlighted in yellow in Figure 36.22) showed good bioavailability and acceptable activity. The maximum serum concentration available through oral administration was significantly higher than the levels required to suppress

FIGURE 36.21 Initial design of an HIV protease inhibitor. This compound was designed by combining part of one compound with good inhibition activity but poor solubility (shown in red) with part of another compound with better solubility (shown in blue).

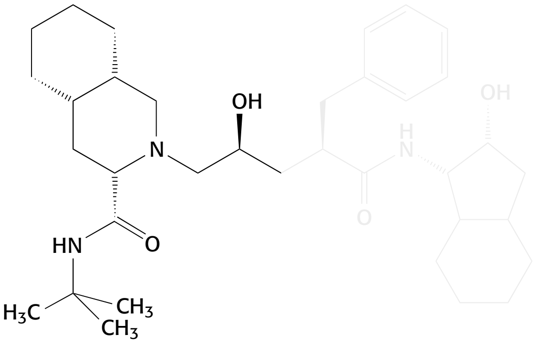

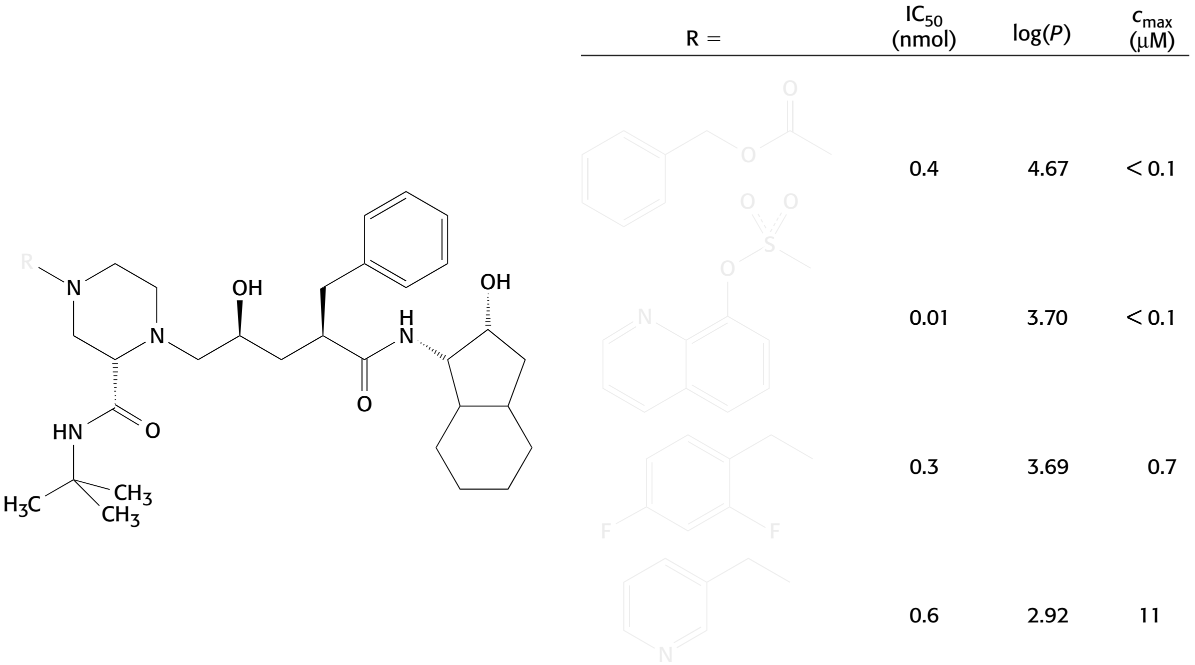

R =	IC_{50} (nmol)	log(*P*)	c_{max} (μM)
	0.4	4.67	< 0.1
	0.01	3.70	< 0.1
	0.3	3.69	0.7
	0.6	2.92	11

FIGURE 36.22 Compound optimization. Four compounds are evaluated for characteristics including the IC_{50}, log(*P*), and c_{max} (the maximal concentration of compound present) measured in the serum of dogs. The compound shown at the bottom (highlighted in yellow) has the weakest inhibitory power (measured by IC_{50}) but by far the best bioavailability (measured by c_{max}). This compound was selected for further development, leading to the drug indinavir (Crixivan).

replication of the virus. This drug, as well as other protease inhibitors developed at about the same time, has been used in combination with other drugs to treat AIDS with much more encouraging results than had been obtained previously (Figure 36.23).

Aspirin targets the cyclooxygenase site in prostaglandin H_2 synthase, as discussed earlier. Animal studies suggested that mammals contain not one but two distinct cyclooxygenase enzymes, both of which are targeted by aspirin. The more recently discovered enzyme, cyclooxygenase 2 (COX2), is expressed primarily as part of the inflammatory response, whereas cyclooxygenase 1 (COX1) is expressed more generally. These observations suggested that a cyclooxygenase inhibitor that was specific for COX2 might be able to reduce inflammation in conditions such as arthritis without producing the gastric and other side effects associated with aspirin.

The amino acid sequences of COX1 and COX2 were deduced from cDNA cloning studies. These sequences are more than 60% identical, clearly indicating that the enzymes have the same overall structure. Nevertheless, there are some differences in the residues around the aspirin-binding site. X-ray crystallography revealed that an extension of the binding pocket was present in COX2, but absent in COX1. This structural difference suggested

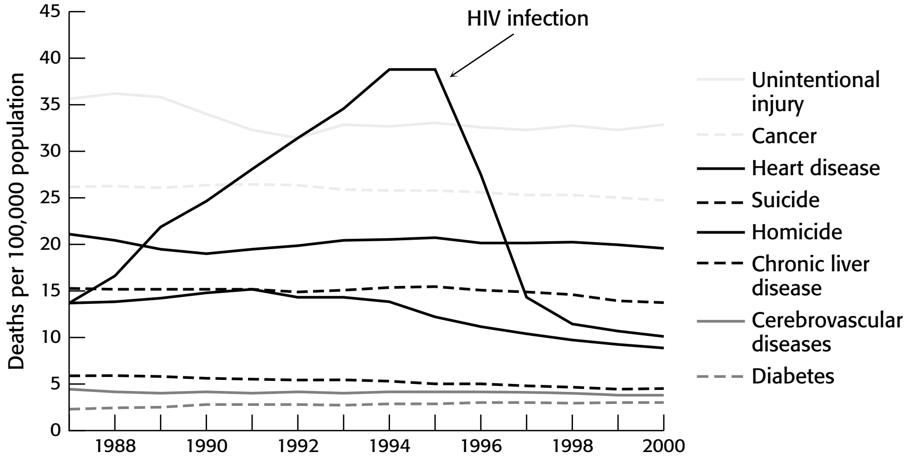

FIGURE 36.23 The effect of anti-HIV drug development. Death rates from HIV infection (AIDS) reveal the tremendous effect of HIV protease inhibitors and their use in combination with inhibitors of HIV reverse transcriptase. The death rates in this graph are from the leading causes of death among persons 24 to 44 years old in the United States. [Data from Centers for Disease Control.]

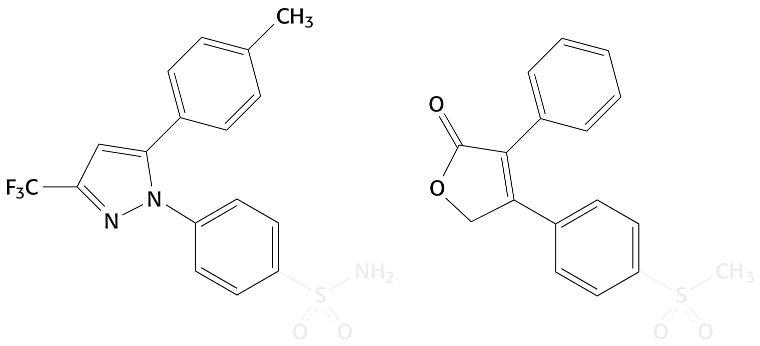

Celecoxib (Celebrex) **Rofecoxib (Vioxx)**

FIGURE 36.24 **COX2-specific inhibitors.** These compounds have protuberances (shown in red) that fit into a pocket in the COX2 isozyme but sterically clash with the COX1 isozyme.

a strategy for constructing COX2-specific inhibitors—namely, to synthesize compounds that had a protuberance that would fit into the pocket in the COX2 enzyme. Such compounds were designed and synthesized and then further refined to produce effective drugs familiar as Celebrex and Vioxx (Figure 36.24). Vioxx was subsequently withdrawn from the market because some people experienced adverse effects. Some of these effects may be due to the inhibition of COX2, the intended target. Thus, although the development of these drugs is a triumph for structure-based drug design, these outcomes highlight the fact that the inhibition of important enzymes can lead to complex physiological responses.

36.3 Analyses of Genomes Hold Great Promise for Drug Discovery

The completion of the sequencing of the human and other genomes is a potentially powerful driving force for the development of new drugs. Genomic sequencing and analysis projects have vastly increased our knowledge of the proteins encoded by the human genome. This new source of knowledge may greatly accelerate early stages of the drug-development process or even allow drugs to be tailored to the individual patient.

Potential targets can be identified in the human proteome

The human genome encodes approximately 21,000 proteins, not counting the variation produced by alternative mRNA splicing and posttranslational modifications. Many of these proteins are potential drug targets, in particular those that are enzymes or receptors and have significant biological effects when activated or inhibited. Several large protein families are particularly rich sources of targets. For example, the human genome includes genes for more than 500 protein kinases that can be recognized by comparing the deduced amino acid sequences. Many of these kinases are known to play a role in the progression of a variety of diseases. For example, Bcr-Abl kinase, a dysregulated kinase formed from a specific chromosomal defect, is known to contribute to certain leukemias and is the target of the drug imatinib mesylate (Gleevec; Section 14.5). Some of the other protein kinases undoubtedly play central roles in particular cancers as well. Similarly, the human genome encodes approximately 800 7TM receptors (Section 14.1), of which approximately 350 are odorant receptors. Many of the remaining 7TM receptors are known or potential drug targets. For example, the beta-blockers, which are widely used to treat hypertension, target the β_1-adrenergic receptor, and the antiulcer medication ranitidine (Zantac) targets the histamine H_2 receptor (a 7TM receptor that participates in the control of gastric acid secretion).

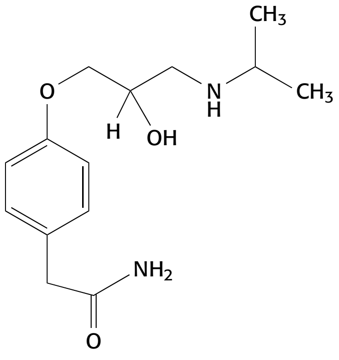

Atenolol

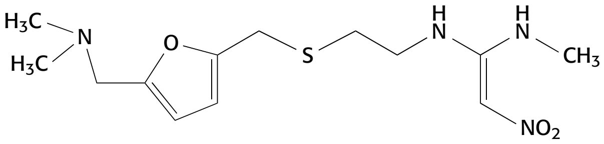

Ranitidine

Novel proteins that are not part of large families already supplying drug targets can be more readily identified through the use of genomic information. There are a number of ways to identify proteins that could serve as targets of drug-development programs. One way is to look for changes in expression patterns, protein localization, or posttranslational modifications in cells from disease-afflicted organisms. Another is to perform studies of tissues or cell types in which particular genes are expressed. Such analyses of the human genome should increase the number of actively pursued drug targets.

Animal models can be developed to test the validity of potential drug targets

The genomes of a number of model organisms have now been sequenced. The most important of these genomes for drug development is that of the mouse. Remarkably, the mouse and human genomes are approximately 85% identical in sequence, and more than 98% of all human genes have recognizable mouse counterparts. Mouse studies provide drug developers with a powerful tool—the ability to disrupt ("knock out") specific genes in the mouse (Section 5.4). If disruption of a gene has a desirable effect, then the product of this gene may represent a promising drug target. The utility of this approach has been demonstrated retrospectively. For example, disruption of the gene for the α subunit of the H^+–K^+ ATPase, the key protein for secreting acid into the stomach, produces mice with a gastric pH of 6.9. Under similar conditions, their wild-type counterparts produce a gastric pH of 3.2. This protein is the target of the drugs omeprazole (Prilosec) and lansoprazole (Prevacid and Takepron), used for treating gastroesophageal reflux disease.

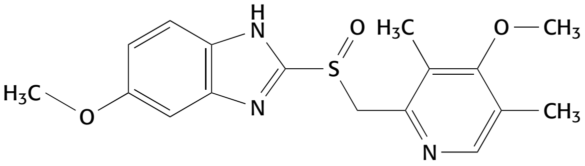

Omeprazole

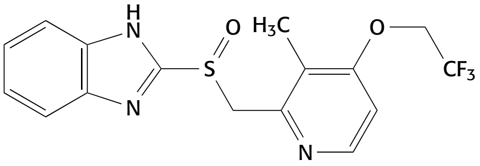

Lansoprazole

Several large-scale efforts are underway to generate hundreds or thousands of mouse strains, each having a different gene disrupted. The phenotypes of these mice are a good indication of whether the protein encoded by a disrupted gene is a promising drug target. This approach allows drug developers to evaluate potential targets without any preconceived notions regarding physiological function.

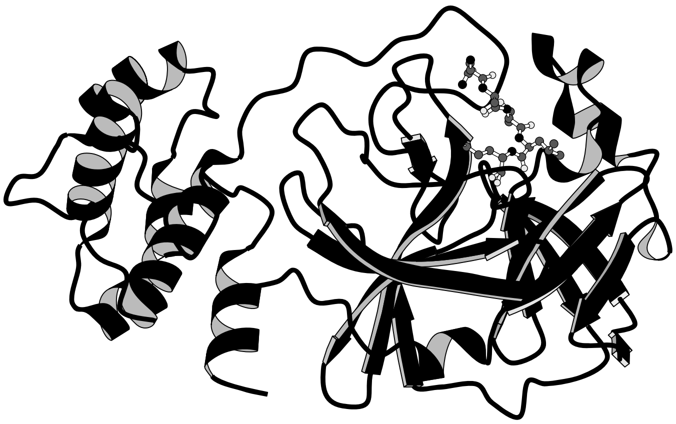

FIGURE 36.25 Emerging drug target. The structure of a protease from the coronavirus that causes SARS (severe acute respiratory syndrome) is shown bound to an inhibitor. This structure was determined less than a year after the identification of the virus. [Drawn from 1P9S.pdb.]

Potential targets can be identified in the genomes of pathogens

Human proteins are not the only important drug targets. Drugs such as penicillin and HIV protease inhibitors act by targeting proteins within a pathogen. The genomes of hundreds of pathogens have now been sequenced, and these genome sequences can be mined for potential targets.

New antibiotics are needed to combat bacteria that are resistant to many existing antibiotics. One approach seeks proteins essential for cell survival that are conserved in a wide range of bacteria. Drugs that inactivate such proteins are expected to be broad-spectrum antibiotics, useful for treating infections from any of a range of different bacteria. One such protein is peptide deformylase, the enzyme that removes formyl groups present at the amino termini of bacterial proteins immediately after translation (Figure 30.19).

Alternatively, a drug may be needed against a specific pathogen. An example of such a pathogen is the strain of coronavirus responsible for severe acute respiratory syndrome (SARS). Within one month of the recognition of this emerging disease, investigators had isolated the virus that causes the syndrome, and, within weeks, completely sequenced its 29,751-base genome. This sequence revealed the presence of a gene encoding a viral protease, known to be essential for viral replication from studies of other members of the coronavirus family to which the SARS virus belongs. This structure has opened the possibility for specific antiviral treatments for this, and related, viruses (Figure 36.25).

Genetic differences influence individual responses to drugs

Many drugs are not effective in everyone, often because of genetic differences among individuals. Nonresponding persons may have slight differences in either a drug's target molecule or the proteins taking part in drug transport and metabolism. The goal of the emerging fields of pharmacogenetics and pharmacogenomics is to design drugs that either act more consistently from person to person or are tailored to individual persons with particular genotypes.

Drugs such as metoprolol that target the β_1-adrenergic receptor are popular treatments for hypertension. These drugs are often referred to as "beta-blockers."

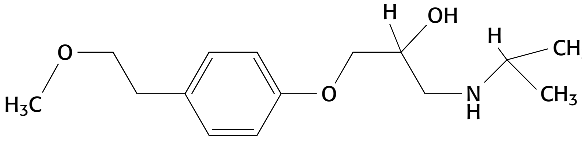

Metoprolol

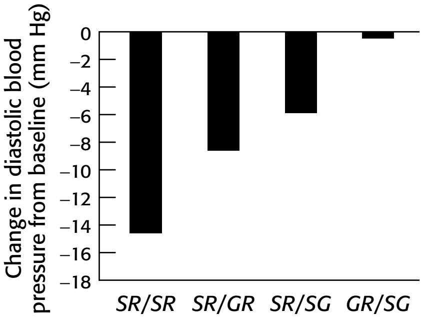

FIGURE 36.26 Phenotype–genotype correlation. Average changes in diastolic blood pressure on treatment with metoprolol. Persons with two copies of the most common allele ($S_{49}R_{389}$) showed significant decreases in blood pressure. Those with one variant allele (*GR* or *SG*) showed more modest decreases, and those with two variant alleles (*GR/SG*) showed no decrease. [Data from J. A. Johnson et al., *Clin. Pharmacol. Ther.* 74:44–52, 2003.]

However, some individuals do not respond well to beta-blockers. Two variants of the gene coding for the β_1-adrenergic receptor are common in the U.S. population. The most common allele has serine in position 49 and arginine in position 389. In some persons, however, glycine replaces one or the other of these residues. In clinical studies, participants with two copies of the most common allele responded well to metoprolol: their daytime diastolic blood pressure was reduced by 14.7 ± 2.9 mm Hg on average. In contrast, participants with one variant allele showed a smaller reduction in blood pressure, and the drug had no significant effect on participants with two variant alleles (Figure 36.26). These observations suggest the potential utility of genotyping individual patients at these positions. One could then predict whether treatment with metoprolol or other beta-blockers is likely to be effective.

Given the importance of ADME and toxicity properties in determining drug efficacy, it is not surprising that variations in proteins participating in drug transport and metabolism can alter a drug's effectiveness. An important example is the use of thiopurine drugs such as 6-thioguanine, 6-mercaptopurine, and azothioprine to treat diseases including leukemia, immune disorders, and inflammatory bowel disease.

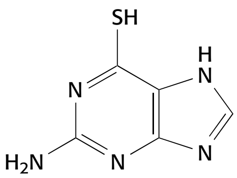

6-Thioguanine

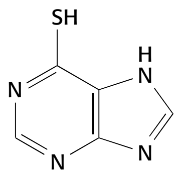

6-Mercaptopurine

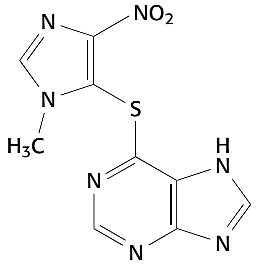

Azathioprine

A minority of patients who are treated with these drugs show signs of toxicity at doses that are well tolerated by most patients. These differences between patients are due to rare variations in the gene encoding the xenobiotic-metabolizing enzyme thiopurine methyltransferase, which adds a methyl group to sulfur atoms.

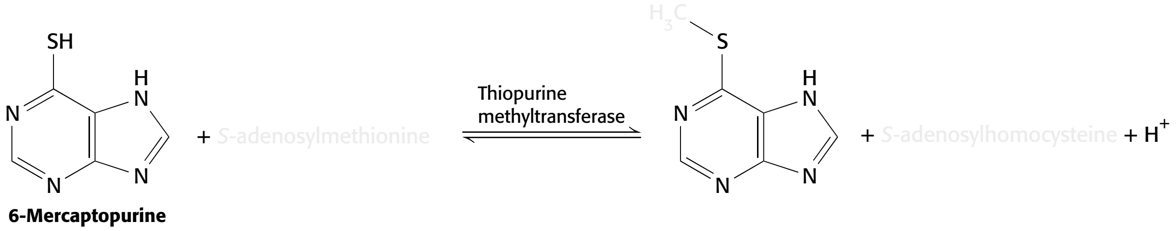

The variant enzyme is less stable. Patients with these variant enzymes can build up toxic levels of the drugs if appropriate care is not taken. Thus, genetic variability in an enzyme participating in drug metabolism plays a large role in determining the variation in the tolerance of different persons to particular drug levels. Many other drug-metabolism enzymes and drug-transport proteins have been implicated in controlling individual reactions to specific drugs. The identification of the genetic factors will allow a deeper understanding of why some drugs work well in some individuals but poorly in others. In the future, doctors may examine a patient's genes to help plan drug-therapy programs.

36.4 The Clinical Development of Drugs Proceeds Through Several Phases

In the United States, the FDA requires demonstration that drug candidates be effective and safe before they may be used in human beings on a large scale. This requirement is particularly true for drug candidates that are to be taken by people who are relatively healthy. More side effects are acceptable for drug candidates intended to treat significantly ill patients such as those with serious forms of cancer, where there are clear, unfavorable consequences for not having an effective treatment.

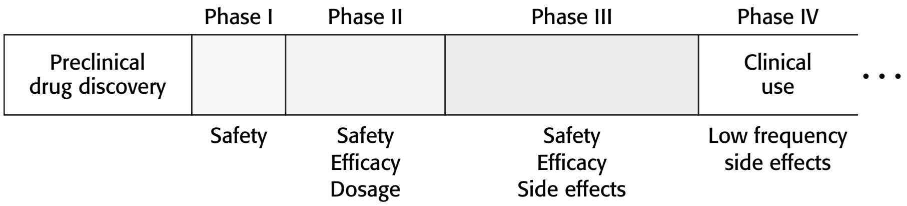

FIGURE 36.27 Clinical-trial phases. Clinical trials proceed in phases examining safety and efficacy in increasingly large groups.

Clinical trials are time consuming and expensive

Clinical trials test the effectiveness and potential side effects of a candidate drug before it is approved by the FDA for general use. These trials proceed in at least three phases (Figure 36.27). In Phase I, a small number (typically from 10 to 100) of usually healthy volunteers take the drug for an initial study of safety. These volunteers are given a range of doses and are monitored for signs of toxicity. The efficacy of the drug candidate is not specifically evaluated.

In Phase II, the efficacy of the drug candidate is tested in a small number of persons who might benefit from the drug. Further data regarding the drug's safety are obtained. Such trials are often controlled and double-blinded. In a controlled study, subjects are divided randomly into two groups. Subjects in the treatment group are given the treatment under investigation. Subjects in the control group are given either a *placebo*—that is, a treatment such as sugar pills known to not have intrinsic value—or the best standard treatment available, if withholding treatment altogether would be unethical. In a double-blinded study, neither the subjects nor the researchers know which subjects are in the treatment group and which are in the control group. A double-blinded study prevents bias in the course of the trial. When the trial has been completed, the assignments of the subjects into treatment and control groups are unsealed and the results for the two groups are compared. A variety of doses are often investigated in Phase II trials to determine which doses appear to be free of serious side effects and which doses appear to be effective.

The power of the *placebo effect*—that is, the tendency to perceive improvement in a subject who believes that he or she is receiving a potentially beneficial treatment—should not be underestimated. In a study of arthroscopic surgical treatment for knee pain, for example, subjects who were led to believe that they had received surgery through the use of videotapes and other means showed the same level of improvement, on average, as subjects who actually received the procedure.

In Phase III, similar studies are performed on a larger and more diverse population. This phase is intended to more firmly establish the efficacy of the drug candidate and to detect side effects that may develop in a small percentage of the subjects who receive treatment. Thousands of subjects may participate in a typical Phase III study.

Clinical trials can be extremely costly. Hundreds or thousands of patients must be recruited and monitored for the duration of the trial. Many physicians, nurses, clinical pharmacologists, statisticians, and others participate in the design and execution of the trial. Costs can run from tens of millions to hundreds of millions of dollars. Extensive records must be kept, including documentation of any adverse reactions. These data are compiled and submitted to the FDA. The full cost of developing a drug is currently estimated to be more than $800 million.

Even after a drug has been approved and is in use, difficulties can arise. Clinical trials run after a drug has entered the market, referred to as Phase IV studies, are designed to identify low-frequency side effects that may only emerge after widespread or long-term use. As mentioned earlier, rofecoxib (Vioxx), for example, was withdrawn from the market after significant cardiac side effects were detected in Phase IV clinical trials. Such events highlight the necessity for users of any drug to balance beneficial effects against potential risks.

The evolution of drug resistance can limit the utility of drugs for infectious agents and cancer

Many drugs are used for long periods of time without any loss of effectiveness. However, in some cases, particularly for the treatment of cancer or infectious diseases, drug treatments that were initially effective become less so. In other words, the disease becomes resistant to the drug therapy. Why does this resistance develop? Infectious diseases and cancer have a common feature—namely, that an affected person contains many cells (or viruses) that can mutate and reproduce. These conditions are necessary for evolution to take place. Thus, an individual microorganism or cancer cell may, by chance, have a genetic variation that makes it more suitable for growth and reproduction in the presence of the drug. These microorganisms or cells are more fit than others in their population, and they will tend to take over the population. As the selective pressure due to the drug is continually applied, the population of microorganisms or cancer cells will tend to become more and more resistant to the presence of the drug. Note that resistance can develop by a number of mechanisms.

The HIV protease inhibitors discussed earlier provide an important example of the evolution of drug resistance. Retroviruses are very well suited to this sort of evolution because reverse transcriptase carries out replication without a proofreading mechanism. In a genome of approximately 9750 bases, each possible single point mutation is estimated to appear in a virus particle more than 1000 times per day in each infected person. Many multiple mutations also occur. Most of these mutations either have no effect or are detrimental to the virus. However, a few of the mutant virus particles encode proteases that are less susceptible to inhibition by the drug. In the presence of an HIV protease inhibitor, these virus particles will tend to replicate more effectively than does the population at large. With the passage of time, the less-susceptible viruses will come to dominate the population and the virus population will become resistant to the drug.

Pathogens may become resistant to antibiotics by completely different mechanisms. Some pathogens contain enzymes that inactivate or degrade specific antibiotics. For example, many bacteria are resistant to β-lactams such as penicillin because they contain β-lactamase enzymes. These enzymes hydrolyze the β-lactam ring and render the drugs inactive.

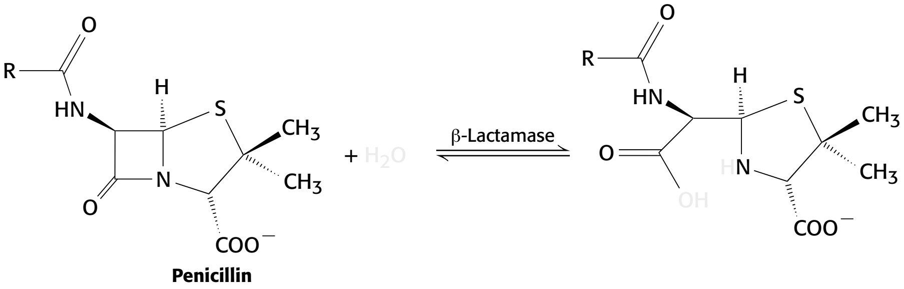

Many of these enzymes are encoded in plasmids, small circular pieces of DNA often carried by bacteria. Many plasmids are readily transferred from one bacterial cell to another, transmitting the capability for antibiotic resistance. Plasmid transfer thus contributes to the spread of antibiotic resistance, a major health-care challenge. On the other hand, plasmids have been harnessed for use in recombinant DNA methods (Section 5.2).

Drug resistance commonly emerges in the course of cancer treatment. Cancer cells are characterized by their ability to grow rapidly without the constraints that apply to normal cells. Many drugs used for cancer chemotherapy inhibit processes that are necessary for this rapid cell growth.

However, individual cancer cells may accumulate genetic changes that mitigate the effects of such drugs. These altered cancer cells will tend to grow more rapidly than others and will become dominant within the cancer-cell population. This ability of cancer cells to mutate quickly has been a challenge to one of the major breakthroughs in cancer treatment: the development of inhibitors for proteins specific to cancer cells present in certain leukemias (Section 14.5). For example, tumors become undetectable in patients treated with imatinib mesylate, which is directed against the Bcr-Abl protein kinase. Unfortunately, the tumors of many of the patients treated with imatinib mesylate recur after a period of years. In many of these cases, mutations have altered the Bcr-Abl protein so that it is no longer inhibited by the concentrations of imatinib mesylate used in therapy.

Cancer patients often take multiple drugs concurrently in the course of chemotherapy and, in many cases, cancer cells become simultaneously resistant to many or all of them. This multiple-drug resistance can be due to the proliferation of cancer cells that overexpress a number of ABC transporter proteins that pump drugs out of the cell (Section 13.2). Thus, cancer cells can evolve drug resistance by over expressing normal human proteins or by modifying proteins responsible for the cancer phenotype.

SUMMARY

36.1 The Development of Drugs Presents Huge Challenges

Most drugs act by binding to enzymes or receptors and modulating their activities. To be effective, drugs must bind to these targets with high affinity and specificity. However, compounds with the desired affinity and specificity do not necessarily make suitable drugs. Most compounds are poorly absorbed or rapidly excreted from the body or they are modified by metabolic pathways that target foreign compounds. Consequently, when taken orally, these compounds do not reach their targets at appropriate concentrations for a sufficient period of time. A drug's properties related to its absorption, distribution, metabolism, and excretion are called ADME properties. Oral bioavailability is a measure of a drug's ability to be absorbed; it is the ratio of the peak concentration of a compound given orally to the peak concentration of the same dose directly injected. The structure of a compound can affect its bioavailability in complicated ways, but generalizations called Lipinski's rules provide useful guidelines. Drug-metabolism pathways include oxidation by cytochrome P450 enzymes (phase I metabolism) and conjugation to glutathione, glucuronic acid, and sulfate (phase II metabolism). A compound may also not be a useful drug because it is toxic, either because it modulates the target molecule too effectively or because it also binds to proteins other than the target. The liver and kidneys play central roles in drug metabolism and excretion.

36.2 Drug Candidates Can Be Discovered by Serendipity, Screening, or Design

Many drugs have been discovered by serendipity—that is, by chance observation. The antibiotic penicillin is produced by a mold that accidentally contaminated a culture dish, killing nearby bacteria. Drugs such as chlorpromazine and sildenafil were discovered to have beneficial, but unexpected, effects on human physiology. The cholesterol-lowering statin drugs were developed after large collections of compounds were screened for potentially interesting activities. Combinatorial chemistry methods have been developed to generate large collections of chemically related yet diverse compounds for screening. In some cases, the three-dimensional structure of a drug target is available and can be used to aid the design of potent and specific inhibitors. Examples of drugs designed in this manner are the HIV protease inhibitor indinavir and cyclooxygenase 2 inhibitors such as celecoxib.

36.3 Analyses of Genomes Hold Great Promise for Drug Discovery

The human genome encodes approximately 21,000 proteins, and many more if derivatives due to alternative mRNA splicing and post-translational modification are included. The genome sequences can be examined for potential drug targets. Large families of proteins known to participate in key physiological processes such as the protein kinases and 7TM receptors have each yielded several targets for which drugs have been developed. The genomes of model organisms also are useful for drug-development studies. Strains of mice with particular genes disrupted have been useful in validating certain drug targets. The genomes of bacteria, viruses, and parasites encode many potential drug targets that can be exploited owing to their important functions and their differences from human proteins, minimizing the potential for side effects. Genetic differences between individuals can be examined and correlated with differences in responses to drugs, potentially aiding both clinical treatments and drug development.

36.4 The Clinical Development of Drugs Proceeds Through Several Phases

Before compounds can be given to human beings as drugs, they must be extensively tested for safety and efficacy. Clinical trials are performed in stages: first testing safety, then safety and efficacy in a small population, and finally safety and efficacy in a larger population to detect rarer adverse effects. Largely due to the expenses associated with clinical trials, the cost of developing a new drug has been estimated to be more than $800 million. Even when a drug has been approved for use, complications can arise. With regard to infectious diseases and cancer, patients often develop resistance to a drug after it has been administered for a period of time because variants of the disease agent that are less susceptible to the drug arise and replicate, even when the drug is present.

KEY TERMS

ligand (p. 1035)
dissociation constant (K_d) (p. 1035)
side effect (p. 1035)
inhibition constant (K_i) (p. 1036)
Cheng–Prusoff equation (p. 1036)
ADME (p. 1036)
oral bioavailability (p. 1036)
Lipinski's rules (p. 1036)
compartment (p. 1037)
blood–brain barrier (p. 1037)
xenobiotic compounds (p. 1037)
drug metabolism (p. 1037)
oxidation (p. 1037)
conjugation (p. 1037)
phase I transformation (p. 1039)
phase II transformation (p. 1039)
first-pass metabolism (p. 1039)
glomeruli (p. 1039)
enterohepatic cycling (p. 1040)
therapeutic index (p. 1041)
atheroma (p. 1043)
myopathy (p. 1044)
high-throughput screening (p. 1045)
combinatorial chemistry (p. 1045)
split-pool synthesis (p. 1045)
structure-based drug design (p. 1046)
structure–activity relationship (SAR) (p. 1046)
placebo (p. 1052)
placebo effect (p. 1052)

PROBLEMS

1. *Routes to discovery.* For each of the following drugs, indicate whether the physiological effects of the drug were known before or after the target was identified.

(a) Penicillin
(b) Sildenafil (Viagra)
(c) Rofecoxib (Vioxx)
(d) Atorvastatin (Lipitor)
(e) Aspirin
(f) Indinavir (Crixivan)

2. *Lipinski's rules.* Which of the following compounds satisfy all of Lipinski's rules? [Log(*P*) values are given in parentheses.]

(a) Atenolol (0.23)
(b) Sildenafil (3.18)
(c) Indinavir (2.78)

3. *Calculating log tables.* Considerable effort has been expended to develop computer programs that can estimate log(P) values entirely on the basis of chemical structure. Why would such programs be useful?

4. *An ounce of prevention.* Legislation has been proposed that would require that N-acetylcysteine be added to acetaminophen tablets. Speculate about the role of this additive.

5. *Clinical-trial design.* Distinguish between Phase I and Phase II clinical trials in regard to number of persons enrolled, the state of health of the subjects, and the goals of the study.

6. *Drug interactions.* As noted in this chapter, coumadin can be a very dangerous drug because too much can cause uncontrolled bleeding. Persons taking coumadin must be careful about taking other drugs, particularly those that bind to albumin. Propose a mechanism for this drug–drug interaction.

7. *A bad combination.* Explain why drugs that inhibit P450 enzymes may be particularly dangerous when used in combination with other medications.

8. *Mechanistically speaking.* Name one advantage of a noncompetitive inhibitor as a potential drug compared with a competitive inhibitor.

9. *A helping hand.* You have developed a drug that is capable of inhibiting the ABC transporter MDR. Suggest a possible application for this drug in cancer chemotherapy.

10. *Find the target.* Trypanosomes are unicellular parasites that cause sleeping sickness. During one stage of their life cycle, these organisms live in the bloodstream and derive all of their energy from glycolysis, which takes place in a specialized organelle called a glycosome inside the parasite. Propose potential targets for treating sleeping sickness. What are some potential difficulties with your approach?

11. *Knowledge is power.* How might genomic information be helpful for the effective use of imatinib mesylate (Gleevec) in cancer chemotherapy?

12. *Multiple targets, same goal.* Sildenafil induces its physiological effects by increasing the intracellular concentrations of cGMP, leading to muscle relaxation. On the basis of the scheme shown in Figure 36.17, identify another approach for increasing cGMP levels with a small molecule.

Mechanism Problem

13. *Variations on a theme.* The metabolism of amphetamine by cytochrome P450 enzymes results in the conversion shown here. Propose a mechanism and indicate any additional products.

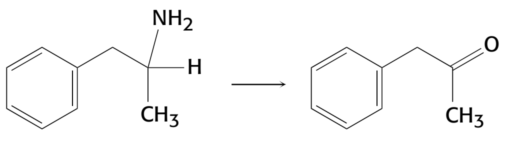

Amphetamine

Data Interpretation Problem

14. *HIV protease inhibitor design.* Compound A is one of a series that were designed to be potent inhibitors of HIV protease.

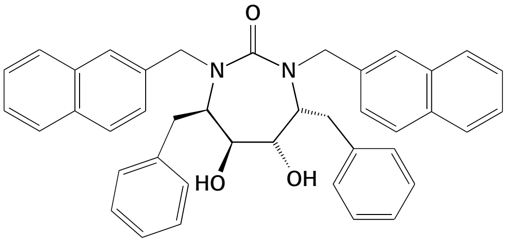

Compound A

Compound A was tested by using two assays: (1) direct inhibition of HIV protease in vitro and (2) inhibition of viral RNA production in HIV-infected cells, a measure of viral replication. The results of these assays are shown below. The HIV protease activity is measured with a substrate peptide present at a concentration equal to its K_M value.

Compound A (nM)	HIV protease activity (arbitrary units)
0	11.2
0.2	9.9
0.4	7.4
0.6	5.6
0.8	4.8
1	4.0
2	2.2
10	0.9
100	0.2

Compound A (nM)	Viral RNA production (arbitrary units)
0	760
1.0	740
2.0	380
3.0	280
4.0	180
5.0	100
10	30
50	20

Estimate the values for the K_I of compound A in the protease-activity assay and for its IC_{50} in the viral-RNA-production assay.

Treating rats with the relatively high oral dose of 20 mg kg^{-1} results in a maximum concentration of compound A of 0.4 μM. On the basis of this value, do you expect compound A to be effective in preventing HIV replication when taken orally?

ANSWERS TO PROBLEMS

Chapter 1

1. The hydrogen-bond donors are the NH and NH_2 groups. The hydrogen-bond acceptors are the carbonyl oxygen atoms and those ring nitrogen atoms that are not bonded to hydrogen or to deoxyribose.
2. Interchange the positions of the single and double bonds in the six-membered ring.
3. (a) Ionic interactions; (b) van der Waals interactions.
4. Processes *a* and *b*.
5. $\Delta S_{\text{system}} = -661\ \text{J mol}^{-1}\ \text{K}^{-1}(-158\ \text{kcal mol}^{-1}\ \text{K}^{-1})$

$\Delta S_{\text{surroundings}} = +842\ \text{J mol}^{-1}\ \text{K}^{-1}(+201\ \text{cal mol}^{-1}\ \text{K}^{-1})$

6. (a) 1.0; (b) 13.0; (c) 1.3; (d) 12.7
7. 2.88
8. 1.96
9. 55.5 M
10. 11.83
11. 447; 0.00050
12. 0.00066 M
13. 6.0
14. 5.53
15. 6.48
16. 7.8
17. 100
18. (a) 1.6; (b) 0.51; (c) 0.16.
19.

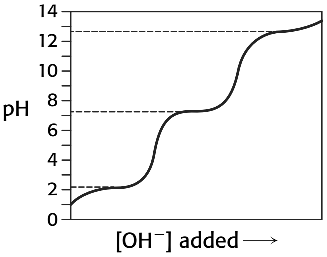

20. 0.1 M sodium acetate solution: 6.34; 6.03; 5.70; 4.75.
0.01 M sodium acetate solution: 5.90; 4.75; 3.38; 1.40.
21. 90 mM acetic acid; 160 mM sodium acetate, 0.18 moles acetic acid; 0.32 moles sodium acetate; 10.81 g acetic acid; 26.25 g sodium acetate.
22. 0.50 moles of acetic acid; 0.32 moles of NaOH; 30.03 g of acetic acid; 12.80 g of NaOH.
23. 250 mM; yes; no, it will also contain 90 mM NaCl.
24. 8.63 g Na_2HPO_4; 4.71 g NaH_2PO_4
25. 7.0; this buffer will not be very useful, because the pH value is far from the pK_a value.
26. $+1.45\ \text{kJ mol}^{-1}$ ($+0.35\ \text{kcal mol}^{-1}$); $+57.9\ \text{kJ mol}^{-1}$ ($+13.8\ \text{kcal mol}^{-1}$)
27. There will be approximately 15 million differences.
28. (20!)/(10!*10!) = 184,756
29. 7.9%

Chapter 2

1. (A) Proline, Pro, P; (B) tyrosine, Tyr, Y; (C) leucine, Leu, L; (D) lysine, Lys, K.
2. (a) C, B, A; (b) D; (c) D, B; (d) B, D; (e) B.
3. (a) 6; (b) 2; (c) 3; (d) 1; (e) 4; (f) 5.
4. (a) Ala; (b) Tyr; (c) Ser; (d) His.
5. Ser, Glu, Tyr, Thr
6. (a) Alanine-glycine-serine; (b) Alanine; (c and d):

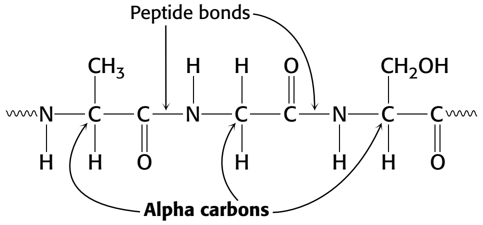

7. At pH 5.5, the net charge is +1:

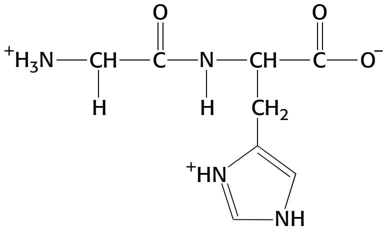

At pH 7.5, the net charge is 0:

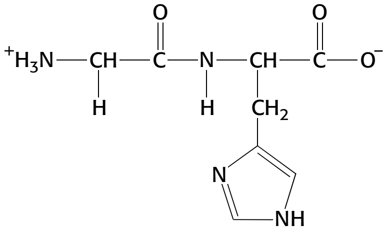

8. There are 20 choices for each of the 50 amino acids: 20^{50}, or 1×10^{65}.
9.

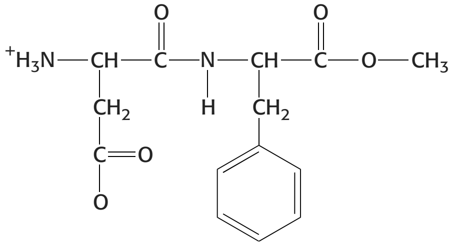

10. The (nitrogen–α carbon–carbonyl carbon) repeating unit.
11. Side chain is the functional group attached to the α-carbon atom of an amino acid.
12. Amino acid composition refers simply to the amino acids that make up the protein. The order is not specified. Amino acid sequence is the same as the primary structure—the sequence of amino acids from the amino terminal to the carboxyl terminal of the protein. Different proteins may have the same amino acid composition, but amino acid sequence identifies a unique protein.
13. (a) Each strand is 35 kDa and hence has about 318 residues (the mean residue mass is 110 daltons). Because the rise per residue in an α helix is 1.5 Å, the length is 477 Å. More precisely, for an α-helical coiled coil, the rise per residue is 1.46 Å; so the length is 464 Å. (b) Eighteen residues in each strand (40 minus 4 divided by 2) are in a β-sheet conformation. Because the rise per residue is 3.5 Å, the length is 63 Å.
14. The methyl group attached to the β-carbon atom of isoleucine sterically interferes with α-helix formation. In leucine, this methyl group is attached to the γ-carbon atom, which is farther from the main chain and hence does not interfere.

15. Proline and glycine. The cyclic side chain of proline linking the nitrogen and α-carbon atoms limits ϕ to a very narrow range (around -60 degrees). The lack of steric hindrance exhibited by the side chain hydrogen atom of glycine enables this amino acid to access a much greater area of the Ramachandran plot.
16. The first mutation destroys activity because valine occupies more space than alanine does, and so the protein must take a different shape, assuming that this residue lies in the closely packed interior. The second mutation restores activity because of a compensatory reduction of volume; glycine is smaller than isoleucine.
17. Loops invariably are on the surface of proteins, exposed to the environment. Because many proteins exist in aqueous environments, the exposed loops will be hydrophilic to interact with water.
18. The native conformation of insulin is not the thermodynamically most stable form, because it contains two separate chains linked by disulfide bonds. Insulin is formed from proinsulin, a single-chain precursor, that is cleaved to form insulin, a 51-residue molecule, after the disulfide bonds have formed.
19. A segment of the main chain of the protease could hydrogen bond to the main chain of the substrate to form an extended parallel or antiparallel pair of β strands.
20. Glycine has the smallest side chain of any amino acid. Its size is often critical in allowing polypeptide chains to make tight turns or to approach one another closely.
21. Glutamate, aspartate, and the terminal carboxylate can form salt bridges with the guanidinium group of arginine. In addition, this group can be a hydrogen-bond donor to the side chains of glutamine, asparagine, serine, threonine, aspartate, tyrosine, and glutamate and to the main-chain carbonyl group. Histidine can form hydrogen bonds with arginine at pH 7.
22. Disulfide bonds in hair are broken by adding a thiol-containing reagent and applying gentle heat. The hair is curled, and an oxidizing agent is added to re-form disulfide bonds to stabilize the desired shape.
23. Some proteins that span biological membranes are "the exceptions that prove the rule" because they have the reverse distribution of hydrophobic and hydrophilic amino acids. For example, consider *porins,* proteins found in the outer membranes of many bacteria. Membranes are built largely of hydrophobic chains. Thus, porins are covered on the outside largely with hydrophobic residues that interact with the neighboring hydrophobic chains. In contrast, the center of the protein contains many charged and polar amino acids that surround a water-filled channel running through the middle of the protein. Thus, because porins function in hydrophobic environments, they are "inside out" relative to proteins that function in aqueous solution.
24. The amino acids would be hydrophobic in nature. An α helix is especially suited to crossing a membrane because all of the amide hydrogen atoms and carbonyl oxygen atoms of the peptide backbone take part in intrachain hydrogen bonds, thus stabilizing these polar atoms in a hydrophobic environment.
25. This example demonstrates that the pK_a values are affected by the environment. A given amino acid can have a variety of pK_a values, depending on the chemical environment inside the protein.
26. Recall that hemoglobin exists as a tetramer while myoglobin is a monomer. Consequently, the hydrophobic residues on the surface of hemoglobin subunits are probably involved in van der Waals interactions with similar regions on the other subunits, and will be shielded from the aqueous environment by this interaction.
27. A possible explanation is that the severity of the symptoms corresponds to the degree of structural disruption. Hence, substitution of alanine for glycine might result in mild symptoms, but substitution of the much larger tryptophan may result in little or no collagen triple-helix formation.
28. The energy barrier that must be crossed to go from the polymerized state to the hydrolyzed state is large even though the reaction is thermodynamically favorable.
29. Using the Henderson–Hasselbach equation, we find the ratio of alanine-COOH to alanine-COO$^-$ at pH 7 to be 10^{-4}. The ratio of alanine-NH$_2$ to alanine-NH$_3{}^+$, determined in the same fashion, is 10^{-1}. Thus, the ratio of neutral alanine to the zwitterionic species is $10^{-4} \times 10^{-1} = 10^{-5}$.
30. The assignment of absolute configuration requires the assignment of priorities to the four groups connected to a tetrahedral carbon atom. For all amino acids except cysteine, the priorities are: (1) amino group; (2) carbonyl group; (3) side chain; (4) hydrogen. For cysteine, because of the sulfur atom in its side chain, the side chain has a greater priority than does the carbonyl group, leading to the assignment of an *R* rather than *S* configuration.
31. ELVISISLIVINGINLASVEGAS
32. No, Pro–X would have the characteristics of any other peptide bond. The steric hindrance in X–Pro arises because the R group of Pro is bonded to the amino group. Hence, in X–Pro, the proline R group is near the R group of X, which would not be the case in Pro–X.
33. A, c; B, e; C, d; D, a; E, b.
34. The reason is that the wrong disulfides formed pairs in urea. There are 105 different ways of pairing eight cysteine molecules to form four disulfides; only one of these combinations is enzymatically active. The 104 wrong pairings have been picturesquely termed "scrambled" ribonuclease.

Chapter 3

1. (a) Phenyl isothiocyanate; (b) urea; β-mercaptoethanol to reduce disulfides; (c) chymotrypsin; (d) CNBr; (e) trypsin.
2. For each cell within an organism, the genome is a fixed property. However, the proteome is dynamic, reflecting different environmental conditions and external stimuli. Two different cell types will likely express different subsets of proteins encoded within the genome.
3. The *S*-aminoethylcysteine side chain resembles that of lysine. The only difference is a sulfur atom in place of a methylene group.
4. A 1 mg ml^{-1} solution of myoglobin (17.8 kDa; Table 3.2) corresponds to 5.62×10^{-5} M. The absorbance of a 1-cm path length is 0.84, which corresponds to an I_0/I ratio of 6.96. Hence 14.4% of the incident light is transmitted.
5. The sample was diluted 1000-fold. The concentration after dialysis is thus 0.001 M, or 1 mM. You could reduce the salt concentration by dialyzing your sample, now 1 mM, in more buffer free of $(NH_4)_2SO_4$.
6. If the salt concentration becomes too high, the salt ions interact with the water molecules. Eventually, there will not be enough water molecules to interact with the protein, and the protein will precipitate. If there is lack of salt in a protein solution, the proteins may interact with one another—the positive charges on one protein with the negative charges on another or several others. Such an aggregate becomes too large to be solubilized by water alone. If salt is added, the salt neutralizes the charges on the proteins, preventing protein–protein interactions.
7. Tropomyosin is rod shaped, whereas hemoglobin is approximately spherical.
8. The frictional coefficient, *f*, and the mass, *m*, determine *s*. Specifically, *f* is proportional to *r* (see equation 2 on p. 71). Hence, *f* is proportional to $m^{1/3}$, and so *s* is proportional to $m^{2/3}$ (see the

equation on p. 76). An 80-kDa spherical protein undergoes sedimentation 1.59 times as rapidly as a 40-kDa spherical protein.

9. The long hydrophobic tail on the SDS molecule (see p. 72) disrupts the hydrophobic interactions in the interior of the protein. The protein unfolds, with the hydrophobic R groups now interacting with SDS rather than with one another.

10. 50 kDa

11. The protein may be modified. For instance, asparagine residues in the protein may be modified with carbohydrate units (Section 2.6).

12. A fluorescence-labeled derivative of a bacterial degradation product (e.g., a formylmethionyl peptide) would bind to cells containing the receptor of interest.

13. (a) Trypsin cleaves after arginine (R) and lysine (K), generating AVGWR, VK, and S. Because they differ in size, these products could be separated by molecular exclusion chromatography. (b) Chymotrypsin, which cleaves after large aliphatic or aromatic R groups, generates two peptides of equal size (AVGW) and (RVKS). Separation based on size would not be effective. The peptide RVKS has two positive charges (R and K), whereas the other peptide is neutral. Therefore, the two products could be separated by ion-exchange chromatography.

14. Antibody molecules bound to a solid support can be used for affinity purification of proteins for which a ligand molecule is not known or unavailable.

15. If the product of the enzyme-catalyzed reaction is highly antigenic, it may be possible to obtain antibodies to this particular molecule. These antibodies can be used to detect the presence of product by ELISA, providing an assay format suitable for the purification of this enzyme.

16. An inhibitor of the enzyme being purified might have been present and subsequently removed by a purification step. This removal would lead to an apparent increase in the total amount of enzyme present.

17. Many proteins have similar masses but different sequences and different patterns when digested with trypsin. The set of masses of tryptic peptides forms a detailed "fingerprint" of a protein that is very unlikely to appear at random in other proteins regardless of size. (A conceivable analogy is: "Just as similarly sized fingers will give different individual fingerprints, so also similarly sized proteins will give different digestion patterns with trypsin.")

18. Isoleucine and leucine are isomers and, hence, have identical masses. Peptide sequencing by mass spectrometry as described in this chapter is incapable of distinguishing these residues. Further analytical techniques are required to differentiate these residues.

19. See the table at the bottom of the page.

20. (a) Ion exchange chromatography will remove Proteins A and D, which have substantially lower isoelectric point; then gel filtration chromatography will remove Protein C, which has a lower molecular weight. (b) If Protein B carries a His tag, a single affinity chromatography step with an immobilized nickel(II) column may be sufficient to isolate the desired protein from the others.

21. Protein crystal formation requires the ordered arrangement of identically positioned molecules. Proteins with flexible linkers can introduce disorder into this arrangement and prevent the formation of suitable crystals. A ligand or binding partner may induce an ordered conformation to this linker and could be included in the solution to facilitate crystal growth. Alternatively, the individual domains separated by the linker may be expressed by recombinant methods and their crystal structures solved separately.

22. Treatment with urea will disrupt noncovalent bonds. Thus the original 60-kDa protein must be made of two 30-kDa subunits. When these subunits are treated with urea and β-mercaptoethanol, a single 15-kDa species results, suggesting that disulfide bonds link the 30-kDa subunits.

23. (a) Electrostatic repulsion between positively charged ε-amino groups hinders α-helix formation at pH 7. At pH 10, the side chains become deprotonated, allowing α-helix formation. (b) Poly-L-glutamate is a random coil at pH 7 and becomes α helical below pH 4.5 because the γ-carboxylate groups become protonated.

24. The difference between the predicted and the observed masses for this fragment equals 28.0, exactly the mass shift that would be expected in a formylated peptide. This peptide is likely formylated at its amino terminus, and corresponds to the most N-terminal fragment of the protein.

25. Light was used to direct the synthesis of these peptides. Each amino acid added to the solid support contained a photolabile protecting group instead of a *t*-Boc protecting group at its α-amino group. Illumination of selected regions of the solid support led to the release of the protecting group, which exposed the amino groups in these sites to make them reactive. The pattern of masks used in these illuminations and the sequence of reactants define the ultimate products and their locations.

26. Mass spectrometry is highly sensitive and capable of detecting the mass difference between a protein and its deuterated counterpart. Fragmentation techniques can be used to identify the amino acids that retained the isotope label. Alternatively, NMR spectroscopy can be used to detect the isotopically labeled atoms because the deuteron and the proton have very different nuclear-spin properties.

27. First amino acid: A
Last amino acid: R (not cleaved by carboxypeptidase).
Sequence of N-terminal tryptic peptide: AVR (tryptic peptide ends in K)
Sequence of N-terminal chymotryptic peptide: AVRY (chymotryptic peptide ends in Y)
Sequence: AVRYSR

28. First amino acid: S
Last amino acid: L
Cyanogen bromide cleavage: M is 10th position
C-terminal residues are: (2S,L,W)
Amino-terminal residues: (G,K,S,Y), tryptic peptide, ends in K
Amino-terminal sequence: SYGK
Chymotryptic peptide order: (S,Y), (G,K,L), (F,I,S), (M,T), (S,W), (S,L)
Sequence: SYGKLSIFTMSWSL

Purification procedure	**Total protein (mg)**	**Total activity (units)**	**Specific activity (units mg^{-1})**	**Purification level**	**Yield (%)**
Crude extract	20,000	4,000,000	200	1	100
$(NH_4)_2SO_4$ precipitation	5,000	3,000,000	600	3	75
DEAE–cellulose chromatography	1,500	1,000,000	667	3.3	25
Gel-filtration chromatography	500	750,000	1,500	7.5	19
Affinity chromatography	45	675,000	15,000	75	17

29. If the protein did not contain any disulfide bonds, then the electrophoretic mobility of the trypsin fragments would be the same before and after performic acid treatment: all the fragments would lie along the diagonal of the paper. If one disulfide bond were present, the disulfide-linked trypsin fragments would run as a single peak in the first direction, then would run as two separate peaks after performic acid treatment. The result would be two peaks appearing off the diagonal:

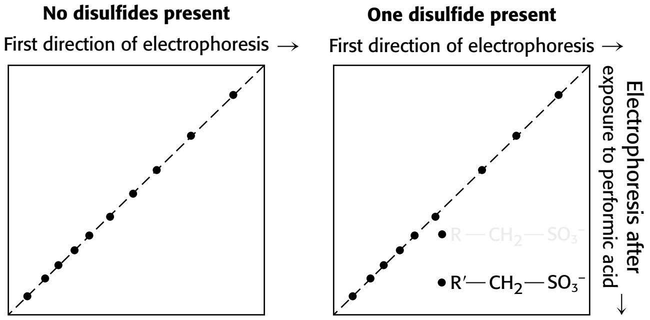
No disulfides present
First direction of electrophoresis →
One disulfide present
First direction of electrophoresis →
Electrophoresis after exposure to performic acid ↓
R — CH₂ — SO₃⁻
R′— CH₂— SO₃⁻

These fragments could then be isolated from the chromatography paper and analyzed by mass spectrometry to determine their amino acid composition and thus identify the cysteines participating in the disulfide bond.

Chapter 4

1. A nucleoside is a base attached to a ribose or deoxyribose sugar. A nucleotide is a nucleoside with one or more phosphoryl groups attached to the ribose or deoxyribose.
2. Hydrogen-bond pairing between the base A and the base T as well as hydrogen-bond pairing between the base G and the base C in DNA.
3. T is always equal to A, and so these two nucleotides constitute 40% of the bases. G is always equal to C, and so the remaining 60% must be 30% G and 30% C.
4. Nothing, because the base-pair rules do not apply to single-stranded nucleic acids.
5. (a) TTGATC; (b) GTTCGA; (c) ACGCGT; (d) ATGGTA.
6. (a) $[T] + [C] = 0.46$. (b) $[T] = 0.30$, $[C] = 0.24$, and $[A] + [G] = 0.46$.
7. Stable hydrogen bonding occurs only between GC and AT pairs. Moreover, two purines are too large to fit inside the double helix, and two pyrimidines are too small to form base pairs with each other.
8. The thermal energy causes the chains to wiggle about, which disrupts the hydrogen bonds between base pairs and the stacking forces between bases and thereby causes the strands to separate.
9. The probability that any sequence will appear is $1/4^n$, where 4 is the number of nucleotides and n is the length of the sequence. The probability of any 15-base sequence appearing is $1/4^{15}$, or 1/1,073,741,824. Thus, a 15-nucleotide sequence would be likely to appear approximately three times (3 billion × probability of appearance). The probability of a 16-base sequence appearing is $1/4^{16}$, which is equal to 1/4,294,967,296. Such a sequence will be unlikely to appear more than once.
10. One end of a nucleic acid polymer ends with a free 5′-hydroxyl group (or a phosphoryl group esterified to the hydroxyl group), and the other end has a free 3′-hydroxyl group. Thus, the ends are different. Two strands of DNA can form a double helix only if the strands are running in different directions—that is, have opposite polarity.
11. Although the individual bonds are weak, the population of thousands to millions of such bonds provides much stability. There is strength in numbers.
12. There would be too much charge repulsion from the negative charges on the phosphoryl groups. These charges must be countered by the addition of cations.
13. The three forms are the A-DNA, the B-DNA and the Z-DNA, with B-DNA being the most common. There are many differences (Table 4.2). Some key differences are: A-DNA and B-DNA are right-handed, whereas Z-DNA is left-handed. A-DNA forms in less-hydrated conditions than does B-DNA. The A form is shorter and wider than the B form.
14. 5.88×10^3 base pairs.
15. The diameter of DNA is 20 Å and 1 Å = 0.1 nm, so the diameter is 2 nm. Because 1 μm = 10^3 nm, the length is 2×10^4 nm. Thus, the axial ratio is 1×10^4.
16. A template is the sequence of DNA or RNA that directs the synthesis of a complementary sequence. A primer is the initial segment of a polymer that is to be extended during elongation.
17. In conservative replication, after 1.0 generation, half of the molecules would be ^{15}N-^{15}N, the other half ^{14}N-^{14}N. After 2.0 generations, one-quarter of the molecules would be ^{15}N-^{15}N, the other three-quarters ^{14}N-^{14}N. Hybrid ^{14}N-^{15}N molecules would not be observed in conservative replication.
18. The nucleotides used for DNA synthesis have the triphosphate attached to the 5′-hydroxyl group with free 3′-hydroxyl groups. Such nucleotides can be utilized only for 5′-to-3′ DNA synthesis.
19. (a) Tritiated thymine or tritiated thymidine. (b) dATP, dGTP, dCTP, and TTP labeled with ^{32}P in the innermost (α) phosphorus atom.
20. Molecules in parts *a* and *b* would not lead to DNA synthesis, because they lack a 3′-OH group (a primer). The molecule in part *d* has a free 3′-OH group at one end of each strand but no template strand beyond. Only the molecule in part *c* would lead to DNA synthesis.
21. A retrovirus is a virus that has RNA as its genetic material. However, for the information to be expressed, it must first be converted into DNA, a reaction catalyzed by the enzyme reverse transcriptase. Thus, at least initially, information flow is opposite that of a normal cell: RNA → DNA rather than DNA → RNA.
22. A thymidylate oligonucleotide should be used as the primer. The poly(A) template specifies the incorporation of T; hence, radioactive thymidine triphosphate (labeled in the α phosphoryl group) should be used in the assay.
23. The ribonuclease serves to degrade the RNA strand, a necessary step in forming duplex DNA from the RNA–DNA hybrid.
24. Treat one aliquot of the sample with ribonuclease and another with deoxyribonuclease. Test these nuclease-treated samples for infectivity.
25. Deamination changes the original G · C base pair into a G · U pair. After one round of replication, one daughter duplex will contain a G · C pair and the other duplex will contain an A · U pair. After two rounds of replication, there will be two G · C pairs, one A · U pair, and one A · T pair.
26. (a) $4^8 = 65{,}536$. In computer terminology, there are 64K 8-mers of DNA.
(b) A bit specifies two bases (say, A and C) and a second bit specifies the other two (G and T). Hence, two bits are needed to specify a single nucleotide (base pair) in DNA. For example, 00, 01, 10, and 11 could encode A, C, G, and T. An 8-mer stores 16 bits ($2^{16} = 65{,}536$), the *E. coli* genome (4.6×10^6 bp) stores 9.2×10^6 bits, and the human genome (3.0×10^9 bases) stores 6.0×10^9 bits of genetic information.
(c) A standard CD can hold about 700 megabytes, which is equal to 5.6×10^9 bits. A large number of 8-mer sequences could be

stored on such a CD. The DNA sequence of *E. coli* could be written on a single CD with room to spare for a lot of music. One CD would not be quite enough to record the entire human genome.

27. (a) Deoxyribonucleoside triphosphates versus ribonucleoside triphosphates.
(b) 5′ → 3′ for both.
(c) Semiconserved for DNA polymerase I; conserved for RNA polymerase.
(d) DNA polymerase I needs a primer, whereas RNA polymerase does not.

28. The template strand has a sequence complementary to that of the RNA transcript. The coding strand has the same sequence as that of the RNA transcript except for thymine (T) in place of uracil (U).

29. Messenger RNA encodes the information that, on translation, yields a protein. Ribosomal RNA is the catalytic component of ribosomes, the molecular complexes that synthesize proteins. Transfer RNA is an adaptor molecule, capable of binding a specific amino acid and recognizing a corresponding codon. Transfer RNAs with attached amino acids are substrates for the ribosome.

30. Three nucleotides encode an amino acid; the code is nonoverlapping; the code has no punctuation; the code exhibits directionality; the code is degenerate.

31. (a) 5′-UAACGGUACGAU-3′
(b) Leu-Pro-Ser-Asp-Trp-Met
(c) Poly(Leu-Leu-Thr-Tyr)

32. The 2′-OH group in RNA acts as an intramolecular nucleophile. In the alkaline hydrolysis of RNA, it forms a 2′-3′ cyclic intermediate.

33.

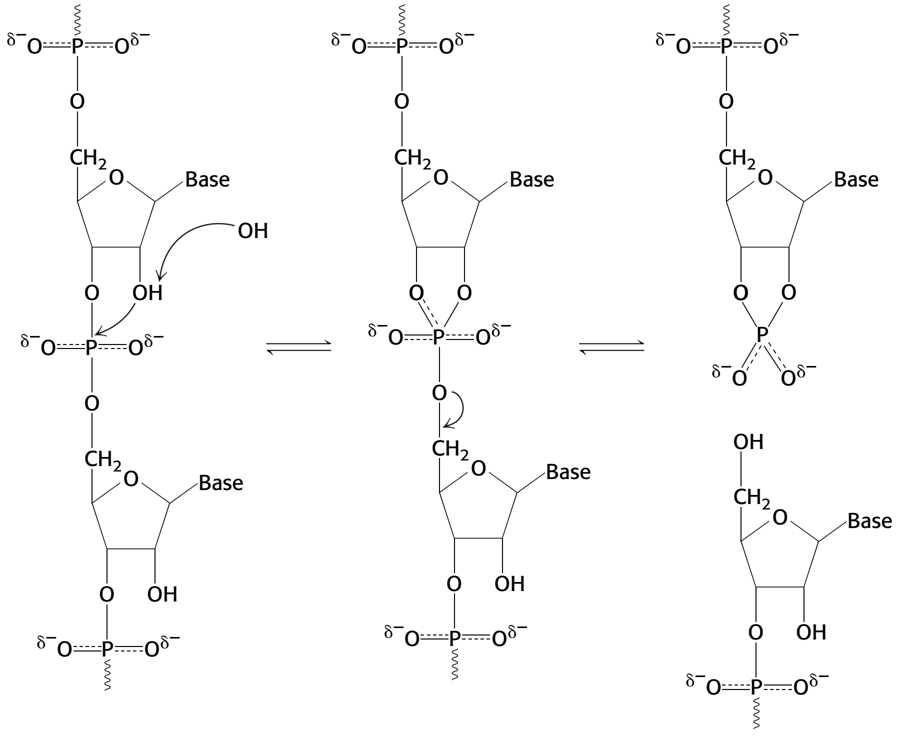

34. Gene expression is the process of expressing the information of a gene in its functional molecular form. For many genes, the functional information is a protein molecule. Thus, gene expression includes transcription and translation.

35. A nucleotide sequence whose bases represent the most-common, but not necessarily the only, members of the sequence. A consensus sequence can be thought of as the average of many similar sequences.

36. Cordycepin terminates RNA synthesis. An RNA chain containing cordycepin lacks a 3′-OH group.

37. Only single-stranded RNA can serve as a template for protein synthesis.

38. Degeneracy of the code refers to the fact that most amino acids are encoded by more than one codon.

39. If only 20 of the 64 possible codons encoded amino acids, then a mutation that changed a codon would likely result in a nonsense codon, leading to termination of protein synthesis. With degeneracy, a nucleotide change might yield a synonym or a codon for an amino acid with similar chemical properties.

40. (a) 2, 4, 8; (b) 1, 6, 10; (c) 3, 5, 7, 9.

41. (a) 3; (b) 6; (c) 2; (d) 5; (e) 7; (f) 1; (g) 4.

42. Incubation with RNA polymerase and only UTP, ATP, and CTP led to the synthesis of only poly(UAC). Only poly(GUA) was formed when GTP was used in place of CTP.

43. A peptide terminating with Lys (UGA is a stop codon), another containing -Asn-Glu-, and a third containing -Met-Arg-.

44. Phe-Cys-His-Val-Ala-Ala

45. Exon shuffling is a molecular process that can lead to the generation of new proteins by the rearrangement of exons within genes. Because many exons encode functional protein domains, exon shuffling is a rapid and efficient means of generating new genes.

46. Alternate splicing allows one gene to code for several different but related proteins.

47. It shows that the genetic code and the biochemical means of interpreting the code are common to even very distantly related life forms. It also testifies to the unity of life: that all life arose from a common ancestor.

48. (a) A codon for lysine cannot be changed to one for aspartate by the mutation of a single nucleotide. (b) Arg, Asn, Gln, Glu, Ile, Met, or Thr.

49. The genetic code is degenerate. Of the 20 amino acids, 18 are specified by more than one codon. Hence, many nucleotide changes (especially in the third base of a codon) do not alter the nature of the encoded amino acid. Mutations leading to an altered amino acid are usually more deleterious than those that do not and hence are subject to more stringent selection.

50. GC base pairs have three hydrogen bonds compared with two for AT base pairs. Thus, the higher content of GC means more hydrogen bonds and greater helix stability.

51. C_0t value essentially corresponds to the complexity of the DNA sequence—in other words, how long it will take for a sequence of DNA to find its complementary strand to form a double helix. The more complex the DNA, the slower it reassociates to make the double-stranded form.

52. Increasing salt increases the melting temperature. Because the DNA backbone is negatively charged, there is a tendency for charge repulsion to destabilize the helix and cause it to melt. The addition of salt neutralizes the charge repulsion, thereby stabilizing

the double helix. The results show that within the parameters of the experiment, more salt results in more stabilization, which is reflected as a higher melting temperature.

Chapter 5

1. *Taq* polymerase is the DNA polymerase from the thermophilic bacterium that lives in hot springs. Consequently, it is heat stable and can withstand the high temperatures required for PCR without denaturing.
2. Ovalbumin cDNA should be used. *E. coli* lacks the machinery to splice the primary transcript arising from genomic DNA.
3. Consistent with its planar, aromatic structure, ethidium bromide is a DNA intercalator: it aligns itself between the paired bases in a DNA duplex.
4. The presence of the AluI sequence would, on average, be $(1/4)^4$, or 1/256, because the likelihood of any base being at any position is one-fourth and there are four positions. By the same reasoning, the presence of the NotI sequence would be $(1/4)^8$, or 1/65,536. Thus, the average product of digestion by AluI would be 250 base pairs (0.25 kb) in length, whereas that by NotI would be 66,000 base pairs (66 kb) in length.
5. No, because most human genes are much longer than 4 kb. A fragment would contain only a small part of a complete gene.
6. Southern blotting of an MstII digest would distinguish between the normal and the mutant genes. The loss of a restriction site would lead to the replacement of two fragments on the Southern blot by a single longer fragment. Such a finding would not prove that GTG replaced GAG; other sequence changes at the restriction site could yield the same result.
7. Although the two enzymes cleave the same recognition site, they each break different bonds within the 6-bp sequence. Cleavage by KpnI yields an overhang on the 3′ strand, whereas cleavage by Acc65I produces an overhang on the 5′ strand. These sticky ends do not overlap.

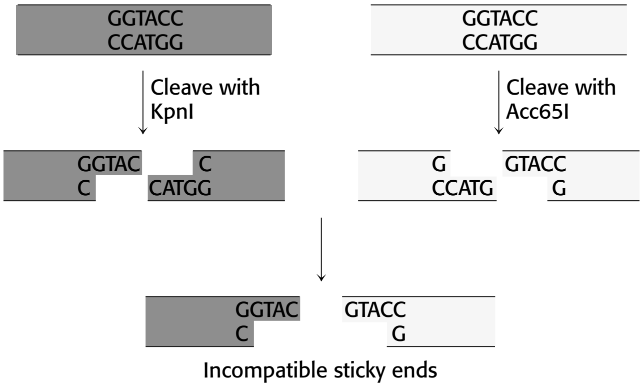

8. A simple strategy for generating many mutants is to synthesize a degenerate set of cassettes by using a mixture of activated nucleosides in particular rounds of oligonucleotide synthesis. Suppose that the 30-bp coding region begins with GTT, which encodes valine. If a mixture of all four nucleotides is used in the first and second rounds of synthesis, the resulting oligonucleotides will begin with the sequence XYT (where X and Y denote A, C, G, or T). These 16 different versions of the cassette will encode proteins containing either Phe, Leu, Ile, Val, Ser, Pro, Thr, Ala, Tyr, His, Asn, Asp, Cys, Arg, or Gly at the first position. Likewise, degenerate cassettes can be made in which two or more codons are simultaneously varied.
9. Because PCR can amplify as little as one molecule of DNA, statements claiming the isolation of ancient DNA need to be greeted with some skepticism. The DNA would need to be sequenced. Is it similar to human, bacterial, or fungal DNA? If so, contamination is the likely source of the amplified DNA. Is it similar to that of birds or crocodiles? This sequence similarity would strengthen the case that it is dinosaur DNA because these species are evolutionarily close to dinosaurs.
10. PCR amplification is greatly hindered by the presence of G–C-rich regions within the template. Owing to their high melting temperatures, these templates do not denature easily, preventing the initiation of an amplification cycle. In addition, rigid secondary structures prevent the progress of DNA polymerase along the template strand during elongation.
11. At high temperatures of hybridization, only very close matches between primer and target would be stable because all (or most) of the bases would need to find partners to stabilize the primer–target helix. As the temperature is lowered, more mismatches would be tolerated; so the amplification is likely to yield genes with less sequence similarity. In regard to the yeast gene, synthesize primers corresponding to the ends of the gene, and then use these primers and human DNA as the target. If nothing is amplified at 54°C, the human gene differs from the yeast gene, but a counterpart may still be present. Repeat the experiment at a lower temperature of hybridization.
12. Digest genomic DNA with a restriction enzyme, and select the fragment that contains the known sequence. Circularize this fragment. Then carry out PCR with the use of a pair of primers that serve as templates for the synthesis of DNA away from the known sequence.
13. The encoded protein contains four repeats of a specific sequence.
14. Use chemical synthesis or the polymerase chain reaction to prepare hybridization probes that are complementary to both ends of the known (previously isolated) DNA fragment. Challenge clones representing the library of DNA fragments with both of the hybridization probes. Select clones that hybridize to one of the probes but not the other; such clones are likely to represent DNA fragments that contain one end of the known fragment along with the adjacent region of the particular chromosome.
15. The codon(s) for each amino acid can be used to determine the number of possible nucleotide sequences that encode each peptide sequence (Table 4.5):

Ala–Met–Ser–Leu–Pro–Trp:
$4 \times 1 \times 6 \times 6 \times 4 \times 1 = 576$ total sequences

Gly–Trp–Asp–Met–His–Lys:
$4 \times 1 \times 2 \times 1 \times 2 \times 2 = 32$ total sequences

Cys–Val–Trp–Asn–Lys–Ile:
$2 \times 4 \times 1 \times 2 \times 2 \times 3 = 96$ total sequences

Arg–Ser–Met–Leu–Gln–Asn:
$6 \times 6 \times 1 \times 6 \times 2 \times 2 = 864$ total sequences

The set of DNA sequences encoding the peptide Gly-Trp-Asp-Met-His-Lys would be most ideal for probe design because it encompasses only 32 total oligonucleotides.
16. Within a single species, individual dogs show enormous variation in body size and substantial diversity in other physical characteristics. Therefore, genomic analysis of individual dogs would provide valuable clues concerning the genes responsible for the diversity within the species.
17. On the basis of the comparative genome map shown in Figure 5.28, the region of greatest overlap with human chromosome 20 can be found on mouse chromosome 2.
18. T_m is the melting temperature of a double-stranded nucleic acid. If the melting temperatures of the primers are too different,

the extent of hybridization with the target DNA will differ during the annealing phase, which would result in differential replications of the strands.

19. Careful comparison of the sequences reveals that there is a 7-bp region of complementarity at the 3′ ends of these two primers:

5′-GGATCGATGCTCGCGA-3′
| | | | | | |
3′-GAGCGCTGGGCTAGGA-5′

In a PCR experiment, these primers would likely anneal to one another, preventing their interaction with the template DNA. During DNA synthesis by the polymerase, each primer would act as a template for the other primer, leading to the amplification of a 25-bp sequence corresponding to the overlapped primers.

20. A mutation in person B has altered one of the alleles for gene *X,* leaving the other intact. The fact that the mutated allele is smaller suggests that a deletion has occurred in one copy of the gene. The one functioning copy is transcribed and translated and apparently produces enough protein to render the person asymptomatic.

Person C has only the smaller version of the gene. This gene is neither transcribed (negative northern blot) nor translated (negative western blot).

Person D has a normal-size copy of the gene but no corresponding RNA or protein. There may be a mutation in the promoter region of the gene that prevents transcription.

Person E has a normal-size copy of the gene that is transcribed, but no protein is made, which suggests that a mutation prevents translation. There are a number of possible explanations, including a mutation that introduced a premature stop codon in the mRNA.

Person F has a normal amount of protein but still displays the metabolic problem. This finding suggests that the mutation affects the activity of the protein—for instance, a mutation that compromises the active site of enzyme Y.

21. Chongqing: residue 2, L → R, CTG → CGG
Karachi: residue 5, A → P, GCC → CCC
Swan River: residue 6, D → G, GAC → GGC

22. This particular person is heterozygous for this particular mutation: one allele is wild type, whereas the other carries a point mutation at this position. Both alleles are PCR amplified in this experiment, yielding the "dual peak" appearance on the sequencing chromatogram.

Chapter 6

1. There are 26 identities and two gaps for a score of 210. The two sequences are approximately 26% identical. This level of homology is likely to be statistically significant.

2. They are likely related by divergent evolution, because three-dimensional structure is more conserved than is sequence identity.

3. (1) Identity score = −25; Blosum score = 14; (2) identity score = 15; Blosum score = 3.

4. U. One possible structure:

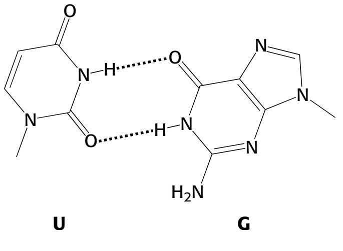

5. There are 4^{40}, or 1.2×10^{24}, different molecules. Each molecule has a mass of 2.2×10^{-20}, because 1 mol of polymer has a mass of 330 g $\text{mol}^{-1} \times 40$, and there are 6.02×10^{23} molecules per mole. Therefore, 26.4 kg of RNA would be required.

6. Because three-dimensional structure is much more closely associated with function than is sequence, tertiary structure is more evolutionarily conserved than is primary structure. In other words, protein function is the most important characteristic, and protein function is determined by structure. Thus, the structure must be conserved but not necessarily a specific amino acid sequence.

7. Alignment score of sequences (1) and (2) is 6 × 10 = 60. Many answers are possible, depending on the randomly reordered sequence. A possible result is

Shuffled sequence: (2) `TKADKAGEYL`
Alignment: (1) `ASNFLDKAGK`
(2) `TKADKAGEYL`

Alignment score is 4 × 10 = 40.

8. (a) Almost certainly diverged from a common ancestor. (b) Almost certainly diverged from a common ancestor. (c) May have diverged from a common ancestor, but the sequence alignment may not provide supporting evidence. (d) May have diverged from a common ancestor, but the sequence alignment is unlikely to provide supporting evidence.

9. Replacement of cysteine, glycine, and proline never yields a positive score. Each of these residues exhibits features unlike those of its other 19 counterparts: cysteine is the only amino acid capable of forming disulfide bonds, glycine is the only amino acid without a side-chain and is highly flexible, and proline is the only amino acid that is highly constrained through the bonding of its side chain to its amine nitrogen.

10. Protein A is clearly homologous to protein B, given 65% sequence identity, and so A and B are expected to have quite similar three-dimensional structures. Likewise, proteins B and C are clearly homologous, given 55% sequence identity, and so B and C are expected to have quite similar three-dimensional structures. Thus, proteins A and C are likely to have similar three-dimensional structures, even though they are only 15% identical in sequence.

11. The likely secondary structure is

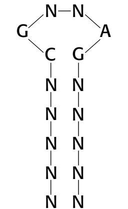

12. To detect pairs of residues with correlated mutations, there must be variability in these sequences. If the alignment is over-represented by closely related organisms, there may not be enough changes in their sequences to allow the identification of potential base-pairing patterns.

13. After RNA molecules have been selected and reverse transcribed, PCR is performed to introduce additional mutations into these strands. The use of this error-prone, thermostable polymerase in the amplification step would enhance the efficiency of this random mutagenesis.

14. The initial pool of RNA molecules used in a molecular-evolution experiment is typically much smaller than the total number of possible sequences. Hence, the best possible RNA sequences will likely not be represented in the initial set of oligonucleotides.

Mutagenesis of the initial selected RNA molecules allows for the iterative improvement of these sequences for the desired property.
15. 107 or 108 identities (depending on which annotated human sequence is chosen).

Chapter 7

1. The whale swims long distances between breaths. A high concentration of myoglobin in the whale muscle maintains a ready supply of oxygen for the muscle between breathing episodes.
2. (a) 2.96×10^{-11} g
(b) 2.74×10^{8} molecules
(c) No. There would be 3.17×10^{8} hemoglobin molecules in a red cell if they were packed in a cubic crystalline array. Hence, the actual packing density is about 84% of the maximum possible.
3. 2.65 g (or 4.75×10^{-2} mol) of Fe
4. (a) In human beings, 1.44×10^{-2} g (4.49×10^{-4} mol) of O_2 per kilogram of muscle. In sperm whale, 0.144 g (4.49×10^{-3} mol) of O_2 per kilogram.
(b) 128
5. The pK_a is (a) lowered; (b) raised; and (c) raised.
6. Deoxy Hb A contains a complementary site, and so it can add on to a fiber of deoxy Hb S. The fiber cannot then grow further, because the terminal deoxy Hb A molecule lacks a sticky patch.
7. 62.7% oxygen-carrying capacity
8. Myoglobin does not exhibit a Bohr effect. The interactions responsible for mediating the Bohr effect in hemoglobin are dependent upon a tetrameric structure. Myoglobin is a monomer.
9. A higher concentration of BPG would shift the oxygen-binding curve to the right, causing an increase in P_{50}. The larger value of P_{50} would promote dissociation of oxygen in the tissues and would thereby increase the percentage of oxygen delivered to the tissues.
10. (a) The transfusion would increase the number of red blood cells, which increases the oxygen-carrying capacity of the blood, allowing more sustained effort.
(b) BPG stabilizes the T-state of hemoglobin, which results in a more efficient release of oxygen. If BPG is depleted, the oxygen will not be released even though the red blood cells are carrying more oxygen.
11. Oxygen binding appears to cause the copper ions and their associated histidine ligands to move closer to one another, thereby also moving the helices to which the histidines are attached (in similar fashion to the conformational change in hemoglobin).
12. The modified hemoglobin should not show cooperativity. Although the imidazole in solution will bind to the heme iron (in place of histidine) and will facilitate oxygen binding, the imidazole lacks the crucial connection to the particular α helix that must move so as to transmit the change in conformation.
13. Inositol pentaphosphate (part *c*) is highly anionic, much like 2,3-bisphosphoglycerate.
14.

(a)

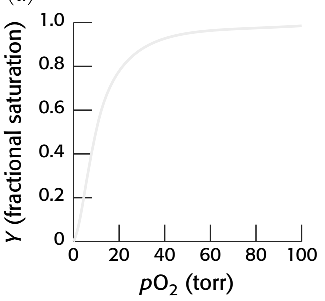

(b)

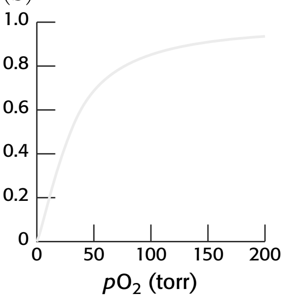

15. Release of acid will lower the pH. A lower pH promotes oxygen dissociation in the tissues. However, the enhanced release of oxygen in the tissues will increase the concentration of deoxy-Hb, thereby increasing the likelihood that the cells will sickle.
16. (a) $Y = 0.5$ when $pO_2 = 10$ torr. The plot of Y versus pO_2 appears to indicate little or no cooperativity.

(A)

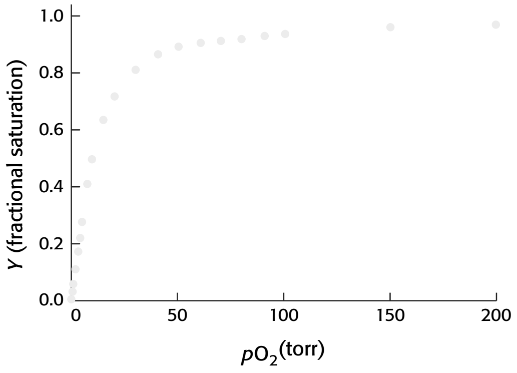

(b) The Hill plot shows slight cooperativity with $n = 1.3$ in the central region.

(B)

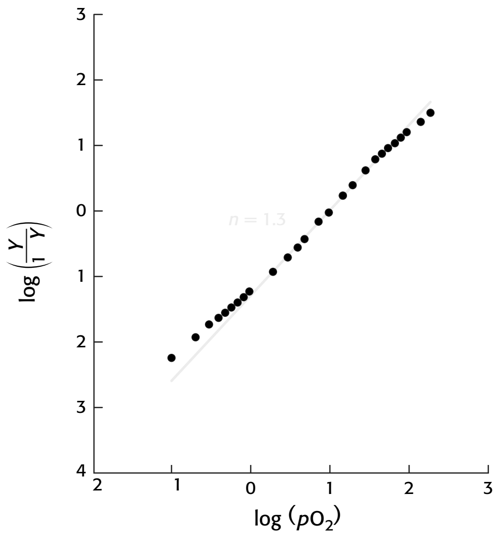

(c) Deoxy dimers of lamprey hemoglobin could have lower affinity for oxygen than do the monomers. If the binding of the first oxygen atom to a dimer causes dissociation of the dimer to give two monomers, then the process would be cooperative. In this mechanism, oxygen binding to each monomer would be easier than binding the first oxygen atom to a deoxy dimer.
17. (a) 2; (b) 4; (c) 2; (d) 1.
18. The electrostatic interactions between BPG and hemoglobin would be weakened by competition with water molecules. The T state would not be stabilized.
19. Fetal hemoglobin contains two α chains and two γ chains. The increase in levels of the γ chain provides an alternative to the mutated β chain in sickle-cell anemia patients. Hence, by increasing fetal hemoglobin expression, hydroxyurea reduces the potential for the formation of insoluble hemoglobin aggregates.

Chapter 8

1. Rate enhancement and substrate specificity.
2. A cofactor.
3. Coenzymes and metals.

4. Vitamins are converted into coenzymes.

5. Enzymes facilitate the formation of the transition state.

6. The intricate three-dimensional structure of proteins allows the construction of active sites that will recognize only specific substrates.

7. The energy required to reach the transition state (the activation energy) is returned when the transition state proceeds to product.

8. (a) $K = \frac{[P]}{[S]} = \frac{k_F}{k_R} = \frac{10^{-4}}{10^{-6}} = 100$. Using equation 5 in the text, $\Delta G^{\circ\prime} = -11.42$ kJ mol^{-1} (-2.73 kcal mol^{-1})

(b) $k_F = 10^{-2}$ s^{-1} and $k_R = 10^{-4}$ s^{-1}. The equilibrium constant and $\Delta G^{\circ\prime}$ values are the same for both the uncatalyzed and catalyzed reactions.

9. Protein hydrolysis has a large activation energy. Protein synthesis must require energy to proceed.

10. The enzymes help protect the fluid that surrounds eyes from bacterial infection.

11. Binding energy is the free energy released when two molecules bind together, such as when an enzyme and a substrate interact.

12. Binding energy is maximized when an enzyme interacts with the transition state, thereby facilitating the formation of the transition state and enhancing the rate of the reaction.

13. There would be no catalytic activity. If the enzyme–substrate complex is more stable than the enzyme–transition-state complex, the transition state would not form and catalysis would not take place.

14. Transition states are very unstable. Consequently, molecules that resemble transition states are themselves likely to be unstable and, hence, difficult to synthesize.

15. (a) 0; (b) $+28.53$; (c) -22.84; (d) -11.42; (e) $+5.69$.

16. (a) $\Delta G^{\circ\prime} = -RT \ln K'_{eq}$

$$+1.8 = -(1.98 \times 10^{-3}\,\text{kcal}^{-1}\,\text{K}^{-1}\,\text{mol}^{-1})(298\,\text{K})\,(\ln[\text{G1P}]/[\text{G6P}])$$

$$-3.05 = \ln[\text{G1P}]/[\text{G6P}]$$

$$+3.05 = \ln[\text{G6P}]/[\text{G1P}]$$

$$K'^{-1}_{eq} = 21 \quad \text{or} \quad K'_{eq} = 4.8 \times 10^{-2}$$

Because [G6P]/[G1P] = 21, there is 1 molecule of G1P for every 21 molecules of G6P. Because we started with 0.1 M, the [G1P] is 1/22(0.1 M) = 0.0045 M and [G6P] must be 21/22(0.1 M) or 0.096 M. Consequently, the reaction does not proceed as written to a significant extent.

(b) Supply G6P at a high rate and remove G1P at a high rate by other reactions. In other words, make sure that the [G6P]/[G1P] is kept large.

17. $K_{eq} = 19$, $\Delta G^{\circ\prime} = -7.3$ kJ mol^{-1} (-1.77 kcal mol^{-1})

18. The three-dimensional structure of an enzyme is stabilized by interactions with the substrate, reaction intermediates, and products. This stabilization minimizes thermal denaturation.

19. At substrate concentrations near the K_M, the enzyme displays significant catalysis yet is sensitive to changes in substrate concentration.

20. No, K_M is not equal to the dissociation constant, because the numerator also contains k_2, the rate constant for the conversion of the enzyme–substrate complex into enzyme and product. If, however, k_2 is much smaller than k_{-1}, $K_M \approx K_d$.

21. When [S] = 10 K_M, $V_0 = 0.91\ V_{max}$. When [S] = 20 K_M, $V_0 = 95\ V_{max}$.

So any Michaelis–Menten curves showing that the enzyme actually attains V_{max} are pernicious lies.

22. (a) 31.1 μmol; (b) 0.05 μmol; (c) 622 s^{-1}, a midrange value for enzymes (Table 8.5).

23. (a) Yes, $K_M = 5.2 \times 10^{-6}$ M; (b) $V_{max} = 6.8 \times 10^{-10}$ mol minute^{-1}; (c) 337 s^{-1}.

24. Penicillinase, like glycopeptide transpeptidase, forms an acyl-enzyme intermediate with its substrate but transfers the intermediate to water rather than to the terminal glycine residue of the pentaglycine bridge.

25. (a) V_{max} is 9.5 μmol minute^{-1}. K_M is 1.1×10^{-5} M, the same as without inhibitor.

(b) Noncompetitive.

(c) 2.5×10^{-5} M

(d) $f_{ES} = 0.73$, in the presence or absence of this noncompetitive inhibitor.

26. (a) $V_0 = V_{max} - (V_0/[S])\,K_M$

(b) Slope = $-K_M$, y-intercept = V_{max}, x-intercept = V_{max}/K_M

(c) An Eadie–Hofstee plot.

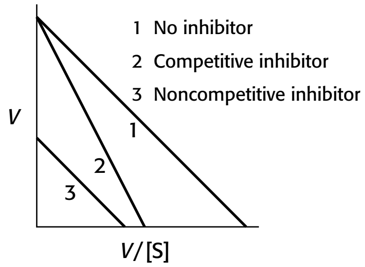

27. Sequential reactions are characterized by the formation of a ternary complex consisting of the enzyme and both substrates. Double-displacement reactions always require the formation of a temporarily substituted enzyme intermediate.

28. The rates of utilization of substrates A and B are given by

$$V_A = \left(\frac{k_{cat}}{K_M}\right)_A [E][A]$$

and

$$V_B = \left(\frac{k_{cat}}{K_M}\right)_B [E][B]$$

Hence, the ratio of these rates is

$$V_A/V_B = \left(\frac{k_{cat}}{K_M}\right)_B [A] / \left(\frac{k_{cat}}{K_M}\right)_A [B]$$

Thus, an enzyme discriminates between competing substrates on the basis of their values of k_{cat}/K_M rather than of K_M alone.

29. The mutation slows the reaction by a factor of 100 because the activation free energy is increased by $+11.42$ kJ mol^{-1} ($+2.73$ kcal mol^{-1}). Strong binding of the substrate relative to the transition state slows catalysis.

30. 11 μmol minute^{-1}

31. (a) This piece of information is necessary for determining the correct dosage of succinylcholine to administer.

(b) The duration of the paralysis depends on the ability of the serum cholinesterase to clear the drug. If there were one-eighth the amount of enzyme activity, paralysis could last eight times as long.

(c) K_M is the concentration needed by the enzyme to reach ½ V_{max}. Consequently, for a given concentration of substrate, the reaction catalyzed by the enzyme with the lower K_M will have the higher rate. The mutant patient with the higher K_M will clear the drug at a much lower rate.

32. (a) K_M is a measure of affinity *only* if k_2 is rate limiting, which is the case here. Therefore, the lower K_M means higher affinity. The mutant enzyme has a higher affinity.

(b) 50 μmol minute^{-1}. 10 mM is K_M, and K_M yields ½ V_{max}. V_{max} is 100 μmol minute^{-1}, and so. . .
(c) Enzymes do not alter the equilibrium of the reaction.
33. Enzyme 2. Despite the fact that enzyme 1 has a higher V_{max} than enzyme 2, enzyme 2 shows greater activity at the concentration of the substrate in the environment because enzyme 2 has a lower K_M for the substrate.
34. (a) The most effective means of measuring the efficiency of any enzyme–substrate complex is to determine the k_{cat}/K_M values. For the three substrates in question, the respective values of k_{cat}/K_M are: 6, 15, and 36. Thus, the enzyme exhibits a strong preference for cleaving peptide bonds in which the second amino acid is a large hydrophobic amino acid.
(b) The k_{cat}/K_M for this substrate is 2. Not very effective. This value suggests that the enzyme prefers to cleave peptide bonds with the following specificity: small R group—large hydrophobic R group.
35. If the total amount of enzyme (E_T) is increased, V_{max} will increase, because $V_{max} = k_2[E]_T$. But $K_M = (k_{-1} + k_2)/k_1$; that is, it is independent of substrate concentration. The middle graph describes this situation.
36.

Experimental condition	V_{max}	K_M
a. Twice as much enzyme is used	Doubles	No change
b. Half as much enzyme is used	Half as large	No change
c. A competitive inhibitor is present	No change	Increases
d. An uncompetitive inhibitor is present	Decreases	Decreases
e. A pure non-competitive is present	Decreases	No change

37. (a)

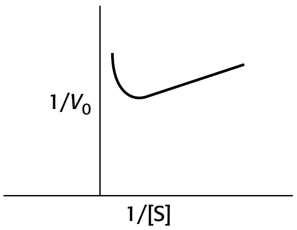

(b) This behavior is substrate inhibition: at high concentrations, the substrate forms unproductive complexes at the active site. The adjoining drawing shows what might happen. Substrate normally binds in a defined orientation, shown in the drawing as red to red and blue to blue. At high concentrations, the substrate may bind at the active site such that the proper orientation is met for each end of the molecule, but two different substrate molecules are binding.

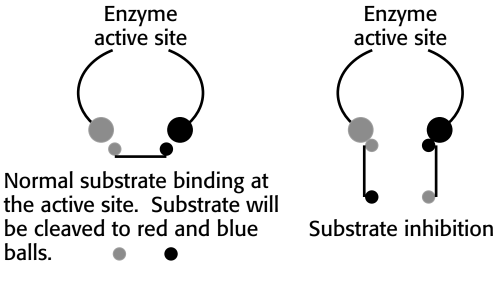
Enzyme active site
Enzyme active site
Normal substrate binding at the active site. Substrate will be cleaved to red and blue balls.
Substrate inhibition

38. The first step will be the rate-limiting step. Enzymes E_B and E_C are operating at ½ V_{max}, whereas the K_M for enzyme E_A is greater than the substrate concentration. E_A would be operating at approximately $10^{-2}V_{max}$.
39. The fluorescence spectroscopy reveals the existence of an enzyme–serine complex and of an enzyme–serine–indole complex.
40. (a) When [S^+] is much greater than the value of K_M, pH will have a negligible effect on the enzyme because S^+ will interact with E^- as soon as the enzyme becomes available.

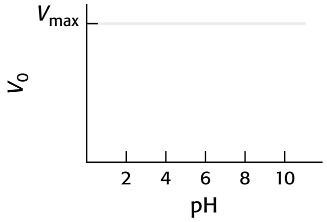

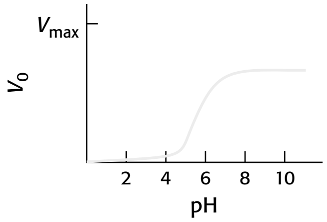

(b) When [S^+] is much less than the value of K_M, the plot of V_0 versus pH becomes essentially a titration curve for the ionizable groups, with enzyme activity being the titration marker. At low pH, the high concentration of H^+ will keep the enzyme in the EH form and inactive. As the pH rises, more and more of the enzyme will be in the E^- form and active. At high pH (low H^+), all of the enzyme is E^-.
(c) The midpoint on this curve will be the pK_a of the ionizable group, which is stated to be pH 6.
41. (a) Incubating the enzyme at 37°C leads to a denaturation of enzyme structure and a loss of activity. For this reason, most enzymes must be kept cool if they are not actively catalyzing their reactions.
(b) The coenzyme apparently helps to stabilize enzyme structure, because enzyme from PLP-deficient cells denatures faster. Cofactors often help stabilize enzyme structure.
42. The slow second order step occurs when complementary sequences on two different molecules bind with one another. Once the initial sequence alignment occurs, the remainder of the molecule can quickly locate complementary sequences from this nucleation site and reanneal, a first order reaction.

Chapter 9

1. For the amide substrate, the formation of the acyl-enzyme intermediate is slower than the hydrolysis of the acyl-enzyme intermediate, and so no burst is observed. A burst is observed for ester substrates; the formation of the acyl-enzyme intermediate is faster, leading to the observed burst.
2. The histidine residue in the substrate can substitute to some extent for the missing histidine residue of the catalytic triad of the mutant enzyme.
3. No. The catalytic triad works as a unit. After this unit has been made ineffective by the mutation of histidine to alanine, the further mutation of serine to alanine should have only a small effect.
4. The substitution corresponds to one of the key differences between trypsin and chymotrypsin, and so trypsin-like specificity (cleavage after lysine and arginine) might be predicted.

In fact, additional changes are required to effect this specificity change.

5. Imidazole is apparently small enough to reach the active site of carbonic anhydrase and compensate for the missing histidine. Buffers with large molecular components cannot do so, and the effects of the mutation are more evident.

6. No. The odds of such a sequence being present are approximately 1 in $4^{10} = 1{,}048{,}576$. Because a typical viral genome has only 50,000 bp, the target sequence would be unlikely to be present.

7. No, because the enzyme would destroy the host DNA before protective methylation could take place.

8. No. The bacteria receiving the enzyme would have their own DNA destroyed because they would likely lack the appropriate protective methylase.

9. EDTA will bind to Zn^{2+} and remove the ion, which is required for enzyme activity, from the enzyme.

10. (a) The aldehyde reacts with the active-site serine. (b) A hemiacetal is formed.

11. Trypsin.

12. The reaction is expected to be slower by a factor of 10 because the rate depends on the pK_a of the zinc-bound water. $k_{cat} = 60{,}000\ s^{-1}$.

13. EDTA binds the magnesium necessary for the reaction.

14. ATP hydrolysis is reversible within the active site. ATP hydrolysis takes place within the active site with the incorporation of ^{18}O, ATP is re-formed, and the ATP is released back into solution.

15. If the aspartate is mutated, the protease is inactive and the virus will not be viable.

16. Water substitutes for the hydroxyl group of serine 236 in mediating proton transfer from the attacking water and the γ-phosphoryl group.

17. For subtilisin, the catalytic power is approximately $30\ s^{-1}/10^{-8}\ s^{-1} = 3 \times 10^9$. For carbonic anhydrase (at pH 7), the catalytic power is approximately $500{,}000\ s^{-1}/0.15\ s^{-1} = 3.3 \times 10^6$. Subtilisin is the more powerful enzyme by this criterion.

18. The triple mutant still catalyzes the reaction by a factor of approximately 1000-fold compared to the uncatalyzed reaction. This could be due to the enzyme binding the substrate and holding it in a conformation that is susceptible to attack by water.

19. (a) Cysteine protease: The same as Figure 9.8, except that cysteine replaces serine in the active site and no aspartate is present.

(b) Aspartyl protease:

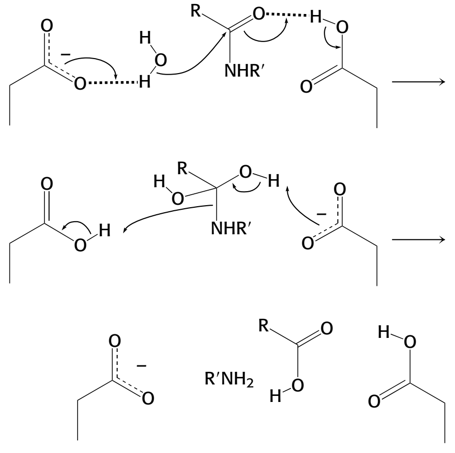

(c) Metalloprotease:

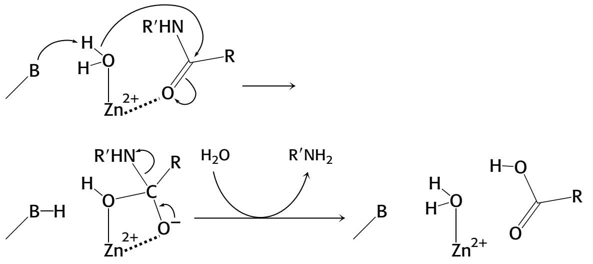

Chapter 10

1. The enzyme catalyzes the first step in the synthesis of pyrimidines. It facilitates the condensation of carbamoyl phosphate and aspartate to form *N*-carbamoylaspartate and inorganic phosphate.

2. The protonated form of histidine probably stabilizes the negatively charged carbonyl oxygen atom of the scissile bond (bond to be broken) in the transition state. Deprotonation would lead to a loss of activity. Hence, the rate is expected to be half maximal at a pH of about 6.5 (the p*K* of an unperturbed histidine side chain in a protein) and to decrease as the pH is raised.

3. The inhibition of an allosteric enzyme by the end product of the pathway controlled by the enzyme. It prevents the production of too much end product and the consumption of substrates when product is not required.

4. High concentrations of ATP might signal two overlapping situations. The high levels of ATP might suggest that some *nucleotides* are available for nucleic acid synthesis, and consequently, UTP and CTP should be synthesized. The high levels of ATP indicate that *energy* is available for nucleic acid synthesis, and so UTP and CTP should be produced.

5. All of the enzyme would be in the R form all of the time. There would be no cooperativity. The kinetics would look like that of a Michaelis–Menten enzyme.

6. The enzyme would show simple Michaelis–Menten kinetics because it is essentially always in the R state.

7. CTP is formed by the addition of an amino group to UTP. Evidence indicates the UTP is also capable of inhibiting ATCase in the presence of CTP.

8. Homotropic effectors are the substrates of allosteric enzymes. Heterotropic effectors are the regulators of allosteric enzymes. Homotropic effectors account for the sigmoidal nature of the velocity versus substrate concentration curve, whereas heterotropic effectors alter the K_M of the curve. Ultimately, both types of effectors work by altering the T/R ratio.

9. The reconstitution shows that the complex quaternary structure and the resulting catalytic and regulatory properties are ultimately encoded in the primary structure of individual components.

10. If substrates had been used, the enzyme would catalyze the reaction. Intermediates would not accumulate on the enzyme. Consequently, any enzyme that crystallized would have been free of substrates or products.

11. (a) 100. The change in the [R]/[T] ratio on binding one substrate molecule must be the same as the ratio of the substrate affinities of the two forms.

(b) 10. The binding of four substrate molecules changes the [R]/[T] by a factor of $100^4 = 10^8$. The ratio in the absence of substrate is 10^{-7}. Hence, the ratio in the fully liganded molecule is $10^8 \times 10^{-7} = 10$.

12. The fraction of molecules in the R form is 10^{-5}, 0.004, 0.615, 0.998, and 1 when 0, 1, 2, 3, and 4 ligands, respectively, are bound.

13. The sequential model can account for negative cooperativity, whereas the concerted model cannot.

14.

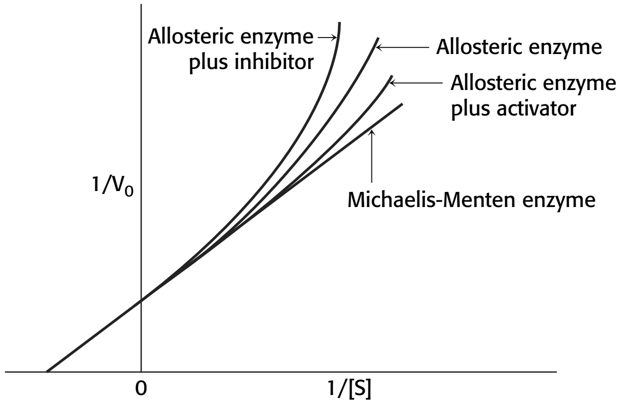

15. The binding of PALA switches ATCase from the T to the R state because PALA acts as a substrate analog. An enzyme molecule containing bound PALA has fewer free catalytic sites than does an unoccupied enzyme molecule. However, the PALA-containing enzyme will be in the R state and, hence, have a higher affinity for the substrates. The dependence of the degree of activation on the concentration of PALA is a complex function of the allosteric constant L_0 and of the binding affinities of the R and T states for the analog and substrates.

16. The net outcome of the two reactions is the hydrolysis of ATP to ADP and P_i, which has a ΔG of -50 kJ mol^{-1} (-12 kcal mol^{-1}) under cellular conditions.

17. Isozymes are homologous enzymes that catalyze the same reaction but have different kinetic or regulatory properties.

18. Although the same reaction may be required in a variety of tissues, the biochemical properties of tissues will differ according to their biological function. Isozymes allow the fine-tuning of catalytic and regulatory properties to meet the specific needs of the tissue.

19. (a) 7; (b) 8; (c) 11; (d) 6; (e) 1; (f) 12; (g) 3; (h) 4; (i) 5; (j) 2; (k) 10; (l) 9.

20. When phosphorylation takes place at the expense of ATP, sufficient energy is expended to dramatically alter the structure and hence activity of a protein. Moreover, because ATP is the cellular energy currency, protein modification is linked to the energy status of the cell.

21. Covalent modification is reversible, whereas proteolytic cleavage is irreversible.

22. Activation is independent of zymogen concentration because the reaction is intramolecular.

23. Although quite rare, cases of enteropeptidase deficiency have been reported. The affected person has diarrhea and fails to thrive because digestion is inadequate. In particular, protein digestion is impaired.

24. Add blood from the second patient to a sample from the first. If the mixture clots, the second patient has a defect different from that of the first. This type of assay is called a complementation test.

25. Activated factor X remains bound to blood-platelet membranes, which accelerates its activation of prothrombin.

26. Antithrombin III is a very slowly hydrolyzed substrate of thrombin. Hence, its interaction with thrombin requires a fully formed active site on the enzyme.

27. Replacing methionine with leucine would be a good choice. Leucine is resistant to oxidation and has nearly the same volume and degree of hydrophobicity as methionine has.

28. Inappropriate clot formation could block arteries in the brain, causing a stroke, or the heart, causing a heart attack.

29. Thrombin catalyzes the hydrolysis of fibrinogen to form active fibrin. But it also has a role in shutting down the cascade by activating protein C, a protease that digests other clotting enzymes V_a and $VIII_a$.

30. Tissue-type plasminogen activator, or TPA, is a serine protease that leads to the dissolution of blood clots. TPA activates plasminogen that is bound to a fibrin clot, converting it into active plasmin, which then hydrolyzes the fibrin of the clot.

31. A mature clot is stabilized by amide linkages between the side chains of lysine and glutamine that are absent in a soft clot. The linkages are formed by transglutaminase.

32. The simple sequential model predicts that the fraction of catalytic chains in the R state, f_R, is equal to the fraction containing bound substrate, Y. The concerted model, in contrast, predicts that f_R increases more rapidly than Y as the substrate concentration is increased. The change in f_R leads to the change in Y on addition of substrate, as predicted by the concerted model.

33. The binding of succinate to the functional catalytic sites of the native c_3 moiety changed the visible absorption spectrum of nitrotyrosine residues in the *other* c_3 moiety of the hybrid enzyme. Thus, the binding of substrate analog to the active sites of one trimer altered the structure of the other trimer.

34. According to the concerted model, an allosteric activator shifts the conformational equilibrium of all subunits toward the R state, whereas an allosteric inhibitor shifts it toward the T state. Thus, ATP (an allosteric activator) shifted the equilibrium to the R form, resulting in an absorption change similar to that obtained when substrate is bound. CTP had a different effect. Hence, this allosteric inhibitor shifted the equilibrium to the T form. Thus, the concerted model accounts for the ATP-induced and CTP-induced (heterotropic), as well as for the substrate-induced (homotropic), allosteric interactions of ATCase.

35. (a) When crowded, the control group displays gregarious behavior. (b) Inhibition of PKA appears to prevent gregarious behavior, while inhibition of PKG has no effect on the behavior. (c) The effect of PKG inhibition was investigated to establish that the effect seen with PKA inhibition is specific and not just due to the inhibition of any kinase. (d) PKA plays a role in altering behavior of insects. (e) Gregariousness in locusts that are always gregarious is not affected by PKA inhibition, suggesting that PKA may play a role in modifying behavior patterns but not in establishing the patterns.

36. Residues *a* and *d* are located in the interior of an α-helical coiled coil, near the axis of the superhelix. Hydrophobic interactions between these side chains contribute to the stability of the coiled coil.

37. In the R state, ATCase expands and becomes less dense. This decrease in density results in a decrease in the sedimentation value (see the formula on p. 76).

38. The interaction between trypsin and the inhibitor is so stable that the transition state is rarely formed. Recall that maximal binding energy is released when an enzyme binds to the transition state. If the substrate-enzyme interaction is too stable, the transition state rarely forms.

39. Dicoumarol is a competitive inhibitor of γ-glutamyl carboxylase. Consequently, γ-carboxyglutamate, which is required for prothrombin to be converted into thrombin, is not formed. Amino acid composition is determined by

hydrolyzing the protein at elevated temperatures in the presence of strong acid. Under these conditions, the carboxyl group of γ-carboxyglutamate is removed from the normal prothrombin, leaving simply glutamate.

40.

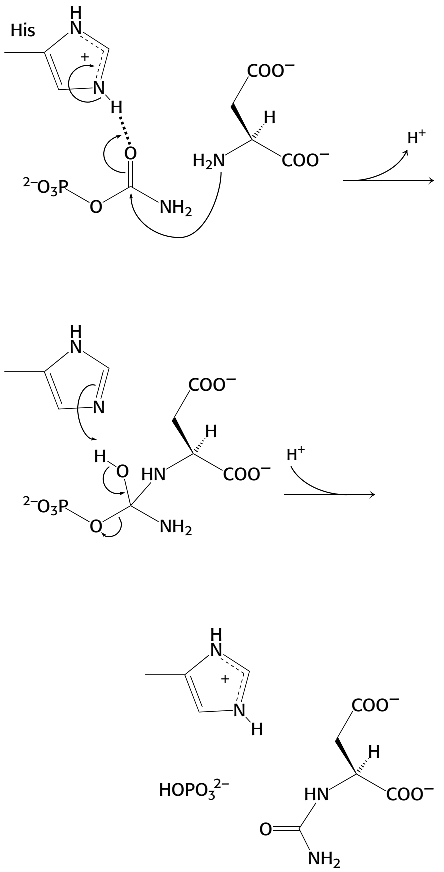
His
H
N
+
N
H
O
$^{2-}O_3P$
O
NH_2
COO^-
H
H_2N
COO^-
H^+
H
N
N
COO^-
H
H
O
HN
COO^-
H^+
$^{2-}O_3P$
O
NH_2
H
N
+
N
H
COO^-
H
$HOPO_3^{2-}$
HN
COO^-
O
NH_2

41.

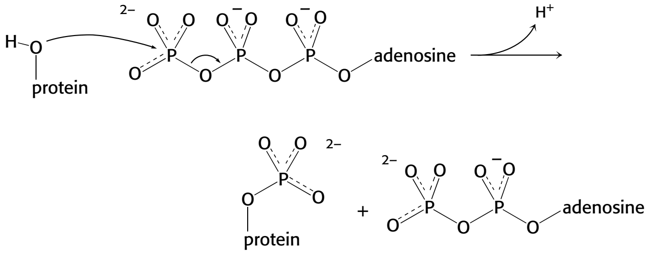
H
O
protein
2−
O O O − O O − O
P P P
O O O O
adenosine
H^+
O O 2−
P
O
O
protein
+
2− O O O − O
P P
O O O
adenosine

Chapter 11

1. Carbohydrates were originally regarded as *hydrates* of *carbon* because the empirical formula of many of them is $(CH_2O)_n$.

2. Three amino acids can be linked by peptide bonds in only six different ways. However, three different monosaccharides can be linked in a plethora of ways. The monosaccharides can be linked in a linear or branched manner, with α or β linkages, with bonds between C-1 and C-3, between C-1 and C-4, between C-1 and C-6, and so forth. In fact, the three monosaccharides can form 12,288 different trisaccharides.

3. (a) 10; (b) 6; (c) 8; (d) 9; (e) 2; (f) 4; (g) 1; (h) 5; (i) 7; (j) 3.

4. (a) aldose-ketose; (b) epimers; (c) aldose-ketose (d) anomers; (e) aldose-ketose; (f) epimers.

5. Erythrose: tetrose aldose; ribose: pentose aldose; glyceraldehyde: triose aldose; dihydroxyacetone: triose ketose; erythrulose: tetrose ketose; ribulose: pentose ketose; fructose: hexose ketose.

6.

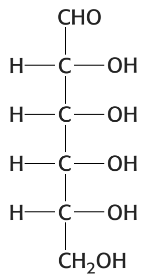
CHO
H—C—OH
H—C—OH
H—C—OH
H—C—OH
CH_2OH

D-Allose

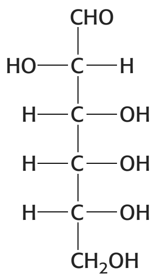
CHO
HO—C—H
H—C—OH
H—C—OH
H—C—OH
CH_2OH

D-Altrose

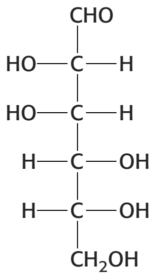
CHO
HO—C—H
HO—C—H
H—C—OH
H—C—OH
CH_2OH

D-Mannose

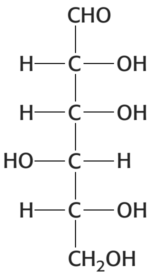
CHO
H—C—OH
H—C—OH
HO—C—H
H—C—OH
CH_2OH

D-Gulose

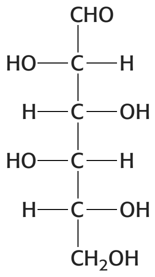
CHO
HO—C—H
H—C—OH
HO—C—H
H—C—OH
CH_2OH

D-Idose

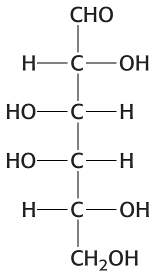
CHO
H—C—OH
HO—C—H
HO—C—H
H—C—OH
CH_2OH

D-Galactose

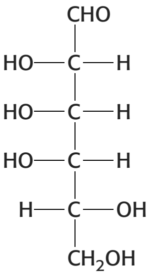
CHO
HO—C—H
HO—C—H
HO—C—H
H—C—OH
CH_2OH

D-Talose

7.

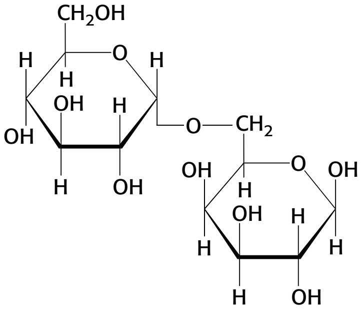
CH_2OH
H
O
H
H
OH
H
OH
H
OH
O
CH_2
OH
O
OH
H
OH
H
H
H
H
OH

-Glucosyl-(1 →6)-galactose

8. The proportion of the α anomer is 0.36, and that of the β anomer is 0.64.

9. Glucose is reactive because of the presence of an aldehyde group in its open-chain form. The aldehyde group slowly condenses with amino groups to form aldimine products of a type called Schiff-base adducts.

10. A pyranoside reacts with two molecules of periodate; formate is one of the products. A furanoside reacts with only one molecule of periodate; formate is not formed.

11. (a) β-D-Mannose; (b) β-D-galactose; (c) β-D-fructose; (d) β-D-glucosamine.

12. The trisaccharide itself should be a competitive inhibitor of cell adhesion if the trisaccharide unit of the glycoprotein is critical for the interaction.

13. Reducing ends would form 1,2,3,6-tetramethylglucose. The branch points would yield 2,3-dimethylglucose. The remainder of the molecule would yield 2,3,6-trimethylglucose.

14. (a) Not a reducing sugar; no open-chain forms are possible. (b) D-galactose, D-glucose, D-fructose. (c) D-galactose and sucrose (glucose + fructose).

15. The hemiketal linkage of the α anomer is broken to form the open form. Rotation about the C-1 and C-2 bonds allows the formation of the β anomer, and a mixture of isomers results.

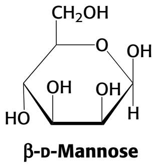

β-D-Mannose

16. Heating converts the very sweet pyranose form into the more-stable but less-sweet furanose form. Consequently, the sweetness of the preparation is difficult to accurately control, which also accounts for why honey loses sweetness with time. See Figure 11.5 for structures.

17. (a) Each glycogen molecule has one reducing end, whereas the number of nonreducing ends is determined by the number of branches, or α-1,6 linkages. (b) Because the number of nonreducing ends greatly exceeds the number of reducing ends in a collection of glycogen molecules, all of the degradation and synthesis of glycogen takes place at the nonreducing ends, thus maximizing the rate of degradation and synthesis.

18. No, sucrose is not a reducing sugar. The anomeric carbon atom acts as the reducing agent in both glucose and fructose but, in sucrose, the anomeric carbon atoms of fructose and glucose are joined by a covalent bond and are thus not available to react.

19. Glycogen is a polymer of glucose linked by α-1,4-glycosidic bonds with branches formed approximately every 10 glucose units by α-1,6-glycosidic bonds. Starch consists of two polymers of glucose. Amylose is a straight-chain polymer formed by α-1,4-glycosidic bonds. Amylopectin is similar to glycogen but amylopectin has fewer branches, one branch per 30 or so glucose units.

20. Cellulose is a linear polymer of glucose joined by β-1,4 linkages. Glycogen is a branched polymer with the main chain being formed by α-1,4-glycosidic bonds. The β-1,4 linkages allow the formation of a linear polymer ideal for structural roles. The α-1,4 linkages of glycogen form a helical structure, which allows the storage of many glucose moieties in a small space.

21. Simple glycoproteins are often secreted proteins and thus play a variety of roles. For example, the hormone EPO is a glycoprotein. Usually, the protein component constitutes the bulk of the glycoprotein by mass. In contrast, proteoglycans and mucoproteins are predominantly carbohydrates. Proteoglycans have glycosaminoglycans attached, and play structural roles as in cartilage and the extracellular matrix. Mucoproteins often serve as lubricants and have multiple carbohydrates attached through an *N*-acetylgalactosamine moiety.

22. The attachment of the carbohydrate allows the EPO to stay in circulation longer and thus to function for longer periods of time than would a carbohydrate-free EPO.

23. The glycosaminoglycan, because it is heavily charged, binds many water molecules. When cartilage is stressed, such as when your heel hits the ground, the water is released, thus cushioning the impact. When you lift your heel, the water rebinds.

24. The lectin that binds the mannose 6-phosphate might be defective and not recognize a correctly addressed protein.

25. Asparagine, serine, and threonine.

26. Different molecular forms of a glycoprotein that differ in the amount of carbohydrate attached or the location of attachment or both.

27. The total collection of carbohydrates synthesized by a cell at particular times and under particular environmental conditions.

28. The genome comprises all of the genes present in an organism. The proteome includes all of the possible protein products and modified proteins that a cell expresses under any particular set of circumstances. The glycome consists of all of the carbohydrates synthesized by the cell under any particular set of circumstances. Because the genome is static, but any given protein can be variously expressed and modified, the proteome is more complex than the genome. The glycome, which includes not only glycoforms of proteins, but also many possible carbohydrate structures, must be even more complex.

29. An asparagine residue can be glycosylated if the residue is part of an Asn-X-Ser or Asn-X-Thr sequence, in which X can be any residue, except proline. Your roommate's hedging is because not all potential sites are glycosylated.

30. It suggests that carbohydrates are on the cell surfaces of all organisms for the purpose of recognition by other cells, organisms, or the environment.

31. A glycoprotein is a protein that is decorated with carbohydrates. A lectin is a protein that specifically recognizes carbohydrates. A lectin can also be a glycoprotein.

32. Each site either is or is not glycosylated, and so there are $2^6 = 64$ possible proteins.

33. The 20 amino acid components of proteins and the 4 nucleotide components of nucleic acids are linked by the same type of bond—the peptide bond in proteins and the 5′-to-3′ phosphodiester linkage in nucleic acids. In contrast, there are many different carbohydrates that can be modified and linked in a variety of ways. Moreover, oligosaccharides can be branched. Finally, many sugars have the same or similar chemical formula, and similar chemical properties, making specific identification and linkage difficult.

34. As discussed in Chapter 9, many enzymes display stereochemical specificity. Clearly, the enzymes of sucrose synthesis are able to distinguish between the isomers of the substrates and link only the correct pair.

35. If the carbohydrate specificity of the lectin is known, an affinity column with the appropriate carbohydrate attached could be prepared. The protein preparation containing the lectin of interest could be passed over the column. The use of this method was indeed how the glucose-binding lectin concanavalin A was purified.

36. (a) Aggrecan is heavily decorated with glycosaminoglycans. If glycosaminoglycans are released into the media, aggrecan must be undergoing degradation.

(b) Another enzyme might be present that cleaves glycosaminoglycans from aggrecan without degrading aggrecan. Other experiments not shown established that glycosaminoglycan release is an accurate measure of aggrecan destruction.

(c) The control provides a baseline of "background" degradation inherent in the assay.

(d) Aggrecan degradation is greatly enhanced.

(e) Aggrecan degradation is reduced to the background system.
(f) It is an in vitro system in which not all the factors contributing to cartilage stabilization in vivo are present.

Chapter 12

1. 2.86×10^6 molecules, because each leaflet of the bilayer contains 1.43×10^6 molecules.
2. Essentially an "inside-out" membrane. The hydrophilic groups would come together on the interior of the structure, away from the solvent, whereas the hydrocarbon chains would interact with the solvent.
3. 2×10^{-7} cm, 6×10^{-6} cm, and 2×10^{-4} cm.
4. The radius of this molecule is 3.1×10^{-7} cm, and its diffusion coefficient is 7.4×10^{-9} cm^2 s^{-1}. The average distances traversed are 1.7×10^{-7} cm in 1 μs, 5.4×10^{-6} cm in 1 ms, and 1.7×10^{-4} cm in 1 s.
5. The membrane underwent a phase transition from a highly fluid to a nearly frozen state when the temperature was lowered. A carrier can shuttle ions across a membrane only when the bilayer is highly fluid. A channel, in contrast, allows ions to traverse its pore even when the bilayer is quite rigid.
6. The presence of a cis double bond introduces a kink in the fatty acid chain that prevents tight packing and reduces the number of atoms in van der Waals contact. The kink lowers the melting point compared with that of a saturated fatty acid. Trans fatty acids do not have the kink, and so their melting temperatures are higher, more similar to those of saturated fatty acids. Because trans fatty acids have no structural effect, they are rarely observed.
7. Palmitic acid is shorter than stearic acid. Thus, when the chains pack together, there is less opportunity for van der Waals interaction and the melting point is thus lower than that of the longer stearic acid.
8. Hibernators selectively feed on plants that have a high proportion of polyunsaturated fatty acids with lower melting temperature.
9. The initial decrease in fluorescence with the first addition of sodium dithionite results from the quenching of NBD-PS molecules in the outer leaflet of the bilayer. Sodium dithionite does not traverse the membrane under these experimental conditions; hence, it does not quench the labeled phospholipids in the inner leaflet. A second addition of sodium dithionite has no effect, as the NBD-PS molecules in the outer leaflet remain quenched. However, after a 6.5-hour incubation, about half the NBD-PS has flipped over to the outer leaflet of the bilayer, resulting in the 50% decrease in fluorescence when sodium dithionite is added.
10. The addition of the carbohydrate introduces a significant energy barrier to the flip-flop because a hydrophilic carbohydrate moiety would need to be moved through a hydrophobic environment. This energetic barrier enhances membrane asymmetry.
11. The C_{16} alkyl chain is attached by an ether linkage. The C-2 carbon atom of glycerol has only an acetyl group attached by an ester linkage instead of a fatty acid, as is the case with most phospholipids.
12. In a hydrophobic environment, the formation of intrachain hydrogen bonds stabilizes the amide hydrogen atoms and carbonyl oxygen atoms of the polypeptide chain, and so an α helix forms. In an aqueous environment, these groups are stabilized by interaction with water, and so there is no energetic reason to form an α helix. Thus, the α helix would be more likely to form in a hydrophobic environment.
13. The protein may contain an α helix that passes through the hydrophobic core of the protein. This helix is likely to feature a stretch of hydrophobic amino acids similar to those observed in transmembrane helices.
14. The shift to the lower temperature would decrease fluidity by enhancing the packing of the hydrophobic chains by van der Waals interactions. To prevent this packing, new phospholipids having shorter chains and a greater number of cis double bonds would be synthesized. The shorter chains would reduce the number of van der Waals interactions, and the cis double bonds, which cause the kink in structure, would prevent the packing of the fatty acid tails of the phospholipids.
15. Each of the 21 v-SNARE proteins could interact with each of 7 t-SNARE partners. Multiplication gives the total number of different interacting pairs: $7 \times 21 = 147$ different v-SNARE–t-SNARE pairs.
16. (a) The graph shows that, as temperature increases, the phospholipid bilayer becomes more fluid. T_m is the temperature of the transition from the predominantly less fluid state to the predominantly more fluid state. Cholesterol broadens the transition from the less-fluid to the more-fluid state. In essence, cholesterol makes membrane fluidity less sensitive to temperature changes.
(b) This effect is important because the presence of cholesterol tends to stabilize membrane fluidity by preventing sharp transitions. Because protein function depends on the proper fluidity of the membrane, cholesterol maintains the proper environment for membrane-protein function.
17. The protein plotted in part *c* is a transmembrane protein from *C. elegans.* It spans the membrane with four α helices that are prominently displayed as hydrophobic peaks in the hydropathy plot. Interestingly, the protein plotted in part *a* also is a membrane protein, a porin. This protein is made primarily of β strands, which lack the prominent hydrophobic window of membrane helices. This example shows that, although hydropathy plots are useful, they are not infallible.
18. (a) Prostaglandin H_2 synthase-1 recovers its activity immediately after removal of ibuprofen, suggesting that this inhibitor dissociates rapidly from the enzyme. In contrast, the enzyme remains significantly inhibited 30 minutes after removal of indomethacin, suggesting that this inhibitor dissociates slowly from its active site.
(b) Aspirin covalently modifies prostaglandin H_2 synthase-1, indicating that it would dissociate very slowly (if at all). Hence, one would anticipate that very low activity would be evident in all conditions where inhibitor has been added (columns 2, 3, and 4).
19. To purify any protein, the protein must first be solubilized. For a membrane protein, solubilization usually requires a detergent—hydrophobic molecules that bind to the protein and thus replace the lipid environment of the membrane. If the detergent is removed, the protein aggregates and precipitates from solution. Often, the steps in purification, such as ion-exchange chromatography, are difficult to perform in the presence of sufficient detergent to solubilize the protein. Crystals of appropriate protein–detergent complexes must be generated.

Chapter 13

1. In simple diffusion, the substance in question can diffuse down its concentration gradient through the membrane. In facilitated diffusion, the substance is not lipophilic and cannot directly diffuse through the membrane. A channel or carrier is required to facilitate movement down the gradient.

2. The two forms are (1) ATP hydrolysis and (2) the movement of one molecule down its concentration gradient coupled with the movement of another molecule up its concentration gradient.
3. The three types of carriers are symporters, antiporters, and uniporters. Symporters and antiporters can mediate secondary active transport.

4. The free-energy cost is +32 kJ mol^{-1} (+7.6 kcal mol^{-1}). The chemical work performed is +20.4 kJ mol^{-1} (+4.9 kcal mol^{-1}), and the electrical work performed is +11.5 kJ mol^{-1} (+2.8 kcal mol^{-1}).
5. For chloride, $z = -1$; for calcium $z = +2$. At the concentrations given, the equilibrium potential for chloride is −97 mV and the equlibrium potential for calcium is +122 mV.
6. The concentration of glucose inside the cell is 66 times as great as that outside the cell $[(c_2/c_1) = 66]$ when the free-energy input is +10.8 kJ mol^{-1} (+2.6 kcal mol^{-1}).
7. By analogy with the Ca^{2+} ATPase, with three Na^+ ions binding from inside the cell to the E_1 conformation and with two K^+ ions binding from outside the cell to the E_2 conformation, a plausible mechanism is as follows:

(i) A catalytic cycle could begin with the enzyme in its unphosphorylated state (E_1) with three sodium ions bound.
(ii) The E_1 conformation binds ATP. A conformational change traps sodium ions inside the enzyme.
(iii) The phosphoryl group is transferred from ATP to an aspartyl residue.
(iv) On ADP release, the enzyme changes its overall conformation, including the membrane domain. This new conformation (E_2) releases the sodium ions to the side of the membrane opposite that at which they entered and binds two potassium ions from the side where sodium ions are released.
(v) The phosphorylaspartate residue is hydrolyzed to release inorganic phosphate. With the release of phosphate, the interactions stabilizing E_2 are lost, and the enzyme everts to the E_1 conformation. Potassium ions are released to the cytoplasmic side of the membrane. The binding of three sodium ions from the cytoplasmic side of the membrane completes the cycle.

8. Establish a lactose gradient across vesicle membranes that contain properly oriented lactose permease. Initially, the pH should be the same on both sides of the membrane and the lactose concentration should be higher on the "exit" side of lactose permease. As the lactose flows "in reverse" through the permease, down its concentration gradient, it can be tested whether or not a pH gradient becomes established as the lactose gradient is dissipated.
9. Ligand-gated channels open in response to the binding of a molecule by the channel, whereas voltage-gated channels open in response to changes in the membrane potential.
10. An ion channel must transport ions in either direction at the same rate. The net flow of ions is determined only by the composition of the solutions on either side of the membrane.
11. Uniporters act as enzymes do; their transport cycles include large conformational changes, and only a few molecules interact with the protein per transport cycle. In contrast, channels, after having opened, provide a pore in the membrane through which many ions may pass. As such, channels mediate transport at a much higher rate than do uniporters.
12. FCCP effectively creates a pore in the bacterial membrane through which protons can pass rapidly. Protons that are pumped out of the bacteria will pass through this pore preferentially (the "path of least resistance"), rather than participate in H^+/lactose symport.
13. Cardiac muscle must contract in a highly coordinated manner in order to pump blood effectively. Gap junctions mediate the orderly cell-to-cell propagation of the action potential through the heart during each beat.
14. The positively charged guanidinium group resembles Na^+ and binds to negatively charged carboxylate groups in the mouth of the channel.
15. SERCA, a P-type ATPase, uses a mechanism by which a covalent phosphorylated intermediate (at an aspartate residue) is formed. At steady state, a subset of the SERCA molecules is trapped in the E_2-P state and, as a result, radiolabeled. The MDR protein is an ABC transporter and does not operate through a phosphorylated intermediate. Hence, a radiolabeled band would not be observed for MDR.
16. The blockage of ion channels inhibits action potentials, leading to loss of nervous function. Like tetrodotoxin, these toxin molecules are useful for isolating and specifically inhibiting particular ion channels.
17. After repolarization, the ball domains of the ion channels engage the channel pore, rendering them inactive for a short period of time. During this time, the channels cannot be reopened until the ball domains disengage and the channel returns to the "closed" state.
18. Because sodium ions are charged and because sodium channels carry only sodium ions (but not anions), the accumulation of excess positive charge on one side of the membrane dominates the chemical gradients.
19. A mutation that impairs the ability of the sodium channel to inactivate would prolong the duration of the depolarizing sodium current, thus lengthening the cardiac action potential.
20. No. Channels will likely open or close in response to an external stimulus, but the unit conductance of the open channel will be influenced very little.
21. The ratio of closed to open forms of the channel is 10^5, 5000, 250, 12.5, and 0.625 when zero, one, two, three, and four ligands, respectively, are bound. Hence, the fraction of open channels is 1.0×10^{-5}, 2.0×10^{-4}, 4.0×10^{-3}, 7.4×10^{-2}, and 0.62.
22. These organic phosphates inhibit acetylcholinesterase by reacting with the active-site serine residue to form a stable phosphorylated derivative. They cause respiratory paralysis by blocking synaptic transmission at cholinergic synapses.
23. (a) The binding of the first acetylcholine molecule increases the open-to-closed ratio by a factor of 240, and the binding of the second increases it by a factor of 11,700. (b) The free-energy contributions are +14 kJ mol^{-1} (+3.3 kcal mol^{-1}) and +23 kJ mol^{-1} (+5.6 kcal mol^{-1}), respectively. (c) No; the MWC model predicts that the binding of each ligand will have the same effect on the open-to-closed ratio.
24. Batrachotoxin blocks the transition from the open to the closed state.
25. (a) Chloride ions flow into the cell. (b) Chloride flux is inhibitory because it hyperpolarizes the membrane. (c) The channel consists of five subunits.
26. After the addition of ATP and calcium, SERCA will pump Ca^{2+} ions into the vesicle. However, the accumulation of Ca^{2+} ions inside the vesicle will rapidly lead to the formation of an electrical gradient that cannot be overcome by ATP hydrolysis. The addition of calcimycin will allow the pumped Ca^{2+} ions to flow back out of the vesicle, dissipating the charge buildup, and enabling the pump to operate continuously.
27. The catalytic prowess of acetylcholinesterase ensures that the duration of the nerve stimulus will be short.

28. See reaction below.

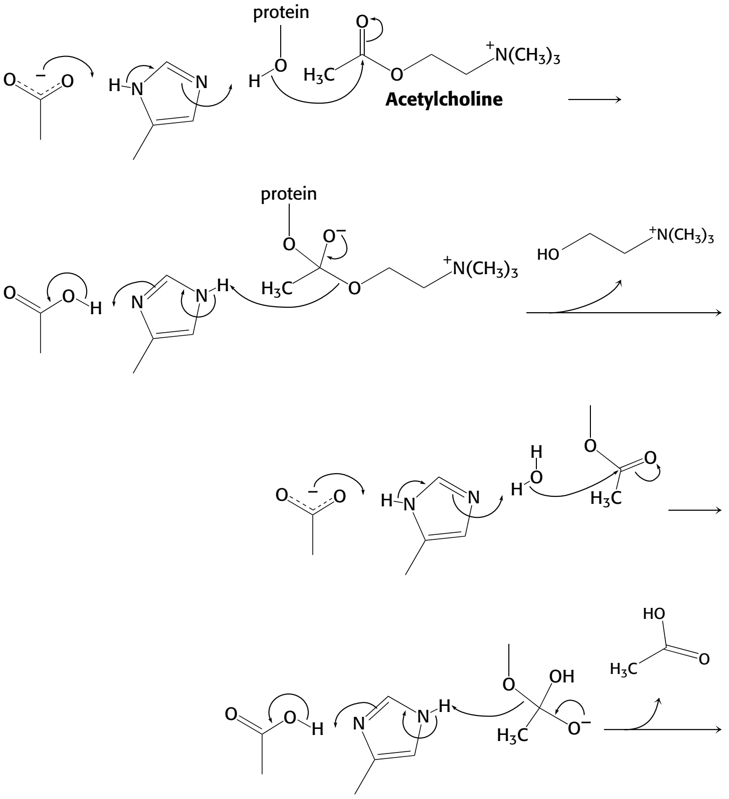

29. (a) Only ASIC1a is inhibited by the toxin. (b) Yes; when the toxin was removed, the activity of the acid-sensing channel began to be restored. (c) 0.9 nM.

30. This mutation is one of a class of mutations that result in slow-channel syndrome (SCS). The results suggest a defect in channel closing; so the channel remains open for prolonged periods. Alternatively, the channel may have a higher affinity for acetylcholine than does the control channel.

31. The mutation reduces the affinity of acetylcholine for the receptor. The recordings would show the channel opening only infrequently.

32. Glucose displays a transport curve that suggests the participation of a carrier because the initial rate is high but then levels off at higher concentrations, consistent with saturation of the carrier, which is reminiscent of Michaelis–Menten enzymes (Section 8.4). Indole shows no such saturation phenomenon, which implies that the molecule is lipophilic and simply diffuses across the membrane. Ouabain is a specific inhibitor the Na^+–K^+ pump. If ouabain were to inhibit glucose transport, then a Na^+-glucose cotransporter would be assisting in transport.

Chapter 14

1. The negatively charged glutamate residues mimic the negatively charged phosphoserine or phosphothreonine residues and stabilize the active conformation of the enzyme.

2. No. Phosphoserine and phosphothreonine are considerably shorter than phosphotyrosine.

3. The GTPase activity terminates the signal. Without such activity, after a pathway has been activated, it remains activated and is unresponsive to changes in the initial signal. If the GTPase activity were more efficient, the lifetime of the GTP-bound G_α subunit would be too short to achieve downstream signaling.

4. Two identical receptor molecules must recognize different aspects of the same signal molecule.

5. Growth-factor receptors can be activated by dimerization. If an antibody causes a receptor to dimerize, the signal-transduction pathway in a cell will be activated.

6. The mutated α subunit will always be in the GTP form and, hence, in the active form, which would stimulate its signaling pathway.

7. A G protein is a component of the signal-transduction pathway. GTPγS is not hydrolyzed by the G_α subunit, leading to prolonged activation.

8. Calcium ions diffuse slowly because they bind to many protein surfaces within a cell, impeding their free motion. Cyclic AMP does not bind as frequently, and so it diffuses more rapidly.

9. Fura-2 is a highly negatively charged molecule, with five carboxylate groups. Its charge prevents it from effectively crossing the hydrophobic region of the plasma membrane.

10. $G_{\alpha s}$ stimulates adenylate cyclase, leading to the generation of cAMP. This signal then leads to glucose mobilization (Chapter 21). If cAMP phosphodiesterase were inhibited, then cAMP levels would remain high even after the termination of the epinephrine signal, and glucose mobilization would continue.

11. If the two kinase domains are forced to be within close proximity of each other, the activation loop of one kinase, in its inactivating conformation, can be displaced by the activation loop of the neighboring kinase, which acts as a substrate for phosphorylation.

12. The full network of pathways initiated by insulin includes a large number of proteins and is substantially more elaborate than indicated in Figure 14.26. Furthermore, many additional proteins take part in the termination of insulin signaling. A defect in any of the proteins in the insulin signaling pathways or in the subsequent termination of the insulin response could potentially cause problems. Therefore, it is not surprising that many different gene defects can cause type 2 diabetes.

13. The binding of growth hormone causes its monomeric receptor to dimerize. The dimeric receptor can then activate a separate tyrosine kinase to which the receptor binds. The signaling pathway can then continue in similar fashion to the pathways that are activated by the insulin receptor or other mammalian EGF receptors.

14. The truncated receptor will dimerize with the full-length monomers on EGF-binding, but cross-phosphorylation cannot take place, because the truncated receptor possesses neither the substrate for the neighboring kinase domain nor its own kinase domain to phosphorylate the C-terminal tail of the other monomer. Hence, these mutant receptors will block normal EGF signaling.

15. Insulin would elicit the response that is normally caused by EGF. Insulin binding will likely stimulate dimerization and phosphorylation of the chimeric receptor and thereby signal the downstream events that are normally triggered by EGF binding. Exposure of these cells to EGF would have no effect.

16. 10^5

17. The formation of diacylglycerol implies the participation of phospholipase C. A simple pathway would entail receptor activation by cross-phosphorylation, followed by the binding of phospholipase C (through its SH2 domains). The participation of phospholipase C indicates that IP_3 would be formed and, hence, calcium concentrations would increase.

18. Other potential drug targets within the EGF signaling cascade include, but are not limited to, the kinase active sites of the EGF receptor, Raf, MEK, or ERK.
19. In the reaction catalyzed by adenylate cyclase, the 3′-OH group nucleophilically attacks the α-phosphorus atom attached to the 5′-OH group, leading to displacement of pyrophosphate. The reaction catalyzed by DNA polymerase is similar except that the 3′-OH group is on a different nucleotide.
20. ATP-competitive inhibitors are likely to act on multiple kinases because every kinase domain contains an ATP-binding site. Hence, these drugs may not be selective for the desired kinase target.
21. (a) X $\approx 10^{-7}$ M; Y $\approx 5 \times 10^{-6}$ M; Z $\approx 10^{-3}$ M. (b) Because much less X is required to fill half of the sites, X displays the highest affinity. (c) The binding affinity almost perfectly matches the ability to stimulate adenylate cyclase, suggesting that the hormone–receptor complex leads to the stimulation of adenylate cyclase. (d) Try performing the experiment in the presence of antibodies to $G_{\alpha s}$.
22. (a) The total binding does not distinguish binding to a specific receptor from binding to different receptors or from nonspecific binding to the membrane.
(b) The rationale is that the receptor will have a high affinity for the ligand. Thus, in the presence of excess nonradioactive ligand, the receptor will bind to nonradioactive ligand. Therefore, any binding of the radioactive ligand must be nonspecific.
(c) The plateau suggests that the number of receptor-binding sites in the cell membrane is limited.
23. Number of receptors per cell =

$$\frac{10^4\ \text{cpm}}{\text{mg of membrane protein}} \times \frac{\text{mg of membrane protein}}{10^{10}\ \text{cells}} \times \frac{\text{mmol}}{10^{12}\ \text{cpm}} \times \frac{6.023 \times 10^{20}\ \text{molecules}}{\text{mmol}} = 600$$

Chapter 15

1. The highly integrated biochemical reactions that take place inside the cell.
2. Anabolism is the set of biochemical reactions that use energy to build new molecules and ultimately new cells. Catabolism is the set of biochemical reactions that extract energy from fuel sources or break down biomolecules.
3. You reply that vandalism is disrespectful and expensive. Part of your tuition money will now have to pay to remove the vandalism. Plus, the fool should know that Gibbs free energy is at a minimum when a system is in equilibrium.
4. Cellular movements and the performance of mechanical work; active transport; biosynthetic reactions.
5. 1. f; 2. h; 3. i; 4. a; 5. g; 6. b; 7. c; 8. e; 9. j; 10. d.
6. These ions neutralize the charges on the ATP and also facilitate interactions with macromolecules that bind ATP.
7. Charge repulsion, resonance stabilization, increase in entropy, and stabilization by hydration.
8. Trick question. The answer is not known. Adenine appears to form more readily under prebiotic conditions, so ATP may have predominated initially.
9. Having only one nucleotide represent the available energy allows the cell to better monitor its energy status.
10. Increasing the concentration of ATP or decreasing the concentration cellular ADP or P_i (by rapid removal by other reactions, for instance) would make the reaction more exergonic. Likewise, altering the Mg^{2+} concentration could raise or lower the ΔG of the reaction.
11. The free-energy changes of the individual steps in a pathway are summed to determine the overall free-energy change of the entire pathway. Consequently, a reaction with a positive free-energy value can be powered to take place if coupled to a sufficiently exergonic reaction.
12. Reactions in parts *a* and *c*, to the left; reactions in parts *b* and *d*, to the right.
13. None whatsoever.
14. (a) $\Delta G^{\circ\prime} = +31.4$ kJ mol^{-1} ($+7.5$ kcal mol^{-1}) and $K'_{\text{eq}} = 3.06 \times 10^{-6}$; (b) 3.28×10^4.
15. $\Delta G^{\circ\prime} = +7.1$ kJ mol^{-1} ($+1.7$ kcal mol^{-1}). The equilibrium ratio is 17.5.
16. (a) Acetate + CoA + H^+ goes to acetyl CoA + H_2O, $\Delta G^{\circ\prime} = -31.4$ kJ mol^{-1} (-7.5 kcal mol^{-1}). ATP hydrolysis to AMP and PP_i, $\Delta G^{\circ\prime} = -45.6$ kJ mol^{-1} (-10.9 kcal mol^{-1}). Overall reaction, $\Delta G^{\circ\prime} = -14.2$ kJ mol^{-1} (-3.4 kcal mol^{-1}).
(b) With pyrophosphate hydrolysis, $\Delta G^{\circ\prime} = -33.4$ kJ mol^{-1} (-7.98 kcal mol^{-1}). Pyrophosphate hydrolysis makes the overall reaction even more exergonic.
17. (a) For an acid AH,

$$\text{AH} \rightleftharpoons \text{A}^- + \text{H}^+ \quad K = \frac{[\text{A}^-][\text{H}^+]}{[\text{AH}]}$$

The p*K* is defined as p$K = -\log_{10} K$. $\Delta G^{\circ\prime}$ is the standard free-energy change at pH 7. Thus, $\Delta G^{\circ\prime} = -RT \ln K = -2.303\, RT \log_{10} K = +2.303\, RT\, \text{p}K$.
(b) $\Delta G^{\circ\prime} = +27.32$ kJ mol^{-1} ($+6.53$ kcal mol^{-1}).
18. Arginine phosphate in invertebrate muscle, like creatine phosphate in vertebrate muscle, serves as a reservoir of high-potential phosphoryl groups. Arginine phosphate maintains a high level of ATP in muscular exertion.
19. An ADP unit.
20. (a) The rationale behind creatine supplementation is that it would be converted into creatine phosphate and thus serve as a rapid means of replenishing ATP after muscle contraction. (b) If creatine supplementation is beneficial, it would affect activities that depend on short bursts of activity; any sustained activity would require ATP generation by fuel metabolism, which, as Figure 15.7 shows, requires more time.
21. Under standard conditions, $\Delta G^{\circ\prime} = -RT \ln$ [products]/[reactants]. Substituting $+23.8$ kJ mol^{-1} ($+5.7$ kcal mol^{-1}) for $\Delta G^{\circ\prime}$ and solving for [products]/[reactants] yields 9.9×10^{-5}. In other words, the forward reaction does not take place to a significant extent. Under intracellular conditions, ΔG is -1.3 kJ mol^{-1} (-0.3 kcal mol^{-1}). Using the equation $\Delta G = \Delta G^{\circ\prime} + RT \ln$ [products]/[reactants] and solving for [products]/[reactants] gives a ratio of 5.96×10^{-5}. Thus, a reaction that is endergonic under standard conditions can be converted into an exergonic reaction by maintaining the [products]/[reactants] ratio below the equilibrium value. This conversion is usually attained by using the products in another coupled reaction as soon as they are formed.
22. Under standard conditions,

$$K'_{\text{eq}} = \frac{[\text{B}]_{\text{eq}}}{[\text{A}]_{\text{eq}}} \times \frac{[\text{ADP}]_{\text{eq}}[\text{P}_\text{i}]_{\text{eq}}}{[\text{ATP}]_{\text{eq}}} = 10^{33/1.36} = 2.67 \times 10^2$$

At equilibrium, the ratio of [B] to [A] is given by

$$\frac{[\text{B}]_{\text{eq}}}{[\text{A}]_{\text{eq}}} = K'_{\text{eq}} \frac{[\text{ATP}]_{\text{eq}}}{[\text{ADP}]_{\text{eq}}[\text{P}_\text{i}]_{\text{eq}}}$$

The ATP-generating system of cells maintains the [ATP]/[ADP] [P_i] ratio at a high level, typically about 500 M^{-1}. For this ratio,

$$\frac{[\text{B}]_{\text{eq}}}{[\text{A}]_{\text{eq}}} = 2.67 \times 10^2 \times 500 = 1.34 \times 10^5$$

This equilibrium ratio is strikingly different from the value of 1.15×10^{-3} for the reaction $A \rightarrow B$ in the absence of ATP hydrolysis. In other words, coupling the hydrolysis of ATP with the conversion of A into B has changed the equilibrium ratio of B to A by a factor of about 10^8.

23. Liver: -45.2 kJ mol^{-1} (-10.8 kcal mol^{-1}); muscle: -48.1 kJ mol^{-1} (-11.5 kcal mol^{-1}); brain: -48.5 kJ mol^{-1} (-11.6 kcal mol^{-1}). The ΔG is most negative in brain cells.

24. (a) Ethanol; (b) lactate; (c) succinate; (d) isocitrate; (e) malate.

25. Recall that $\Delta G = \Delta G^{\circ\prime} + RT \ln [\text{products}]/[\text{reactants}]$. Altering the ratio of products to reactants will cause ΔG to vary. In glycolysis, the concentrations of the components of the pathway result in a value of ΔG greater than that of $\Delta G^{\circ\prime}$.

26. Higher organisms cannot make vitamins, and thus are dependent on obtaining them from other organisms.

27. Unless the ingested food is converted into molecules capable of being absorbed by the intestine, no energy can ever be extracted by the body.

28. NADH and $FADH_2$ are electron carriers for catabolism; NADPH is the carrier for anabolism.

29. The electrons of the C–O bond cannot form resonance structures with the C–S bond that are as stable as those that they can form with the C–O bond. Thus, the thioester is not stabilized by resonance to the same degree as an oxygen ester is stabilized.

30. Oxidation–reduction reactions; ligation reactions; isomerization reactions; group-transfer reactions; hydrolytic reactions; cleavage of bonds by means other than hydrolysis or oxidation.

31. Controlling the amount of enzymes; controlling enzyme activity; controlling the availability of substrates.

32. Although the reaction is thermodynamically favorable, the reactants are kinetically stable because of the large activation energy. Enzymes lower the activation energy so that reactions take place on time scales required by the cell.

33. The activated form of sulfate in most organisms is 3′-phosphoadenosine-5′-phosphosulfate.

34. (a) As the Mg^{2+} concentration falls, the ΔG of hydrolysis rises. Note that pMg is a logarithmic plot, and so each number on the x-axis represents a 10-fold change in $[Mg^{2+}]$.
(b) Mg^{2+} would bind to the phosphates of ATP and help to mitigate charge repulsion. As the $[Mg^{2+}]$ falls, charge stabilization of ATP would be less, leading to greater charge repulsion and an increase in ΔG on hydrolysis.

Chapter 16

1. Two molecules of ATP are produced per molecule of glyceraldehyde 3-phosphate and, because two molecules of GAP are produced per molecule of glucose, the total ATP yield is four. However, two molecules of ATP are required to convert glucose into fructose 1,6-bisphosphate. Thus, the net yield is only two molecules of ATP.

2. (a) 4; (b) 3; (c) 1; (d) 6; (e) 8; (f) 2; (g) 10; (h) 9; (i) 7; (j) 5.

3. In both cases, the electron donor is glyceraldehyde 3-phosphate. In lactic acid fermentation, the electron acceptor is pyruvate, converting it into lactate. In alcoholic fermentation, acetaldehyde is the electron acceptor, forming ethanol.

4. (a) 3 ATP; (b) 2 ATP; (c) 2 ATP; (d) 2 ATP; (e) 4 ATP.

5. Glucokinase enables the liver to remove glucose from the blood when hexokinase is saturated, ensuring that glucose is captured for later use.

6. The GAP formed is immediately removed by subsequent reactions, resulting in the conversion of DHAP into GAP by the enzyme.

7. A thioester couples the oxidation of glyceraldehyde 3-phosphate to 3-phosphoglycerate with the formation of 1,3-bisphosphoglycerate. 1,3-Bisphosphoglycerate can subsequently power the formation of ATP.

8. Glycolysis is a component of alcoholic fermentation, the pathway that produces alcohol for beer and wine. The belief was that understanding the biochemical basis of alcohol production might lead to a more-efficient means of producing beer.

9. The conversion of glyceraldehyde 3-phosphate into 1,3- bisphosphoglycerate would be impaired. Glycolysis would be less effective.

10. Glucose 6-phosphate must have other fates. Indeed, it can be converted into glycogen (Chapter 21) or be processed to yield reducing power for biosynthesis (Chapter 20).

11. The energy needs of a muscle cell vary widely, from rest to intense exercise. Consequently, the regulation of phosphofructokinase by energy charge is vital. In other tissues, such as the liver, ATP concentration is less likely to fluctuate and will not be a key regulator of phosphofructokinase.

12. (a) 6; (b) 1; (c) 7; (d) 3; (e) 2; (f) 5 ; (g) 4.

13. The $\Delta G^{\circ\prime}$ for the reverse of glycolysis is $+90$ kJ mol^{-1} ($+22$ kcal mol^{-1}), far too endergonic to take place.

14. The conversion of glucose into glucose 6-phosphate by hexokinase; the conversion of fructose 6-phosphate into fructose 1,6-bisphosphate by phosphofructokinase; the formation of pyruvate from phosphoenolpyruvate by pyruvate kinase.

15. Lactic acid is a strong acid. If it remained in the cell, the pH of the cell would fall, which could lead to the denaturation of muscle protein and result in muscle damage.

16. GLUT2 transports glucose only when the blood concentration of glucose is high, which is precisely the condition in which the β cells of the pancreas secrete insulin.

17. Fructose + ATP $\longrightarrow$ fructose 1-phosphate + ADP: Fructokinase

Fructose 1-phosphate $\longrightarrow$ dihydroxyacetone phosphate + glyceraldehyde: Fructose 1-phosphate aldolase

Glyceraldehyde + ATP $\longrightarrow$ glyceraldehyde 3-phosphate + ADP: Triose kinase

The primary controlling step of glycolysis catalyzed by phosphofructokinase is bypassed by the preceding reactions. Glycolysis will proceed in an unregulated fashion.

18. (a) A, B; (b) C, D; (c) D; (d) A; (e) B; (f) C; (g) A; (h) D; (i) none; (j) A; (k) A.

19. (a) 4; (b) 10; (c) 1; (d) 5; (e) 7; (f) 8; (g) 9; (h) 2; (i) 3; (j) 6.

20. Without triose isomerase, only one of the two three-carbon molecules generated by aldolase could be used to generate ATP. Only two molecules of ATP would result from the metabolism of each glucose. But two molecules of ATP would still be required to form fructose 1,6-bisphosphate, the substrate for aldolase. The net yield of ATP would be zero, a yield incompatible with life.

21. Glucose is reactive because its open-chain form contains an aldehyde group.

22. (a) The label is in the methyl carbon atom of pyruvate. (b) 5 mCi mM^{-1}. The specific activity is halved because the number of moles of product (pyruvate) is twice that of the labeled substrate (glucose).

23. (a) Glucose + 2 P_i + 2 ADP $\rightarrow$ 2 lactate + 2 ATP.
(b) $\Delta G = -114$ kJ mol^{-1} (-27.2 kcal mol^{-1}).

24. 3.06×10^{-5}

25. The equilibrium concentrations of fructose 1,6-bisphosphate, dihydroxyacetone phosphate, and glyceraldehyde 3-phosphate are 7.8×10^{-4} M, 2.2×10^{-4} M, and 2.2×10^{-4} M, respectively.

26. All three carbon atoms of 2,3-BPG are ^{14}C labeled. The phosphorus atom attached to the C-2 hydroxyl group is ^{32}P labeled.

27. Hexokinase has a low ATPase activity in the absence of a sugar because it is in a catalytically inactive conformation. The addition of xylose closes the cleft between the two lobes of the enzyme. However, xylose lacks a hydroxymethyl group, and so it cannot be phosphorylated. Instead, a water molecule at the site normally occupied by the C-6 hydroxymethyl group acts as the acceptor of the phosphoryl group from ATP.
28. (a) The fructose 1-phosphate pathway forms glyceraldehyde 3-phosphate.
(b) Phosphofructokinase, a key control enzyme, is bypassed.
29. The reverse of glycolysis is highly endergonic under cellular conditions. The expenditure of six NTP molecules in gluconeogenesis renders gluconeogenesis exergonic.
30. (a) 2, 3, 6, 9; (b) 1, 4, 5, 7, 8.
31. Lactic acid is capable of being further oxidized and is thus useful energy. The conversion of this acid into glucose saves the carbon atoms for future combustion.
32. In glycolysis, the formation of pyruvate and ATP by pyruvate kinase is irreversible. This step is bypassed by two reactions in gluconeogenesis: (1) the formation of oxaloacetate from pyruvate and CO_2 by pyruvate carboxylase and (2) the formation of phosphoenolpyruvate from oxaloacetate and GTP by phosphoenolpyruvate carboxykinase. The formation of fructose 1,6-bisphosphate by phosphofructokinase is bypassed by fructose 1,6-bisphosphatase in gluconeogenesis, which catalyzes the conversion of fructose 1,6-bisphosphate into fructose 6-phosphate. Finally, the hexokinase-catalyzed formation of glucose 6-phosphate in glycolysis is bypassed by glucose 6-phosphatase, but only in the liver.
33. Reciprocal regulation at the key allosteric enzymes in the two pathways. For instance, PFK is stimulated by fructose 2,6-bisphosphate and AMP. The effect of these signals is opposite that of fructose 1,6-bisphosphatase. If both pathways were operating simultaneously, a futile cycle would result. ATP would be hydrolyzed, yielding only heat.
34. Muscle is likely to produce lactic acid during contraction. Lactic acid is a strong acid and cannot accumulate in muscle or blood. Liver removes the lactic acid from the blood and converts it into glucose. The glucose can be released into the blood or stored as glycogen for later use.
35. Glucose produced by the liver could not be released into the blood. Tissues that rely on glucose as an energy source would not function as well unless glucose was provided in the diet.
36. Glucose is an important energy source for both tissues and is essentially the only energy source for the brain. Consequently, these tissues should never release glucose. Glucose release is prevented by the absence of glucose 6-phosphatase.
37. 6 NTP (4 ATP and 2 GTP); 2 NADH.
38. (a) None; (b) none; (c) 4 (2 ATP and 2 GTP); (d) none.
39. If the amino groups are removed from alanine and aspartate, the ketoacids pyruvate and oxaloacetate are formed. Both of these molecules are components of the gluconeogenic pathway.
40. (a) Increased; (b) increased; (c) increased; (d) decreased.
41. Fructose 2,6-bisphosphate, present at high concentration when glucose is abundant, normally inhibits gluconeogenesis by blocking fructose 1,6-bisphosphatase. In this genetic disorder, the phosphatase is active irrespective of the glucose level. Hence, substrate cycling is increased. The level of fructose 1,6-bisphosphate is consequently lower than normal. Less pyruvate is formed and thus less ATP is generated.
42. Reactions in parts *b* and *e* would be blocked.
43. There will be no labeled carbons. The CO_2 added to pyruvate (formed from the lactate) to form oxaloacetate is lost with the conversion of oxaloacetate into phosphoenolpyruvate.
44. The net reaction in the presence of arsenate is

$$\text{Glyceraldehyde 3-phosphate} + \text{NAD}^+ + \text{H}_2\text{O} \longrightarrow \text{3-phosphoglycerate} + \text{NADH} + 2\,\text{H}^+$$

Glycolysis proceeds in the presence of arsenate, but the ATP normally formed in the conversion of 1,3-bisphosphoglycerate into 3-phosphoglycerate is lost. Thus, arsenate uncouples oxidation and phosphorylation by forming a highly labile acyl arsenate.
45. This example illustrates the difference between the *stoichiometric* and the *catalytic* use of a molecule. If cells used NAD^+ stoichiometrically, a new molecule of NAD^+ would be required each time a molecule of lactate was produced. As we will see, the synthesis of NAD^+ requires ATP. On the other hand, if the NAD^+ that is converted into NADH could be recycled and reused, a small amount of the molecule could regenerate a vast amount of lactate, which is the case in the cell. NAD^+ is regenerated by the oxidation of NADH and reused. NAD^+ is thus used catalytically.
46. Consider the equilibrium equation of adenylate kinase:

$$K_{\text{eq}} = [\text{ATP}][\text{AMP}]/\,[\text{ADP}]^2\,(1)$$

or

$$\text{AMP} = K_{\text{eq}}\,[\text{ADP}]^2/[\text{ATP}](2)$$

Recall that [ATP] > [ADP] > [AMP] in the cell. As ATP is utilized, a small decrease in its concentration will result in a larger percentage increase in [ADP] because its concentration is greater than that of ADP. This larger percentage increase in [ADP] will result in an even greater percentage increase in [AMP] because the concentration of AMP is related to the square of [ADP]. In essence, equation 2 shows that monitoring the energy status with AMP magnifies small changes in [ATP], leading to tighter control.
47. The synthesis of glucose during intense exercise provides a good example of interorgan cooperation in higher organisms. When muscle is actively contracting, lactate is produced from glucose by glycolysis. The lactate is released into the blood and absorbed by the liver, where it is converted by gluconeogenesis into glucose. The newly synthesized glucose is then released and taken up by the muscle for energy generation.
48. The input of four additional high-phosphoryl-transfer-potential molecules in gluconeogenesis changes the equilibrium constant by a factor of 10^{32}, which makes the conversion of pyruvate into glucose thermodynamically feasible. Without this energetic input, gluconeogenesis would not take place.
49. The mechanism is analogous to that for triose phosphate isomerase (Figure 16.5). It proceeds through an enediol intermediate. The active site would be expected to have a general base (analogous to Glu 165 in TPI) and a general acid (analogous to His 95 in TPI).
50. Galactose is a component of glycoproteins. Possibly, the absence of galactose leads to the improper formation or function of glycoproteins required in the central nervous system. More generally, the fact that the symptoms arise in the absence of galactose suggests that galactose is required in some fashion.
51. Using the Michaelis–Menten equation to solve for [S] when $K_M = 50\ \mu\text{M}$ and $V_o = 0.9V_{max}$ shows that a substrate concentration of 0.45 mM yields 90% of V_{max}. Under normal conditions, the enzyme is essentially working at V_{max}.
52. Fructose 2,6-bisphosphate stabilizes the R state of the enzyme.
53. (a) Curiously, the enzyme uses ADP as the phosphoryl donor rather than ATP.
(b) Both AMP and ATP behave as competitive inhibitors of ADP, the phosphoryl donor. Apparently, the *P. furiosus* enzyme is not allosterically inhibited by ATP.

54. (a) If both enzymes operated simultaneously, the following reactions would take place:

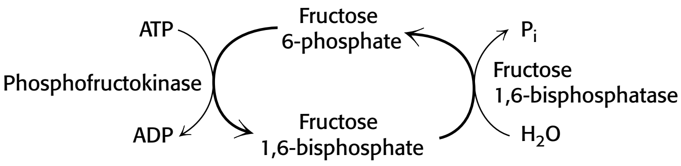

The net result would be simply:

$$ATP + H_2O \longrightarrow ADP + P_i$$

The energy of ATP hydrolysis would be released as heat.
(b) Not really. For the cycle to generate heat, both enzymes must be functional at the same time in the same cell.
(c) The species *B. terrestris* and *B. rufocinctus* might show some futile cycling because both enzymes are active to a substantial degree.
(d) No. These results simply suggest that simultaneous activity of phosphofructokinase and fructose 1,6-bisphosphatase is unlikely to be employed to generate heat in the species shown.
55. ATP initially stimulates PFK activity, as would be expected for a substrate. Higher concentrations of ATP inhibit the enzyme. Although this effect seems counterintuitive for a substrate, recall that the function of glycolysis in muscle is to generate ATP. Consequently, high concentrations of ATP signal that the ATP needs are met and glycolysis should stop. In addition to being a substrate, ATP is an allosteric inhibitor of PFK.

Chapter 17

1. The pyruvate dehydrogenase complex catalyzes the following reaction, linking glycolysis and the citric acid cycle:

$$\text{Pyruvate} + \text{CoA} + \text{NAD}^+ \longrightarrow \text{acetyl CoA} + \text{NADH} + \text{H}^+ + \text{CO}_2$$

2. Pyruvate dehydrogenase catalyzes the decarboxylation of pyruvate and the formation of acetyllipoamide. Dihydrolipoyl transacetylase catalyzes the formation of acetyl CoA. Dihydrolipoyl dehydrogenase catalyzes the reduction of the oxidized lipoic acid. The kinase associated with the complex phosphorylates and inactivates the complex, whereas the phosphatase dephosphorylates and activates the complex.
3. Thiamine pyrophosphate plays a role in the decarboxylation of pyruvate. Lipoic acid (as lipoamide) transfers the acetyl group. Coenzyme A accepts the acetyl group from lipoic acid to form acetyl CoA. FAD accepts the electrons and hydrogen ions when reduced lipoic acid is oxidized. NAD^+ accepts electrons from $FADH_2$.
4. Catalytic coenzymes (TPP, lipoic acid, and FAD) are modified but regenerated in each reaction cycle. Thus, they can play a role in the processing of many molecules of pyruvate. Stoichiometric coenzymes (coenzyme A and NAD^+) are used in only one reaction because they are the components of products of the reaction.
5. The remaining steps regenerate oxidized lipoamide, which is required to begin the next reaction cycle. Moreover, this regeneration results in the production of high-energy electrons in the form of NADH.
6. The advantages are as follows:
   The reaction is facilitated by having the active sites in proximity.
   The reactants do not leave the enzyme until the final product is formed.
   Constraining the reactants minimizes loss due to diffusion and minimizes side reactions.
   All of the enzymes are present in the correct amounts.
   Regulation is more efficient because the regulatory enzymes—the kinase and phosphatase—are part of the complex.
7. (a) After one round of the citric acid cycle, the label emerges in C-2 and C-3 of oxaloacetate. (b) The label emerges in CO_2 in the formation of acetyl CoA from pyruvate. (c) After one round of the citric acid cycle, the label emerges in C-1 and C-4 of oxaloacetate. (d) and (e) Same fate as that in part *a*.
8. (a) Isocitrate lyase and malate synthase are required in addition to the enzymes of the citric acid cycle.
(b) $2\ \text{Acetyl CoA} + 2\ \text{NAD}^+ + \text{FAD} + 3\ \text{H}_2\text{O} \longrightarrow \text{oxaloacetate} + 2\ \text{CoA} + 2\ \text{NADH} + \text{FADH}_2 + 3\ \text{H}^+$.
(c) No. Hence, mammals cannot carry out the net synthesis of oxaloacetate from acetyl CoA.
9. $-41.0\ \text{kJ mol}^{-1} (-9.8\ \text{kcal mol}^{-1})$
10. Enzymes or enzyme complexes are biological catalysts. Recall that a catalyst facilitates a chemical reaction without the catalyst itself being permanently altered. Oxaloacetate can be thought of as a catalyst because it binds to an acetyl group, leads to the oxidative decarboxylation of the two carbon atoms, and is regenerated at the completion of a cycle. In essence, oxaloacetate (and any cycle intermediate) acts as a catalyst.
11. Thiamine thiazolone pyrophosphate is a transition-state analog. The sulfur-containing ring of this analog is uncharged, and so it closely resembles the transition state of the normal coenzyme in thiamine-catalyzed reactions (e.g., the uncharged resonance form of hydroxyethyl-TPP).
12. (a) 6; (b) 10; (c) 1; (d) 7; (e) 2; (f) 8; (g) 3; (h) 4; (i) 5; (j) 9.
13. A decrease in the amount of O_2 will necessitate an increase in anaerobic glycolysis for energy production, leading to the generation of a large amount of lactic acid. Under conditions of shock, the kinase inhibitor is administered to ensure that pyruvate dehydrogenase is operating maximally.
14. (a) As is stated in the previous problem, DCA inhibits pyruvate dehydrogenase kinase.
(b) The fact that inhibiting the kinase results in more dehydrogenase activity suggests that there must be some residual activity that is being inhibited by the kinase.
15. Acetyllipoamide and acetyl CoA.
16. In muscle, the acetyl CoA generated by the complex is used for energy generation. Consequently, signals that indicate an energy-rich state (high ratios of ATP/ADP and $NADH/NAD^+$) inhibit the complex, whereas the reverse conditions stimulate the enzyme. Calcium as the signal for muscle contraction (and, hence, energy need) also stimulates the enzyme. In liver, acetyl CoA derived from pyruvate is used for biosynthetic purposes, such as fatty acid synthesis. Insulin, the hormone denoting the fed state, stimulates the complex.
17. (a) Enhanced kinase activity will result in a decrease in the activity of the PDH complex because phosphorylation by the kinase inhibits the complex.
(b) Phosphatase activates the complex by removing a phosphate. If the phosphatase activity is diminished, the activity of the PDH complex also will decrease.
18. She might have been ingesting, in some fashion, the arsenite from the peeling paint or the wallpaper. Also, she might have been breathing arsine gas from the wallpaper, which would be oxidized to arsenite in her body. In any of these circumstances, the arsenite inhibited enzymes that require lipoic acid—notably, the PDH complex.
19. (a) 5; (b) 7; (c) 1; (d) 10; (e) 2; (f) 4; (g) 9; (h) 3; (i) 8; (j) 6.
20. The TCA cycle depends on a steady supply of NAD^+ as an oxidant, generating NADH. O_2 is never directly utilized in the cycle. However, NAD^+ is regenerated via donation of electrons to O_2 by way of the electron transport chain, so eventually a lack of O_2 will cause the cycle to cease due to a lack of NAD^+.

21. Succinate dehydrogenase is the only enzyme in the citric acid cycle that is embedded in the mitochondrial membrane, which makes it associated with the electron-transport chain.

22. (a) The steady-state concentrations of the products are low compared with those of the substrates. (b) The ratio of malate to oxaloacetate must be greater than 1.57×10^4 for oxaloacetate to be formed.

23.

$$\text{Pyruvate} + \text{CoA} + \text{NAD}^+ \xrightarrow{\text{Pyruvate dehydrogenase complex}} \text{acetyl CoA} + \text{CO}_2 + \text{NADH}$$

$$\text{Pyruvate} + \text{CO}_2 + \text{ATP} + \text{H}_2\text{O} \xrightarrow{\text{Pyruvate carboxylase}} \text{oxaloacetate} + \text{ADP} + \text{P}_i + \text{H}^+$$

$$\text{Oxaloacetate} + \text{acetyl CoA} + \text{H}_2\text{O} \xrightarrow{\text{Citrate synthase}} \text{citrate} + \text{CoA} + \text{H}^+$$

$$\text{Citrate} \xrightarrow{\text{Aconitase}} \text{isocitrate}$$

$$\text{Isocitrate} + \text{NAD}^+ \xrightarrow{\text{Isocitrate dehydrogenase}} \alpha\text{-ketoglutarate} + \text{CO}_2 + \text{NADH}$$

$$\text{Net: } 2\ \text{Pyruvate} + 2\ \text{NAD}^+ + \text{ATP} + \text{H}_2\text{O} \longrightarrow \alpha\text{-ketoglutarate} + \text{CO}_2 + \text{ADP} + \text{P}_i + 2\ \text{NADH} + 3\ \text{H}^+$$

24. Succinate will increase in concentration, followed by α-ketoglutarate and the other intermediates "upstream" of the site of inhibition. Succinate has two methylene groups that are required for the dehydrogenation, whereas malonate has but one.

25. Pyruvate carboxylase should be active only when the acetyl CoA concentration is high. Acetyl CoA might accumulate if the energy needs of the cell are not being met, because of a deficiency of oxaloacetate. Under these conditions the pyruvate carboxylase catalyzes an anaplerotic reaction. Alternatively, acetyl CoA might accumulate because the energy needs of the cell have been met. In this circumstance, pyruvate will be converted back into glucose, and the first step in this conversion is the formation of oxaloacetate.

26. The energy released when succinate is oxidized to fumarate is not sufficient to power the synthesis of NADH but is sufficient to reduce FAD.

27. Citrate is a tertiary alcohol that cannot be oxidized, because oxidation requires a hydrogen atom to be removed from the alcohol and a hydrogen atom to be removed from the carbon atom bonded to the alcohol. No such hydrogen exists in citrate. The isomerization converts the tertiary alcohol into isocitrate, which is a secondary alcohol that can be oxidized.

28. The enzyme nucleoside diphosphokinase transfers a phosphoryl group from GTP (or any nucleoside triphosphate) to ADP according to the reversible reaction:

$$\text{GTP} + \text{ADP} \rightleftharpoons \text{GDP} + \text{ATP}$$

29. The reaction is powered by the hydrolysis of a thioester. Acetyl CoA provides the thioester that is converted into citryl CoA. When this thioester is hydrolyzed, citrate is formed in an irreversible reaction.

30. It enables organisms such as plants and bacteria to convert fats, through acetyl CoA, into glucose.

31. We cannot get the net conversion of fats into glucose, because the only means to get the carbon atoms from fats into oxaloacetate, the precursor of glucose, is through the citric acid cycle. However, although two carbon atoms enter the cycle as acetyl CoA, two carbon atoms are lost as CO_2 before oxaloacetate is formed. Thus, although some carbon atoms from fats may end up as carbon atoms in glucose, we cannot obtain a *net* synthesis of glucose from fats.

32. Acetyl CoA will inhibit the complex. Glucose metabolism to pyruvate will be slowed because acetyl CoA is being derived from an alternative source.

33. The enol intermediate of acetyl CoA attacks the carbonyl carbon atom of glyoxylate to form a C–C bond. This reaction is like the condensation of oxaloacetate with the enol intermediate of acetyl CoA in the reaction catalyzed by citrate synthase. Glyoxylate contains a hydrogen atom in place of the $-\text{CH}_2\text{COO}^-$ group of oxaloacetate; the reactions are otherwise nearly identical.

34. Citrate is a symmetric molecule. Consequently, the investigators assumed that the two $-\text{CH}_2\text{COO}^-$ groups in it would react identically. Thus, for every citrate molecule undergoing the reactions shown in path 1, they thought that another citrate molecule would react as shown in path 2. If so, then only *half* the label should have emerged in the CO_2.

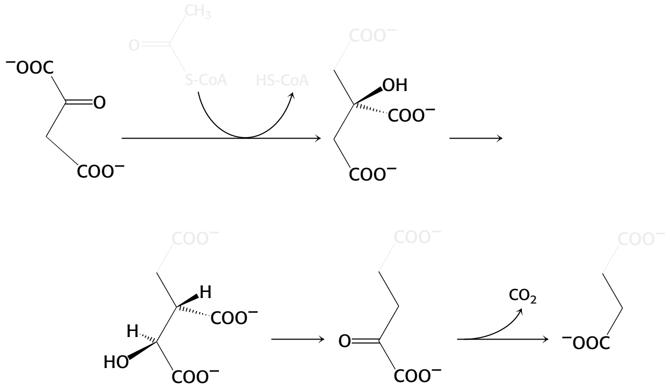

Path 1

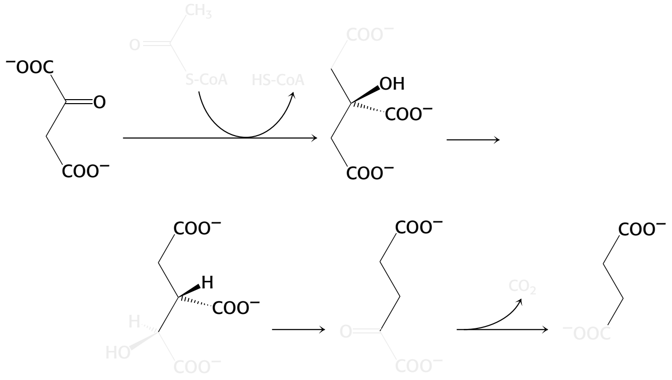

Path 2 (does not occur)

35. Call one hydrogen atom A and the other B. Now suppose that an enzyme binds three groups of this substrate—X, Y, and H—at three complementary sites. The adjoining diagram shows X, Y, and H_A bound to three points on the enzyme. In contrast, X, Y, and H_B cannot be bound to this active site; two of these three groups can be bound, but not all three. Thus, H_A and H_B will have different fates.

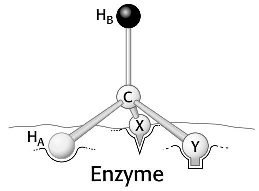

Sterically nonequivalent groups such as H_A and H_B will almost always be distinguished in enzymatic reactions. The essence of the differentiation of these groups is that the enzyme holds the substrate in a specific orientation. Attachment at three points, as depicted in the diagram, is a readily visualized way of achieving a particular orientation of the substrate, but it is not the only means of doing so.

36. (a) The complete oxidation of citrate requires 4.5 μmol of O_2 for every micromole of citrate.

$$C_6H_8O_7 + 4.5\,O_2 \longrightarrow 6\,CO_2 + 4\,H_2O$$

Thus, 13.5 μmol of O_2 would be consumed by 3 μmol of citrate. (b) Citrate led to the consumption of far more O_2 than can be accounted for simply by the oxidation of citrate itself. Citrate thus facilitated O_2 consumption.

37. (a) In the absence of arsenite, the amount of citrate remained constant. In its presence, the concentration of citrate fell, suggesting that it was being metabolized.
(b) The action of arsenite is not altered. Citrate still disappears.
(c) Arsenite is preventing the regeneration of citrate. Recall (pp. 515–516) that arsenite inhibits the pyruvate dehydrogenase complex.

38. (a) The initial infection is unaffected by the absence of isocitrate lyase, but the absence of this enzyme inhibits the latent phase of the infection.
(b) Yes.
(c) A critic could say that, in the process of deleting the isocitrate lyase gene, some other gene was damaged, and it is the absence of this other gene that prevents latent infection. Reinserting the isocitrate lyase gene into the bacteria from which it had been removed renders the criticism less valid.
(d) Isocitrate lyase enables the bacteria to synthesize carbohydrates that are necessary for survival, including carbohydrate components of the cell membrane.

Chapter 18

1. In fermentations, organic compounds are both the donors and the acceptors of electrons. In respiration, the electron donor is usually an organic compound, whereas the electron acceptor is an inorganic molecule, such as oxygen.

2. Biochemists use E_0', the value at pH 7, whereas chemists use E_0, the value in 1 M H^+. The prime denotes that pH 7 is the standard state.

3. The reduction potential of $FADH_2$ is less than that of NADH (Table 18.1). Consequently, when those electrons are passed along to oxygen, less energy is released. The consequence of the difference is that electron flow from $FADH_2$ to O_2 pumps fewer protons than do the electrons from NADH.

4. The $\Delta G^{\circ\prime}$ for the reduction of oxygen by $FADH_2$ is -200 kJ mol^{-1} (-48 kcal mol^{-1}).

5. $\Delta G^{\circ\prime}$ is $+67$ kJ mol^{-1} ($+16.1$ kcal mol^{-1}) for oxidation by NAD^+ and -3.8 kJ mol^{-1} (-0.92 kcal mol^{-1}) for oxidation by FAD. The oxidation of succinate by NAD^+ is not thermodynamically feasible.

6. An oxidizing agent, or oxidant, accepts electrons in oxidation–reduction reactions. A reducing reagent, or reductant, donates electrons in such reactions.

7. Pyruvate accepts electrons and is thus the oxidant. NADH gives up electrons and is the reductant.

8. $\Delta G^{\circ\prime} = -nF\Delta E_0'$

9. The $\Delta E_0'$ value of iron can be altered by changing the environment of the ion.

10. c, e, b, a, d.

11. (a) 4; (b) 5; (c) 2; (d) 10; (e) 3; (f) 8; (g) 9; (h) 7; (i) 1; (j) 6.

12. (a) 4; (b) 3; (c) 1; (d) 5; (e) 2.

13. The 10 isoprene units render coenzyme Q soluble in the hydrophobic environment of the inner mitochondrial membrane. The two oxygen atoms can reversibly bind two electrons and two protons as the molecule transitions between the quinone form and quinol form.

14. Rotenone: NADH, NADH-Q oxidoreductase will be reduced. The remainder will be oxidized. Antimycin A: NADH, NADH-Q oxidoreductase and coenzyme Q will be reduced. The remainder will be oxidized. Cyanide: All will be reduced.

15. Complex I would be reduced, whereas Complexes II, III, and IV would be oxidized. The citric acid cycle would halt because it has no way to oxidize NADH.

16. The respirasome is another example of the use of supramolecular complexes in biochemistry. Having the three complexes that are proton pumps associated with one another will enhance the efficiency of electron flow from complex to complex, which in turn will cause more-efficient proton pumping.

17. Succinate dehydrogenase is a component of Complex II.

18. Hydroxyl radical ($OH\,\cdot$), hydrogen peroxide (H_2O_2), superoxide ion ($O_2^{\cdot-}$), and peroxide (O_2^{2-}). These small molecules react with a host of macromolecules—including proteins, nucleotides, and membranes—to disrupt cell structure and function.

19. The ATP is recycled by ATP-generating processes, most notably oxidative phosphorylation.

20. (a) 12.5; (b) 14; (c) 32; (d) 13.5; (e) 30; (f) 16.

21. (a) It blocks electron transport and proton pumping at Complex IV. (b) It blocks electron transport and ATP synthesis by inhibiting the exchange of ATP and ADP across the inner mitochondrial membrane. (c) It blocks electron transport and proton pumping at Complex I. (d) It blocks ATP synthesis without inhibiting electron transport by dissipating the proton gradient. (e) It blocks electron transport and proton pumping at Complex IV. (f) It blocks electron transport and proton pumping at Complex III.

22. If the proton gradient is not dissipated by the influx of protons into a mitochondrion with the generation of ATP, eventually the outside of the mitochondrion develops such a large positive charge that the electron-transport chain can no longer pump protons against the gradient.

23. The subunits are jostled by background thermal energy (Brownian motion). The proton gradient makes clockwise rotation more likely because that direction results in protons flowing down their concentration gradient.

24. Dicyclohexylcarbodiimide reacts readily with carboxyl groups. Hence, the most likely targets are aspartate and glutamate side chains. In fact, Asp 61 of subunit **c** of *E. coli* F_0 is specifically modified by this reagent. The conversion of Asp 61 into asparagine by site-specific mutagenesis eliminates proton conduction.

25. In the presence of poorly functioning mitochondria, the only means of generating ATP is by anaerobic glycolysis, which will lead to an accumulation of lactic acid in blood.

26. If ADP cannot get into mitochondria, the electron-transport chain will cease to function because there will be no acceptor for

the energy. NADH will build up in the matrix. Recall that NADH inhibits some citric acid cycle enzymes and that NAD^+ is required by several citric acid cycle enzymes. Glycolysis will switch to lactic acid fermenation so that the NADH can be reoxidized to NAD^+ by lactate dehydrogenase.

27. (a) No effect; mitochondria cannot metabolize glucose.
(b) No effect; no fuel is present to power the synthesis of ATP.
(c) The $[O_2]$ falls because citrate is a fuel and ATP can be formed from ADP and P_i.
(d) Oxygen consumption stops because oligomycin inhibits ATP synthesis, which is coupled to the activity of the electron-transport chain.
(e) No effect, for the reasons given in part *d*.
(f) $[O_2]$ falls rapidly because the system is uncoupled and does not require ATP synthesis to lower the proton-motive force.
(g) $[O_2]$ falls, though at a lower rate. Rotenone inhibits Complex I, but the presence of succinate will enable electrons to enter at Complex II.
(h) Oxygen consumption ceases because Complex IV is inhibited and the entire chain backs up.

28. (a) The P : O ratio is equal to the product of $(H^+/2\,e^-)$ and (P/H^+). Note that the P : O ratio is identical with the P : 2 e^- ratio.
(b) 2.5 and 1.5, respectively.

29. Cyanide can be lethal because it binds to the ferric form of cytochrome oxidase and thereby inhibits oxidative phosphorylation. Nitrite converts ferrohemoglobin into ferrihemoglobin, which also binds cyanide. Thus, ferrihemoglobin competes with cytochrome *c* oxidase for cyanide. This competition is therapeutically effective because the amount of ferrihemoglobin that can be formed without impairing oxygen transport is much greater than the amount of cytochrome *c* oxidase.

30. Such a defect (called Luft syndrome) was found in a 38-year-old woman who was incapable of performing prolonged physical work. Her basal metabolic rate was more than twice normal, but her thyroid function was normal. A muscle biopsy showed that her mitochondria were highly variable and atypical in structure. Biochemical studies then revealed that oxidation and phosphorylation were not tightly coupled in these mitochondria. In this patient, much of the energy of fuel molecules was converted into heat rather than ATP.

31. Triose phosphate isomerase converts dihydroxyacetone phosphate (a potential dead end) into glyceraldehyde 3-phosphate (a mainstream glycolytic intermediate).

32. This inhibitor (like antimycin A) blocks the reduction of cytochrome c_1 by QH_2, the crossover point.

33. If oxidative phosphorylation were uncoupled, no ATP could be produced. In a futile attempt to generate ATP, much fuel would be consumed. The danger lies in the dose. Too much uncoupling would lead to tissue damage in highly aerobic organs such as the brain and heart, which would have severe consequences for the organism as a whole. The energy that is normally transformed into ATP would be released as heat. To maintain body temperature, sweating might increase, although the very process of sweating itself depends on ATP.

34. If ATP and ADP cannot exchange between the matrix and the mitochondria, ATP synthase will cease to function because its substrate ADP is absent. The proton gradient will eventually become so large that the energy released by the electron-transport chain will not be great enough to pump protons against the larger-than-normal gradient.

35. Add the inhibitor with and without an uncoupler, and monitor the rate of O_2 consumption. If the O_2 consumption increases again in the presence of inhibitor and uncoupler, the inhibitor must be inhibiting ATP synthase. If the uncoupler has no effect on the inhibition, the inhibitor is inhibiting the electron-transport chain.

36. Presumably, because the muscle has greater energy needs, especially during exercise, it will require more ATP. This requirement means that more sites of oxidative phosphorylation are called for, and these sites can be provided by an increase in the amount of cristae.

37. The arginine residue, with its positive charge, will facilitate proton release from aspartic acid by stabilizing the negatively charged aspartate.

38. 4; 4.7

39. The ATP synthase would pump protons at the expense of ATP hydrolysis, thus maintaining the proton-motive force. The synthase would function as an ATPase. There is some evidence that damaged mitochondria use this tactic to maintain, at least temporarily, the proton-motive force.

40. It suggests that malfunctioning mitochondria may play a role in the development of Parkinson disease. Specifically, it implicates Complex I.

41. The extra negative charge on ATP relative to that on ADP accounts for ATP's more-rapid translocation out of the mitochondrial matrix. If the charge differences between ATP and ADP were lessened by the binding of Mg^{2+}, ADP might more readily compete with ATP for transport to the cytoplasm.

42. When all of the available ADP has been converted into ATP, ATP synthase can no longer function. The proton gradient becomes large enough that the energy of the electron-transport chain is not enough to pump against the gradient, and electron transport and, hence, oxygen consumption falls.

43. The effect on the proton gradient is the same in each case.

44 ATP export from the matrix. Phosphate import into the matrix.

45. Recall from the discussion of enzyme-catalyzed reactions that the direction of a reaction is determined by the ΔG difference between substrate and products. An enzyme speeds up the rate of both the forward and the backward reactions. The hydrolysis of ATP is exergonic, and so ATP synthase will enhance the hydrolytic reaction.

46. The cytoplasmic kinases thereby obtain preferential access to the exported ATP.

47. The organic acids in the blood are indications that the mice are deriving a large part of their energy needs through anaerobic glycolysis. Lactate is the end product of anaerobic glycolysis. Alanine is an aminated transport form of pyruvate, which is formed from lactate. Alanine formation plays a role in succinate formation, which is caused by the reduced state of the mitochondria.

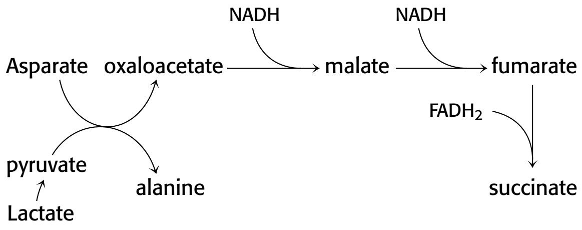

The electron-transport chain is slowed because the inner mitochondrial membrane is hyperpolarized. Without ADP to accept the energy of the proton-motive force, the membrane becomes polarized to such an extent that protons can no longer be pumped. The excess H_2O_2 is probably due to the fact that the superoxide radical is present in higher concentration because the oxygen can no longer be effectively reduced.

$$O_2\cdot^- + O_2\cdot^- + 2\,H^+ \longrightarrow O_2 + H_2O_2$$

Indeed, these mice display evidence of such oxidative damage.

48. (a) Vitamins C and E.
(b) Exercise induces superoxide dismutase, which converts ROS in hydrogen peroxide and oxygen.

(c) The answer to this question is not fully established. Two possibilities are (1) the suppression of ROS by vitamins prevents the expression of more superoxide dismutase and (2) some ROS may be signal molecules required to stimulate insulin-sensitivity pathways.

49. (a) DNP is an uncoupler that prevents the use of the proton-motive force for ATP synthesis. Consequently, the rate of oxygen consumption rises (reflecting the rate of the electron transport chain) in a futile attempt to synthesize ATP. Because mitochondrial ATP synthesis in inhibited, the rate of glycolysis, as measured by ECAR, increases in an attempt meet the cells ATP needs.
(b) Because glycolysis is now inhibited, no lactic acid will be produced and the rate of extracellular acidification will fall. Because DNP is still present, oxygen consumption will still occur at a high rate.
(c) A key step in glycolysis is the isomerization of glucose 6-phosphate to fructose 6-phosphate. 2-Deoxyglucose is incapable of undergoing the isomerization.
(d) Rotenone inhibits electron flow through Complex I, the electron transport chain is inhibited and oxygen consumption ceases.

50. (a) Succinate is oxidized by Complex II, and the electrons are used to establish a proton-motive force that powers ATP synthesis.
(b) The ability to synthesize ATP is greatly reduced.
(c) The goal was to measure ATP hydrolysis. If succinate had been added in the presence of ATP, no reaction would have taken place, because of respiratory control.
(d) The mutation has little effect on the ability of the enzyme to catalyze the hydrolysis of ATP.
(e) They suggest two things: (1) the mutation did not affect the catalytic site on the enzyme, because ATP synthase is still capable of catalyzing the reverse reaction, and (2) the mutation did not affect the amount of enzyme present, given that the controls and patients had similar amounts of activity.

51. The absolute configuration of thiophosphate indicates that inversion at phosphorus has taken place in the reaction catalyzed by ATP synthase. This result is consistent with an inline phosphoryl-transfer reaction taking place in a single step. The retention of configuration in the Ca^{2+}-ATPase reaction points to two phosphoryl-transfer reactions—inversion by the first and a return to the starting configuration by the second. The Ca^{2+}-ATPase reaction proceeds by a phosphorylated enzyme intermediate.

Chapter 19

1. Ultimately, all of the carbon atoms of which we are made, not just carbohydrates, enter the biosphere through the process of photosynthesis. Moreover, the oxygen that we require is produced by photosynthesis.

2. $2\ NADP^+ + 3\ ADP^{3-} + 3\ P_i^{2-} + H^+ \rightarrow O_2 + 2\ NADPH + 3\ ATP^{4-} + H_2O$

3. (a) 7; (b) 5; (c) 4; (d) 10; (e) 1; (f) 2; (g) 9; (h) 3; (i) 8; (j) 6.

4. Photosystem II, in conjunction with the oxygen-generating complex, powers oxygen release. The reaction center of photosystem II absorbs light maximally at 680 nm.

5. Oxygen consumption will be maximal when photosystems I and II are operating cooperatively. Oxygen will be efficiently generated when electrons from photosystem II fill the electron holes in photosystem I, which were generated when the reaction center of photosystem I was illuminated by light of 700 nm.

6. Photosystem I generates ferredoxin, which reduces $NADP^+$ to NADPH, a biosynthetic reducing power. Photosystem II activates the water-oxidizing complex, generating electrons for photosynthesis, and generating protons to form a proton gradient and to reduce ferredoxin and O_2.

7. The light reactions take place on thylakoid membranes. Increasing the membrane surface increases the number of ATP- and NADPH-generating sites.

8. These complexes absorb more light than can a reaction center alone. The light-harvesting complexes funnel light to the reaction centers.

9. $NADP^+$ is the acceptor. H_2O is the donor. Light energy.

10. The charge gradient, a component of the proton-motive force in mitochondria, is neutralized by the influx of Mg^{2+} into the lumen of the thylakoid membranes.

11. Chlorophyll is readily inserted into the hydrophobic interior of the thylakoid membranes.

12. Protons released by the oxidation of water; protons pumped into the lumen by the cytochrome *bf* complex; protons removed from the stroma by the reduction of $NADP^+$ and plastoquinone.

13. 700-nm photons have an energy content of $+172$ kJ mol^{-1}. The absorption of light by photosystem I results in a $\Delta E'_0$ of -1.0 V. Recall that $\Delta G'_0 = -nF\Delta E'_0$, where $F = 96.48$ kJ $mol^{-1}\ V^{-1}$. Under standard conditions, the energy change for the electrons is 96.5 kJ. Thus, the efficiency is $96.5/172 = 56\%$.

14. The electron flow from photosystem II to photosystem I is uphill, or exergonic. For this uphill flow, ATP would need to be consumed, defeating the purpose of photosynthesis.

15. $\Delta E'_0 = 10.11$ V, and $\Delta G^{\circ\prime} = -21.3$ kJ mol^{-1} (-5.1 kcal mol^{-1}).

16. (a) All ecosystems require an energy source from outside the system, because the chemical energy sources will ultimately be limited. The photosynthetic conversion of sunlight is one example of such a conversion.
(b) Not at all. Spock would point out that chemicals other than water can donate electrons and protons.

17. DCMU inhibits electron transfer in the link between photosystems II and I. O_2 can evolve in the presence of DCMU if an artificial electron acceptor such as ferricyanide can accept electrons from Q.

18. DCMU will have no effect, because it blocks photosystem II, and cyclic photophosphorylation uses photosystem I and the cytochrome *bf* complex.

19. (a) $+120$ kJ $einstein^{-1}$ ($+28.7$ kcal $einstein^{-1}$)
(b) 1.24 V
(c) One 1000-nm photon has the free energy content of 2.4 molecules of ATP. A minimum of 0.42 photon is needed to drive the synthesis of a molecule of ATP.

20. At this distance, the expected rate is one electron per second.

21. The distance doubles, and so the rate should decrease by a factor of 64 to 640 ps.

22. The cristae.

23. In eukaryotes, both processes take place in specialized organelles. Both depend on high-energy electrons to generate ATP. In oxidative phosphorylation, the high-energy electrons originate in fuels and are extracted as reducing power in the form of NADH. In photosynthesis, the high-energy electrons are generated by light and are captured as reducing power in the form of NADPH. Both processes use redox reactions to generate a proton gradient, and the enzymes that convert the proton gradient into ATP are very similar in both processes. In both systems, electron transport takes place in membranes inside organelles.

24. We need to factor in the NADPH because it is an energy-rich molecule. Recall from Chapter 18 that NADH is worth 2.5 ATP if oxidized by the electron-transport chain. 12 NADPH = 30 ATP. Eighteen molecules of ATP are used directly, and so the equivalent of 48 molecules of ATP is required for the synthesis of glucose.

25. Both photosynthesis and cellular respiration are powered by high-energy electrons flowing toward a more-stable state. In cellular respiration, the high-energy electrons are derived from the oxidation of carbon fuels as NADH and $FADH_2$. They release their energy as they reduce oxygen. In photosynthesis, high-energy electrons are generated by absorbing light energy, and they find stability in photosystem I and ferridoxin.

26. The electrons flow through photosystem II directly to ferricyanide. No other steps are required.

27. (a) Thioredoxin

(b) The control enzyme is unaffected, but the mitochondrial enzyme with part of the chloroplast γ subunit increases activity as the concentration of DTT increases.

(c) The increase was even larger when thioredoxin was present. Thioredoxin is the natural reductant for the chloroplast enzyme, and so it presumably operates more efficiently than would DTT, which probably functions to keep the thioredoxin reduced.

(d) They seem to have done so.

(e) The enzyme is susceptible to control by the redox state. In plant cells, reduced thioredoxin is generated by photosystem I. Thus, the enzyme is active when photosynthesis is taking place.

(f) Cysteine.

(g) Group-specific modification or site-specific mutagenesis.

Chapter 20

1. The Calvin cycle is the primary means of converting gaseous CO_2 into organic matter—that is, biomolecules. Essentially, every carbon atom in your body passed through rubisco and the Calvin cycle at some time in the past.

2. Autotrophs can use the energy of sunlight, carbon dioxide, and water to synthesize carbohydrates, which can subsequently be used for catabolic or anabolic purposes. Heterotrophs require chemical fuels and are thus ultimately dependent on autotrophs.

3. Nothing grim or secret about these reactions. They are sometimes called the dark reactions because they do not directly depend on light.

4.

Calvin cycle	**Krebs cycle**
Stroma	Matrix
Carbon chemistry for photosynthesis	Carbon chemistry for oxidative phosphorylation
Fixes CO_2	Releases CO_2
Requires high-energy electrons (NADPH)	Generates high-energy electrons (NADH)
Regenerates starting compound (ribulose 1.5-bisphosphate)	Regenerates starting compound (oxaloacetate)
Requires ATP	Generates ATP
Complex stoichiometry	Simple stoichiometry

5. (a) 3-Phosphoglycerate. (b) The other members of the Calvin cycle.

6. Stage 1 is the fixation of CO_2 with ribulose 1,5-bisphosphate and the subsequent formation of 3-phosphoglycerate. Stage 2 is the conversion of some of the 3-phosphoglycerate into hexose. Stage 3 is the regeneration of ribulose 1,5-bisphosphate.

7. It catalyzes a crucial reaction, but it is highly inefficient. Consequently, it is required in large amounts to overcome its slow catalysis.

8. Because carbamate forms only in the presence of CO_2, this property prevents rubisco from catalyzing the oxygenase reaction exclusively when CO_2 is absent.

9. Because NADPH is generated in the chloroplasts by the light reactions.

10. The concentration of 3-phosphoglycerate would increase, whereas that of ribulose 1,5-bisphosphate would decrease.

11. The concentration of 3-phosphoglycerate would decrease, whereas that of ribulose 1,5-bisphosphate would increase.

12. Aspartate + glyoxylate ⟶ oxaloacetate + glycine

13. The oxygenase activity of rubisco increases with temperature. Crabgrass is a C_4 plant, whereas most grasses lack this capability. Consequently, the crabgrass will thrive at the hottest part of the summer because the C_4 pathway provides an ample supply of CO_2.

14. The C_4 pathway allows the CO_2 concentration to increase at the site of carbon fixation. High concentrations of CO_2 inhibit the oxygenase reaction of rubisco. This inhibition is important for tropical plants because the oxygenase activity increases more rapidly with temperature than does the carboxylase activity.

15. ATP is required to form phosphoenolpyruvate (PEP) from pyruvate. The PEP combines with CO_2 to form oxaloacetate and, subsequently, malate. Two ATP molecules are required because a second ATP molecule is required to phosphorylate AMP to ADP.

16. Photorespiration is the consumption of oxygen by plants with the production of CO_2, but it does not generate energy. Photorespiration is due to the oxygenase activity of rubisco. It is wasteful because, instead of fixing CO_2 for conversion into hexoses, rubisco is generating CO_2.

17. As global warming progresses, C_4 plants will invade the higher latitudes, and C_3 plants will retreat to cooler regions.

18. The light reactions lead to an increase in the stromal concentrations of NADPH, reduced ferredoxin, and Mg^{2+}, as well as an increase in pH.

19. (a) 5; (b) 1; (c) 7; (d) 2; (e) 10; (f) 3; (g) 6; (h) 4; (i) 8; (j) 9.

20. The enzymes catalyze the transformation of the five-carbon sugar formed by the oxidative phase of the pentose phosphate pathway into fructose 6-phosphate and glyceraldehyde 3-phosphate, intermediates in glycolysis (and gluconeogenesis).

21. (a) C; (b) B and F; (c) G; (d) F; (e) E; (f) H; (g) I; (h) D; (i) A; (j) F; (k) B.

22. The label emerges at C-5 of ribulose 5-phosphate.

23. Oxidative decarboxylation of isocitrate to α-ketoglutarate. A β-ketoacid intermediate is formed in both reactions.

24. (a) 5 Glucose 6-phosphate + ATP $\rightarrow$
6 ribose 5-phosphate + ADP + H^+.
(b) Glucose 6-phosphate + 12 $NADP^+$ + $7H_2O$ $\rightarrow$
6 CO_2 + 12 NADPH + 12 H^+ + P_i.

25. The nonoxidative phase of the pentose phosphate pathway can be used to convert three molecules of ribose 5-phosphate into two molecules of fructose 6-phosphate and one molecule of glyceraldehyde 3-phosphate. These molecules are components of the glycolytic pathway.

26. The conversion of fructose 6-phosphate into fructose 1,6-bisphosphate by phosphofructokinase requires ATP.

27. When much NADPH is required. The oxidative phase of the pentose phosphate pathway is followed by the nonoxidative phase. The resulting fructose 6-phosphate and glyceraldehyde 3-phosphate are used to generate glucose 6-phosphate through gluconeogenesis, and the cycle is repeated until the equivalent of one glucose molecule is oxidized to CO_2.

28. Fava beans contain vicine, a purine glycoside that can lead to the generation of peroxides—reactive oxygen species that can damage membranes as well as other biomolecules. Glutathione is used to detoxify the ROS. The regeneration of glutathione depends on an adequate supply of NADPH, which is synthesized by the oxidative phase of the pentose phosphate pathway. People with low levels of the dehydrogenase are especially susceptible to vicine toxicity.

29. Because red blood cells do not have mitochondria and the only means to obtain NADPH is through the pentose phosphate pathway. There are biochemical means to convert mitochondrial NADH into cytoplasmic NADPH.

30. Reactive peroxides are a type of reactive oxygen species. The enzyme glutathione peroxidase uses reduced glutathione to neutralize peroxides by converting them into alcohols while generating

oxidized glutathione. Reduced glutathione is regenerated by glutathione reductase with the use of NADPH, the product of the oxidative phase of the pentose phosphate pathway.

31. $\Delta E'_0$ for the reduction of glutathione by NADPH is $+0.09$ V. Hence, $\Delta G^{\circ\prime}$ is -17.4 kJ mol^{-1} (-4.2 kcal mol^{-1}), which corresponds to an equilibrium constant of 1126. The required [NADPH]/[NADP$^+$] ratio is 8.9×10^{-5}.

32.

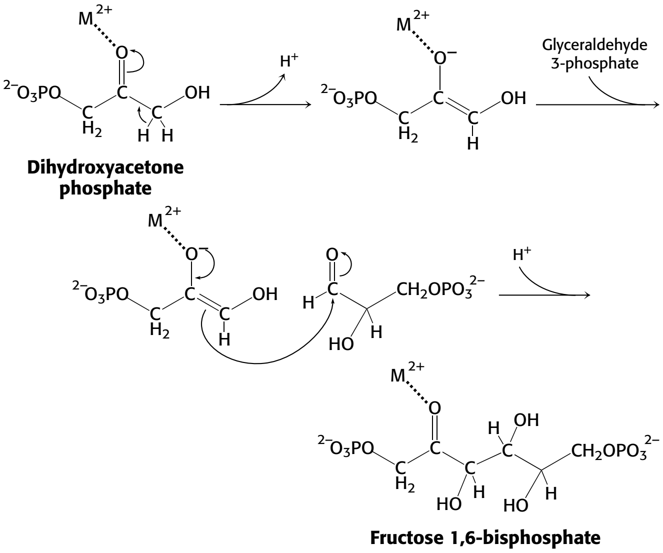
M2+
H+
Glyceraldehyde 3-phosphate
Dihydroxyacetone phosphate
H+
Fructose 1,6-bisphosphate

33.

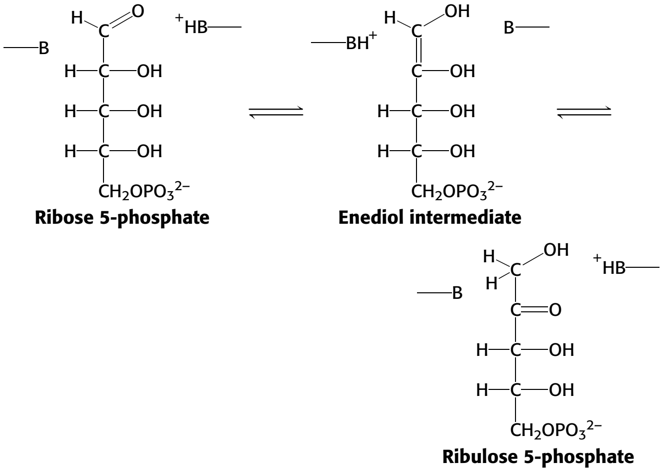

34. Incubate an aliquot of a tissue homogenate with glucose labeled with ^{14}C at C-1, and incubate another with glucose labeled with ^{14}C at C-6. Compare the radioactivity of the CO_2 produced by the two samples. The rationale of this experiment is that only C-1 is decarboxylated by the pentose phosphate pathway, whereas C-1 and C-6 are decarboxylated equally when glucose is metabolized by the glycolytic pathway, the pyruvate dehydrogenase complex, and the citric acid cycle. The reason for the equivalence of C-1 and C-6 in the latter set of reactions is that glyceraldehyde 3-phosphate and dihydroxyacetone phosphate are rapidly interconverted by triose phosphate isomerase.

35. Lacking mitochondria, red blood cells metabolize glucose to lactate to obtain energy in the form of ATP. The CO_2 results from extensive use of the pentose phosphate pathway coupled with gluconeogenesis. This coupling allows the generation of much NADPH with the complete oxidation of glucose by the oxidative branch of the pentose phosphate pathway.

36. (a) $k_{\text{cat}}^{\text{CO}_2}/K_{\text{M}}^{\text{CO}_2} = 3 \times 10^6\ \text{s}^{-1}\text{M}^{-1}$

$k_{\text{cat}}^{\text{O}_2}/K_{\text{M}}^{\text{O}_2} = 4 \times 10^3\ \text{s}^{-1}\text{M}^{-1}$

(b) Despite the fact that the specificity constant for CO_2 as a substrate is much greater than that of O_2, the concentration of O_2 in the atmosphere is higher than that of CO_2, allowing the oxygenation reaction to occur.

37. The reduction of each mole of CO_2 to the level of a hexose requires two moles of NADPH. The reduction of NADP$^+$ is a two-electron process. Hence, the formation of two moles of NADPH requires the pumping of four moles of electrons by photosystem I. The electrons given up by photosystem I are replenished by photosystem II, which needs to absorb an equal number of photons. Hence, eight photons are needed to generate the required NADPH. The energy input of eight moles of photons is $+1594$ kJ ($+381$ kcal). Thus, the overall efficiency of photosynthesis under standard conditions is at least 477/1594, or 30%.

38. It is neither a violation nor a miracle. The equation on page 597 requires not only 18 ATP, but also 12 NADPH. These electrons, if transferred to NAD$^+$ and used in the electron-transport chain, would yield 30 ATP. Thus, the synthesis of glucose requires the equivalent of 48 ATP.

39. (a) The curve on the right in graph A was generated by the C_4 plant. Recall that the oxygenase activity of rubisco increases with temperature more rapidly than does the carboxylase activity. Consequently, at higher temperatures, the C_3 plants would fix less carbon. Because C_4 plants can maintain a higher CO_2 concentration, the rise in temperature is less deleterious.

(b) The oxygenase activity will predominate. Additionally, when the temperature rise is very high, the evaporation of water might become a problem. The higher temperatures can begin to damage protein structures as well.

(c) The C_4 pathway is a very effective active-transport system for concentrating CO_2, even when environmental concentrations are very low.

(d) With the assumption that the plants have approximately the same capability to fix CO_2, the C_4 pathway is apparently the rate-limiting step in C_4 plants.

Chapter 21

1. Step 1 is the release of glucose 1-phosphate from glycogen by glycogen phosphorylase. Step 2 is the formation of glucose 6-phosphate from glucose 1-phosphate, a reaction catalyzed by phosphoglucomutase. Step 3 is the remodeling of the glycogen by the transferase and the glucosidase.

2. (a) 8; (b) 3; (c) 6; (d) 5; (e) 9; (f) 2; (g) 10; (h) 1; (i) 4; (j) 7.

3. Glycogen is an important fuel reserve for several reasons. The controlled breakdown of glycogen and release of glucose increase the amount of glucose that is available between meals. Hence, glycogen serves as a buffer to maintain blood-glucose levels. Glycogen's role in maintaining blood-glucose levels is especially important because glucose is virtually the only fuel used by the brain, except during prolonged starvation. Moreover, the glucose from glycogen is readily mobilized and is therefore a good source of energy for sudden, strenuous activity. Unlike fatty acids, the released glucose can provide energy in the absence of oxygen and can thus supply energy for anaerobic activity.

4. As an unbranched polymer, α-amylose has only one nonreducing end. Therefore, only one glycogen phosphorylase molecule could degrade each α-amylose molecule. Because glycogen is highly branched, there are many nonreducing ends per molecule.

Consequently, many phosphorylase molecules can release many glucose molecules per glycogen molecule.
5. The patient has a deficiency of the branching enzyme.
6. In muscle, the *b* form of phosphorylase is activated by AMP. In the liver, the *a* form is inhibited by glucose. The difference corresponds to the difference in the metabolic role of glycogen in each tissue. Muscle uses glycogen as a fuel for contraction, whereas the liver uses glycogen to maintain blood-glucose levels.
7. Cells maintain the $[P_i]/[\text{glucose 1-phosphate}]$ ratio at greater than 100, substantially favoring phosphorolysis. We see here an example of how the cell can alter the free-energy change to favor a reaction taking place by altering the ratio of substrate and product.
8. The high level of glucose 6-phosphate in von Gierke disease, resulting from the absence of glucose 6-phosphatase or the transporter, shifts the allosteric equilibrium of phosphorylated glycogen synthase toward the active form.
9. The phosphoryl donor is glucose 1,6-bisphosphate, which is formed from glucose 1-phosphate and ATP in a reaction catalyzed by phosphoglucokinase.
10. The different manifestations correspond to the different roles of the liver and muscle. Liver glycogen phosphorylase plays a crucial role in the maintenance of blood-glucose levels. Recall that glucose is the primary fuel for the brain. Muscle glycogen phosphorylase provides glucose only for the muscle and, even then, only when the energy needs of the muscle are high, as during exercise. The fact that there are two different diseases suggests that there are two different isozymic forms of the glycogen phosphorylase—a liver-specific isozyme and a muscle-specific isozyme.
11. Water is excluded from the active site to prevent hydrolysis. The entry of water could lead to the formation of glucose rather than glucose 1-phosphate. A site-specific mutagenesis experiment is revealing in this regard. In phosphorylase, Tyr 573 is hydrogen bonded to the 2′-OH group of a glucose residue. The ratio of glucose 1-phosphate to glucose product is 9000 : 1 for the wild-type enzyme, and 500 : 1 for the Phe 573 mutant. Model building suggests that a water molecule occupies the site normally filled by the phenolic OH group of tyrosine and occasionally attacks the oxocarbonium ion intermediate to form glucose.
12. The amylase activity was necessary to remove all of the glycogen from the glycogenin. Recall that glycogenin synthesizes oligosaccharides of about eight glucose units, and then activity stops. Consequently, if the glucose residues are not removed by extensive amylase treatment, glycogenin will not function.
13. The substrate can be handed directly from the transferase site to the debranching site.
14. During exercise, [ATP] falls and [AMP] rises. Recall that AMP is an allosteric activator of glycogen phosphorylase *b*. Thus, even in the absence of covalent modification by phosphorylase kinase, glycogen is degraded.
15. Although glucose 1-phosphate is the actual product of the phosphorylase reaction, glucose 6-phosphate is a more versatile molecule with respect to metabolism. Among other fates, glucose-6-phosphate can be processed to yield energy or building blocks. In the liver, glucose 6-phosphate can be converted into glucose and released into the blood.
16. Epinephrine binds to its G-protein-coupled receptor. The resulting structural changes activate a G_α protein, which in turn activates adenylate cyclase. Adenylate cyclase synthesizes cAMP, which activates protein kinase A. Protein kinase A partly activates phosphoryl kinase, which phosphorylates and activates glycogen phosphorylase. The calcium released during muscle contraction also activates the phosphorylase kinase, leading to further stimulation of glycogen phosphorylase.
17. First, the signal-transduction pathway is shut down when the initiating hormone is no longer present. Second, the inherent GTPase activity of the G protein converts the bound GTP into inactive GDP. Third, phosphodiesterases convert cyclic AMP into AMP. Fourth, PP1 removes the phosphoryl group from glycogen phosphorylase, converting the enzyme into the usually inactive *b* form.
18. It prevents both from operating simultaneously, which would lead to a useless expenditure of energy.
19. All these symptoms suggest central nervous system problems. If exercise is exhaustive enough or the athlete has not prepared well enough or both, liver glycogen also can be depleted. The brain depends on glucose derived from liver glycogen. The symptoms suggest that the brain is not getting enough fuel (hypoglycemia).
20. Liver phosphorylase *a* is inhibited by glucose, which facilitates the R → T transition. This transition releases PP1, which inactivates glycogen breakdown and stimulates glycogen synthesis. Muscle phosphorylase is insensitive to glucose.
21. (a) 4; (b) 1; (c) 5; (d) 10; (e) 7; (f) 2; (g) 8; (h) 9; (i) 6; (j) 3.
22. Phosphoglucomutase, UDP-glucose pyrophosphorylase, pyrophosphatase, glycogenin, glycogen synthase, and branching enzyme.
23. The enzyme pyrophosphatase converts the pyrophosphate into two molecules of inorganic phosphate. This conversion renders the overall reaction irreversible.

$$\begin{array}{c}\text{Glucose 1-phosphate} + \text{UTP} \rightleftharpoons \text{UDP-glucose} + \text{PP}_i\\ \text{PP}_i + \text{H}_2\text{O} \longrightarrow 2\text{P}_i\\ \hline \text{Glucose 1-phosphate} + \text{UTP} \longrightarrow \text{UDP-glucose} + 2\text{Pi}\end{array}$$

24. The presence of high concentrations of glucose 6-phosphate indicates that glucose is abundant and that it is not being used by glycolysis. Therefore, this valuable resource is saved by incorporation into glycogen.
25. Free glucose must be phosphorylated at the expense of a molecule of ATP. Glucose 6-phosphate derived from glycogen is formed by phosphorolytic cleavage, sparing one molecule of ATP. Thus, the net yield of ATP when glycogen-derived glucose is processed to pyruvate is three molecules of ATP compared with two molecules of ATP from free glucose.
26. Breakdown: Phosphoglucomutase converts glucose 1-phosphate, liberated from glycogen breakdown, into glucose 6-phosphate, which can be released as free glucose (liver) or processed in glycolysis (muscle and liver). Synthesis: Converts glucose 6-phosphate into glucose 1-phosphate, which reacts with UTP to form UDP-glucose, the substrate for glycogen synthase.
27. $\text{Glycogen}_n + \text{P}_i \longrightarrow \text{glycogen}_{n-1} + \text{glucose 6-phosphate}$

$$\text{Glucose 6-phosphate} \longrightarrow \text{glucose 1-phosphate}$$

$$\text{UTP} + \text{glucose 1-phosphate} \longrightarrow \text{UDP-glucose} + 2\ \text{P}_i$$

$$\text{Glycogen}_{n-1} + \text{UDP-glucose} \longrightarrow \text{glycogen}_n + \text{UDP}$$

$$\text{Sum: Glycogen}_n + \text{UTP} \longrightarrow \text{glycogen}_n + \text{UDP} + \text{P}_i$$

28. In principle, having glycogen be the only primer for the further synthesis of glycogen should be a successful strategy. However, if the glycogen granules were not evenly divided between daughter cells, glycogen stores for future generations of cells might be compromised. Glycogenin synthesizes the primer for glycogen synthase.
29. Insulin binds to its receptor and activates the tyrosine kinase activity of the receptor, which in turn triggers a pathway that activates protein kinases. The kinases phosphorylate and inactivate glycogen synthase kinase. Protein phosphatase 1 then removes the phosphate from glycogen synthase and thereby activates the synthase.

30.

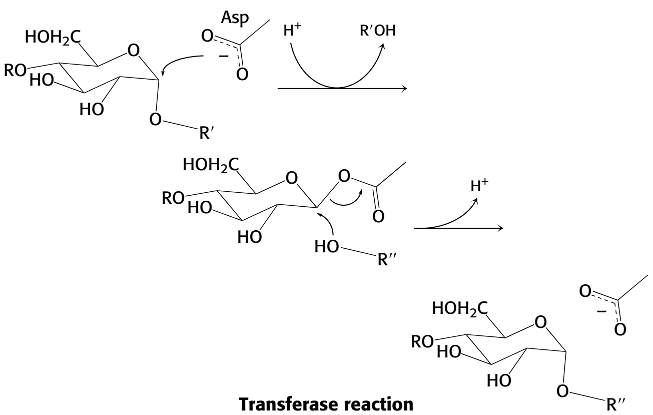

Transferase reaction

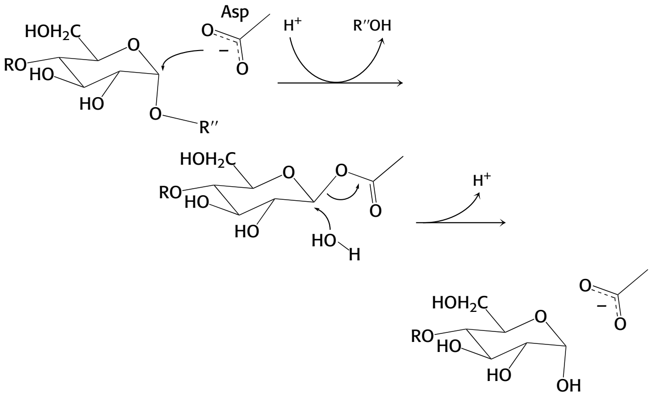

α-1,6-Glucosidase reaction

31. In the liver, glucagon stimulates the cAMP-dependent pathway that activates protein kinase A. Epinephrine binds to a 7TM α-adrenergic receptor in the liver plasma membrane, which activates phospholipase C and the phosphoinositide cascade. This activation causes calcium ions to be released from the endoplasmic reticulum, which bind to calmodulin, and further stimulates phosphorylase kinase and glycogen breakdown.

32. Galactose + ATP + UTP + H_2O + glycogen$_n$ $\longrightarrow$ glycogen$_{n+1}$ + ADP + UDP + 2 P_i + H^+.

33. Phosphorylase, transferase, glucosidase, phosphoglucomutase, and glucose 6-phosphatase.

34. Glucose is an allosteric inhibitor of phosphorylase *a.* Hence, crystals grown in its presence are in the T state. The addition of glucose 1-phosphate, a substrate, shifts the R-to-T equilibrium toward the R state. The conformational differences between these states are sufficiently large that the crystal shatters unless it is stabilized by chemical cross-links.

35. Galactose is converted into UDP-galactose to eventually form glucose 6-phosphate.

36. This disease can also be produced by a mutation in the gene that encodes the glucose 6-phosphate transporter. Recall that glucose 6-phosphate must be transported into the lumen of the endoplasmic reticulum to be hydrolyzed by phosphatase. Mutations in the other three essential proteins of this system can likewise lead to von Gierke disease.

37. (a) Apparently, the glutamate, with its negatively charged R group, can mimic to some extent the presence of a phosphoryl group on serine. That the stimulation is not as great is not surprising in that the carboxyl group is smaller and not as charged as the phosphate.
(b) Substitution of aspartate would give some stimulation, but because it is smaller than the glutamate, the stimulation would be smaller.

38. (a) Glycogen was too large to enter the gel and, because analysis was by western blot with the use of an antibody specific to glycogenin, we would not expect to see background proteins.
(b) α-Amylase degrades glycogen, releasing the protein glycogenin, which can be visualized by a western blot.
(c) Glycogen phosphorylase, glycogen synthase, and protein phosphatase 1. These proteins might be visible if the gel were stained for protein, but a western analysis reveals the presence of glycogenin only.

39. (a) The smear was due to molecules of glycogenin with increasingly large amounts of glycogen attached to them.
(b) In the absence of glucose in the medium, glycogen is metabolized, resulting in a loss of the high-molecular-weight material.
(c) Glycogen could have been resynthesized and added to the glycogenin when the cells were fed glucose again.
(d) No difference between lanes 3 and 4 suggests that, by 1 hour, the glycogen molecules had attained maximum size in this cell line. Prolonged incubation does not apparently increase the amount of glycogen.
(e) α-Amylase removes essentially all of the glycogen, and so only the glycogenin remains.

Chapter 22

1. (a) 5; (b) 11; (c) 1; (d) 10; (e) 2; (f) 6; (g) 9; (h) 3; (i) 4; (j) 7; (k) 8.

2. Glycerol + 2 NAD^+ + P_i + ADP $\longrightarrow$ pyruvate + ATP + H_2O + 2 NADH + H^+

Glycerol kinase and glycerol phosphate dehydrogenase

3. The ready reversibility is due to the high-energy nature of the thioester in the acyl CoA.

4. To return the AMP to a form that can be phosphorylated by oxidative phosphorylation or substrate-level phosphorylation, another molecule of ATP must be expended in the reaction:

$$\text{ATP} + \text{AMP} \rightleftharpoons 2\ \text{ADP}$$

5. b, c, a, g, h, d, e, f.

6. The citric acid cycle. The reactions that take succinate to oxaloacetate, or the reverse, are similar to those of fatty acid metabolism (Section 17.2).

7. The next-to-last degradation product, acetoacetyl CoA, yields two molecules of acetyl CoA with the thiolysis by only one molecule of CoA.

8. Palmitic acid yields 106 molecules of ATP. Palmitoleic acid has a double bond between carbons C-9 and C-10. When palmitoleic acid is processed in β oxidation, one of the oxidation steps (to introduce a double bond before the addition of water) will not take place, because a double bond already exists. Thus, $FADH_2$ will not be generated, and palmitoleic acid will yield 1.5 fewer molecules of ATP than palmitic acid, for a total of 104.5 molecules of ATP.

9.

Activation fee to form the acyl CoA	−2 ATP
Seven rounds of yield:	
7 acetyl CoA at 10 ATP/acetyl CoA	+ 70 ATP
7 NADH at 2.5 ATP/NADH	+ 17.5 ATP
7 $FADH_2$ at 1.5 ATP/$FADH_2$	+ 10.5 ATP
Propionyl CoA, which requires an ATP to be converted into succinyl CoA	− 1 ATP
Succinyl CoA → succinate	+ 1 ATP
Succinate → fumarate + $FADH_2$ $FADH_2$ at 1.5 ATP/$FADH_2$	+ 1.5 ATP
Fumarate → malate	
Malate → oxaloacetate + NADH NADH at 2.5 ATP/NADH	+ 2.5 ATP
Total	120 ATP

10. You might hate yourself in the morning, but at least you won't have to worry about energy. To form stearoyl CoA requires the equivalent of 2 molecules of ATP.

$$\text{Stearoyl CoA} + 8\ \text{FAD} + 8\ \text{NAD}^+ + 8\ \text{CoA} + 8\ H_2O \longrightarrow 9\ \text{acetyl CoA} + 8\ \text{FADH}_2 + 8\ \text{NADH} + 8\ H^+$$

9 acetyl CoA at 10 ATP/acetyl CoA	+ 90 ATP
8 NADH at 2.5 ATP/NADH	+ 20 ATP
8 $FADH_2$ at 1.5 ATP/$FADH_2$	+ 12 ATP
Activation fee	−2.0
Total	122 ATP

11. Keep in mind that, in the citric acid cycle, 1 molecule of $FADH_2$ yields 1.5 ATP, 1 molecule of NADH yields 2.5 ATP, and 1 molecule of acetyl CoA yields 10 ATP. Two molecules of ATP are produced when glucose is degraded to 2 molecules of pyruvate. Two molecules of NADH also are produced, but the electrons are transferred to $FADH_2$ to enter the electron transport chain. Each molecule of $FADH_2$ can generate 1.5 ATP. Each molecule of pyruvate will produce 1 molecule of NADH. Each molecule of acetyl CoA generates 3 molecules of NADH, 1 molecule of $FADH_2$, and 1 molecule of ATP. So, we have a total of 10 ATP per acetyl CoA, or 20 for the 2 molecules of acetyl CoA. The total for glucose is 30 ATP. Now, what about hexanoic acid? Caprioic acid is activated to caprioic CoA at the expense of 2 ATP, and so we are 2 ATP in the hole. The first cycle of β oxidation generates 1 $FADH_2$, 1 NADH, and 1 acetyl CoA. After the acetyl CoA has been run through the citric acid cycle, this step will have generated a total of 14 ATP. The second cycle of β oxidation generates 1 $FADH_2$ and 1 NADH but 2 acetyl CoA. After the acetyl CoA has been run through the citric acid cycle, this step will have generated a total of 24 ATP. The total is 36 ATP. Thus, the foul-smelling caprioic acid has a net yield of 36 ATP. So on a per carbon basis, this fat yields 20% more ATP than does glucose, a manifestation of the fact that fats are more reduced than carbohydrates.

12. Stearate + ATP + 13.5 H_2O + 8 FAD + 8 $NAD^+ \rightarrow$ 4.5 acetoacetate + 14.5 H^+ + 8 $FADH_2$ + 8 NADH + AMP + 2 P_i.

13. Palmitate is activated and then processed by β oxidation according to the following reactions.

$$\text{Palmitate} + \text{CoA} + \text{ATP} \longrightarrow \text{palmitoyl CoA} + \text{AMP} + 2\ P_i$$

$$\text{Palmitoyl CoA} + 7\ \text{FAD} + 7\ \text{NAD}^+ + 7\ \text{CoASH} + H_2O \longrightarrow 8\ \text{acetyl CoA} + 7\ \text{FADH}_2 + 7\ \text{NADH} + 7\ H^+$$

The eight molecules of acetyl CoA combine to form four molecules of acetoacetate for release into the blood, and so they do not contribute to the energy yield in the liver. However, the $FADH_2$ and NADH generated in the preparation of acetyl CoA can be processed by oxidative phosphorylation to yield ATP.

$$1.5\ \text{ATP}/\text{FADH}_2 \times 7 = 10.5\ \text{ATP}$$

$$2.5\ \text{ATP}/\text{NADH} \times 7 = 17.5\ \text{ATP}$$

The equivalent of 2 ATP were used to form palmitoyl CoA. Thus, 26 ATP were generated for use by the liver.

14. NADH produced with the oxidation to acetoacetate = 2.5 ATP. Acetoacetate is converted into acetoacetyl CoA. Two molecules of acetyl CoA result from the hydrolysis of acetoacetyl CoA, each worth 10 ATP when processed by the citric acid cycle. Total ATP yield is 22.5.

15. Because a molecule of succinyl CoA is used to form acetoacetyl CoA. Succinyl CoA could be used to generate one molecule of ATP, and so someone could argue that the yield is 21.5.

16. For fats to be combusted, not only must they be converted into acetyl CoA, but the acetyl CoA must be processed by the citric acid cycle. In order for acetyl CoA to enter the citric acid cycle, there must be a supply of oxaloacetate. Oxaloacetate can be formed by the metabolism of glucose to pyruvate and the subsequent carboxylation of pyruvate to form oxaloacetate.

17. (a)

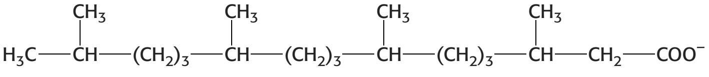

$$H_3C{-}\overset{CH_3}{CH}{-}(CH_2)_3{-}\overset{CH_3}{CH}{-}(CH_2)_3{-}\overset{CH_3}{CH}{-}(CH_2)_3{-}\overset{CH_3}{CH}{-}CH_2{-}COO^-$$

Phytanic acid

The problem with phytanic acid is that, as it undergoes β oxidation, we encounter the dreaded pentavalent carbon atom. Because the pentavalent carbon atom doesn't exist, β oxidation cannot take place and phytanic acid accumulates.

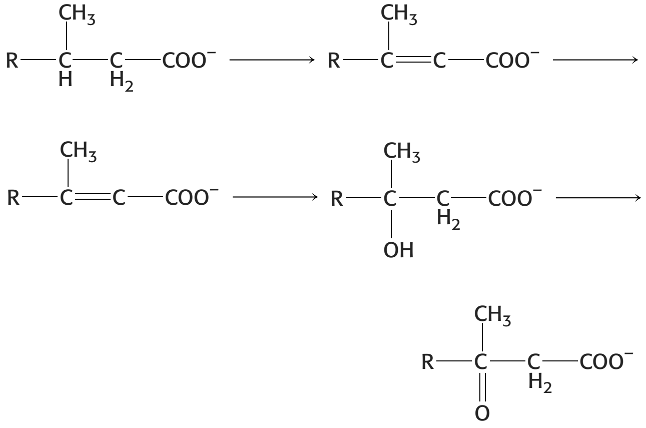

The dreaded pentavalent carbon atom

(b) Removing methyl groups, though theoretically possible, would be time consuming and lacking in elegance. What would we do with the methyl groups? Our livers solve the problem by inventing α oxidation.

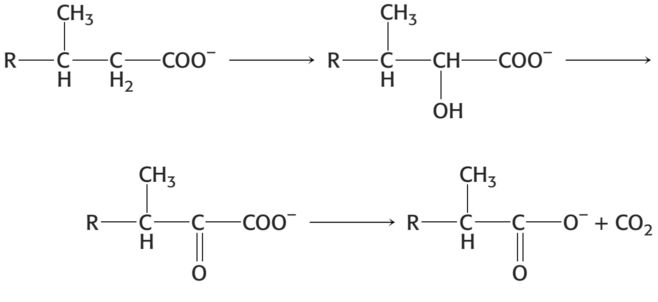

One round of α oxidation rather than β oxidation converts phytanic acid into a β-oxidation substrate.

18. The first oxidation removes two tritium atoms. The hydration adds nonradioactive H and OH. The second oxidation removes another tritium atom from the β-carbon atom. Thiolysis removes an acetyl CoA with only one tritium atom; so the tritium-to-carbon ratio is 1/2. This ratio will be the same for two of the acetates. The last one, however, does not undergo oxidation, and so all tritium remains. The ratio for this acetate is 3/2. The ratio for the entire molecule is then 5/6.

19. In the absence of insulin, lipid mobilization will take place to an extent that it overwhelms the ability of the liver to convert the lipids into ketone bodies.

20. (a) 10; (b) 1; (c) 5; (d) 8; (e) 3; (f) 9; (g) 6; (h) 7; (i) 4; (j) 2.

21. (a) Oxidation in mitochondria; synthesis in the cytoplasm.
(b) Coenzyme A in oxidation; acyl carrier protein for synthesis.
(c) FAD and NAD^+ in oxidation; NADPH for synthesis.
(d) The L isomer of 3-hydroxyacyl CoA in oxidation; the D isomer in synthesis.
(e) From carboxyl to methyl in oxidation; from methyl to carboxyl in synthesis.
(f) The enzymes of fatty acid synthesis, but not those of oxidation, are organized in a multienzyme complex.

22. Bicarbonate is required for the synthesis of malonyl CoA from acetyl CoA by acetyl CoA carboxylase.

23. $$\text{7 acetyl CoA} + \text{6 ATP} + \text{12 NADPH} + 12\ H^+ \longrightarrow \text{myristate} + \text{7 CoA} + \text{6 ADP} + 6\ P_i + 12\ NADP^+ + 5H_2O.$$

24. We will need six acetyl CoA units. One acetyl CoA unit will be used directly to become the two carbon atoms farthest from the acid end. The other five units must be converted into malonyl CoA. The synthesis of each malonyl CoA molecule costs a molecule of ATP; so 5 molecules of ATP will be required. Each round of elongation requires 2 molecules of NADPH, 1 molecule to reduce the keto group to an alcohol and 1 molecule to reduce the double bond. As a result, 10 molecules of NADPH will be required. Therefore, 5 molecules of ATP and 10 molecules of NADPH are required to synthesize lauric acid.

25. e, b, d, a, c.

26. Such a mutation would inhibit fatty acid synthesis because the enzyme cleaves cytoplasmic citrate to yield acetyl CoA for fatty acid synthesis.

27. (a) False. Biotin is required for acetyl CoA carboxylase activity.
(b) True.
(c) False. ATP is required to synthesize malonyl CoA.
(d) True.
(e) True.
(f) False. Fatty acid synthase is a dimer.
(g) True.
(h) False. Acetyl CoA carboxylase is stimulated by citrate, which is cleaved to yield its substrate acetyl CoA.

28. Fatty acids with odd numbers of carbon atoms are synthesized starting with propionyl ACP (instead of acetyl ACP), which is formed from propionyl CoA by acetyl transacetylase.

29. All of the labeled carbon atoms will be retained. Because we need 8 acetyl CoA molecules and only 1 carbon atom is labeled in the acetyl group, we will have 8 labeled carbon atoms. The only acetyl CoA used directly will retain 3 tritium atoms. The 7 acetyl CoA molecules used to make malonyl CoA will lose 1 tritium atom on addition of the CO_2 and another one at the dehydration step. Each of the 7 malonyl CoA molecules will retain 1 tritium atom. Therefore, the total retained tritium is 10 atoms. The ratio of tritium to carbon is 1.25.

30. With a diet rich in raw eggs, avidin will inhibit fatty acid synthesis by reducing the amount of biotin required by acetyl CoA carboxylase. Cooking the eggs will denature avidin, and so it will no longer bind biotin.

31. The only acetyl CoA used directly, not in the form of malonyl CoA, provides the two carbon atoms at the ω end of the fatty acid chain. Because palmitic acid is a C_{16} fatty acid, acetyl CoA will have provided carbons 15 and 16.

32. HCO_3^- is attached to acetyl CoA to form malonyl CoA. When malonyl CoA condenses with acetyl CoA to form the four-carbon ketoacyl CoA, the HCO_3^- is lost as CO_2.

33. Phosphofructokinase controls the flux down the glycolytic pathway. Glycolysis functions to generate ATP or building blocks for biosynthesis, depending on the tissue. The presence of citrate in the cytoplasm indicates that those needs are met, and there is no need to metabolize glucose.

34. C-1 is more radioactive.

35. The mutant enzyme will be persistently active because it cannot be inhibited by phosphorylation. Fatty acid synthesis will be abnormally active. Such a mutation might lead to obesity.

36. (a) Palmitoleate; (b) linoleate; (c) linoleate; (d) oleate; (e) oleate; (f) linolenate.

37. Decarboxylation drives the condensation of malonyl ACP and acetyl ACP. In contrast, the condensation of two molecules of acetyl ACP is energetically unfavorable. In gluconeogenesis, decarboxylation drives the formation of phosphoenolpyruvate from oxaloacetate.

38. Fat mobilization in adipocytes is activated by phosphorylation. Hence, overproduction of the cAMP-activated kinase will lead to an accelerated breakdown of triacylglycerols and a depletion of fat stores.

39. Carnitine translocase deficiency and glucose 6-phosphate transporter deficiency.

40. In the fifth round of β oxidation, *cis*-Δ^2-enoyl CoA is formed. Dehydration by the classic hydratase yields D-3-hydroxyacyl CoA, the wrong isomer for the next enzyme in β oxidation. This dead end is circumvented by a second hydratase that removes water to give *trans*-Δ^2-enoyl CoA. The addition of water by the classic hydratase then yields L-3-hydroxyacyl CoA, the appropriate isomer. Thus, hydratases of opposite stereospecificities serve to epimerize (invert the configuration of) the 3-hydroxyl group of the acyl CoA intermediate.

41. An advantage of this arrangement is that the synthetic activity of different enzymes is coordinated. In addition, intermediates can be efficiently handed from one active site to another without leaving the assembly. Furthermore, a complex of covalently joined enzymes is more stable than one formed by noncovalent attractions. Each of the component enzymes is recognizably homologous to its bacterial counterpart.

42. The probability of synthesizing an error-free polypeptide chain decreases as the length of the chain increases. A single mistake can make the entire polypeptide ineffective. In contrast, a defective subunit can be spurned in the formation of a noncovalent multienzyme complex; the good subunits are not wasted.

43. The absence of ketone bodies is due to the fact that the liver, the source of ketone bodies in the blood, cannot oxidize fatty acids to produce acetyl CoA. Moreover, because of the impaired fatty acid oxidation, the liver becomes more dependent on glucose as an energy source. This dependency results in a decrease in gluconeogenesis and a drop in blood-glucose levels, which is exacerbated by the lack of fatty acid oxidation in muscle and a subsequent increase in glucose uptake from the blood.

44. Peroxisomes enhance the degradation of very long chain fatty acids. Consequently, increasing the activity of peroxisomes could help to lower levels of blood triglycerides. In fact, clofibrate is rarely used because of serious side effects.

45. Citrate works by facilitating, in cooperation with the protein MIG12, the formation of active filaments from inactive monomers. In essence, it increases the number of active sites available, or the concentration of enzyme. Consequently, its effect is visible as an increase in the value of $V_{\max}$. Allosteric enzymes that alter their $V_{\max}$ values in response to regulators are sometimes called V-class enzymes. The more common type of allosteric enzyme, in which K_m is altered, comprises K-class enzymes. Palmitoyl CoA causes depolymerization and thus inactivation.

46. The thiolate anion of CoA attacks the 3-keto group to form a tetrahedral intermediate. This intermediate collapses to form acyl CoA and the enolate anion of acetyl CoA. Protonation of the enolate yields acetyl CoA.

47.

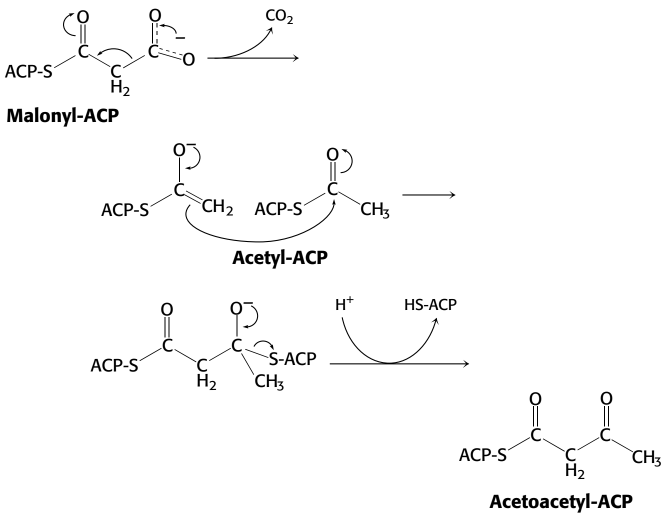

48. (a) Fats burn in the flame of carbohydrates. Without carbohydrates, there would be no anapleurotic reactions to replenish the components of the citric acid cycle. With a diet of fats only, the acetyl CoA from fatty acid degradation would build up.
(b) Acetone from ketone bodies.
(c) Yes. Odd-chain fatty acids would lead to the production of propionyl CoA, which can be converted into succinyl CoA, a citric acid cycle component. It would serve to replenish the citric acid cycle, allow glucose synthesis and mitigate the halitosis.

49. A labeled fat can enter the citric acid cycle as acetyl CoA and yield labeled oxaloacetate, but only after two carbon atoms have been lost as CO_2. Consequently, even though oxaloacetate may be labeled, there can be no net synthesis of oxaloacetate and hence no net synthesis of glucose or glycogen.

50. (a) Glucose is the primary fuel used by the brain. Lack of pyruvate dehydrogenase would prevent complete oxidation of glucose-derived pyruvate by cellular respiration. (b) Because ATP cannot be generated aerobically, glucose would be metabolized to lactate to obtain some ATP. (c) Such a diet would generate ketone bodies for use as fuel by the brain.

51. I-cell disease (Section 11.3) results when lysosomal enzymes are secreted instead of imported into the lysosome.

52. (a) The V_{max} is decreased and the K_m is increased. V_{max} (wild type) = 13 nmol minute^{-1} mg^{-1}; K_m (wild type) = 45 μM; V_{max} (mutant) = 8.3 nmol minute^{-1} mg^{-1}; K_m (mutant) = 74 μM.
(b) Both the V_{max} and the K_m are decreased. V_{max} (wild type) = 41 nmol minute^{-1} mg^{-1}; K_m (wild type) = 104 μM; V_{max} (mutant) = 23 nmol minute^{-1} mg^{-1}; K_m (mutant) = 69 μM.
(c) The wild type is significantly more sensitive to malonyl CoA.
(d) With respect to carnitine, the mutant displays approximately 65% of the activity of the wild type; with respect to palmitoyl CoA, approximately 50% activity. On the other hand, 10 μM of malonyl CoA inhibits approximately 80% of the wild type but has essentially no effect on the mutant enzyme.
(e) The glutamate appears to play a more prominent role in regulation by malonyl CoA than in catalysis.

53. (a) Leucine is changed to alanine.
(b) No change relative to control.
(c) Tyrosine to alanine.
(d) Greatly reduced lipase binding compared to the control.
(e) Lipase activity was diminished.
(f) This suggests that they are separate. The L16A mutation allows binding of the lipase but apparently does not allow activation of the lipase.
(g) This mutation decreased both binding and activity, suggesting that the tyrosine is involved in both aspects of colipase activity.

54. (a) Soraphen A inhibits fatty acid synthesis in a dose-dependent manner.
(b) Fatty acid oxidation is increased in the presence of soraphen A.
(c) Recall that acetyl CoA carboxylase 2 synthesizes malonyl CoA to inhibit the transport of fatty acids into the mitochondria, thereby preventing fatty acid oxidation. Soraphen A apparently inhibits both forms of the carboxylase.
(d) Phospholipid synthesis was inhibited in a dose-dependent manner.
(e) Phospholipids are required for membrane synthesis.
(f) Soraphen A inhibits cell proliferation, especially at higher concentrations.

Chapter 23

1. When the proteins are denatured, all of the peptide bonds are accessible to proteolytic enzymes. If the three-dimensional structure of a protein is maintained, access to many peptide bonds is denied to the proteolytic enzymes.

2. First, the ubiquitin-activating enzyme (E1) links ubiquitin to a sulfhydryl group on E1 itself. Next, the ubiquitin is transferred to a cysteine residue on the ubiquitin-conjugating enzyme (E2) by E2. The ubiquitin–protein ligase (E3), using the ubiquitinated E2 as a substrate, transfers the ubiquitin to the target protein.

3. (a) 7; (b) 4; (c) 2; (d) 10; (e) 5; (f) 3; (g) 9; (h) 1; (i) 6; (j) 8.

4. (a) The ATPase activity of the 26S proteasome resides in the 19S subunit. The energy of ATP hydrolysis is used to unfold the substrate, which is too large to enter the catalytic barrel. ATP may also be required for translocation of the substrate into the barrel.
(b) Substantiates the answer in part *a*. Because they are small, the peptides do not need to be unfolded. Moreover, small peptides could probably enter all at once and not require translocation.

5. (a) Pyruvate; (b) oxaloacetate; (c) α-ketoglutarate; (d) α-ketoisocaproate; (e) phenylpyruvate; (f) hydroxyphenylpyruvate.

6. (a) Aspartate + α-ketoglutarate + GTP + ATP + 2 H_2O + NADH + H^+ → ½ glucose + glutamate + CO_2 + ADP + GDP + NAD^+ + 2 P_i.
The required coenzymes are pyridoxal phosphate in the transamination reaction and NAD^+/NADH in the redox reactions.
(b) Aspartate + CO_2 + NH_4^+ + 3 ATP + NAD^+ + 4 H_2O → oxaloacetate + urea + 2 ADP + 4 P_i + AMP + NADH + H^+.

7. In the eukaryotic proteasome, the distinct β subunits have different substrate specificities, allowing proteins to be more thoroughly degraded.

8. The six subunits probably exist as a heterohexamer. Cross-linking experiments could test the model and help determine which subunits are adjacent to one another.

9. Thiamine pyrophosphate.

10. Aminotransferases transfer the α-amino group to α-ketoglutarate to form glutamate. Glutamate is oxidatively deaminated to form an ammonium ion.

11. Aspartate (oxaloacetate), glutamate (α-ketoglutarate), alanine (pyruvate).

12. Serine and threonine.

13. They are either fuels for the citric acid cycle, components of the citric acid cycle, or molecules that can be converted into a fuel for the citric acid cycle in one step.

14. It acts as an electron sink.
15. Carbamoyl phosphate and aspartate.
16. (a) 4; (b) 5; (c) 1; (d) 6; (e) 7; (f) 3; (g) 2.
17. A, arginine; B, citrulline; C, ornithine; D, arginosuccinate. The order of appearance: C, B, D, A.
18. $$CO_2 + NH_4^+ + 3\,ATP + NAD^+ + \text{aspartate} + 3\,H_2O \longrightarrow \text{urea} + 2\,ADP + 2\,P_i + AMP + PP_i + NADH + H^+ + \text{oxaloacetate}.$$

Four high-transfer-potential phosphoryl groups are spent. Note, however, that an NADH is generated if fumarate is converted into oxaloacetate. NADH can generate 2.5 ATP in the electron-transport chain. Taking these ATP into account, only 1.5 high-transfer-potential phosphoryl groups are spent.
19. The synthesis of fumarate by the urea cycle is important because it links the urea cycle and the citric acid cycle. Fumarate is hydrated to malate, which, in turn, is oxidized to oxaloacetate. Oxaloacetate has several possible fates: (1) transamination to aspartate, (2) conversion into glucose by the gluconeogenic pathway, (3) condensation with acetyl CoA to form citrate, or (4) conversion into pyruvate. You can collect.
20. Ornithine transcarbamoylase (Compound A is analogous to PALA; Chapter 10).
21. Ammonia could lead to the amination of α-ketoglutarate, producing a high concentration of glutamate in an unregulated fashion. α-Ketoglutarate for glutamate synthesis could be removed from the citric acid cycle, thereby diminishing the cell's respiration capacity.
22. The mass spectrometric analysis strongly suggests that three enzymes—pyruvate dehydrogenase, α-ketoglutarate dehydrogenase, and the branched-chain α-ketoacid dehydrogenase—are deficient. Most likely, the common E_3 component of these enzymes is missing or defective. This proposal could be tested by purifying these three enzymes and assaying their ability to catalyze the regeneration of lipoamide.
23. Benzoate, phenylacetate, and arginine would be given to supplement a protein-restricted diet. Nitrogen would emerge in hippurate, phenylacetylglutamine, and citrulline.
24. The liver is the primary tissue for capturing nitrogen as urea. If the liver is damaged (for instance, by hepatitis or the excessive consumption of alcohol), free ammonia is released into the blood.
25. This defect can be partly bypassed by providing a surplus of arginine in the diet and restricting the total protein intake. In the liver, arginine is split into urea and ornithine, which then reacts with carbamoyl phosphate to form citrulline. This urea-cycle intermediate condenses with aspartate to yield argininosuccinate, which is then excreted. Note that two nitrogen atoms—one from carbamoyl phosphate and the other from aspartate—are eliminated from the body per molecule of arginine provided in the diet. In essence, argininosuccinate substitutes for urea in carrying nitrogen out of the body. The formation of argininosuccinate removes the nitrogen, and the restriction on protein intake relieves the aciduria.
26. Aspartame, a dipeptide ester (L-aspartyl- L-phenylalanine methyl ester), is hydrolyzed to L-aspartate and L-phenylalanine. High levels of phenylalanine are harmful in phenylketonurics.
27. *N*-Acetylglutamate is synthesized from acetyl CoA and glutamate. Once again, acetyl CoA serves as an activated acetyl donor. This reaction is catalyzed by *N*-acetylglutamate synthase.
28. Not all proteins are created equal: some are more important than others. Some proteins would be degraded to provide the missing amino acid. The nitrogen from the other amino acids would be excreted as urea. Consequently, more nitrogen would be excreted than ingested.
29. The carbon skeletons of ketogenic amino acids can be converted into ketone bodies or fatty acids. Only leucine and lysine are purely ketogenic. Glucogenic amino acids are those whose carbon skeletons can be converted into glucose.
30. As shown in Figure 23.28, alanine, a gluconeogenic amino acid, is released during the metabolism of tryptophan to acetyl CoA and acetoacetyl CoA.
31. The branched-chain amino acids leucine, isoleucine, and valine. The required enzyme is the branched-chain α-ketoacid dehydrogenase complex.
32. Pyruvate (glycolysis and gluconeogenesis), acetyl CoA (citric acid cycle and fatty acid synthesis), acetoacetyl CoA (ketone-body formation), α-ketoglutarate (citric acid cycle), succinyl CoA (citric acid cycle), fumarate (citric acid cycle), and oxaloacetate (citric acid cycle and gluconeogenesis).

33.

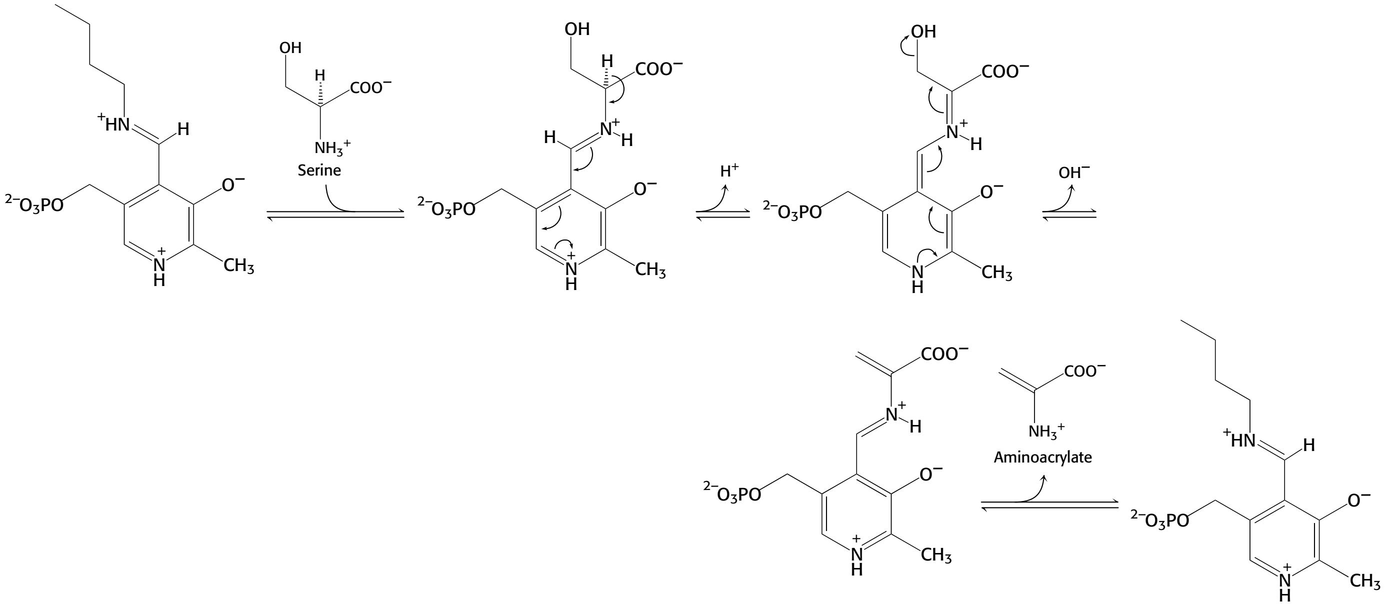

34.

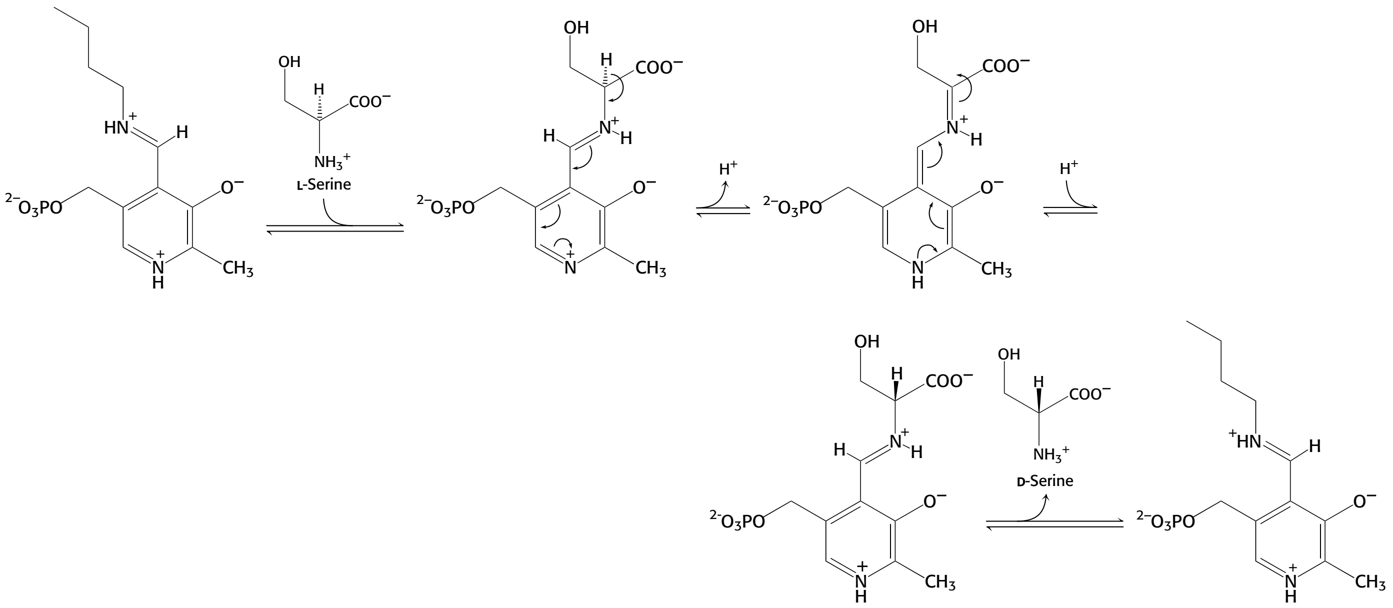

The equilibrium constant for the interconversion of L-serine and D-serine is exactly 1.

35. Double-displacement. A substituted enzyme intermediate is formed.

36. Exposure of such a domain suggests that a component of a multiprotein complex has failed to form properly or that one component has been synthesized in excess. This exposure leads to rapid degradation and the restoration of appropriate stoichiometries.

37. (a) Depletion of glycogen stores. When they are gone, proteins must be degraded to meet the glucose needs of the brain. The resulting amino acids are deaminated, and the nitrogen atoms are excreted as urea.
(b) The brain has adapted to the use of ketone bodies, which are derived from fatty acid catabolism. In other words, the brain is being powered by fatty acid breakdown.
(c) When the glycogen and lipid stores are gone, the only available energy source is protein.

38. The precise cause of all of the symptoms is not firmly established, but a likely explanation depends on the centrality of oxaloacetate to metabolism. A lack of pyruvate carboxylase would reduce the amount of oxaloacetate. The lack of oxaloacetate would reduce the activity of the citric acid cycle and so ATP would be generated by lactic acid formation. If the concentration of oxaloacetate is low, aspartate cannot be formed and the urea cycle would be compromised. Oxaloacetate is also required to form citrate, which transports acetyl CoA to the cytoplasm for fatty acid synthesis. Finally, oxaloacetate is required for gluconeogenesis.

39. Deamination to α-keto-β-methylvalerate; oxidative decarboxylation to α-methylbutyryl CoA; oxidation to tiglyl CoA; hydration, oxidation, and thiolysis yield acetyl CoA and propionyl CoA; propionyl CoA to succinyl CoA.

40. Glycogen phosphorylase. The coenzyme serves as an acid–base catalyst.

41. In the Cori cycle, the carbon atoms are transferred from muscle to liver as lactate. For lactate to be of any use, it must be reduced to pyruvate. This reduction requires high-energy electrons in the form of NADH. When the carbon atoms are transferred as alanine, transamination yields pyruvate directly.

42. (a) Virtually no digestion in the absence of nucleotides.
(b) Protein digestion is greatly stimulated by the presence of ATP.
(c) AMP-PNP, a nonhydrolyzable analog of ATP, is no more effective than ADP.
(d) The proteasome requires neither ATP nor PAN to digest small substrates.
(e) PAN and ATP hydrolysis may be required to unfold the peptide and translocate it into the proteasome.
(f) Although *Thermoplasma* PAN is not as effective with the other proteasomes, it nonetheless results in threefold to fourfold stimulation of digestion.
(g) In light of the fact that the archaea and eukarya diverged several billion years ago, the fact that *Thermoplasma* PAN can stimulate rabbit muscle suggests homology not only between the proteasomes, but also between PAN and the 19S subunit (most likely the ATPases) of the mammalian 26S proteasome.

Chapter 24

1. Nitrogen fixation is the conversion of atmospheric N_2 into NH_4^+. Diazotrophic (nitrogen-fixing) microorganisms are able to fix nitrogen.

2. (a) 4; (b) 8; (c) 10; (d) 6; (e) 7; (f) 9; (g) 3; (h) 5; (i) 2; (j) 1.

3. The reductase provides electrons with high reducing power, whereas the nitrogenase, which requires ATP hydrolysis, uses the electrons to reduce N_2 to NH_3.

4. False. Nitrogen is thermodynamically favored. ATP expenditure by the nitrogenase is required to make the reaction kinetically possible.

5. The bacteria provide the plant with ammonia by reducing atmospheric nitrogen. This reduction is energetically expensive, and the bacteria use ATP from the plant.

6. Oxaloacetate, pyruvate, ribose-5-phosphate, phosphoenolpyruvate, erythrose-4-phosphate, α-ketoglutarate, and 3-phosphoglycerate.

7. Human beings do not have the biochemical pathways to synthesize certain amino acids from simpler precursors. Consequently, these amino acids are "essential" and must be obtained from the diet.

8. Glucose + 2 ADP + 2 P_i + 2 NAD^+ + 2 glutamate ⟶ 2 alanine + 2 α-ketoglutrate + 2 ATP + 2 NADH + 2 H_2O + 2 H^+.

9. $N_2 \longrightarrow NH_4^+ \longrightarrow$ glutamate ⟶ serine ⟶ glycine ⟶ δ-aminolevulinate ⟶ porphobilinogen ⟶ heme.

10. Pyridoxal phosphate (PLP).

11. *S*-Adenosylmethionine, tetrahydrofolate, and methylcobalamin.

12. (a) N^5,N^{10}-Methylenetetrahydrofolate; (b) N^5-methyltetrahydrofolate.

13. γ-Glutamyl phosphate is a likely reaction intermediate.

14. The synthesis of asparagine from aspartate passes through an acyl-adenylate intermediate. One of the products of the reaction will be ^{18}O-labeled AMP.

15. The administration of glycine leads to the formation of isovalerylglycine. This water-soluble conjugate, in contrast with isovaleric acid, is excreted very rapidly by the kidneys.

16. The nitrogen atom shaded red is derived from glutamine. The carbon atom shaded blue is derived from serine.

17. They carry out nitrogen fixation. The absence of photosystem II provides an environment in which O_2 is not produced. Recall that the nitrogenase is very rapidly inactivated by O_2.

18. The cytoplasm is a reducing environment, whereas the extracellular milieu is an oxidizing environment.

19. (a) None; (b) D-glutamate and oxaloacetate.

20. Succinyl CoA is formed in the mitochondrial matrix as part of the citric acid cycle.

21. Alanine from pyruvate; aspartate from oxaloacetate; glutamate from α-ketoglutarate.

22. Lysine cyclodeaminase converts L-lysine into the six-membered ring analog of proline, also referred to as L-homoproline or L-pipecolate:

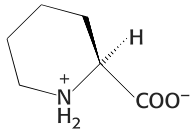

Pipecolate

23. Y could inhibit the C → D step, Z could inhibit the C → F step, and C could inhibit A → B. This scheme is an example of sequential feedback inhibition. Alternatively, Y could inhibit the C → D step, Z could inhibit the C → F step, and the A → B step would be inhibited only in the presence of both Y and Z. This scheme is called concerted feedback inhibition.

24. The rate of the A → B step in the presence of high levels of Y and Z would be 24 s^{-1} (0.6 × 0.4 × 100 s^{-1}).

25. Lysine 258 is absolutely essential for the activity of aspartate aminotransferase, as it is responsible both for the formation of the internal aldimine with the pyridoxal phosphate cofactor and for transferring the proton between the ketimine and quinonoid intermediates. Mutation of this residue to cysteine would be expected to dramatically impair catalysis, as cysteine cannot occupy the same space as lysine and also exhibits differing pK_a properties. Upon treatment with 2-bromoethylamine, however, the resulting thioether now has a shape and pK_a similar to the original lysine side chain. Hence, some catalytic activity is restored.

26. An external aldimine forms with SAM, which is deprotonated to form the quinonoid intermediate. The deprotonated carbon atom attacks the carbon atom adjacent to the sulfur atom to form the cyclopropane ring and release methylthioadenosine, the other product.

27. An external aldimine forms with L-serine, which is deprotonated to form the quinonoid intermediate. This intermediate is reprotonated on its opposite face to form an aldimine with D-serine. This compound is cleaved to release D-serine. The equilibrium constant for a racemization reaction is 1 because the reactant and product are exact mirror images of each other.

28. (a) In the first step, histidine attacks the methylene group from the methionine subgroup of SAM (rather than the usual methyl substituent), resulting in the transfer of an aminocarboxypropyl group. Three subsequent conventional SAM-mediated methylations of the primary amine yield diphthine.

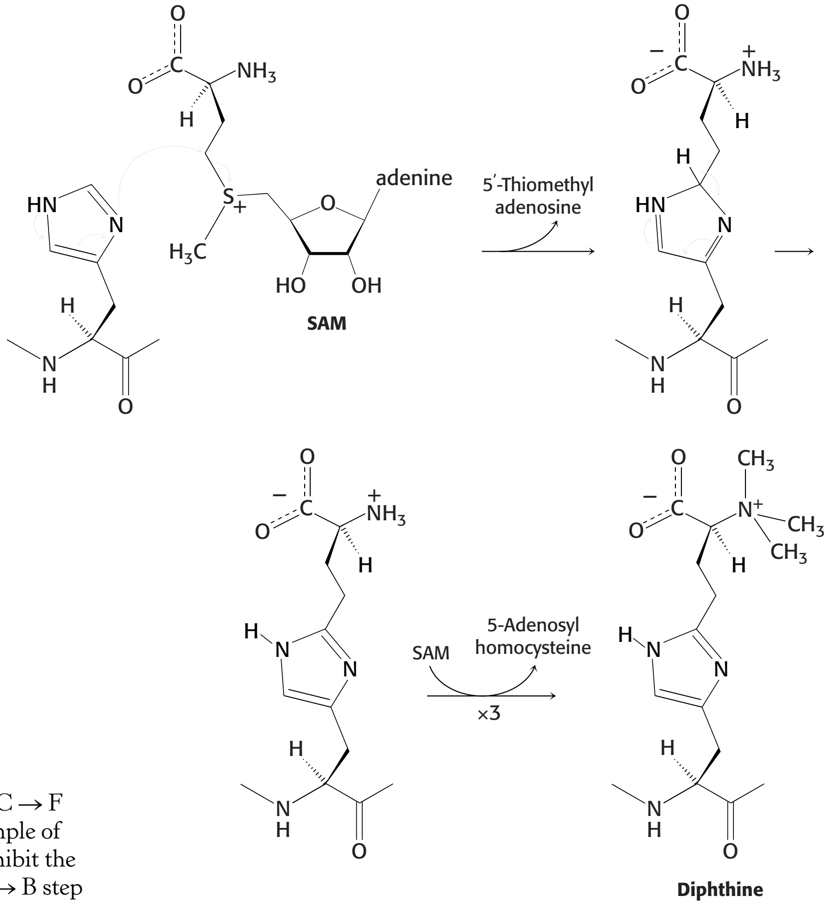

(b) In this chapter, we have observed two examples of an ATP-dependent conversion of a carboxylate into an amide: glutamine synthetase, which uses an acyl-phosphate intermediate, and asparagine synthetase, which uses an acyl-adenylate intermediate. Either mechanism is possible in formation of diphthamide from diphthine.

29. Biotin.

30. Synthesis from oxaloacetate and α-ketoglutarate would deplete the citric acid cycle, which would decrease ATP production. Anapleurotic reactions would be required to replenish the citric acid cycle.

31. SAM is the donor for DNA methylation reactions that protect a host from digestion by its own restriction enzymes. A lack of SAM would render the bacterial DNA susceptible to digestion by the cell's own restriction enzymes.

32. Acetate → acetyl-CoA → citrate → isocitrate → α-ketoglutarate → succinyl-CoA.
33. The value of K_M of glutamate dehydrogenase for NH_4^+ is high (>> 1 mM), and so this enzyme is not saturated when NH_4^+ is limiting. In contrast, glutamine synthetase has very high affinity for NH_4^+. Thus, ATP hydrolysis is required to capture ammonia when it is scarce.
34. (a) Asparagine is much more abundant in the dark. More glutamine is present in the light. These amino acids show the most dramatic effects. Glycine also is more abundant in the light.
(b) Glutamine is a more metabolically reactive amino acid, used in the synthesis of many other compounds. Consequently, when energy is available as light, glutamine will be preferentially synthesized. Asparagine, which carries more nitrogen per carbon atom and is thus a more-efficient means of storing nitrogen when energy is short, is synthesized in the dark. Glycine is more prevalent in the light because of photorespiration.
(c) White asparagus has an especially high concentration of asparagine, which accounts for its intense taste. All asparagus has a large amount of asparagine. In fact, as suggested by its name, asparagine was first isolated from asparagus.

Chapter 25

1. In de novo synthesis, the nucleotides are synthesized from simpler precursor compounds, in essence from scratch. In salvage pathways, preformed bases are recovered and attached to riboses.
2. Carbon 2 and nitrogen 3 come from carbamoyl phosphate. Nitrogen 1 and carbons 4, 5, and 6 are derived from aspartate.
3. Nitrogen 1: aspartate; carbon 2: N^{10}-formyltetrahydrofolate; nitrogen 3: glutamine; carbons 4 and 5 and nitrogen 7: glycine; carbon 6: CO_2; carbon 8: N^{10}-formyltetrahydrofolate; nitrogen 9: glutamine.
4. Energy currency: ATP; signal transduction: ATP and GTP; RNA synthesis: ATP, GTP, CTP, and UTP; DNA synthesis: dATP, dCTP, dGTP, and TTP; components of coenzymes: ATP in CoA, FAD, and $NAD(P)^+$; carbohydrate synthesis: UDP-glucose. These are just some of the uses.
5. A nucleoside is a base attached to ribose. A nucleotide is a nucleoside with the ribose bearing one or more phosphates.
6. (a) 9; (b) 7; (c) 6; (d) 10; (e) 2; (f) 4; (g) 1; (h) 11; (i) 8; (j) 3; (k) 5.
7. Substrate channeling is the process whereby the product of one active site moves to become a substrate at another active site without ever leaving the enzyme. A channel connects the active sites. Substrate channeling greatly enhances enzyme efficiency and minimizes the diffusion of a substrate to an active site.
8. $\text{Glucose} + 2\,\text{ATP} + 2\,\text{NADP}^+ + \text{H}_2\text{O} \longrightarrow \text{PRPP} + \text{CO}_2 + \text{ADP} + \text{AMP} + 2\,\text{NADPH} + 3\,\text{H}^+$.
9. $\text{Glutamine} + \text{aspartate} + \text{CO}_2 + 2\,\text{ATP} + \text{NAD}^+ \longrightarrow \text{orotate} + 2\,\text{ADP} + 2\,\text{P}_i + \text{glutamate} + \text{NADH} + \text{H}^+$.
10. (a, c, and d) PRPP; (b) carbamoyl phosphate.
11. PRPP and formylglycinamide ribonucleotide
12. $\text{dUMP} + \text{serine} + \text{NADPH} + \text{H}^+ \longrightarrow \text{TMP} + \text{NADP}^+ + \text{glycine}$.
13. There is a deficiency of N^{10}-formyltetrahydrofolate. Sulfanilamide inhibits the synthesis of folate by acting as an analog of *p*-aminobenzoate, one of the precursors of folate.
14. (a) Cell A cannot grow in a HAT medium, because it cannot synthesize TMP either from thymidine or from dUMP. Cell B cannot grow in this medium, because it cannot synthesize purines by either the de novo pathway or the salvage pathway. Cell C can grow in a HAT medium because it contains active thymidine kinase from cell B (enabling it to phosphorylate thymidine to TMP) and hypoxanthine guanine phosphoribosyltransferase from cell A (enabling it to synthesize purines from hypoxanthine by the salvage pathway).
(b) Transform cell A with a plasmid containing foreign genes of interest and a functional thymidine kinase gene. The only cells that will grow in a HAT medium are those that have acquired a thymidylate kinase gene; nearly all of these transformed cells will also contain the other genes on the plasmid.
15. The folate derivative N^5, N^{10}-methylenetetrahydrofolate is required by thymidylate synthase to add a methyl group to dUMP, forming TMP. Insufficient folate could result in spina bifida.
16. The reciprocal substrate relation refers to the fact that AMP synthesis requires GTP, whereas GMP synthesis requires ATP. These requirements tend to balance the synthesis of ATP and GTP.
17. Ring carbon 6 in cytosine will be labeled. In guanine, only carbon 5 will be labeled with ^{13}C.
18. UTP is first converted into UDP. Ribonucleotide reductase generates dUDP. DeoxyUDP is converted to dUMP. Thymidylate synthase generates TMP from dUMP. Monophosphate and diphosphate kinases subsequently form TTP.
19. These patients have a high level of urate because of the breakdown of nucleic acids. Allopurinol prevents the formation of kidney stones and blocks other deleterious consequences of hyperuricemia by preventing the formation of urate.
20. The free energies of binding are −57.7 (wild type), −49.8 (Asn 27), and −38.1 (Ser 27) kJ mol^{-1} (−13.8, −11.9, and −9.1 kcal mol^{-1}, respectively). The loss in binding energy is +7.9 kJ mol^{-1} (+1.9 kcal mol^{-1}) and +19.7 kJ mol^{-1} (+4.7 kcal mol^{-1}).
21. By their nature, cancer cells divide rapidly and thus require frequent DNA synthesis. Inhibitors of TMP synthesis will impair DNA synthesis and cancer growth.
22. Uridine and cytidine are administered to by-pass the defective enzyme in orotic aciduria.
23. Inosine or hypoxanthine could be administered.
24. N-1 in both cases, and the amine group linked to C-6 in ATP.
25. Nitrogen atoms 3 and 9 in the purine ring
26. Allopurinol, an analog of hypoxanthine, is a suicide inhibitor of xanthine oxidase.
27. An oxygen atom is added to allopurinol to form alloxanthine.

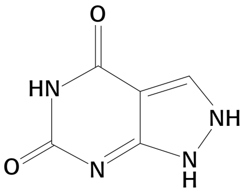

Alloxanthine

28.

The synthesis of carbamoyl phosphate requires 2 ATP	2 ATP
The formation of PRPP from ribose 5-phosphate yields an AMP*	2 ATP
The conversion of UMP to UTP requires 2 ATP	2 ATP
The conversion of UTP to CTP requires 1 ATP	1 ATP
Total	7 ATP

*Remember that AMP is the equivalent of 2 ATP because an ATP must be expended to generate ADP, the substrate for ATP synthesis.

29. (a) Carboxyaminoimidazole ribonucleotide; (b) glycinamide ribonucleotide; (c) phosphoribosyl amine; (d) formylglycinamide ribonucleotide.

30. The first reaction proceeds by phosphorylation of glycine to form an acyl phosphate followed by nucleophilic attack by the amine of phosphoribosylamine to displace orthophosphate. The second reaction consists of adenylation of the carbonyl group of xanthylate followed by nucleophilic attack by ammonia to displace AMP.

31. The $-NH_2$ group attacks the carbonyl carbon atom to form a tetrahedral intermediate. Removal of a proton leads to the elimination of water to form inosinate.

32. The enzyme that uses ammonia, carbamoyl phosphate synthetase I, forms carbamoyl phosphate for a reaction with ornithine, the first step of the urea cycle. The enzyme that uses glutamine, carbamoyl phosphate synthetase II, generates carbamoyl phosphate for use in the first step of pyrimidine biosynthesis.

33. PRPP is the activated intermediate in the synthesis of phosphoribosylamine in the de novo pathway of purine formation; of purine nucleotides from free bases by the salvage pathway; of orotidylate in the formation of pyrimidines; of nicotinate ribonucleotide; of phosphoribosyl ATP in the pathway leading to histidine; and of phosphoribosylanthranilate in the pathway leading to tryptophan.

34. (a) cAMP; (b) ATP; (c) UDP-glucose; (d) acetyl CoA; (e) NAD^+, FAD; (f) dideoxynucleotides; (g) fluorouracil; (h) CTP inhibits ATCase.

35. In vitamin B_{12} deficiency, methyltetrahydrofolate cannot donate its methyl group to homocysteine to regenerate methionine. Because the synthesis of methyltetrahydrofolate is irreversible, the cell's tetrahydrofolate will ultimately be converted into this form. No formyl or methylene tetrahydrofolate will be left for nucleotide synthesis. Vitamin B_{12} is also required to metabolize propionyl CoA generated in the oxidation of odd-chain fatty acids and in the degradation of methionine.

36. Because folate is required for nucleotide synthesis, cells that are dividing rapidly would be most readily affected. They would include cells of the intestine, which are constantly replaced, and precursors to blood cells. A lack of intestinal cells and blood cells would account for the symptoms often observed.

37. In patients with glucose 6-phosphatase deficiency, the cytoplasmic level of ATP in the liver falls as a result of increased glycogenolysis. In all three conditions, AMP rises above normal, and the excess AMP is degraded to urate.

38. Succinate → malate → oxaloacetate by the citric acid cycle. Oxaloacetate → aspartate by transamination, followed by pyrimidine synthesis. Carbons 4, 5, and 6 are labeled.

39. Glucose will most likely be converted into two molecules of pyruvate, one of which will be labeled in the 2 position:

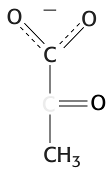

Now consider two common fates of pyruvate—conversion into acetyl CoA and subsequent processing by the citric acid cycle or carboxylation by pyruvate carboxylase to form oxaloacetate. Formation of citrate by condensing the labeled pyruvate with oxaloacetate will yield labeled citrate:

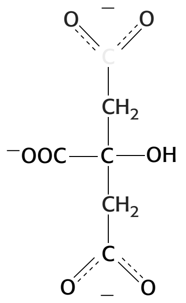

The labeled carbon will be retained through one round of the citric acid cycle but, on the formation of the symmetric succinate, the label will appear in two different positions. Thus, when succinate is metabolized to oxaloacetate, which may be aminated to form aspartate, two carbons will be labeled:

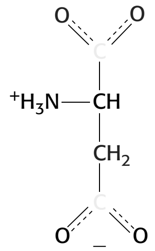

When this aspartate is used to form uracil, the labeled COO^- attached to the α-carbon is lost and the other COO^- becomes incorporated into uracil as carbon 4.

Suppose, instead, that labeled 2-[^{14}C]pyruvate is carboxylated to form oxaloacetate and processed to form aspartate. In this case, the α-carbon of aspartate bears the label.

When this aspartate is used to synthesize uracil, carbon 6 bears the label:

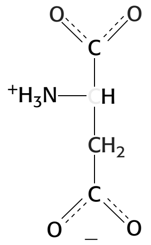

40. HGPRT, which is nonfunctional in Lesch–Nyhan patients, is required to form 6-mercaptopurine ribose monophosphate. Consequently, de novo purine synthesis continues.

41. (a) Some ATP can be salvaged from the ADP that is being generated. (b) There are equal numbers of high-phosphoryl-transfer-potential groups on each side of the equation. (c) Because the adenylate kinase reaction is at equilibrium, the removal of AMP would lead to the formation of more ATP. (d) Essentially, the cycle serves as an anaplerotic reaction for the generation of the citric acid cycle intermediate fumarate.

42. (i) The formation of 5-aminoididazole-4-carboxamide ribonucleotide from 5-aminoimidazole-4-(*N*-succinylcarboxamide) ribonucleotide in the synthesis of IMP. (ii) The formation of AMP from adenylosuccinate. (iii) The formation of arginine from argininosuccinate in the urea cycle.

43. Allopurinol is an inhibitor of xanthine oxidase, which is on the pathway for urate synthesis. In your pet duck, this pathway is the

means by which excess nitrogen is excreted. If xanthine oxidase were inhibited in your duck, nitrogen could not be excreted, with severe consequences such as the formation of a dead duck.

44. (a) The enzyme from the LND 2 patient showed much less activity than the normal enzyme, suggesting that the defect in the enzyme impaired its catalytic ability. The results for LND 1 are puzzling. The enzyme displays activity similar to the enzyme from the normal cell line, and yet the patient was suffering from Lesch–Nyhan disease.

(b) Possible explanations include: there may be an inhibitor in the cells that prevents the enzyme from acting in vivo but is lost during the purification procedure; the enzyme may be degraded more rapidly in vivo than the normal enzyme; the enzyme may be inherently less stable than the normal enzyme.

(c) The enzyme from LND 1 lost activity much faster than the normal enzyme, suggesting that the enzyme was structurally unstable and would lose enzyme activity in the cell, accounting for the appearance of the disease.

Chapter 26

1. Glycerol 3-phosphate is the foundation for both triacylglycerol and phospholipid synthesis. Glycerol 3-phosphate is acylated twice to form phosphatidate. In triacylglycerol synthesis, the phosphoryl group is removed from glycerol 3-phosphate to form diacylglycerol, which is then acylated to form triacylglycerol. In phospholipid synthesis, phosphatidate commonly reacts with CTP to form CDP-diacylglycerol, which then reacts with an alcohol to form a phospholipid. Alternatively, diacylglycerol may react with a CDP-alcohol to form a phospholipid.

2. Glycerol 3-phosphate is formed primarily by the reduction of dihydroxyacetone phosphate, a gluconeogenic intermediate, and to a lesser extent by the phosphorylation of glycerol.

3. Glycerol + 4 ATP + 3 fatty acids + 4 $H_2O \longrightarrow$ triacylglycerol + ADP + 3 AMP + 7 P_i + 4 H^+.

4. Glycerol + 3 ATP + 2 fatty acids + 2 H_2O + CTP + ethanolamine $\longrightarrow$ phosphatidylethanolamine + CMP + ADP + 2 AMP + 6 P_i + 3 H^+.

5. Three. One molecule of ATP to form phosphorylethanolamine and two molecules of ATP to regenerate CTP from CMP.

6. All are synthesized from ceramide. In sphingomyelin, the terminal hydroxyl group of ceramide is modified with phosphorylcholine. In a cerebroside, the hydroxyl group has a glucose or galactose attached. In a ganglioside, oligosaccharide chains are attached to the hydroxyl group.

7. (i) Activate the diacylglycerol as CDP-DAG. (ii) Activate the alcohol as CDP-alcohol. (iii) Use the base-exchange reaction.

8. (a) CDP-diacylglycerol; (b) CDP-ethanolamine; (c) acyl CoA; (d) phosphatidylcholine; (e) UDP-glucose or UDP-galactose; (f) UDP-galactose; (g) geranyl pyrophosphate.

9. Such mutations are seen in mice. The amount of adipose tissue would decrease severely because diacylglycerol could not be formed. Normally, diacylglycerol is acylated to form triacylglycerols. If there were deficient phosphatidic acid phosphatase activity, no triacylglycerols would form.

10. (a) 8; (b) 4; (c) 1; (d) 9; (e) 3; (f) 10; (g) 5; (h) 2; (i) 6; (j) 7.

11. (i) The synthesis of activated isoprene units (isopentyl pyrophosphate), (ii) the condensation of six of the activated isoprene units to form squalene, and (iii) cyclization of the squalene to form cholesterol.

12. The amount of reductase and its activity control the regulation of cholesterol biosynthesis. Transcriptional control is mediated by SREBP. Translation of the reductase mRNA also is controlled. The reductase itself may undergo regulated proteolysis. Finally, the activity of the reductase is inhibited by phosphorylation by AMP kinase when ATP levels are low.

13. (a and b) None, because the label is lost as CO_2.

14. The hallmark of this genetic disease is elevated cholesterol levels in the blood of even young children. The excess cholesterol is taken up by marcrophages, which eventually results in the formation of plaques and heart disease. There are many mutations that cause the disease, but all result in malfunctioning of the LDL receptor.

15. The categories of mutations are: (i) no receptor is synthesized; (ii) receptors are synthesized but do not reach the plasma membrane, because they lack signals for intracellular transport or do not fold properly; (iii) receptors reach the cell surface, but they fail to bind LDL normally because of a defect in the LDL-binding domain; (iv) receptors reach the cell surface and bind LDL, but they fail to cluster in coated pits because of a defect in their carboxyl-terminal regions.

16. "None of your business" and "I don't talk biochemistry until after breakfast" are appropriate but rude and uninformative answers. A better answer might be: "Although it is true that cholesterol is a precursor to steroid hormones, the rest of the statement is oversimplified. Cholesterol is a component of membranes, and membranes literally define cells, and cells make up tissues. But to say that cholesterol 'makes' cells and tissues is wrong."

17. Statins are competitive inhibitors of HMG-CoA reductase. They are used as drugs to inhibit cholesterol synthesis in patients with high levels of cholesterol.

18. No. Cholesterol is essential for membrane function and as a precursor for bile salts and steroid hormones. The complete lack of cholesterol would be lethal.

19. Deamination of cytidine to uridine changes CAA (Gln) into UAA (stop).

20. The LDL contains apolipoprotein B-100, which binds to an LDL receptor on the cell surface in a region known as a coated pit. On binding, the complex is internalized by endocytosis to form an internal vesicle. The vesicle is separated into two components. One, with the receptor, is transported back to the cell surface and fuses with the membrane, allowing continued use of the receptor. The other vesicle fuses with lysosomes inside the cell. The cholesteryl esters are hydrolyzed, and free cholesterol is made available for cellular use. The LDL protein is hydrolyzed to free amino acids.

21. Benign prostatic hypertrophy can be treated by inhibiting 5α-reductase. Finasteride, the 4-azasteroid analog of dihydrotestosterone, competitively inhibits the reductase but does not act on androgen receptors. Patients taking finasteride have a markedly lower plasma level of dihydrotestosterone and a nearly normal level of testosterone. The prostate gland becomes smaller, whereas testosterone-dependent processes such as fertility, libido, and muscle strength appear to be unaffected.

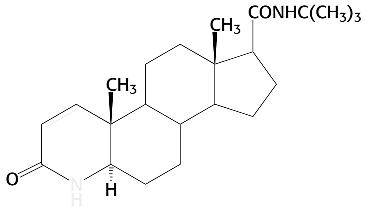

Finasteride

22. Patients who are most sensitive to debrisoquine have a deficiency of a liver P450 enzyme encoded by a member of the *CYP*2 subfamily. This characteristic is inherited as an autosomal recessive

trait. The capacity to degrade other drugs may be impaired in people who hydroxylate debrisoquine at a slow rate, because a single P450 enzyme usually handles a broad range of substrates.

23. Many hydrophobic odorants are deactivated by hydroxylation. Molecular oxygen is activated by a cytochrome P450 monooxygenase. NADPH serves as the reductant. One oxygen atom of O_2 goes into the odorant substrate, whereas the other is reduced to water.

24. Recall that dihydrotestosterone is crucial for the development of male characteristics in the embryo. If a pregnant woman were to be exposed to Propecia, the 5α-reductase of the male embryo would be inhibited, which could result in severe developmental abnormalities.

25. The oxygenation reactions catalyzed by the cytochrome P450 family permit greater flexibility in biosynthesis. Because plants are not mobile, they must rely on physical defenses, such as thorns, and chemical defenses, such as toxic alkaloids. The larger P450 array might permit greater biosynthetic versatility.

26. This knowledge might enable clinicians to characterize the likelihood of a patient's having an adverse drug reaction or being susceptible to chemical-induced illnesses. It might also permit a personalized and especially effective drug-treatment regime for diseases such as cancer.

27. The honeybees may be especially sensitive to environmental toxins, including pesticides, because these chemicals are not readily detoxified, owing to the minimal P450 system.

28. A deficiency of the hydroxylase will cause a build-up of progesterone, which will then be converted into estradiol and testosterone.

29. The core structure of a steroid is four fused rings: three cyclohexane rings and one cyclopentane ring. In vitamin D, the B ring is split by ultraviolet light.

30. The negatively charged phosphoserine residue interacts with the positively charged protonated histidine residue and decreases its ability to transfer a proton to the thiolate.

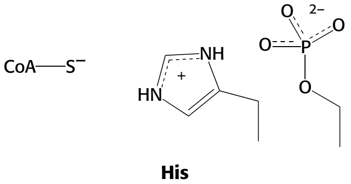

31. The methyl group is first hydroxylated. The hydroxymethylamine eliminates formaldehyde to form methylamine.

32. Note that a cytidine nucleotide plays the same role in the synthesis of these phosphoglycerides as a uridine nucleotide does in the formation of glycogen (Section 21.4). In all of these biosyntheses, an activated intermediate (UDP-glucose, CDP-diacylglycerol, or CDP-alcohol) is formed from a phosphorylated substrate (glucose 1-phosphate, phosphatidate, or a phosphorylalcohol) and a nucleoside triphosphate (UTP or CTP). The activated intermediate then reacts with a hydroxyl group (the terminus of glycogen, the side chain of serine, or a diacylglycerol).

33. The attachment of isoprenoid side chains confers hydrophobic character. Proteins having such a modification are targeted to membranes.

34. 3-Hydroxy-3-methylglutaryl CoA is also a precursor for ketone-body synthesis. If fuel is needed elsewhere in the body, as might be the case during a fast, 3-hydroxy-3-methylglutaryl CoA is converted into the ketone body acetoacetate. If energy needs are met, the liver will synthesize cholesterol. Remember also that cholesterol synthesis occurs in the cytoplasm while ketone bodies are synthesized in the mitochondria.

35. One way in which phosphatidylcholine can be synthesized is by the addition of three methyl groups to phosphatidylethanolamine. The methyl donor is a modified form of methionine, *S*-adenosylmethionine or SAM (Section 24.2).

36. Mutations could occur in the gene encoding the sodium channel that would prevent the action of DDT. Alternatively, P450 enzyme synthesis could be increased to accelerate metabolism of the insecticide to inactive metabolites. In fact, both types of responses to insecticides have been observed.

37. Citrate is transported out of the mitochondria in times of plenty. ATP-citrate lyase yields acetyl CoA and oxaloacetate. The acetyl CoA can then be used to synthesize cholesterol.

38. (a) There is no effect. (b) Because actin is not controlled by cholesterol, the amount isolated should be the same in both experimental groups; a difference would suggest a problem in the RNA isolation. (c) The presence of cholesterol in the diet dramatically reduces the amount of HMG-CoA reductase protein. (d) A common means of regulating the amount of a protein present is to regulate transcription, which is clearly not the case here. (e) The translation of mRNA could be inhibited, and the protein could be rapidly degraded.

39. (a) The activity of the enzyme from the GD patient is the same as that from the control. This suggests that GD is not caused by a mutation that impairs enzyme activity.
(b) There is much less GCase in the GD sample. Because the same number of cells were used in the two samples (confirmed by the identical levels of actin in both samples), we know that the difference in amount of GCase is not due to different quantities of cells. Two possible explanations are that transcription is impaired in the GD sample or that the enzyme in GD is more readily destroyed than the control.
(c) Apparently, the enzyme is being synthesized but then degraded.
(d) The defect in the enzyme from the GD patient seems to result in more rapid degradation of the enzyme by the proteasome. The fact that the amount of GCase present in the control increased upon proteasomal inhibition suggests that GCase may undergo rapid turnover under normal conditions.

Chapter 27

1. Over the 40 years under consideration, our test subject will have consumed

$$\begin{aligned}40 \text{ years} \times 365 \text{ days year}^{-1} \times 8400 \text{ kJ } (2000 \text{ kcal}) \text{ day}^{-1} \\ = 1.2 \times 10^8 \text{ kJ } (2.9 \times 10^7 \text{ kcals}) \text{ in } 40 \text{ years}\end{aligned}$$

Thus, over the 40-year span, our subject has ingested

$$\begin{aligned}1.2 \times 108(2.9 \times 10^7 \text{ kcal})/38 \text{ kJ } (9 \text{ kcal g}^{-1}) \\ = 3.2 \times 10^6 \text{ g} = 3200 \text{ kg of food}\end{aligned}$$

which is equivalent to more than 6 tons of food!

2. 55 pounds = 25 kg = 25,000 g = total weight gain

$$40 \text{ years} \times 365 \text{ days year}^{-1} = 14{,}600 \text{ days}$$
$$25{,}000 \text{ g}/14{,}600 \text{ days} = 1.7 \text{ g day}^{-1}$$

which is equivalent to an extra pat of butter per day. Her BMI is 26.5, and she would be considered overweight but not obese.

3. Adipose tissue is now known to be an active endocrine organ, secreting signal molecules called adipokines.

4. Caloric homeostasis is the condition in which the energy expenditure of an organism is equal to the energy intake.

5. Leptin and insulin.

6. CCK produces a feeling of satiety and stimulates the secretion of digestive enzymes by the pancreas and the secretion of bile salts

by the gall bladder. GLP-1 also produces a feeling of satiety; in addition, it potentiates the glucose-induced secretion of insulin by the β cells of the pancreas.

7. Obviously, something is amiss. Although the answer is not known, the leptin-signaling pathway appears to be inhibited by suppressors of cytokine signaling, the regulatory proteins.

8. 1: a, b; 2: f; 3: c, d, f; 4: c, d; 5: c; 6: f; 7: e; 8: e; 9: e.

9. Phosphorylation of dietary glucose after it enters the liver; gluconeogenesis; glycogen breakdown.

10. Type 1 diabetes is due to autoimmune destruction of the insulin-producing cells of the pancreas. Type 1 diabetes is also called insulin-dependent diabetes because affected people require insulin to survive. Type 2 diabetes is characterized by insulin resistance. Insulin is produced, but the tissues that should respond to insulin, such as muscle, do not.

11. Leptin stimulates processes impaired in diabetes. For instance, leptin stimulates fatty acid oxidation, inhibits triacylglycerol synthesis, and increases the sensitivity of muscle and the liver to insulin.

12. (a) A watt is equal to 1 joule (J) per second (0.239 calorie per second). Hence, 70 W is equivalent to 0.07 kJ s^{-1} (0.017 kcal s^{-1}).
(b) A watt is a current of 1 ampere (A) across a potential of 1 volt (V). For simplicity, let us assume that all the electron flow is from NADH to O_2 (a potential drop of 1.14 V). Hence, the current is 61.4 A, which corresponds to 3.86×10^{20} electrons per second (1 A = 1 coulomb s^{-1} = 6.28×10^{18} charge s^{-1}).
(c) About 2.5 molecules of ATP are formed per molecule of NADH oxidized (two electrons). Hence, 1 molecule of ATP is formed per 0.8 electron transferred. A flow of 3.86×10^{20} electrons per second therefore leads to the generation of 4.83×10^{20} molecules of ATP per second, or 0.80 mmol s^{-1}.
(d) The molecular weight of ATP is 507. The total body content of ATP of 50 g is equal to 0.099 mol. Hence, ATP turns over about once in 125 seconds when the body is at rest.

13. (a) The stoichiometry of the complete oxidation of glucose is

$$C_6H_{12}O_6 + 6\,O_2 \longrightarrow 6\,CO_2 + 6\,H_2O$$

and that of tripalmitoylglycerol is

$$C_{51}H_{98}O_2 + 72.5\,O_2 \longrightarrow 51\,CO_2 + 49\,H_2O$$

Hence, the RQ values are 1.0 and 0.703, respectively.
(b) An RQ value reveals the relative use of carbohydrates and fats as fuels. The RQ of a marathon runner typically decreases from 0.97 to 0.77 in the course of a race. The lowering of the RQ indicates the shift in fuel from carbohydrates to fat.

14. One gram of glucose (molecular weight 180.2) is equal to 5.55 mmol, and one gram of tripalmitoylglycerol (molecular weight 807.3) is equal to 1.24 mmol. The reaction stoichiometries (Problem 13) indicate that 6 mol of H_2O is produced per mole of glucose oxidized, and 49 mol of H_2O is produced per mole of tripalmitoylglycerol oxidized. Hence, the H_2O yields per gram of fuel are 33.3 mmol (0.6 g) for glucose and 60.8 mmol (1.09 g) for tripalmitoylglycerol. Thus, complete oxidation of this fat gives 1.82 times as much water as does glucose. Another advantage of triacylglycerols is that they can be stored in essentially anhydrous form, whereas glucose is stored as glycogen, a highly hydrated polymer. A hump consisting mainly of glycogen would be an intolerable burden—far more than the straw that broke the camel's back.

15. The starved–fed cycle is the nightly hormonal cycle that humans experience during sleep and on eating. The cycle maintains adequate amounts of blood glucose. The starved part—sleep—is characterized by increased glucagon secretion and decreased insulin secretion. After a meal, glucagon concentration falls and insulin concentration rises.

16. Ethanol is oxidized to yield acetaldehyde by alcohol dehydrogenase, which is subsequently oxidized to acetate and acetaldehyde. Ethanol is also metabolized to acetaldehyde by the P450 enzymes, with the subsequent depletion of NADPH.

17. First, fatty liver develops owing to the increased amounts of NADH that inhibit fatty acid oxidation and stimulate fatty acid synthesis. Second, alcoholic hepatitis begins owing to oxidative damage and damage due to excess acetaldehyde that results in cell death. Finally, fibrous tissues form, creating scars that impair blood flow and biochemical function. Ammonia cannot be converted into urea, and its toxicity leads to coma and death.

18. A typical macadamia nut has a mass of about 2 g. Because it consists mainly of fats (~37 kJ g^{-1}, ~9 kcal g^{-1}), a nut has a value of about 75 kJ (18 kcal). The ingestion of 10 nuts results in an intake of about 753 kJ (180 kcal). As stated in the answer to Problem 12, a power consumption of 1 W corresponds to 1 J s^{-1} (0.239 cal s^{-1}), and so 400-W running requires 0.4 kJ s^{-1} (0.0956 kcal s^{-1}). Hence, a person would have to run 1882 s, or about 31 minutes, to spend the calories provided by 10 nuts.

19. A high blood-glucose level triggers the secretion of insulin, which stimulates the synthesis of glycogen and triacylglycerols. A high insulin level would impede the mobilization of fuel reserves during the marathon.

20. A lack of adipose tissue leads to an accumulation of fats in the muscle, with the generation of insulin resistance. The experiment shows that adipokines secreted by the adipose tissue, here leptin, facilitate in some fashion the action of insulin in muscle.

21. Such a mutation would increase the phosphorylation of the insulin receptor and IRS in muscle and would improve insulin sensitivity. Indeed, PTP1B is an attractive therapeutic target for type 2 diabetes.

22. Lipid mobilization can be so rapid that it exceeds the ability of the liver to oxidize the lipids or convert them into ketone bodies. The excess is reesterified and released into the blood as VLDLs.

23. A role of the liver is to provide glucose for other tissues. In the liver, glycolysis is used not for energy production but for biosynthetic purposes. Consequently, in the presence of glucagon, liver glycolysis stops so that the glucose can be released into the blood.

24. The urea cycle and gluconeogenesis.

25. (a) Insulin inhibits lipid utilization.
(b) Insulin stimulates protein synthesis, but there are no amino acids in the children's diet. Moreover, insulin inhibits protein breakdown. Consequently, muscle proteins cannot be broken down and used for the synthesis of essential proteins.
(c) Because proteins cannot be synthesized, blood osmolarity is too low. Consequently, fluid leaves the blood. An especially important protein for maintaining blood osmolarity is albumin.

26. During strenuous exercise, muscle converts glucose into pyruvate through glycolysis. Some of the pyruvate is processed by cellular respiration. However, some of it is converted into lactate and released into the blood. The liver takes up the lactate and converts it into glucose through gluconeogenesis. Muscle may process the carbon skeletons of branched-chain amino acids aerobically. The nitrogens of these amino acids are transferred to pyruvate to form alanine, which is released into the blood and taken up by the liver. After the transamination of the amino group to α-ketoglutarate, the resulting pyruvate is converted into glucose. Finally, muscle glycogen may be mobilized, and the released glucose can be used by muscle.

27. This conversion allows muscle to function anaerobically. NAD^+ is regenerated when pyruvate is reduced to lactate, and so energy can continue to be extracted from glucose during strenuous exercise. The liver converts the lactate into glucose.

28. Fatty acids and glucose, respectively.

29. This practice is called carbo-loading. Depleting the glycogen stores will initially cause the muscles to synthesis a large amount of glycogen when dietary carbohydrates are provided and will lead to the supercompensation of glycogen stores.

30. The oxygen consumption at the end of exercise is used to replenish ATP and creatine phosphate and to oxidize any lactate produced.

31. Oxygen is used in oxidative phosphorylation to resynthesize ATP and creatine phosphate. The liver converts lactate released by the muscle into glucose. Blood must be circulated to return the body temperature to normal, and so the heart cannot return to its resting rate immediately. Hemoglobin must be reoxygenated to replace the oxygen used in exercise. The muscles that power breathing must continue working at the same time as the exercised muscles are returning to resting states. In essence, all the biochemical systems activated in intense exercise need increased oxygen to return to the resting state.

32. Ethanol may replace water that is hydrogen bonded to proteins and membrane surfaces. This alteration of the hydration state of the protein would alter its conformation and hence function. Ethanol may also alter phospholipid packing in membranes. The two effects suggest that integral membrane proteins would be most sensitive to ethanol, as indeed seems to be the case.

33. Cells from the type I fiber would be rich in mitochondria, whereas those of the type II fiber would have few mitochondria.

34. (a) The ATP expended during this race amounts to about 8380 kg, or 18,400 pounds. (b) The cyclist would need about $1,260,000,000 to complete the race.

35. Exercise greatly enhances the ATP needs of muscle cells. To more efficiently meet these needs, more mitochondria are synthesized.

36. AMPK activity increases as ATP is used for muscle contraction. AMPK inactivates acetyl CoA carboxylase. Recall that malonyl CoA, the product of acetyl CoA carboxylase, inhibits transport of fatty acids into the mitochondria. The decrease in muscle malonyl CoA allows fatty acid oxidation in muscle.

37. After the first several days of starvation, most tissues are using fatty acids. Ketone bodies provide much of the brain's energy, decreasing glucose requirement. The low insulin/high glucagon ration stimulates lipolysis and gluconeogenesis. However, gluconeogenesis will not occur because the increase in fatty acid oxidation increases acetyl CoA and NADH. The high concentration of NADH inhibits the TCA cycle as well as gluconeogenesis. The acetyl CoA forms ketone bodies.

38. (a) The increase in all of the ratios is due to the NADH glut caused by the metabolism of alcohol.
(b) The increased amounts of lactate and D-3-hydroxybutyrate are released into the blood, accounting for the acidosis.
(c) Drinking on an empty stomach suggests that glycogen stores are low. Because of the NADH glut, gluconeogenesis cannot occur. Consequently, hypoglycemia results. A well-fed drinker will have glucose in the blood from the meal and thus will not experience hypoglycemia.

39. If glucose is always provided, even in small amounts, the brain will use glucose as a fuel rather than adapting to ketone body use. During the fast, muscle protein will be broken down to meet the brains glucose needs. This protein degradation will lead to organ failure sooner than if the brain had adapted to ketone body utilization.

40. The inability of muscle mitochondria to process all of the fatty acids produced by overnutrition leads to excessive levels of diacylglycerol and ceramide in the muscle cytoplasm. These second-messenger molecules activate enzymes that impair insulin signaling.

41. Both are due to a lack of thiamine (vitamin B_1). Thiamine, which is sometimes called aneurin, is required most notably for the proper functioning of pyruvate dehydrogenase.

42. (a) Red blood cells always produce lactate, and fast-twitch or type II, muscle fibers (Problem 33) also produce a large amount of lactate.
(b) At that point, the athlete is beginning to move into anaerobic exercise, in which most energy is produced by anaerobic glycolysis.
(c) The lactate threshold is essentially the point at which the athlete switches from aerobic exercise, which can be done for extended periods, to anaerobic exercise, essentially sprinting, which can be done for only short periods. The idea is to race at the extreme of his or her aerobic capacity until the finish line is in sight and then to switch to anaerobic.
(d) Training increases the amount of blood vessels and the number of muscle mitochondria. Together, they increase the ability to process glucose aerobically. Consequently, a greater effort can be expended before the switch to anaerobic energy production.

43. Consider the graph of lactate production as a function of effort shown in Problem 42. For an athlete racing at her lactate threshold or just below it, the RQ value will be 1. With the finish line in sight, our runner ups her pace so that she is now also processing glucose to lactic acid in addition to processing glucose aerobically; that is, she begins running above her lactate threshold. The lactic acid released into the blood will ionize

$$\underset{\text{Lactic acid}}{\mathrm{CH_3CH(OH)COOH}} \rightleftharpoons \mathrm{CH_3CH(OH)COO^-}$$

The increase in H^+ will alter the blood buffer system, leading to the formation of carbonic acid

$$\mathrm{H^+ + HCO_3^-} \rightleftharpoons \underset{\text{Carbonic acid}}{\mathrm{H_2CO_3}}$$

The carbonic acid will dissociate into water and carbon dioxide

$$\mathrm{H_2CO_3} \rightleftharpoons \mathrm{CO_2 + H_2O}$$

This carbon dioxide will be superimposed on the carbon dioxide generated by the combustion of glucose aerobically, leading to an RQ greated than 1.

44. The increase in ATP resulting from the processing of glucose in the β cells closes a potassium channel. The closing of the potassium channel alters the voltage across the cell membrane, which leads to an opening of a calcium channel. The influx of calcium causes the insulin-containing secretory granules to fuse with the cell membrane, resulting in the release of insulin.

Chapter 28

1. DNA polymerase I uses deoxyribonucleoside triphosphates; pyrophosphate is the leaving group. DNA ligase uses DNA–adenylate (AMP joined to the 5′-phosphoryl group) as a reaction partner; AMP is the leaving group. Topoisomerase I uses a DNA–tyrosyl intermediate (5′-phosphoryl group linked to the phenolic OH group); the tyrosine residue of the enzyme is the leaving group.

2. Positive supercoiling resists the unwinding of DNA. The melting temperature of DNA increases in proceeding from negatively supercoiled to relaxed to positively supercoiled DNA. Positive supercoiling is probably an adaptation to high temperature.

3. The nucleotides used for DNA synthesis have the triphosphate attached to the 5′-hydroxyl group with free 3′-hydroxyl groups. Such nucleotides can be utilized only for 5′-to-3′ DNA synthesis.

4. DNA replication requires RNA primers. Without appropriate ribonucleotides, such primers cannot be synthesized.
5. This close contact prevents the incorporation of ribonucleotides rather than $2'$-deoxyribonucleotides.
6. (a) 96.2 revolutions per second (1000 nucleotides per second divided by 10.4 nucleotides per turn for B-DNA gives 96.2 rps).
(b) $0.34\ \mu\text{m s}^{-1}$ (1000 nucleotides per second corresponds to $3400\ \text{Å s}^{-1}$ because the axial distance between nucleotides in B-DNA is 3.4 Å).
7. Eventually, the DNA would become so tightly wound that movement of the replication complex would be energetically impossible.
8. Linking number $Lk = Tw + Wr = 48 + 3 = 51$. If $Tw = 50$, then $Wr = 1$.
9. A hallmark of most cancer cells is prolific cell division, which requires DNA replication. If the telomerase were not activated, the chromosomes would shorten until they became nonfunctional, leading to cell death.
10. No.
11. Treat the DNA briefly with endonuclease to occasionally nick each strand. Add the polymerase with the radioactive dNTPs. At the broken bond, or nick, the polymerase will degrade the existing strand with its $5' \rightarrow 3'$ exonuclease activity and replace it with a radioactive complementary copy by using its polymerase activity. This reaction scheme is referred to as "nick translation" because the nick is moved, or translated, along the DNA molecule without ever becoming sealed.
12. If replication were unidirectional, tracks with a low grain density at one end and a high grain density at the other end would be seen. On the other hand, if replication were bidirectional, the middle of a track would have a low density, as shown in the diagram below. For *E. coli,* the grain tracks are denser on both ends than in the middle, indicating that replication is bidirectional.

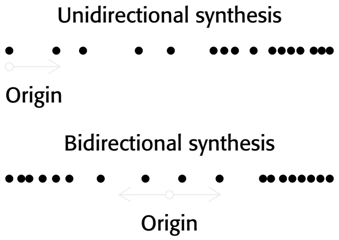

13. Pro (CCC), Ser (UCC), Leu (CUC), and Phe (UUC). Alternatively, the last base of each of these codons could be U.
14. Potentially deleterious side reactions are prevented. The enzyme itself might be damaged by light if it could be activated by light in the absence of bound DNA harboring a pyrimidine dimer.
15. The free DNA ends that appear in the absence of telomeres are repaired by DNA fusion.
16. The free energy of ATP hydrolysis under standard conditions is $-30.5\ \text{kJ mol}^{-1}$ ($-7.3\ \text{kcal mol}^{-1}$). In principle, it could be used to break three base pairs.
17. The oxidation of guanine could lead to DNA repair: DNA strand cleavage could allow looping out of the triplet repeat regions and triplet expansion.
18. The release of DNA topoisomerase II after the enzyme has acted on its DNA substrate requires ATP hydrolysis. Negative supercoiling requires only the binding of ATP, not its hydrolysis.
19. (a) Size; the top is relaxed and the bottom is supercoiled DNA. (b) Topoisomers. (c) The DNA is becoming progressively more unwound, or relaxed, and thus slower moving.
20. (a) It was used to determine the number of spontaneous revertants—that is, the background mutation rate.
(b) To firmly establish that the system was working. A known mutagen's failure to produce revertants would indicate that something was wrong with the experimental system.
(c) The chemical itself has little mutagenic ability but is apparently activated into a mutagen by the liver homogenate.
(d) Cytochrome P450 system.

Chapter 29

1. The sequence of the coding (+, sense) strand is

5′-ATGGGGAACAGCAAGAGTGGGGCCCTGTCCAAGGAG-3′

and the sequence of the template (–, antisense) strand is

3′-TACCCCTTGTCGTTCTCACCCCGGGACAGGTTCCTC-5′

2. An error will affect only one molecule of mRNA of many synthesized from a gene. In addition, the errors do not become a permanent part of the genomic information.
3. At any given instant, only a fraction of the genome (total DNA) is being transcribed. Consequently, speed is not essential.
4. The active sites are related by convergent evolution.
5. Heparin, a glycosaminoglycan, is highly anionic. Its negative charges, like the phosphodiester bridges of DNA templates, allow it to bind to lysine and arginine residues of RNA polymerase.
6. This mutant σ will competitively inhibit the binding of holoenzyme and prevent the specific initiation of RNA chains at promoter sites.
7. The core enzyme without σ binds more tightly to the DNA template than does the holoenzyme. The retention of σ after chain initiation would make the mutant RNA polymerase slower. The mutant enzyme would also be unlikely to bind alternative σ factors.
8. A 100-kDa protein contains about 910 residues, which are encoded by 2730 nucleotides. At a maximal transcription rate of 50 nucleotides per second, the mRNA would be synthesized in 55 s.
9. The RNA polymerase slides along the DNA rapidly rather than simply diffusing through three-dimensional space.
10. The start site is in red:

5′-GCCGTTGACACCGTTCGGCGATCGATCCGCTATAATGTGTGGATCCGCTT-3′

11. Initiation at strong promoters takes place every 2 s. In this interval, 100 nucleotides are transcribed. Hence, centers of transcription bubbles are 34 nm (340 Å) apart.
12. (a) The lowest band on the gel will be that of strand 3 alone (*i*). Band *ii* will be at the same position as band *i* because the RNA is not complementary to the nontemplate strand, whereas band *iii* will be higher because a complex is formed between RNA and the template strand. Band *iv* will be higher than the others because strand 1 is complexed to 2, and strand 2 is complexed to 3. Band *v* is the highest because core polymerase associates with the three strands.
(b) None, because rifampicin acts before the formation of the open complex.
(c) RNA polymerase is processive. When the template is bound, heparin cannot enter the DNA-binding site.
(d) When GTP is absent, synthesis stops when the first cytosine residue downstream of the bubble is encountered in the template strand. In contrast, with all four nucleoside triphosphates present, synthesis will continue to the end of the template.
13. Backtracking must occur prior to cleavage leading to dinucleotide products.
14. The base-pairing energy of the di- and trinucleotide DNA–RNA hybrids formed at the very beginning of transcription is not sufficient to prevent strand separation and loss of product.

15. (a) Because cordycepin lacks a 3′-OH group, it cannot participate in $3' \rightarrow 5'$ bond formation. (b) Because the poly(A) tail is a long stretch of adenosine nucleotides, the likelihood that a molecule of cordycepin would become incorporated is higher than with most RNA. (c) Yes, it must be converted into cordycepin 5′-triphosphate.
16. There are $2^8 = 256$ possible products.
17. The relationship between the −10 and −35 sequences could be affected by torsional strain. Since topoisomerase II introduces negative supercoils in DNA, this prevents this enzyme from overstimulating the expression of its own gene.
18. Ser-Ile-Phe-His-Pro-Stop
19. A mutation that disrupted the normal AAUAAA recognition sequence for the endonuclease could account for this finding. In fact, a change from U to C in this sequence caused this defect in a thalassemic patient. Cleavage occurred at the AAUAAA 900 nucleotides downstream from this mutant AACAAA site.
20. One possibility is that the 3′ end of the poly(U) donor strand cleaves the phosphodiester bond on the 5′ side of the insertion site. The newly formed 3′ terminus of the acceptor strand then cleaves the poly(U) strand on the 5′ side of the nucleotide that initiated the attack. In other words, a uridine residue could be added by two transesterification reactions. This postulated mechanism is similar to the one in RNA splicing.
21. Alternative splicing, RNA editing. Covalent modification of the proteins subsequent to synthesis.
22. Attach an oligo(dT) or oligo(U) sequence to an inert support to create an affinity column. When RNA is passed through the column, only poly(A)-containing RNA will be retained.
23. (a) Different amounts of RNA are present for the various genes.
(b) Although all of the tissues have the same genes, the genes are expressed to different extents in different tissues.
(c) These genes are called housekeeping genes—genes that most tissues express. They might include genes for glycolysis or citric acid cycle enzymes.
(d) The point of the experiment is to determine which genes are initiated in vivo. The initiation inhibitor is added to prevent initiation at start sites that may have been activated during the isolation of the nuclei.
24. DNA is the single strand that forms the trunk of the tree. Strands of increasing length are RNA molecules; the beginning of transcription is where growing chains are the smallest; the end of transcription is where chain growth stops. Direction is left to right. Many enzymes are actively transcribing each gene.

Chapter 30

1. The Oxford English Dictionary defines translation as the action or process of turning from one language into another. Protein synthesis converts nucleic acid sequence information into amino acid sequence information.
2. An error frequency of 1 incorrect amino acid every 10^4 incorporations allows for the rapid and accurate synthesis of proteins as large as 1000 amino acids. Higher error rates would result in too many defective proteins. Lower error rates would likely slow the rate of protein synthesis without a significant gain in accuracy.
3. (i) Each is a single chain. (ii) They contain unusual bases.
(iii) Approximately half of the bases are base-paired to form double helices. (iv) The 5′ end is phosphorylated and is usually pG. (v) The amino acid is attached to the hydroxyl group of the A residue of the CCA sequence at the 3′ end of the tRNA.
(vi) The anticodon is located in a loop near the center of the tRNA sequence. (vii) The molecules are L-shaped.
4. First is the formation of the aminoacyl adenylate, which then reacts with the tRNA to form the aminoacyl-tRNA. Both steps are catalyzed by aminoacyl-tRNA synthetase.
5. Unique features are required so that the aminoacyl-tRNA synthetases can distinguish among the tRNAs and attach the correct amino acid to the proper tRNA. Common features are required because all tRNAs must interact with the same protein-synthesizing machinery.
6. An activated amino acid is one linked to the appropriate tRNA.
7. (a) No; (b) no; (c) yes.
8. The ATP is cleaved to AMP and PP_i. Consequently, a second ATP is required to convert AMP into ADP, the substrate for oxidative phosphorylation.
9. Amino acids larger than the correct amino acid cannot fit into the active site of the tRNA. Smaller but incorrect amino acids that become attached to the tRNA fit into the editing site and are cleaved from the tRNA.
10. Recognition sites on both faces of the tRNAs may be required to uniquely identify the 20 different tRNAs.
11. The first two bases in a codon form Watson–Crick base pairs that are checked for fidelity by bases of the 16S rRNA. The third base is not inspected for accuracy, and so some variation is tolerated.
12. Four bands: light, heavy, a hybrid of light 30S and heavy 50S, and a hybrid of heavy 30S and light 50S.
13. Two hundred molecules of ATP are converted into 200 AMP + 400 P_i to activate the 200 amino acids, which is equivalent to 400 molecules of ATP. One molecule of GTP is required for initiation, and 398 molecules of GTP are needed to form 199 peptide bonds.
14. The reading frame is a set of contiguous, nonoverlapping three-nucleotide codons that begins with a start codon and ends with a stop codon.
15. A mutation caused by the insertion of an extra base can be suppressed by a tRNA that contains a fourth base in its anticodon. For example, UUUC rather than UUU is read as the codon for phenylalanine by a tRNA that contains 3′-AAAG-5′ as its anticodon.
16. One approach is to synthesize a tRNA that is acylated with a reactive amino acid analog. For example, bromoacetyl-phenylalanyl-tRNA is an affinity-labeling reagent for the P site of *E. coli* ribosomes.
17. The sequence GAGGU is complementary to a sequence of five bases at the 3′ end of 16S rRNA and is located several bases upstream of an AUG start codon. Hence, this region is a start signal for protein synthesis. The replacement of G by A would be expected to weaken the interaction of this mRNA with the 16S rRNA and thereby diminish its effectiveness as an initiation signal. In fact, this mutation results in a 10-fold decrease in the rate of synthesis of the protein specified by this mRNA.
18. The peptide would be Phe-Cys-His-Val-Ala-Ala. The codons UGC and UGU encode cysteine but, because the cysteine was modified to alanine, alanine is incorporated in place of cysteine.
19. Proteins are synthesized from the amino to the carboxyl end on ribosomes, whereas they are synthesized in the reverse direction in the solid-phase method. The activated intermediate in ribosomal synthesis is an aminoacyl-tRNA; in the solid-phase method, it is the adduct of the amino acid and dicyclohexylcarbodiimide.
20. GTP is not hydrolyzed until aminoacyl-tRNA is delivered to the A site of the ribosome. An earlier hydrolysis of GTP would be wasteful because EF-Tu–GDP has little affinity for aminoacyl-tRNA.
21. The translation of an mRNA molecule can be blocked by antisense RNA, an RNA molecule with the complementary sequence. The antisense–sense RNA duplex cannot serve as a template for translation; single-stranded mRNA is required. Furthermore, the antisense–sense duplex is degraded by nucleases. Antisense RNA added to the external medium is spontaneously taken up by

many cells. A precise quantity can be delivered by microinjection. Alternatively, a plasmid encoding the antisense RNA can be introduced into target cells.

22. (a) A_5. (b) $A_5 > A_4 > A_3 > A_2$. (c) Synthesis is from the amino terminus to the carboxyl terminus.

23. These enzymes convert nucleic acid information into protein information by interpreting the tRNA and linking it to the proper amino acid.

24. The rate would fall because the elongation step requires that the GTP be hydrolyzed before any further elongation can take place.

25. Protein factors modulate the initiation of protein synthesis. The role of IF1 and IF3 is to prevent premature binding of the 30S and 50S ribosomal subunits, whereas IF2 delivers Met-tRNA$_f$ to the ribosome. Protein factors are also required for elongation (EF-G and EF-Tu), for termination (release factors, RFs), and for ribosome dissociation (ribosome release factors, RRFs).

26. The signal sequence, signal-recognition particle (SRP), the SRP receptor, and the translocon.

27. The formation of peptide bonds, which in turn are powered by the hydrolysis of the aminoacyl-tRNAs.

28. The Shine–Dalgarno sequence of the mRNA base-pairs with a part of the 16S rRNA of the 30S subunit, which positions the subunit so that the initiator AUG is recognized.

29.

	Bacteria	**Eukaryote**
Ribosome size	70S	80S
mRNA	Polycistronic	Not polycistronic
Initiation	Shine–Dalgarno is required	First AUG is used
Protein factors	Required	Many more required
Relation to transcription	Translation can start before transcription is completed	Transcription and translation are spatially separated
First amino acid	fMet	Met

30. The SRP binds to the signal sequence and inhibits further translation. The SRP ushers the inhibited ribosome to the ER, where it interacts with the SRP receptor (SR). The SRP–SR complex binds the translocon and simultaneously hydrolyzes GTP. On GTP hydrolysis, SRP and SR dissociate from each other and from the ribosome. Protein synthesis resumes and the nascent protein is channeled through the translocon.

31. The alternative would be to have a single ribosome translating a single mRNA molecule. The use of polysomes allows more protein synthesis per mRNA molecule in a given period of time and thus the production of more protein.

32. (a) 1, 2, 3, 5, 6, 10; (b) 1, 2, 7, 8; (c) 1, 4, 8, 9.

33. Transfer RNAs have roles in several recognition processes. A tRNA must be recognized by the appropriate aminoacyl-tRNA synthetase, and the tRNA must interact with the ribosome and, in particular, with the peptidyl transferase.

34. The aminoacyl-tRNA can be initially synthesized. However, the side-chain amino group attacks the ester linkage to form a six-membered amide, releasing the tRNA.

35. (a, d, and e) Type 2; (b, c, and f) Type 1.

36. The error rates of DNA, RNA, and protein synthesis are of the order of 10^{-10}, 10^{-5}, and 10^{-4}, respectively, per nucleotide (or amino acid) incorporated. The fidelity of all three processes depends on the precision of base-pairing to the DNA or mRNA template. Few errors are corrected in RNA synthesis. In contrast, the fidelity of DNA synthesis is markedly increased by the $3' \rightarrow 5'$ proofreading nuclease activity and by postreplicative repair. In protein synthesis, the mischarging of some tRNAs is corrected by the hydrolytic action of aminoacyl-tRNA synthetase. Proofreading also takes place when aminoacyl-tRNA occupies the A site on the ribosome; the GTPase activity of EF-Tu sets the pace of this final stage of editing.

37. EF-Ts catalyzes the exchange of GTP for GDP bound to EF-Tu. In G-protein cascades, an activated 7TM receptor catalyzes GTP–GDP exchange in a G protein.

38. The α subunits of G proteins are inhibited by a similar mechanism in cholera and whooping cough (Section 14.5).

39. Glu-tRNA^{Gln} is formed by misacylation. The activated glutamate is subsequently amidated to form Gln-tRNA^{Gln}. Ways in which glutamine is formed from glutamate were discussed in Section 24.2. In regard to *H. pylori,* a specific enzyme, Glu-tRNA^{Gln} amidotransferase, catalyzes the following reaction:

$$\text{Gln} + \text{Glu-tRNA}^{\text{Gln}} + \text{ATP} \longrightarrow \text{Gln-tRNA}^{\text{Gln}} + \text{Glu} + \text{ADP} + \text{P}_i$$

Glu-tRNA^{Glu} is not a substrate for the enzyme; so the transferase must also recognize aspects of the structure of tRNA^{Gln}.

40. The primary structure determines the three-dimensional structure of the protein. Thus, the final phase of information transfer from DNA to RNA to protein synthesis is the folding of the protein into its functional state.

41. (a) eIF-4H has two effects: (1) the extent of unwinding is increased and (2) the rate of unwinding is increased, as indicated by the increased rise in activity at early reaction times.
(b) To firmly establish that the effect of eIF-H4 was not due to any inherent helicase activity.
(c) Half-maximal activity was achieved at 0.11 μM of eIF-4H. Therefore, maximal stimulation would be achieved at a ratio of 1:1.
(d) eIF-4H enhances the rate of unwinding of all helices, but the effect is greater as the helices increase in stability.
(e) The results in graph C suggest that eIF-4H increases the processivity.

42. (a) The three peaks represent, from left to right, the 40S ribosomal subunit, the 60S ribosomal subunit, and the 80S ribosome.
(b) Not only are ribosomal subunits and the 80S ribosome present, but polysomes of various lengths also are apparent. The individual peaks in the polysome region represent polysomes of discrete length.
(c) The treatment significantly inhibited the number of polysomes while increasing the number of free ribosomal subunits. This outcome could be due to inhibited protein-synthesis initiation or inhibited transcription.

Chapter 31

1. (a) Cells will express β-galactosidase, *lac* permease, and thiogalactoside transacetylase even in the absence of lactose. (b) Cells will express β-galactosidase, *lac* permease, and thiogalactoside transacetylase even in the absence of lactose. (c) The levels of catabolic enzymes such as β-galactosidase and arabinose isomerase will remain low even at low levels of glucose.

2. The concentration is $1/(6 \times 10^{23})$ moles per 10^{-15} liter $= 1.7 \times 10^{-9}$ M. Because $K_d = 10^{-13}$ M, the single molecule should be bound to its specific binding site.

3. The number of possible 8-bp sites is $4^8 = 65{,}536$. In a genome of 4.6×10^6 base pairs, the average site should appear $4.6 \times 10^6/65{,}536 = 70$ times. Each 10-bp site should appear 4 times. Each 12-bp site should appear 0.27 times (many 12-bp sites will not appear at all).

4. The *lac* repressor does not bind DNA when the repressor is bound to a small molecule (the inducer), whereas the *pur* repressor binds

DNA only when the repressor is bound to a small molecule (the corepressor). The *E. coli* genome contains only a single *lac* repressor-binding region, whereas it has many sites for the *pur* repressor.

5. Anti-inducers bind to the conformation of repressors, such as the *lac* repressor, that are capable of binding DNA. They occupy a site that overlaps that for the inducer and, therefore, compete for binding to the repressor.

6. The inverted repeat may be a binding site for a dimeric DNA-binding protein or it may correspond to a stem-loop structure in the encoded RNA.

7. Bacteriophage λ would be more likely to enter the lytic phase because the cooperative binding of the λ repressor to O_R2 and O_R1, which supports the lysogenic pathway, would be disrupted.

8. λ repressor gene −10 region GATTTA −35 region TAGATA
Cro gene −10 region TAATGG −35 region TTGACT
There are four differences in the −10 region and three differences in the −35 region.

9. Increased Cro concentration reduces the expression of the λ repressor gene. Increased λ repressor concentration reduces the expression of the Cro gene. At low λ repressor concentrations, increased λ repressor concentration increases the expression of the λ repressor gene. At higher λ repressor concentrations, increased λ repressor concentration decreases the expression of the λ repressor gene.

10. Normally, bacterial mRNAs have a leader sequence in which a Shine–Dalgarno sequence precedes the AUG start codon. The absence of a leader would be expected to lead to inefficient translation.

11. Add each compound to a culture of *V. fischeri* at low density and look for the development of luminescence.

12. ACC, 7; ACA, 1; ACU, 0; ACG, 0.

13. Retention. The reaction likely proceeds in two steps: Attack of Glu 537 on the carbon of the galactose moiety (with inversion) followed by attack of water on this carbon (with a second inversion) to release the galactose from the enzyme.

14. The footprint appears to have approximately 50% of its intensity near 3.7 nM so that the dissociation constant is approximately 3.7 nM, corresponding to a standard free energy of binding of −48 kJ/mol (−11 kcal/mol) at T = 298K.

Chapter 32

1. The distribution of charged amino acids is H2A (13 K, 13 R, 2 D, 7 E, charge = +17), H2B (20 K, 8 R, 3 D, 7 E, charge = +18), H3 (13 K, 18 R, 4 D, 7 E, charge = +20), H4 (11 K, 14 R, 3 D, 4 E, charge = +18). The total charge of the histone octamer is estimated to be $2 \times (17 + 18 + 20 + 18) = +146$. The total charge on 150 base pairs of DNA is −300. Thus, the histone octamer neutralizes approximately one-half of the charge.

2. The presence of a particular DNA fragment could be detected by hybridization, by PCR, or by direct sequencing.

3. The total length of the DNA is estimated to be $145 \text{ bp} \times 3.4 \text{ Å/bp} = 493 \text{ Å}$, which represents 1.75 turns or $1.75 \times 2\pi r = 11.0r$. Thus, the radius is estimated to be $r = 493 \text{ Å}/11.0 = 44.8 \text{ Å}$.

4. 5-Azacytidine cannot be methylated. Some genes, normally repressed by methylation, will be active. 5-Azacytidine is also an inhibitor of DNA methyltransferase, resulting in lower levels of methylation and, hence, lower levels of gene repression.

5. Proteins containing these domains will be targeted to methylated DNA in repressed promoter regions. They would likely bind in the major groove because that is where the methyl group is located.

6. Gene expression is not expected to respond to the presence of estrogen. However, genes for which expression normally responds to estrogen will respond to the presence of progesterone.

7. The acetylation of lysine will reduce the charge from +1 to 0. The methylation of lysine will not reduce the charge.

8. On the basis of the pattern of cysteine and histidine residues, this region appears to contain three zinc-finger domains.

9. 10/4000 = 0.25%. 0.25% of 12 Mb = 30 kilobase pairs.

10. Monomethylated-activated; Trimethylated-repressed.

11. The addition of an IRE to the 5′ end of the mRNA is expected to block translation in the absence of iron. The addition of an IRE to the 3′ end of the mRNA is not expected to block translation, but it might affect mRNA stability.

12. The sequences of all of the mRNAs would be searched for sequences that are fully or nearly complementary to the sequence of the miRNA. These sequences would be candidates for regulation by this mRNA.

13. The amino group of the lysine residue, formed from the protonated form by a base, attacks the carbonyl group of acetyl CoA to generate a tetrahedral intermediate. This intermediate collapses to form the amide bond and release CoA.

14. In mouse DNA, most of the HpaII sites are methylated and therefore not cut by the enzyme, resulting in large fragments. Some small fragments are produced from CpG islands that are unmethylated. For *Drosophila* and *E. coli* DNA, there is no methylation and all sites are cut.

Chapter 33

1. The transgenic nematode would avoid the compound. The identity of the ligand is determined by the receptor, whereas the behavioral response is dictated by the neuron in which the receptor is expressed.

2. Only a mixture of compounds C_5-COOH and HOOC-C_7-COOH is predicted to yield this pattern.

3. Bitter and sweet sensations are mediated by G proteins coupled to 7TM receptors, leading to millisecond time resolution. Salty and sour sensations are mediated directly by ion channels, which may lead to faster time resolution.

4. Sound travels 0.15 m in 428 μs. The human hearing system is capable of sensing time differences of close to a microsecond, and so the difference in arrival times at the two ears is substantial. A system based on G proteins is unlikely to be able to reliably distinguish between signals arriving at the two ears, because G proteins typically respond in milliseconds.

5. If a plant tastes bitter, animals will avoid eating it even if it is nontoxic, which may provide a selective advantage to the plant.

6. Using mice in which either the gene for T1R1 or the gene for T1R3 has been disrupted, test the taste responses of these mice to glutamate, aspartate, and a wide variety of other amino acids.

7. 530 nm light will be absorbed to some degree by all three photoreceptors, with the largest absorption from the "green" receptor.

8. These women have four functional color receptors: blue, red, green, and a red–green hybrid. The additional color receptor allows some colors that appear identical to most people to be distinguished.

9. 380 (one for each receptor); there are $(380 \times 379)/2! = 72{,}010$ combinations of two receptors; $(380 \times 379 \times 378)/3! = 9{,}073{,}260$ combinations of three receptors.

10. The absorption of light converts 11-*cis*-retinal into all-*trans*-retinal.

11. These compounds are enantiomers and must bind to protein receptors to elicit a smell. Even these subtle structural differences can affect relative receptor binding affinities and, hence, the elicited odor.

12. Vision: cGMP-gated channel; taste: amiloride-sensitive sodium channel; hearing; tip-link channel.

13. For all senses, ATP hydrolysis is required to generate and maintain ion gradients and membrane potential. Olfaction: ATP is required for the synthesis of cAMP. Gustation: ATP is required for the synthesis of cyclic nucleotides, and GTP is required for the action of gustducin in the detection of bitter and sweet tastes. Vision: GTP is required for the synthesis of cGMP and for the action of transducin. Hearing and touch: ATP hydrolysis is required to generate and maintain ion gradients and membrane potential and may be required for other roles as well.

14.

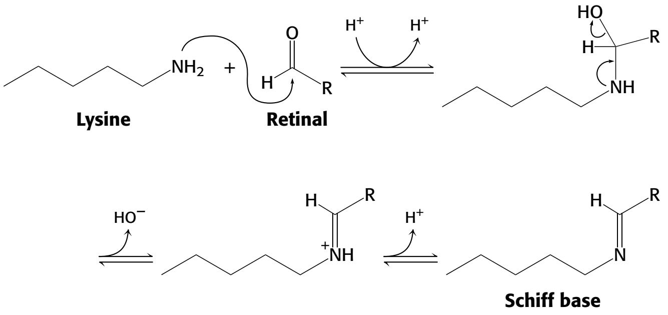

Chapter 34

1. The innate immune system responds rapidly to common features present in many pathogens. The genes for the innate immune system's key molecules are expressed without substantial modification. In contrast, the adaptive immune system responds to specific features present only in a given pathogen. Its genes undergo significant rearrangement and mutation to enable specific recognition of a vast number of potential binding surfaces.

2. VJ and V(D)J recombination; variability in segment joining by the action of terminal deoxyribonucleotidyl transferase; somatic mutation.

3. *Affinity* refers to the strength of a single interaction; *avidity* refers to the cumulative strength of multiple independent binding interactions. Avidity may play a significant role in the interaction between IgM and antigen because this immunoglobulin class features 10 binding sites.

4. The intracellular signaling domain common to each of the TLRs is responsible for docking other proteins and reporting that a targeted pathogen-associated molecular pattern (PAMP), such as LPS, has been detected. If a mutation within this domain interfered with the intracellular docking and signal transduction, then TLR4 would not respond to LPS.

5. Viruses that contain dsRNA genomes would be expected to stimulate a TLR3-mediated immune response.

6. (a) $\Delta G^{\circ\prime} = -37 \text{ kJ mol}^{-1} (-8.9 \text{ kcal mol}^{-1})$

(b) $K_a = 3.3 \times 10^6 \text{ M}^{-1}$

(c) $k_{on} = 4 \times 10^8 \text{ M}^{-1} \text{ s}^{-1}$. This value is close to the diffusion-controlled limit for the combination of a small molecule with a protein (p. 231). Hence, the extent of structural change is likely to be small; extensive conformational transitions take time.

7. The fluorescence enhancement and the shift to blue indicate that water is largely excluded from the binding site when the hapten is bound. Hydrophobic interactions contribute significantly to the formation of most antigen–antibody complexes.

8. (a) An antibody combining site is formed by CDRs from both the H and the L chains. The V_H and V_L domains are essential. A small proportion of F_{ab} fragments can be further digested to produce F_v, a fragment that contains just these two domains. C_H1 and C_L contribute to the stability of F_{ab} but not to antigen binding.

(b) A synthetic F_v analog 248 residues long was prepared by expressing a synthetic gene consisting of a V_H gene joined to a V_L gene through a linker. [J. S. Huston et al., *Proc. Natl. Acad. Sci. U.S.A.* 85:5879–5883, 1988.]

9. (a) Multivalent antigens lead to the dimerization or oligomerization of transmembrane immunoglobulins, an essential step in their activation. This mode of activation is reminiscent of that of receptor tyrosine kinases (Section 14.2).

(b) An antibody specific for a transmembrane immunoglobulin will activate a B cell by cross-linking these receptors. This experiment can be carried out by using, for example, a goat antibody to cross-link receptors on a mouse B cell.

10. B cells do not express T-cell receptors. The hybridization of T-cell cDNAs with B-cell mRNAs removes cDNAs that are expressed in both cells. Hence, the mixture of cDNAs subsequent to this hybridization are enriched in those encoding T-cell receptors. This procedure, called subtractive hybridization, is generally useful in isolating low-abundance cDNAs. Hybridization should be carried out by using mRNAs from a closely related cell that does not express the gene of interest. [See S. M. Hedrick, D. I. Cohen, E. A. Nielsen, and M. M. Davis, *Nature* 308:149–153, 1984, for an interesting account of how this method was used to obtain genes for T-cell receptors.]

11. TLR4 is the receptor for LPS, a toxin found specifically in the walls of Gram-negative bacteria. Mutations that inhibit the function of TLR4 impair an affected person's defenses against this class of bacteria.

12. If the HLA alleles are not matched, then the recipient's T cell receptors will identify the MHC proteins of the transplanted tissue as nonself and transplant rejection is likely.

13. Purify an antibody with a specificity to one antigen. Unfold the antibody and allow it to re-fold either in the presence of the antigen or in the absence of the antigen. Test the re-folded antibodies for antigen-binding ability.

14. In some cases, V–D–J rearrangement will result in combining V, D, and J segments out of frame. mRNA molecules produced from such rearranged genes will produce truncated molecules if translated. This possibility is excluded by degrading the mRNA.

15. The mutant bacteria may still stimulate an immune response without causing disease. Hence, they may be valuable starting points for the design of a live attenuated vaccine for the original pathogenic strain.

16. The peptide is LLQATYSAV (L in second position, V in last).

17. Catalysis is likely to require a base for removing a proton from a water molecule. A histidine, glutamate, or aspartate residue is most likely. In addition, a potential hydrogen-bond donor may be present and will interact with the negatively charged oxygen atom that forms in the transition state.

18. A phosphotyrosine residue in the carboxyl terminus of Src and related protein tyrosine kinases binds to its own SH2 domain to generate the inhibited form of Src (Section 14.5). Removal of the phosphoryl group from this residue will activate the kinase.

19. (a) $K_d = 10^{-7}$ M; (b) $K_d = 10^{-9}$ M. The gene was probably generated by a point mutation in the gene for antibody A rather than by de novo rearrangement.

Chapter 35

1. (a) Skeletal muscle and eukaryotic cilia derive their free energy from ATP hydrolysis; the bacterial flagellar motor uses a proton-motive force.

(b) Skeletal muscle requires myosin and actin. Eukaryotic cilia require microtubules and dynein. The bacterial flagellar motor requires MotA, MotB, and FliG, as well as many ancillary components.

2. 6400 Å/80 Å = 80 body lengths per second. For a 10-foot automobile, this body-length speed corresponds to a speed of 80 × 10 feet = 800 feet per second, or 545 miles per hour.

3. 4 pN = 8.8×10^{-13} pounds. The weight of a single motor domain is 100,000 g $\text{mol}^{-1}/(6.023 \times 10^{23}$ molecules $\text{mol}^{-1}) = 1.7 \times 10^{-19}$ g $= 3.7 \times 10^{-22}$ pounds. Thus, a motor domain can lift $(8.8 \times 10^{-13}/3.7 \times 10^{-22}) = 2.4 \times 10^{9}$ times its weight.

4. Both actin filaments and microtubules are built from subunits and these subunits bind and hydrolyze nucleoside triphosphates. Actin filaments are built of a single type of subunit and these subunits bind ATP. Microtubules are built of two different types of subunits and these subunits bind GTP.

5. The light chains in myosin stiffen the lever arm. The light chains in kinesin bind cargo to be transported.

6. After death, the ratio of ADP to ATP increases rapidly. In the ADP form, myosin motor domains bind tightly to actin. Myosin–actin interactions are possible because the drop in ATP concentration also allows the calcium concentration to rise, clearing the blockage of actin by tropomyosin through the action of the troponin complex.

7. Above its critical concentration, ATP-actin will polymerize. The ATP will hydrolyze through time to form ADP-actin, which has a higher critical concentration. Thus, if the initial subunit concentration is between the critical concentrations of ATP-actin and ADP-actin, filaments will form initially and then disappear on ATP hydrolysis.

8. A one-base step is approximately 3.4 Å = 3.4×10^{-4} μm. If a stoichiometry of one molecule of ATP per step is assumed, this distance corresponds to a velocity of 0.017 μm s^{-1}. Kinesin moves at a velocity of 6400 Å per second, or 0.64 μm s^{-1}.

9. A proton-motive force across the plasma membrane is necessary to drive the flagellar motor. Under conditions of starvation, this proton-motive force is depleted. In acidic solution, the pH difference across the membrane is sufficient to power the motor.

10. The mean distance between tumbles would be longer when the bacterium is moving up a gradient of a chemoattractant.

11. (a) 1.13×10^{-9} dyne
(b) 6.8×10^{14} erg
(c) 6.6×10^{-11} erg per 80 molecules of ATP. A single kinesin motor provides more than enough free energy to power the transport of micrometer-size cargoes at micrometer-per-second velocities.

12. The spacing between identical subunits on microtubules is 8 nm. Thus, a kinesin molecule with a step size that is not a multiple of 8 nm would have to be able to bind at more than one type of site on the microtubule surface.

13. KIF1A must be tethered to an additional microtubule-binding element that retains an attachment to the microtubule when the motor domain releases.

14. Filaments built from subunits can be arbitrarily long, can be dynamically assembled and disassembled, and require only a small amount of genetic information to encode.

15. Protons still flow from outside to inside the cell. Each proton might pass into the outer half-channel of one MotA–MotB complex, bind to the MS ring, rotate clockwise, and pass into the inner half-channel of the neighboring MotA–MotB complex.

16. At a high concentration of calcium ion, Ca^{2+} binds to calmodulin. In turn, calmodulin binds to a protein kinase that phosphorylates myosin light chains and activates it. At low calcium ion concentration, the light chains are dephosphorylated by a Ca^{2+}-independent phosphatase.

17. (a) The value of k_{cat} is approximately 13 molecules per second, whereas the K_{M} value for ATP is approximately 12 μM.
(b) The step size is approximately $(380 - 120)/7 = 37$ nm.
(c) The step size is very large, which is consistent with the presence of six light-chain-binding sites and, hence, very long lever arms. The rate of ADP release is essentially identical with the overall k_{cat}; so ADP release is rate limiting, which suggests that both motor domains can bind to sites 37 nm apart simultaneously. ADP release from the hindmost domain allows ATP to bind, leading to actin release and lever-arm motion.

Chapter 36

1. (a) Before; (b) after; (c) after; (d) after; (e) before; (f) after.

2. (a) Yes; (b) yes; (c) no (MW > 600).

3. If computer programs could estimate log(P) values on the basis of chemical structure, then the required laboratory time for drug development could be shortened. The determination of the relative solubilities of pharmaceutical candidates by allowing each compound to equilibrate between water and an organic phase would no longer be necessary.

4. Perhaps *N*-acetylcysteine would conjugate to some of the *N*-acetyl-*p*-benzoquinone imine that is produced by the metabolism of acetaminophen, thereby preventing the depletion of the liver's supply of glutathione.

5. In Phase I clinical trials, approximately 10 to 100 usually healthy volunteers are typically enrolled in a study designed to assess safety. In contrast, a larger number of subjects are enrolled in a typical Phase II trial. Moreover, these persons may benefit from the drug administered. In a Phase II trial, efficacy, dosage, and safety can be assessed.

6. The binding of other drugs to albumin could cause extra coumadin to be released. (Albumin is a general carrier for hydrophobic molecules.)

7. A drug that inhibits a P450 enzyme may dramatically affect the disposition of another drug that is metabolized by that same enzyme. If this inhibited metabolism is not accounted for when dosing, the second drug may reach very high, and sometimes toxic, levels in the blood.

8. Unlike competitive inhibition, noncompetitive inhibition cannot be overcome with additional substrate. Hence, a drug that acts by a noncompetitive mechanism will be unaffected by changing levels of the physiological substrate.

9. An inhibitor of MDR could prevent the efflux of a chemotherapeutic drug from tumor cells. Hence, this type of an inhibitor could be useful in averting resistance to cancer chemotherapy.

10. Agents that inhibit one or more enzymes of the glycolytic pathway could act to deprive trypanosomes of energy and thus be useful for treating sleeping sickness. A difficulty is that glycolysis in the host cells also would be inhibited.

11. Imatinib is an inhibitor of the Bcr-Abl kinase, a mutant kinase present only in tumor cells that have undergone a translocation between chromosomes 9 and 22 (Figure 14.34). Before initiating treatment with imatinib, we could sequence the DNA of the tumor cells and determine (a) whether this translocation has taken place and (b) whether the sequence of *bcr-abl* carries any mutations that would render the kinase resistant

to imatinib. If the translocation has not taken place or if the gene carries resistance mutations, then imatinib would likely not be an effective treatment for the patient carrying this particular tumor.

12. Sildenafil increases cGMP levels by inhibiting the phosphodiesterase-mediated breakdown of cGMP to GMP. Intracellular cGMP levels can also be increased by activating its synthesis. This activation can be achieved with the use of NO donors (such as sodium nitroprusside and nitroglycerin) or compounds that activate guanylate cyclase activity. Drugs that act by the latter mechanism are currently in clinical trials.

13. A reasonable mechanism would be an oxidative deamination following an overall mechanism similar to that in Figure 36.10, with release of ammonia.

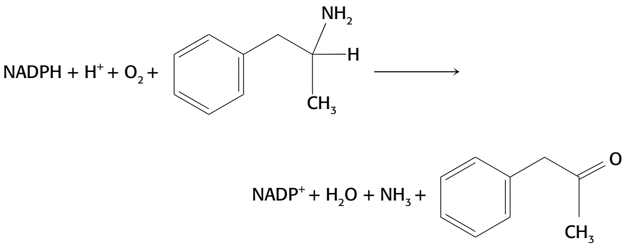

14. $K_I \approx 0.3$ nM. $IC_{50} \approx 2.0$ nM. Yes, compound A should be effective when taken orally because 400 nM is much greater than the estimated values of K_I and IC_{50}.

SELECTED READINGS

Chapter 2

Where to Start

Service, R. F. 2008. Problem solved* (*sort of) (a brief review of protein folding). *Science* 321:784–786.

Doolittle, R. F. 1985. Proteins. *Sci. Am.* 253(4):88–99.

Richards, F. M. 1991. The protein folding problem. *Sci. Am.* 264(1):54–57.

Weber, A. L., and Miller, S. L. 1981. Reasons for the occurrence of the twenty coded protein amino acids. *J. Mol. Evol.* 17:273–284.

Books

Petsko, G. A., and Ringe, D. 2004. *Protein Structure and Function*. New Science Press.

Tanford, C., and Reynolds, J. 2004. *Nature's Robots: A History of Proteins.* Oxford.

Branden, C., and Tooze, J. 1999. *Introduction to Protein Structure* (2d ed.). Garland.

Creighton, T. E. 1992. *Proteins: Structures and Molecular Principles* (2d ed.). W. H. Freeman and Company.

Conformation of Proteins

Smock, R. G., and Gierasch, L. M. 2009. Sending signals dynamically. *Science* 324:198–203.

Tokuriki, N., and Tawfik, D. S. 2009. Protein dynamism and evolvability. *Science* 324:203–207.

Pace, C. N., Grimsley, G. R., and Scholtz, J. M. 2009. Protein ionizable groups: p*K* values and their contribution to protein stability and solubility. *J. Biol. Chem.* 284:13285–13289.

Breslow, R., and Cheng, Z.-L. 2009. On the origin of terrestrial homochirality for nucleosides and amino acids. *Proc. Natl. Acad. Sci. U.S.A.* 106:9144–9146.

Secondary Structure

Shoulders, M. D., and Raines, R. T. 2009. Collagen structure and stability. *Annu. Rev. Biochem.* 78:929–958.

O'Neil, K. T., and DeGrado, W. F. 1990. A thermodynamic scale for the helix-forming tendencies of the commonly occurring amino acids. *Science* 250:646–651.

Zhang, C., and Kim, S. H. 2000. The anatomy of protein beta-sheet topology. *J. Mol. Biol.* 299:1075–1089.

Regan, L. 1994. Protein structure: Born to be beta. *Curr. Biol.* 4:656–658.

Srinivasan, R., and Rose, G. D. 1999. A physical basis for protein secondary structure. *Proc. Natl. Acad. Sci. U.S.A.* 96:14258–14263.

Intrinsically Unstructured Proteins

Galea, C. A., Wang, Y., Sivakolundu, S. G., and Kriwacki, R. W. 2008. Regulation of cell division by intrinsically unstructured proteins: Intrinsic flexibility, modularity, and signaling conduits. *Biochemistry* 47:7598–7609.

Raychaudhuri, S., Dey, S., Bhattacharyya, N. P., and Mukhopadhyay, D. 2009. The role of intrinsically unstructured proteins in neurodegenerative diseases. *PLoS One* 4:e5566.

Tompa, P., and Fuxreiter, M. 2008. Fuzzy complexes: Polymorphism and structural disorder in protein–protein interactions. *Trends Biochem. Sci.* 33:2–8.

Tuinstra, R. L., Peterson, F. C., Kutlesa, E. S., Elgin, S., Kron, M. A., and Volkman, B. F. 2008. Interconversion between two unrelated protein folds in the lymphotactin native state. *Proc. Natl. Acad. Sci. U.S.A.* 105:5057–5062.

Domains

Jin, J., Xie, X., Chen, C., Park, J. G., Stark, C., James, D. A., Olhovsky, M., Lindinger, R., Mao, Y., and Pawson, T. 2009. Eukaryotic protein domains as functional units of cellular evolution. *Sci. Signal.* 2:ra76.

Bennett, M. J., Choe, S., and Eisenberg, D. 1994. Domain swapping: Entangling alliances between proteins. *Proc. Natl. Acad. Sci. U.S.A.* 91:3127–3131.

Bergdoll, M., Eltis, L. D., Cameron, A. D., Dumas, P., and Bolin, J. T. 1998. All in the family: Structural and evolutionary relationships among three modular proteins with diverse functions and variable assembly. *Protein Sci.* 7:1661–1670.

Hopfner, K. P., Kopetzki, E., Kresse, G. B., Bode, W., Huber, R., and Engh, R. A. 1998. New enzyme lineages by subdomain shuffling. *Proc. Natl. Acad. Sci. U.S.A.* 95:9813–9818.

Ponting, C. P., Schultz, J., Copley, R. R., Andrade, M. A., and Bork, P. 2000. Evolution of domain families. *Adv. Protein Chem.* 54:185–244.

Protein Folding

Caughey, B., Baron, G. S., Chesebro, B., and Jeffrey, M. 2009. Getting a grip on prions: Oligomers, amyloids, and pathological membrane interactions. *Annu. Rev. Biochem.* 78:177–204.

Cobb, N. J., and Surewicz, W. K. 2009. Prion diseases and their biochemical mechanisms. *Biochemistry* 48:2574–2585.

Soto, C. 2011. Prion diseases: The end of the controversy? *Trends Biochem. Sci.* 36:151–158.

Daggett, V., and Fersht, A. R. 2003. Is there a unifying mechanism for protein folding? *Trends Biochem. Sci.* 28:18–25.

Selkoe, D. J. 2003. Folding proteins in fatal ways. *Nature* 426:900–904.

Anfinsen, C. B. 1973. Principles that govern the folding of protein chains. *Science* 181:223–230.

Baldwin, R. L., and Rose, G. D. 1999. Is protein folding hierarchic? I. Local structure and peptide folding. *Trends Biochem. Sci.* 24:26–33.

Baldwin, R. L., and Rose, G. D. 1999. Is protein folding hierarchic? II. Folding intermediates and transition states. *Trends Biochem. Sci.* 24:77–83.

Kuhlman, B., Dantas, G., Ireton, G. C., Varani, G., Stoddard, B. L., and Baker, D. 2003. Design of a novel globular protein with atomic-level accuracy. *Science* 302:1364–1368.

Staley, J. P., and Kim, P. S. 1990. Role of a subdomain in the folding of bovine pancreatic trypsin inhibitor. *Nature* 344:685–688.

Covalent Modification of Proteins

Tarrant, M. K., and Cole, P. A. 2009. The chemical biology of protein phosphorylation. *Annu. Rev. Biochem.* 78:797–825.

Krishna, R. G., and Wold, F. 1993. Post-translational modification of proteins. *Adv. Enzymol. Relat. Areas. Mol. Biol.* 67:265–298.

Aletta, J. M., Cimato, T. R., and Ettinger, M. J. 1998. Protein methylation: A signal event in post-translational modification. *Trends Biochem. Sci.* 23:89–91.

Tsien, R. Y. 1998. The green fluorescent protein. *Annu. Rev. Biochem.* 67:509–544.

Chapter 3

Where to Start

Sanger, F. 1988. Sequences, sequences, sequences. *Annu. Rev. Biochem.* 57:1–28.

Merrifield, B. 1986. Solid phase synthesis. *Science* 232:341–347.

Hunkapiller, M. W., and Hood, L. E. 1983. Protein sequence analysis: Automated microsequencing. *Science* 219:650–659.

Milstein, C. 1980. Monoclonal antibodies. *Sci. Am.* 243(4):66–74.

Moore, S., and Stein, W. H. 1973. Chemical structures of pancreatic ribonuclease and deoxyribonuclease. *Science* 180:458–464.

Books

Methods in Enzymology. Academic Press.

Wilson, K., and Walker, J. (Eds.). 2010. *Principles and Techniques of Practical Biochemistry* (7th ed.). Cambridge University Press.

Van Holde, K. E., Johnson, W. C., and Ho, P.-S. 1998. *Principles of Physical Biochemistry.* Prentice Hall.

Wilkins, M. R., Williams, K. L., Appel, R. D., and Hochstrasser, D. F. 1997. *Proteome Research: New Frontiers in Functional Genomics (Principles and Practice).* Springer Verlag.

Johnstone, R. A. W. 1996. *Mass Spectroscopy for Chemists and Biochemists* (2d ed.). Cambridge University Press.

Kyte, J. 1994. *Structure in Protein Chemistry.* Garland.

Creighton, T. E. 1993. *Proteins: Structure and Molecular Properties* (2d ed.). W. H. Freeman and Company.

Cantor, C. R., and Schimmel, P. R. 1980. *Biophysical Chemistry.* W. H. Freeman and Company.

Protein Purification and Analysis

Blackstock, W. P., and Weir, M. P. 1999. Proteomics: Quantitative and physical mapping of cellular proteins. *Trends Biotechnol.* 17:121–127.

Deutscher, M. (Ed.). 1997. *Guide to Protein Purification.* Academic Press.

Dunn, M. J. 1997. Quantitative two-dimensional gel electrophoresis: From proteins to proteomes. *Biochem. Soc. Trans.* 25:248–254.

Scopes, R. K., and Cantor, C. 1994. *Protein Purification: Principles and Practice* (3d ed.). Springer Verlag.

Aebersold, R., Pipes, G. D., Wettenhall, R. E., Nika, H., and Hood, L. E. 1990. Covalent attachment of peptides for high sensitivity solid-phase sequence analysis. *Anal. Biochem.* 187:56–65.

Ultracentrifugation and Mass Spectrometry

Steen, H., and Mann, M. 2004. The ABC's (and XYZ's) of peptide sequencing. *Nat. Rev. Mol. Cell Biol.* 5:699–711.

Glish, G. L., and Vachet, R. W. 2003. The basics of mass spectrometry in the twenty-first century. *Nat. Rev. Drug Discov*. 2:140–150.

Li, L., Garden, R. W., and Sweedler, J. V. 2000. Single-cell MALDI: A new tool for direct peptide profiling. *Trends Biotechnol.* 18:151–160.

Yates, J. R., 3d. 1998. Mass spectrometry and the age of the proteome. *J. Mass Spectrom.* 33:1–19.

Pappin, D. J. 1997. Peptide mass fingerprinting using MALDI-TOF mass spectrometry. *Methods Mol. Biol.* 64:165–173.

Schuster, T. M., and Laue, T. M. 1994. *Modern Analytical Ultracentrifugation.* Springer Verlag.

Arnott, D., Shabanowitz, J., and Hunt, D. F. 1993. Mass spectrometry of proteins and peptides: Sensitive and accurate mass measurement and sequence analysis. *Clin. Chem.* 39:2005–2010.

Chait, B. T., and Kent, S. B. H. 1992. Weighing naked proteins: Practical, high-accuracy mass measurement of peptides and proteins. *Science* 257:1885–1894.

Edmonds, C. G., Loo, J. A., Loo, R. R., Udseth, H. R., Barinaga, C. J., and Smith, R. D. 1991. Application of electrospray ionization mass spectrometry and tandem mass spectrometry in combination with capillary electrophoresis for biochemical investigations. *Biochem. Soc. Trans.* 19:943–947.

Jardine, I. 1990. Molecular weight analysis of proteins. *Methods Enzymol.* 193:441–455.

Proteomics

Yates, J. R., 3rd. 2004. Mass spectral analysis in proteomics. *Annu. Rev. Biophys. Biomol. Struct.* 33:297–316.

Weston, A. D., and Hood, L. 2004. Systems biology, proteomics, and the future of health care: Toward predictive, preventative, and personalized medicine. *J. Proteome Res*. 3:179–196.

Pandey, A., and Mann, M. 2000. Proteomics to study genes and genomes. *Nature* 405:837–846.

Dutt, M. J., and Lee, K. H. 2000. Proteomic analysis. *Curr. Opin. Biotechnol.* 11:176–179.

Rout, M. P., Aitchison, J. D., Suprapto, A., Hjertaas, K., Zhao, Y., and Chait, B. T. 2000. The yeast nuclear pore complex: Composition, architecture, and transport mechanism. *J. Cell Biol.* 148:635–651.

X-ray Crystallography and NMR Spectroscopy

Rhodes, G. 2006. *Crystallography Made Crystal Clear.* Elsevier/Academic Press.

Moffat, K. 2003. The frontiers of time-resolved macromolecular crystallography: Movies and chirped X-ray pulses. *Faraday Discuss.* 122:65–88.

Bax, A. 2003. Weak alignment offers new NMR opportunities to study protein structure and dynamics. *Protein Sci.* 12:1–16.

Wery, J. P., and Schevitz, R. W. 1997. New trends in macromolecular x-ray crystallography. *Curr. Opin. Chem. Biol.* 1:365–369.

Glusker, J. P. 1994. X-ray crystallography of proteins. *Methods Biochem. Anal.* 37:1–72.

Clore, G. M., and Gronenborn, A. M. 1991. Structures of larger proteins in solution: Three- and four-dimensional heteronuclear NMR spectroscopy. *Science* 252:1390–1399.

Wüthrich, K. 1989. Protein structure determination in solution by nuclear magnetic resonance spectroscopy. *Science* 243:45–50.

Wüthrich, K. 1986. *NMR of Proteins and Nucleic Acids.* Wiley-Interscience.

Monoclonal Antibodies and Fluorescent Molecules

Immunology Today. 2000. Volume 21, issue 8.

Tsien, R. Y. 1998. The green fluorescent protein. *Annu. Rev. Biochem.* 67:509–544.

Kendall, J. M., and Badminton, M. N. 1998. *Aequorea victoria* bioluminescence moves into an exciting era. *Trends Biotechnol.* 16:216–234.

Goding, J. W. 1996. *Monoclonal Antibodies: Principles and Practice.* Academic Press.

Köhler, G., and Milstein, C. 1975. Continuous cultures of fused cells secreting antibody of predefined specificity. *Nature* 256:495–497.

Chemical Synthesis of Proteins

Bang, D., Chopra, N., and Kent, S. B. 2004. Total chemical synthesis of crambin. *J. Am. Chem. Soc.* 126:1377–1383.

Dawson, P. E., and Kent, S. B. 2000. Synthesis of native proteins by chemical ligation. *Annu. Rev. Biochem.* 69:923–960.

Mayo, K. H. 2000. Recent advances in the design and construction of synthetic peptides: For the love of basics or just for the technology of it. *Trends Biotechnol.* 18:212–217.

Chapter 4

Where to Start

Felsenfeld, G. 1985. DNA. *Sci. Am.* 253(4):58–67.

Darnell, J. E., Jr. 1985. RNA. *Sci. Am.* 253(4):68–78.

Dickerson, R. E. 1983. The DNA helix and how it is read. *Sci. Am.* 249(6):94–111.

Crick, F. H. C. 1954. The structure of the hereditary material. *Sci. Am.* 191(4):54–61.

Chambon, P. 1981. Split genes. *Sci. Am.* 244(5):60–71.

Watson, J. D., and Crick, F. H. C. 1953. Molecular structure of nucleic acids: A structure for deoxyribose nucleic acid. *Nature* 171:737–738.

Watson, J. D., and Crick, F. H. C. 1953. Genetic implications of the structure of deoxyribonucleic acid. *Nature* 171:964–967.

Meselson, M., and Stahl, F. W. 1958. The replication of DNA in *Escherichia coli*. *Proc. Natl. Acad. Sci. U.S.A.* 44:671–682.

Books

Bloomfield, V. A., Crothers, D. M., Tinoco, I., and Hearst, J. 2000. *Nucleic Acids: Structures, Properties, and Functions.* University Science Books.

Singer, M., and Berg, P. 1991. *Genes and Genomes: A Changing Perspective*. University Science Books.

Lodish, H., Berk, A., Kaiser, C. A., Krieger, M. Bretscher, A., Ploegh, H., Amon, A., and Scott, M. P. 2012. *Molecular Cell Biology* (7th ed.). W. H. Freeman and Company.

Krebs, J. E, Goldstein, E. S. and Kilpatrick, S. T. 2012. *Lewin's Genes XI*. (11th ed.). Jones and Bartlett.

Watson, J. D., Baker, T. A., Bell, S. P., Gann, A., Levine, M., and Losick, R. 2013. *Molecular Biology of the Gene* (7th ed.). Benjamin Cummings.

DNA Structure

Neidle, S. 2007. *Principles of Nucleic Acid Structure*. Academic Press.

Dickerson, R. E., Drew, H. R., Conner, B. N., Wing, R. M., Fratini, A. V., and Kopka, M. L. 1982. The anatomy of A-, B-, and Z-DNA. *Science* 216:475–485.

Sinden, R. R. 1994. *DNA Structure and Function*. Academic Press.

DNA Replication

Lehman, I. R. 2003. Discovery of DNA polymerase. *J. Biol. Chem.* 278:34733–34738.

Hübscher, U., Maga, G., and Spardari, S. 2002. Eukaryotic DNA polymerases. *Annu. Rev. Biochem.* 71:133–163.

Hübscher, U., Nasheuer, H.-P., and Syväoja, J. E. 2000. Eukaryotic DNA polymerases: A growing family. *Trends Biochem. Sci.* 25:143–147.

Brautigam, C. A., and Steitz, T. A. 1998. Structural and functional insights provided by crystal structures of DNA polymerases and their substrate complexes. *Curr. Opin. Struct. Biol.* 8:54–63.

Kornberg, A. 2005. *DNA Replication* (2d ed.). University Science Books.

Discovery of Messenger RNA

Jacob, F., and Monod, J. 1961. Genetic regulatory mechanisms in the synthesis of proteins. *J. Mol. Biol.* 3:318–356.

Brenner, S., Jacob, F., and Meselson, M. 1961. An unstable intermediate carrying information from genes to ribosomes for protein synthesis. *Nature* 190:576–581.

Hall, B. D., and Spiegelman, S. 1961. Sequence complementarity of T2-DNA and T2-specific RNA. *Proc. Natl. Acad. Sci. U.S.A.* 47:137–146.

Genetic Code

Novoa, E. M., and Ribas de Pouplana, L. 2012. Speeding with control: Codon usage, tRNAs, and ribosomes. *Trends Genet.* 28:574–581.

Koonin, E. V., and Novozhilov, A. S. 2009. Origin and evolution of the genetic code: The universal enigma. *IUBMB Life* 61:99–111.

Yarus, M., Caporaso, J. G., and Knight, R. 2005. Origins of the genetic code: The escaped triplet theory. *Annu. Rev. Biochem.* 74:179–198.

Freeland, S. J., and Hurst, L. D. 2004. Evolution encoded. *Sci. Am.* 290(4):84–91.

Crick, F. H. C., Barnett, L., Brenner, S., and Watts-Tobin, R. J. 1961. General nature of the genetic code for proteins. *Nature* 192:1227–1232.

Knight, R. D., Freeland, S. J., and Landweber L. F. 1999. Selection, history and chemistry: The three faces of the genetic code. *Trends Biochem. Sci.* 24(6):241–247.

Introns, Exons, and Split Genes

Liu, M., and Grigoriev, A. 2004. Protein domains correlate strongly with exons in multiple eukaryotic genomes—evidence of exon shuffling? *Trends Genet.* 20:399–403.

Dorit, R. L., Schoenbach, L., and Gilbert, W. 1990. How big is the universe of exons? *Science* 250:1377–1382.

Cochet, M., Gannon, F., Hen, R., Maroteaux, L., Perrin, F., and Chambon, P. 1979. Organization and sequence studies of the 17-piece chicken conalbumin gene. *Nature* 282:567–574.

Tilghman, S. M., Tiemeier, D. C., Seidman, J. G., Peterlin, B. M., Sullivan, M., Maizel, J. V., and Leder, P. 1978. Intervening sequence of DNA identified in the structural portion of a mouse β-globin gene. *Proc. Natl. Acad. Sci. U.S.A.* 75:725–729.

Reminiscences and Historical Accounts

Watson, J. D., Gann, A., and Witkowski, J. (Eds.). 2012. *The Annotated and Illustrated Double Helix*. Simon and Shuster.

Nirenberg, M. 2004. Deciphering the genetic code—a personal account. *Trends Biochem. Sci.* 29:46–54.

Clayton, J., and Dennis, C. (Eds.). 2003. *50 Years of DNA*. Palgrave Macmillan.

Watson, J. D. 1968. *The Double Helix*. Atheneum.

McCarty, M. 1985. *The Transforming Principle: Discovering That Genes Are Made of DNA*. Norton.

Cairns, J., Stent, G. S., and Watson, J. D. 2000. *Phage and the Origins of Molecular Biology*. Cold Spring Harbor Laboratory.

Olby, R. 1974. *The Path to the Double Helix*. University of Washington Press.

Judson, H. F. 1996. *The Eighth Day of Creation*. Cold Spring Harbor Laboratory.

Sayre, A. 2000. *Rosalind Franklin and DNA*. Norton.

Chapter 5

Where to Start

Berg, P. 1981. Dissections and reconstructions of genes and chromosomes. *Science* 213:296–303.

Gilbert, W. 1981. DNA sequencing and gene structure. *Science* 214:1305–1312.

Sanger, F. 1981. Determination of nucleotide sequences in DNA. *Science* 214:1205–1210.

Mullis, K. B. 1990. The unusual origin of the polymerase chain reaction. *Sci. Am.* 262(4):56–65.

Books on Recombinant DNA Technology

Watson, J. D., Myers, R. M., Caudy, A. A., and Witkowski, J. 2007. *Recombinant DNA: Genes and Genomes* (3d ed.). W. H. Freeman and Company.

Grierson, D. (Ed.). 1991. *Plant Genetic Engineering*. Chapman and Hall.

Mullis, K. B., Ferré, F., and Gibbs, R. A. (Eds.). 1994. *The Polymerase Chain Reaction*. Birkhaüser.

Green, M. R., and Sambrook, S. 2014. *Molecular Cloning: A Laboratory Manual* (4th ed.). Cold Spring Harbor Laboratory Press.

Ausubel, F. M., Brent, R., Kingston, R. E., and Moore, D. D. (Eds.). 2002. *Short Protocols in Molecular Biology: A Compendium of Methods from Current Protocols in Molecular Biology*. Wiley.

Birren, B., Green, E. D., Klapholz, S., Myers, R. M., Roskams, J., Riethamn, H., and Hieter, P. (Eds.). 1999. *Genome Analysis* (vols. 1–4). Cold Spring Harbor Laboratory Press.

Methods in Enzymology. Academic Press. [Many volumes in this series deal with recombinant DNA technology.]

DNA Sequencing and Synthesis

Hunkapiller, T., Kaiser, R. J., Koop, B. F., and Hood, L. 1991. Large-scale and automated DNA sequence determination. *Science* 254:59–67.

Sanger, F., Nicklen, S., and Coulson, A. R. 1977. DNA sequencing with chain-terminating inhibitors. *Proc. Natl. Acad. Sci. U.S.A.* 74:5463–5467.

Maxam, A. M., and Gilbert, W. 1977. A new method for sequencing DNA. *Proc. Natl. Acad. Sci. U.S.A.* 74:560–564.

Smith, L. M., Sanders, J. Z., Kaiser, R. J., Hughes, P., Dodd, C., Connell, C. R., Heiner, C., Kent, S. B. H., and Hood, L. E. 1986. Fluorescence detection in automated DNA sequence analysis. *Nature* 321:674–679.

Pease, A. C., Solas, D., Sullivan, E. J., Cronin, M. T., Holmes, C. P., and Fodor, S. P. A. 1994. Light-generated oligonucleotide arrays for rapid DNA sequence analysis. *Proc. Natl. Acad. Sci. U.S.A.* 91:5022–5026.

Venter, J. C., Adams, M. D., Sutton, G. G., Kerlavage, A. R., Smith, H. O., and Hunkapiller, M. 1998. Shotgun sequencing of the human genome. *Science* 280:1540–1542.

Mardis, E. R. 2008. Next-generation DNA sequencing methods. *Annu. Rev. Genomics Hum. Genet.* 9:387–402.

Metzker, M. L. 2010. Sequencing technologies—the next generation. *Nature Rev. Genet.* 11:31–46.

Rothberg, J. M., Hinz, W., Rearick, T. M., Schultz, J., Mileski, W., Davey, M., Leamon, J. H., Johnson, K., Milgrew, M. J., Edwards, M., et al. 2011. An integrated semi-conductor device enabling non-optical genome sequencing. *Nature*. 475:348–352.

Polymerase Chain Reaction

Arnheim, N., and Erlich, H. 1992. Polymerase chain reaction strategy. *Annu. Rev. Biochem.* 61:131–156.

Kirby, L. T. (Ed.). 1997. *DNA Fingerprinting: An Introduction.* Stockton Press.

Eisenstein, B. I. 1990. The polymerase chain reaction: A new method for using molecular genetics for medical diagnosis. *New Engl. J. Med.* 322:178–183.

Foley, K. P., Leonard, M. W., and Engel, J. D. 1993. Quantitation of RNA using the polymerase chain reaction. *Trends Genet.* 9:380–386.

Pääbo, S. 1993. Ancient DNA. *Sci. Am.* 269(5):86–92.

Hagelberg, E., Gray, I. C., and Jeffreys, A. J. 1991. Identification of the skeletal remains of a murder victim by DNA analysis. *Nature* 352:427–429.

Lawlor, D. A., Dickel, C. D., Hauswirth, W. W., and Parham, P. 1991. Ancient HLA genes from 7500-year-old archaeological remains. *Nature* 349:785–788.

Krings, M., Geisert, H., Schmitz, R. W., Krainitzki, H., and Pääbo, S. 1999. DNA sequence of the mitochondrial hypervariable region II for the Neanderthal type specimen. *Proc. Natl. Acad. Sci. U.S.A.* 96:5581–5585.

Ovchinnikov, I. V., Götherström, A., Romanova, G. P., Kharitonov, V. M., Lidén, K., and Goodwin, W. 2000. Molecular analysis of Neanderthal DNA from the northern Caucasus. *Nature* 404: 490–493.

Genome Sequencing

International Human Genome Sequencing Consortium. 2004. Finishing the euchromatic sequence of the human genome. *Nature* 431:931–945.

Lander, E. S., Linton, L. M., Birren, B., Nusbaum, C., Zody, M. C., Baldwin, J., Devon, K., Dewar, K., Doyle, M., FitzHugh, W., et al. 2001. Initial sequencing and analysis of the human genome. *Nature* 409:860–921.

Venter, J. C., Adams, M. D., Myers, E. W., Li, P. W., Mural, R. J., Sutton, G. G., Smith, H. O., Yandell, M., Evans, C. A., Holt, R. A., et al. 2001. The sequence of the human genome. *Science* 291:1304–1351.

Waterston, R. H., Lindblad-Toh, K., Birney, E., Rogers, J., Abril, J. F., Agarwal, P., Agarwala, R., Ainscough, R., Alexandersson, M., An, P., et al. 2002. Initial sequencing and comparative analysis of the mouse genome. *Nature* 420:520–562.

Koonin, E. V. 2003. Comparative genomics, minimal gene-sets and the last universal common ancestor. *Nat. Rev. Microbiol.* 1:127–236.

Gilligan, P., Brenner, S., and Venkatesh, B. 2002. Fugu and human sequence comparison identifies novel human genes and conserved non-coding sequences. *Gene* 294:35–44.

Enard, W., and Pääbo, S. 2004. Comparative primate genomics. *Annu. Rev. Genomics Hum. Genet.* 5:351–378.

Quantitative PCR and DNA Arrays

Duggan, D. J., Bittner, J. M., Chen, Y., Meltzer, P., and Trent, J. M. 1999. Expression profiling using cDNA microarrays. *Nat. Genet.* 21:10–14.

Golub, T. R., Slonim, D. K., Tamayo, P., Huard, C., Gaasenbeek, M., Mesirov, J. P., Coller, H., Loh, M. L., Downing, J. R., Caligiuri, M. A., et al. 1999. Molecular classification of cancer: Class discovery and class prediction by gene expression monitoring. *Science* 286:531–537.

Perou, C. M., Sørlie, T., Eisen, M. B., van de Rijn, M., Jeffery, S. S., Rees, C. A., Pollack, J. R., Ross, D. T., Johnsen, H., Akslen, L. A., et al. 2000. Molecular portraits of human breast tumours. *Nature* 406:747–752.

Walker, N. J. 2002. A technique whose time has come. *Science* 296:557–559.

Manipulation of Eukaryotic Genes

Anderson, W. F. 1992. Human gene therapy. *Science* 256:808–813.

Friedmann, T. 1997. Overcoming the obstacles to gene therapy. *Sci. Am.* 277(6):96–101.

Blaese, R. M. 1997. Gene therapy for cancer. *Sci. Am.* 277(6):111–115.

Brinster, R. L., and Palmiter, R. D. 1986. Introduction of genes into the germ lines of animals. *Harvey Lect.* 80:1–38.

Capecchi, M. R. 1989. Altering the genome by homologous recombination. *Science* 244:1288–1292.

Hasty, P., Bradley, A., Morris, J. H., Edmondson, D. G., Venuti, J. M., Olson, E. N., and Klein, W. H. 1993. Muscle deficiency and neonatal death in mice with a targeted mutation in the myogenin gene. *Nature* 364:501–506.

Parkmann, R., Weinberg, K., Crooks, G., Nolta, J., Kapoor, N., and Kohn, D. 2000. Gene therapy for adenosine deaminase deficiency. *Annu. Rev. Med.* 51:33–47.

Gaj, T., Gersbach, C. A., and Barbas III, C. F. 2013. ZFN, TALEN, and CRISPR/Cas-based methods for genome engineering. *Trends Biotechnol.* 31:397–405.

RNA Interference

Rana, T. M. 2007. Illuminating the silence: Understanding the structure and function of small RNAs. *Nat. Rev. Mol. Cell Biol.* 8:23–36.

Novina, C. D., and Sharp, P. A. 2004. The RNAi revolution. *Nature* 430:161–164.

Hannon, G. J., and Rossi, J. J. 2004. Unlocking the potential of the human genome with RNA interference. *Nature* 431:371–378.

Meister, G., and Tuschl, T. 2004. Mechanisms of gene silencing by double-stranded RNA. *Nature* 431:343–349.

Elbashir, S. M., Harborth, J., Lendeckel, W., Yalcin, A., Weber, K., and Tuschl, T. 2001. Duplexes of 21-nucleotide RNAs mediate RNA interference in cultured mammalian cells. *Nature* 411:494–498.

Fire, A., Xu, S., Montgomery, M. K., Kostas, S. A., Driver, S. E., and Mello, C. C. 1998. Potent and specific genetic interference by double-stranded RNA in *Caenorhabditis elegans*. *Nature* 391:806–811.

Genetic Engineering of Plants

Gasser, C. S., and Fraley, R. T. 1992. Transgenic crops. *Sci. Am.* 266(6):62–69.

Gasser, C. S., and Fraley, R. T. 1989. Genetically engineering plants for crop improvement. *Science* 244:1293–1299.

Shimamoto, K., Terada, R., Izawa, T., and Fujimoto, H. 1989. Fertile transgenic rice plants regenerated from transformed protoplasts. *Nature* 338:274–276.

Chilton, M.-D. 1983. A vector for introducing new genes into plants. *Sci. Am.* 248(6):50–59.

Hansen, G., and Wright, M. S. 1999. Recent advances in the transformation of plants. *Trends Plant Sci.* 4:226–231.

Hammond, J. 1999. Overview: The many uses of transgenic plants. *Curr. Top. Microbiol. Immunol.* 240:1–20.

Finer, J. J., Finer, K. R., and Ponappa, T. 1999. Particle bombardment mediated transformation. *Curr. Top. Microbiol. Immunol.* 240: 60–80.

Amyotrophic Lateral Sclerosis

Siddique, T., Figlewicz, D. A., Pericak-Vance, M. A., Haines, J. L., Rouleau, G., Jeffers, A. J., Sapp, P., Hung, W.-Y., Bebout, J., McKenna-Yasek, D., et al. 1991. Linkage of a gene causing familial amyotrophic lateral sclerosis to chromosome 21 and evidence of genetic-locus heterogeneity. *New Engl. J. Med.* 324:1381–1384.

Rosen, D. R., Siddique, T., Patterson, D., Figlewicz, D. A., Sapp, P., Hentati, A., Donaldson, D., Goto, J., O'Regan, J. P., Deng, H.-X., et al. 1993. Mutations in Cu/Zn superoxide dismutase gene are associated with familial amyotrophic lateral sclerosis. *Nature* 362:59–62.

Gurney, M. E., Pu, H., Chiu, A. Y., Dal Canto, M. C., Polchow, C. Y., Alexander, D. D., Caliendo, J., Hentati, A., Kwon, Y. W., Deng, H.-X., et al. 1994. Motor neuron degeneration in mice that express a human Cu, Zn superoxide dismutase mutation. *Science* 264:1772–1774.

Borchelt, D. R., Lee, M. K., Slunt, H. S., Guarnieri, M., Xu, Z.-S., Wong, P. C., Brown, R. H., Jr., Price, D. L., Sisodia, S. S., and Cleveland, D. W. 1994. Superoxide dismutase 1 with mutations linked to familial amyotrophic lateral sclerosis possesses significant activity. *Proc. Natl. Acad. Sci. U.S.A.* 91:8292–8296.

Chapter 6

Where to Start

Hogewer, P. 2011. The roots of bioinformatics in theoretical biology. *PLoS Comp. Biol.* 7:e1002021.

Searls, D. B. 2010. The roots of bioinformatics. *PLoS Comp. Biol.* 6: e1000809.

Books

Claverie, J.-M., and Notredame, C. 2003. *Bioinformatics for Dummies*. Wiley.

Pevsner, J. 2003. *Bioinformatics and Functional Genomics*. Wiley-Liss.

Doolittle, R. F. 1987. *Of URFS and ORFS*. University Science Books.

Sequence Alignment

Schaffer, A. A., Aravind, L., Madden, T. L., Shavirin, S., Spouge, J. L., Wolf, Y. I., Koonin, E. V., and Altschul, S. F. 2001. Improving the accuracy of PSI-BLAST protein database searches with composition-based statistics and other refinements. *Nucleic Acids Res.* 29: 2994–3005.

Henikoff, S., and Henikoff, J. G. 1992. Amino acid substitution matrices from protein blocks. *Proc. Natl. Acad. Sci. U.S.A.* 89:10915–10919.

Johnson, M. S., and Overington, J. P. 1993. A structural basis for sequence comparisons: An evaluation of scoring methodologies. *J. Mol. Biol.* 233:716–738.

Eddy, S. R. 2004. Where did the BLOSUM62 alignment score matrix come from? *Nat. Biotechnol.* 22:1035–1036.

Aravind, L., and Koonin, E. V. 1999. Gleaning non-trivial structural, functional and evolutionary information about proteins by iterative database searches. *J. Mol. Biol.* 287:1023–1040.

Altschul, S. F., Madden, T. L., Schaffer, A. A., Zhang, J., Zhang, Z., Miller, W., and Lipman, D. J. 1997. Gapped BLAST and PSI-BLAST: A new generation of protein database search programs. *Nucleic Acids Res.* 25:3389–3402.

Structure Comparison

Orengo, C. A., Bray, J. E., Buchan, D. W., Harrison, A., Lee, D., Pearl, F. M., Sillitoe, I., Todd, A. E., and Thornton, J. M. 2002. The CATH protein family database: A resource for structural and functional annotation of genomes. *Proteomics* 2:11–21.

Bashford, D., Chothia, C., and Lesk, A. M. 1987. Determinants of a protein fold: Unique features of the globin amino acid sequences. *J. Mol. Biol.* 196:199–216.

Harutyunyan, E. H., Safonova, T. N., Kuranova, I. P., Popov, A. N., Teplyakov, A. V., Obmolova, G. V., Rusakov, A. A., Vainshtein, B. K., Dodson, G. G., Wilson, J. C., et al. 1995. The structure of deoxy- and oxy-leghaemoglobin from lupin. *J. Mol. Biol.* 251:104–115.

Flaherty, K. M., McKay, D. B., Kabsch, W., and Holmes, K. C. 1991. Similarity of the three-dimensional structures of actin and the ATPase fragment of a 70-kDa heat shock cognate protein. *Proc. Natl. Acad. Sci. U.S.A.* 88:5041–5045.

Murzin, A. G., Brenner, S. E., Hubbard, T., and Chothia, C. 1995. SCOP: A structural classification of proteins database for the investigation of sequences and structures. *J. Mol. Biol.* 247:536–540.

Hadley, C., and Jones, D. T. 1999. A systematic comparison of protein structure classification: SCOP, CATH and FSSP. *Struct. Fold. Des.* 7:1099–1112.

Domain Detection

Marchler-Bauer, A., Anderson, J. B., DeWeese-Scott, C., Fedorova, N. D., Geer, L. Y., He, S., Hurwitz, D. I., Jackson, J. D., Jacobs, A. R., Lanczycki, C. J., et al. 2003. CDD: A curated Entrez database of conserved domain alignments. *Nucleic Acids Res.* 31:383–387.

Ploegman, J. H., Drent, G., Kalk, K. H., and Hol, W. G. 1978. Structure of bovine liver rhodanese I: Structure determination at 2.5 Å resolution and a comparison of the conformation and sequence of its two domains. *J. Mol. Biol.* 123:557–594.

Nikolov, D. B., Hu, S. H., Lin, J., Gasch, A., Hoffmann, A., Horikoshi, M., Chua, N. H., Roeder, R. G., and Burley, S. K. 1992. Crystal structure of TFIID TATA-box binding protein. *Nature* 360:40–46.

Doolittle, R. F. 1995. The multiplicity of domains in proteins. *Annu. Rev. Biochem.* 64:287–314.

Heger, A., and Holm, L. 2000. Rapid automatic detection and alignment of repeats in protein sequences. *Proteins* 41:224–237.

Evolutionary Trees

Wolf, Y. I., Rogozin, I. B., Grishin, N. V., and Koonin, E. V. 2002. Genome trees and the tree of life. *Trends Genet.* 18:472–479.

Doolittle, R. F. 1992. Stein and Moore Award address. Reconstructing history with amino acid sequences. *Protein Sci.* 1:191–200.

Zuckerkandl, E., and Pauling, L. 1965. Molecules as documents of evolutionary history. *J. Theor. Biol.* 8:357–366.

Schönknecht, G., Chen, W.-H., Ternes, C. M., Barbier, G. G., Shrestha, R. P., Stanke, M., Bräutigam, A., Baker, B. J., Banfield, J. F., Garavito, R. M., et al. 2013. Gene transfer from bacteria and archaea facilitated evolution of an extremophilic eukaryote. *Science* 339:1207–1210.

Ancient DNA

Prüfer, K., Racimo, F., Patterson, N., Jay, F., Sankararaman, S., Sawyer, S., Heinze, A., Renaud, G., Sudmant, P. H., de Filippo C., et al. 2014. The complete genome sequence of a Neanderthal from the Altai Mountains. *Nature* 505:43–49.

Meyer, M., Kircher, M., Gansauge, M. T., Li, H., Racimo, F., Mallick, S., Schraiber, J. G., Jay, F., Prüfer, K., de Filippo, C., et al. 2012. A high-coverage genome sequence from an archaic Denisovan individual. *Science* 338:222–226.

Green, R. E., Malaspinas, A.-S., Krause, J., Briggs, A. W., Johnson, P. L. F., Uhler, C., Meyer, M., Good, J. M., Maricic, T., Stenzel, U., et al. 2008. A complete Neandertal mitochondrial genome sequence determined by high-throughput sequencing. *Cell* 134:416–426.

Pääbo, S., Poinar, H., Serre, D., Jaenicke-Despres, V., Hebler, J., Rohland, N., Kuch, M., Krause, J., Vigilant, L., and Hofreiter, M. 2004. Genetic analyses from ancient DNA. *Annu. Rev. Genet.* 38:645–679.

Evolution in the Laboratory

Sassanfar, M., and Szostak, J. W. 1993. An RNA motif that binds ATP. *Nature* 364:550–553.

Gold, L., Polisky, B., Uhlenbeck, O., and Yarus, M. 1995. Diversity of oligonucleotide functions. *Annu. Rev. Biochem.* 64:763–797.

Wilson, D. S., and Szostak, J. W. 1999. In vitro selection of functional nucleic acids. *Annu. Rev. Biochem.* 68:611–647.

Hermann, T., and Patel, D. J. 2000. Adaptive recognition by nucleic acid aptamers. *Science* 287:820–825.

Keefe, A. D., Pai, S., and Ellington, A. 2010. Aptamers as therapeutics. *Nat. Rev. Drug Discov.* 9:537–550.

Radom, F., Jurek, P. M., Mazurek, M. P., Otlewski, J., and Jeleń, F. 2013. Aptamers: Molecules of great potential. *Biotechnol. Adv.* 31:1260–1274.

Web Sites

The Protein Data Bank (PDB) site is the repository for three-dimensional macromolecular structures. It currently contains more than 100,000 structures. (http://www.pdb.org).

National Center for Biotechnology Information (NCBI) contains molecular biological databases and software for analysis. (http://www.ncbi.nlm.nih.gov/).

Chapter 7

Where to Start

Changeux, J.-P. 2011. 50th anniversary of the word "Allosteric." *Protein Sci.* 20:1119–1124.

Perutz, M. F. 1978. Hemoglobin structure and respiratory transport. *Sci. Am.* 239(6):92–125.

Perutz, M. F. 1980. Stereochemical mechanism of oxygen transport by haemoglobin. *Proc. R. Soc. Lond. Biol. Sci.* 208:135–162.

Kilmartin, J. V. 1976. Interaction of haemoglobin with protons, CO_2, and 2,3-diphosphoglycerate. *Brit. Med. Bull.* 32:209–222.

Structure

Kendrew, J. C., Bodo, G., Dintzis, H. M., Parrish, R. G., Wyckoff, H., and Phillips, D. C. 1958. A three-dimensional model of the myoglobin molecule obtained by x-ray analysis. *Nature* 181:662–666.

Shaanan, B. 1983. Structure of human oxyhaemoglobin at 2.1 Å resolution. *J. Mol. Biol.* 171:31–59.

Frier, J. A., and Perutz, M. F. 1977. Structure of human foetal deoxyhaemoglobin. *J. Mol. Biol.* 112:97–112.

Perutz, M. F. 1969. Structure and function of hemoglobin. *Harvey Lect.* 63:213–261.

Perutz, M. F. 1962. Relation between structure and sequence of haemoglobin. *Nature* 194:914–917.

Harrington, D. J., Adachi, K., and Royer, W. E., Jr. 1997. The high resolution crystal structure of deoxyhemoglobin S. *J. Mol. Biol.* 272:398–407.

Interaction of Hemoglobin with Allosteric Effectors

Benesch, R., and Beesch, R. E. 1969. Intracellular organic phosphates as regulators of oxygen release by haemoglobin. *Nature* 221:618–622.

Fang, T. Y., Zou, M., Simplaceanu, V., Ho, N. T., and Ho, C. 1999. Assessment of roles of surface histidyl residues in the molecular basis of the Bohr effect and of β 143 histidine in the binding of 2,3-bisphosphoglycerate in human normal adult hemoglobin. *Biochemistry* 38:13423–13432.

Arnone, A. 1992. X-ray diffraction study of binding of 2,3-diphosphoglycerate to human deoxyhaemoglobin. *Nature* 237:146–149.

Models for Cooperativity

Changeux, J.-P. 2012. Allostery and the Monod-Wyman-Changeux model after 50 years. *Annu. Rev. Biophys.* 41:103–133.

Monod, J., Wyman, J., and Changeux, J.-P. 1965. On the nature of allosteric interactions: A plausible model. *J. Mol. Biol.* 12:88–118.

Koshland, D. L., Jr., Nemethy, G., and Filmer, D. 1966. Comparison of experimental binding data and theoretical models in proteins containing subunits. *Biochemistry* 5:365–385.

Ackers, G. K., Doyle, M. L., Myers, D., and Daugherty, M. A. 1992. Molecular code for cooperativity in hemoglobin. *Science* 255:54–63.

Sickle-Cell Anemia and Thalassemia

Herrick, J. B. 1910. Peculiar elongated and sickle-shaped red blood corpuscles in a case of severe anemia. *Arch. Intern. Med.* 6:517–521.

Pauling, L., Itano, H. A., Singer, S. J., and Wells, L. C. 1949. Sickle cell anemia: A molecular disease. *Science* 110:543–548.

Ingram, V. M. 1957. Gene mutation in human hemoglobin: The chemical difference between normal and sickle cell haemoglobin. *Nature* 180:326–328.

Eaton, W. A., and Hofrichter, J. 1990. Sickle cell hemoglobin polymerization. *Adv. Prot. Chem.* 40:63–279.

Weatherall, D. J. 2001. Phenotype genotype relationships in monogenic disease: Lessons from the thalassemias. *Nat. Rev. Genet.* 2:245–255.

Tsaras, G., Owusu-Ansah, A., Boateng, F. O., and Amoateng-Adjepong, Y. 2009. Complications associated with sickle cell trait: A brief narrative review. *Am. J. Med.* 122:507–512.

Globin-Binding Proteins and Other Globins

Helbo, S., Weber, R. E., and Fago, A. 2013. Expression patterns and adaptive functional diversity of vertebrate myoglobins. *Biochim. Biophys. Acta* 1834:1832–1839.

Kihm, A. J., Kong, Y., Hong, W., Russell, J. E., Rouda, S., Adachi, K., Simon, M. C., Blobel, G. A., and Weiss, M. J. 2002. An abundant erythroid protein that stabilizes free α-haemoglobin. *Nature* 417:758–763.

Feng, L., Zhou, S., Gu, L., Gell, D. A., Mackay, J. P., Weiss, M. J., Gow, A. J., and Shi, Y. 2005. Structure of oxidized α-haemoglobin bound to AHSP reveals a protective mechanism for haem. *Nature* 435:697–701.

Yu, X., Kong, Y., Dore, L. C., Abdulmalik, O., Katein, A. M., Zhou, S., Choi, J. K., Gell, D., Mackay, J. P., Gow, A. J., et al. 2007. An erythroid chaperone that facilitates folding of α-globin subunits for hemoglobin synthesis. *J. Clin. Invest.* 117:1856–1865.

Burmester, T., Haberkamp, M., Mitz, S., Roesner, A., Schmidt, M., Ebner, B., Gerlach, F., Fuchs, C., and Hankeln, T. 2004. Neuroglobin and cytoglobin: Genes, proteins and evolution. *IUBMB Life* 56:703–707.

Hankeln, T., Ebner, B., Fuchs, C., Gerlach, F., Haberkamp, M., Laufs, T. L., Roesner, A., Schmidt, M., Weich, B., Wystub, S., et al. 2005. Neuroglobin and cytoglobin in search of their role in the vertebrate globin family. *J. Inorg. Biochem.* 99:110–119.

Burmester, T., Ebner, B., Weich, B., and Hankeln, T. 2002. Cytoglobin: A novel globin type ubiquitously expressed in vertebrate tissues. *Mol. Biol. Evol.* 19:416–421.

Zhang, C., Wang, C., Deng, M., Li, L., Wang, H., Fan, M., Xu, W., Meng, F., Qian, L., and He, F. 2002. Full-length cDNA cloning of human neuroglobin and tissue expression of rat neuroglobin. *Biochem. Biophys. Res. Commun.* 290:1411–1419.

Chapter 8

Where to Start

Zalatan, J. G., and Herschlag, D. 2009. The far reaches of enzymology. *Nat. Chem. Biol.* 5:516–520.

Hammes, G. G. 2008. How do enzymes really work? *J. Biol. Chem.* 283:22337–22346.

Koshland, D. E., Jr. 1987. Evolution of catalytic function. *Cold Spring Harbor Symp. Quant. Biol.* 52:1–7.

Jencks, W. P. 1987. Economics of enzyme catalysis. *Cold Spring Harbor Symp. Quant. Biol.* 52:65–73.

Lerner, R. A., and Tramontano, A. 1988. Catalytic antibodies. *Sci. Am.* 258(3):58–70.

Books

Cook, P. F., and Cleland, W. W. 2007. *Enzyme Kinetics and Mechanism.* Garland Press.

Fersht, A. 1999. *Structure and Mechanism in Protein Science: A Guide to Enzyme Catalysis and Protein Folding.* W. H. Freeman and Company.

Walsh, C. 1979. *Enzymatic Reaction Mechanisms.* W. H. Freeman and Company.

Bender, M. L., Bergeron, R. J., and Komiyama, M. 1984. *The Bioorganic Chemistry of Enzymatic Catalysis.* Wiley-Interscience.

Abelson, J. N., and Simon, M. I. (Eds.). 1992. *Methods in Enzymology.* Academic Press.

Friedmann, H. C. (Ed.). 1981. *Benchmark Papers in Biochemistry,* vol. 1, *Enzymes.* Hutchinson Ross.

Transition-State Stabilization, Analogs, and Other Enzyme Inhibitors

Schramm, V. L. 2007. Enzymatic transition state theory and transition state analog design. *J. Biol. Chem.* 282:28297–28300.

Pauling, L. 1948. Nature of forces between large molecules of biological interest. *Nature* 161:707–709.

Leinhard, G. E. 1973. Enzymatic catalysis and transition-state theory. *Science* 180:149–154.

Kraut, J. 1988. How do enzymes work? *Science* 242:533–540.

Waxman, D. J., and Strominger, J. L. 1983. Penicillin-binding proteins and the mechanism of action of β-lactam antibiotics. *Annu. Rev. Biochem.* 52:825–869.

Abraham, E. P. 1981. The β-lactam antibiotics. *Sci. Am.* 244(6):76–86.

Walsh, C. T. 1984. Suicide substrates, mechanism-based enzyme inactivators: Recent developments. *Annu. Rev. Biochem.* 53:493–535.

Catalytic Antibodies

Hilvert, D. 2000. Critical analysis of antibody catalysis. *Annu. Rev. Biochem.* 69:751–794.

Wade, H., and Scanlan, T. S. 1997. The structural and functional basis of antibody catalysis. *Annu. Rev. Biophys. Biomol. Struct.* 26:461–493.

Lerner, R. A., Benkovic, S. J., and Schultz, P. G. 1991. At the crossroads of chemistry and immunology: Catalytic antibodies. *Science* 252:659–667.

Cochran, A. G., and Schultz, P. G. 1990. Antibody-catalyzed porphyrin metallation. *Science* 249:781–783.

Enzyme Kinetics and Mechanisms

Hammes, G. G., Benkovic, S. J., and Hammes-Schiffer, S. 2011. Flexibility, Diversity, and Cooperativity: Pillars of Enzyme Catalysis. *Biochemistry* 50:10422–10430.

Johnson, K. A., and Goody, R. S. 2011. The Original Michaelis Constant: Translation of the 1913 Michaelis–Menten Paper. *Biochemistry* 50:8264–8269.

Hammes-Schiller, S., and Benkovic, S. J. 2006. Relating protein motion to catalysis. *Annu. Rev. Biochem.* 75:519–541.

Benkovic, S. J., and Hammes-Schiller, S. 2003. A perspective on enzyme catalysis. *Science* 301:1196–1202.

Hur, S., and Bruice, T. C. 2003. The near attack conformation approach to the study of the chorismate to prephenate reaction. *Proc. Natl. Acad. Sci. U.S.A.* 100:12015–12020.

Miles, E. W., Rhee, S., and Davies, D. R. 1999. The molecular basis of substrate channeling. *J. Biol. Chem.* 274:12193–12196.

Warshel, A. 1998. Electrostatic origin of the catalytic power of enzymes and the role of preorganized active sites. *J. Biol. Chem.* 273:27035–27038.

Cannon, W. R., and Benkovic, S. J. 1999. Solvation, reorganization energy, and biological catalysis. *J. Biol. Chem.* 273:26257–26260.

Cleland, W. W., Frey, P. A., and Gerlt, J. A. 1998. The low barrier hydrogen bond in enzymatic catalysis. *J. Biol. Chem.* 273: 25529–25532.

Romesberg, F. E., Santarsiero, B. D., Spiller, B., Yin, J., Barnes, D., Schultz, P. G., and Stevens, R. C. 1998. Structural and kinetic evidence for strain in biological catalysis. *Biochemistry* 37:14404–14409.

Fersht, A. R., Leatherbarrow, R. J., and Wells, T. N. C. 1986. Binding energy and catalysis: A lesson from protein engineering of the tyrosyl-tRNA synthetase. *Trends Biochem. Sci.* 11:321–325.

Jencks, W. P. 1975. Binding energy, specificity, and enzymic catalysis: The Circe effect. *Adv. Enzymol.* 43:219–410.

Knowles, J. R., and Albery, W. J. 1976. Evolution of enzyme function and the development of catalytic efficiency. *Biochemistry* 15:5631–5640.

Single Molecule Studies

Allewell, N. M. 2010. Thematic Minireview Series: Single-molecule Measurements in Biochemistry and Molecular Biology. *J. Biol. Chem.* 285:18959–18983. A series of reviews on single-molecule studies.

Min, W., English, B. P., Lou, G., Cherayil, B. J., Kou, S. C., and Xie, X. S. 2005. Fluctuating Enzymes: Lessons from Single-Molecule Studies. *Acc. Chem. Res.* 38: 923–931.

Xie, X. S., and Lu, H. P. 1999. Single-molecule enzymology. *J. Biol. Chem.* 274:15967–15970.

Lu, H. P., Xun, L., and Xie, X. S. 1998. Single-molecule enzymatic dynamics. *Science* 282:1877–1882.

Chapter 9

Where to Start

Stroud, R. M. 1974. A family of protein-cutting proteins. *Sci. Am.* 231(1):74–88.

Kraut, J. 1977. Serine proteases: Structure and mechanism of catalysis. *Annu. Rev. Biochem.* 46:331–358.

Lindskog, S. 1997. Structure and mechanism of carbonic anhydrase. *Pharmacol. Ther.* 74:1–20.

Jeltsch, A., Alves, J., Maass, G., and Pingoud, A. 1992. On the catalytic mechanism of EcoRI and EcoRV: A detailed proposal based on biochemical results, structural data and molecular modelling. *FEBS Lett.* 304:4–8.

Bauer, C. B., Holden, H. M., Thoden, J. B., Smith, R., and Rayment, I. 2000. X-ray structures of the apo and MgATP-bound states of *Dictyostelium discoideum* myosin motor domain. *J. Biol. Chem.* 275:38494–38499.

Lolis, E., and Petsko, G. A. 1990. Transition-state analogues in protein crystallography: Probes of the structural source of enzyme catalysis. *Annu. Rev. Biochem.* 59:597–630.

Books

Fersht, A. 1999. *Structure and Mechanism in Protein Science: A Guide to Enzyme Catalysis and Protein Folding.* W. H. Freeman and Company.

Silverman, R. B. 2000. *The Organic Chemistry of Enzyme-Catalyzed Reactions*. Academic Press.

Page, M., and Williams, A. 1997. *Organic and Bio-organic Mechanisms*. Addison Wesley Longman.

Chymotrypsin and Other Serine Proteases

Fastrez, J., and Fersht, A. R. 1973. Demonstration of the acyl-enzyme mechanism for the hydrolysis of peptides and anilides by chymotrypsin. *Biochemistry* 12:2025–2034.

Sigler, P. B., Blow, D. M., Matthews, B. W., and Henderson, R. 1968. Structure of crystalline-chymotrypsin II: A preliminary report including a hypothesis for the activation mechanism. *J. Mol. Biol.* 35:143–164.

Kossiakoff, A. A., and Spencer, S. A. 1981. Direct determination of the protonation states of aspartic acid-102 and histidine-57 in the tetrahedral intermediate of the serine proteases: Neutron structure of trypsin. *Biochemistry* 20:6462–6474.

Carter, P., and Wells, J. A. 1988. Dissecting the catalytic triad of a serine protease. *Nature* 332:564–568.

Carter, P., and Wells, J. A. 1990. Functional interaction among catalytic residues in subtilisin BPN′. *Proteins* 7:335–342.

Koepke, J., Ermler, U., Warkentin, E., Wenzl, G., and Flecker, P. 2000. Crystal structure of cancer chemopreventive Bowman-Birk inhibitor in ternary complex with bovine trypsin at 2.3 Å resolution: Structural basis of Janus-faced serine protease inhibitor specificity. *J. Mol. Biol.* 298:477–491.

Gaboriaud, C., Rossi, V., Bally, I., Arlaud, G. J., and Fontecilla-Camps, J. C. 2000. Crystal structure of the catalytic domain of human complement C1s: A serine protease with a handle. *EMBO J.* 19:1755–1765.

Bachovchin D. A., and Cravatt B. F. 2012. The pharmacological landscape and therapeutic potential of serine hydrolases. *Nature Reviews Drug Discovery*. 11:52–68.

Other Proteases

Vega, S., Kang, L. W., Velazquez-Campoy, A., Kiso, Y., Amzel, L. M., and Freire, E. 2004. A structural and thermodynamic escape mechanism from a drug resistant mutation of the HIV-1 protease. *Proteins* 55:594–602.

Kamphuis, I. G., Kalk, K. H., Swarte, M. B., and Drenth, J. 1984. Structure of papain refined at 1.65 Å resolution. *J. Mol. Biol.* 179:233–256.

Kamphuis, I. G., Drenth, J., and Baker, E. N. 1985. Thiol proteases: Comparative studies based on the high-resolution structures of papain and actinidin, and on amino acid sequence information for cathepsins B and H, and stem bromelain. *J. Mol. Biol.* 182:317–329.

Sivaraman, J., Nagler, D. K., Zhang, R., Menard, R., and Cygler, M. 2000. Crystal structure of human procathepsin X: A cysteine protease with the proregion covalently linked to the active site cysteine. *J. Mol. Biol.* 295:939–951.

Davies, D. R. 1990. The structure and function of the aspartic proteinases. *Annu. Rev. Biophys. Biophys. Chem.* 19:189–215.

Dorsey, B. D., Levin, R. B., McDaniel, S. L., Vacca, J. P., Guare, J. P., Darke, P. L., Zugay, J. A., Emini, E. A., Schleif, W. A., Quintero, J. C., et al. 1994. L-735,524: The design of a potent and orally bio-available HIV protease inhibitor. *J. Med. Chem.* 37:3443–3451.

Chen, Z., Li, Y., Chen, E., Hall, D. L., Darke, P. L., Culberson, C., Shafer, J. A., and Kuo, L. C. 1994. Crystal structure at 1.9-Å resolution of human immunodeficiency virus (HIV) II protease complexed with L-735,524, an orally bioavailable inhibitor of the HIV proteases. *J. Biol. Chem.* 269:26344–26348.

Ollis, D. L., Cheah, E., Cygler, M., Dijkstra, B., Frolow, F., Franken, S. M., Harel, M., Remington, S. J., Silman, I., Schrag, J., et al. 1992. The α/β hydrolase fold. *Protein Eng.* 5:197–211.

Carbonic Anhydrase

Lindskog, S., and Coleman, J. E. 1973. The catalytic mechanism of carbonic anhydrase. *Proc. Natl. Acad. Sci. U.S.A.* 70:2505–2508.

Kannan, K. K., Notstrand, B., Fridborg, K., Lovgren, S., Ohlsson, A., and Petef, M. 1975. Crystal structure of human erythrocyte carbonic anhydrase B: Three-dimensional structure at a nominal 2.2-Å resolution. *Proc. Natl. Acad. Sci. U.S.A.* 72:51–55.

Boriack-Sjodin, P. A., Zeitlin, S., Chen, H. H., Crenshaw, L., Gross, S., Dantanarayana, A., Delgado, P., May, J. A., Dean, T., and Christianson, D. W. 1998. Structural analysis of inhibitor binding to human carbonic anhydrase II. *Protein Sci.* 7:2483–2489.

Wooley, P. 1975. Models for metal ion function in carbonic anhydrase. *Nature* 258:677–682.

Jonsson, B. H., Steiner, H., and Lindskog, S. 1976. Participation of buffer in the catalytic mechanism of carbonic anhydrase. *FEBS Lett.* 64:310–314.

Sly, W. S., and Hu, P. Y. 1995. Human carbonic anhydrases and carbonic anhydrase deficiencies. *Annu. Rev. Biochem.* 64:375–401.

Maren, T. H. 1988. The kinetics of HCO_3^- synthesis related to fluid secretion, pH control, and CO_2 elimination. *Annu. Rev. Physiol.* 50:695–717.

Roy, A., and Taraphder, S. 2010. Role of protein motions on proton transfer pathways in human carbonic anhydrase II. *Biochim. Biophys. Acta* 1804:352–361.

Restriction Enzymes

Selvaraj, S., Kono, H., and Sarai, A. 2002. Specificity of protein-DNA recognition revealed by structure-based potentials: Symmetric/asymmetric and cognate/non-cognate binding. *J. Mol. Biol.* 322:907–915.

Winkler, F. K., Banner, D. W., Oefner, C., Tsernoglou, D., Brown, R. S., Heathman, S. P., Bryan, R. K., Martin, P. D., Petratos, K., and Wilson, K. S. 1993. The crystal structure of EcoRV endonuclease and of its complexes with cognate and non-cognate DNA fragments. *EMBO J.* 12:1781–1795.

Kostrewa, D., and Winkler, F. K. 1995. Mg^{2+} binding to the active site of EcoRV endonuclease: A crystallographic study of complexes with substrate and product DNA at 2 Å resolution. *Biochemistry* 34:683–696.

Athanasiadis, A., Vlassi, M., Kotsifaki, D., Tucker, P. A., Wilson, K. S., and Kokkinidis, M. 1994. Crystal structure of PvuII endonuclease reveals extensive structural homologies to EcoRV. *Nat. Struct. Biol.* 1:469–475.

Sam, M. D., and Perona, J. J. 1999. Catalytic roles of divalent metal ions in phosphoryl transfer by EcoRV endonuclease. *Biochemistry* 38:6576–6586.

Jeltsch, A., and Pingoud, A. 1996. Horizontal gene transfer contributes to the wide distribution and evolution of type II restriction-modification systems. *J. Mol. Evol.* 42:91–96.

Advani S., Mishra P., Dubey S., and Thakur S. 2010. Categoric prediction of metal ion mechanisms in the active sites of 17 select type II restriction endonucleases. *Biochem. Biophys. Res. Commun.* 402:177–179.

Myosins

Grigorenko, B. L., Rogov, A. V., Topol, I. A., Burt, S. K., Martinez, H. M., and Nemukhin, A. V. 2007. Mechanism of the myosin catalyzed hydrolysis of ATP as rationalized by molecular modeling. *Proc. Natl. Acad. Sci. U.S.A.* 104:7057–7061.

Gulick, A. M., Bauer, C. B., Thoden, J. B., and Rayment, I. 1997. X-ray structures of the MgADP, MgATPγ S, and MgAMPPNP complexes of the *Dictyostelium discoideum* myosin motor domain. *Biochemistry* 36:11619–11628.

Kovacs, M., Malnasi-Csizmadia, A., Woolley, R. J., and Bagshaw, C. R. 2002. Analysis of nucleotide binding to *Dictyostelium* myosin II motor domains containing a single tryptophan near the active site. *J. Biol. Chem.* 277:28459–28467.

Kuhlman, P. A., and Bagshaw, C. R. 1998. ATPase kinetics of the *Dictyostelium discoideum* myosin II motor domain. *J. Muscle Res. Cell Motil.* 19:491–504.

Smith, C. A., and Rayment, I. 1996. X-ray structure of the magnesium(II) ADP vanadate complex of the *Dictyostelium discoideum* myosin motor domain to 1.9 Å resolution. *Biochemistry* 35:5404–5417.

Yildiz A., Forkey J. N., McKinney S. A., Ha T., Goldman Y. E., and Selvin P. R. 2003. Myosin V walks hand-over-hand: Single fluorophore imaging with 1.5-nm localization. *Science*. 300:2061–2065.

Chapter 10

Where to Start

Kyriakis, J. M. 2014. In the beginning, there was protein phosphorylation. *J. Biol. Chem.* 289:9460—9462.

Changeux, J.-P. 2011. 50th anniversary of the word "Allosteric." *Protein Sci.* 20:1119–1124.

Kantrowitz, E. R., and Lipscomb, W. N. 1990. *Escherichia coli* aspartate transcarbamoylase: The molecular basis for a concerted allosteric transition. *Trends Biochem. Sci.* 15:53–59.

Schachman, H. K. 1988. Can a simple model account for the allosteric transition of aspartate transcarbamoylase? *J. Biol. Chem.* 263:18583–18586.

Neurath, H. 1989. Proteolytic processing and physiological regulation. *Trends Biochem. Sci.* 14:268–271.

Bode, W., and Huber, R. 1992. Natural protein proteinase inhibitors and their interaction with proteinases. *Eur. J. Biochem.* 204: 433–451.

Aspartate Transcarbamoylase and Allosteric Interactions

Changeux, J.-P. 2012. Allostery and the Monod-Wyman-Changeux Model After 50 Years. *Annu. Rev. Biophys.* 41:103–133.

Peterson, A. W., Cockrell, G. M., and Kantrowitz, E. R. 2012. A second allosteric site in *Escherichia coli* aspartate transcarbamoylase. *Biochemistry* 51:4776−4778.

Rabinowitz, J. D., Hsiao, J. J., Gryncel, K. R., Kantrowitz, E. R., Feng, X.-J., Li, G., and Rabitz H. 2008. Dissecting enzyme regulation by multiple allosteric effectors: Nucleotide regulation of aspartate transcarbamoylase. *Biochemistry* 47:5881–5888.

West, J. M., Tsuruta, H., and Kantrowitz, E. R. 2004. A fluorescent probe-labeled *Escherichia coli* aspartate transcarbamoylase that monitors the allosteric conformation state. *J. Biol. Chem.* 279:945–951.

Endrizzi, J. A., Beernink, P. T., Alber, T., and Schachman, H. K. 2000. Binding of bisubstrate analog promotes large structural changes in the unregulated catalytic trimer of aspartate transcarbamoylase: Implications for allosteric regulation. *Proc. Natl. Acad. Sci. U.S.A.* 97:5077–5082.

Beernink, P. T., Endrizzi, J. A., Alber, T., and Schachman, H. K. 1999. Assessment of the allosteric mechanism of aspartate transcarbamoylase based on the crystalline structure of the unregulated catalytic subunit. *Proc. Natl. Acad. Sci. U.S.A.* 96:5388–5393.

Wales, M. E., Madison, L. L., Glaser, S. S., and Wild, J. R. 1999. Divergent allosteric patterns verify the regulatory paradigm for aspartate transcarbamoylase. *J. Mol. Biol.* 294:1387–1400.

Newell, J. O., Markby, D. W., and Schachman, H. K. 1989. Cooperative binding of the bisubstrate analog *N*-(phosphonacetyl)-L-aspartate to aspartate transcarbamoylase and the heterotropic effects of ATP and CTP. *J. Biol. Chem.* 264:2476–2481.

Stevens, R. C., Gouaux, J. E., and Lipscomb, W. N. 1990. Structural consequences of effector binding to the T state of aspartate carbamoyl-transferase: Crystal structures of the unligated and ATP- and CTP-complexed enzymes at 2.6-Å resolution. *Biochemistry* 29:7691–7701.

Gouaux, J. E., and Lipscomb, W. N. 1990. Crystal structures of phosphonoacetamide ligated T and phosphonoacetamide and malonate ligated R states of aspartate carbamoyltransferase at 2.8-Å resolution and neutral pH. *Biochemistry* 29:389–402.

Labedan, B., Boyen, A., Baetens, M., Charlier, D., Chen, P., Cunin, R., Durbeco, V., Glansdorff, N., Herve, G., Legrain, C., et al. 1999. The evolutionary history of carbamoyltransferases: A complex set of paralogous genes was already present in the last universal common ancestor. *J. Mol. Evol.* 49:461–473.

Covalent Modification

Endicott, J. A., Noble, M. E. M., and Johnson, L. N. 2012. The structural basis for control of eukaryotic protein kinases. *Annu. Rev. Biochem.* 81:587–613.

Tarrant, M. K., and Cole, P. A. 2009. The chemical biology of protein phosphorylation *Annu. Rev. Biochem.* 78:797–825.

Guarente, L. 2011. The logic linking protein acetylation and metabolism. *Cell Metab.* 14:151–153.

Guan, K-L., and Xiong, Y. 2011. Regulation of intermediary metabolism by protein acetylation. *Trends Biochem. Sci.* 36:108–116.

Johnson, L. N., and Barford, D. 1993. The effects of phosphorylation on the structure and function of proteins. *Annu. Rev. Biophys. Biomol. Struct.* 22:199–232.

Barford, D., Das, A. K., and Egloff, M. P. 1998. The structure and mechanism of protein phosphatases: Insights into catalysis and regulation. *Annu. Rev. Biophys. Biomol. Struct.* 27:133–164.

Protein Kinase A

Taylor, S. S., Ilouz, R., Zhang, P., and Kornev, A. P. 2012. Assembly of allosteric macromolecular switches: Lessons from PKA. *Nature Rev. Mol. Cell Biol.* 13:646–658.

Zhang, P., Smith-Nguyen, E. V., Keshwani, M. M., Deal, M. S., Kornev, A. P., and Taylor, S. S. 2012. Structure and allostery of the PKA RIIb tetrameric holoenzyme. *Science* 334:712–716.

Taylor, S. S., and Kornev, A. P. 2011. Protein kinases: evolution of dynamic regulatory proteins. *Trends Biochem. Sci.* 36:65–77.

Pearlman, S. M., Serber, Z., and Ferrell Jr., J. E. 2011. A mechanism for the evolution of phosphorylation sites. *Cell* 147:934–946.

Knighton, D. R., Zheng, J. H., TenEyck, L., Xuong, N. H., Taylor, S. S., and Sowadski, J. M. 1991. Structure of a peptide inhibitor bound to the catalytic subunit of cyclic adenosine monophosphate-dependent protein kinase. *Science* 253:414–420.

Zymogen Activation

Artenstein, A. W., and Opal, S. M. 2011. Proprotein convertases in health and disease. *New Engl. J. Med.* 65:2507–2518.

Neurath, H. 1986. The versatility of proteolytic enzymes. *J. Cell. Biochem.* 32:35–49.

Bode, W., and Huber, R. 1986. Crystal structure of pancreatic serine endopeptidases. In *Molecular and Cellular Basis of Digestion* (pp. 213–234), edited by P. Desnuelle, H. Sjostrom, and O. Noren. Elsevier.

James, M. N. 1991. Refined structure of porcine pepsinogen at 1.8 Å resolution. *J. Mol. Biol.* 219:671–692.

Protease Inhibitors

Gooptu, B., and Lomas, D. A. 2009. Conformational Pathology of the Serpins: Themes, Variations, and Therapeutic Strategies. *Annu. Rev. Biochem.* 78:147–167.

Carrell, R., and Travis, J. 1985. α_1-Antitrypsin and the serpins: Variation and countervariation. *Trends Biochem. Sci.* 10:20–24.

Carp, H., Miller, F., Hoidal, J. R., and Janoff, A. 1982. Potential mechanism of emphysema: α_1-Proteinase inhibitor recovered from lungs of cigarette smokers contains oxidized methionine and has decreased elastase inhibitory capacity. *Proc. Natl. Acad. Sci. U.S.A.* 79:2041–2045.

Owen, M. C., Brennan, S. O., Lewis, J. H., and Carrell, R. W. 1983. Mutation of antitrypsin to antithrombin. *New Engl. J. Med.* 309: 694–698.

Travis, J., and Salvesen, G. S. 1983. Human plasma proteinase inhibitors. *Annu. Rev. Biochem.* 52:655–709.

Clotting Cascade

Kollman, J. M., Pandi, L., Sawaya, M. R., Riley, M., and Doolittle, R. F. 2009. Crystal structure of human fibrinogen. *Biochemistry* 48: 3877–3886.

Furie, B., and Furie, B. C. 2008. Mechanisms of thrombus formation. *New Engl. J. Med.* 359:938–949.

Orfeo, T., Brufatto, N., Nesheim, M. E., Xu, H., Butenas, S., and Mann, K. G. 2004. The factor V activation paradox. *J. Biol. Chem.* 279:19580–19591.

Mann, K. G. 2003. Thrombin formation. *Chest* 124:4S–10S.

Rose, T., and Di Cera, E. 2002. Three-dimensional modeling of thrombin–fibrinogen interaction. *J. Biol. Chem.* 277:18875–18880.

Krem, M. M., and Di Cera, E. 2002. Evolution of cascades from embryonic development to blood coagulation. *Trends Biochem. Sci.* 27:67–74.

Fuentes-Prior, P., Iwanaga, Y., Huber, R., Pagila, R., Rumennik, G., Seto, M., Morser, J., Light, D. R., and Bode, W. 2000. Structural basis for the anticoagulant activity of the thrombin–thrombomodulin complex. *Nature* 404:518–525.

Lawn, R. M., and Vehar, G. A. 1986. The molecular genetics of hemophilia. *Sci. Am.* 254(3):48–65.

Chapter 11

Where to Start

Glycochemistry and glycobiology. A series of review articles. 2007. *Nature* 446:999–1051.

Maeder, T. 2002. Sweet medicines. *Sci. Am.* 287(1):40–47.

Freeze, H. H. 2013. Understanding human glycosylation disorders. *J. Biol. Chem.* 288:6936–6945.

Coutinho, M. F., Prata M., J., and Alves, S. 2012. Mannose-6-phosphate pathway: A review on its role in lysosomal function and dysfunction. *Mol. Gen. Metab.* 105:542–550.

Books

Varki, A., Cummings, R., Esko, J., Freeze, H., Stanley, P., Bertozzi, C., Hart, G., and Etzler, M. E. 2009. *Essentials of Glycobiology* (2d ed.). Cold Spring Harbor Laboratory Press.

Stick, R. V., and Williams, S. 2008. *Carbohydrates: The Essential Molecules of Life* (2d ed.). Elsevier Science.

Sansome, C., and Markman, O. 2007. *Glycobiology*. Scion.

Lindhorst, T. K. 2007. *Essentials of Carbohydrate Chemistry and Biochemistry* (3d ed.). Wiley-VCH.

Taylor, M. E. 2006. *Introduction to Glycobiology* (2d ed.). Oxford University Press.

Glycoproteins

Tran, D. T., and Hagen, K. G. T. 2013. Mucin-type O-glycosylation during development. *J. Biol. Chem.* 288:6921–6929.

Gill, D. J., Clausen H., and Bard, F. 2011. Location, location, location: New insights into O-GalNAc protein glycosylation. *Trends Cell Biol.* 21:149–158.

Foley, R. N. 2008. Erythropoietin: Physiology and molecular mechanisms. *Heart Failure Rev.* 13:404–414.

Fisher, J. W. 2003. Erythropoietin: Physiology and pharmacology update. *Exp. Biol. Med.* 228:1–14.

Cheetham, J. C., Smith, D. M., Aoki, K. H., Stevenson, J. L., Hoeffel, T. J., Syed, R. S., Egrie, J., and Harvey, T. S. 1998. NMR structure of human erythropoietin and a comparison with its receptor bound conformation. *Nat. Struct. Biol.* 5:861–866.

Hattrup, C. L., and Gendler, S. J. 2008. Structure and function of the cell surface (tethered) mucins. *Annu. Rev. Physiol.* 70:431–457.

Thorton, D. J., Rousseau, K., and McGuckin, M. A. 2008. Structure and function of mucins in airways mucus. *Annu. Rev. Physiol.* 70:459–486.

Rose, M. C., and Voynow, J. A. 2007. Respiratory tract mucin genes and mucin glycoproteins in health and disease. *Physiol. Rev.* 86:245–278.

Lamoureux, F., Baud'huin, M., Duplomb, L., Heymann, D., and Rédini, F. 2007. Proteoglycans: Key partners in bone cell biology. *Bioessays* 29:758–771.

Carraway, K. L., Funes, M., Workman, H. C., and Sweeney, C. 2007. Contribution of membrane mucins to tumor progression through modulation of cellular growth signaling pathways. *Curr. Top. Dev. Biol.* 78:1–22.

Yan, A., and Lennarz, W. J. 2005. Unraveling the mechanism of protein *N*-glycosylation. *J. Biol. Chem.* 280:3121–3124.

Pratta, M. A., Yao, W., Decicco, C., Tortorella, M., Liu, R.-Q., Copeland, R. A., Magolda, R., Newton, R. C., Trzaskos, J. M., and Arner, E. C. 2003. Aggrecan protects cartilage collagen from proteolytic cleavage. *J. Biol. Chem.* 278:45539–45545.

Glycosyltransferases

Wells, L. 2013. The O-mannosylation pathway: Glycosyltransferases and proteins implicated in congenital muscular dystrophy. *J. Biol. Chem.* 288:6930–6935.

Vocadlo, D. J. 2012. O-GlcNAc processing enzymes: Catalytic mechanisms, substrate specificity, and enzyme regulation. *Curr. Opin. Chem. Biol.* 16:488–497.

Hurtado-Guerrero, R., and Davies, G. J. 2012. Recent structural and mechanistic insights into post-translational enzymatic glycosylation. *Curr. Opin. Chem. Biol.* 16:479–487.

Hart, G. W., Slawson, C., Ramirez-Correa, G., and Lagerlof, O. 2011. Cross talk between O-GlcNAcylation and phosphorylation: Roles in signaling, transcription, and chronic disease. *Annu. Rev. Biochem.* 80:825–858.

Lazarus, M. B., Nam, Y., Jiang, J., Sliz, P., and Walker, S. 2011. Structure of human O-GlcNAc transferase and its complex with a peptide substrate. *Nature* 469:564–569.

Lee, W.-S., Kang, C., Drayna, D., and Kornfeld, S. 2011. Analysis of mannose 6-phosphate uncovering enzyme mutations associated with persistent stuttering. *J. Biol. Chem.* 286:39786–39793.

Lairson, L. L., Henrissat, B., Davies, G. J., and Withers, S. G. 2008. Glycosyltransferases: Structures, functions and mechanisms. *Annu. Rev. Biochem.* 77:521–555.

Qasba, P. K., Ramakrishnan, B., and Boeggeman, E. 2005. Substrate-induced conformational changes in glycosyltransferases. *Trends Biochem. Sci.* 30:53–62.

Carbohydrate-Binding Proteins

Gabius, H.-J., André, S., Jiménez-Barbero, J., Romero, A., and Solís, D. 2011. From lectin structure to functional glycomics: Principles of the sugar code. *Trends Biochem. Sci.* 36:298–313.

Wasserman, P. M. 2008. Zona pellucida glycoproteins. *J. Biol. Chem.* 283:24285–24289.

Sharon, N. 2008. Lectins: Past, present and future. *Biochem. Soc. Trans.* 36:1457–1460.

Balzarini, J. 2007. Targeting the glycans of glycoproteins: A novel paradigm for antiviral therapy. *Nat. Rev. Microbiol.* 5:583–597.

Sharon, N. 2007. Lectins: Carbohydrate-specific reagents and biological recognition molecules. *J. Biol. Chem.* 282:2753–2764.

Stevens, J., Blixt, O., Tumpey, T. M., Taubenberger, J. K., Paulson, J. C., and Wilson, I. A. 2006. Structure and receptor specificity of hemagglutinin from an H5N1 influenza virus. *Science* 312:404–409.

Cambi, A., Koopman, M., and Figdor, C. G. 2005. How C-type lectins detect pathogens. *Cell. Microbiol.* 7:481–488.

Clothia, C., and Jones, E. V. 1997. The molecular structure of cell adhesion molecules. *Annu. Rev. Biochem.* 66:823–862.

Bouckaert, J., Hamelryck, T., Wyns, L., and Loris, R. 1999. Novel structures of plant lectins and their complexes with carbohydrates. *Curr. Opin. Struct. Biol.* 9:572–577.

Weis, W. I., and Drickamer, K. 1996. Structural basis of lectin–carbohydrate recognition. *Annu. Rev. Biochem.* 65:441–473.

Carbohydrate Sequencing

Venkataraman, G., Shriver, Z., Raman, R., and Sasisekharan, R. 1999. Sequencing complex polysaccharides. *Science* 286:537–542.

Zhao, Y., Kent, S. B. H., and Chait, B. T. 1997. Rapid, sensitive structure analysis of oligosaccharides. *Proc. Natl. Acad. Sci. U.S.A.* 94:1629–1633.

Rudd, P. M., Guile, G. R., Küster, B., Harvey, D. J., Opdenakker, G., and Dwek, R. A. 1997. Oligosaccharide sequencing technology. *Nature* 388:205–207.

Chapter 12

Where to Start

De Weer, P. 2000. A century of thinking about cell membranes. *Annu. Rev. Physiol.* 62:919–926.

Bretscher, M. S. 1985. The molecules of the cell membrane. *Sci. Am.* 253(4):100–108.

Unwin, N., and Henderson, R. 1984. The structure of proteins in biological membranes. *Sci. Am.* 250(2):78–94.

Deisenhofer, J., and Michel, H. 1989. The photosynthetic reaction centre from the purple bacterium *Rhodopseudomonas viridis. EMBO J.* 8:2149–2170.

Singer, S. J., and Nicolson, G. L. 1972. The fluid mosaic model of the structure of cell membranes. *Science* 175:720–731.

Jacobson, K., Sheets, E. D., and Simson, R., 1995. Revisiting the fluid mosaic model of membranes. *Science* 268:1441–1442.

Books

Gennis, R. B. 1989. *Biomembranes: Molecular Structure and Function.* Springer Verlag.

Vance, D. E., and Vance, J. E. (Eds.). 2008. *Biochemistry of Lipids, Lipoproteins, and Membranes* (5th ed.). Elsevier.

Lipowsky, R., and Sackmann, E. 1995. *The Structure and Dynamics of Membranes.* Elsevier.

Racker, E. 1985. *Reconstitutions of Transporters, Receptors, and Pathological States.* Academic Press.

Tanford, C. 1980. *The Hydrophobic Effect: Formation of Micelles and Biological Membranes* (2d ed.). Wiley-Interscience.

Membrane Lipids and Dynamics

Lingwood, D., and Simons, K. 2010. Lipid rafts as a membrane-organizing principle. *Science.* 327:46–50.

Pike, L. J. 2009. The challenge of lipid rafts. *J. Lipid Res.* 50:S323–S328.

Simons, K., and Vaz, W. L. 2004. Model systems, lipid rafts, and cell membranes. *Annu. Rev. Biophys. Biomol. Struct.* 33:269–295.

Anderson, T. G., and McConnell, H. M. 2002. A thermodynamic model for extended complexes of cholesterol and phospholipid. *Biophys. J.* 83:2039–2052.

Saxton, M. J., and Jacobson, K. 1997. Single-particle tracking: Applications to membrane dynamics. *Annu. Rev. Biophys. Biomol. Struct.* 26:373–399.

Bloom, M., Evans, E., and Mouritsen, O. G. 1991. Physical properties of the fluid lipid-bilayer component of cell membranes: A perspective. *Q. Rev. Biophys.* 24:293–397.

Elson, E. L. 1986. Membrane dynamics studied by fluorescence correlation spectroscopy and photobleaching recovery. *Soc. Gen. Physiol. Ser.* 40:367–383.

Zachowski, A., and Devaux, P. F. 1990. Transmembrane movements of lipids. *Experientia* 46:644–656.

Devaux, P. F. 1992. Protein involvement in transmembrane lipid asymmetry. *Annu. Rev. Biophys. Biomol. Struct.* 21:417–439.

Silvius, J. R. 1992. Solubilization and functional reconstitution of biomembrane components. *Annu. Rev. Biophys. Biomol. Struct.* 21:323–348.

Yeagle, P. L., Albert, A. D., Boesze-Battaglia, K., Young, J., and Frye, J. 1990. Cholesterol dynamics in membranes. *Biophys. J.* 57:413–424.

Nagle, J. F., and Tristram-Nagle, S. 2000. Lipid bilayer structure. *Curr. Opin. Struct. Biol.* 10:474–480.

Dowhan, W. 1997. Molecular basis for membrane phospholipid diversity: Why are there so many lipids? *Annu. Rev. Biochem.* 66:199–232.

Huijbregts, R. P. H., de Kroon, A. I. P. M., and de Kruijff, B. 1998. Rapid transmembrane movement of newly synthesized phosphatidylethanolamine across the inner membrane of *Escherichia coli. J. Biol. Chem.* 273:18936–18942.

Structure of Membrane Proteins

Walian, P., Cross, T. A., and Jap, B. K. 2004. Structural genomics of membrane proteins. *Genome Biol.* 5:215.

Werten, P. J., Remigy, H. W., de Groot, B. L., Fotiadis, D., Philippsen, A., Stahlberg, H., Grubmuller, H., and Engel, A. 2002. Progress in the analysis of membrane protein structure and function. *FEBS Lett.* 529:65–72.

Popot, J.-L., and Engleman, D. M. 2000. Helical membrane protein folding, stability and evolution. *Annu. Rev. Biochem.* 69:881–922.

White, S. H., and Wimley, W. C. 1999. Membrane protein folding and stability: Physical principles. *Annu. Rev. Biophys. Biomol. Struct.* 28:319–365.

Marassi, F. M., and Opella, S. J. 1998. NMR structural studies of membrane proteins. *Curr. Opin. Struct. Biol.* 8:640–648.

Lipowsky, R. 1991. The conformation of membranes. *Nature* 349:475–481.

Altenbach, C., Marti, T., Khorana, H. G., and Hubbell, W. L. 1990. Transmembrane protein structure: Spin labeling of bacteriorhodopsin mutants. *Science* 248:1088–1092.

Fasman, G. D., and Gilbert, W. A. 1990. The prediction of transmembrane protein sequences and their conformation: An evaluation. *Trends Biochem. Sci.* 15:89–92.

Jennings, M. L. 1989. Topography of membrane proteins. *Annu. Rev. Biochem.* 58:999–1027.

Engelman, D. M., Steitz, T. A., and Goldman, A. 1986. Identifying non-polar transbilayer helices in amino acid sequences of membrane proteins. *Annu. Rev. Biophys. Biophys. Chem.* 15:321–353.

Udenfriend, S., and Kodukola, K. 1995. How glycosyl-phosphatidylinositol-anchored membrane proteins are made. *Annu. Rev. Biochem.* 64:563–591.

Intracellular Membranes

Skehel, J. J., and Wiley, D. C. 2000. Receptor binding and membrane fusion in virus entry: The influenza hemagglutinin. *Annu. Rev. Biochem.* 69:531–569.

Roth, M. G. 1999. Lipid regulators of membrane traffic through the Golgi complex. *Trends Cell Biol.* 9:174–179.

Jahn, R., and Sudhof, T. C. 1999. Membrane fusion and exocytosis. *Annu. Rev. Biochem.* 68:863–911.

Stroud, R. M., and Walter, P. 1999. Signal sequence recognition and protein targeting. *Curr. Opin. Struct. Biol.* 9:754–759.

Teter, S. A., and Klionsky, D. J. 1999. How to get a folded protein across a membrane. *Trends Cell Biol.* 9:428–431.

Hettema, E. H., Distel, B., and Tabak, H. F. 1999. Import of proteins into peroxisomes. *Biochim. Biophys. Acta* 1451:17–34.

Membrane Fusion

Sollner, T. H., and Rothman, J. E. 1996. Molecular machinery mediating vesicle budding, docking and fusion. *Experientia* 52:1021–1025.

Ungar, D., and Hughson, F. M. 2003. SNARE protein structure and function. *Annu. Rev. Cell Dev. Biol.* 19:493–517.

Martens, S., and McMahon, H. T. 2008. Mechanisms of membrane fusion: Disparate players and common principles. *Nat. Rev. Mol. Cell Biol.* 9:543–556.

Chapter 13

Where to Start

Lancaster, C. R. 2004. Structural biology: Ion pump in the movies. *Nature* 432:286–287.

Unwin, N. 2003. Structure and action of the nicotinic acetylcholine receptor explored by electron microscopy. *FEBS Lett.* 555:91–95.

Abramson, J., Smirnova, I., Kasho, V., Verner, G., Iwata, S., and Kaback, H. R. 2003. The lactose permease of *Escherichia coli:* Overall structure, the sugar-binding site and the alternating access model for transport. *FEBS Lett.* 555:96–101.

Lienhard, G. E., Slot, J. W., James, D. E., and Mueckler, M. M. 1992. How cells absorb glucose. *Sci. Am.* 266(1):86–91.

King, L. S., Kozono, D., and Agre, P. 2004. From structure to disease: The evolving tale of aquaporin biology. *Nat. Rev. Mol. Cell Biol.* 5:687–698.

Neher, E., and Sakmann, B. 1992. The patch clamp technique. *Sci. Am.* 266(3):28–35.

Sakmann, B. 1992. Elementary steps in synaptic transmission revealed by currents through single ion channels. *Science* 256:503–512.

Books

Ashcroft, F. M. 2000. *Ion Channels and Disease.* Academic Press.

Conn, P. M. (Ed.). 1998. *Ion Channels,* vol. 293, *Methods in Enzymology.* Academic Press.

Aidley, D. J., and Stanfield, P. R. 1996. *Ion Channels: Molecules in Action.* Cambridge University Press.

Hille, B. 2001. *Ionic Channels of Excitable Membranes* (3d ed.). Sinauer.

Läuger, P. 1991. *Electrogenic Ion Pumps.* Sinauer.

Stein, W. D. 1990. *Channels, Carriers, and Pumps: An Introduction to Membrane Transport.* Academic Press.

Hodgkin, A. 1992. *Chance and Design: Reminiscences of Science in Peace and War.* Cambridge University Press.

P-Type ATPases

Sorensen, T. L., Moller, J. V., and Nissen, P. 2004. Phosphoryl transfer and calcium ion occlusion in the calcium pump. *Science* 304:1672–1675.

Sweadner, K. J., and Donnet, C. 2001. Structural similarities of Na, K-ATPase and SERCA, the Ca^{2+}-ATPase of the sarcoplasmic reticulum. *Biochem. J.* 356:685–704.

Toyoshima, C., and Mizutani, T. 2004. Crystal structure of the calcium pump with a bound ATP analogue. *Nature* 430:529–535.

Toyoshima, C., Nakasako, M., Nomura, H., and Ogawa, H. 2000. Crystal structure of the calcium pump of sarcoplasmic reticulum at 2.6 Å resolution. *Nature* 405:647–655.

Auer, M., Scarborough, G. A., and Kuhlbrandt, W. 1998. Three-dimensional map of the plasma membrane H^+-ATPase in the open conformation. *Nature* 392:840–843.

Axelsen, K. B., and Palmgren, M. G. 1998. Evolution of substrate specificities in the P-type ATPase superfamily. *J. Mol. Evol.* 46:84–101.

Pedersen, P. A., Jorgensen, J. R., and Jorgensen, P. L. 2000. Importance of conserved α-subunit segment ^{709}GDGVND for Mg^{2+} binding, phosphorylation, energy transduction in Na, K-ATPase. *J. Biol. Chem.* 275:37588–37595.

Blanco, G., and Mercer, R. W. 1998. Isozymes of the Na-K-ATPase: Heterogeneity in structure, diversity in function. *Am. J. Physiol.* 275:F633–F650.

Estes, J. W., and White, P. D. 1965. William Withering and the purple foxglove. *Sci. Am.* 212(6):110–117.

ATP-Binding Cassette Proteins

Locher, K. P. 2009. Structure and mechanism of ATP-binding cassette transporters. *Phil. Trans. R. Soc. B* 364:239–245.

Rees, D. C., Johnson, E., and Lewinson, O. 2009. ABC transporters: The power to change. *Nat. Rev. Mol. Cell Biol.* 10:218–227.

Ward, A., Reyes, C. L., Yu, J., Roth, C. B., and Chang, G. 2007. Flexibility in the ABC transporter MsbA: Alternating access with a twist. *Proc. Natl. Acad. Sci. U.S.A.* 104:19005–19010.

Locher, K. P., Lee, A. T., and Rees, D. C. 2002. The *E. coli* BtuCD structure: A framework for ABC transporter architecture and mechanism. *Science* 296:1091–1098.

Borths, E. L., Locher, K. P., Lee, A. T., and Rees, D. C. 2002. The structure of *Escherichia coli* BtuF and binding to its cognate ATP binding cassette transporter. *Proc. Natl. Acad. Sci. U.S.A.* 99:16642–16647.

Dong, J., Yang, G., and McHaourab, H. S. 2005. Structural basis of energy transduction in the transport cycle of MsbA. *Science* 308:1023–1028.

Akabas, M. H. 2000. Cystic fibrosis transmembrane conductance regulator: Structure and function of an epithelial chloride channel. *J. Biol. Chem.* 275:3729–3732.

Chen, J., Sharma, S., Quiocho, F. A., and Davidson, A. L. 2001. Trapping the transition state of an ATP-binding cassette transporter: Evidence for a concerted mechanism of maltose transport. *Proc. Natl. Acad. Sci. U.S.A.* 98:1525–1530.

Sheppard, D. N., and Welsh, M. J. 1999. Structure and function of the CFTR chloride channel. *Physiol. Rev.* 79:S23–S45.

Chen, Y., and Simon, S. M. 2000. In situ biochemical demonstration that P-glycoprotein is a drug efflux pump with broad specificity. *J. Cell Biol.* 148:863–870.

Saier, M. H., Jr., Paulsen, I. T., Sliwinski, M. K., Pao, S. S., Skurray, R. A., and Nikaido, H. 1998. Evolutionary origins of multidrug and drug-specific efflux pumps in bacteria. *FASEB J.* 12:265–274.

Symporters and Antiporters

Abramson, J., Smirnova, I., Kasho, V., Verner, G., Kaback, H. R., and Iwata, S. 2003. Structure and mechanism of the lactose permease of *Escherichia coli. Science* 301:610–615.

Philipson, K. D., and Nicoll, D. A. 2000. Sodium-calcium exchange: A molecular perspective. *Annu. Rev. Physiol.* 62:111–133.

Pao, S. S., Paulsen, I. T., and Saier, M. H., Jr. 1998. Major facilitator superfamily. *Microbiol. Mol. Biol. Rev.* 62:1–34.

Wright, E. M., Hirsch, J. R., Loo, D. D., and Zampighi, G. A. 1997. Regulation of Na^+/glucose cotransporters. *J. Exp. Biol.* 200:287–293.

Kaback, H. R., Bibi, E., and Roepe, P. D. 1990. β-Galactoside transport in *E. coli:* A functional dissection of lac permease. *Trends Biochem. Sci.* 8:309–314.

Hilgemann, D. W., Nicoll, D. A., and Philipson, K. D. 1991. Charge movement during Na^+ translocation by native and cloned cardiac Na^+/Ca^{2+} exchanger. *Nature* 352:715–718.

Hediger, M. A., Turk, E., and Wright, E. M. 1989. Homology of the human intestinal Na^+/glucose and *Escherichia coli* Na^+/proline cotransporters. *Proc. Natl. Acad. Sci. U.S.A.* 86: 5748–5752.

Ion Channels

Zhou, Y., and MacKinnon, R. 2003. The occupancy of ions in the K1 selectivity filter: Charge balance and coupling of ion binding to a protein conformational change underlie high conduction rates. *J. Mol. Biol.* 333:965–975.

Zhou, Y., Morais-Cabral, J. H., Kaufman, A., and MacKinnon, R. 2001. Chemistry of ion coordination and hydration revealed by a K^+ channel-Fab complex at 2.0 Å resolution. *Nature* 414:43–48.

Jiang, Y., Lee, A., Chen, J., Cadene, M., Chait, B. T., and MacKinnon, R. 2002. The open pore conformation of potassium channels. *Nature* 417:523–526.

Jiang, Y., Lee, A., Chen, J., Ruta, V., Cadene, M., Chait, B. T., and MacKinnon, R. 2003. X-ray structure of a voltage-dependent K^+ channel. *Nature* 423:33–41.

Jiang, Y., Ruta, V., Chen, J., Lee, A., and MacKinnon, R. 2003. The principle of gating charge movement in a voltage-dependent K^+ channel. *Nature* 423:42–48.

Mackinnon, R. 2004. Structural biology: Voltage sensor meets lipid membrane. *Science* 306:1304–1305.

Noskov, S. Y., Bernèche, S., and Roux, B. 2004. Control of ion selectivity in potassium channels by electrostatic and dynamic properties of carbonyl ligands. *Nature* 431:830–834.

Bezanilla, F. 2000. The voltage sensor in voltage-dependent ion channels. *Physiol. Rev.* 80:555–592.

Shieh, C.-C., Coghlan, M., Sullivan, J. P., and Gopalakrishnan, M. 2000. Potassium channels: Molecular defects, diseases, and therapeutic opportunities. *Pharmacol. Rev.* 52:557–594.

Horn, R. 2000. Conversation between voltage sensors and gates of ion channels. *Biochemistry* 39:15653–15658.

Perozo, E., Cortes, D. M., and Cuello, L. G. 1999. Structural rearrangements underlying K^+-channel activation gating. *Science* 285:73–78.

Doyle, D. A., Morais Cabral, J., Pfuetzner, R. A., Kuo, A., Gulbis, J. M., Cohen, S. L., Chait, B. T., and MacKinnon R. 1998. The structure of the potassium channel: Molecular basis of K^+ conduction and selectivity. *Science* 280:69–77.

Marban, E., Yamagishi, T., and Tomaselli, G. F. 1998. Structure and function of the voltage-gated Na^+ channel. *J. Physiol.* 508: 647–657.

Miller, R. J. 1992. Voltage-sensitive Ca^{2+} channels. *J. Biol. Chem.* 267: 1403–1406.

Catterall, W. A. 1991. Excitation-contraction coupling in vertebrate skeletal muscle: A tale of two calcium channels. *Cell* 64:871–874.

Ligand-Gated Ion Channels

Unwin, N. 2005. Refined structure of the nicotinic acetylcholine receptor at 4 Å resolution. *J. Mol. Biol.* 346:967–989.

Miyazawa, A., Fujiyoshi, Y., Stowell, M., and Unwin, N. 1999. Nicotinic acetylcholine receptor at 4.6 Å resolution: Transverse tunnels in the channel wall. *J. Mol. Biol.* 288:765–786.

Jiang, Y., Lee, A., Chen, J., Cadene, M., Chait, B. T., and MacKinnon, R. 2002. Crystal structure and mechanism of a calcium-gated potassium channel. *Nature* 417:515–522.

Barrantes, F. J., Antollini, S. S., Blanton, M. P., and Prieto, M. 2000. Topography of the nicotinic acetylcholine receptor membrane-embedded domains. *J. Biol. Chem.* 275:37333–37339.

Cordero-Erausquin, M., Marubio, L. M., Klink, R., and Changeux, J. P. 2000. Nicotinic receptor function: New perspectives from knockout mice. *Trends Pharmacol. Sci.* 21:211–217.

Le Novère, N., and Changeux, J. P. 1995. Molecular evolution of the nicotinic acetylcholine receptor: An example of multigene family in excitable cells. *J. Mol. Evol.* 40:155–172.

Kunishima, N., Shimada, Y., Tsuji, Y., Sato, T., Yamamoto, M., Kumasaka, T., Nakanishi, S., Jingami, H., and Morikawa, K. 2000. Structural basis of glutamate recognition by dimeric metabotropic glutamate receptor. *Nature* 407:971–978.

Betz, H., Kuhse, J., Schmieden, V., Laube, B., Kirsch, J., and Harvey, R. J. 1999. Structure and functions of inhibitory and excitatory glycine receptors. *Ann. N. Y. Acad. Sci.* 868:667–676.

Unwin, N. 1995. Acetylcholine receptor channel imaged in the open state. *Nature* 373:37–43.

Colquhoun, D., and Sakmann, B. 1981. Fluctuations in the microsecond time range of the current through single acetylcholine receptor ion channels. *Nature* 294:464–466.

Long QT Syndrome and hERG

Saenen, J. B., and Vrints, C. J. 2008. Molecular aspects of the congenital and acquired Long QT Syndrome: Clinical implications. *J. Mol. Cell. Cardiol.* 44:633–646.

Zaręba, W. 2007. Drug induced QT prolongation. *Cardiol. J.* 14:523–533.

Fernandez, D., Ghanta, A., Kauffman, G. W., and Sanguinetti, M. C. 2004. Physicochemical features of the hERG channel drug binding site. *J. Biol. Chem.* 279:10120–10127.

Mitcheson, J. S., Chen, J., Lin, M., Culberson, C., and Sanguinetti, M. C. 2000. A structural basis for drug-induced long QT syndrome. *Proc. Natl. Acad. Sci. U.S.A.* 97:12329–12333.

Gap Junctions

Maeda, S., Nakagawa, S., Suga, M., Yamashita, E., Oshima, A., Fujiyoshi, Y., and Tsukihara, T. 2009. Structure of the connexin 26 gap junction channel at 3.5 Å resolution. *Nature* 458:597–604.

Saez, J. C., Berthoud, V. M., Branes, M. C., Martinez, A. D., and Beyer, E. C. 2003. Plasma membrane channels formed by connexins: Their regulation and functions. *Physiol. Rev.* 83:1359–1400.

Revilla, A., Bennett, M. V. L., and Barrio, L. C. 2000. Molecular determinants of membrane potential dependence in vertebrate gap junction channels. *Proc. Natl. Acad. Sci. U.S.A.* 97:14760–14765.

Unger, V. M., Kumar, N. M., Gilula, N. B., and Yeager, M. 1999. Three-dimensional structure of a recombinant gap junction membrane channel. *Science* 283:1176–1180.

Simon, A. M. 1999. Gap junctions: More roles and new structural data. *Trends Cell Biol.* 9:169–170.

Beltramello, M., Piazza, V., Bukauskas, F. F., Pozzan, T., and Mammano, F. 2005. Impaired permeability to Ins(1,4,5)P3 in a mutant connexin underlies recessive hereditary deafness. *Nat. Cell Biol.* 7:63–69.

White, T. W., and Paul, D. L. 1999. Genetic diseases and gene knockouts reveal diverse connexin functions. *Annu. Rev. Physiol.* 61:283–310.

Water Channels

Agre, P., King, L. S., Yasui, M., Guggino, W. B., Ottersen, O. P., Fujiyoshi, Y., Engel, A., and Nielsen, S. 2002. Aquaporin water channels: From atomic structure to clinical medicine. *J. Physiol.* 542:3–16.

Agre, P., and Kozono, D. 2003. Aquaporin water channels: Molecular mechanisms for human diseases. *FEBS Lett.* 555:72–78.

de Groot, B. L., Engel, A., and Grubmuller, H. 2003. The structure of the aquaporin-1 water channel: A comparison between cryo-electron microscopy and X-ray crystallography. *J. Mol. Biol.* 325:485–493.

Chapter 14

Where to Start

Scott, J. D., and Pawson, T. 2000. Cell communication: The inside story. *Sci. Am.* 282(6):7279.

Pawson, T. 1995. Protein modules and signalling networks. *Nature* 373:573–580.

Okada, T., Ernst, O. P., Palczewski, K., and Hofmann, K. P. 2001. Activation of rhodopsin: New insights from structural and biochemical studies. *Trends Biochem. Sci.* 26:318–324.

Tsien, R. Y. 1992. Intracellular signal transduction in four dimensions: From molecular design to physiology. *Am. J. Physiol.* 263: C723–C728.

Loewenstein, W. R. 1999. *Touchstone of Life: Molecular Information, Cell Communication, and the Foundations of Life.* Oxford University Press.

G Proteins and 7TM Receptors

Palczewski, K., Kumasaka, T., Hori, T., Behnke, C. A., Motoshima, H., Fox, B. A., Le Trong, I., Teller, D. C., Okada, T., Stenkamp, R. E., et al. 2000. Crystal structure of rhodopsin: A G protein-coupled receptor. *Science* 289:739–745.

Rasmussen, S. G. F., Choi, H.-J., Rosenbaum, D. M., Kobilka, T. S., Thian, F. S., Edwards, P. C., Burghammer, M., Ratnala, V. R. P., Sanishvili, R., Fischetti, R. F., et al. 2007. Crystal structure of the human β_2 adrenergic G-protein-coupled receptor. *Nature* 450:383–387.

Rosenbaum, D. M., Cherezov, V., Hanson, M. A., Rasmussen, S. G. F., Thian, F. S., Kobilka, T. S., Choi, H.-J., Yao, X.-J., Weis, W. I., Stevens, R. C., et al. 2007. GPCR engineering yields high-resolution structural insights into β_2-adrenergic receptor function. *Science* 318:1266–1273.

Rasmussen, S. G. F., DeVree, B. T., Zou, Y., Kruse, A. C., Chung, K. Y., Kobilka, T. S., Thian, F. S., Chae, P. S., Pardon, E., Calinski, D., et al. 2011. Crystal structure of the β_2 adrenergic receptor–Gs protein complex. *Nature* 477:549–555.

Lefkowitz, R. J. 2000. The superfamily of heptahelical receptors. *Nat. Cell Biol.* 2:E133–E136.

Audet, M., and Bouvier, M. 2012. Restructuring G-protein-coupled receptor activation. *Cell* 151:14–22.

Bourne, H. R., Sanders, D. A., and McCormick, F. 1991. The GTPase superfamily: Conserved structure and molecular mechanism. *Nature* 349:117–127.

Lambright, D. G., Noel, J. P., Hamm, H. E., and Sigler, P. B. 1994. Structural determinants for activation of the α-subunit of a heterotrimeric G protein. *Nature* 369:621–628.

Noel, J. P., Hamm, H. E., and Sigler, P. B. 1993. The 2.2 Å crystal structure of transducin-α complexed with GTPγS. *Nature* 366: 654–663.

Sondek, J., Lambright, D. G., Noel, J. P., Hamm, H. E., and Sigler, P. B. 1994. GTPase mechanism of G proteins from the 1.7-Å crystal structure of transducin α-GDP-AIF$_4^-$. *Nature* 372:276–279.

Sondek, J., Bohm, A., Lambright, D. G., Hamm, H. E., and Sigler, P. B. 1996. Crystal structure of a G-protein βγ dimer at 2.1 Å resolution. *Nature* 379:369–374.

Wedegaertner, P. B., Wilson, P. T., and Bourne, H. R. 1995. Lipid modifications of trimeric G proteins. *J. Biol. Chem.* 270: 503–506.

Farfel, Z., Bourne, H. R., and Iiri, T. 1999. The expanding spectrum of G protein diseases. *New Engl. J. Med.* 340:1012–1020.

Bockaert, J., and Pin, J. P. 1999. Molecular tinkering of G protein-coupled receptors: An evolutionary success. *EMBO J.* 18: 1723–1729.

Cyclic AMP Cascade

Hurley, J. H. 1999. Structure, mechanism, and regulation of mammalian adenylyl cyclase. *J. Biol. Chem.* 274:7599–7602.

Kim, C., Xuong, N. H., and Taylor, S. S. 2005. Crystal structure of a complex between the catalytic and regulatory (RI) subunits of PKA. *Science* 307:690–696.

Tesmer, J. J., Sunahara, R. K., Gilman, A. G., and Sprang, S. R. 1997. Crystal structure of the catalytic domains of adenylyl cyclase in a complex with $G_{s\alpha}$-GTPγS. *Science* 278:1907–1916.

Smith, C. M., Radzio-Andzelm, E., Madhusudan, Akamine, P., and Taylor, S. S. 1999. The catalytic subunit of cAMP-dependent protein kinase: Prototype for an extended network of communication. *Prog. Biophys. Mol. Biol.* 71:313–341.

Taylor, S. S., Buechler, J. A., and Yonemoto, W. 1990. cAMP-dependent protein kinase: Framework for a diverse family of regulatory enzymes. *Annu. Rev. Biochem.* 59:971–1005.

Phosphoinositide Cascade

Berridge, M. J., and Irvine, R. F. 1989. Inositol phosphates and cell signalling. *Nature* 341:197–205.

Berridge, M. J. 1993. Inositol trisphosphate and calcium signalling. *Nature* 361:315–325.

Essen, L. O., Perisic, O., Cheung, R., Katan, M., and Williams, R. L. 1996. Crystal structure of a mammalian phosphoinositide-specific phospholipase C δ. *Nature* 380:595–602.

Ferguson, K. M., Lemmon, M. A., Schlessinger, J., and Sigler, P. B. 1995. Structure of the high affinity complex of inositol trisphosphate with a phospholipase C pleckstrin homology domain. *Cell* 83:1037–1046.

Baraldi, E., Carugo, K. D., Hyvonen, M., Surdo, P. L., Riley, A. M., Potter, B. V., O'Brien, R., Ladbury, J. E., and Saraste, M. 1999. Structure of the PH domain from Bruton's tyrosine kinase in complex with inositol 1,3,4,5-tetrakisphosphate. *Struct. Fold. Design* 7:449–460.

Waldo, G. L., Ricks, T. K., Hicks, S. N., Cheever, M. L., Kawano, T., Tsuboi, K., Wang, X., Montell, C., Kozasa, T., Sondek, J., et al. 2010. Kinetic scaffolding mediated by a phospholipase C-β and G_q signaling complex. *Science* 330:974–980.

Calcium

Ikura, M., Clore, G. M., Gronenborn, A. M., Zhu, G., Klee, C. B., and Bax, A. 1992. Solution structure of a calmodulin-target peptide complex by multidimensional NMR. *Science* 256:632–638.

Kuboniwa, H., Tjandra, N., Grzesiek, S., Ren, H., Klee, C. B., and Bax, A. 1995. Solution structure of calcium-free calmodulin. *Nat. Struct. Biol.* 2:768–776.

Grynkiewicz, G., Poenie, M., and Tsien, R. Y. 1985. A new generation of Ca^{2+} indicators with greatly improved fluorescence properties. *J. Biol. Chem.* 260:3440–3450.

Kerr, R., Lev-Ram, V., Baird, G., Vincent, P., Tsien, R. Y., and Schafer, W. R. 2000. Optical imaging of calcium transients in neurons and pharyngeal muscle of *C. elegans*. *Neuron* 26:583–594.

Chin, D., and Means, A. R. 2000. Calmodulin: A prototypical calcium sensor. *Trends Cell Biol.* 10:322–328.

Dawson, A. P. 1997. Calcium signalling: How do IP3 receptors work? *Curr. Biol.* 7:R544–R547.

Protein Kinases, Including Receptor Tyrosine Kinases

Riedel, H., Dull, T. J., Honegger, A. M., Schlessinger, J., and Ullrich, A. 1989. Cytoplasmic domains determine signal specificity, cellular routing characteristics and influence ligand binding of epidermal growth factor and insulin receptors. *EMBO J.* 8:2943–2954.

Taylor, S. S., Knighton, D. R., Zheng, J., Sowadski, J. M., Gibbs, C. S., and Zoller, M. J. 1993. A template for the protein kinase family. *Trends Biochem. Sci.* 18:84–89.

Sicheri, F., Moarefi, I., and Kuriyan, J. 1997. Crystal structure of the Src family tyrosine kinase Hck. *Nature* 385:602–609.

Waksman, G., Shoelson, S. E., Pant, N., Cowburn, D., and Kuriyan, J. 1993. Binding of a high affinity phosphotyrosyl peptide to the Src SH2 domain: Crystal structures of the complexed and peptide-free forms. *Cell* 72:779–790.

Schlessinger, J. 2000. Cell signaling by receptor tyrosine kinases. *Cell* 103:211–225.

Simon, M. A. 2000. Receptor tyrosine kinases: Specific outcomes from general signals. *Cell* 103:13–15.

Robinson, D. R., Wu, Y. M., and Lin, S. F. 2000. The protein tyrosine kinase family of the human genome. *Oncogene* 19:5548–5557.

Hubbard, S. R. 1999. Structural analysis of receptor tyrosine kinases. *Prog. Biophys. Mol. Biol.* 71:343–358.

Carter-Su, C., and Smit, L. S. 1998. Signaling via JAK tyrosine kinases: Growth hormone receptor as a model system. *Recent Prog. Horm. Res.* 53:61–82.

Insulin Signaling Pathway

Khan, A. H., and Pessin, J. E. 2002. Insulin regulation of glucose uptake: A complex interplay of intracellular signalling pathways. *Diabetologia* 45:1475–1483.

Bevan, P. 2001. Insulin signalling. *J. Cell Sci.* 114:1429–1430.

De Meyts, P., and Whittaker, J. 2002. Structural biology of insulin and IGF1 receptors: Implications for drug design. *Nat. Rev. Drug Discov.* 1:769–783.

Dhe-Paganon, S., Ottinger, E. A., Nolte, R. T., Eck, M. J., and Shoelson, S. E. 1999. Crystal structure of the pleckstrin homology-phosphotyrosine binding (PH-PTB) targeting region of insulin receptor substrate 1. *Proc. Natl. Acad. Sci. U.S.A.* 96:8378–8383.

Domin, J., and Waterfield, M. D. 1997. Using structure to define the function of phosphoinositide 3-kinase family members. *FEBS Lett.* 410:91–95.

Hubbard, S. R. 1997. Crystal structure of the activated insulin receptor tyrosine kinase in complex with peptide substrate and ATP analog. *EMBO J.* 16:5572–5581.

Hubbard, S. R., Wei, L., Ellis, L., and Hendrickson, W. A. 1994. Crystal structure of the tyrosine kinase domain of the human insulin receptor. *Nature* 372:746–754.

EGF Signaling Pathway

Burgess, A. W., Cho, H. S., Eigenbrot, C., Ferguson, K. M., Garrett, T. P., Leahy, D. J., Lemmon, M. A., Sliwkowski, M. X., Ward, C. W., and Yokoyama, S. 2003. An open-and-shut case? Recent insights into the activation of EGF/ErbB receptors. *Mol. Cell* 12:541–552.

Cho, H. S., Mason, K., Ramyar, K. X., Stanley, A. M., Gabelli, S. B., Denney, D. W., Jr., and Leahy, D. J. 2003. Structure of the extracellular region of HER2 alone and in complex with the Herceptin Fab. *Nature* 421:756–760.

Chong, H., Vikis, H. G., and Guan, K. L. 2003. Mechanisms of regulating the Raf kinase family. *Cell. Signal.* 15:463–469.

Stamos, J., Sliwkowski, M. X., and Eigenbrot, C. 2002. Structure of the epidermal growth factor receptor kinase domain alone and in complex with a 4-anilinoquinazoline inhibitor. *J. Biol. Chem.* 277:46265–46272.

Ras

Milburn, M. V., Tong, L., deVos, A. M., Brunger, A., Yamaizumi, Z., Nishimura, S., and Kim, S. H. 1990. Molecular switch for signal transduction: Structural differences between active and inactive forms of protooncogenic Ras proteins. *Science* 247:939–945.

Boriack-Sjodin, P. A., Margarit, S. M., Bar-Sagi, D., and Kuriyan, J. 1998. The structural basis of the activation of Ras by Sos. *Nature* 394:337–343.

Maignan, S., Guilloteau, J. P., Fromage, N., Arnoux, B., Becquart, J., and Ducruix, A. 1995. Crystal structure of the mammalian Grb2 adaptor. *Science* 268:291–293.

Takai, Y., Sasaki, T., and Matozaki, T. 2001. Small GTP-binding proteins. *Physiol. Rev.* 81:153–208.

Cancer

Druker, B. J., Sawyers, C. L., Kantarjian, H., Resta, D. J., Reese, S. F., Ford, J. M., Capdeville, R., and Talpaz, M. 2001. Activity of a specific inhibitor of the BCR-ABL tyrosine kinase in the blast crisis of chronic myeloid leukemia and acute lymphoblastic leukemia with the Philadelphia chromosome. *New Engl. J. Med.* 344:1038–1042.

Vogelstein, B., and Kinzler, K. W. 1993. The multistep nature of cancer. *Trends Genet.* 9:138–141.

Ellis, C. A., and Clark, G. 2000. The importance of being K-Ras. *Cell. Signal.* 12:425–434.

Hanahan, D., and Weinberg, R. A. 2000. The hallmarks of cancer. *Cell* 100:57–70.

McCormick, F. 1999. Signalling networks that cause cancer. *Trends Cell Biol.* 9:M53–M56.

Chapter 15

Where to Start

Stipanuk, M. H. (Ed.). 2006. *Biochemical, Physiological, Molecular Aspects of Human Nutrition.* Saunders-Elsevier.

McGrane, M. M., Yun, J. S., Patel, Y. M., and Hanson, R. W. 1992. Metabolic control of gene expression: In vivo studies with transgenic mice. *Trends Biochem. Sci.* 17:40–44.

Westheimer, F. H. 1987. Why nature chose phosphates. *Science* 235:1173–1178.

Kamerlin, S. C. L., Sharma, P. K., Prasad, R. B., and Warshel, A. 2013. Why nature really chose phosphate. *Q. Rev. Biophys.* 46:1–132.

Books

Atkins, P., and de Paula, J. 2011. *Physical Chemistry for the Life Sciences* (2d ed.). W. H. Freeman and Company.

Harold, F. M. 1986. *The Vital Force: A Study of Bioenergetics.* W. H. Freeman and Company.

Krebs, H. A., and Kornberg, H. L. 1957. *Energy Transformations in Living Matter.* Springer Verlag.

Nicholls, D. G., and Ferguson, S. J. 2013. *Bioenergetics* (4th ed.). Academic Press.

Frayn, K. N. 2010. *Metabolic Regulation: A Human Perspective* (3d ed.). Wiley-Blackwell.

Fell, D. 1997. *Understanding the Control of Metabolism.* Portland Press.

Harris, D. A. 1995. *Bioenergetics at a Glance.* Blackwell Scientific.

Von Baeyer, H. C. 1999. *Warmth Disperses and Time Passes: A History of Heat.* Modern Library.

Thermodynamics

Alberty, R. A. 1993. Levels of thermodynamic treatment of biochemical reaction systems. *Biophys. J.* 65:1243–1254.

Alberty, R. A., and Goldberg, R. N. 1992. Standard thermodynamic formation properties for the adenosine 5′-triphosphate series. *Biochemistry* 31:10610–10615.

Alberty, R. A. 1968. Effect of pH and metal ion concentration on the equilibrium hydrolysis of adenosine triphosphate to adenosine diphosphate. *J. Biol. Chem.* 243:1337–1343.

Goldberg, R. N. 1984. *Compiled Thermodynamic Data Sources for Aqueous and Biochemical Systems: An Annotated Bibliography (1930–1983).* National Bureau of Standards Special Publication 685, U.S. Government Printing Office.

Frey, P. A., and Arabshahi, A. 1995. Standard free energy change for the hydrolysis of the α,β-phosphoanhydride bridge in ATP. *Biochemistry* 34:11307–11310.

Bioenergetics and Metabolism

Schilling, C. H., Letscher, D., and Palsson, B. O. 2000. Theory for the systemic definition of metabolic pathways and their use in interpreting metabolic function from a pathway-oriented perspective. *J. Theor. Biol.* 203:229–248.

DeCoursey, T. E., and Cherny, V. V. 2000. Common themes and problems of bioenergetics and voltage-gated proton channels. *Biochim. Biophys. Acta* 1458:104–119.

Giersch, C. 2000. Mathematical modelling of metabolism. *Curr. Opin. Plant Biol.* 3:249–253.

Rees, D. C., and Howard, J. B. 1999. Structural bioenergetics and energy transduction mechanisms. *J. Mol. Biol.* 293:343–350.

Regulation of Metabolism

Kemp, G. J. 2000. Studying metabolic regulation in human muscle. *Biochem. Soc. Trans.* 28:100–103.

Towle, H. C., Kaytor, E. N., and Shih, H. M. 1996. Metabolic regulation of hepatic gene expression. *Biochem. Soc. Trans.* 24:364–368.

Hofmeyr, J. H. 1995. Metabolic regulation: A control analytic perspective. *J. Bioenerg. Biomembr.* 27:479–490.

Historical Aspects

Kalckar, H. M. 1991. 50 years of biological research: From oxidative phosphorylation to energy requiring transport regulation. *Annu. Rev. Biochem.* 60:1–37.

Kalckar, H. M. (Ed.). 1969. *Biological Phosphorylations.* Prentice Hall.

Fruton, J. S. 1972. *Molecules and Life.* Wiley-Interscience.

Lipmann, F. 1971. *Wanderings of a Biochemist.* Wiley-Interscience.

Chapter 16

Where to Start

McCracken, A. N., and Edinger, A. L. 2013. Nutrient transporters: The Achilles' heel of anabolism. *Trends Endocrin. Met.* 24:200–208.

Curry, A. 2013. The milk revolution. *Nature* 500:20–22.

Bar-Even, A., Flamholz, A., Noor, E., and Milo, R. 2012. Rethinking glycolysis: On the biochemical logic of metabolic pathways. *Nature Chem. Biol.* 8:509–517.

Ward, P. S., and Thompson, C. B. 2012. Metabolic reprogramming: A cancer hallmark even Warburg did not anticipate. *Cancer Cell* 21:297–308.

Herling, A., König, M., Bulik, S., and Holzhütter, H.-G. 2011. Enzymatic features of the glucose metabolism in tumor cells. *FEBS J.* 278:2436–2459.

Lin, H. V., and Accili, D. 2011. Hormonal regulation of hepatic glucose production in health and disease. *Cell Metab.* 14:9–19.

Hirabayashi, J. 1996. On the origin of elementary hexoses. *Quart. Rev. Biol.*71:365–380.

Books and Reviews

Tong, L. 2013. Structure and function of biotin-dependent carboxylases. *Cell. Mol. Life Sci.* 70:863–891.

Frayn, K. N. 2010. *Metabolic Regulation: A Human Perspective* (3d ed.). Wiley-Blackwell.

Fell, D. 1997. *Understanding the Control of Metabolism.* Portland.

Fersht, A. 1999. *Structure and Mechanism in Protein Science: A Guide to Enzyme Catalysis and Protein Folding.* W. H. Freeman and Company.

Poortmans, J. R. (Ed.). 2004. *Principles of Exercise Biochemistry.* Krager.

Structure of Glycolytic and Gluconeogenic Enzymes

Lietzan, A. D., and St. Maurice, M. 2013. A substrate-induced biotin binding pocket in the carboxyltransferase domain of pyruvate carboxylase. *J. Biol. Chem.* 288:19915−19925.

Banaszak, L., Mechin, I., Obmolova, G., Oldham, M., Chang, S. H., Ruiz, T., Radermacher, M., Kopperschläger, G., and Rypniewski, W. 2011. The crystal structures of eukaryotic phosphofructokinases from baker's yeast and rabbit skeletal muscle. *J. Mol. Biol.* 407:284–297.

Lasso, G., Yu, L. P. C., Gil, D., Xiang, S., Tong, L., and Valle, M. 2010. Cryo-EM analysis reveals new insights into the mechanism of action of pyruvate carboxylase. *Structure* 18:1300–1310.

Ferreras, C., Hernández, E. D., Martínez-Costa, O. H., and Aragón, J. J. 2009. Subunit interactions and composition of the fructose 6-phosphate catalytic site and the fructose 2,6-bisphosphate allosteric site of mammalian phosphofructokinase. *J. Biol. Chem.* 284:9124–9131.

Hines, J. K., Chen, X., Nix, J. C., Fromm, H. J., and Honzatko. R. B. 2007. Structures of mammalian and bacterial fructose-1, 6-bisphosphatase reveal the basis for synergism in AMP/fructose-2, 6-bisphosphate inhibition. *J. Biol. Chem.* 282:36121–36131.

Ferreira-da-Silva, F., Pereira, P. J., Gales, L., Roessle, M., Svergun, D. I., Moradas-Ferreira, P., and Damas, A. M. 2006. The crystal and solution structures of glyceraldehyde-3-phosphate dehydrogenase reveal different quaternary structures. *J. Biol. Chem.* 281:33433–33440.

Kim, S.-G., Manes, N. P., El-Maghrabi, M. R., and Lee, Y.-H. 2006. Crystal structure of the hypoxia-inducible form of 6-phosphofructo-2-kinase/fructose-2,6-phosphatase (PFKFB3): A possible target for cancer therapy. *J. Biol. Chem.* 281:2939–2944.

Aleshin, A. E., Kirby, C., Liu, X., Bourenkov, G. P., Bartunik, H. D., Fromm, H. J., and Honzatko, R. B. 2000. Crystal structures of mutant monomeric hexokinase I reveal multiple ADP binding sites and conformational changes relevant to allosteric regulation. *J. Mol. Biol.* 296:1001–1015.

Jeffery, C. J., Bahnson, B. J., Chien, W., Ringe, D., and Petsko, G. A. 2000. Crystal structure of rabbit phosphoglucose isomerase, a glycolytic enzyme that moonlights as neuroleukin, autocrine motility factor, and differentiation mediator. *Biochemistry* 39:955–964.

Bernstein, B. E., and Hol, W. G. 1998. Crystal structures of substrates and products bound to the phosphoglycerate kinase active site reveal the catalytic mechanism. *Biochemistry* 37:4429–4436.

Rigden, D. J., Alexeev, D., Phillips, S. E. V., and Fothergill-Gilmore, L. A. 1998. The 2.3 Å X-ray crystal structure of *S. cerevisiae* phosphoglycerate mutase. *J. Mol. Biol.* 276:449–459.

Zhang, E., Brewer, J. M., Minor, W., Carreira, L. A., and Lebioda, L. 1997. Mechanism of enolase: The crystal structure of asymmetric dimer enolase-2-phospho-D-glycerate/enolase-phosphoenolpyruvate at 2.0 Å resolution. *Biochemistry* 36:12526–12534.

Hasemann, C. A., Istvan E. S., Uyeda, K., and Deisenhofer, J. 1996. The crystal structure of the bifunctional enzyme 6-phosphofructo-2-kinase/fructose-2,6-biphosphatase reveals distinct domain homologies. *Structure* 4:1017–1029.

Tari, L. W., Matte, A., Pugazhenthi, U., Goldie, H., and Delbaere, L. T. J. 1996. Snapshot of an enzyme reaction intermediate in the structure of the ATP-Mg^{2+}-oxalate ternary complex of *Escherichia coli* PEP carboxykinase. *Nat. Struct. Biol.* 3:355–363.

Catalytic Mechanisms

Soukri, A., Mougin, A., Corbier, C., Wonacott, A., Branlant, C., and Branlant, G. 1989. Role of the histidine 176 residue in glyceraldehyde-3-phosphate dehydrogenase as probed by site-directed mutagenesis. *Biochemistry* 28:2586–2592.

Bash, P. A., Field, M. J., Davenport, R. C., Petsko, G. A., Ringe, D., and Karplus, M. 1991. Computer simulation and analysis of the reaction pathway of triosephosphate isomerase. *Biochemistry* 30:5826–5832.

Knowles, J. R., and Albery, W. J. 1977. Perfection in enzyme catalysis: The energetics of triosephosphate isomerase. *Acc. Chem. Res.* 10: 105–111.

Regulation

Liu, S., Ammirati, M. J., Song, X., Knafels, J. D., Zhang, J., Greasley, S. E., Pfefferkorn, J. A., and Qiu, X. 2012. Insights into mechanism of glucokinase activation: Observation of multiple distinct protein conformations. *J. Biol. Chem.* 287:13598–13610.

Brüser, A., Kirchberger, J., Kloos, M., Sträter, N., and Schöneberg, T. 2012. Functional linkage of adenine nucleotide binding sites in mammalian muscle 6-phosphofructokinase. *J. Biol. Chem.* 287: 17546–17553.

Anderka, O., Boyken, J., Aschenbach, U., Batzer, A., Boscheinen, O., and Schmoll, D. 2008. Biophysical characterization of the interaction between hepatic glucokinase and its regulatory protein: Impact of physiological and pharmacological effectors. *J. Biol. Chem.* 283:31333–31340.

Iancu, C. V., Mukund, S., Fromm, H. J., and Honzatko, R. B. 2005. R-state AMP complex reveals initial steps of the quaternary transition of fructose-l,6-bisphosphatase. *J. Biol. Chem.* 280: 19737–19745.

Lee, Y. H., Li, Y., Uyeda, K., and Hasemann, C. A. 2003. Tissue-specific structure/function differentiation of the five isoforms of 6-phosphofructo-2-kinase/fructose-2,6-bisphosphatase. *J. Biol. Chem.* 278:523–530.

Gleeson, T. T. 1996. Post-exercise lactate metabolism: A comparative review of sites, pathways, and regulation. *Annu. Rev. Physiol.* 58:556–581.

Jitrapakdee, S., and Wallace, J. C. 1999. Structure, function and regulation of pyruvate carboxylase. *Biochem. J.* 340:1–16.

van de Werve, G., Lange, A., Newgard, C., Mechin, M. C., Li, Y., and Berteloot, A. 2000. New lessons in the regulation of glucose metabolism taught by the glucose 6-phosphatase system. *Eur. J. Biochem.* 267:1533–1549.

Sugar Transporters

Blodgett, D. M., Graybill, C. and Carruthers, A. 2008. Analysis of glucose transporter topology and structural dynamics. *J. Biol. Chem.* 283:36416–36424.

Huang, S., and Czech, M. P. 2007. The GLUT4 glucose transporter. *Cell Metab.* 5:237–252.

Czech, M. P., and Corvera, S. 1999. Signaling mechanisms that regulate glucose transport. *J Biol. Chem.* 274:1865–1868.

Silverman, M. 1991. Structure and function of hexose transporters. *Annu. Rev. Biochem.* 60:757–794.

Thorens, B., Charron, M. J., and Lodish, H. F. 1990. Molecular physiology of glucose transporters. *Diabetes Care* 13:209–218.

Glycolysis and Cancer

Morgan, H. P., O'Reilly, F. J., Wear, M. A., O'Neill, J. R., Fothergill-Gilmore, L. A., Hupp, T., and Walkinshaw, M. D. 2013. M2 pyruvate kinase provides a mechanism for nutrient sensing and regulation of cell proliferation. *Proc. Natl. Acad. Sci. U.S.A.* 110: 5881–5886.

Schulze, A., and Harris, A. L. 2012. How cancer metabolism is tuned for proliferation and vulnerable to disruption. *Nature* 491:364–373.

Lunt, S. Y., and Vander Heiden, M. G. 2011. Aerobic glycolysis: Meeting the metabolic requirements of cell proliferation. *Annu. Rev. Cell Dev. Biol.* 27:441–64.

Vander Heiden, M. G., Cantley, L. C., and Thompson, C. B. 2009. Understanding the Warburg effect: The metabolic requirements of cell proliferation. *Science* 324:1029–1033.

Mathupala, S. P., Ko, Y. H., and Pedersen, P. L. 2009. Hexokinase-2 bound to mitochondria: Cancer's stygian link to the "Warburg effect" and a pivotal target for effective therapy. *Sem. Cancer Biol.* 19:17–24.

Kroemer, G. K., and Pouyssegur, J. 2008. Tumor cell metabolism: Cancer's Achilles' heel. *Cancer Cell* 12:472–482.

Hsu, P. P., and Sabatini, D. M. 2008. Cancer cell metabolism: Warburg and beyond. *Cell* 134:703–707.

Genetic Diseases

Orosz, F., Oláh, J., and Ovádi, J. 2009. Triosephosphate isomerase deficiency: New insights into an enigmatic disease. *Biochim. Biophys. Acta* 1792:1168–1174.

Scriver, C. R., Beaudet, A. L., Valle, D., Sly, W. S., Childs, B., Kinzler, K., and Vogelstein, B. (Eds.). 2001. *The Metabolic and Molecular Basis of Inherited Disease* (8th ed.). McGraw-Hill.

Evolution

Dandekar, T., Schuster, S., Snel, B., Huynen, M., and Bork, P. 1999. Pathway alignment: Application to the comparative analysis of glycolytic enzymes. *Biochem. J.* 343:115–124.

Heinrich, R., Melendez-Hevia, E., Montero, F., Nuno, J. C., Stephani, A., and Waddell, T. G. 1999. The structural design of glycolysis: An evolutionary approach. *Biochem. Soc. Trans.* 27:294–298.

Walmsley, A. R., Barrett, M. P., Bringaud, F., and Gould, G. W. 1998. Sugar transporters from bacteria, parasites and mammals: Structure-activity relationships. *Trends Biochem. Sci.* 23: 476–480.

Maes, D., Zeelen, J. P., Thanki, N., Beaucamp, N., Alvarez, M., Thi, M. H., Backmann, J., Martial, J. A., Wyns, L., Jaenicke, R., et al. 1999. The crystal structure of triosephosphate isomerase (TIM) from *Thermotoga maritima:* A comparative thermostability structural analysis of ten different TIM structures. *Proteins* 37:441–453.

Historical Aspects

Friedmann, H. C. 2004. From *Butyribacterium* to *E. coli:* An essay on unity in biochemistry. *Perspect. Biol. Med.* 47:47–66.

Fruton, J. S. 1999. *Proteins, Enzymes, Genes: The Interplay of Chemistry and Biology.* Yale University Press.

Kalckar, H. M. (Ed.). 1969. *Biological Phosphorylations: Development of Concepts*. Prentice Hall.

Chapter 17

Where to Start

Sugden, M. C., and Holness, M. J. 2003. Recent advances in mechanisms regulating glucose oxidation at the level of the pyruvate dehydrogenase complex by PDKs. *Am. J. Physiol. Endocrinol. Metab.* 284:E855–E862.

Owen, O. E., Kalhan, S. C., and Hanson, R. W. 2002. The key role of anaplerosis and cataplerosis for citric acid function. *J. Biol. Chem.* 277:30409–30412.

Pyruvate Dehydrogenase Complex

Patel, K. P., O'Brien, T. W., Subramony, S. H., Shuster, J., and Stacpoole, P. W. 2012. The spectrum of pyruvate dehydrogenase complex deficiency: Clinical, biochemical and genetic features in 371 patients. *Mol. Genet. Metab.* 105:34–43.

Vijayakrishnan, S., Callow, P., Nutley, M. A., Mcgow, D. P., Gilbert, D., Kropholler, P., Cooper, A., Byron, O., And Lindsay, J. G. 2011. Variation in the organization and subunit composition of the mammalian pyruvate dehydrogenase complex E2/E3BP core assembly. *Biochem. J.* 437:565–574.

Vijayakrishnan, S., Kelly, S. M., Gilbert, R. J., Callow, P., Bhella, D., Forsyth, T., Lindsay, J. G., and Byron, O. 2010. Solution structure and characterization of the human pyruvate dehydrogenase complex core assembly. *J. Mol. Biol.* 399:71–93.

Brautigam, C. A., Wynn, R. M., Chuang, J. L., and Chuang, D. T. 2009. Subunit and catalytic component stoichiometries of an in vitro reconstituted human pyruvate dehydrogenase complex. *J. Biol. Chem.* 284:13086–13098.

Hiromasa, Y., Fujisawa, T., Aso, Y., and Roche, T. E. 2004. Organization of the cores of the mammalian pyruvate dehydrogenase complex formed by E2 and E2 plus the E3-binding proteins and their capacities to bind the E1 and E3 components. *J. Biol Chem.* 279:6921–6933.

Domingo, G. J., Chauhan, H. J., Lessard, I. A., Fuller, C., and Perham, R. N. 1999. Self-assembly and catalytic activity of the pyruvate dehydrogenase multienzyme complex from *Bacillus stearothermophilus. Eur. J. Biochem.* 266:1136–1146.

Structure of Citric Acid Cycle Enzymes

Fraser, M. E., Hayakawa, K., Hume, M. S., Ryan, D. G., and Brownie, E. R. 2006. Interactions of GTP with the ATP-grasp domain of GTP-specific succinyl-CoA synthetase. *J. Biol. Chem.* 281:11058–11065.

Yankovskaya, V., Horsefield, R., Törnroth, S., Luna-Chavez, C., Miyoshi, H., Léger, C., Byrne, B., Cecchini, G., and Iowata, S. 2003. Architecture of succinate dehydrogenase and reactive oxygen species generation. *Science* 299:700–704.

Fraser, M. E., James, M. N., Bridger, W. A., and Wolodko, W. T. 1999. A detailed structural description of *Escherichia coli* succinyl-CoA synthetase. *J. Mol. Biol.* 285:1633–1653. [Published erratum appears in May 7, 1999, issue of *J. Mol. Biol.* 288(3):501.]

Lloyd, S. J., Lauble, H., Prasad, G. S., and Stout, C. D. 1999. The mechanism of aconitase: 1.8 Å resolution crystal structure of the S642A:citrate complex. *Protein Sci.* 8:2655–2662.

Rose, I. A. 1998. How fumarase recycles after the malate → fumarate reaction: Insights into the reaction mechanism. *Biochemistry* 37:17651–17658.

Organization of the Citric Acid Cycle

Lambeth, D. O., Tews, K. N., Adkins, S., Frohlich, D., and Milavetz, B. I. 2004. Expression of two succinyl-CoA specificities in mammalian tissues. *J. Biol. Chem.* 279:36621–36624.

Velot, C., Mixon, M. B., Teige, M., and Srere, P. A. 1997. Model of a quinary structure between Krebs TCA cycle enzymes: A model for the metabolon. *Biochemistry* 36:14271–14276.

Haggie, P. M., and Brindle, K. M. 1999. Mitochondrial citrate synthase is immobilized in vivo. *J. Biol. Chem.* 274:3941–3945.

Morgunov, I., and Srere, P. A. 1998. Interaction between citrate synthase and malate dehydrogenase: Substrate channeling of oxaloacetate. *J. Biol. Chem.* 273:29540–29544.

Regulation

Shi, Q., Xu, H., Yu, H., Zhang, N., Ye, Y., Estevez, A. G., Deng, H., and Gibson, G. E. 2011. Inactivation and reactivation of the mitochondrial α-ketoglutarate dehydrogenase complex. *J. Biol. Chem.* 286:17640–17648.

Phillips, D., Aponte, A. M., French, S. A., Chess, D. J., and Balaban, R. S. 2009. Succinyl-CoA synthetase is a phosphate target for the activation of mitochondrial metabolism. *Biochemistry* 48: 7140–7149.

Taylor, A. B., Hu, G., Hart, P. J., and McAlister-Henn, L. 2008. Allosteric motions in structures of yeast NAD^+-specific isocitrate dehydrogenase. *J. Biol. Chem.* 283:10872–10880.

Green, T., Grigorian, A., Klyuyeva, A., Tuganova, A., Luo, M., and Popov, K. M. 2008. Structural and functional insights into the molecular mechanisms responsible for the regulation of pyruvate dehydrogenase kinase. *J. Biol. Chem.* 283:15789–15798.

Hiromasa, Y., and Roche, T. E. 2003. Facilitated interaction between the pyruvate dehydrogenase kinase isoform 2 and the dihydrolipoyl acetyltransferases. *J. Biol. Chem.* 278:33681–33693.

Jitrapakdee, S., and Wallace, J. C. 1999. Structure, function and regulation of pyruvate carboxylase. *Biochem. J.* 340:1–16.

The Citric Acid Cycle and Cancer

Wang, F., Travins, J., DeLaBarre, B., Penard-Lacronique, V., Schalm, S., Hansen, E., Straley, K., Kernytsky, A., Liu, W., Gliser, C., et al. 2013. Targeted inhibition of mutant IDH2 in leukemia cells induces cellular differentiation. *Science* 340:622–626.

Rohle, D., Popovici-Muller, J., Palaskas, N., Turcan, S., Grommes, C., Campos, C., Tsoi, J., Clark, O., Oldrini, B., Komisopoulou, E., et al. 2013. An inhibitor of mutant IDH1 delays growth and promotes differentiation of glioma cells. *Science* 340:626–630.

Losman, J.-A., Koivunen, P., Lee, S., Schneider, R. K., McMahon, C., Cowley, G. S., Root, D. E., Ebert, B. L., Kaelin, W. G. Jr., et al. 2013. (*R*)-2-Hydroxyglutarate is sufficient to promote leukemogenesis and its effects are reversible. *Science* 339:1621–1625.

Sakai, C., Tomitsuka, T., Esumi, H., Harada, S., and Kita, K. 2012. Mitochondrial fumarate reductase as a target of chemotherapy: From parasites to cancer cells. *Biochim. Biophys. Acta* 1820:643–651.

Xekouki P., and Stratakis, C. A. 2012. Succinate dehydrogenase (SDHx) mutations in pituitary tumors: Could this be a new role for mitochondrial complex II and/or Krebs cycle defects? *Endocr.-Relat. Cancer* 19:C33–C40.

Thompson, C. B. 2009. Metabolic enzymes as oncogenes or tumor suppressors. *New Engl. J. Med.* 360:813–815.

McFate, T., Mohyeldin, A., Lu, H., Thakar, J., Henriques, J., Halim, N. D., Wu, H., Schell, M. J., Tsang, T. M., Teahan, O., Zhou, S., Califano, J. A., Jeoung, M. N., Harris, R. A., and Verma, A. 2008. Pyruvate dehydrogenase complex activity controls metabolic and malignant phenotype in cancer cells. *J. Biol. Chem.* 283:22700–22708.

Gogvadze, V., Orrenius, S., and Zhivotovsky, B. 2008. Mitochondria in cancer cells: What is so special about them? *Trends Cell Biol.* 18:165–173.

Evolutionary Aspects

Meléndez-Hevia, E., Waddell, T. G., and Cascante, M. 1996. The puzzle of the Krebs citric acid cycle: Assembling the pieces of chemically feasible reactions, and opportunism in the design of metabolic pathways in evolution. *J. Mol. Evol.* 43:293–303.

Baldwin, J. E., and Krebs, H. 1981. The evolution of metabolic cycles. *Nature* 291:381–382.

Gest, H. 1987. Evolutionary roots of the citric acid cycle in prokaryotes. *Biochem. Soc. Symp.* 54:3–16.

Weitzman, P. D. J. 1981. Unity and diversity in some bacterial citric acid cycle enzymes. *Adv. Microbiol. Physiol.* 22:185–244.

Discovery of the Citric Acid Cycle

Kornberg, H. 2000. Krebs and his trinity of cycles. *Nat. Rev. Mol. Cell. Biol.* 1:225–228.

Krebs, H. A., and Johnson, W. A. 1937. The role of citric acid in intermediate metabolism in animal tissues. *Enzymologia* 4:148–156.

Krebs, H. A. 1970. The history of the tricarboxylic acid cycle. *Perspect. Biol. Med.* 14:154–170.

Krebs, H. A., and Martin, A. 1981. *Reminiscences and Reflections.* Clarendon Press.

Chapter 18

Where to Start

Guarente, L. 2008. Mitochondria: A nexus for aging, calorie restriction, and sirtuins? *Cell* 132:171–176.

Wallace, D. C. 2007. Why do we still have a maternally inherited mitochondrial DNA? Insights from evolutionary medicine. *Annu. Rev. Biochem.* 76:781–821.

Hosler, J. P., Ferguson-Miller, S., and Mills, D. A. 2006. Energy transduction: Proton transfer through the respiratory complexes. *Annu. Rev. Biochem.* 75:165–187.

Gray, M. W., Burger, G., and Lang, B. F. 1999. Mitochondrial evolution. *Science* 283:1476–1481.

Shultz, B. E., and Chan, S. I. 2001. Structures and proton-pumping strategies of mitochondrial respiratory enzymes. *Annu. Rev. Biophys. Biomol. Struct.* 30:23–65.

Books

Scheffler, I. E. 2007. *Mitochondria.* Wiley.

Lane, N. 2005. *Power, Sex, Suicide: Mitochondria and the Meaning of Life.* Oxford.

Nicholls, D. G., and Ferguson, S. J. 2013. *Bioenergetics* (4th ed.). Academic Press.

Electron-Transport Chain

Baradaran, R., Berrisford, J. M., Minhas, G. S., and Sazanov, L. A. 2013. Crystal structure of the entire respiratory complex I. *Nature* 494:443–448.

Lapuente-Brun, E., Moreno-Loshuertos, R., Acín-Pérez, R., Latorre-Pellicer, A., Colás, C., Balsa, E., Perales-Clemente, E., Quirós, P. M., Calvo, E., Rodríguez-Hernández, M. A., et al. 2013. Supercomplex assembly determines electron flux in the mitochondrial electron transport chain. *Science* 340:1567–1570.

Cammack, R. 2012. Iron-sulfur proteins. *The Biochemist* 35:14–17.

Yoshikawa, S., Muramoto, K., and Shinzawa-Itoh, K. 2011. Proton-pumping mechanism of cytochrome *c* oxidase. *Annu. Rev. Biophys.* 40:205–23.

Qin, L., Liu, J., Mills, D. A., Proshlyakov, D. A., Hiser, C., and Ferguson-Miller, S. 2009. Redox-dependent conformational changes in cytochrome *c* oxidase suggest a gating mechanism for proton uptake. *Biochemistry* 48:5121–5130.

Lill, R. 2009. Function and biogenesis of iron–sulphur proteins. *Nature* 460:831–838.

Cooley, C. W., Lee, D.-W., and Daldal, F. 2009. Across membrane communication between the Q_o and Q_i active sites of cytochrome bc_1. *Biochemistry* 48:1888–1899.

Verkhovskaya, M. L., Belevich, N., Euro, L., Wikström, M., and. Verkhovsky, M. I. 2008. Real-time electron transfer in respiratory complex I. *Proc. Natl. Acad. Sci. U.S.A.* 105:3763–3767.

Acín-Pérez, R., Fernández-Silva, P., Peleato, M. L., Pérez-Martos, A., and Enriquez, J. A. 2008. Respiratory active mitochondrial supercomplexes. *Mol. Cell* 32:529–539.

Kruse, S. E., Watt, W. C., Marcinek, D. J., Kapur, R. P., Schenkman, K. A., and Palmiter, R. D. 2008. Mice with mitochondrial Complex I deficiency develop a fatal encephalomyopathy. *Cell Metab.* 7:312–320.

Sun, F., Huo, X., Zhai, Y., Wang, A., Xu, J., Su, D., Bartlam, M., and Ral, Z. 2005. Crystal structure of mitochondrial respiratory membrane protein complex II. *Cell* 121:1043–1057.

Crofts, A. R. 2004. The cytochrome bc_1 complex: Function in the context of structure. *Annu. Rev. Physio*l. 66:689–733.

Bianchi, C., Genova, M. L., Castelli, G. P., and Lenaz, G. 2004. The mitochondrial respiratory chain is partially organized in a supramolecular complex. *J. Biol. Chem.* 279:36562–36569.

Cecchini, G. 2003. Function and structure of Complex II of the respiratory chain. *Annu. Rev. Biochem.* 72:77–109.

Lange, C., and Hunte, C. 2002. Crystal structure of the yeast cytochrome bc_1 complex with its bound substrate cytochrome *c. Proc. Natl. Acad. Sci. U.S.A.* 99:2800–2805.

ATP Synthase

Toei, M., and Noji, H. 2013. Single-molecule analysis of F_0F_1-ATP synthase inhibited by N, N-dicyclohexylcarbodiimide. *J. Biol. Chem.* 288:25717–25726.

Watt, I. N., Montgomery, M. G., Runswick, M. J., Leslie, A. G. W., and Walker, J. E. 2010. Bioenergetic cost of making an adenosine triphosphate molecule in animal mitochondria. *Proc. Natl. Acad. Sci. U.S.A.* 107:16823–16827.

Wittig, I., and Hermann, S. 2009. Supramolecular organization of ATP synthase and respiratory chain in mitochondrial membranes. *Biochim. Biophys. Acta* 1787:672–680.

Junge, W., Sielaff, H., and Engelbrecht S. 2009. Torque generation and elastic power transmission in the rotary F_0F_1-ATPase. *Nature* 459:364–370.

von Ballmoos, C., Cook, G. M., and Dimroth, P. 2008. Unique rotary ATP synthase and its biological diversity. *Annu. Rev. Biophys.* 37:43–64.

Adachi, K., Oiwa, K., Nishizaka, T., Furuike, S., Noji, H., Itoh, H., Yoshida, M., and Kinosita, K., Jr. 2007. Coupling of rotation and catalysis in F_1-ATPase revealed by single-molecule imaging and manipulation. *Cell* 130:309–321.

Chen, C., Ko, Y., Delannoy, M., Ludtke, S. J., Chiu, W., and Pedersen, P. L. 2004. Mitochondrial ATP synthasome: Three-dimensional structure by electron microscopy of the ATP synthase in complex formation with the carriers for P_i and ADP/ATP. *J. Biol. Chem.* 279:31761–31768.

Noji, H., and Yoshida, M. 2001. The rotary machine in the cell: ATP synthase. *J. Biol. Chem.* 276:1665–1668.

Yasuda, R., Noji, H., Kinosita, K., Jr., and Yoshida, M. 1998. F_1-ATPase is a highly efficient molecular motor that rotates with discrete 120 degree steps. *Cell* 93:1117–1124.

Noji, H., Yasuda, R., Yoshida, M., and Kinosita, K., Jr., 1997. Direct observation of the rotation of F_1-ATPase. *Nature* 386:299–302.

Tsunoda, S. P., Aggeler, R., Yoshida, M., and Capaldi, R. A. 2001. Rotation of the *c* subunit oligomer in fully functional F_1 F_0 ATP synthase. *Proc. Natl. Acad. Sci. U.S.A.* 987:898–902.

Gibbons, C., Montgomery, M. G., Leslie, A. G. W., and Walker, J. 2000. The structure of the central stalk in F_1-ATPase at 2.4 Å resolution. *Nat. Struct. Biol.* 7:1055–1061.

Sambongi, Y., Iko, Y., Tanabe, M., Omote, H., Iwamoto-Kihara, A., Ueda, I., Yanagida, T., Wada, Y., and Futai, M. 1999. Mechanical rotation of the *c* subunit oligomer in ATP synthase (F_0F_1): Direct observation. *Science* 286:1722–1724.

Translocators and Channels

Villarroya, F., and Vidal-Puig, A. 2013. Beyond the sympathetic tone: The new brown fat activators. *Cell Metab.*17:638–643.

Rey, M., Forest, E., and Pelosi, L. 2012. Exploring the conformational dynamics of the bovine ADP/ATP carrier in mitochondria. *Biochemistry* 51:9727–9735.

Divakaruni, A. S., Humphrey, D. M., and Brand, M. D. 2012. Fatty acids change the conformation of uncoupling protein 1 (UCP1). *J. Biol. Chem.* 44:36845–36853.

Fedorenko, A., Lishko, P. V., and Kirichok, Y. 2012. Mechanism of fatty-acid-dependent UCP1 uncoupling in brown fat mitochondria. *Cell* 151:400–413.

van Marken Lichtenbelt, W. D., Vanhommerig, J. W., Smulders, N. M., Drossaerts, J. M., Kemerink, G. J., Bouvy, N. D., Schrauwen, P., and Teule, G. J. 2009. Cold-activated brown adipose tissue in healthy men. *New Engl. J. Med.* 360:1500–1508.

Cypess, A. M., Sanaz Lehman, S., Gethin Williams, G., Tal, I., Rodman, D., Goldfine, A. B., Kuo, F. C., Palmer, E. L., Tseng, Y.-H., Doria, A., et al. 2009. Identification and importance of brown adipose tissue in adult humans. *New Engl. J. Med.* 360:1509–1517.

Virtanen, K. A., Lidell, M. E., Orava, J., Heglind, M., Westergren, R., Niemi, T., Taittonen, M., Laine, J., Savisto, N.-J., Enerbäck, S., et al. 2009. Functional brown adipose tissue in healthy adults. *New Engl. J. Med.* 360:1518–1525.

Bayrhuber, M., Meins, T., Habeck, M., Becker, S., Giller, K., Villinger, S., Vonrhein, C., Griesinger, C., Zweckstetter, M., and Zeth, K. 2008. Structure of the human voltage-dependent anion channel. *Proc. Natl. Acad. Sci. U.S.A.* 105:15370–15375.

Bamber, L., Harding, M., Monné, M., Slotboom, D.-J., and Kunji, E. R. 2007. The yeast mitochondrial ADP/ATP carrier functions as a monomer in mitochondrial membranes. *Proc. Natl. Acad. Sci. U.S.A.* 10:10830–10843.

Pebay-Peyroula, E., Dahout, C., Kahn, R., Trézéguet, V., Lauquin, G. J.-M., and Brandolin, G. 2003. Structure of mitochondrial ADP/ATP carrier in complex with carboxyatractyloside. *Nature* 246:39–44.

Reactive Oxygen Species, Superoxide Dismutase, and Catalase

Sena, L. A., and Chandel, N. S. 2012. Physiological roles of mitochondrial reactive oxygen species. *Mol. Cell* 48:158–167.

Forman, H. J., Maiorino, M., and Ursini, F. 2010. Signaling functions of reactive oxygen species. *Biochemistry* 49:835–842.

Murphy, M. P. 2009. How mitochondria produce reactive oxygen species. *Biochem. J.* 417:1–13.

Leitch, J. M., Yick, P. J., and Culotta, V. V. 2009. The right to choose: Multiple pathways for activating copper, zinc superoxide dismutase. *J. Biol. Chem.* 284:24679–24683.

Winterbourn, C. C. 2008. Reconciling the chemistry and biology of reactive oxygen species. *Nat. Chem. Biol.* 4:278–286.

Veal, E. A., Day, A. M., and Morgan, B. A. 2007. Hydrogen peroxide sensing and signaling. *Mol. Cell* 26:1–14.

Stone, J. R., and Yang, S. 2006. Hydrogen peroxide: A signaling messenger. *Antioxid. Redox Signal.* 8:243–270.

Valentine, J. S., Doucette, P. A., and Potter S. Z. 2005. Copper-zinc superoxide dismutase and amyotrophic lateral sclerosis. *Annu. Rev. Biochem.* 74:563–593.

Mitochondrial Diseases

Papa, S., and De Rasmo, D. 2013. Complex I deficiencies in neurological disorders. *Trends Mol. Med.* 19:61–69.

Koopman, W. J. H., Willems, P. H. G. M., and Smeitink, J. A. M. 2012. Monogenic mitochondrial disorders. *New Engl. J. Med.* 366:1132–41.

Lina, C. S., Sharpley, M. S., Fan W., Waymire, K. G., Sadun, A. A., Carelli, V., Ross-Cisneros, F. N., Baciu, P., Sung, E., McManus, M. J., et al. 2012. Mouse mtDNA mutant model of Leber hereditary optic neuropathy. *Proc. Natl. Acad. Sci. U.S.A.* 109:20065–20070.

Mitochondria Disease. 2009. A compendium of nine articles on mitochondrial diseases. *Biochem. Biophys. Acta Mol. Basis Disease* 1792:1095–1167.

Cicchetti, F., Drouin-Ouellet, J., and Gross, R. E. 2009. Environmental toxins and Parkinson's disease: What have we learned from pesticide-induced animal models? *Trends Pharm. Sci.* 30:475–483.

DiMauro, S., and Schon, E. A. 2003. Mitochondrial respiratory-chain disease. *New Engl. J. Med.* 348:2656–2668.

Smeitink, J., van den Heuvel, L., and DiMauro, S. 2001. The genetics and pathology of oxidative phosphorylation. *Nat. Rev. Genet.* 2:342–352.

Apoptosis

Qi, S., Pang, Y., Hu, Q., Liu, Q., Li, H., Zhou, Y., He, T., Liang, Q., Liu, Y., Yuan, X., et al. 2010. Crystal structure of the *Caenorhabditis elegans* apoptosome reveals an octameric assembly of CED-4. *Cell* 141:446–457.

Chan, D. C. 2006. Mitochondria: Dynamic organelles in disease, aging, and development. *Cell* 125:1241–1252.

Green, D. R. 2005. Apoptotic pathways: Ten minutes to dead. *Cell* 121:671–674.

Historical Aspects

Prebble, J., and Weber, B. 2003. *Wandering in the Gardens of the Mind: Peter Mitchell and the Making of Glynn.* Oxford.

Mitchell, P. 1979. Keilin's respiratory chain concept and its chemiosmotic consequences. *Science* 206:1148–1159.

Preeble, J. 2002. Peter Mitchell and the ox phos wars. *Trends Biochem. Sci.* 27:209–212.

Mitchell, P. 1976. Vectorial chemistry and the molecular mechanics of chemiosmotic coupling: Power transmission by proticity. *Biochem. Soc. Trans.* 4:399–430.

Racker, E. 1980. From Pasteur to Mitchell: A hundred years of bioenergetics. *Fed. Proc.* 39:210–215.

Kalckar, H. M. 1991. Fifty years of biological research: From oxidative phosphorylation to energy requiring transport and regulation. *Annu. Rev. Biochem.* 60:1–37.

Chapter 19

Where to Start

Huber, R. 1989. A structural basis of light energy and electron transfer in biology. *EMBO J.* 8:2125–2147.

Deisenhofer, J., and Michel, H. 1989. The photosynthetic reaction centre from the purple bacterium *Rhodopseudomonas viridis. EMBO J.* 8:2149–2170.

Barber, J., and Andersson, B. 1994. Revealing the blueprint of photosynthesis. *Nature* 370:31–34.

Books and General Reviews

Nelson, N., and Yocum, C. 2006. Structure and functions of photosystems I and II. *Annu. Rev. Plant Biol.* 57:521–565.

Merchant, S., and Sawaya, M. R. 2005. The light reactions: A guide to recent acquisitions for the picture gallery. *Plant Cell* 17:648–663.

Blankenship, R. E. 2009. *Molecular Mechanisms of Photosynthesis.* Wiley-Blackwell.

Nicholls, D. G., and Ferguson, S. J. 2013. *Bioenergetics* (4th ed.). Academic Press.

Electron-Transfer Mechanisms

Beratan, D., and Skourtis, S. 1998. Electron transfer mechanisms. *Curr. Opin. Chem. Biol.* 2:235–243.

Moser, C. C., Keske, J. M., Warncke, K., Farid, R. S., and Dutton, P. L. 1992. Nature of biological electron transfer. *Nature* 355:796–802.

Boxer, S. G. 1990. Mechanisms of long-distance electron transfer in proteins: Lessons from photosynthetic reaction centers. *Annu. Rev. Biophys. Biophys. Chem.* 19:267–299.

Photosystem II

Vinyard, D. J., Ananyev, G. M., and Dismukes, G. C. 2013. Photosystem II: The reaction center of oxygenic photosynthesis. *Annu. Rev. Biochem.* 82:577–606.

Kirchhoff, H., Tremmel, I., Haase, W., and Kubitscheck, U. 2004. Supramolecular photosystem II organization in grana of thylakoid membranes: Evidence for a structured arrangement. *Biochemistry* 43:9204–9213.

Diner, B. A., and Rappaport, F. 2002. Structure, dynamics, and energetics of the primary photochemistry of photosystem II of oxygenic photosynthesis. *Annu. Rev. Plant Biol.* 54:551–580.

Zouni, A., Witt, H. T., Kern, J., Fromme, P., Krauss, N., Saenger, W., and Orth, P. 2001. Crystal structure of photosystem II from *Synechococcus elongatus* at 3.8 Å resolution. *Nature* 409:739–743.

Deisenhofer, J., and Michel, H. 1991. High-resolution structures of photosynthetic reaction centers. *Annu. Rev. Biophys. Biophys. Chem.* 20:247–266.

Oxygen Evolution

Umena, Y., Kawakami, K., Shen, J.-R. and Kamiya, N. 2011. Crystal structure of oxygen-evolving photosystem II at a resolution of 1.9Å. *Nature* 473:55–60.

Barber, J. 2008. Crystal structure of the oxygen-evolving complex of photosystem II. *Inorg. Chem.* 47:1700–1710.

Pushkar, Y., Yano, J., Sauer, K., Boussac, A., and Yachandra, V. K. 2008. Structural changes in the Mn_4Ca cluster and the mechanism of photosynthetic water splitting. *Proc. Natl. Acad. Sci. U.S.A.* 105:1879–1884.

Renger, G. 2007. Oxidative photosynthetic water splitting: Energetics, kinetics and mechanism. *Photosynth. Res.* 92:407–425.

Renger, G., and Kühn, P. 2007. Reaction pattern and mechanism of light induced oxidative water splitting in photosynthesis. *Biochim. Biophys. Acta* 1767:458–471.

Photosystem I and Cytochrome *bf*

Schöttler, M. A., Albus, C. A., and Bock, R. 2011. Photosystem I: Its biogenesis and function in higher plants. *J. Plant Physiol.* 168:1452–1461.

Iwai, M., Takizawa, K., Tokutsu, R., Okamuro, A., Takahashi, Y., and Minagawa, J. 2010. Isolation of the elusive supercomplex that drives cyclic electron flow in photosynthesis. *Nature* 464:1210–1214.

Amunts, A., Drory, O., and Nelson, N. 2007. The structure of photosystem I supercomplex at 3.4 Å resolution. *Nature* 447:58–63.

Cramer, W. A., Zhang, H., Yan, J., Kurisu, G., and Smith, J. L. 2004. Evolution of photosynthesis: Time-independent structure of the cytochrome b_6f complex. *Biochemistry* 43:5921–5929.

Kargul, J., Nield, J., and Barber, J. 2003. Three-dimensional reconstruction of a light-harvesting complex I-photosystem I (LHCI-PSI) supercomplex from the green alga *Chlamydomonas reinhardtii. J. Biol. Chem.* 278:16135–16141.

Schubert, W. D., Klukas, O., Saenger, W., Witt, H. T., Fromme, P., and Krauss, N. 1998. A common ancestor for oxygenic and anoxygenic photosynthetic systems: A comparison based on the structural model of photosystem I. *J. Mol. Biol.* 280:297–314.

ATP Synthase

Kohzuma, K., Dal Bosco, C., Meurer, J., and Kramer, D. M. 2013. Light- and metabolism-related regulation of the chloroplast ATP synthase has distinct mechanisms and functions. *J. Biol. Chem.* 288:13156–13163.

Vollmar, M., Schlieper, D., Winn, D., Büchner, C., and Groth, G. 2009. Structure of the c14 rotor ring of the proton translocating chloroplast ATP synthase. *J. Biol. Chem.* 284:18228–18235.

Varco-Merth, B., Fromme, R., Wang, M., and Fromme, P. 2008. Crystallization of the c14-rotor of the chloroplast ATP synthase reveals that it contains pigments. *Biochim. Biophys. Acta* 1777:605–612.

Oster, G., and Wang, H. 1999. ATP synthase: Two motors, two fuels. *Structure* 7:R67–R72.

Weber, J., and Senior, A. E. 2000. ATP synthase: What we know about ATP hydrolysis and what we do not know about ATP synthesis. *Biochim. Biophys. Acta* 1458:300–309.

Light-Harvesting Assemblies

Collins, A. M., Qian, P., Tang, Q., Bocian, D. F., Hunter, C. N., Blankenship, R. E. 2010. Light-harvesting antenna system from the phototrophic bacterium *Roseiflexus castenholzii. Biochemistry* 49:7524–7531.

Melkozernov, A. N., Barber, J., and Blankenship, R. E. 2006. Light harvesting in photosystem I supercomplexes. *Biochemistry* 45:331–345.

Conroy, M. J., Westerhuis, W. H., Parkes-Loach, P. S., Loach, P. A., Hunter, C. N., and Williamson, M. P. 2000. The solution structure of *Rhodobacter sphaeroides* LH1b reveals two helical domains separated by a more flexible region: Structural consequences for the LH1 complex. *J. Mol. Biol.* 298:83–94.

Koepke, J., Hu, X., Muenke, C., Schulten, K., and Michel, H. 1996. The crystal structure of the light-harvesting complex II (B800–850) from *Rhodospirillum molischianum. Structure* 4:581–597.

Grossman, A. R., Bhaya, D., Apt, K. E., and Kehoe, D. M. 1995. Light-harvesting complexes in oxygenic photosynthesis: Diversity, control, and evolution. *Annu. Rev. Genet.* 29:231–288.

Evolution

Hohmann-Marriott, M. F., and Blankenship, R. E. 2011. Evolution of photosynthesis. *Annu. Rev. Plant Biol.* 62:515–48.

Chen, M., and Zhang, Y. 2008. Tracking the molecular evolution of photosynthesis through characterization of atomic contents of the photosynthetic units. *Photosynth. Res.* 97:255–261.

Iverson, T. M. 2006. Evolution and unique bioenergetic mechanisms in oxygenic photosynthesis. *Curr. Opin. Chem. Biol.* 10:91–100.

Cavalier-Smith, T. 2002. Chloroplast evolution: Secondary symbiogenesis and multiple losses. *Curr. Biol.* 12:R62–64.

Nelson, N., and Ben-Shem, A. 2005. The structure of photosystem I and evolution of photosynthesis. *BioEssays* 27:914–922.

Green, B. R. 2001. Was "molecular opportunism" a factor in the evolution of different photosynthetic light-harvesting pigment systems? *Proc. Natl. Acad. Sci. U.S.A.* 98:2119–2121.

Dismukes, G. C., Klimov, V. V., Baranov, S. V., Nozlov, Y. N., Das Gupta, J., and Tyryshkin, A. 2001. The origin of atmospheric oxygen on Earth: The innovation of oxygenic photosynthesis. *Proc. Natl. Acad. Sci. U.S.A.* 98:2170–2175.

Moreira, D., Le Guyader, H., and Phillippe, H. 2000. The origin of red algae and the evolution of chloroplasts. *Nature* 405:69–72.

Cavalier-Smith, T. 2000. Membrane heredity and early chloroplast evolution. *Trends Plant Sci.* 5:174–182.

Chapter 20

Where to Start

Buchanan, B. B., and Wong, J. H. 2013. A conversation with Andrew Benson: reflections on the discovery of the Calvin–Benson cycle. *Photosynth. Res.* 114:207–214.

Ellis, R. J. 2010. Tackling unintelligent design. *Nature* 463:164–165.

Gutteridge, S., and Pierce, J. 2006. A unified theory for the basis of the limitations of the primary reaction of photosynthetic CO_2 fixation: Was Dr. Pangloss right? *Proc. Natl. Acad. Sci. U.S.A.* 103:7203–7204.

Horecker, B. L. 1976. Unravelling the pentose phosphate pathway. In *Reflections on Biochemistry* (pp. 65–72), edited by A. Kornberg, L. Cornudella, B. L. Horecker, and J. Oro. Pergamon.

Levi, P. 1984. Carbon. In *The Periodic Table.* Random House.

Books and General Reviews

Parry, M. A. J., Andralojc, P. J., Mitchell, R. A. C., Madgwick, P. J., and Keys, A. J. 2003. Manipulation of rubisco: The amount, activity, function and regulation. *J. Exp. Bot.* 54:1321–1333.

Spreitzer, R. J., and Salvucci, M. E. 2002. Rubisco: Structure, regulatory interactions, and possibilities for a better enzyme. *Annu. Rev. Plant Biol.* 53:449–475.

Wood, T. 1985. *The Pentose Phosphate Pathway.* Academic Press.

Buchanan, B. B., Gruissem, W., and Jones, R. L. 2000. *Biochemistry and Molecular Biology of Plants.* American Society of Plant Physiologists.

Enzymes and Reaction Mechanisms

Harrison, D. H., Runquist, J. A., Holub, A., and Miziorko, H. M. 1998. The crystal structure of phosphoribulokinase from *Rhodobacter sphaeroides* reveals a fold similar to that of adenylate kinase. *Biochemistry* 37:5074–5085.

Miziorko, H. M. 2000. Phosphoribulokinase: Current perspectives on the structure/function basis for regulation and catalysis. *Adv. Enzymol. Relat. Areas Mol. Biol.* 74:95–127.

Thorell, S., Gergely, P., Jr., Banki, K., Perl, A., and Schneider, G. 2000. The three-dimensional structure of human transaldolase. *FEBS Lett.* 475:205–208.

Carbon Dioxide Fixation and Rubisco

Satagopan, S., Scott, S. S., Smith, T. G., and Tabita, F. R. 2009. A rubisco mutant that confers growth under a normally "inhibitory" oxygen concentration. *Biochemistry* 48:9076–9083.

Tcherkez, G. G. B., Farquhar, G. D., and Andrews, J. T. 2006. Despite slow catalysis and confused substrate specificity, all ribulose bisphosphate carboxylases may be nearly perfectly optimized. *Proc. Natl. Acad. Sci. U.S.A.* 103:7246–7251.

Sugawara, H., Yamamoto, H., Shibata, N., Inoue, T., Okada, S., Miyake, C., Yokota, A., and Kai, Y. 1999. Crystal structure of carboxylase reaction-oriented ribulose 1,5-bisphosphate carboxylase/oxygenase from a thermophilic red alga, *Galdieria partita. J. Biol. Chem.* 274:15655–15661.

Hansen, S., Vollan, V. B., Hough, E., and Andersen, K. 1999. The crystal structure of rubisco from *Alcaligenes eutrophus* reveals a novel central eight-stranded β-barrel formed by β-strands from four subunits. *J. Mol. Biol.* 288:609–621.

Knight, S., Andersson, I., and Branden, C. I. 1990. Crystallographic analysis of ribulose 1,5-bisphosphate carboxylase from spinach at 2.4 Å resolution: Subunit interactions and active site. *J. Mol. Biol.* 215:113–160.

Taylor, T. C., and Andersson, I. 1997. The structure of the complex between rubisco and its natural substrate ribulose 1,5-bisphosphate. *J. Mol. Biol.* 265:432–444.

Cleland, W. W., Andrews, T. J., Gutteridge, S., Hartman, F. C., and Lorimer, G. H. 1998. Mechanism of rubisco: The carbamate as general base. *Chem. Rev.* 98:549–561.

Buchanan, B. B. 1992. Carbon dioxide assimilation in oxygenic and anoxygenic photosynthesis. *Photosynth. Res.* 33:147–162.

Hatch, M. D. 1987. C_4 photosynthesis: A unique blend of modified biochemistry, anatomy, and ultrastructure. *Biochim. Biophys. Acta* 895:81–106.

Regulation

Keown, J. R., Griffin, M. D. W., Mertens, H. D. T., and Pearce, F. G. 2013. Small oligomers of ribulose-bisphosphate carboxylase/oxygenase (rubisco) activase are required for biological activity. *J. Biol. Chem.* 288:20607–20615.

Carmo-Silva, A. E., and Salvucci, M. E. 2013. The regulatory properties of rubisco activase differ among species and affect photosynthetic induction during light transitions. *Plant Physiol.* 161:1645–1655.

Gontero, B., and Maberly, S. C. 2012. An intrinsically disordered protein, CP12: Jack of all trades and master of the Calvin cycle. *Biochem. Soc. Trans.* 40:995–999.

Stotz, M., Mueller-Cajar, O., Ciniawsky, S., Wendler, P., Hartl, F.-U., Bracher, A., Hayer-Hartl, M. 2011. Structure of green-type Rubisco activase from tobacco. *Nature Struct. Mol. Biol.* 18:1366–1370.

Lebreton, S., Andreescu, S., Graciet, E., and Gontero, B. 2006. Mapping of the interaction site of CP12 with glyceraldehyde-3-phosphate dehydrogenase from *Chlamydomonas reinhardtii*. Functional consequences for glyceraldehyde-3-phosphate dehydrogenase. *FEBS J.* 273:3358–3369.

Graciet, E., Lebreton, S., and Gontero, B. 2004. The emergence of new regulatory mechanisms in the Benson-Calvin pathway via protein-protein interactions: A glyceraldehyde-3-phosphate dehydrogenase/CP12/phosphoribulokinase complex. *J. Exp. Bot.* 55:1245–1254.

Balmer, Y., Koller, A., del Val, G., Manieri, W., Schürmann, P., and Buchanan, B. B. 2003. Proteomics gives insight into the regulatory function of chloroplast thioredoxins. *Proc. Natl. Acad. Sci. U.S.A.* 100:370–375.

Wedel, N., Soll, J., and Paap, B. K. 1997. CP12 provides a new mode of light regulation of Calvin cycle activity in higher plants. *Proc. Natl. Acad. Sci. U.S.A.* 94:10479–10484.

Avilan, L., Lebreton, S., and Gontero, B. 2000. Thioredoxin activation of phosphoribulokinase in a bi-enzyme complex from *Chlamydomonas reinhardtii* chloroplasts. *J. Biol. Chem.* 275:9447–9451.

Irihimovitch, V., and Shapira, M. 2000. Glutathione redox potential modulated by reactive oxygen species regulates translation of rubisco large subunit in the chloroplast. *J. Biol. Chem.* 275:16289–16295.

Glucose 6-phosphate Dehydrogenase

Howes, R. E., Piel, F. B., Patil, A. P., Nyangiri, O. A., Gething, P. W., Dewi, M., Hogg, M. M., Battle, K. E., Padilla, C. D., Baird, et al. 2012. G6PD deficiency prevalence and estimates of affected populations in malaria endemic countries: A geostatistical model-based map. *PLoS Med.* 9:e1001339.

Wang, X.-T., and Engel, P. C. 2009. Clinical mutants of human glucose 6-phosphate dehydrogenase: Impairment of $NADP^+$ binding affects both folding and stability. *Biochim. Biophys. Acta* 1792:804–809.

Au, S. W., Gover, S., Lam, V. M., and Adams, M. J. 2000. Human glucose-6-phosphate dehydrogenase: The crystal structure reveals a structural NADP(+) molecule and provides insights into enzyme deficiency. *Struct. Fold. Des.* 8:293–303.

Salvemini, F., Franze, A., Iervolino, A., Filosa, S., Salzano, S., and Ursini, M. V. 1999. Enhanced glutathione levels and oxidoresistance mediated by increased glucose-6-phosphate dehydrogenase expression. *J. Biol. Chem.* 274:2750–2757.

Tian, W. N., Braunstein, L. D., Apse, K., Pang, J., Rose, M., Tian, X., and Stanton, R. C. 1999. Importance of glucose-6-phosphate dehydrogenase activity in cell death. *Am. J. Physiol.* 276:C1121–C1131.

Tian, W. N., Braunstein, L. D., Pang, J., Stuhlmeier, K. M., Xi, Q. C., Tian, X., and Stanton, R. C. 1998. Importance of glucose-6-phosphate dehydrogenase activity for cell growth. *J. Biol. Chem.* 273:10609–10617.

Ursini, M. V., Parrella, A., Rosa, G., Salzano, S., and Martini, G. 1997. Enhanced expression of glucose-6-phosphate dehydrogenase in human cells sustaining oxidative stress. *Biochem. J.* 323:801–806.

Evolution

Williams, B. P., Aubry S., and Hibberd, J. M. 2012. Molecular evolution of genes recruited into C_4 photosynthesis. *Trends Plant Sci.* 4:213–220.

Sage, R. F., Sage, T. L., and Kocacinar, F. 2012. Photorespiration and the evolution of C_4 photosynthesis. *Annu. Rev. Plant Biol.* 63:19–47.

Deschamps, P., Haferkamp, I., d'Hulst, C., Neuhaus, H. E., and Ball, S. G. 2008. The relocation of starch metabolism to chloroplasts: When, why and how. *Trends Plant Sci.* 13:574–582.

Coy, J. F., Dubel, S., Kioschis, P., Thomas, K., Micklem, G., Delius, H., and Poustka, A. 1996. Molecular cloning of tissue-specific transcripts of a transketolase-related gene: Implications for the evolution of new vertebrate genes. *Genomics* 32:309–316.

Schenk, G., Layfield, R., Candy, J. M., Duggleby, R. G., and Nixon, P. F. 1997. Molecular evolutionary analysis of the thiamine-diphosphate-dependent enzyme, transketolase. *J. Mol. Evol.* 44:552–572.

Notaro, R., Afolayan, A., and Luzzatto, L. 2000. Human mutations in glucose 6-phosphate dehydrogenase reflect evolutionary history. *FASEB J.* 14:485–494.

Wedel, N., and Soll, J. 1998. Evolutionary conserved light regulation of Calvin cycle activity by NADPH-mediated reversible phosphoribulokinase/CP12/glyceraldehyde-3-phosphate dehydrogenase complex dissociation. *Proc. Natl. Acad. Sci. U.S.A.* 95:9699–9704.

Martin, W., and Schnarrenberger, C. 1997. The evolution of the Calvin cycle from prokaryotic to eukaryotic chromosomes: A case study of functional redundancy in ancient pathways through endosymbiosis. *Curr. Genet.* 32:1–18.

Ku, M. S., Kano-Murakami, Y., and Matsuoka, M. 1996. Evolution and expression of C4 photosynthesis genes. *Plant Physiol.* 111:949–957.

Pereto, J. G., Velasco, A. M., Becerra, A., and Lazcano, A. 1999. Comparative biochemistry of CO_2 fixation and the evolution of autotrophy. *Int. Microbiol.* 2:3–10.

Chapter 21

Where to Start

Fisher, E. H. 2013. Cellular regulation by protein phosphorylation. *Biochem. Biophys. Res. Commun.* 430:865–867.

Greenberg, C. C., Jurczak, M. J., Danos, A. M., and Brady, M. J. 2006. Glycogen branches out: New perspectives on the role of glycogen metabolism in the integration of metabolic pathways. *Am. J. Physiol. Endocrinol. Metab.* 291:E1–E8.

Books and General Reviews

Roach, P. J, Depaoli-Roach, A. A., Hurley, T. D., and Tagliabracci, V. S. 2012. Glycogen and its metabolism: Some new developments and old themes. *Biochem. J.* 441:763–787.

Palm, D. C., Rohwer J. M., and Hofmeyr, J.-H. S. 2013. Regulation of glycogen synthase from mammalian skeletal muscle: A unifying view of allosteric and covalent regulation. *FEBS J.* 280:2–27.

Agius, L. 2008. Glucokinase and molecular aspects of liver glycogen metabolism. *Biochem. J.* 414:1–18.

Structural Studies

Nadeau, O. W., Lane, L. A., Xu, D., Sage, J., Priddy, T. S., Artigues, A., Villar, M. T., Yang, Q., Robinson, C. V., Zhang, Y. et al. 2012. Structure and location of the regulatory β subunits in the $(\alpha\beta\gamma\delta)_4$ phosphorylase kinase complex. *J. Biol. Chem.* 287:36651–36661.

Horcajada, C., Guinovart, J. J., Fita, I., and Ferrer, J. C. 2006. Crystal structure of an archaeal glycogen synthase: Insights into oligomerization and substrate binding of eukaryotic glycogen synthases. *J. Biol. Chem.* 281:2923–2931.

Buschiazzo, A., Ugalde, J. E., Guerin, M. E., Shepard, W., Ugalde, R. A., and Alzari, P. M. 2004. Crystal structure of glycogen synthase: Homologous enzymes catalyze glycogen synthesis and degradation. *EMBO J.* 23:3196–3205.

Gibbons, B. J., Roach, P. J., and Hurley, T. D. 2002. Crystal structure of the autocatalytic initiator of glycogen biosynthesis, glycogenin. *J. Mol. Biol.* 319:463–477.

Priming of Glycogen Synthesis

Lomako, J., Lomako, W. M., and Whelan, W. J. 2004. Glycogenin: The primer for mammalian and yeast glycogen synthesis. *Biochim. Biophys. Acta* 1673:45–55.

Lin, A., Mu, J., Yang, J., and Roach, P. J. 1999. Self-glucosylation of glycogenin, the initiator of glycogen biosynthesis, involves an intersubunit reaction. *Arch. Biochem. Biophys.* 363:163–170.

Roach, P. J., and Skurat, A. V. 1997. Self-glucosylating initiator proteins and their role in glycogen biosynthesis. *Prog. Nucleic Acid Res. Mol. Biol.* 57:289–316.

Catalytic Mechanisms

Skamnaki, V. T., Owen, D. J., Noble, M. E., Lowe, E. D., Lowe, G., Oikonomakos, N. G., and Johnson, L. N. 1999. Catalytic mechanism of phosphorylase kinase probed by mutational studies. *Biochemistry* 38:14718–14730.

Buchbinder, J. L., and Fletterick, R. J. 1996. Role of the active site gate of glycogen phosphorylase in allosteric inhibition and substrate binding. *J. Biol. Chem.* 271:22305–22309.

Regulation of Glycogen Metabolism

Zhang, T., Wang, S., Lin, Y., Xu, W., Ye, D., Xiong, Y., Zhao, S., and Guan, K.-L. 2012. Acetylation negatively regulates glycogen phosphorylase by recruiting protein phosphatase 1. *Cell Metab.* 15:75–87.

Díaz, A., Martínez-Pons, C., Fita, I., Ferrer, J. C., Guinovart, J. J. 2011. Processivity and subcellular localization of glycogen synthase depend on a non-catalytic high affinity glycogen-binding site. *J. Biol. Chem.* 286:18505–18514.

Bouskila, M., Hunter, R. W., Ibrahim, A. D. F., Delattre, L., Peggie, M., van Diepen, J. A., Voshol, P. J., Jensen, J., Sakamoto, K. 2010. Allosteric regulation of glycogen synthase controls glycogen synthesis in muscle. *Cell Metab.*12:456–466.

Ros, S., García-Rocha, M., Domínguez, J., Ferrer, J. C., Guinovart, J. J. 2009. Control of liver glycogen synthase activity and intracellular distribution by phosphorylation. *J. Biol. Chem.* 284:6370–6378.

Danos, A. M., Osmanovic, S., and Brady, M. J. 2009. Differential regulation of glycogenolysis by mutant protein phosphatase-1 glycogen-targeting subunits. *J. Biol. Chem.* 284:19544–19553.

Pautsch, A., Stadler, N., Wissdorf, O., Langkopf, E., Moreth, W., Streicher, R. 2008. Molecular recognition of the protein phosphatase 1 glycogen targeting subunit by glycogen phosphorylase. *J. Biol. Chem.* 283:8913–8918.

Boulatnikov, I. G., Peters, J. L., Nadeau, O. W., Sage, J. M., Daniels, P. J., Kumar, P., Walsh, D. A., and Carlson, G. M. 2009. Expressed phosphorylase *b* kinase and its $\alpha\gamma\delta$ subcomplex as regulatory models for the rabbit skeletal muscle holoenzyme. *Biochemistry* 48:10183–10191.

Ros, S., García-Rocha, M., Domínguez, J., Ferrer, J. C., and Guinovart, J. J. 2009. Control of liver glycogen synthase activity and intracellular distribution by phosphorylation. *J. Biol. Chem.* 284:6370–6378.

Danos, A. M., Osmanovic, S., and Brady, M. J. 2009. Differential regulation of glycogenolysis by mutant protein phosphatase-1 glycogen-targeting subunits. *J. Biol. Chem.* 284:19544–19553.

Pautsch, A., Stadler, N., Wissdorf, O., Langkopf, E., Moreth, M., and Streicher, R. 2008. Molecular recognition of the protein phosphatase 1 glycogen targeting subunit by glycogen phosphorylase. *J. Biol. Chem.* 283:8913–8918.

Jope, R. S., and Johnson, G. V. W. 2004. The glamour and gloom of glycogen synthase kinase-3. *Trends Biochem. Sci.* 29:95–102.

Doble, B. W., and Woodgett, J. R. 2003. GSK-3: Tricks of the trade for a multi-tasking kinase. *J. Cell Sci.* 116:1175–1186.

Pederson, B. A., Cheng, C., Wilson, W. A., and Roach, P. J. 2000. Regulation of glycogen synthase: Identification of residues involved in regulation by the allosteric ligand glucose-6-P and by phosphorylation. *J. Biol. Chem.* 275:27753–27761.

Melendez, R., Melendez-Hevia, E., and Canela, E. I. 1999. The fractal structure of glycogen: A clever solution to optimize cell metabolism. *Biophys. J.* 77:1327–1332.

Franch, J., Aslesen, R., and Jensen, J. 1999. Regulation of glycogen synthesis in rat skeletal muscle after glycogen-depleting contractile activity: Effects of adrenaline on glycogen synthesis and activation of glycogen synthase and glycogen phosphorylase. *Biochem. J.* 344:231–235.

Aggen, J. B., Nairn, A. C., and Chamberlin, R. 2000. Regulation of protein phosphatase-1. *Chem. Biol.* 7:R13–R23.

Egloff, M. P., Johnson, D. F., Moorhead, G., Cohen, P. T., Cohen, P., and Barford, D. 1997. Structural basis for the recognition of regulatory subunits by the catalytic subunit of protein phosphatase 1. *EMBO J.* 16:1876–1887.

Wu, J., Liu, J., Thompson, I., Oliver, C. J., Shenolikar, S., and Brautigan, D. L. 1998. A conserved domain for glycogen binding in protein phosphatase-1 targeting subunits. *FEBS Lett.* 439:185–191.

Genetic Diseases

Nyhan, W. L., Barshop, B. A., and Ozand, P. T. 2005. *Atlas of Metabolic Diseases*. (2d ed., pp. 373–408). Hodder Arnold.

Chen, Y.-T. 2001. Glycogen storage diseases. In *The Metabolic and Molecular Bases of Inherited Diseases* (8th ed., pp. 1521–1552), edited by C. R. Scriver., W. S. Sly, B. Childs, A. L. Beaudet, D. Valle, K. W. Kinzler, and B. Vogelstein. McGraw-Hill.

Burchell, A., and Waddell, I. D. 1991. The molecular basis of the hepatic microsomal glucose-6-phosphatase system. *Biochim. Biophys. Acta* 1092:129–137.

Lei, K. J., Shelley, L. L., Pan, C. J., Sidbury, J. B., and Chou, J. Y. 1993. Mutations in the glucose-6-phosphatase gene that cause glycogen storage disease type Ia. *Science* 262:580–583.

Ross, B. D., Radda, G. K., Gadian, D. G., Rocker, G., Esiri, M., and Falconer-Smith, J. 1981. Examination of a case of suspected McArdle's syndrome by ^{31}P NMR. *New Engl. J. Med.* 304:1338–1342.

Evolution

Holm, L., and Sander, C. 1995. Evolutionary link between glycogen phosphorylase and a DNA modifying enzyme. *EMBO J.* 14: 1287–1293.

Hudson, J. W., Golding, G. B., and Crerar, M. M. 1993. Evolution of allosteric control in glycogen phosphorylase. *J. Mol. Biol.* 234:700–721.

Rath, V. L., and Fletterick, R. J. 1994. Parallel evolution in two homologues of phosphorylase. *Nat. Struct. Biol.* 1:681–690.

Melendez, R., Melendez-Hevia, E., and Cascante, M. 1997. How did glycogen structure evolve to satisfy the requirement for rapid mobilization of glucose? A problem of physical constraints in structure building. *J. Mol. Evol.* 45:446–455.

Rath, V. L., Lin, K., Hwang, P. K., and Fletterick, R. J. 1996. The evolution of an allosteric site in phosphorylase. *Structure* 4:463–473.

Chapter 22

Where to Start

Walther, T. C., and Farese Jr., R. V. 2012. Lipid droplets and cellular lipid metabolism. *Annu. Rev. Biochem.* 81:687–714.

Granneman, J. G., and Moore, H.-P. 2008. Location, location: Protein trafficking and lipolysis in adipocytes. *Trends Endocrinol. Metab.* 19:3–9.

Yang, L., Ding, Y., Chen, Y., Zhang, S., Huo, C., Wang, Y., Yu, J., Zhang, P., Na, H., Zhang, H., et al. 2012. The proteomics of lipid droplets: Structure, dynamics, and functions of the organelle conserved from bacteria to humans. *J. Lipid Res.* 53:1245–1253.

Rinaldo, P., Matern, D., and Bennet, M. J. 2002. Fatty acid oxidation disorders. *Annu. Rev. Physiol.* 64:477–502.

Rasmussen, B. B., and Wolfe, R. R. 1999. Regulation of fatty acid oxidation in skeletal muscle. *Annu. Rev. Nutr.* 19:463–484.

Semenkovich, C. F. 1997. Regulation of fatty acid synthase (FAS). *Prog. Lipid Res.* 36:43–53.

Wolf, G. 1996. Nutritional and hormonal regulation of fatty acid synthase. *Nutr. Rev.* 54:122–123.

Books

Lawrence, G. D. 2010. *The Fats of Life: Essential Fatty Acids in Health and Disease.* Rutgers University Press.

Vance, D. E., and Vance, J. E. (Eds.). 2008. *Biochemistry of Lipids, Lipoproteins, and Membranes.* Elsevier.

Stipanuk, M. H. (Ed.). 2006. *Biochemical and Physiological Aspects of Human Nutrition.* Saunders.

Fatty Acid Oxidation

Ross, L. E., Xiao, X., and Lowe, M. E. 2013. Identification of amino acids in human colipase that mediate adsorption to lipid emulsions and mixed micelles. *Biochim. Biophys. Acta* 1831: 1052–1059.

Badin, P. M., Loubière, C., Coonen, M., Louche, K., Tavernier, G., Bourlier, V., Mairal, A., Rustan, A. C., Smith, S. R., Langin, D., et al. 2012. Regulation of skeletal muscle lipolysis and oxidative metabolism by the co-lipase CGI-58. *J. Lipid Res.* 53:839–848.

Yang, X., Lu, X., Lombès, M., Rha, G. B., Chi, Y. I., Guerin, T. M., Smart, E. J., Liu, J. 2010. The G_0/G_1 switch gene 2 regulates adipose lipolysis through association with adipose triglyceride lipase. *Cell Metab.* 11:194–205.

Wang, Y., Mohsen, A.-W., Mihalik, S. J., Goetzman, E. S., Vockley, J. 2010. Evidence for physical association of mitochondrial fatty acid oxidation and oxidative phosphorylation complexes. *J. Biol.Chem.* 285:29834–29841.

Ahmadian, M., Duncan, R. E., and Sul, H. S. 2009. The skinny on fat: Lipolysis and fatty acid utilization in adipocytes. *Trends Endocrinol. Metab.* 20:424–428.

Farese, R. V., Jr., and Walther, T. C. 2009. Lipid droplets finally get a little R-E-S-P-E-C-T. *Cell* 139:855–860.

Goodman, J. L. 2008. The gregarious lipid droplet. *J. Biol. Chem.* 283: 28005–28009.

Saha, P. K., Kojima, H., Marinez-Botas, J., Sunehag, A. L., and Chan, L. 2004. Metabolic adaptations in absence of perilipin. *J. Biol. Chem.* 279:35150–35158.

Barycki, J. J., O'Brien, L. K., Strauss, A. W., and Banaszak, L. J. 2000. Sequestration of the active site by interdomain shifting: Crystallographic and spectroscopic evidence for distinct conformations of L-3-hydroxyacyl-CoA dehydrogenase. *J. Biol. Chem.* 275:27186–27196.

Ramsay, R. R. 2000. The carnitine acyltransferases: Modulators of acyl-CoA-dependent reactions. *Biochem. Soc. Trans.* 28:182–186.

Fatty Acid Synthesis

Sun, T., Hayakawa, K., Bateman, K. S., and Fraser, M. E. 2010. Identification of the citrate-binding site of human ATP-citrate lyase using x-ray crystallography. *J. Biol. Chem.* 285: 27418–27428.

Fan, F., Williams, H. J., Boyer, J. G., Graham, T. L., Zhao, H., Lehr, R., Qi, H., Schwartz, B., Raushel, F. M., and Meek, T. D. 2012. On the catalytic mechanism of human ATP citrate lyase. *Biochemistry* 51:5198−5211.

Chypre, M., Zaidi, N., and Smans, K. 2012. ATP-citrate lyase: A minireview. *Biochem. Biophys. Res. Commun.* 422:1–4.

Maier, T., Leibundgut, M., and Ban, N. 2008. The crystal structure of a mammalian fatty acid synthase. *Science* 321:1315–1322.

Ming, D., Kong, Y., Wakil, S. J., Brink, J., and Ma, J. 2002. Domain movements in human fatty acid synthase by quantized elastic deformational model. *Proc. Natl. Acad. Sci. U.S.A.* 99:7895–7899.

Zhang, Y.-M., Rao, M. S., Heath, R. J., Price, A. C., Olson, A. J., Rock, C. O., and White, S. W. 2001. Identification and analysis of the acyl carrier protein (ACP) docking site on β-ketoacyl-ACP synthase III. *J. Biol. Chem.* 276:8231–8238.

Davies, C., Heath, R. J., White, S. W., and Rock, C. O. 2000. The 1.8 Å crystal structure and active-site architecture of β-ketoacyl-acyl carrier protein synthase III (FabH) from *Escherichia coli*. *Struct. Fold. Design* 8:185–195.

Loftus, T. M., Jaworsky, D. E., Frehywot, G. L., Townsend, C. A., Ronnett, G. V., Lane, M. D., and Kuhajda, F. P. 2000. Reduced food intake and body weight in mice treated with fatty acid synthase inhibitors. *Science* 288:2379–2381.

Acetyl CoA Carboxylase

Kim, C.-W., Moon, Y.-A., Park, S. W., Cheng, D., Kwon, H. J., and Horton, J. D. 2010. Induced polymerization of mammalian acetyl-CoA carboxylase by MIG12 provides a tertiary level of regulation of fatty acid synthesis. *Proc. Natl. Acad. Sci. U.S.A.* 107:9626–9631.

Brownsey, R. W., Boone, A. N., Elliott, J. E., Kulpa, J. E., and Lee, W. M. 2006. Regulation of acetyl-CoA carboxylase. *Biochem. Soc. Trans.* 34:223–227.

Hardie, D. G., Ross, F. A., and Hawley, S. A. 2013. AMP-activated protein kinase: A target for drugs both ancient and modern. *Chem. Biol.* 19:1222–1236.

Munday, M. R. 2002. Regulation of acetyl CoA carboxylase. *Biochem. Soc. Trans.* 30:1059–1064.

Thoden, J. B., Blanchard, C. Z., Holden, H. M., and Waldrop, G. L. 2000. Movement of the biotin carboxylase B-domain as a result of ATP binding. *J. Biol. Chem.* 275:16183–16190.

Eicosanoids

De Caterina, R. 2011. n–3 Fatty acids in cardiovascular disease. *New Engl. J. Med.* 364:2439–2450.

Harizi, H., Corcuff, J.-B., and Gualde, N. 2008. Arachidonic-acid-derived eicosanoids: Roles in biology and immunopathology. *Trends Mol. Med.* 14:461–469.

Nakamura, M. T., and Nara, T. Y. 2004. Structure, function, and dietary regulation of $\Delta 6$, $\Delta 5$, and $\Delta 9$ desaturases. *Annu. Rev. Nutr.* 24:345–376.

Malkowski, M. G., Ginell, S. L., Smith, W. L., and Garavito, R. M. 2000. The productive conformation of arachidonic acid bound to prostaglandin synthase. *Science* 289:1933–1937.

Smith, T., McCracken, J., Shin, Y.-K., and DeWitt, D. 2000. Arachidonic acid and nonsteroidal anti-inflammatory drugs induce conformational changes in the human prostaglandin endoperoxide H2 synthase-2 (cyclooxygenase-2). *J. Biol. Chem.* 275: 40407–40415.

Kalgutkar, A. S., Crews, B. C., Rowlinson, S. W., Garner, C., Seibert, K., and Marnett L. J. 1998. Aspirin-like molecules that covalently inactivate cyclooxygenase-2. *Science* 280:1268–1270.

Lands, W. E. 1991. Biosynthesis of prostaglandins. *Annu. Rev. Nutr.* 11:41–60.

Sigal, E. 1991. The molecular biology of mammalian arachidonic acid metabolism. *Am. J. Physiol.* 260:L13–L28.

Weissmann, G. 1991. Aspirin. *Sci. Am.* 264(1):84–90.

Vane, J. R., Flower, R. J., and Botting, R. M. 1990. History of aspirin and its mechanism of action. *Stroke* (12 suppl.):IV12–IV23.

Genetic Diseases and Cancer

Celestino-Soper, P. B. S., Violante, S., Crawford, E. L., Luo, R., Lionel, A. C., Delaby, E., Cai, G., Sadikovic, B., Lee, K., Lo, C., et al. 2012. A common X-linked inborn error of carnitine biosynthesis may be a risk factor for nondysmorphic autism. *Proc. Natl. Acad. Sci. U.S.A.* 109:7947–7981.

Currie, E., Schulze, A., Zechner, R., Walther, T. C., and Farese, Jr. R. V. 2013. Cellular fatty acid metabolism and cancer. *Cell. Metab.* 18: 153–161.

Lutas, A. and Yellen, G. 2013. The ketogenic diet: Metabolic influences on brain excitability and epilepsy. *Trends Neurosci.* 36:32–40.

Beckers, A., Organe, S., Timmermans, L., Scheys, K., Peeters, A., Brusselmans, K., Verhoeven, G., and Swinnen, J. V. 2007. Chemical inhibition of acetyl-CoA carboxylase induces growth arrest and cytotoxicity selectively in cancer cells. *Cancer Res.* 67:8180–8187.

Kuhajda, F. P. 2006. Fatty acid synthase and cancer: New application of an old pathway. *Cancer Res.* 66:5977–5980.

Nyhan, W. L., Barshop, B. A., and Ozand, P. T. 2005. *Atlas of Metabolic Diseases* (2d ed., pp. 339–300). Hodder Arnold.

Roe, C. R., and Coates, P. M. 2001. Mitochondrial fatty acid oxidation disorders. In *The Metabolic and Molecular Bases of Inherited Diseases* (8th ed., pp. 2297–2326), edited by C. R. Scriver., W. S. Sly, B. Childs, A. L. Beaudet, D. Valle, K. W. Kinzler, and B. Vogelstein. McGraw-Hill.

Brivet, M., Boutron, A., Slama, A., Costa, C., Thuillier, L., Demaugre, F., Rabier, D., Saudubray, J. M., and Bonnefont, J. P. 1999. Defects in activation and transport of fatty acids. *J. Inherit. Metab. Dis.* 22:428–441.

Wanders, R. J., van Grunsven, E. G., and Jansen, G. A. 2000. Lipid metabolism in peroxisomes: Enzymology, functions and dysfunctions of the fatty acid α-and β-oxidation systems in humans. *Biochem. Soc. Trans.* 28:141–149.

Wanders, R. J., Vreken, P., den Boer, M. E., Wijburg, F. A., van Gennip, A. H., and Ijist, L. 1999. Disorders of mitochondrial fatty acyl-CoA β-oxidation. *J. Inherit. Metab. Dis.* 22:442–487.

Kerner, J., and Hoppel, C. 1998. Genetic disorders of carnitine metabolism and their nutritional management. *Annu. Rev. Nutr.* 18: 179–206.

Bartlett, K., and Pourfarzam, M. 1998. Recent developments in the detection of inherited disorders of mitochondrial β-oxidation. *Biochem. Soc. Trans.* 26:145–152.

Pollitt, R. J. 1995. Disorders of mitochondrial long-chain fatty acid oxidation. *J. Inherit. Metab. Dis.* 18:473–490.

Chapter 23

Where to Start

Varshavsky, A. 2012. The Ubiquitin System, an Immense Realm. *Annu. Rev. Biochem.* 81:167–76.

Ubiquitin-Mediated Protein Regulation. 2009. *Annu. Rev. Biochem.* 78: A series of reviews on the various roles of ubiquitin.

Torchinsky, Y. M. 1989. Transamination: Its discovery, biological and chemical aspects. *Trends Biochem. Sci.* 12:115–117.

Watford, M. 2003. The urea cycle. *Biochem. Mol. Biol. Ed.* 31: 289–297.

Books

Magnusson, S. 2010. *Life of Pee: The Story of How Urine Got Everywhere*. Aurum.

Bender, D. A. 2012. *Amino Acid Metabolism* (3rd ed.). Wiley-Blackwell.

Lippard, S. J., and Berg, J. M. 1994. *Principles of Bioinorganic Chemistry.* University Science Books.

Walsh, C. 1979. *Enzymatic Reaction Mechanisms.* W. H. Freeman and Company.

Christen, P., and Metzler, D. E. 1985. *Transaminases.* Wiley.

Ubiquitin and the Proteasome

Shemorry, A., Hwang, C.-S., and Varshavsky, A. 2013. Control of protein quality and stoichiometries by N-terminal acetylation and the N-end rule pathway. *Mol. Cell* 50:540–551.

Liu, C.-W., and Jacobson, A. D. 2013. Functions of the 19S complex in proteasomal degradation. *Trends Biochem. Sci.* 38:103−110.

Ehlinger, A., and Walters, K. J. 2013. Structural insights into proteasome activation by the 19S regulatory particle. *Biochemistry* 52:3618−3628.

Peth, A. Nathan, J. A. and Goldberg, A. L. 2013. The ATP costs and time required to degrade ubiquitinated proteins by the 26 S proteasome. *J. Biol. Chem.* 288:29215–29222.

Tomko, Jr., R. J., and Hochstrasser, M. 2013. Molecular architecture and assembly of the eukaryotic proteasome. *Annu. Rev. Biochem.* 82:415–445.

Komander, D., and Rape, M. 2012. The ubiquitin code. *Annu. Rev. Biochem.* 81:203–229.

Greer, P. L., Hanayama, R., Bloodgood, B. L., Mardinly, A. R., Lipton, D. M., Flavell, S. W., Kim, T.-K., Griffith, E. C., Waldon, Z., Maehr, R., et al. 2010. The Angelman syndrome protein Ube3A regulates synapse development by ubiquitinating Arc. *Cell* 140:704–716.

Peth, A., Besche, H. C., and Goldberg A. L. 2009. Ubiquitinated proteins activate the proteasome by binding to Usp14/Ubp6, which causes 20S gate opening. *Mol. Cell* 36:794–804.

Lin, G., Li, D., Carvalho, L. P. S., Deng, H., Tao, H., Vogt, G., Wu, K., Schneider, J., Chidawanyika, T., Warren, J. D., et al. 2009. Inhibitors selective for mycobacterial versus human proteasomes. *Nature* 461:621–626.

Giasson, B. I., and Lee, V. M.-Y. 2003. Are ubiquitination pathways central to Parkinson's disease? *Cell* 114:1–8.

Pagano, M., and Benmaamar, R. 2003. When protein destruction runs amok, malignancy is on the loose. *Cancer Cell* 4:251–256.

Hochstrasser, M. 2000. Evolution and function of ubiquitin-like protein-conjugation systems. *Nat. Cell Biol.* 2:E153–E157.

Pyridoxal Phosphate-Dependent Enzymes

Eliot, A. C., and Kirsch, J. F. 2004. Pyridoxal phosphate enzymes: Mechanistic, structural, and evolutionary considerations. *Annu. Rev. Biochem.* 73:383–415.

Mehta, P. K., and Christen, P. 2000. The molecular evolution of pyridoxal-$5'$-phosphate-dependent enzymes. *Adv. Enzymol. Relat. Areas Mol. Biol.* 74:129–184.

Schneider, G., Kack, H., and Lindqvist, Y. 2000. The manifold of vitamin B_6 dependent enzymes. *Structure Fold Des.* 8:R1–R6.

Urea Cycle Enzymes

Haeussinger, D., and Sies, H. 2013. Hepatic encephalopathy: Clinical aspects and pathogenetic concept. *Arch. Biochem. Biophys.* 536:97–100.

Li, M., Li, C., Allen, A., Stanley, C. A., and Smith, T. J. 2012. The structure and allosteric regulation of mammalian glutamate dehydrogenase. *Arch. Biochem. Biophys.* 519:69–80.

Nakagawa, T., Lomb, D. J., Haigis, M. C., and Guarente, L. 2009. SIRT5 deacetylates carbamoyl phosphate synthetase 1 and regulates the urea cycle. *Cell* 137:560–570.

Lawson, F. S., Charlebois, R. L., and Dillon, J. A. 1996. Phylogenetic analysis of carbamoylphosphate synthetase genes: Complex evolutionary history includes an internal duplication within a gene which can root the tree of life. *Mol. Biol. Evol.* 13:970–977.

McCudden, C. R., and Powers-Lee, S. G. 1996. Required allosteric effector site for *N*-acetylglutamate on carbamoyl-phosphate synthetase I. *J. Biol. Chem.* 271:18285–18294.

Amino Acid Degradation

Li, M., Smith, C. J., Walker, M. T., and Smith, T. J. 2009. Novel inhibitors complexed with glutamate dehydrogenase: Allosteric regulation by control of protein dynamics. *J. Biol. Chem.* 284:22988–23000.

Smith, T. J., and Stanley, C. A. 2008. Untangling the glutamate dehydrogenase allosteric nightmare. *Trends Biochem. Sci.* 33:557–564.

Fusetti, F., Erlandsen, H., Flatmark, T., and Stevens, R. C. 1998. Structure of tetrameric human phenylalanine hydroxylase and its implications for phenylketonuria. *J. Biol. Chem.* 273: 16962–16967.

Titus, G. P., Mueller, H. A., Burgner, J., Rodriguez De Cordoba, S., Penalva, M. A., and Timm, D. E. 2000. Crystal structure of human homogentisate dioxygenase. *Nat. Struct. Biol.* 7:542–546.

Erlandsen, H., and Stevens, R. C. 1999. The structural basis of phenylketonuria. *Mol. Genet. Metab.* 68:103–125.

Genetic Diseases

Jayakumar, A. R., Liu, M., Moriyama, M. Ramakrishnan, R., Forbush III, B., Reddy, P. V. V., and Norenberg, M. D. 2008. Na-K-Cl cotransporter-1 in the mechanism of ammonia-induced astrocyte swelling. *J. Biol. Chem.* 283:33874–33882.

Scriver, C. R., and Sly, W. S. (Eds.), Childs, B., Beaudet, A. L., Valle, D., Kinzler, K. W., and Vogelstein, B. 2001. *The Metabolic Basis of Inherited Disease* (8th ed.). McGraw-Hill.

Historical Aspects and the Process of Discovery

Cooper, A. J. L., and Meister, A. 1989. An appreciation of Professor Alexander E. Braunstein: The discovery and scope of enzymatic transamination. *Biochimie* 71:387–404.

Garrod, A. E. 1909. *Inborn Errors in Metabolism.* Oxford University Press (reprinted in 1963 with a supplement by H. Harris).

Childs, B. 1970. Sir Archibald Garrod's conception of chemical individuality: A modern appreciation. *New Engl. J. Med.* 282:71–78.

Holmes, F. L. 1980. Hans Krebs and the discovery of the ornithine cycle. *Fed. Proc.* 39:216–225.

Chapter 24

Where to Start

Brewin, N. J. 2013. Legume root nodule symbiosis. *The Biochemist* 35:14–18.

Christen, P., Jaussi, R., Juretic, N., Mehta, P. K., Hale, T. I., and Ziak, M. 1990. Evolutionary and biosynthetic aspects of aspartate aminotransferase isoenzymes and other aminotransferases. *Ann. N. Y. Acad. Sci.* 585:331–338.

Schneider, G., Kack, H., and Lindqvist, Y. 2000. The manifold of vitamin B_6 dependent enzymes. *Structure Fold Des.* 8:R1–R6.

Rhee, S. G., Chock, P. B., and Stadtman, E. R. 1989. Regulation of *Escherichia coli* glutamine synthetase. *Adv. Enzymol. Mol. Biol.* 62:37–92.

Shemin, D. 1989. An illustration of the use of isotopes: The biosynthesis of porphyrins. *Bioessays* 10:30–35.

Books

Wu, G. 2013. *Amino Acids: Biochemistry and Nutrition*. CRC Press.

Bender, D. A. 2012. *Amino Acid Metabolism* (3rd ed.). Wiley-Blackwell.

Jordan, P. M. (Ed.). 1991. *Biosynthesis of Tetrapyrroles.* Elsevier.

Scriver, C. R. (Ed.), Sly, W. S. (Ed.), Childs, B., Beaudet, A. L., Valle, D., Kinzler, K. W., and Vogelstein, B. 2001. *The Metabolic Basis of Inherited Disease* (8th ed.). McGraw-Hill.

McMurry, J. E., and Begley, T. P. 2005. *The Organic Chemistry of Biological Pathways.* Roberts and Company.

Blakley, R. L., and Benkovic, S. J. 1989. *Folates and Pterins* (vol. 2). Wiley.

Walsh, C. 1979. *Enzymatic Reaction Mechanisms.* W. H. Freeman and Company.

Nitrogen Fixation

Spatzal, T., Aksoyoglu, M., Zhang, L., Andrade, S. L. A., Schleicher, E., Weber, S., Rees, D. C., Einsle, O. 2011. Evidence for interstitial carbon in nitrogenase FeMo Cofactor. *Science* 334:940.

Lancaster, K. M., Roemelt, M., Ettenhuber, P., Hu, Y., Ribbe, M. W., Neese, F., Bergmann, U., DeBeer, S. 2011. X-ray emission spectroscopy evidences a central carbon in the nitrogenase iron-molybdenum cofactor. *Science* 334:974–977.

Seefeldt, L. C., Hoffman, B. M., and Dean, D. R. 2009. Mechanism of Mo-dependent nitrogenase. *Annu. Rev. Biochem.* 79:701–722.

Halbleib, C. M., and Ludden, P. W. 2000. Regulation of biological nitrogen fixation. *J. Nutr.* 130:1081–1084.

Einsle, O., Tezcan, F. A., Andrade, S. L., Schmid, B., Yoshida, M., Howard, J. B., and Rees, D. C. 2002. Nitrogenase MoFe-protein at 1.16 Å resolution: A central ligand in the FeMo-cofactor. *Science* 297:1696–1700.

Benton, P. M., Laryukhin, M., Mayer, S. M., Hoffman, B. M., Dean, D. R., and Seefeldt, L. C. 2003. Localization of a substrate binding site on the FeMo-cofactor in nitrogenase: Trapping propargyl alcohol with an α-70-substituted MoFe protein. *Biochemistry* 42:9102–9109.

Regulation of Amino Acid Biosynthesis

Li, Y., Zhang, H., Jiang, C., Xu, M., Pang, Y., Feng, J., Xiang, X., Kong, W., Xu, G., Li, Y., et al. 2013. Hyperhomocysteinemia promotes insulin resistance by inducing endoplasmic reticulum stress in adipose tissue. *J. Biol. Chem.* 288:9583–9592.

Eisenberg, D., Gill, H. S., Pfluegl, G. M., and Rotstein, S. H. 2000. Structure-function relationships of glutamine synthetases. *Biochim. Biophys. Acta* 1477:122–145.

Purich, D. L. 1998. Advances in the enzymology of glutamine synthesis. *Adv. Enzymol. Relat. Areas Mol. Biol.* 72:9–42.

Yamashita, M. M., Almassy, R. J., Janson, C. A., Cascio, D., and Eisenberg, D. 1989. Refined atomic model of glutamine synthetase at 3.5 Å resolution. *J. Biol. Chem.* 264:17681–17690.

Schuller, D. J., Grant, G. A., and Banaszak, L. J. 1995. The allosteric ligand site in the $V_{\max}$-type cooperative enzyme phosphoglycerate dehydrogenase. *Nat. Struct. Biol.* 2:69–76.

Rhee, S. G., Park, R., Chock, P. B., and Stadtman, E. R. 1978. Allosteric regulation of monocyclic interconvertible enzyme cascade systems: Use of *Escherichia coli* glutamine synthetase as an experimental model. *Proc. Natl. Acad. Sci. U.S.A.* 75:3138–3142.

Wessel, P. M., Graciet, E., Douce, R., and Dumas, R. 2000. Evidence for two distinct effector-binding sites in threonine deaminase by site-directed mutagenesis, kinetic, and binding experiments. *Biochemistry* 39:15136–15143.

James, C. L., and Viola, R. E. 2002. Production and characterization of bifunctional enzymes: Domain swapping to produce new bifunctional enzymes in the aspartate pathway. *Biochemistry* 41:3720–3725.

Xu, Y., Carr, P. D., Huber, T., Vasudevan, S. G., and Ollis, D. L. 2001. The structure of the PII-ATP complex. *Eur. J. Biochem.* 268:2028–2037.

Krappmann, S., Lipscomb, W. N., and Braus, G. H. 2000. Coevolution of transcriptional and allosteric regulation at the chorismate metabolic branch point of *Saccharomyces cerevisiae*. *Proc. Natl. Acad. Sci. U.S.A.* 97:13585–13590.

Aromatic Amino Acid Biosynthesis

Brown, K. A., Carpenter, E. P., Watson, K. A., Coggins, J. R., Hawkins, A. R., Koch, M. H., and Svergun, D. I. 2003. Twists and turns: A tale of two shikimate-pathway enzymes. *Biochem. Soc. Trans.* 31:543–547.

Pan, P., Woehl, E., and Dunn, M. F. 1997. Protein architecture, dynamics and allostery in tryptophan synthase channeling. *Trends Biochem. Sci.* 22:22–27.

Sachpatzidis, A., Dealwis, C., Lubetsky, J. B., Liang, P. H., Anderson, K. S., and Lolis, E. 1999. Crystallographic studies of phosphonate-based α-reaction transition-state analogues complexed to tryptophan synthase. *Biochemistry* 38:12665–12674.

Weyand, M., and Schlichting, I. 1999. Crystal structure of wild-type tryptophan synthase complexed with the natural substrate indole-3-glycerol phosphate. *Biochemistry* 38:16469–16480.

Crawford, I. P. 1989. Evolution of a biosynthetic pathway: The tryptophan paradigm. *Annu. Rev. Microbiol.* 43:567–600.

Carpenter, E. P., Hawkins, A. R., Frost, J. W., and Brown, K. A. 1998. Structure of dehydroquinate synthase reveals an active site capable of multistep catalysis. *Nature* 394:299–302.

Schlichting, I., Yang, X. J., Miles, E. W., Kim, A. Y., and Anderson, K. S. 1994. Structural and kinetic analysis of a channel-impaired mutant of tryptophan synthase. *J. Biol. Chem.* 269:26591–26593.

Glutathione

Edwards, R., Dixon, D. P., and Walbot, V. 2000. Plant glutathione *S*-transferases: Enzymes with multiple functions in sickness and in health. *Trends Plant Sci.* 5:193–198.

Lu, S. C. 2000. Regulation of glutathione synthesis. *Curr. Top. Cell Regul.* 36:95–116.

Schulz, J. B., Lindenau, J., Seyfried, J., and Dichgans, J. 2000. Glutathione, oxidative stress and neurodegeneration. *Eur. J. Biochem.* 267:4904–4911.

Lu, S. C. 1999. Regulation of hepatic glutathione synthesis: Current concepts and controversies. *FASEB J.* 13:1169–1183.

Ethylene and Nitric Oxide

Hill, B. G., Dranka, B. P., Baily, S. M., Lancaster, Jr., J. R., and Darley-Usmar, V. M. 2010. What part of NO don't you understand? Some answers to the cardinal questions in nitric oxide biology. *J. Biol. Chem.* 285:19699–19704.

Nisoli, E., Falcone, S., Tonello, C., Cozzi, V., Palomba, L., Fiorani, M., Pisconti, A., Brunelli, S., Cardile, A., Francolini, M., et al. 2004. Mitochondrial biogenesis by NO yields functionally active mitochondria in mammals. *Proc. Natl. Acad. Sci U.S.A.* 101: 16507–16512.

Bretscher, L. E., Li, H., Poulos, T. L. and Griffith, O. W. 2003. Structural characterization and kinetics of nitric oxide synthase inhibition by novel N_5-(iminoalkyl)- and N_5-(iminoalkenyl)-ornithines. *J. Biol. Chem.* 278:46789–46797.

Haendeler, J., Zeiher, A. M., and Dimmeler, S. 1999. Nitric oxide and apoptosis. *Vitam. Horm.* 57:49–77.

Capitani, G., Hohenester, E., Feng, L., Storici, P., Kirsch, J. F., and Jansonius, J. N. 1999. Structure of 1-aminocyclopropane-1-carboxylate synthase, a key enzyme in the biosynthesis of the plant hormone ethylene. *J. Mol. Biol.* 294:745–756.

Hobbs, A. J., Higgs, A., and Moncada, S. 1999. Inhibition of nitric oxide synthase as a potential therapeutic target. *Annu. Rev. Pharmacol. Toxicol.* 39:191–220.

Stuehr, D. J. 1999. Mammalian nitric oxide synthases. *Biochim. Biophys. Acta* 1411:217–230.

Chang, C., and Shockey, J. A. 1999. The ethylene-response pathway: Signal perception to gene regulation. *Curr. Opin. Plant Biol.* 2:352–358.

Theologis, A. 1992. One rotten apple spoils the whole bushel: The role of ethylene in fruit ripening. *Cell* 70:181–184.

Biosynthesis of Porphyrins

Kaasik, K., and Lee, C. C. 2004. Reciprocal regulation of haem biosynthesis and the circadian clock in mammals. *Nature* 430:467–471.

Leeper, F. J. 1989. The biosynthesis of porphyrins, chlorophylls, and vitamin B_{12}. *Nat. Prod. Rep.* 6:171–199.

Porra, R. J., and Meisch, H.-U. 1984. The biosynthesis of chlorophyll. *Trends Biochem. Sci.* 9:99–104.

Chapter 25

Where to Start

Sutherland, J. D. 2010. Ribonucleotides. *Cold Spring Harb. Perspect. Biol.* 2:a005439.

Ipata, P. L. 2011. Origin, utilization, and recycling of nucleosides in the central nervous system. *Adv. Physiol. Educ.* 35:342–346.

Ordi, J., Alonso, P. L., de Zulueta, J., Esteban, J., Velasco, M., Mas, E., Campo, E., and Fernández, P. L. 2006. The severe gout of Holy Roman Emperor Charles V. *New Eng. J. Med.* 355:516–520.

Kappock, T. J., Ealick, S. E., and Stubbe, J. 2000. Modular evolution of the purine biosynthetic pathway. *Curr. Opin. Chem. Biol.* 4:567–572.

Jordan, A., and Reichard, P. 1998. Ribonucleotide reductases. *Annu. Rev. Biochem.* 67:71–98.

Pyrimidine Biosynthesis

Raushel, F. M., Thoden, J. B., Reinhart, G. D., and Holden, H. M. 1998. Carbamoyl phosphate synthetase: A crooked path from substrates to products. *Curr. Opin. Chem. Biol.* 2:624–632.

Huang, X., Holden, H. M., and Raushel, F. M. 2001. Channeling of substrates and intermediates in enzyme-catalyzed reactions. *Annu. Rev. Biochem.* 70:149–180.

Begley, T. P., Appleby, T. C., and Ealick, S. E. 2000. The structural basis for the remarkable proficiency of orotidine 5′-monophosphate decarboxylase. *Curr. Opin. Struct. Biol.* 10:711–718.

Traut, T. W., and Temple, B. R. 2000. The chemistry of the reaction determines the invariant amino acids during the evolution and divergence of orotidine 5′-monophosphate decarboxylase. *J. Biol. Chem.* 275:28675–28681.

Purine Biosynthesis

Zhao, H., French, J. B., Fang, Y., and Benkovic, S. J. 2013. The purinosome, a multi-protein complex involved in the de novo biosynthesis of purines in humans. *Chem. Commun.* 49:4444–4452.

Verrier, F., An, S., Ferrie, A. M., Sun, H., Kyoung, M., Deng, H., Fang, Y., and Benkovic, S. J. 2011. GPCRs regulate the assembly of a multienzyme complex for purine biosynthesis. *Nat. Chem. Biol.* 7:909–915.

Mastrangelo, L., Kim, J.-E., Miyanohara, A., Kang, T. H., and Friedmann, T. 2012. Purinergic signaling in human pluripotent stem cells is regulated by the housekeeping gene encoding hypoxanthine guanine phosphoribosyltransferase. *Proc. Natl. Acad. Sci. U.S.A.* 109:3377–3382.

An, S., Kyoung, M., Allen, J. J., Shokat, K. M., and Benkovic, S. J. 2010. Dynamic regulation of a metabolic multi-enzyme complex by protein kinase CK2. *J. Biol. Chem.* 285:11093–11099.

Thoden, J. B., Firestine, S., Nixon, A., Benkovic, S. J., and Holden, H. M. 2000. Molecular structure of *Escherichia coli* PurT-encoded glycinamide ribonucleotide transformylase. *Biochemistry* 39:8791–8802.

McMillan, F. M., Cahoon, M., White, A., Hedstrom, L., Petsko, G. A., and Ringe, D. 2000. Crystal structure at 2.4 Å resolution of *Borrelia burgdorferi* inosine 5′-monophosphate dehydrogenase: Evidence of a substrate-induced hinged-lid motion by loop 6. *Biochemistry* 39:4533–4542.

Levdikov, V. M., Barynin, V. V., Grebenko, A. I., Melik-Adamyan, W. R., Lamzin, V. S., and Wilson, K. S. 1998. The structure of SAICAR synthase: An enzyme in the de novo pathway of purine nucleotide biosynthesis. *Structure* 6:363–376.

Ribonucleotide Reductases

Ahmad, M. F., and Dealwis, C. G. 2013. The structural basis for the allosteric regulation of ribonucleotide reductase. *Prog. Mol. Biol. Transl. Sci.* 117:389–410.

Minnihan, E. C., Nocera, D. G., and Stubbe, J. 2013. Reversible, long-range radical transfer in *E. coli* class Ia ribonucleotide reductase. *Acc. Chem. Res.* 46:2524−2535.

Reichard, P. 2010. Ribonucleotide reductases: Substrate specificity by allostery. *Biochem. Biophys. Res. Commun.* 396:19–23

Avval, F. Z., and Holmgren, A. 2009. Molecular mechanisms of thioredoxin and glutaredoxin as hydrogen donors for mammalian S phase ribonucleotide reductase. *J. Biol. Chem.* 284:8233–8240.

Rofougaran, R., Crona M., Vodnala, M., Sjöberg, B. M., and Hofer, A. 2008. Oligomerization status directs overall activity regulation of the *Escherichia coli* class Ia ribonucleotide reductase. *J. Biol. Chem.* 283:35310–35318.

Nordlund, P., and Reichard, P. 2006. Ribonucleotide reductases. *Annu. Rev. Biochem.* 75:681–706.

Eklund, H., Uhlin, U., Farnegardh, M., Logan, D. T., and Nordlund, P. 2001. Structure and function of the radical enzyme ribonucleotide reductase. *Prog. Biophys. Mol. Biol.* 77:177–268.

Reichard, P. 1997. The evolution of ribonucleotide reduction. *Trends Biochem. Sci.* 22:81–85.

Stubbe, J. 2000. Ribonucleotide reductases: The link between an RNA and a DNA world? *Curr. Opin. Struct. Biol.* 10:731–736.

Logan, D. T., Andersson, J., Sjoberg, B. M., and Nordlund, P. 1999. A glycyl radical site in the crystal structure of a class III ribonucleotide reductase. *Science* 283:1499–1504.

Tauer, A., and Benner, S. A. 1997. The B_{12}-dependent ribonucleotide reductase from the archaebacterium *Thermoplasma acidophila:* An evolutionary solution to the ribonucleotide reductase conundrum. *Proc. Natl. Acad. Sci. U.S.A.* 94:53–58.

Stubbe, J., Nocera, D. G., Yee, C. S. and Chang, M. C. 2003. Radical initiation in the class I ribonucleotide reductase: Long-range proton-coupled electron transfer? *Chem. Rev.* 103:2167–2201.

Stubbe, J., and Riggs-Gelasco, P. 1998. Harnessing free radicals: Formation and function of the tyrosyl radical in ribonucleotide reductase. *Trends Biochem. Sci.* 23:438–443.

Thymidylate Synthase and Dihydrofolate Reductase

Liu, C. T., Hanoian, P., French, J. B., Pringle, T. H., Hammes-Schiffer, S., and Benkovic, S. J. 2013. Functional significance of evolving protein sequence in dihydrofolate reductase from bacteria to humans. *Proc. Natl. Acad. Sci. U.S.A.* 110: 10159–10164.

Abali, E. E., Skacel, N. E., Celikkaya, H., and Hsieh, Y.-C. 2008. Regulation of human dihydrofolate reductase activity and expression. *Vitam. Horm.* 79:267–292.

Schnell, J. R., Dyson, H. J., and Wright, P. E. 2004. Structure, dynamics, and catalytic function of dihydrofolate reductase. *Annu. Rev. Biophys. Biomol. Struct.* 33:119–140.

Li, R., Sirawaraporn, R., Chitnumsub, P., Sirawaraporn, W., Wooden, J., Athappilly, F., Turley, S., and Hol, W. G. 2000. Three-dimensional structure of *M. tuberculosis* dihydrofolate reductase reveals opportunities for the design of novel tuberculosis drugs. *J. Mol. Biol.* 295:307–323.

Liang, P. H., and Anderson, K. S. 1998. Substrate channeling and domain-domain interactions in bifunctional thymidylate synthase-dihydrofolate reductase. *Biochemistry* 37:12195–12205.

Miller, G. P., and Benkovic, S. J. 1998. Stretching exercises: Flexibility in dihydrofolate reductase catalysis. *Chem. Biol.* 5:R105–R113.

Carreras, C. W., and Santi, D. V. 1995. The catalytic mechanism and structure of thymidylate synthase. *Annu. Rev. Biochem.* 64:721–762.

Defects in Nucleotide Biosynthesis

Grunebaum, E., Cohen, A., and Roifman, C. M. 2013. Recent advances in understanding and managing adenosine deaminase and purine nucleoside phosphorylase deficiencies. *Curr. Opin. Allergy Clin. Immunol.* 13:630–638.

Fu, R., and Jinnah, H. A. 2012. Genotype-phenotype correlations in Lesch-Nyhan Disease: Moving beyond the gene. *J. Biol. Chem.* 287:2997−3008.

Richette, P. and Bardin, T. 2010. Gout. *Lancet* 375:318–328.

Aiuti, A., Cattaneo, F., Galimberti, S., Benninghoff, U., Cassani, B., Callegaro, L., Scaramuzza, S., Andolfi, G., Mirolo, M., Brigida, I., et al. 2009. Gene therapy for immunodeficiency due to adenosine deaminase deficiency. *New Engl. J. Med.* 360:447–458.

Jurecka, A. 2009. Inborn errors of purine and pyrimidine metabolism. *J. Inherit. Metab. Dis.* 32:247–263.

Nyhan, W. L., Barshop, B. A., and Ozand, P. T. 2005. *Atlas of Metabolic Diseases*. (2d ed., pp. 429–462). Hodder Arnold.

Scriver, C. R., Sly, W. S., Childs, B., Beaudet, A. L., Valle, D., Kinzler, K. W., and Vogelstein, B. (Eds.). 2001. *The Metabolic and Molecular Bases of Inherited Diseases* (8th ed., pp. 2513–2704). McGraw-Hill.

Nyhan, W. L. 1997. The recognition of Lesch-Nyhan syndrome as an inborn error of purine metabolism. *J. Inherited Metab. Dis.* 20:171–178.

Wong, D. F., Harris, J. C., Naidu, S., Yokoi, F., Marenco, S., Dannals, R. F., Ravert, H. T., Yaster, M., Evans, A., Rousset, O., et al. 1996. Dopamine transporters are markedly reduced in Lesch-Nyhan disease in vivo. *Proc. Natl. Acad. Sci. U.S.A.* 93:5539–5543.

Neychev, V. K., and Mitev, V. I. 2004. The biochemical basis of the neurobehavioral abnormalities in the Lesch-Nyhan syndrome: A hypothesis. *Med. Hypotheses* 63:131–134.

Chapter 26

Where to Start

Vickers, K. C., and Remaley, A. T. 2014. HDL and cholesterol: Life after the divorce? *J. Lipid Res.* 55:4–12.

Lambert, G., Sjouke, B., Choque, B., Kastelein, J. J. P., and Hovingh, G. K. 2012. The PCSK9 decade. *J. Lipid Res.* 53:2515–2524.

Brown, M. S., and Goldstein, J. L. 2009. Cholesterol feedback: From Schoenheimer's bottle to Scap's MELADL. *J. Lipid Res.* 50:S15–S27.

Gimpl, G., Burger, K., and Fahrenholz, F. 2002. A closer look at the cholesterol sensor. *Trends Biochem. Sci.* 27:595–599.

Oram, J. F. 2002. Molecular basis of cholesterol homeostasis: Lessons from Tangier disease and ABCA1. *Trends Mol. Med.* 8:168–173.

Endo, A. 1992. The discovery and development of HMG-CoA reductase inhibitors. *J. Lipid Res.* 33:1569–1582.

Books

Vance, J. E., and Vance, D. E. (Eds.). 2008. *Biochemistry of Lipids, Lipoproteins and Membranes.* Elsevier.

Nyhan, W. L., Barshop, B. A., and Al-Aqeel, A. I. 2011. *Atlas of Metabolic Diseases*. (3d ed., pp. 659–780). Hodder Arnold.

Scriver, C. R., Sly, W. S., Childs, B., Beaudet, A. L., Valle, D., Kinzler, K. W., and Vogelstein, B. (Eds.). 2001. *The Metabolic and Molecular Bases of Inherited Diseases* (8th ed., pp. 2707–2960). McGraw-Hill.

Phospholipids and Sphingolipids

Lee, J., Taneva, S. G., Holland, B. W., Tieleman, D. P., and Cornell, R. B. 2014. Structural basis for autoinhibition of CTP: phosphocholine cytidylyltransferase (CCT), the regulatory enzyme in phosphatidylcholine synthesis, by its membrane-binding amphipathic helix. *J. Biol. Chem*. 289:1742–1755.

Tang, W. H. W., Wang, Z., Levison, B. S., Koeth, R. A., Britt, E. B., Fu, F., Wu, Y., and Hazen, S. L. 2013. Intestinal microbial metabolism of phosphatidylcholine and cardiovascular risk. *New Engl. J. Med*. 368:1575–1584.

Pascual, F., and Carman, G. M. 2013. Phosphatidate phosphatase, a key regulator of lipid homeostasis. *Biochim. Biophys. Acta* 1831:514–522.

Bennett, B. J., de Aguiar Vallim, T. Q., Wang, Z., Shih, D. M., Meng, Y., Gregory, J., Allayee, H., Lee, R., Graham, M., Crooke, R., et al. 2013. Trimethylamine-N-oxide, a metabolite associated with atherosclerosis, exhibits complex genetic and dietary regulation. *Cell Metab*. 17:49–60.

Claypool, S. M., and Koehler C. M. 2012. The complexity of cardiolipin in health and disease. *Trends Biochem. Sci.* 37:32–41.

Carman, G. M., and Han, G.-S. 2009. Phosphatidic acid phosphatase, a key enzyme in the regulation of lipid synthesis. *J. Biol. Chem.* 284:2593–2597.

Bartke, N., and Hannun, Y. A. 2009. Bioactive sphingolipids: Metabolism and function. *J. Lipid Res*. 50:S91–S96.

Lee, J., Johnson, J., Ding, Z., Paetzel, M., and Cornell, R. B. 2009. Crystal structure of a mammalian CTP: Phosphocholine cytidylyltransferase catalytic domain reveals novel active site residues within a highly conserved nucleotidyltransferase fold. *J. Biol. Chem*. 284:33535–33548.

Nye, C. K., Hanson, R. W., and Kalhan, S. C. 2008. Glyceroneogenesis is the dominant pathway for triglyceride glycerol synthesis *in vivo* in the rat. *J. Biol. Chem.* 283:27565–27574.

Biosynthesis of Cholesterol and Steroids

Radhakrishnan, A., Goldstein, J. L., McDonald, J. G., and Brown, M. S. 2008. Switch-like control of SREBP-2 transport triggered by small changes in ER cholesterol: A delicate balance. *Cell Metab*. 8:512–521.

DeBose-Boyd, R. A. 2008. Feedback regulation of cholesterol synthesis: Sterol-accelerated ubiquitination and degradation of HMG CoA reductase. *Cell Res.* 18:609–621.

Hampton, R. Y. 2002. Proteolysis and sterol regulation. *Annu. Rev. Cell Dev. Biol.* 18:345–378.

Kelley, R. I., and Herman, G. E. 2001. Inborn errors of sterol biosynthesis. *Annu. Rev. Genom. Hum. Genet.* 2:299–341.

Istvan, E. S., and Deisenhofer, J. 2001. Structural mechanism for statin inhibition of HMG-CoA reductase. *Science* 292:1160–1164.

Lipoproteins and Their Receptors

Gustafsen, C., Kjolby, M., Nyegaard, M., Mattheisen, M., Lundhede, J., Buttenschøn, H., Mors, O., Bentzon, J. F., Madsen, P., Nykjaer, A., et al. 2014. The hypercholesterolemia-risk gene SORT1 facilitates PCSK9 secretion. *Cell Metab*. 19:310–318.

Rye, K-A., Bursill, C. A., Lambert, G., Tabet, F., and Barter, P. J. 2009. The metabolism and anti-atherogenic properties of HDL. *J. Lipid Res*. 50:S195–S200.

Rader, D. J., Alexander, E. T., Weibel, G. L., Billheimer, J., and Rothblat, G. H. 2009. The role of reverse cholesterol transport in animals and humans and relationship to atherosclerosis. *J. Lipid Res*. 50:S189–S194.

Tall, A. R., Yvan-Charvet, L., Terasaka, N., Pagler, T., and Wang, N. 2008. HDL, ABC transporters, and cholesterol efflux: Implications for the treatment of atherosclerosis. *Cell Metab*. 7:365–375.

Jeon, H., and Blacklow, S. C. 2005. Structure and physiologic function of the low-density lipoprotein receptor. *Annu. Rev. Biochem.* 74:535–562.

Beglova, N., and Blacklow, S. C. 2005. The LDL receptor: How acid pulls the trigger. *Trends Biochem. Sci*. 30:309–316.

Oxygen Activation and P450 Catalysis

Stiles, A. R., McDonald, J. G., Bauman, D. R., and Russell, D. W. 2009. CYP7B1: One cytochrome P450, two human genetic diseases, and multiple physiological functions. *J. Biol. Chem*. 284:28485–28489.

Zhou, S.-F., Liu, J.-P., and Chowbay, B. 2009. Polymorphism of human cytochrome P450 enzymes and its clinical impact. *Drug Metab. Rev*. 4:89–295.

Williams, P. A., Cosme, J., Vinkovic, D. M., Ward, A., Angove, H. C., Day, P. J., Vonrhein, C., Tickle, I. J., and Jhoti, H. 2004. Crystal structure of human cytochrome P450 3A4 bound to metyrapone and progesterone. *Science* 305:683–686.

Chapter 27

Where to Start

Cahill, Jr. G. F. 2006. Fuel metabolism in starvation. *Annu. Rev. Nutr.* 26:1–22.

Dunn, R. 2013. Everything you know about calories is wrong. *Sci. Am.* (3) 309:57−59.

Kenny, P. J. 2013. The food addiction. *Sci. Am.* (3) 309:44−49.

Taubes, G. 2013. Which one will make you fat? *Sci. Am.* (3) 309:60−65.

Hardie, D. G. 2012. Organismal carbohydrate and lipid homeostasis. *Cold Spring Harb. Perspect. Biol.* 4:a006031.

Books

Kessler, D. A. 2010. *The End of Overeating: Taking Control of the Insatiable American Appetite.* Rodale.

Wrangham, R. 2009. *Catching Fire: How Cooking Made Us Human*. Basic Books.

Stipanuk, M. H. (Ed.). 2006. *Biochemical, Physiological, & Molecular Aspects of Human Nutrition.* Saunders-Elsevier.

Fell, D. 1997. *Understanding the Control of Metabolism.* Portland Press.

Frayn, K. N. 1996. *Metabolic Regulation: A Human Perspective*. Portland Press.

Poortmans, J. R. (Ed.). 2004. *Principles of Exercise Biochemistry*. Karger.

Harris, R. A., and Crabb, D. W. 2011. Metabolic interrelationships. In *Textbook of Biochemistry with Clinical Correlations* (pp. 839–882), edited by T. M. Devlin. Wiley-Liss.

Caloric Homeostasis

Woods, S. C. 2009. The control of food intake: Behavioral versus molecular perspectives. *Cell Metab.* 9:489–498.

Figlewicz, D. P., and Benoit, S. C. 2009. Insulin, leptin, and food reward: Update 2008. *Am. J. Physiol. Integr. Comp. Physiol.* 296:R9–R19.

Israel, D., and Chua, S. Jr. 2009. Leptin receptor modulation of adiposity and fertility. *Trends Endocrinol. Metab*. 21:10–16.

Meyers, M. G., Cowley, M. A., and Münzberg, H. 2008. Mechanisms of leptin action and leptin resistance. *Annu. Rev. Physiol*. 70:537–556.

Sowers, J. R. 2008. Endocrine functions of adipose tissue: Focus on adiponectin. *Clin. Cornerstone* 9:32–38.

Brehma, B. J., and D'Alessio, D. A. 2008. Benefits of high-protein weight loss diets: Enough evidence for practice? *Curr. Opin. Endocrinol., Diabetes, Obesity* 15:416–421.

Coll, A. P., Farooqi, I. S., and O'Rahillt, S. O. 2007. The hormonal control of food intake. *Cell* 129:251–262.

Muoio, D. M., and Newgard, C. B. 2006. Obesity-related derangements in metabolic regulation. *Annu. Rev. Biochem*. 75:367–401.

Diabetes Mellitus

Lee, J., and Ozcan, U. 2014. Unfolded protein response signaling and metabolic diseases. *J. Biol. Chem*. 289:1203−1211.

Yamauchi, T., and Kadowaki, T. 2013. Adiponectin receptor as a key player in healthy longevity and obesity-related diseases. *Cell Metab*. 17:185−196.

Könner, A. C., and Brüning, J. C. 2012. Selective insulin and leptin resistance in metabolic disorders. *Cell Metab*. 16:144−152.

Zhang, B. B., Zhou, G., and Li, C. 2009. AMPK: An emerging drug target for diabetes and the metabolic syndrome. *Cell Metab*. 9:407–416.

Magkos, F., Yannakoulia, M., Chan, J. L., and Mantzoros, C. S. 2009. Management of the metabolic syndrome and type 2 diabetes through lifestyle modification. *Annu. Rev. Nutr*. 29:8.1–8.34.

Muoio, D. M., and Newgard, C. B. 2008. Molecular and metabolic mechanisms of insulin resistance and β-cell failure in type 2 diabetes. *Nat. Rev. Mol. Cell. Biol*. 9:193–205.

Leibiger, I. B., Leibiger, B., and Berggren, P.-O. 2008. Insulin signaling in the pancreatic β-cell. *Annu. Rev. Nutr*. 28:233–251.

Doria, A., Patti, M. E., and Kahn, C. R. 2008. The emerging architecture of type 2 diabetes. *Cell Metab*. 8:186–200.

Croker, B. A., Kiu, H., and Nicholson, S. E. 2008. SOCS regulation of the JAK/STAT signalling pathway. *Semin. Cell Dev. Biol*. 19:414–422.

Eizirik, D. L., Cardozo, A. K., and Cnop, M. 2008. The role of endoplasmic reticulum stress in diabetes mellitus. *Endocrinol. Rev*. 29:42–61.

Howard, J. K., and Flier, J. S. 2006. Attenuation of leptin and insulin signaling by SOCS proteins. *Trends Endocrinol. Metab*. 9:365–371.

Lowel, B. B., and Shulman, G. 2005. Mitochondrial dysfunction and type 2 diabetes. *Science* 307:384–387.

Taylor, S. I. 2001. Diabetes mellitus. In *The Metabolic Basis of Inherited Diseases* (8th ed., pp. 1433–1469), edited by C. R. Scriver, W. S. Sly, B. Childs, A. L. Beaudet, D. Valle, K. W. Kinzler, and B. Vogelstein. McGraw-Hill.

Exercise Metabolism

Egan, B., and Zierath, J. R. 2013. Exercise metabolism and the molecular regulation of skeletal muscle adaptation. *Cell Metab*. 17:162−184.

Hood, D. A. 2001. Contractile activity-induced mitochondrial biogenesis in skeletal muscle. *J. Appl. Physiol*. 90:1137–1157.

Shulman, R. G., and Rothman, D. L. 2001. The "glycogen shunt" in exercising muscle: A role for glycogen in muscle energetics and fatigue. *Proc. Natl. Acad. Sci. U.S.A*. 98:457–461.

Gleason, T. 1996. Post-exercise lactate metabolism: A comparative review of sites, pathways, and regulation. *Annu. Rev. Physiol*. 58:556–581.

Holloszy, J. O., and Kohrt, W. M. 1996. Regulation of carbohydrate and fat metabolism during and after exercise. *Annu. Rev. Nutr*. 16:121–138.

Hochachka, P. W., and McClelland, G. B. 1997. Cellular metabolic homeostasis during large-scale change in ATP turnover rates in muscles. *J. Exp. Biol*. 200:381–386.

Horowitz, J. F., and Klein, S. 2000. Lipid metabolism during endurance exercise. *Am. J. Clin. Nutr*. 72:558S–563S.

Wagenmakers, A. J. 1999. Muscle amino acid metabolism at rest and during exercise. *Diabetes Nutr. Metab*. 12:316–322.

Metabolic Adaptations in Starvation

Baverel, G., Ferrier, B., and Martin, M. 1995. Fuel selection by the kidney: Adaptation to starvation. *Proc. Nutr. Soc*. 54:197–212.

MacDonald, I. A., and Webber, J. 1995. Feeding, fasting and starvation: Factors affecting fuel utilization. *Proc. Nutr. Soc*. 54:267–274.

Cahill, G. F., Jr. 1976. Starvation in man. *Clin. Endocrinol. Metab*. 5:397–415.

Sugden, M. C., Holness, M. J., and Palmer, T. N. 1989. Fuel selection and carbon flux during the starved-to-fed transition. *Biochem. J*. 263:313–323.

Ethanol Metabolism

Nagy, L. E. 2004. Molecular aspects of alcohol metabolism: Transcription factors involved in early-induced liver injury. *Annu. Rev. Nutr*. 24:55–78.

Molotkov, A., and Duester, G. 2002. Retinol/ethanol drug interaction during acute alcohol intoxication involves inhibition of retinol metabolism to retinoic acid by alcohol dehydrogenase. *J. Biol. Chem*. 277:22553–22557.

Stewart, S., Jones, D., and Day, C. P. 2001. Alcoholic liver disease: New insights into mechanisms and preventive strategies. *Trends Mol. Med*. 7:408–413.

Lieber, C. S. 2000. Alcohol: Its metabolism and interaction with nutrients. *Annu. Rev. Nutr*. 20:395–430.

Niemela, O. 1999. Aldehyde-protein adducts in the liver as a result of ethanol-induced oxidative stress. *Front. Biosci*. 1:D506–D513.

Riveros-Rosas, H., Julian-Sanchez, A., and Pina, E. 1997. Enzymology of ethanol and acetaldehyde metabolism in mammals. *Arch. Med. Res*. 28:453–471.

Chapter 28

Where to Start

O'Donnell, M., Langston, L. and Stillman, B. 2013. Principles and concepts of DNA replication in bacteria, archaea, and eukarya. *Cold Spring Harb. Perspect. Biol*. 5:1–13.

Johnson, A., and O'Donnell, M. 2005. Cellular DNA replicases: Components and dynamics at the replication fork. *Annu. Rev. Biochem*. 74:283–315.

Kornberg, A. 1988. DNA replication. *J. Biol. Chem*. 263:1–4.

Wang, J. C. 1982. DNA topoisomerases. *Sci. Am*. 247(1):94–109.

Lindahl, T. 1993. Instability and decay of the primary structure of DNA. *Nature* 362:709–715.

Greider, C. W., and Blackburn, E. H. 1996. Telomeres, telomerase, and cancer. *Sci. Am*. 274(2):92–97.

Books

Kornberg, A., and Baker, T. A. 1992. *DNA Replication* (2d ed.). W. H. Freeman and Company.

Bloomfield, V. A., Crothers, D., Tinoco, I., and Hearst, J. 2000. *Nucleic Acids: Structures, Properties and Functions*. University Science Books.

Friedberg, E. C., Walker, G. C., and Siede, W. 1995. *DNA Repair and Mutagenesis*. American Society for Microbiology.

Cozzarelli, N. R., and Wang, J. C. (Eds.). 1990. *DNA Topology and Its Biological Effects*. Cold Spring Harbor Laboratory Press.

DNA Topology and Topoisomerases

Graille, M., Cladiere, L., Durand, D., Lecointe, F., Gadelle, D., Quevillon-Cheruel, S., Vachette, P., Forterre, P., and van Tilbeurgh, H. 2008.

Crystal structure of an intact type II DNA topoisomerase: Insights into DNA transfer mechanisms. *Structure* 16:360–370.

Charvin, G., Strick, T. R., Bensimon, D., and Croquette, V. 2005. Tracking topoisomerase activity at the single-molecule level. *Annu. Rev. Biophys. Biomol. Struct.* 34:201–219.

Sikder, D., Unniraman, S., Bhaduri, T., and Nagaraja, V. 2001. Functional cooperation between topoisomerase I and single strand DNA-binding protein. *J. Mol. Biol.* 306:669–679.

Fortune, J. M., and Osheroff, N. 2000. Topoisomerase II as a target for anticancer drugs: When enzymes stop being nice. *Prog. Nucleic Acid Res. Mol. Biol.* 64:221–253.

Isaacs, R. J., Davies, S. L., Sandri, M. I., Redwood, C., Wells, N. J., and Hickson, I. D. 1998. Physiological regulation of eukaryotic topoisomerase II. *Biochim. Biophys. Acta* 1400:121–137.

Wang, J. C. 1998. Moving one DNA double helix through another by a type II DNA topoisomerase: The story of a simple molecular machine. *Q. Rev. Biophys.* 31:107–144.

Baird, C. L., Harkins, T. T., Morris, S. K., and Lindsley, J. E. 1999. Topoisomerase II drives DNA transport by hydrolyzing one ATP. *Proc. Natl. Acad. Sci. U.S.A.* 96:13685–13690.

Vologodskii, A. V., Levene, S. D., Klenin, K. V., Frank, K. M., and Cozzarelli, N. R. 1992. Conformational and thermodynamic properties of supercoiled DNA. *J. Mol. Biol.* 227:1224–1243.

Fisher, L. M., Austin, C. A., Hopewell, R., Margerrison, M., Oram, M., Patel, S., Wigley, D. B., Davies, G. J., Dodson, E. J., Maxwell, A., et al. 1991. Crystal structure of an N-terminal fragment of the DNA gyrase B protein. *Nature* 351:624–629.

Mechanism of Replication

Davey, M. J., and O'Donnell, M. 2000. Mechanisms of DNA replication. *Curr. Opin. Chem. Biol.* 4:581–586.

Keck, J. L., and Berger, J. M. 2000. DNA replication at high resolution. *Chem. Biol.* 7:R63–R71.

Kunkel, T. A., and Bebenek, K. 2000. DNA replication fidelity. *Annu. Rev. Biochem.* 69:497–529.

Waga, S., and Stillman, B. 1998. The DNA replication fork in eukaryotic cells. *Annu. Rev. Biochem.* 67:721–751.

Marians, K. J. 1992. Prokaryotic DNA replication. *Annu. Rev. Biochem.* 61:673–719.

DNA Polymerases and Other Enzymes of Replication

Kurth, I., and O'Donnell, M. 2013. New insights into replisome fluidity during chromosome replication. *Trends Biochem. Sci.* 38:195–203.

Nandakumar, J., and Cech, T. R. 2013. Finding the end: Recruitment of telomerase to telomeres. *Nat. Rev. Mol. Cell. Biol.* 14:69–82.

Singleton, M. R., Sawaya, M. R., Ellenberger, T., and Wigley, D. B. 2000. Crystal structure of T7 gene 4 ring helicase indicates a mechanism for sequential hydrolysis of nucleotides. *Cell* 101:589–600.

Donmez, I., and Patel, S. S. 2006. Mechanisms of a ring shaped helicase. *Nucleic Acids Res.* 34:4216–4224.

Johnson, D. S., Bai, L., Smith, B. Y., Patel, S. S., and Wang, M. D. 2007. Single-molecule studies reveal dynamics of DNA unwinding by the ring-shaped T7 helicase. *Cell* 129:1299–1309.

Lee, S. J., Qimron, U., and Richardson, C. C. 2008. Communication between subunits critical to DNA binding by hexameric helicase of bacteriophage T7. *Proc. Natl. Acad. Sci. U.S.A.* 105:8908–8913.

Toth, E. A., Li, Y., Sawaya, M. R., Cheng, Y., and Ellenberger, T. 2003. The crystal structure of the bifunctional primase-helicase of bacteriophage T7. *Mol. Cell* 12:1113–1123.

Hubscher, U., Maga, G., and Spadari, S. 2002. Eukaryotic DNA polymerases. *Annu. Rev. Biochem.* 71:133–163.

Doublié, S., Tabor, S., Long, A. M., Richardson, C. C., and Ellenberger, T. 1998. Crystal structure of a bacteriophage T7 DNA replication complex at 2.2 Å resolution. *Nature* 391:251–258.

Arezi, B., and Kuchta, R. D. 2000. Eukaryotic DNA primase. *Trends Biochem. Sci.* 25:572–576.

Jager, J., and Pata, J. D. 1999. Getting a grip: Polymerases and their substrate complexes. *Curr. Opin. Struct. Biol.* 9:21–28.

Steitz, T. A. 1999. DNA polymerases: Structural diversity and common mechanisms. *J. Biol. Chem.* 274:17395–17398.

Beese, L. S., Derbyshire, V., and Steitz, T. A. 1993. Structure of DNA polymerase I Klenow fragment bound to duplex DNA. *Science* 260:352–355.

McHenry, C. S. 1991. DNA polymerase III holoenzyme: Components, structure, and mechanism of a true replicative complex. *J. Biol. Chem.* 266:19127–19130.

Kong, X. P., Onrust, R., O'Donnell, M., and Kuriyan, J. 1992. Three-dimensional structure of the β subunit of *E. coli* DNA polymerase III holoenzyme: A sliding DNA clamp. *Cell* 69: 425–437.

Polesky, A. H., Steitz, T. A., Grindley, N. D., and Joyce, C. M. 1990. Identification of residues critical for the polymerase activity of the Klenow fragment of DNA polymerase I from *Escherichia coli. J. Biol. Chem.* 265:14579–14591.

Lee, J. Y., Chang, C., Song, H. K., Moon, J., Yang, J. K., Kim, H. K., Kwon, S. T., and Suh, S. W. 2000. Crystal structure of NAD$^+$ dependent DNA ligase: Modular architecture and functional implications. *EMBO J.* 19:1119–1129.

Timson, D. J., and Wigley, D. B. 1999. Functional domains of an NAD$^+$-dependent DNA ligase. *J. Mol. Biol.* 285:73–83.

Doherty, A. J., and Wigley, D. B. 1999. Functional domains of an ATP-dependent DNA ligase. *J. Mol. Biol.* 285:63–71.

von Hippel, P. H., and Delagoutte, E. 2001. A general model for nucleic acid helicases and their "coupling" within macromolecular machines. *Cell* 104:177–190.

Tye, B. K., and Sawyer, S. 2000. The hexameric eukaryotic MCM helicase: Building symmetry from nonidentical parts. *J. Biol. Chem.* 275:34833–34836.

Marians, K. J. 2000. Crawling and wiggling on DNA: Structural insights to the mechanism of DNA unwinding by helicases. *Struct. Fold. Des.* 5:R227–R235.

Soultanas, P., and Wigley, D. B. 2000. DNA helicases: "Inching forward." *Curr. Opin. Struct. Biol.* 10:124–128.

de Lange, T. 2009. How telomeres solve the end-protection problem. *Science* 326:948–952.

Bachand, F., and Autexier, C. 2001. Functional regions of human telomerase reverse transcriptase and human telomerase RNA required for telomerase activity and RNA-protein interactions. *Mol. Cell Biol.* 21:1888–1897.

Griffith, J. D., Comeau, L., Rosenfield, S., Stansel, R. M., Bianchi, A., Moss, H., and de Lange, T. 1999. Mammalian telomeres end in a large duplex loop. *Cell* 97:503–514.

McEachern, M. J., Krauskopf, A., and Blackburn, E. H. 2000. Telomeres and their control. *Annu. Rev. Genet.* 34:331–358.

Mutations and DNA Repair

Yang, W. 2003. Damage repair DNA polymerases Y. *Curr. Opin. Struct. Biol.* 13:23–30.

Wood, R. D., Mitchell, M., Sgouros, J., and Lindahl, T. 2001. Human DNA repair genes. *Science* 291:1284–1289.

Shin, D. S., Chahwan, C., Huffman, J. L., and Tainer, J. A. 2004. Structure and function of the double-strand break repair machinery. *DNA Repair (Amst.)* 3:863–873.

Michelson, R. J., and Weinert, T. 2000. Closing the gaps among a web of DNA repair disorders. *BioEssays* 22:966–969.

Aravind, L., Walker, D. R., and Koonin, E. V. 1999. Conserved domains in DNA repair proteins and evolution of repair systems. *Nucleic Acids Res.* 27:1223–1242.

Mol, C. D., Parikh, S. S., Putnam, C. D., Lo, T. P., and Tainer, J. A. 1999. DNA repair mechanisms for the recognition and removal of damaged DNA bases. *Annu. Rev. Biophys. Biomol. Struct.* 28:101–128.

Parikh, S. S., Mol, C. D., and Tainer, J. A. 1997. Base excision repair enzyme family portrait: Integrating the structure and chemistry of an entire DNA repair pathway. *Structure* 5:1543–1550.

Vassylyev, D. G., and Morikawa, K. 1997. DNA-repair enzymes. *Curr. Opin. Struct. Biol.* 7:103–109.

Verdine, G. L., and Bruner, S. D. 1997. How do DNA repair proteins locate damaged bases in the genome? *Chem. Biol.* 4:329–334.

Bowater, R. P., and Wells, R. D. 2000. The intrinsically unstable life of DNA triplet repeats associated with human hereditary disorders. *Prog. Nucleic Acid Res. Mol. Biol.* 66:159–202.

Cummings, C. J., and Zoghbi, H. Y. 2000. Fourteen and counting: Unraveling trinucleotide repeat diseases. *Hum. Mol. Genet.* 9: 909–916.

Defective DNA Repair and Cancer

Dever, S. M., White, E. R., Hartman, M. C., and Valerie, K. 2012. BRCA1-directed, enhanced and aberrant homologous recombination: Mechanism and potential treatment strategies. *Cell Cycle* 11:687–94.

Berneburg, M., and Lehmann, A. R. 2001. Xeroderma pigmentosum and related disorders: Defects in DNA repair and transcription. *Adv. Genet.* 43:71–102.

Lambert, M. W., and Lambert, W. C. 1999. DNA repair and chromatin structure in genetic diseases. *Prog. Nucleic Acid Res. Mol. Biol.* 63:257–310.

Buys, C. H. 2000. Telomeres, telomerase, and cancer. *New Engl. J. Med.* 342:1282–1283.

Urquidi, V., Tarin, D., and Goodison, S. 2000. Role of telomerase in cell senescence and oncogenesis. *Annu. Rev. Med.* 51:65–79.

Lynch, H. T., Smyrk, T. C., Watson, P., Lanspa, S. J., Lynch, J. F., Lynch, P. M., Cavalieri, R. J., and Boland, C. R. 1993. Genetics, natural history, tumor spectrum, and pathology of hereditary nonpolyposis colorectal cancer: An updated review. *Gastroenterology* 104:1535–1549.

Fishel, R., Lescoe, M. K., Rao, M. R. S., Copeland, N. G., Jenkins, N. A., Garber, J., Kane, M., and Kolodner, R. 1993. The human mutator gene homolog *MSH2* and its association with hereditary nonpolyposis colon cancer. *Cell* 75:1027–1038.

Ames, B. N., and Gold, L. S. 1991. Endogenous mutagens and the causes of aging and cancer. *Mutat. Res.* 250:3–16.

Ames, B. N. 1979. Identifying environmental chemicals causing mutations and cancer. *Science* 204:587–593.

Recombination and Recombinases

Singleton, M. R., Dillingham, M. S., Gaudier, M., Kowalczykowski, S. C., and Wigley, D. B. 2004. Crystal structure of RecBCD enzyme reveals a machine for processing DNA breaks. *Nature* 432: 187–193.

Spies, M., Bianco, P. R., Dillingham, M. S., Handa, N., Baskin, R. J., and Kowalczykowski, S. C. 2003. A molecular throttle: The recombination hotspot chi controls DNA translocation by the RecBCD helicase. *Cell* 114:647–654.

Kowalczykowski, S. C. 2000. Initiation of genetic recombination and recombination-dependent replication. *Trends Biochem. Sci.* 25:1562165.

Prevost, C., and Takahashi, M. 2003. Geometry of the DNA strands within the RecA nucleofilament: Role in homologous recombination. *Q. Rev. Biophys.* 36:429–453.

Van Duyne, G. D. 2001. A structural view of Cre-loxP site-specific recombination. *Annu. Rev. Biophys. Biomol. Struct.* 30:87–104.

Chen, Y., Narendra, U., Iype, L. E., Cox, M. M., and Rice, P. A. 2000. Crystal structure of a Flp recombinase-Holliday junction complex: Assembly of an active oligomer by helix swapping. *Mol. Cell* 6:885–897.

Craig, N. L. 1997. Target site selection in transposition. *Annu. Rev. Biochem.* 66:437–474.

Gopaul, D. N., Guo, F., and Van Duyne, G. D. 1998. Structure of the Holliday junction intermediate in Cre-loxP site-specific recombination. *EMBO J.* 17:4175–4187.

Gopaul, D. N., and Van Duyne, G. D. 1999. Structure and mechanism in site-specific recombination. *Curr. Opin. Struct. Biol.* 9:14–20.

Chapter 29

Where to Start

Liu, X., Bushnell, D. A., and Kornberg, R. D. 2013. RNA polymerase II transcription: Structure and mechanism. *Biochim. Biophys. Acta* 1829:2–8.

Kornberg, R. D. 2007. The molecular basis of eukaryotic transcription. *Proc. Natl. Acad. Sci. U.S.A.* 104:12955–12961.

Woychik, N. A. 1998. Fractions to functions: RNA polymerase II thirty years later. *Cold Spring Harbor Symp. Quant. Biol.* 63:311–317.

Losick, R. 1998. Summary: Three decades after sigma. *Cold Spring Harbor Symp. Quant. Biol.* 63:653–666.

Sharp, P. A. 1994. Split genes and RNA splicing (Nobel Lecture). *Angew. Chem. Int. Ed. Engl.* 33:1229–1240.

Cech, T. R. 1990. Nobel lecture: Self-splicing and enzymatic activity of an intervening sequence RNA from *Tetrahymena*. *Biosci. Rep.* 10:239–261.

Villa, T., Pleiss, J. A., and Guthrie, C. 2002. Spliceosomal snRNAs: Mg^{2+} dependent chemistry at the catalytic core? *Cell* 109: 149–152.

Books

Krebs, J. E., and Goldstein, E. S. 2012. *Lewin's Genes XI* (11th ed.). Jones and Bartlett.

Kornberg, A., and Baker, T. A. 1992. *DNA Replication* (2d ed.). W. H. Freeman and Company.

Lodish, H., Berk, A., Kaiser, C. A., Krieger, M., Bretscher, A., Ploegh, H., Amon, A., and Scott, M. P. 2012. *Molecular Cell Biology* (7th ed.). W. H. Freeman and Company.

Watson, J. D., Baker, T. A., Bell, S. P., Gann, A., Levine, M., and Losick, R. 2013. *Molecular Biology of the Gene* (7th ed.). Benjamin Cummings.

Gesteland, R. F., Cech, T., and Atkins, J. F. 2006. *The RNA World: The Nature of Modern RNA Suggests a Prebiotic RNA* (3d ed.). Cold Spring Harbor Laboratory Press.

RNA Polymerases

Liu, X., Bushnell, D. A., Wang, D., Calero, G., and Kornberg, R. D. 2010. Structure of an RNA polymerase II-TFIIB complex and the transcription initiation mechanism. *Science* 327:206–209.

Wang, D., Bushnell, D. A., Huang, X., Westover, K. D., Levitt, M., and Kornberg, R. D. 2009. Structural basis of transcription: Backtracked RNA polymerase II at 3.4 Å resolution. *Science* 324:1203–1206.

Darst, S. A. 2001. Bacterial RNA polymerase. *Curr. Opin. Struct. Biol.* 11:155–162.

Ross, W., Gosink, K. K., Salomon, J., Igarashi, K., Zou, C., Ishihama, A., Severinov, K., and Gourse, R. L. 1993. A third recognition element in bacterial promoters: DNA binding by the alpha subunit of RNA polymerase. *Science* 262:1407–1413.

Cramer, P., Bushnell, D. A., and Kornberg, R. D. 2001. Structural basis of transcription: RNA polymerase II at 2.8 Å resolution. *Science* 292:1863–1875.

Gnatt, A. L., Cramer, P., Fu, J., Bushnell, D. A., and Kornberg, R. D. 2001. Structural basis of transcription: An RNA polymerase II elongation complex at 3.3 Å resolution. *Science* 292:1876–1882.

Zhang, G., Campbell, E. A., Minakhin, L., Richter, C., Severinov, K., and Darst, S. A. 1999. Crystal structure of *Thermus aquaticus* core RNA polymerase at 3.3 Å resolution. *Cell* 98:811–824.

Campbell, E. A., Korzheva, N., Mustaev, A., Murakami, K., Nair, S., Goldfarb, A., and Darst, S. A. 2001. Structural mechanism for rifampicin inhibition of bacterial RNA polymerase. *Cell* 104:901–912.

Darst, S. A. 2004. New inhibitors targeting bacterial RNA polymerase. *Trends Biochem. Sci.* 29:159–160.

Cheetham, G. M., and Steitz, T. A. 1999. Structure of a transcribing T7 RNA polymerase initiation complex. *Science* 286:2305–2309.

Ebright, R. H. 2000. RNA polymerase: Structural similarities between bacterial RNA polymerase and eukaryotic RNA polymerase II. *J. Mol. Biol.* 304:687–698.

Paule, M. R., and White, R. J. 2000. Survey and summary: Transcription by RNA polymerases I and III. *Nucleic Acids Res.* 28:1283–1298.

Initiation and Elongation

Murakami, K. S., and Darst, S. A. 2003. Bacterial RNA polymerases: The whole story. *Curr. Opin. Struct. Biol.* 13:31–39.

Buratowski, S. 2000. Snapshots of RNA polymerase II transcription initiation. *Curr. Opin. Cell Biol.* 12:320–325.

Conaway, J. W., and Conaway, R. C. 1999. Transcription elongation and human disease. *Annu. Rev. Biochem.* 68:301–319.

Conaway, J. W., Shilatifard, A., Dvir, A., and Conaway, R. C. 2000. Control of elongation by RNA polymerase II. *Trends Biochem. Sci.* 25:375–380.

Korzheva, N., Mustaev, A., Kozlov, M., Malhotra, A., Nikiforov, V., Goldfarb, A., and Darst, S. A. 2000. A structural model of transcription elongation. *Science* 289:619–625.

Reines, D., Conaway, R. C., and Conaway, J. W. 1999. Mechanism and regulation of transcriptional elongation by RNA polymerase II. *Curr. Opin. Cell Biol.* 11:342–346.

Promoters, Enhancers, and Transcription Factors

Merika, M., and Thanos, D. 2001. Enhanceosomes. *Curr. Opin. Genet. Dev.* 11:205–208.

Park, J. M., Gim, B. S., Kim, J. M., Yoon, J. H., Kim, H. S., Kang, J. G., and Kim, Y. J. 2001. *Drosophila* mediator complex is broadly utilized by diverse gene-specific transcription factors at different types of core promoters. *Mol. Cell. Biol.* 21:2312–2323.

Smale, S. T., and Kadonaga, J. T. 2003. The RNA polymerase II core promoter. *Annu. Rev. Biochem.* 72:449–479.

Gourse, R. L., Ross, W., and Gaal, T. 2000. Ups and downs in bacterial transcription initiation: The role of the alpha subunit of RNA polymerase in promoter recognition. *Mol. Microbiol.* 37:687– 695.

Fiering, S., Whitelaw, E., and Martin, D. I. 2000. To be or not to be active: The stochastic nature of enhancer action. *BioEssays* 22:381–387.

Hampsey, M., and Reinberg, D. 1999. RNA polymerase II as a control panel for multiple coactivator complexes. *Curr. Opin. Genet. Dev.* 9:132–139.

Chen, L. 1999. Combinatorial gene regulation by eukaryotic transcription factors. *Curr. Opin. Struct. Biol.* 9:48–55.

Muller, C. W. 2001. Transcription factors: Global and detailed views. *Curr. Opin. Struct. Biol.* 11:26–32.

Reese, J. C. 2003. Basal transcription factors. *Curr. Opin. Genet. Dev.* 13:114–118.

Kadonaga, J. T. 2004. Regulation of RNA polymerase II transcription by sequence-specific DNA binding factors. *Cell* 116:247–257.

Harrison, S. C. 1991. A structural taxonomy of DNA-binding domains. *Nature* 353:715–719.

Sakurai, H., and Fukasawa, T. 2000. Functional connections between mediator components and general transcription factors of *Saccharomyces cerevisiae*. *J. Biol. Chem.* 275:37251–37256.

Droge, P., and Muller-Hill, B. 2001. High local protein concentrations at promoters: Strategies in prokaryotic and eukaryotic cells. *Bioessays* 23:179–183.

Smale, S. T., Jain, A., Kaufmann, J., Emami, K. H., Lo, K., and Garraway, I. P. 1998. The initiator element: A paradigm for core promoter heterogeneity within metazoan protein-coding genes. *Cold Spring Harbor Symp. Quant. Biol.* 63:21–31.

Kim, Y., Geiger, J. H., Hahn, S., and Sigler, P. B., 1993. Crystal structure of a yeast TBP/TATA-box complex. *Nature* 365:512–520.

Kim, J. L., Nikolov, D. B., and Burley, S. K., 1993. Co-crystal structure of TBP recognizing the minor groove of a TATA element. *Nature* 365:520–527.

White, R. J., and Jackson, S. P., 1992. The TATA-binding protein: A central role in transcription by RNA polymerases I, II and III. *Trends Genet.* 8:284–288.

Martinez, E. 2002. Multi-protein complexes in eukaryotic gene transcription. *Plant Mol. Biol.* 50:925–947.

Meinhart, A., Kamenski, T., Hoeppner, S., Baumli, S., and Cramer, P. 2005. A structural perspective of CTD function. *Genes Dev.* 19: 1401–1415.

Palancade, B., and Bensaude, O. 2003. Investigating RNA polymerase II carboxyl-terminal domain (CTD) phosphorylation. *Eur. J. Biochem.* 270:3859–3870.

Termination

Burgess, B. R., and Richardson, J. P. 2001. RNA passes through the hole of the protein hexamer in the complex with *Escherichia coli* Rho factor. *J. Biol. Chem.* 276:4182–4189.

Yu, X., Horiguchi, T., Shigesada, K., and Egelman, E. H. 2000. Three-dimensional reconstruction of transcription termination factor rho: Orientation of the N-terminal domain and visualization of an RNA-binding site. *J. Mol. Biol.* 299:1279–1287.

Stitt, B. L. 2001. *Escherichia coli* transcription termination factor Rho binds and hydrolyzes ATP using a single class of three sites. *Biochemistry* 40:2276–2281.

Henkin, T. M. 2000. Transcription termination control in bacteria. *Curr. Opin. Microbiol.* 3:149–153.

Gusarov, I., and Nudler, E. 1999. The mechanism of intrinsic transcription termination. *Mol. Cell* 3:495–504.

Riboswitches

Barrick, J. E., and Breaker, R. R. 2007. The distributions, mechanisms, and structures of metabolite-binding riboswitches. *Genome Biol.* 8:R239.

Cheah, M. T., Wachter, A., Sudarsan, N., and Breaker, R. R. 2007. Control of alternative RNA splicing and gene expression by eukaryotic riboswitches. *Nature* 447:497–500.

Serganov, A., Huang, L., and Patel, D. J. 2009. Coenzyme recognition and gene regulation by a flavin mononucleotide riboswitch. *Nature* 458:233–237.

Noncoding RNA

Cech, T. R. and Steitz, J. A. 2014. The noncoding RNA revolution-trashing old rules to forge new ones. *Cell* 157:77–94.

Peculis, B. A. 2002. Ribosome biogenesis: Ribosomal RNA synthesis as a package deal. *Curr. Biol.* 12:R623–R624.

Decatur, W. A., and Fournier, M. J. 2002. rRNA modifications and ribosome function. *Trends Biochem. Sci.* 27:344–351.

Hopper, A. K., and Phizicky, E. M. 2003. tRNA transfers to the limelight. *Genes Dev.* 17:162–180.

Weiner, A. M. 2004. tRNA maturation: RNA polymerization without a nucleic acid template. *Curr. Biol.* 14:R883–R885.

5′-Cap Formation and Polyadenylation

Shatkin, A. J., and Manley, J. L. 2000. The ends of the affair: Capping and polyadenylation. *Nat. Struct. Biol.* 7:838–842.

Bentley, D. L. 2005. Rules of engagement: Co-transcriptional recruitment of pre-mRNA processing factors. *Curr. Opin. Cell Biol.* 17:251–256.

Aguilera, A. 2005. Cotranscriptional mRNP assembly: From the DNA to the nuclear pore. *Curr. Opin. Cell Biol.* 17:242–250.

Ro-Choi, T. S. 1999. Nuclear snRNA and nuclear function (discovery of 5′ cap structures in RNA). *Crit. Rev. Eukaryotic Gene Expr.* 9:107–158.

Bard, J., Zhelkovsky, A. M., Helmling, S., Earnest, T. N., Moore, C. L., and Bohm, A. 2000. Structure of yeast poly(A) polymerase alone and in complex with 3′-dATP. *Science* 289:1346–1349.

Martin, G., Keller, W., and Doublie, S. 2000. Crystal structure of mammalian poly(A) polymerase in complex with an analog of ATP. *EMBO J.* 19:4193–4203.

Zhao, J., Hyman, L., and Moore, C. 1999. Formation of mRNA 3′ ends in eukaryotes: Mechanism, regulation, and interrelationships with other steps in mRNA synthesis. *Microbiol. Mol. Biol. Rev.* 63:405–445.

Minvielle-Sebastia, L., and Keller, W. 1999. mRNA polyadenylation and its coupling to other RNA processing reactions and to transcription. *Curr. Opin. Cell Biol.* 11:352–357.

Small Regulatory RNAs

Winter, J., Jung, S., Keller, S., Gregory, R. I., and Diederichs, S. 2009. Many roads to maturity: MicroRNA biogenesis pathways and their regulation. *Nat. Cell Biol.* 11:228–234.

Ruvkun, G., Wightman, B., and Ha, I. 2004. The 20 years it took to recognize the importance of tiny RNAs. *Cell* 116:S93–S96.

RNA Editing

Gott, J. M., and Emeson, R. B. 2000. Functions and mechanisms of RNA editing. *Annu. Rev. Genet.* 34:499–531.

Simpson, L., Thiemann, O. H., Savill, N. J., Alfonzo, J. D., and Maslov, D. A. 2000. Evolution of RNA editing in trypanosome mitochondria. *Proc. Natl. Acad. Sci. U.S.A.* 97:6986–6993.

Chester, A., Scott, J., Anant, S., and Navaratnam, N. 2000. RNA editing: Cytidine to uridine conversion in apolipoprotein B mRNA. *Biochim. Biophys. Acta* 1494:1–3.

Maas, S., and Rich, A. 2000. Changing genetic information through RNA editing. *BioEssays* 22:790–802.

Splicing of mRNA Precursors

Caceres, J. F., and Kornblihtt, A. R. 2002. Alternative splicing: Multiple control mechanisms and involvement in human disease. *Trends Genet*. 18:186–193.

Faustino, N. A., and Cooper, T. A. 2003. Pre-mRNA splicing and human disease. *Genes Dev*. 17:419–437.

Lou, H., and Gagel, R. F. 1998. Alternative RNA processing: Its role in regulating expression of calcitonin/calcitonin gene-related peptide. *J. Endocrinol*. 156:401–405.

Matlin, A. J., Clark, F., and Smith, C. W. 2005. Understanding alternative splicing: Towards a cellular code. *Nat. Rev. Mol. Cell Biol.* 6:386–398.

McKie, A. B., McHale, J. C., Keen, T. J., Tarttelin, E. E., Goliath, R., van Lith-Verhoeven, J. J., Greenberg, J., Ramesar, R. S., Hoyng, C. B., Cremers, F. P., et al. 2001. Mutations in the pre-mRNA splicing factor gene PRPC8 in autosomal dominant retinitis pigmentosa (RP13). *Hum. Mol. Genet*. 10:1555–1562.

Nilsen, T. W. 2003. The spliceosome: The most complex macromolecular machine in the cell? *BioEssays* 25:1147–1149.

Rund, D., and Rachmilewitz, E. 2005. β-Thalassemia. *New Engl. J. Med.* 353:1135–1146.

Patel, A. A., and Steitz, J. A. 2003. Splicing double: Insights from the second spliceosome. *Nat. Rev. Mol. Cell Biol*. 4:960–970.

Sharp, P. A. 2005. The discovery of split genes and RNA splicing. *Trends Biochem. Sci*. 30:279–281.

Valadkhan, S., and Manley, J. L. 2001. Splicing-related catalysis by protein-free snRNAs. *Nature* 413:701–707.

Zhou, Z., Licklider, L. J., Gygi, S. P., and Reed, R. 2002. Comprehensive proteomic analysis of the human spliceosome. *Nature* 419: 182–185.

Stark, H., Dube, P., Luhrmann, R., and Kastner, B. 2001. Arrangement of RNA and proteins in the spliceosomal U1 small nuclear ribonucleoprotein particle. *Nature* 409:539–542.

Strehler, E. E., and Zacharias, D. A. 2001. Role of alternative splicing in generating isoform diversity among plasma membrane calcium pumps. *Physiol. Rev.* 81:21–50.

Graveley, B. R. 2001. Alternative splicing: Increasing diversity in the proteomic world. *Trends Genet.* 17:100–107.

Newman, A. 1998. RNA splicing. *Curr. Biol.* 8:R903–R905.

Reed, R. 2000. Mechanisms of fidelity in pre-mRNA splicing. *Curr. Opin. Cell Biol.* 12:340–345.

Sleeman, J. E., and Lamond, A. I. 1999. Nuclear organization of pre-mRNA splicing factors. *Curr. Opin. Cell Biol.* 11:372–377.

Black, D. L. 2000. Protein diversity from alternative splicing: A challenge for bioinformatics and post-genome biology. *Cell* 103:367–370.

Collins, C. A., and Guthrie, C. 2000. The question remains: Is the spliceosome a ribozyme? *Nat. Struct. Biol.* 7:850–854.

Self-Splicing and RNA Catalysis

Adams, P. L., Stanley, M. R., Kosek, A. B., Wang, J., and Strobel, S. A. 2004. Crystal structure of a self-splicing group I intron with both exons. *Nature* 430:45–50.

Adams, P. L., Stanley, M. R., Gill, M. L., Kosek, A. B., Wang, J., and Strobel, S. A. 2004. Crystal structure of a group I intron splicing intermediate. *RNA* 10:1867–1887.

Stahley, M. R., and Strobel, S. A. 2005. Structural evidence for a two-metal-ion mechanism of group I intron splicing. *Science* 309:1587–1590.

Carola, C., and Eckstein, F. 1999. Nucleic acid enzymes. *Curr. Opin. Chem. Biol.* 3:274–283.

Doherty, E. A., and Doudna, J. A. 2000. Ribozyme structures and mechanisms. *Annu. Rev. Biochem.* 69:597–615.

Fedor, M. J. 2000. Structure and function of the hairpin ribozyme. *J. Mol. Biol.* 297:269–291.

Hanna, R., and Doudna, J. A. 2000. Metal ions in ribozyme folding and catalysis. *Curr. Opin. Chem. Biol.* 4:166–170.

Scott, W. G. 1998. RNA catalysis. *Curr. Opin. Struct. Biol.* 8:720–726.

Chapter 30

Where to Start

Yusupova, G., and Yusupov, M. 2014. High-resolution structure of the eukaryotic 80S ribosome. *Annu. Rev. Biochem.* 83:467–486.

Anger, A. M., Armache, J.-P., Berninghausen, O., Habeck, M., Subklewe, M., Wilson. D. N., and Beckmann, R. 2013. Structures of the human and Drosophila 80S ribosome. *Nature* 497:80–87.

Novoa, E. M., and Ribas de Pouplana, L. 2012. Speeding with control: Codon usage, tRNAs, and ribosomes. *Trends Genet*. 28:574−581.

Ibba, M., Curnow, A. W., and Söll, D. 1997. Aminoacyl-tRNA synthesis: Divergent routes to a common goal. *Trends Biochem. Sci.* 22:39–42.

Koonin, E. V., and Novozhilov, A. S. 2009. Origin and evolution of the genetic code: The universal enigma. *IUBMB Life* 61:99–111.

Schimmel, P., and Ribas de Pouplana, L. 2000. Footprints of aminoacyl-tRNA synthetases are everywhere. *Trends Biochem. Sci.* 25:207–209.

Books

Rodnina, M. V., Wintermeyer, W., and Green, R. 2011 (Eds.). *Ribosome Structure, Function and Dynamics*. Springer.

Cold Spring Harbor Symposia on Quantitative Biology. 2001. Volume 66. *The Ribosome*. Cold Spring Harbor Laboratory Press.

Gesteland, R. F., Atkins, J. F., and Cech, T. (Eds.). 2005. *The RNA World* (3d ed.). Cold Spring Harbor Laboratory Press.

Garrett, R., Douthwaite, S. R., Liljas, A., Matheson, A. T., Moore, P. B., and Noller, H. F. 2000. *The Ribosome: Structure, Function, Antibiotics, and Cellular Interactions.* The American Society for Microbiology.

Aminoacyl-tRNA Synthetases

Kaminska, M., Havrylenko, S., Decottignies, P., Le Maréchal, P., Negrutskii, B., and Mirande, M. 2009. Dynamic organization of aminoacyl-tRNA synthetase complexes in the cytoplasm of human cells. *J. Biol. Chem.* 284:13746–13754.

Park, S. G., Schimmel, P., and Kim, S. 2008. Aminoacyl tRNA synthetases and their connections to disease. *Proc. Natl. Acad. Sci. U.S.A.* 105:11043–11049.

Ibba, M., and Söll, D. 2000. Aminoacyl-tRNA synthesis. *Annu. Rev. Biochem.* 69:617–650.

Sankaranarayanan, R., Dock-Bregeon, A. C., Rees, B., Bovee, M., Caillet, J., Romby, P., Francklyn, C. S., and Moras, D. 2000. Zinc ion mediated amino acid discrimination by threonyl-tRNA synthetase. *Nat. Struct. Biol.* 7:461–465.

Sankaranarayanan, R., Dock-Bregeon, A. C., Romby, P., Caillet, J., Springer, M., Rees, B., Ehresmann, C., Ehresmann, B., and Moras, D. 1999. The structure of threonyl-tRNA synthetase-tRNA^{Thr} complex enlightens its repressor activity and reveals an essential zinc ion in the active site. *Cell* 97:371–381.

Dock-Bregeon, A., Sankaranarayanan, R., Romby, P., Caillet, J., Springer, M., Rees, B., Francklyn, C. S., Ehresmann, C., and Moras, D. 2000. Transfer RNA-mediated editing in threonyl-tRNA synthetase: The class II solution to the double discrimination problem. *Cell* 103:877–884.

de Pouplana, L. R., and Schimmel, P. 2000. A view into the origin of life: Aminoacyl-tRNA synthetases. *Cell. Mol. Life Sci.* 57:865–870.

Transfer RNA

Ibba, M., Becker, H. D., Stathopoulos, C., Tumbula, D. L., and Söll, D. 2000. The adaptor hypothesis revisited. *Trends Biochem. Sci.* 25:311–316.

Weisblum, B. 1999. Back to Camelot: Defining the specific role of tRNA in protein synthesis. *Trends Biochem. Sci.* 24:247–250.

Ribosomes and Ribosomal RNAs

Klinge, S., Voigts-Hoffmann, F., Leibundgut, M., and Ban, N. 2012. Atomic structures of the eukaryotic ribosome. *Trends Biochem. Sci.* 37:189–198.

Jin, H., Kelley, A. C., Loakes, D., and Ramakrishnan, V. 2010. Structure of the 70S ribosome bound to release factor 2 and a substrate analog provides insights into catalysis of peptide release. *Proc. Natl. Acad. Sci. U.S.A.* 107:8593–8598.

Rodnina, M. V., and Wintermeyer, W. 2009. Recent mechanistic insights into eukaryotic ribosomes. *Curr. Opin. Cell Biol.* 21:435–443.

Dinman, J. D. 2008. The eukaryotic ribosome: Current status and challenges. *J. Biol. Chem.* 284:11761–11765.

Wen, J.-D., Lancaster, L., Hodges, C., Zeri, A.-C., Yoshimura, S. H., Noller, H. F., Bustamante, C., and Tinoco, I., Jr. 2008. Following translation by single ribosomes one codon at a time. *Nature* 452:598–603.

Korostelev, A., and Noller, H. F. 2007. The ribosome in focus: New structures bring insights. *Trends Biochem. Sci.* 32:434–441.

Brandt, F., Etchells, S. A., Ortiz, J. O., Elcock, A. H., Hartl, F. U., and Baumeister, W. 2009. The native 3D organization of bacterial polysomes. *Cell* 136:261–271.

Initiation Factors

Søgaard, B., Sørensen, H. P., Mortensen, K. K., and Sperling-Petersen, H. U. 2005. Initiation of protein synthesis in bacteria. *Microbiol. Mol. Biol. Rev.* 69:101–123.

Carter, A. P., Clemons, W. M., Jr., Brodersen, D. E., Morgan-Warren, R. J., Hartsch, T., Wimberly, B. T., and Ramakrishnan, V. 2001. Crystal structure of an initiation factor bound to the 30S ribosomal subunit. *Science* 291:498–501.

Guenneugues, M., Caserta, E., Brandi, L., Spurio, R., Meunier, S., Pon, C. L., Boelens, R., and Gualerzi, C. O. 2000. Mapping the fMet-$\text{tRNA}_{\text{f}}^{\text{Met}}$ binding site of initiation factor IF2. *EMBO J.* 19:5233–5240.

Meunier, S., Spurio, R., Czisch, M., Wechselberger, R., Guenneugues, M., Gualerzi, C. O., and Boelens, R. 2000. Structure of the fMet-$\text{tRNA}_{\text{f}}^{\text{Met}}$-binding domain of *B. stearothermophilus* initiation factor IF2. *EMBO J.* 19:1918–1926.

Elongation Factors

Voorhees R. M., and Ramakrishnan, V. 2013. Structural basis of the translational elongation cycle. *Annu. Rev. Biochem.* 82:203–236.

Liu, S., Bachran, C., Gupta, P., Miller-Randolph, S., Wang, H., Crown, D., Zhang, Y., Kavaliauskas, D., Nissen, P., and Knudsen, C. R. 2012. The busiest of all ribosomal assistants: Elongation factor Tu. *Biochemistry* 51:2642−2651.

Schuette, J.-C., Murphy, F. V., Kelley, A. C., Weir, J. R., Giesebrecht, J., Connell, S. R., Loerke, J., Mielke, T., Zhang, W., Penczek, P. A., et al. 2009. GTPase activation of elongation factor EF-Tu by the ribosome during decoding. *EMBO J.* 28:755–765.

Stark, H., Rodnina, M. V., Wieden, H. J., van Heel, M., and Wintermeyer, W. 2000. Large-scale movement of elongation factor G and extensive conformational change of the ribosome during translocation. *Cell* 100:301–309.

Baensch, M., Frank, R., and Kohl, J. 1998. Conservation of the amino-terminal epitope of elongation factor Tu in Eubacteria and Archaea. *Microbiology* 144:2241–2246.

Krasny, L., Mesters, J. R., Tieleman, L. N., Kraal, B., Fucik, V., Hilgenfeld, R., and Jonak, J. 1998. Structure and expression of elongation factor Tu from *Bacillus stearothermophilus. J. Mol. Biol.* 283:371–381.

Pape, T., Wintermeyer, W., and Rodnina, M. V. 1998. Complete kinetic mechanism of elongation factor Tu-dependent binding of aminoacyl-tRNA to the A site of the *E. coli* ribosome. *EMBO J.* 17:7490–7497.

Piepenburg, O., Pape, T., Pleiss, J. A., Wintermeyer, W., Uhlenbeck, O. C., and Rodnina, M. V. 2000. Intact aminoacyl-tRNA is required to trigger GTP hydrolysis by elongation factor Tu on the ribosome. *Biochemistry* 39:1734–1738.

Peptide-Bond Formation and Translocation

Rodnina, M. V. 2013. The ribosome as a versatile catalyst: Reactions at the peptidyl transferase center. *Curr. Opin. Struct. Biol.* 23:595–602.

Uemura, S., Aitken, C. E., Korlach, J., Flusberg, B. A., Turner, S. W., and Puglisi, J. D. 2010. Real-time tRNA transit on single translating ribosomes at codon resolution. *Nature* 464:1012–1018.

Beringer, M., and. Rodnina, M. V. 2007. The ribosomal peptidyl transferase. *Mol. Cell* 26:311–321.

Yarus, M., and Welch, M. 2000. Peptidyl transferase: Ancient and exiguous. *Chem. Biol.* 7:R187–R190.

Vladimirov, S. N., Druzina, Z., Wang, R., and Cooperman, B. S. 2000. Identification of 50S components neighboring 23S rRNA nucleotides A2448 and U2604 within the peptidyl transferase center of *Escherichia coli* ribosomes. *Biochemistry* 39:183–193.

Frank, J., and Agrawal, R. K. 2000. A ratchet-like inter-subunit reorganization of the ribosome during translocation. *Nature* 406:318–322.

Termination

Weixlbaumer, A., Jin, H., Neubauer, C., Voorhees, R. M., Petry, S., Kelley, A. C., and Ramakrishnan, V. 2008. Insights into translational termination from the structure of RF2 bound to the ribosome. *Science* 322:953–956.

Trobro, S., and Åqvist, S. 2007. A model for how ribosomal release factors induce peptidyl-tRNA cleavage in termination of protein synthesis. *Mol. Cell* 27:758–766.

Korostelev, A., Asahara, H., Lancaster, L., Laurberg, M., Hirschi, A., Zhu, J., Trakhanov, S., Scott, W. G., and Noller, H. F. 2008. Crystal structure of a translation termination complex formed with release factor RF2. *Proc. Natl. Acad. Sci. U.S.A.* 105: 19684–19689.

Wilson, D. N., Schluenzen, F., Harms, J. M., Yoshida, T., Ohkubo, T., Albrecht, A., Buerger, J., Kobayashi, Y., and Fucini, P. 2005. X-ray crystallography study on ribosome recycling: The mechanism of binding and action of RRF on the 50S ribosomal subunit. *EMBO J.* 24:251–260.

Kisselev, L. L., and Buckingham, R. H. 2000. Translational termination comes of age. *Trends Biochem. Sci.* 25:561–566.

Fidelity and Proofreading

Zaher, H. S., and Green, R. 2009. Quality control by the ribosome following peptide bond formation. *Nature* 457:161–166.

Zaher, H. S., and Green, R. 2009. Fidelity at the molecular level: Lessons from protein synthesis. *Cell* 136:746–762.

Ogle, J. M., and Ramakrishnan, V. 2005. Structural insights into translational fidelity. *Annu. Rev. Biochem.* 74:129–177.

Eukaryotic Protein Synthesis

Hinnebusch, A. G. 2014. The scanning mechanism of eukaryotic translation initiation. *Annu. Rev. Biochem.* 83:779–812.

Wein, A. N., Singh, R., Fattah, R., and Leppla, S. H. 2012. Diphthamide modification on eukaryotic elongation factor 2 is needed to assure fidelity of mRNA translation and mouse development. *Proc. Natl. Acad. Sci. U.S.A.* 109:13817–13822.

Rhoads, R. E. 2009. eIF4E: New family members, new binding partners, new roles. *J. Biol. Chem.* 284:16711–16715.

Marintchev, A., Edmonds, K. A., Marintcheva, B., Hendrickson, E., Oberer, M., Suzuki, C., Herdy, B., Sonenberg, N., and Wagner, G. 2009. Topology and regulation of the human eIF4A/4G/4H helicase complex in translation initiation. *Cell* 136:447–460.

Fitzgerald, K. D., and Semler, B. L. 2009. Bridging IRES elements in mRNAs to the eukaryotic translation apparatus. *Biochim. Biophys. Acta* 1789:518–528.

Mitchell, S. F., and Lorsch, J. R. 2008. Should I stay or should I go? Eukaryotic translation initiation factors 1 and 1A control start codon recognition. *J. Biol. Chem.* 283:27345–27349.

Amrani, A., Ghosh, S., Mangus, D. A., and Jacobson, A. 2008. Translation factors promote the formation of two states of the closed-loop mRNP. *Nature* 453:1276–1280.

Sachs, A. B., and Varani, G. 2000. Eukaryotic translation initiation: There are (at least) two sides to every story. *Nat. Struct. Biol.* 7:356–361.

Kozak, M. 1999. Initiation of translation in prokaryotes and eukaryotes. *Gene* 234:187–208.

Bushell, M., Wood, W., Clemens, M. J., and Morley, S. J. 2000. Changes in integrity and association of eukaryotic protein synthesis initiation factors during apoptosis. *Eur. J. Biochem.* 267:1083–1091.

Das, S., Ghosh, R., and Maitra, U. 2001. Eukaryotic translation initiation factor 5 functions as a GTPase-activating protein. *J. Biol. Chem.* 276:6720–6726.

Lee, J. H., Choi, S. K., Roll-Mecak, A., Burley, S. K., and Dever, T. E. 1999. Universal conservation in translation initiation revealed by human and archaeal homologs of bacterial translation initiation factor IF2. *Proc. Natl. Acad. Sci. U.S.A.* 96:4342–4347.

Pestova, T. V., and Hellen, C. U. 2000. The structure and function of initiation factors in eukaryotic protein synthesis. *Cell. Mol. Life Sci.* 57:651–674.

Antibiotics and Toxins

Belova, L., Tenson, T., Xiong, L., McNicholas, P. M., and Mankin, A. S. 2001. A novel site of antibiotic action in the ribosome: Interaction of evernimicin with the large ribosomal subunit. *Proc. Natl. Acad. Sci. U.S.A.* 98:3726–3731.

Brodersen, D. E., Clemons, W. M., Jr., Carter, A. P., Morgan-Warren, R. J., Wimberly, B. T., and Ramakrishnan, V. 2000. The structural basis for the action of the antibiotics tetracycline, pactamycin, and hygromycin B on the 30S ribosomal subunit. *Cell* 103:1143–1154.

Porse, B. T., and Garrett, R. A. 1999. Ribosomal mechanics, antibiotics, and GTP hydrolysis. *Cell* 97:423–426.

Lord, M. J., Jolliffe, N. A., Marsden, C. J., Pateman, C. S., Smith, D. S., Spooner, R. A., Watson, P. D., and Roberts, L. M. 2003. Ricin: Mechanisms of toxicity. *Toxicol. Rev.* 22:53–64.

Protein Transport Across Membranes

Akopian, D., Shen, K., Zhang, X., and Shan, S. 2013. Signal recognition particle: An essential protein-targeting machine. *Annu. Rev. Biochem.* 82:693–721.

Nyathi, Y., Wilkinson, B. M., and Pool, M. R. 2013. Co-translational targeting and translocation of proteins to the endoplasmic reticulum. *Biochim. Biophys. Acta* 1833:2392–2402.

Janda, C. Y., Li, J., Oubridge, C., Hernández, H., Robinson, C. V., and Nagai, K. 2010. Recognition of a signal peptide by the signal recognition particle. *Nature* 465:507–510.

Cross, B. C. S., Sinning, I., Luirink, J., and High, S. 2009. Delivering proteins for export from the cytosol. *Nat. Rev. Mol. Cell. Biol.* 10:255–264.

Shan, S., Schmid, S. L., and Zhang, X. 2009. Signal recognition particle (SRP) and SRP receptor: A new paradigm for multistate regulatory GTPases. *Biochemistry* 48:6696–6704.

Johnson, A. E. 2009. The structural and functional coupling of two molecular machines, the ribosome and the translocon. *J. Cell Biol.* 185:765–767.

Pool, R. P. 2009. A trans-membrane segment inside the ribosome exit tunnel triggers RAMP4 recruitment to the Sec61p translocase. *J. Cell Biol.* 185:889–902.

Egea, P. F., Stroud, R. M., and Walter, P. 2005. Targeting proteins to membranes: Structure of the signal recognition particle. *Curr. Opin. Struct. Biol.* 15:213–220.

Halic, M., and Beckmann, R. 2005. The signal recognition particle and its interactions during protein targeting. *Curr. Opin. Struct. Biol.*15:116–125.

Doudna, J. A., and Batey, R. T. 2004. Structural insights into the signal recognition particle. *Annu. Rev. Biochem.* 73:539–557.

Schnell, D. J., and Hebert, D. N. 2003. Protein translocons: Multifunctional mediators of protein translocation across membranes. *Cell* 112:491–505.

Chapter 31

Where to Start

Ptashne, M. 2014. The chemistry of regulation of genes and other things. *J. Biol. Chem.* 289:5417–5435.

Pabo, C. O., and Sauer, R. T. 1984. Protein–DNA recognition. *Annu. Rev. Biochem.* 53:293–321.

Ptashne, M., Johnson, A. D., and Pabo, C. O. 1982. A genetic switch in a bacterial virus. *Sci. Am.* 247:128–140.

Ptashne, M., Jeffrey, A., Johnson, A. D., Maurer, R., Meyer, B. J., Pabo, C. O., Roberts, T. M., and Sauer, R. T. 1980. How the lambda repressor and Cro work. *Cell* 19:1–11.

Books

Ptashne, M. 2004. *A Genetic Switch: Phage 3 Revisited* (3d ed.). Cold Spring Harbor Laboratory Press.

McKnight, S. L., and Yamamoto, K. R. (Eds.). 1992. *Transcriptional Regulation* (vols. 1 and 2). Cold Spring Harbor Laboratory Press.

Lodish, H., Berk, A., Kaiser, C. A., Krieger, M., Bretscher, A., Pleogh, H., Amon, A., and Scott, M. P. 2012. *Molecular Cell Biology* (7th ed.). W. H. Freeman and Company.

DNA-Binding Proteins

Balaeff, A., Mahadevan, L., and Schulten, K. 2004. Structural basis for cooperative DNA binding by CAP and *lac* repressor. *Structure* 12:123–132.

Bell, C. E., and Lewis, M. 2001. The Lac repressor: A second generation of structural and functional studies. *Curr. Opin. Struct. Biol.* 11:19–25.

Lewis, M., Chang, G., Horton, N. C., Kercher, M. A., Pace, H. C., Schumacher, M. A., Brennan, R. G., and Lu, P. 1996. Crystal structure of the lactose operon repressor and its complexes with DNA and inducer. *Science* 271:1247–1254.

Niu, W., Kim, Y., Tau, G., Heyduk, T., and Ebright, R. H. 1996. Transcription activation at class II CAP-dependent promoters: Two interactions between CAP and RNA polymerase. *Cell* 87:1123–1134.

Schultz, S. C., Shields, G. C., and Steitz, T. A. 1991. Crystal structure of a CAP-DNA complex: The DNA is bent by 90 degrees. *Science* 253:1001–1007.

Parkinson, G., Wilson, C., Gunasekera, A., Ebright, Y. W., Ebright, R. E., and Berman, H. M. 1996. Structure of the CAP-DNA complex at 2.5 Å resolution: A complete picture of the protein–DNA interface. *J. Mol. Biol.* 260:395–408.

Busby, S., and Ebright, R. H. 1999. Transcription activation by catabolite activator protein (CAP). *J. Mol. Biol.* 293:199–213.

Somers, W. S., and Phillips, S. E. 1992. Crystal structure of the met repressor-operator complex at 2.8 Å resolution reveals DNA recognition by β-strands. *Nature* 359:387–393.

Gene-Regulatory Circuits

Johnson, A. D., Poteete, A. R., Lauer, G., Sauer, R. T., Ackers, G. K., and Ptashne, M. 1981. Lambda repressor and Cro: Components of an efficient molecular switch. *Nature* 294:217–223.

Stayrook, S., Jaru-Ampornpan, P., Ni, J., Hochschild, A., and Lewis, M. 2008. Crystal structure of the lambda repressor and a model for pairwise cooperative operator binding. *Nature* 452:1022–1025.

Arkin, A., Ross, J., and McAdams, H. H. 1998. Stochastic kinetic analysis of developmental pathway bifurcation in phage lambda-infected *Escherichia coli* cells. *Genetics* 149:1633–1648.

Post-transcriptional Regulation

Kolter, R., and Yanofsky, C. 1982. Attenuation in amino acid biosynthetic operons. *Annu. Rev. Genet.* 16:113–134.

Yanofsky, C. 1981. Attenuation in the control of expression of bacterial operons. *Nature* 289:751–758.

Miller, M. B., and Bassler, B. L. 2001. Quorum sensing in bacteria. *Annu. Rev. Microbiol.* 55:165–199.

Zhang, R. G., Pappas, T., Brace, J. L., Miller, P. C., Oulmassov, T., Molyneaux, J. M., Anderson, J. C., Bashkin, J. K., Winans, S. C., and Joachimiak, A. 2002. Structure of a bacterial quorum-sensing transcription factor complexed with pheromone and DNA. *Nature* 417:971–974.

Soberon-Chavez, G., Aguirre-Ramirez, M., and Ordonez, L. 2005. Is *Pseudomonas aeruginosa* only "sensing quorum"? *Crit. Rev. Microbiol.* 31:171–182.

Historical Aspects

Lewis, M. 2005. The lac repressor. *C. R. Biol.* 328:521–548.

Jacob, F., and Monod, J. 1961. Genetic regulatory mechanisms in the synthesis of proteins. *J. Mol. Biol.* 3:318–356.

Ptashne, M., and Gilbert, W. 1970. Genetic repressors. *Sci. Am.* 222(6):36–44.

Lwoff, A., and Ullmann, A. (Eds.). 1979. *Origins of Molecular Biology: A Tribute to Jacques Monod*. Academic Press.

Judson, H. 1996. *The Eighth Day of Creation: Makers of the Revolution in Biology*. Cold Spring Harbor Laboratory Press.

Chapter 32

Where to Start

Liu, X., Bushnell, D. A., and Kornberg, R. D. 2013. RNA polymerase II transcription: Structure and mechanism. *Biochim. Biophys. Acta* 1829:2–8.

Kornberg, R. D. 2007. The molecular basis of eukaryotic transcription. *Proc. Natl. Acad. Sci. U.S.A.* 104:12955–12961.

Pabo, C. O., and Sauer, R. T. 1984. Protein–DNA recognition. *Annu. Rev. Biochem.* 53:293–321.

Struhl, K. 1989. Helix-turn-helix, zinc-finger, and leucine-zipper motifs for eukaryotic transcriptional regulatory proteins. *Trends Biochem. Sci.* 14:137–140.

Struhl, K. 1999. Fundamentally different logic of gene regulation in eukaryotes and prokaryotes. *Cell* 98:1–4.

Korzus, E., Torchia, J., Rose, D. W., Xu, L., Kurokawa, R., McInerney, E. M., Mullen, T. M., Glass, C. K., and Rosenfeld, M. G. 1998. Transcription factor-specific requirements for coactivators and their acetyltransferase functions. *Science* 279:703–707.

Aalfs, J. D., and Kingston, R. E. 2000. What does "chromatin remodeling" mean? *Trends Biochem. Sci.* 25:548–555.

Books

McKnight, S. L., and Yamamoto, K. R. (Eds.). 1992. *Transcriptional Regulation* (vols. 1 and 2). Cold Spring Harbor Laboratory Press.

Latchman, D. S. 2004. *Eukaryotic Transcription Factors* (4th ed.). Academic Press.

Wolffe, A. 1992. *Chromatin Structure and Function*. Academic Press.

Lodish, H., Berk, A., Kaiser, C. A., Krieger, M., Bretscher, A., Pleogh, H., Amon, A., and Scott, M. P. 2012. *Molecular Cell Biology* (7th ed.). W. H. Freeman and Company.

Chromatin and Chromatin Remodeling

Sadeh, R. and Allis, C. D. 2011. Genome-wide "re"-modeling of nucleosome positions. *Cell* 147:263–266.

Lorch, Y., Maier-Davis, B., and Kornberg, R. D. 2010. Mechanism of chromatin remodeling. *Proc. Natl. Acad. Sci. U.S.A.* 107:3458–3462.

Tang, L., Nogales, E., and Ciferri, C. 2010. Structure and function of SWI/SNF chromatin remodeling complexes and mechanistic implications for transcription. *Prog. Biophys. Mol. Biol.* 102:122–128.

Jenuwein, T., and Allis, C. D. 2001. Translating the histone code. *Science* 293:1074–1080.

Jiang, C., and Pugh, B. F. 2009. Nucleosome positioning and gene regulation: Advances through genomics. *Nat. Rev. Genet.* 10:161–172.

Barski, A., Cuddapah, S., Cui, K., Roh, T. Y., Schones, D. E., Wang, Z., Wei, G., Chepelev, I., and Zhao, K. 2007. High-resolution profiling of histone methylations in the human genome. *Cell* 129:823–837.

Weintraub, H., Larsen, A., and Groudine, M. 1981. β-Globin-gene switching during the development of chicken embryos: Expression and chromosome structure. *Cell* 24:333–344.

Ren, B., Robert, F., Wyrick, J. J., Aparicio, O., Jennings, E. G., Simon, I., Zeitlinger, J., Schreiber, J., Hannett, N., Kanin, E., et al. 2000. Genome-wide location and function of DNA-binding proteins. *Science* 290:2306–2309.

Goodrich, J. A., and Tjian, R. 1994. TBP-TAF complexes: Selectivity factors for eukaryotic transcription. *Curr. Opin. Cell. Biol.* 6:403–409.

Bird, A. P., and Wolffe, A. P. 1999. Methylation-induced repression: Belts, braces, and chromatin. *Cell* 99:451–454.

Cairns, B. R. 1998. Chromatin remodeling machines: Similar motors, ulterior motives. *Trends Biochem. Sci.* 23:20–25.

Albright, S. R., and Tjian, R. 2000. TAFs revisited: More data reveal new twists and confirm old ideas. *Gene* 242:1–13.

Urnov, F. D., and Wolffe, A. P. 2001. Chromatin remodeling and transcriptional activation: The cast (in order of appearance). *Oncogene* 20:2991–3006.

Luger, K., Mader, A. W., Richmond, R. K., Sargent, D. F., and Richmond, T. J. 1997. Crystal structure of the nucleosome core particle at 2.8 Å resolution. *Nature* 389:251–260.

Arents, G., and Moudrianakis, E. N. 1995. The histone fold: A ubiquitous architectural motif utilized in DNA compaction and protein dimerization. *Proc. Natl. Acad. Sci. U.S.A.* 92:11170–11174.

Baxevanis, A. D., Arents, G., Moudrianakis, E. N., and Landsman, D. 1995. A variety of DNA-binding and multimeric proteins contain the histone fold motif. *Nucleic Acids Res.* 23:2685–2691.

Transcription Factors

Green, M. R. 2005. Eukaryotic transcription activation: Right on target. *Mol. Cell* 18:399–402.

Kornberg, R. D. 2005. Mediator and the mechanism of transcriptional activation. *Trends Biochem. Sci.* 30:235–239.

Clements, A., Rojas, J. R., Trievel, R. C., Wang, L., Berger, S. L., and Marmorstein, R. 1999. Crystal structure of the histone acetyltransferase domain of the human PCAF transcriptional regulator bound to coenzyme A. *EMBO J.* 18:3521–3532.

Deckert, J., and Struhl, K. 2001. Histone acetylation at promoters is differentially affected by specific activators and repressors. *Mol. Cell. Biol.* 21:2726–2735.

Dutnall, R. N., Tafrov, S. T., Sternglanz, R., and Ramakrishnan, V. 1998. Structure of the histone acetyltransferase Hat1: A paradigm for the GCN5-related *N*-acetyltransferase superfamily. *Cell* 94:427–438.

Finnin, M. S., Donigian, J. R., Cohen, A., Richon, V. M., Rifkind, R. A., Marks, P. A., Breslow, R., and Pavletich, N. P. 1999. Structures of a histone deacetylase homologue bound to the TSA and SAHA inhibitors. *Nature* 401:188–193.

Finnin, M. S., Donigian, J. R., and Pavletich, N. P. 2001. Structure of the histone deacetylase SIR2. *Nat. Struct. Biol.* 8:621–625.

Jacobson, R. H., Ladurner, A. G., King, D. S., and Tjian, R. 2000. Structure and function of a human TAFII250 double bromodomain module. *Science* 288:1422–1425.

Rojas, J. R., Trievel, R. C., Zhou, J., Mo, Y., Li, X., Berger, S. L., Allis, C. D., and Marmorstein, R. 1999. Structure of *Tetrahymena* GCN5 bound to coenzyme A and a histone H3 peptide. *Nature* 401:93–98.

Induced Pluripotent Stem Cells

Takahashi, K., Tanabe, K., Ohnuki, M., Narita, M., Ichisaka, T., Tomoda, K., and Yamanaka, S. 2007. Induction of pluripotent stem cells from adult human fibroblasts by defined factors. *Cell* 131:861–872.

Takahashi, K., and Yamanaka, S. 2006. Induction of pluripotent stem cells from mouse embryonic and adult fibroblast cultures by defined factors. *Cell* 126:663–676.

Park, I. H., Arora, N., Huo, H., Maherali, N., Ahfeldt, T., Shimamura, A., Lensch, M. W., Cowan, C., Hochedlinger, K., and Daley, G. Q. 2008. Disease-specific induced pluripotent stem cells. *Cell* 134:877–886.

Yamanaka, S. 2009. A fresh look at iPS cells. *Cell* 137:13–17.

Yu, J., Hu, K., Smuga-Otto, K., Tian, S., Stewart, R., Slukvin, I. I., and Thomson, J. A. 2009. Human induced pluripotent stem cells free of vector and transgene sequences. *Science* 324:797–801.

Nuclear Hormone Receptors

Downes, M., Verdecia, M. A., Roecker, A. J., Hughes, R., Hogenesch, J. B., Kast-Woelbern, H. R., Bowman, M. E., Ferrer, J. L., Anisfeld, A. M., Edwards, et al. 2003. A chemical, genetic, and structural analysis of the nuclear bile acid receptor FXR. *Mol. Cell* 11:1079–1092.

Evans, R. M. 2005. The nuclear receptor superfamily: A Rosetta stone for physiology. *Mol. Endocrinol.* 19:1429–1438.

Xu, W., Cho, H., Kadam, S., Banayo, E. M., Anderson, S., Yates, J. R., III, Emerson, B. M., and Evans, R. M. 2004. A methylation-mediator complex in hormone signaling. *Genes Dev.* 18:144–156.

Evans, R. M. 1988. The steroid and thyroid hormone receptor superfamily. *Science* 240:889–895.

Yamamoto, K. R. 1985. Steroid receptor regulated transcription of specific genes and gene networks. *Annu. Rev. Genet.* 19:209–252.

Tanenbaum, D. M., Wang, Y., Williams, S. P., and Sigler, P. B. 1998. Crystallographic comparison of the estrogen and progesterone receptor's ligand binding domains. *Proc. Natl. Acad. Sci. U.S.A.* 95:5998–6003.

Schwabe, J. W., Chapman, L., Finch, J. T., and Rhodes, D. 1993. The crystal structure of the estrogen receptor DNA-binding domain bound to DNA: How receptors discriminate between their response elements. *Cell* 75:567–578.

Shiau, A. K., Barstad, D., Loria, P. M., Cheng, L., Kushner, P. J., Agard, D. A., and Greene, G. L. 1998. The structural basis of estrogen receptor/coactivator recognition and the antagonism of this interaction by tamoxifen. *Cell* 95:927–937.

Collingwood, T. N., Urnov, F. D., and Wolffe, A. P. 1999. Nuclear receptors: Coactivators, corepressors and chromatin remodeling in the control of transcription. *J. Mol. Endocrinol.* 23:255–275.

Posttranscriptional Regulation

Rouault, T. A., Stout, C. D., Kaptain, S., Harford, J. B., and Klausner, R. D. 1991. Structural relationship between an iron-regulated RNA-binding protein (IRE-BP) and aconitase: Functional implications. *Cell* 64:881–883.

Klausner, R. D., Rouault, T. A., and Harford, J. B. 1993. Regulating the fate of mRNA: The control of cellular iron metabolism. *Cell* 72:19–28.

Gruer, M. J., Artymiuk, P. J., and Guest, J. R. 1997. The aconitase family: Three structural variations on a common theme. *Trends Biochem. Sci.* 22:3–6.

Theil, E. C. 1994. Iron regulatory elements (IREs): A family of mRNA non-coding sequences. *Biochem. J.* 304:1–11.

MicroRNAs

Ruvkun, G. 2008. The perfect storm of tiny RNAs. *Nat. Med.* 14:1041–1045.

Sethupathy, P., and Collins, F. S. 2008. MicroRNA target site polymorphisms and human disease. *Trends Genet.* 24:489–497.

Adams, B. D., Cowee, D. M., and White, B. A. 2009. The role of miR-206 in the epidermal growth factor (EGF) induced repression of estrogen receptor-α (ERα) signaling and a luminal phenotype in MCF-7 breast cancer cells. *Mol. Endocrinol.* 23:1215–1230.

Jegga, A. G., Chen, J., Gowrisankar, S., Deshmukh, M. A., Gudivada, R., Kong, S., Kaimal, V., and Aronow, B. J. 2007. GenomeTrafac: A whole genome resource for the detection of transcription factor binding site clusters associated with conventional and microRNA encoding genes conserved between mouse and human gene orthologs. *Nucleic Acids Res.* 35:D116–D121.

Chapter 33

Where to Start

Axel, R. 1995. The molecular logic of smell. *Sci. Am.* 273(4):154–159.

Dulac, C. 2000. The physiology of taste, vintage 2000. *Cell* 100:607–610.

Yarmolinsky, D. A., Zuker, C. S., and Ryba, N. J. (2009) Common sense about taste: From mammals to insects. *Cell* 139:234–244.

Stryer, L. 1996. Vision: From photon to perception. *Proc. Natl. Acad. Sci. U.S.A.* 93:557–559.

Hudspeth, A. J. 1989. How the ear's works work. *Nature* 341:397–404.

Olfaction

Buck, L., and Axel, R. 1991. A novel multigene family may encode odorant receptors: A molecular basis for odor recognition. *Cell* 65:175–187.

Saito, H., Chi, Q., Zhuang, H., Matsunami, H., and Mainland, J. D. 2009. Odor coding by a mammalian receptor repertoire. *Sci. Signal.* 2:ra9.

Malnic, B., Hirono, J., Sato, T., and Buck, L. B. 1999. Combinatorial receptor codes for odors. *Cell* 96:713–723.

Zou, D. J., Chesler, A., and Firestein, S. 2009. How the olfactory bulb got its glomeruli: A just so story? *Nat. Rev. Neurosci.* 10:611–618.

De la Cruz, O., Blekhman, R., Zhang, X., Nicolae, D., Firestein, S., and Gilad, Y. 2009. A signature of evolutionary constraint on a subset of ectopically expressed olfactory receptor genes. *Mol. Biol. Evol.* 26:491–494.

Mombaerts, P., Wang, F., Dulac, C., Chao, S. K., Nemes, A., Mendelsohn, M., Edmondson, J., and Axel, R. 1996. Visualizing an olfactory sensory map. *Cell* 87:675–686.

Buck, L. 2005. Unraveling the sense of smell (Nobel lecture). *Angew. Chem. Int. Ed. Engl.* 44:6128–6140.

Belluscio, L., Gold, G. H., Nemes, A., and Axel, R. 1998. Mice deficient in $G_{(\mathrm{olf})}$ are anosmic. *Neuron* 20:69–81.

Vosshall, L. B., Wong, A. M., and Axel, R. 2000. An olfactory sensory map in the fly brain. *Cell* 102:147–159.

Lewcock, J. W., and Reed, R. R. 2003. A feedback mechanism regulates monoallelic odorant receptor expression. *Proc. Natl. Acad. Sci. U.S.A.*101:1069–1074.

Reed, R. R. 2004. After the holy grail: Establishing a molecular mechanism for mammalian olfaction. *Cell* 116:329–336.

Taste

Chandrashekar, J., Yarmolinsky, D., von Buchholtz, L., Oka, Y., Sly, W., Ryba, N. J., and Zuker, C. S. 2009. The taste of carbonation. *Science* 326:443–445.

Chandrashekar, J., Hoon, M. A., Ryba, N. J., and Zuker, C. S. 2006. The receptors and cells for mammalian taste. *Nature* 444:288–294.

Huang, A. L., Chen, X., Hoon, M. A., Chandrashekar, J., Guo, W., Tranker, D., Ryba, N. J., and Zuker, C. S. 2006. The cells and logic for mammalian sour taste detection. *Nature* 442:934–938.

Zhao, G. Q., Zhang, Y., Hoon, M. A., Chandrashekar, J., Erlenbach, I., Ryba, N. J. P., and Zuker, C. S. 2003. The receptors for mammalian sweet and umami taste. *Cell* 115:255–266.

Herness, M. S., and Gilbertson, T. A. 1999. Cellular mechanisms of taste transduction. *Annu. Rev. Physiol.* 61:873–900.

Adler, E., Hoon, M. A., Mueller, K. L., Chandrashekar, J., Ryba, N. J., and Zuker, C. S. 2000. A novel family of mammalian taste receptors. *Cell* 100:693–702.

Chandrashekar, J., Mueller, K. L., Hoon, M. A., Adler, E., Feng, L., Guo, W., Zuker, C. S., and Ryba, N. J. 2000. T2Rs function as bitter taste receptors. *Cell* 100:703–711.

Mano, I., and Driscoll, M. 1999. DEG/ENaC channels: A touchy superfamily that watches its salt. *BioEssays* 21:568–578.

Benos, D. J., and Stanton, B. A. 1999. Functional domains within the degenerin/epithelial sodium channel (Deg/ENaC) superfamily of ion channels. *J. Physiol. (Lond.)* 520(part 3):631–644.

McLaughlin, S. K., McKinnon, P. J., and Margolskee, R. F. 1992. Gustducin is a taste-cell-specific G protein closely related to the transducins. *Nature* 357:563–569.

Nelson, G., Hoon, M. A., Chandrashekar, J., Zhang, Y., Ryba, N. J., and Zuker, C. S. 2001. Mammalian sweet taste receptors. *Cell* 106:381–390.

Vision

Stryer, L. 1988. Molecular basis of visual excitation. *Cold Spring Harbor Symp. Quant. Biol.* 53:283–294.

Jastrzebska, B., Tsybovsky, Y., and Palczewski, K. 2010. Complexes between photoactivated rhodopsin and transducin: Progress and questions. *Biochem. J.* 428:1–10.

Wald, G. 1968. The molecular basis of visual excitation. *Nature* 219:800–807.

Ames, J. B., Dizhoor, A. M., Ikura, M., Palczewski, K., and Stryer, L. 1999. Three-dimensional structure of guanylyl cyclase activating protein-2, a calcium-sensitive modulator of photoreceptor guanylyl cyclases. *J. Biol. Chem.* 274:19329–19337.

Nathans, J. 1994. In the eye of the beholder: Visual pigments and inherited variation in human vision. *Cell* 78:357–360.

Nathans, J. 1999. The evolution and physiology of human color vision: Insights from molecular genetic studies of visual pigments. *Neuron* 24:299–312.

Palczewski, K., Kumasaka, T., Hori, T., Behnke, C. A., Motoshima, H., Fox, B. A., LeTrong, I., Teller, D. C., Okada, T., Stenkamp, R. E., et al. 2000. Crystal structure of rhodopsin: A G protein-coupled receptor. *Science* 289:739–745.

Filipek, S, Teller, D. C., Palczewski, K., and Stemkamp, R. 2003. The crystallographic model of rhodopsin and its use in studies of other G protein-coupled receptors. *Annu. Rev. Biophys. Biomol. Struct.* 32:375–397.

Hearing

Furness, D. N., Hackney, C. M., and Evans, M. G. 2010. Localisation of the mechanotransducer channels in mammalian cochlear hair cells provides clues to their gating. *J. Physiol.* 588:765–772.

Lim, K., and Park, S. 2009. A mechanical model of the gating spring mechanism of stereocilia. *J. Biomech.* 42:2158–2164.

Siemens, J., Lillo, C., Dumont, R. A., Reynolds, A., Williams, D. S., Gillespie, P. G., and Muller, U. 2004. Cadherin 23 is a component of the tip link in hair-cell stereocilia. *Nature* 428:950–955.

Spinelli, K. J., and Gillespie, P. G. 2009. Bottoms up: Transduction channels at tip link bases. *Nat. Neurosci.* 12:529–530.

Hudspeth, A. J. 1997. How hearing happens. *Neuron* 19:947–950.

Pickles, J. O., and Corey, D. P. 1992. Mechanoelectrical transduction by hair cells. *Trends Neurosci.* 15:254–259.

Walker, R. G., Willingham, A. T., and Zuker, C. S. 2000. A *Drosophila* mechanosensory transduction channel. *Science* 287:2229–2234.

Hudspeth, A. J., Choe, Y., Mehta, A. D., and Martin, P. 2000. Putting ion channels to work: Mechanoelectrical transduction, adaptation, and amplification by hair cells. *Proc. Natl. Acad. Sci. U.S.A.* 97:11765–11772.

Touch and Pain Reception

Myers, B. R., Bohlen, C. J., and Julius, D. 2008. A yeast genetic screen reveals a critical role for the pore helix domain in TRP channel gating. *Neuron* 58:362–373.

Lishko, P. V., Procko, E., Jin, X., Phelps, C. B., and Gaudet, R. 2007. The ankyrin repeats of TRPV1 bind multiple ligands and modulate channel sensitivity. *Neuron* 54:905–918.

Franco-Obregon, A., and Clapham, D. E. 1998. Touch channels sense blood pressure. *Neuron* 21:1224–1226.

Caterina, M. J., Schumacher, M. A., Tominaga, M., Rosen, T. A., Levine, J. D., and Julius, D. 1997. The capsaicin receptor: A heat-activated ion channel in the pain pathway. *Nature* 389:816–824.

Tominaga, M., Caterina, M. J., Malmberg, A. B., Rosen, T. A., Gilbert, H., Skinner, K., Raumann, B. E., Basbaum, A. I., and Julius, D. 1998. The cloned capsaicin receptor integrates multiple pain-producing stimuli. *Neuron* 21:531–543.

Caterina, M. J., and Julius, D. 1999. Sense and specificity: A molecular identity for nociceptors. *Curr. Opin. Neurobiol.* 9:525–530.

Clapham, D. E. 2003. TRP channels as cellular sensors. *Nature* 426: 517–524.

Chapter 34

Where to Start

Nossal, G. J. V. 1993. Life, death, and the immune system. *Sci. Am.* 269(3):53–62.

Tonegawa, S. 1985. The molecules of the immune system. *Sci. Am.* 253(4):122–131.

Leder, P. 1982. The genetics of antibody diversity. *Sci. Am.* 246(5):102–115.

Bromley, S. K., Burack, W. R., Johnson, K. G., Somersalo, K., Sims, T. N., Sumen, C., Davis, M. M., Shaw, A. S., Allen, P. M., and Dustin, M. L. 2001. The immunological synapse. *Annu. Rev. Immunol.* 19:375–396.

Books

Owen, J. A., Punt, J., and Stranford, S. A. 2013. *Kuby Immunology* (7th ed.). W. H. Freeman and Company.

Abbas, A. K., Lichtman, A. H. H., and Pillai, S. 2014. *Cellular and Molecular Immunology* (8th ed.). Saunders.

Cold Spring Harbor Symposia on Quantitative Biology. 1989. Volume 54. *Immunological Recognition.* Cold Spring Harbor Laboratory Press.

Weir, D. M. (Ed.). 1996. *Handbook of Experimental Immunology* (5th ed.). Oxford University Press.

Murphy, K. 2011. *Janeway's Immunobiology* (8th ed.). Garland Science.

Innate Immune System

Janeway, C. A., Jr., and Medzhitov, R. 2002. Innate immune recognition. *Annu. Rev. Immunol.* 20:197–216.

Khalturin, K., Panzer, Z., Cooper, M. D., and Bosch, T. C. 2004. Recognition strategies in the innate immune system of ancestral chordates. *Mol. Immunol.* 41:1077–1087.

Beutler, B., and Rietschel, E. T. 2003. Innate immune sensing and its roots: The story of endotoxin. *Nat. Rev. Immunol.* 3:169–176.

Xu, Y., Tao, X., Shen, B., Horng, T., Medzhitov, R., Manley, J. L., and Tong, L. 2000. Structural basis for signal transduction by the Toll/interleukin-1 receptor domains. *Nature* 408:111–115.

Botos, I., Segal, D. M., and Davies, D. R. 2011. The structural biology of the Toll-like receptors. *Structure* 19:447–459.

Structure of Antibodies and Antibody-Antigen Complexes

Davies, D. R., Padlan, E. A., and Sheriff, S. 1990. Antibody-antigen complexes. *Annu. Rev. Biochem.* 59:439–473.

Poljak, R. J. 1991. Structure of antibodies and their complexes with antigens. *Mol. Immunol.* 28:1341–1345.

Davies, D. R., and Cohen, G. H. 1996. Interactions of protein antigens with antibodies. *Proc. Natl. Acad. Sci. U.S.A.* 93:7–12.

Marquart, M., Deisenhofer, J., Huber, R., and Palm, W. 1980. Crystallographic refinement and atomic models of the intact immunoglobulin molecule Kol and its antigen-binding fragment at 3.0 Å and 1.9 Å resolution. *J. Mol. Biol.* 141:369–391.

Silverton, E. W., Navia, M. A., and Davies, D. R. 1977. Three-dimensional structure of an intact human immunoglobulin. *Proc. Natl. Acad. Sci. U.S.A.* 74:5140–5144.

Padlan, E. A., Silverton, E. W., Sheriff, S., Cohen, G. H., Smith, G. S., and Davies, D. R. 1989. Structure of an antibody-antigen complex: Crystal structure of the HyHEL-10 Fab lysozyme complex. *Proc. Natl. Acad. Sci. U.S.A.* 86:5938–5942.

Rini, J., Schultze-Gahmen, U., and Wilson, I. A. 1992. Structural evidence for induced fit as a mechanism for antibody-antigen recognition. *Science* 255:959–965.

Fischmann, T. O., Bentley, G. A., Bhat, T. N., Boulot, G., Mariuzza, R. A., Phillips, S. E., Tello, D., and Poljak, R. J. 1991. Crystallographic refinement of the three-dimensional structure of the FabD1.3-lysozyme complex at 2.5-Å resolution. *J. Biol. Chem.* 266: 12915–12920.

Burton, D. R. 1990. Antibody: The flexible adaptor molecule. *Trends Biochem. Sci.* 15:64–69.

Saphire, E. O., Parren P. W., Pantophlet, R., Zwick, M. B., Morris, G. M., Rudd, P. M., Dwek, R. A., Stanfield, R. L., Burton, D. R., and Wilson, I. A. 2001. Crystal structure of a neutralizing human IgG against HIV-1: A template for vaccine design. *Science* 293:1155–1159.

Calarese, D. A., Scanlan, C. N., Zwick, M. B., Deechongkit, S., Mimura, Y., Kunert R., Zhu, P., Wormald, M. R., Stanfield, R. L., Roux, K. H., et al. 2003. Antibody domain exchange is an immunological solution to carbohydrate cluster recognition. *Science* 300:2065–2071.

Generation of Diversity

Tonegawa, S. 1988. Somatic generation of immune diversity. *Biosci. Rep.* 8:3–26.

Honjo, T., and Habu, S. 1985. Origin of immune diversity: Genetic variation and selection. *Annu. Rev. Biochem.* 54:803–830.

Gellert, M., and McBlane, J. F. 1995. Steps along the pathway of VDJ recombination. *Philos. Trans. R. Soc. Lond. B Biol. Sci.* 347:43–47.

Harris, R. S., Kong, Q., and Maizels, N. 1999. Somatic hypermutation and the three R's: Repair, replication and recombination. *Mutat. Res.* 436:157–178.

Lewis, S. M., and Wu, G. E. 1997. The origins of V(D)J recombination. *Cell* 88:159–162.

Ramsden, D. A., van Gent, D. C., and Gellert, M. 1997. Specificity in V(D)J recombination: New lessons from biochemistry and genetics. *Curr. Opin. Immunol.* 9:114–120.

Roth, D. B., and Craig, N. L. 1998. VDJ recombination: A transposase goes to work. *Cell* 94:411–414.

Sadofsky, M. J. 2001. The RAG proteins in V(D)J recombination: More than just a nuclease. *Nucleic Acids Res.* 29:1399–1409.

MHC Proteins and Antigen Processing

Bjorkman, P. J., and Parham, P. 1990. Structure, function, and diversity of class I major histocompatibility complex molecules. *Annu. Rev. Biochem.* 59:253–288.

Goldberg, A. L., and Rock, K. L. 1992. Proteolysis, proteasomes, and antigen presentation. *Nature* 357:375–379.

Madden, D. R., Gorga, J. C., Strominger, J. L., and Wiley, D. C. 1992. The three-dimensional structure of HLA-B27 at 2.1 Å resolution suggests a general mechanism for tight binding to MHC. *Cell* 70:1035–1048.

Fremont, D. H., Matsumura, M., Stura, E. A., Peterson, P. A., and Wilson, I. A. 1992. Crystal structures of two viral peptides in complex with murine MHC class I H-2Kb. *Science* 257: 880–881.

Matsumura, M., Fremont, D. H., Peterson, P. A., and Wilson, I. A. 1992. Emerging principles for the recognition of peptide antigens by MHC class I. *Science* 257:927–934.

Brown, J. H., Jardetzky, T. S., Gorga, J. C., Stern, L. J., Urban, R. G., Strominger, J. L., and Wiley, D. C. 1993. Three-dimensional structure of the human class II histocompatibility antigen HLA-DR1. *Nature* 364:33–39.

Saper, M. A., Bjorkman, P. J., and Wiley, D. C. 1991. Refined structure of the human histocompatibility antigen HLA-A2 at 2.6 Å resolution. *J. Mol. Biol.* 219:277–319.

Madden, D. R., Gorga, J. C., Strominger, J. L., and Wiley, D. C. 1991. The structure of HLA-B27 reveals nonamer self-peptides bound in an extended conformation. *Nature* 353:321–325.

Cresswell, P., Bangia, N., Dick, T., and Diedrich, G. 1999. The nature of the MHC class I peptide loading complex. *Immunol. Rev.* 172:21–28.

Madden, D. R., Garboczi, D. N., and Wiley, D. C. 1993. The antigenic identity of peptide-MHC complexes: A comparison of the conformations of five viral peptides presented by HLA-A2. *Cell* 75:693–708.

T-Cell Receptors and Signaling Complexes

Hennecke, J., and Wiley, D. C. 2001. T-cell receptor-MHC interactions up close. *Cell* 104:1–4.

Ding, Y. H., Smith, K. J., Garboczi, D. N., Utz, U., Biddison, W. E., and Wiley, D. C. 1998. Two human T cell receptors bind in a similar diagonal mode to the HLA-A2/Tax peptide complex using different TCR amino acids. *Immunity* 8:403–411.

Reinherz, E. L., Tan, K., Tang, L., Kern, P., Liu, J., Xiong, Y., Hussey, R. E., Smolyar, A., Hare, B., Zhang, R., et al. 1999. The crystal structure of a T-cell receptor in complex with peptide and MHC class II. *Science* 286:1913–1921.

Davis, M. M., and Bjorkman, P. J. 1988. T-cell antigen receptor genes and T-cell recognition. *Nature* 334:395–402.

Cochran, J. R., Cameron, T. O., and Stern, L. J. 2000. The relationship of MHC-peptide binding and T cell activation probed using chemically defined MHC class II oligomers. *Immunity* 12:241–250.

Garcia, K. C., Teyton, L., and Wilson, I. A. 1999. Structural basis of T cell recognition. *Annu. Rev. Immunol.* 17:369–397.

Garcia, K. C., Degano, M., Stanfield, R. L., Brunmark, A., Jackson, M. R., Peterson, P. A., Teyton, L. A., and Wilson, I. A. 1996. An αβ T-cell receptor structure at 2.5 Å and its orientation in the TCR-MHC complex. *Science* 274:209–219.

Garboczi, D. N., Ghosh, P., Utz, U., Fan, Q. R., Biddison, W. E., Wiley, D. C. 1996. Structure of the complex between human T-cell receptor, viral peptide and HLA-A2. *Nature* 384:134–141.

Gaul, B. S., Harrison, M. L., Geahlen, R. L., Burton, R. A., and Post, C. B. 2000. Substrate recognition by the Lyn protein-tyrosine kinase: NMR structure of the immunoreceptor tyrosine-based activation motif signaling region of the B cell antigen receptor. *J. Biol. Chem.* 275:16174–16182.

Kern, P. S., Teng, M. K., Smolyar, A., Liu, J. H., Liu, J., Hussey, R. E., Spoerl, R., Chang, H. C., Reinherz, E. L., and Wang, J. H. 1998. Structural basis of CD8 coreceptor function revealed by crystallographic analysis of a murine CD8 αβ ectodomain fragment in complex with H-2Kb. *Immunity* 9:519–530.

Konig, R., Fleury, S., and Germain, R. N. 1996. The structural basis of CD4-MHC class II interactions: Coreceptor contributions to T cell receptor antigen recognition and oligomerization-dependent signal transduction. *Curr. Top. Microbiol. Immunol.* 205:19–46.

Davis, M. M., Boniface, J. J., Reich, Z., Lyons, D., Hampl, J., Arden, B., and Chien, Y. 1998. Ligand recognition by αβ T-cell receptors. *Annu. Rev. Immunol.* 16:523–544.

Janeway, C. J. 1992. The T cell receptor as a multicomponent signalling machine: CD4/CD8 coreceptors and CD45 in T cell activation. *Annu. Rev. Immunol.* 10:645–674.

Podack, E. R., and Kupfer, A. 1991. T-cell effector functions: Mechanisms for delivery of cytotoxicity and help. *Annu. Rev. Cell Biol.* 7:479–504.

Davis, M. M. 1990. T cell receptor gene diversity and selection. *Annu. Rev. Biochem.* 59:475–496.

Leahy, D. J., Axel, R., and Hendrickson, W. A. 1992. Crystal structure of a soluble form of the human T cell coreceptor CD8 at 2.6 Å resolution. *Cell* 68:1145–1162.

Bots, M., and Medema, J. P. 2006. Granzymes at a glance. *J. Cell. Sci.* 119:5011–5014.

Lowin, B., Hahne, M., Mattmann, C., and Tschopp, J. 1994. Cytolytic T-cell cytotoxicity is mediated through perforin and Fas lytic pathways. *Nature* 370:650–652.

Rudolph, M. G., and Wilson, I. A. 2002. The specificity of TCR/pMHC interaction. *Curr. Opin. Immunol.* 14:52–65.

HIV and AIDS

Fauci, A. S. 1988. The human immunodeficiency virus: Infectivity and mechanisms of pathogenesis. *Science* 239:617–622.

Gallo, R. C., and Montagnier, L. 1988. AIDS in 1988. *Sci. Am.* 259(4): 41–48.

Kwong, P. D., Wyatt, R., Robinson, J., Sweet, R. W., Sodroski, J., and Hendrickson, W. A. 1998. Structure of an HIV gp120 envelope glycoprotein in complex with the CD4 receptor and a neutralizing human antibody. *Nature* 393:648–659.

Vaccines

Johnston, M. I. and Fauci, A. S. 2007. An HIV vaccine—evolving concepts. *New Engl. J. Med.* 356:2073–2081.

Burton, D. R., Desrosiers, R. C., Doms, R. W., Koff, W. C., Kwong, P. D., Moore, J. P., Nabel, G. J., Sodroski, J., Wilson, I. A., and Wyatt, R. T. 2004. HIV vaccine design and the neutralizing antibody problem. *Nature Immunol.* 5:233–236.

Ada, G. 2001. Vaccines and vaccination. *New Engl. J. Med.* 345: 1042–1053.

Behbehani, A. M. 1983. The smallpox story: Life and death of an old disease. *Microbiol. Rev.* 47:455–509.

Discovery of Major Concepts

Ada, G. L., and Nossal, G. 1987. The clonal selection theory. *Sci. Am.* 257(2):62–69.

Porter, R. R. 1973. Structural studies of immunoglobulins. *Science* 180:713–716.

Edelman, G. M. 1973. Antibody structure and molecular immunology. *Science* 180:830–840.

Kohler, G. 1986. Derivation and diversification of monoclonal antibodies. *Science* 233:1281–1286.

Milstein, C. 1986. From antibody structure to immunological diversification of immune response. *Science* 231:1261–1268.

Janeway, C. A., Jr. 1989. Approaching the asymptote? Evolution and revolution in immunology. *Cold Spring Harbor Symp. Quant. Biol.* 54:1–13.

Jerne, N. K. 1971. Somatic generation of immune recognition. *Eur. J. Immunol.* 1:1–9.

Chapter 35

Where to Start

Gennerich, A., and Vale, R. D. 2009. Walking the walk: How kinesin and dynein coordinate their steps. *Curr. Opin. Cell Biol.* 21:59–67.

Vale, R. D. 2003. The molecular motor toolbox for intracellular transport. *Cell* 112:467–480.

Vale, R. D., and Milligan, R. A. 2000. The way things move: Looking under the hood of molecular motor proteins. *Science* 288:88–95.

Vale, R. D. 1996. Switches, latches, and amplifiers: Common themes of G proteins and molecular motors. *J. Cell Biol.* 135:291–302.

Mehta, A. D., Rief, M., Spudich, J. A., Smith, D. A., and Simmons, R. M. 1999. Single-molecule biomechanics with optical methods. *Science* 283:1689–1695.

Schuster, S. C., and Khan, S. 1994. The bacterial flagellar motor. *Annu. Rev. Biophys. Biomol. Struct.* 23:509–539.

Books

Howard, J. 2001. *Mechanics of Motor Proteins and the Cytoskeleton.* Sinauer.

Squire, J. M. 1986. *Muscle Design, Diversity, and Disease.* Benjamin Cummings.

Pollack, G. H., and Sugi, H. (Eds.). 1984. *Contractile Mechanisms in Muscle.* Plenum.

Myosin and Actin

Lorenz, M., and Holmes, K. C. 2010. The actin-myosin interface. *Proc. Natl. Acad. Sci. U.S.A.* 107:12529–12534.

Yang, Y., Gourinath, S., Kovacs, M., Nyitray, L., Reutzel, R., Himmel, D. M., O'Neall-Hennessey, E., Reshetnikova, L., Szent-Györgyi, A. G., Brown, J. H., et al. 2007. Rigor-like structures from muscle myosins reveal key mechanical elements in the transduction pathways of this allosteric motor. *Structure* 15:553–564.

Himmel, D. M., Mui, S., O'Neall-Hennessey, E., Szent-Györgyi, A. G., and Cohen, C. 2009. The on-off switch in regulated myosins: Different triggers but related mechanisms. *J. Mol. Biol.* 394: 496–505.

Houdusse, A., Gaucher, J. F., Krementsova, E., Mui, S., Trybus, K. M., and Cohen, C. 2006. Crystal structure of apo-calmodulin bound to the first two IQ motifs of myosin V reveals essential recognition features. *Proc. Natl. Acad. Sci. U.S.A.* 103:19326–19331.

Li, X. E., Holmes, K. C., Lehman, W., Jung, H., and Fischer, S. 2010. The shape and flexibility of tropomyosin coiled coils: Implications for actin filament assembly and regulation. *J. Mol. Biol.* 395: 327–339.

Fischer, S., Windshugel, B., Horak, D., Holmes, K. C., and Smith, J. C. 2005. Structural mechanism of the recovery stroke in the myosin molecular motor. *Proc. Natl. Acad. Sci. U.S.A.* 102:6873–6878.

Holmes, K. C., Angert, I., Kull, F. J., Jahn, W., and Schroder, R. R. 2003. Electron cryo-microscopy shows how strong binding of myosin to actin releases nucleotide. *Nature* 425:423–427.

Holmes, K. C., Schroder, R. R., Sweeney, H. L., and Houdusse, A. 2004. The structure of the rigor complex and its implications for the power stroke. *Philos. Trans. R. Soc. Lond. B Biol. Sci.* 359: 1819–1828.

Purcell, T. J., Morris, C., Spudich, J. A., and Sweeney, H. L. 2002. Role of the lever arm in the processive stepping of myosin V. *Proc. Natl. Acad. Sci. U.S.A.* 99:14159–14164.

Purcell, T. J., Sweeney, H. L., and Spudich, J. A. 2005. A force-dependent state controls the coordination of processive myosin V. *Proc. Natl. Acad. Sci. U.S.A.* 102:13873–13878.

Holmes, K. C. 1997. The swinging lever-arm hypothesis of muscle contraction. *Curr. Biol.* 7:R112–R118.

Berg, J. S., Powell, B. C., and Cheney, R. E. 2001. A millennial myosin census. *Mol. Biol. Cell* 12:780–794.

Houdusse, A., Kalabokis, V. N., Himmel, D., Szent-Györgyi, A. G., and Cohen, C. 1999. Atomic structure of scallop myosin subfragment S1 complexed with MgADP: A novel conformation of the myosin head. *Cell* 97:459–470.

Houdusse, A., Szent-Györgyi, A. G., and Cohen, C. 2000. Three conformational states of scallop myosin S1. *Proc. Natl. Acad. Sci. U.S.A.* 97:11238–11243.

Uyeda, T. Q., Abramson, P. D., and Spudich, J. A. 1996. The neck region of the myosin motor domain acts as a lever arm to generate movement. *Proc. Natl. Acad. Sci. U.S.A.* 93:4459–4464.

Mehta, A. D., Rock, R. S., Rief, M., Spudich, J. A., Mooseker, M. S., and Cheney, R. E. 1999. Myosin-V is a processive actin-based motor. *Nature* 400:590–593.

Otterbein, L. R., Graceffa, P., and Dominguez, R. 2001. The crystal structure of uncomplexed actin in the ADP state. *Science* 293:708–711.

Holmes, K. C., Popp, D., Gebhard, W., and Kabsch, W. 1990. Atomic model of the actin filament. *Nature* 347:44–49.

Schutt, C. E., Myslik, J. C., Rozycki, M. D., Goonesekere, N. C., and Lindberg, U. 1993. The structure of crystalline profilin-β-actin. *Nature* 365:810–816.

van den Ent, F., Amos, L. A., and Lowe, J. 2001. Prokaryotic origin of the actin cytoskeleton. *Nature* 413:39–44.

Schutt, C. E., and Lindberg, U. 1998. Muscle contraction as a Markov process I: Energetics of the process. *Acta Physiol. Scand.* 163:307–323.

Rief, M., Rock, R. S., Mehta, A. D., Mooseker, M. S., Cheney, R. E., and Spudich, J. A. 2000. Myosin-V stepping kinetics: A molecular model for processivity. *Proc. Natl. Acad. Sci. U.S.A.* 97:9482–9486.

Friedman, T. B., Sellers, J. R., and Avraham, K. B. 1999. Unconventional myosins and the genetics of hearing loss. *Am. J. Med. Genet.* 89:147–157.

Kinesin, Dynein, and Microtubules

Cho, C. and Vale, R. D. 2012. The mechanism of dynein motility: Insight from crystal structures of the motor domain. *Biochim. Biophys. Acta* 1823:182–191.

Yildiz, A., Tomishige, M., Gennerich, A., and Vale, R. D. 2008. Intramolecular strain coordinates kinesin stepping behavior along microtubules. *Cell* 134:1030–1041.

Yildiz, A., Tomishige, M., Vale, R. D., and Selvin, P. R. 2004. Kinesin walks hand-over-hand. *Science* 303:676–678.

Rogers, G. C., Rogers, S. L., Schwimmer, T. A., Ems-McClung, S. C., Walczak, C. E., Vale, R. D., Scholey, J. M., and Sharp, D. J. 2004. Two mitotic kinesins cooperate to drive sister chromatid separation during anaphase. *Nature* 427:364–370.

Vale, R. D., and Fletterick, R. J. 1997. The design plan of kinesin motors. *Annu. Rev. Cell. Dev. Biol.* 13:745–777.

Kull, F. J., Sablin, E. P., Lau, R., Fletterick, R. J., and Vale, R. D. 1996. Crystal structure of the kinesin motor domain reveals a structural similarity to myosin. *Nature* 380:550–555.

Kikkawa, M., Sablin, E. P., Okada, Y., Yajima, H., Fletterick, R. J., and Hirokawa, N. 2001. Switch-based mechanism of kinesin motors. *Nature* 411:439–445.

Wade, R. H., and Kozielski, F. 2000. Structural links to kinesin directionality and movement. *Nat. Struct. Biol.* 7:456–460.

Yun, M., Zhang, X., Park, C. G., Park, H. W., and Endow, S. A. 2001. A structural pathway for activation of the kinesin motor ATPase. *EMBO J.* 20:2611–2618.

Kozielski, F., De Bonis, S., Burmeister, W. P., Cohen-Addad, C., and Wade, R. H. 1999. The crystal structure of the minus-end-directed microtubule motor protein ncd reveals variable dimer conformations. *Struct. Fold. Des.* 7:1407–1416.

Lowe, J., Li, H., Downing, K. H., and Nogales, E. 2001. Refined structure of αβ-tubulin at 3.5 Å resolution. *J. Mol. Biol.* 313:1045–1057.

Nogales, E., Downing, K. H., Amos, L. A., and Lowe, J. 1998. Tubulin and FtsZ form a distinct family of GTPases. *Nat. Struct. Biol.* 5:451–458.

Zhao, C., Takita, J., Tanaka, Y., Setou, M., Nakagawa, T., Takeda, S., Yang, H. W., Terada, S., Nakata, T., Takei, Y., et al. 2001. Charcot-Marie-Tooth disease type 2A caused by mutation in a microtubule motor KIF1Bb. *Cell* 105:587–597.

Asai, D. J., and Koonce, M. P. 2001. The dynein heavy chain: Structure, mechanics and evolution. *Trends Cell Biol.* 11:196–202.

Mocz, G., and Gibbons, I. R. 2001. Model for the motor component of dynein heavy chain based on homology to the AAA family of oligomeric ATPases. *Structure* 9:93–103.

Bacterial Motion and Chemotaxis

Baker, M. D., Wolanin, P. M., and Stock, J. B. 2006. Systems biology of bacterial chemotaxis. *Curr. Opin. Microbiol.* 9:187–192.

Wolanin, P. M., Baker, M. D., Francis, N. R., Thomas, D. R., DeRosier, D. J., and Stock, J. B. 2006. Self-assembly of receptor/signaling complexes in bacterial chemotaxis. *Proc. Natl. Acad. Sci. U.S.A.* 103:14313–14318.

Sowa, Y., Rowe, A. D., Leake, M. C., Yakushi, T., Homma, M., Ishijima, A., and Berry, R. M. 2005. Direct observation of steps in rotation of the bacterial flagellar motor. *Nature* 437:916–919.

Berg, H. C. 2000. Constraints on models for the flagellar rotary motor. *Philos. Trans. R. Soc. Lond. B Biol. Sci.* 355:491–501.

DeRosier, D. J. 1998. The turn of the screw: The bacterial flagellar motor. *Cell* 93:17–20.

Ryu, W. S., Berry, R. M., and Berg, H. C. 2000. Torque-generating units of the flagellar motor of *Escherichia coli* have a high duty ratio. *Nature* 403:444–447.

Lloyd, S. A., Whitby, F. G., Blair, D. F., and Hill, C. P. 1999. Structure of the C-terminal domain of FliG, a component of the rotor in the bacterial flagellar motor. *Nature* 400:472–475.

Purcell, E. M. 1977. Life at low Reynolds number. *Am. J. Physiol.* 45:3–11.

Macnab, R. M., and Parkinson, J. S. 1991. Genetic analysis of the bacterial flagellum. *Trends Genet.* 7:196–200.

Historical Aspects

Huxley, H. E. 1965. The mechanism of muscular contraction. *Sci. Am.* 213(6):18–27.

Summers, K. E., and Gibbons, I. R. 1971. ATP-induced sliding of tubules in trypsin-treated flagella of sea-urchin sperm. *Proc. Natl. Acad. Sci. U.S.A.* 68:3092–3096.

Macnab, R. M., and Koshland, D. E., Jr. 1972. The gradient-sensing mechanism in bacterial chemotaxis. *Proc. Natl. Acad. Sci. U.S.A.* 69:2509–2512.

Taylor, E. W. 2001. 1999 E. B. Wilson lecture: The cell as molecular machine. *Mol. Biol. Cell* 12:251–254.

Chapter 36

Where to Start

Gilman, A. G. 2012. Silver spoons and other personal reflections. *Annu. Rev. Pharmacol. Toxicol.* 52:1–19.

Zhang, H.-Y., Chen, L.-L., Xue-Juan Li, X.-J. and Zhang, J. 2010. Evolutionary inspirations for drug discovery. *Trends Pharmacol. Sci.* 31:443–448.

Books

Kenakin, T. P. 2014. *A Pharmacology Primer: Techniques for More Effective and Strategic Drug Discovery* (4th ed.). Academic Press.

Brunton, L., Chabner, B., and Knollman, B. 2011. *Goodman and Gilman's The Pharmacological Basis of Therapeutics* (12th ed.). McGraw-Hill Professional.

Walsh, C. T., and Schwartz-Bloom, R. D. 2004. *Levine's Pharmacology: Drug Actions and Reactions* (7th ed.). Taylor and Francis Group.

Silverman, R. B., and Holladay, M. W. 2014. *Organic Chemistry of Drug Design and Drug Action* (3d ed.). Academic Press.

Walsh, C. 2003. *Antibiotics: Actions, Origins, Resistance.* ASM Press.

ADME and Toxicity

Caldwell, J., Gardner, I., and Swales, N. 1995. An introduction to drug disposition: The basic principles of absorption, distribution, metabolism, and excretion. *Toxicol. Pathol.* 23:102–114.

Lee, W., and Kim, R. B. 2004. Transporters and renal drug elimination. *Annu. Rev. Pharmacol. Toxicol.* 44:137–166.

Lin, J., Sahakian, D. C., de Morais, S. M., Xu, J. J., Polzer, R. J., and Winter, S. M. 2003. The role of absorption, distribution, metabolism, excretion and toxicity in drug discovery. *Curr. Top. Med. Chem.* 3:1125–1154.

Poggesi, I. 2004. Predicting human pharmacokinetics from preclinical data. *Curr. Opin. Drug Discov. Devel.* 7:100–111.

Case Histories

Flower, R. J. 2003. The development of COX2 inhibitors. *Nat. Rev. Drug Discov.* 2:179–191.

Tobert, J. A. 2003. Lovastatin and beyond: The history of the HMG-CoA reductase inhibitors. *Nat. Rev. Drug Discov.* 2:517–526.

Vacca, J. P., Dorsey, B. D., Schleif, W. A., Levin, R. B., McDaniel, S. L., Darke, P. L., Zugay, J., Quintero, J. C., Blahy, O. M., Roth, E., et al. 1994. L-735,524: An orally bioavailable human immunodeficiency virus type 1 protease inhibitor. *Proc. Natl. Acad. Sci. U.S.A.* 91:4096–4100.

Wong, S., and Witte, O. N. 2004. The BCR-ABL story: Bench to bedside and back. *Annu. Rev. Immunol.* 22:247–306.

Structure-Based Drug Design

Kuntz, I. D. 1992. Structure-based strategies for drug design and discovery. *Science* 257:1078–1082.

Dorsey, B. D., Levin, R. B., McDaniel, S. L., Vacca, J. P., Guare, J. P., Darke, P. L., Zugay, J. A., Emini, E. A., Schleif, W. A., Quintero, J. C., et al. 1994. L-735,524: The design of a potent and orally bioavailable HIV protease inhibitor. *J. Med. Chem.* 37:3443–3451.

Chen, Z., Li, Y., Chen, E., Hall, D. L., Darke, P. L., Culberson, C., Shafer, J. A., and Kuo, L. C. 1994. Crystal structure at 1.9-Å resolution of human immunodeficiency virus (HIV) II protease complexed with L-735,524, an orally bioavailable inhibitor of the HIV proteases. *J. Biol. Chem.* 269:26344–26348.

Combinatorial Chemistry

Baldwin, J. J. 1996. Design, synthesis and use of binary encoded synthetic chemical libraries. *Mol. Divers.* 2:81–88.

Burke, M. D., Berger, E. M., and Schreiber, S. L. 2003. Generating diverse skeletons of small molecules combinatorially. *Science* 302:613–618.

Edwards, P. J., and Morrell, A. I. 2002. Solid-phase compound library synthesis in drug design and development. *Curr. Opin. Drug Discov. Devel.* 5:594–605.

Genomics

Zambrowicz, B. P., and Sands, A. T. 2003. Knockouts model the 100 best-selling drugs: Will they model the next 100? *Nat. Rev. Drug Discov.* 2:38–51.

Salemme, F. R. 2003. Chemical genomics as an emerging paradigm for postgenomic drug discovery. *Pharmacogenomics* 4:257–267.

Michelson, S., and Joho, K. 2000. Drug discovery, drug development and the emerging world of pharmacogenomics: Prospecting for information in a data-rich landscape. *Curr. Opin. Mol. Ther.* 2:651–654.

Weinshilboum, R., and Wang, L. 2004. Pharmacogenomics: Bench to bedside. *Nat. Rev. Drug Discov.* 3:739–748.

INDEX

Note: Page numbers followed by f, t, and b refer to figures, tables, and boxed material.
Boldface page numbers indicate structural formulas and ribbon diagrams.

A band, 1020f
A site, ribosomal, 905, 905f
AAA ATPases
  in amino acid degradation, 685
  in dynein, 1012, 1014
ABC transporters
  ATP hydrolysis reaction and, 376
  defined, 367, 374
  domain arrangement of, 374, 374f
  in drug resistance, 1054
  eukaryotic, 376
  mechanism, 375, 375f
  structure of, **375**
ABCA1 (ATP-binding cassette transporter, subfamily A1), 787
ABO blood groups, 331–332, 331f
Abortive complex, 688
Absorption
  of dietary proteins, 682, 683f
  drug, 1036–1037, 1037f
  light, 569, 569f, 971–972
Abzymes, production of, 241
Acceptor control. *See* Respiratory control
Accessory pigments, in photosynthesis, 581–584, 582f, 583f
Acetaminophen, 1040–1041, 1040f
Acetoacetate. *See also* Ketone bodies
  conversion into acetyl CoA, 658–659
  from phenylalanine, 704
  in respiration, 658
  from tryptophan, 704
  utilization as fuel, 659, 659f
Acetoacetyl CoA, 698–699
Acetyl ACP, 663
Acetyl carnitine, 649–650
Acetyl CoA (acetyl coenzyme A)
  acetoacetate conversion into, 658–659
  acetyl-group-transfer potential, **437**
  in amino acid degradation, 698–699, 701–703
  biotin and, 480
  in citric acid cycle, 495, 498–500, 501–503, 503f, 515
  defined, 437
  in fatty acid metabolism, 648–649
  in fatty acid oxidation, 650–652
  in fatty acid synthesis, 512
  formation from ketone bodies, 657–658, 658f
  formation of, 464, 499
  in glyoxylate cycle, 516–517, 517f
  pyruvate dehydrogenase complex and, 499
  structure of, 437, **437**
  synthesis of, 498–500
  transfer to cytoplasm, 666–667, 666f
Acetyl CoA carboxylase
  in citrate concentration, 671, 672f
  in fatty acid metabolism, 662, 662t, 670–671
  filaments of, 671f
  regulation by hormones, 671–672
  regulation of, 671, 671f
Acetyl CoA synthetase, 649
Acetyl groups, 57
Acetyl transacylase, 663, 663t
Acetylation
  defined, 294t
  in gene regulation, 952–953, 954
  in metabolism regulation, 294
  protein, 293–294
Acetylcholine, 385, 386
Acetylcholine receptor
  defined, 385
  as ligand-gated channel, 386
  as nonspecific cation channel, 388
  opening, 387, 387f
  structure of, 386, 386f
N-acetylglucosamine phosphotransferase, 332
N-acetylglutamate, 694
N-acetylglutamate synthase, 694
Acetyllysine-binding domain, 953, 953f
N-acetylneuraminate, 772
N-acetyl-L-phenylalanine *p*-nitrophenyl ester, 254, 255f
Acid-base reactions
  in biological processes, 13–14
  defined, 13
  double helix and, 14–15
  hydrogen ions in, 13
Acids. *See also* Amino acids; Fatty acids; Nucleic acids
  bile, 646, 646f
  protonation/deprotonation of, 15–16
  sialic, 772
Aconitase, 504, 504f, 955, 956f
Acquired immune deficiency syndrome (AIDS). *See* Human immunodeficiency virus (HIV) infection
Actin/actin filaments
  barbed, 1017
  decorated, 1018
  defined, 1016
  F, 1017
  formation of, 1017–1018
  G, 1017
  in muscle contraction, 1019–1021
  myosin and, 1018–1022, 1020f
  pointed, 1017
  polymerization of, 1018
  structure of, 179, **179,** 1016–1017, 1017f
  in thin filaments, 1020
Actinomycin, 869, 870f
Action potentials
  defined, 378
  integration, 387–388
  ion channels and, 378, 378f
  mechanism, 388, 388f
Activated carriers
  as derived from vitamins, 438–440
  of electrons, for fuel oxidation, 435–436
  of electrons, for reductive biosynthesis, 436
  in metabolism, 435–440, 437t
  recurring set of, 437–438
  of two-carbon fragments, 437–438
Activated glycoaldehyde unit, 606
Activated methyl cycle, 725, 725f
Activation domains, 945, 946
Activation energy
  defined, 221
  enzyme decrease of, 221, 221f, 222
  symbol, 221
Active membrane transport, 367, 369
Active sites
  ATCase, 289, 289f, **289**
  chymotrypsin, 255–256, 256f
  concentration of, 230
  as crevice, 223
  defined, 216
  enzyme and substrate interaction, 223
  evolution of, 252
  as microenvironments, 224
  myosin, 279, 279f
  proteases, 261f
  residues, 223, 223f
  RNA polymerase, 861
  volume of enzyme, 223–224
Acute intermittent porphyria, 738
Acyclovir monophosphate, 748
Acyl carrier protein (ACP), 661–662, 662f, **662,** 664–665, 665f
Acyl CoA:cholesterol acyltransferase (ACAT), 784
Acyl intermediates, 239, 240f
Acyl-enzyme intermediates, 255, 255f, 686
Adaptive immune system, 984–985
Adaptor proteins, 410
Adenine, **4,** 5f, 110, **110**
  deamination of, 846, 846f
  methylation of, 274–275, 275f
  resonance structures, 7
Adenine phosphoribosyltransferase, 752
Adenosine, 107
Adenosine 5′-triphosphate. *See* ATP
Adenosine deaminase, 164, 760–761
Adenosine diphosphate. *See* ADP
Adenosine triphosphate. *See* ATP
S-adenosylhomocysteine, 725, **725**
S-adenosylmethionine (SAM)
  in activated methyl cycle, 725, 725f
  in adenylation of methionine, 701

- S-adenosylmethionine (SAM)—(*continued*)
  - in amino acid degradation, 701, **702**
  - in amino acid synthesis, 724–726
  - as ethylene precursor, 726
  - in phospholipid synthesis, 771
- Adenylate, 108, 751
- Adenylate cyclase, 402–403, 402f
- Adenylate kinase, **280**
- Adenylated intermediates, 721
- Adenylation
  - in amino acid activation, 898–899
  - in amino acid synthesis, 732–733, 733f
  - in translation, 899–902
- Adenylosuccinate synthetase, 751
- Adenylyl transferase, 733, 733f
- Adipokines, 805
- Adiponectin, 806
- Adipose cells (fat cells), 645
- Adipose tissue
  - brown, 555, 555f
  - fat in, 815
  - glucose entry into, 816
  - glycerol released from, 817
  - triacylglycerols in, 818
  - white, 555
- Adipose triglyceride lipase (ATGL), 647–648, 647f
- ADME properties, of drugs, 1036–1040, 1037f
- ADP (adenosine diphosphate), **275**
  - ATP hydrolyzed to, 426
  - in citric acid cycle, 406f, 506
  - formation of, 275
  - in kinesin movement, 1025, 1025f
  - in oxidative phosphorylation, 550–551, 551f, 553–554, 554f
  - in random sequential reaction, 232
  - structure of, 426, **427**
- Adrenocorticotropic hormone, 59
- Aerobic glycolysis, 474–476, 510
- Affinity chromatography, 70–71, 70f
- Affinity maturation, 993
- Affinity tags, 78, 237–238, 237f, 238f
- Aflatoxin activation, 846f
- A-form DNA, 111–112, 111f, 112f, 112t
- Aggrecan, 328
- α-glucosidase, 450
- Agonists, 951
- Agouti-related peptide (AgRP), 805–806, 806f
- Agre, Peter, 1
- *Agrobacterium tumefaciens*, 163, 163f
- Alanine
  - defined, 30
  - formation of, 720–721
  - in gluconeogenesis, 486
  - in muscle contraction, 486, 486f
  - structure of, 31f
  - tryptophan in, 700
- Alanine aminotransferase, 688
- Alanyl-tRNA, 895, 895f
- Albinism, 705t
- Albumin, 137f, 1037
- Alcaptonuria, 705
- Alcohol dehydrogenase, 820
- Alcoholic fermentation, 449, 463, 463f
- Alcoholic scurvy, 821
- Alcohols
  - fermentation of, 462–464, 463f
  - formation from pyruvate, 462–464, 463f
  - metabolism of, 819–822
  - monosaccharides and, 322
  - toxicity of, 821–822
- Aldehyde dehydrogenase, 228
- Aldehydes, oxidation of energy, 457–458
- Alder, Julius, 1026
- Aldimine, 690
- Aldolase, 455
  - in Calvin cycle, 595
  - in transaldolase reaction, 606–607
- Aldoses
  - conversion to ketoses, 454
  - defined, 316
- Aldosterone, 789, 792, **793**
- Allolactose, 930
- Allopurinol, 761
- Allosteric constant, 290
- Allosteric control, 285
- Allosteric effector, 200–201
- Allosteric enzymes, 233, 233f
  - allosteric constant, 290
  - concerted model, 290
  - control of, 443
  - homotropic effects on, 290
  - sequential model, 290–291
  - sigmoidal kinetics, 287, 287f
  - substrate concentration and, 291
  - threshold effects, 291, 291f
  - T-to-R equilibrium in, 291–292, 291f, 292f
  - T-to-R state transition, 290–291, 290f
- Allosteric sites, 287
- Alloxanthine, 761
- α helix
  - of membrane proteins, 355–356, 355f, 355t
  - pitch of, 40
  - as right-handed, 41
  - schematic view of, 41f
  - screw sense, 40–41, 40f
  - structure of, 41f, **41**
- α-stabilizing protein (AHSP), 207–208, 207f
- α_1-antiproteinase, 303
- α-amino acids, 29, 35
- α-helical coiled coil, 44
- α-hemoglobin, 207, 207f
  - alignment with gap insertion, 173f
  - amino acid sequences, 171–172, 171f, 172f
- α-thalassemia, 207
- Alternative splicing, 128, 129f, 877
  - defects in, 885t
  - defined, 885
  - example of, 885f
  - pre-mRNA, 885–886
- Altman, Sidney, 859, 870
- Alu sequences, 154
- Alzheimer's disease, 56–57
- *Amanita phalloides*, 873, 873f
- α-amanitin, 872–873
- Ames test, 852, 852f
- Amide bonds. *See* Peptide bonds
- Amiloride-sensitive sodium channel, 969, 969f, 977
- Amines, monosaccharides and, 322
- Amino acid degradation, 681–708
  - acetoacetyl CoA in, 698–699
  - acetyl CoA in, 698–699, 701–703
  - amino acid use through, 681
  - aminotransferases in, 688–691
  - of aromatic amino acids, 703–705
  - of branched-chain amino acids, 687–689, 701–703
  - coenzymes in, 682
  - deamination in, 692
  - digestive enzymes in, 682
  - fumarate in, 698
  - glucose-alanine cycle in, 692–693, 693f
  - glutamate dehydrogenase in, 688–689
  - α-ketobutyrate in, 701
  - α-ketoglutarate in, 698, 700–701, 700f
  - liver in, 687, 692–693
  - metabolism errors and, 705–706, 705t
  - nitrogen removal in, 687–693
  - overview of, 681–682
  - oxaloacetate in, 698, 700
  - oxygenases in, 703–705
  - propionyl CoA in, 701–702
  - proteasomes in, 681, 685–686, 686f
  - in protein turnover, 683–687
  - pyridoxal phosphate (PLP) in, 682, 691–692
  - pyruvate in, 692–693, 698, 699–700, 699f
  - regulation function of, 683–687, 687t
  - Schiff-base intermediates in, 689–690
  - serine dehydratase in, 692
  - succinyl CoA in, 698, 701, 701f
  - threonine dehydratase in, 692
  - transaminases in, 688–691
  - ubiquitin in, 683–685, 684f
  - ubiquitination in, 684–686
  - urea cycle in, 693–698
- Amino acid sequences
  - alignment of, 171–177, 172f, 173f
  - collagen, 45, 45f
  - comparison of, 90
  - determination of, 65, 66
  - directionality of, 35–36, 36f
  - in DNA probe creation, 91
  - DNA sequences and, 90f
  - evolution of, 37
  - gap insertion, 172–173, 173f
  - of hemoglobin, 171–172, 171f, 172f
  - homologous, 177
  - identities, 172
  - importance of, 37
  - information provided by, 90–91
  - of insulin, 37f
  - of myoglobin, 171–172, 171f, 172f
  - porin, 352, 352f

  probes generated from, 147, 147f
  in protein identification, 90–91
  in protein structure determination, 49–59
  protein structures and, 37, 37f
  recombinant DNA technology and, 89–90
  ribonuclease, 49f
  searching for internal repeats, 91, 91f
  shuffled, 173–174, 173f
  as signals, 91
  statistical comparison of alignment, 173, 173f
  substitution in, 174–177, 175f, 176f
  transmembrane helices from, 354–356, 355f
Amino acid side chains
  aliphatic, 32
  aromatic, 32
  charge of, 33–35, 33f, 34f
  covalent modifications, 57f
  defined, 29
  distribution of, 46
  hydrocarbon, 32
  hydrophilic, 33
  hydrophobic, 32
  hydroxyl-containing, 32, 32f
  ionizable, 33–34, 34t
  sulfydryl-containing, 33, 33f
  thiol-containing, 33, 33f
  types of, 30
Amino acid synthesis, 713–739
  S-adenosylmethionine in, 724–726
  adenylation in, 732–733, 733f
  ammonia in, 714–718
  aromatic amino acids, 727–729
  branched pathways in, 731–732
  chorismate in, 727–729, 727f
  enzyme multiplicity in, 732, 732f
  essential amino acids, 719–720, 720f
  feedback inhibition/activation in, 731–732
  glutamine synthetase in, 732–733, 733f
  human, 719–720
  α-ketoglutarate in, 717–718, 720
  nitrogen fixation in, 714–718, 715f
  nonessential amino acids, 719, 720f
  overview of, 713–714
  regulation of, 730–733
  regulatory domains in, 731–732, 732f
  shikimate in, 727–729
  tetrahydrofolate in, 723–724, 723f, 723t, **724**
  threonine deaminase in, 731–732, 731f
  by transamination, 720–721, 720f
Amino acids. *See also* Proteins
  abbreviations for, 34–35, 34t
  acetyl groups, 57
  activation by adenylation, 898–899
  activation sites, 899–900, 900f
  aromatic, 32, 703–705, 727–729
  basic set of, 719t
  branched-chain, 687–689, 701–703
  carbon skeletons of, fates of, 699f
  chirality of, 29, 721, 721f
  code words, 125
  D isomer, 29, 29f
  defined, 21
  dipolar form of, 29–30, 30f
  encoding of, 124–127
  essential, 682, 682t, 719, 720f
  excess, 681
  genetic code, 125, 125t
  glucogenic, 698–703
  in gluconeogenesis, 476
  hydrophilic, 33, 47
  hydrophobic, 30–32, 31f
  hydroxyl groups of, 32–33, 57
  ionization state of, 29–30, 30f
  L isomer, 29, 29f
  metabolism, 705–706, 705t
  negatively charged, 33–34, 34f
  nitrogen in, 714
  nonessential, 719, 720f
  peptide bonds, 35–36, 35f
  polar, 32–33, 32f
  positively charged, 33, 33f
  as precursors, 734–738
  pyruvate formation from, 699, 699f
  reactive, 33
  residue, 35, 47
  in secondary structures, 51t
  tRNA attachment, 123, 123f
  undesirable reactivity in, 35f
Amino-acid signal sequences, 916–918, 916f
Aminoacrylate, Schiff bases of, 729, **729**
Aminoacyl adenylate, 898
Aminoacyl-AMP, 899
Aminoacyl-tRNA, 123, 124f, 896–897, 897f
  defined, 898
  editing of, 900–901, 900f
  elongation factors and, 907–908, 907f
Aminoacyl-tRNA synthetases
  accuracy of, 901
  activation sites of, 899–900, 900f
  amino acid activation sites, 899–900
  classes of, 901–902, 902f
  defined, 894, 898
  double sieve in, 901
  editing sites, 900–901, 900f
  evolution of, 902
  genetic code and, 898–902
  proofreading by, 900–901
  subunit structure, 902, 902t
Aminoglycoside antibiotics, 914
δ-aminolevulinate, 736
δ-aminolevulinate synthase, 736
Aminopeptidase N, 682
Aminopterin, 757
Aminotransferases
  in amino acid degradation, 688–691
  blood levels of, 691
  defined, 688
  Schiff-base intermediates formation in, 689–690
Ammonia
  in amino acid degradation, 687–689
  in amino acid synthesis, 714–718
  conversion to urea, 693–698
  formation of, 687–689
  in glutamate synthesis, 717–718
  in glutamine synthesis, 717–718
  in pyrimidine synthesis, 745
  transport of, 692–693
Ammoniotelic organisms, 698
AMP (adenosine monophosphate)
  ATP hydrolyzed to, 426
  energy charge and, 482
  in purine synthesis, 751–752, 751f
  structure of, 426, **427**
  synthesis of, 758–759, 758f
AMP-activated protein kinase (AMPK), 671, 806, 812
Amphibolic pathways, 425
Amycolatopsis, 869
α-amylase, 324, 450
Amyloid fibers, 56–57, 56f
Amyloid plaques, 56f
Amyloid precursor protein (APP), 57
Amyloidoses, 56–57
Amylopectin, 324
Amyotrophic lateral sclerosis (ALS), 136
Amytal, 556
Anabolic steroids, 951
Anabolism, 424, 714b
Analytes, 85
Anastrozole, 793
Anchor residues, 997–998, 997f
Anderson disease, 637t
Androgens
  functions of, 789
  pathways for formation of, 794f
  synthesis of, 792–793, **794**
Androstenedione, 789, 793, **794**
Anemia, 17–18, 205–206, 207
Anfinsen, Christian, 49
Angelman syndrome, 685
Angiogenin, sequence comparison of, **170**
Animal models, in drug target testing, 1049
Animal testing, in drug development, 1044
Ankyrin repeats, 976–977, 976f
Anomers, 317f, 319
Anosmias, 962
Antagonists, 952
Anthranilate, 728
Anthrax, 839
Antibiotics
  aminoglycoside, 914
  protein synthesis inhibition by, 913–915, 914t
  transcription inhibition by, 869–870, 869f
  translocation inhibition by, 914–915, 915f
Antibodies. *See also* Immunoglobulins
  amino acid sequence data in making, 91
  antibody binding of, 989–990, 989f
  antigen interaction, 80f
  antigen-binding specificity, 995
  class switching in, 994–995, 995f
  constant region of, 988, 988f
  defined, 79, 984
  diversity of, 992–993

Antibodies. *See also* Immunoglobulins—(*continued*)
  formation of, 994–995
  hypervariable loops of, 988–990, 988f
  monoclonal, 80–82, 80f, 81f
  number of, 992
  oligomerization of, 993–994
  polyclonal, 80, 80f
  primary, 83–84
  recombination in, 991–995, 991f, 992f
  secondary, 84
  structures of, 79f, 985–986
  variable region of, 988, 988f, 989f
Antibody-protein interactions, 990, 990f
Anticancer drugs
  in blocking thymidylate synthesis, 757–758
  targets, 757f
Anticoagulants, 307
Anticodon loop, 896
Anticodons
  base/base pair, 898, 898f
  defined, 123
  in translation, 896, 898, 898f, 901
Antidiuretic hormone, 92–93, 93f
Antigenic determinants, 79
Antigens
  ABO blood group, 331–332, 331f
  antibody interaction, 80f
  cross-linking of, 986, 986f
  defined, 79
  synthetic peptides as, 92
Antihemophilic factor, 308
Antiporters, 376, 376f
Antiserum, 80
Antithrombin III, 307–308
AP endonuclease, 849
Apolipoprotein B (apo B), 879, 879f
Apolipoproteins, 646
Apoptosis
  defined, 299, 557
  mitochondria in, 557–558
Apoptosome, 558
Apoptotic peptidase-activating factor 1 (APAF-1), 558
Approximation, catalysis by, 252
Aptamers, 187
Aquaporins, 391, 391f
Arabidopsis thaliana, 154
Arachidonate, 669, 669f
Archaea, 3, 3f
  membranes of, 346–347, 346f
  proteasomes of, 687, 687f
Arginase, 695
Arginine
  argininosuccinase and, 695
  degradation, 701, 701f
  structure of, 33, 33f
  synthesis of, 722, 722f
Argininosuccinase, 695
Argininosuccinase deficiency, 697, 697f
Argininosuccinate, 695, 696
Argininosuccinate synthetase, 695
Argonaute complex, 956, 956f
Aromatase, 793
Aromatase inhibitors, 793
Aromatic amino acids
  degradation of, 703–705
  side chains, 32
  synthesis of, 727–729
Arrestin, 972
Arsenite poisoning, 516, 516f
Artificial photosynthetic systems, 585
Ascorbic acid (vitamin C)
  deficiency of, alcohol related, 821–822
  forms of, 822, 822f
  function of, 439, 439t
Asparaginase, 700
Asparagine
  conversion into oxaloacetate, 700
  structure of, 32f, 33
  synthesis of, 721, 721f
Aspartate
  conversion into oxaloacetate, 700
  formation of, 720–721
  structure of, 33, 34f, **233**
  synthesis of, 721, 721f
Aspartate aminotransferase, 688, 690–691
Aspartate transcarbamoylase. *See* ATCase
Aspartic acid, 33
Aspartokinases, 732, 732f
Aspartyl proteases, 261f, **261,** 262, 262f
Aspirin
  discovery and development of, 1043–1044
  effect on prostaglandin H_2 synthase-1, 354f
  as prostaglandin inhibitor, 669
Assays
  defined, 67
  enzyme-linked immunosorbent (ELISA), 82–83, 83f
  in protein purification, 67
ATCase (aspartate transcarbamoylase)
  active site of, 289, 289f, **289**
  allosteric interactions in, 288–291
  catalytic subunit, 287–288, 288f
  concerted model, 290
  cooperativity, 290
  defined, 285
  feedback inhibition, 287
  inhibition by CTP, 758
  reaction, 286, 286f
  regulatory subunit, 287–288, 288f
  separable subunits, 287–288
  sigmoidal curve, 291, 291f
  sigmoidal kinetics, 287, 287f
  structure of, 288–289, 289f
  T-to-R transition, 290–291, 290f
  ultracentrifugation studies of, 287, 288f
Atherosclerosis, 661, 784–785, 787–788
Atomic motion, 971, 972f
Atorvastatin, 1044, **1044**
ATP (adenosine triphosphate), 108, **108,** **275,** 295t
  as activated carrier, 435
  binding of, 186–187, 186f, 187f
  binding to molecular motors, 1014–1016, 1015f, 1016f
  in Calvin cycle, 597
  catabolism generation, 432
  in catabolism stages, 434–435, 434f
  as cellular energy currency, 297, 744
  in citric acid cycle, 496–497, 508–510, 513, 514
  defined, 424, 426
  effect on ATCase kinetics, 292, 292f
  electrostatic repulsion, 429
  as energy-coupling agent, 428
  as energy-rich molecule, 426
  entropy increase in, 430
  in exercise, 431, 431f, 476, 813–815, 814t
  formation of, 424
  generation by NADH, 436
  hydration stabilization in, 430
  hydrolysis of, 252
  as immediate donor of free energy, 432
  in insulin release, 810, 811f
  ion gradients in, 433–434, 433f
  in mitochondria, 550–551, 551f
  in muscle, 813
  in muscle contraction, 469–470
  in nitrogen fixation, 715–718
  phosphoryl-transfer potential, 429, 430–431, 430f
  in random sequential reaction, 232
  resonance structures, 429, 429f
  structure of, 426, **427**
  synthesis, 432–433
ATP formation
  1,3-bisphosphoglycerate (1,3-BPG) and, 459–460
  citric acid cycle and, 508
  by cyclic photophosphorylation, 580, 580f, 581
  enzyme-bound, 544
  fermentation in, 462
  from glucose to pyruvate conversion, 461–462
  from glycolysis, 459–462
  from phosphoryl transfer, 459–460
  proton-motive force and, 544–545, 545f
  pyruvate in, 460–462
ATP hydrolysis
  ABC transporters and, 376
  ATP as base to promote, 277, 277f
  in DNA replication, 832–833, 833f
  in DNA supercoiling, 837–839, 838f
  in driving metabolism, 427–429
  enzyme use of, 276
  as exergonic, 426–427
  free energy from, 426–431
  γ subunit in, 546
  hydrolysis, 276
  in kinesin motion, 1024–1026, 1025f
  magnesium ions in, 276–277
  myosin and, 276–278
  myosin conformational changes, 278, 278f
  power stroke in, 1019
  reversible, within myosin active site, 279
  rotational motion, 546

  in transcription, 868, 868f
  transition state formation for, 277–278
ATP synthase
  a subunit of, **543,** 544, 546–547, 546f, 578
  α subunit of, 543, **543**
  ATP-driven rotation in, 545–546, 546f
  b subunit of, **543,** 544, 578
  β subunit of, 543, **543,** 545, 546, 578
  bind-change mechanism for, 544–546, 545f
  c ring of, 545, 546–548
  of chloroplasts, 578–580
  defined, 542
  δ subunit of, **543,** 544
  discovery, 542, 542b
  efficiency of, 548, 548b
  ε subunit of, 580
  F_0 subunit of, 543, **543,** 544
  F_1 subunit of, 543, **543,** 544, 545
  G proteins and, 548–549
  γ subunit of, 543, **543,** 545, 548, 1027
  γε stalk, 544, 545
  inhibition of, 556
  nucleotide-binding sites, 545, 545f
  proton flow through, 542, 544–546
  proton motion across membrane in, 547, 547f
  proton path through membrane in, 547, 547f
  proton-conducting unit, 546–547, 546f
  regulation of, 554
  rotational catalysis in, 546, 546f
ATP synthasome, 552
ATP synthesis
  in chloroplasts, 578–580
  efficiency of, 544
  as endergonic process, 542
  mechanism, 544, 544f
  oxidative phosphorylation uncoupling from, 554–556, 555f
  proton flow around **c** ring in, 546–548
  proton gradients in, 541–549
  uncoupling electron transport from, 556–557
ATP yield, 552–553, 553t
ATP-ADP cycle, 427, 432, 432f
ATP-ADP translocase, 550–551, 551f, 557
ATPases
  AAA, 685, 1012, 1014
  domains of myosin, 276, 276f, 277, 277f
  mitochondrial. *See* ATP synthase
  Na^+-K^+, 370, 373
  P-type, 367, 370–373, 374
  SERCA, 370, 371–373, 372f, **372**
ATP-binding cassettes (ABCs). *See also* ABC transporters
  ATP binding with, 375, 375f
  defined, 374
  distance between, 375
ATP-citrate lyase, 666
ATP-grasp fold, 745
Atractyloside, 557
Atrazine, 584, **584**
Attenuation, 935–937, 936f
Autoimmune diseases, 1005, 1005f
Autoinducers, 934, 934f
Autotrophs, 566, 590
Axel, Richard, 963
Axial bonds, 320–321, 321f
Axoneme, 1023
Azothioprine, 1051, **1051**

B cells
  activation of, 993–994, 993f
  defined, 984
  memory, 1006
B vitamins. *See* Vitamins
β_2-microglobulin, 996–997
Bacillus amyloliquefaciens, 259
Bacillus anthracis, 839
Bacillus subtilis, 867
Backbone models, 61–62, 62f
Backbones
  in nucleic acids, 106–107, 106f
  in polypeptide chains, 36, 36f
Bacteria, 3, 3f. *See also Escherichia coli* (*E. coli*)
  carcinogen action on, 852, 852f
  cell membranes of, 359, 359f
  defined, 3
  flagella movement of, 1026–1029
  gene expression in, 925–938
  glyoxylate cycle in, 516–517, 517f
  nitrogen fixation in, 714–718
  photosynthetic, 584, 585t
  rapid growth, 128
  restriction enzymes in, 137
  transcription factors in, 945
  transcription in, 861–871
  translation in, 906
  upstream promoter elements in, 864
Bacterial artificial chromosomes (BACs), 147
Bacterial reaction center
  cyclic electron flow in, 572, 572f
  defined, 569–570
  electron chain in, 570, 570f
Bacteriochlorophylls, 570
Bacteriopheophytins, 570–571
Bacteriorhodopsin, 351–352, 351f
Baculovirus, 160
BAL (British anti-lewisite), 516
Ball-and-chain model, 384–385, 385f
Ball-and-stick models, 22–23, 23f, 61, 61f
Band centrifugation, 77–78, 77f
Basal transcription apparatus, 875
Base-exchange reactions, 771
Base-excision repair, 848, 849f
Base-pair substitutions, tests for, 852
Base-paired hairpins, 123
Bases/base pairs
  adenine, **4,** 5f
  anticodon, 898, 898f
  compositions, 110, 111t
  cytosine, **4,** 5f
  damage to, 846–847
  double helix, 10
  guanine, **4,** 5f
  hydrogen bonds, 5
  minor-groove side of, 830
  mutagenic, 846
  nomenclature of, 744
  non-Watson-Crick, 846, 848, 863
  nucleic acids, 109
  in nucleotides, 107–108
  purine, 107, **107**
  pyrimidine, 107, **107**
  rRNA in, 903
  rules for, 110
  sequence of, 106, 114, 124
  stacking of, 10, 10f, 111, 111f, 116
  thymine, **4,** 5f
  in translation, 896, 903
  tRNA, 896
  uracil, 107, **107**
  Watson-Crick, 110, 110f, 113, 114f, 898
Basic-leucine zipper (bZip), 945, 945f
B-cell receptor, 993, 993f
Bcr-abl gene, 417, 417f
Bcr-Abl kinase, 1048, 1054
B-DNA helix, 111
Bennett, Claude, 991
Benson, Andrew, 589
Benzoate, 697
Benzoyl CoA, 697
Berg, Howard, 1027
Beriberi, 515, 515b
Beta blockers, 1048–1049, 1050
β chains, 205, 205f
β oxidation, 813, 815, 818
β pleated sheets
  amino acid residues in, 51–52, 51t
  antiparallel, 42f
  defined, 42
  mixed, structure of, 43f
  parallel, 43f
  protein rich, 43f
  twisted, schematic, 43f
β strands
  defined, 42
  DNA recognition through, 927, 927f
  of membrane proteins, 352, 352f
  Ramachandran plot for, 42f
  structure of, 42f
β turns, 44, 51–52
β-adrenergic receptor, 399–400, 400f
β-adrenergic-receptor kinase, 404
β-chain, of hemoglobin, 191
β-globin gene
  coding sequences, 127
  structure of, 127, 127f
  transcription and processing of, 127–128, 128f
β-hemoglobin, 207–208
β-lactam ring, 239
β-oxidation pathway, 650–651
β-thalassemia, 207, 208
B-form DNA, 111–112, 111f, 112t
Bile, 788
Bile acids, 646, 646f

Bile salts
  defined, 788
  synthesis of, 788–789, 789f
Bilirubin, 737
Biliverdin, 736
Biliverdin reductase, 737
Bimolecular reactions, 226
Bimolecular sheets
  defined, 348
  formation of, 348–350
Binding-change mechanism, 544–546, 545f
Binding energy, 225, 252
Biochemistry
  defined, 1
  environmental factors influencing, 20
  evolution timeline, 3f
  as evolving science, 1–23
  genome sequencing and, 17–19
  genomic revolution and, 17–22
  unifying concepts, 1–4
Biofilms, 934–935
Biological diversity
  biochemical unity underlying, 1–4
  similarity and, 2f
Biological macromolecules, 2
Biological membranes. *See* Membranes
Biopterin, 703
Biotin
  defined, 479
  in gluconeogenesis, 479–480, 479f
Biotin carboxyl carrier protein (BCCP), 479, 479f
1,3-bisphosphoglycerate (1,3-BPG)
  as acyl phosphate, 457
  ATP formation and, 459–460
  in glycolysis, 433, 457–460, 459f
  oxidation of energy, 433
  phosphoryl-transfer potential, 430
2,3-bisphosphoglycerate (2,3-BPG)
  allosteric effector, 200–201
  binding of, 201, 201f
  defined, 200
  in oxygen affinity determination, 200–201, 201f
Bitter taste, 966, 967–968
Bjorkman, Pamela, 996
Blackburn, Elizabeth, 845
BLAST (Basic Local Alignment Search Tool) search, 177, 178f
Blood, isozymes in, 293
Blood clotting, 286, 299
  clots, 307–308
  enzymatic cascades, 303–304, 303f
  extrinsic pathway of, 304
  hemophilia and, 308
  intrinsic pathway of, 304
  regulation of, 307–308
  vitamin K in, 304, 306–307
  zymogen activation in, 303–304
Blood groups, 331–332, 331f
Blood-brain barrier, 1037
Blosum-62
  alignment of identities only versus, 176f
  defined, 174
  graphic view of, 175f
Blotting techniques, 136, 138
Boat form, 320–321, 321f
Body mass index (BMI), 802, 803f
Body weight, regulation of, 802–804
Bohr, Christian, 202
Bohr effect, 202–203, 203f
Boltzmann's constant, 222
Bombardment-mediated transformation, 163
Bonds
  axial, 320–321
  covalent, 5, 6–7
  disulfide, 36–37, 37f
  electrostatic interactions, 7
  equatorial, 320–321
  glycosidic, 322, 322f, 325, 325f, 326
  hydrogen. *See* hydrogen bonds
  hydrophobic effect and, 9, 9f
  hydrophobic interactions and, 9
  ionic interactions, 7–8, 10f
  isopeptide, 683
  length measurement, 7b
  length of, 7b
  noncovalent, 7–8
  peptide. *See* peptide bonds
  units of measure for, 7b
  van der Waals interactions, 7, 8, 8f, 10, 348, 990
Bonitus, Jacob, 515b
Bordetella pertussis, 418
Bortezomib, 687
Bovine-spongiform encephalopathy, 56
Brain
  in caloric homeostasis, 804–807
  leptin effects in, 806–807, 806f
  role in caloric homeostasis, 804–807
  sensory connections to, 962, 962f
Branch points, 880, 881f
Branched-chain amino acids, 687–689
Branched-chain ketoaciduria, 705
Branching enzyme, 631–632, 632f
Brittle bone disease, 46
Bromodomains, 953, **953**
Brown, Michael, 784
Brown adipose tissue (BAT), 555, 555f
Brown fat mitochondria, 555
Buchner, Edward, 450
Buck, Linda, 963
Buffers
  action, 15f
  pH and, 15–17
  protonation, 16f

C genes, 991–992
C_4 pathway, 599–601, 600f
C_3 plants, 601
C_4 plants, 601
CAAT box, 874, 874f
Caenorhabditis elegans, 66, 956
  genome of, 153
  RNA interference in, 163
Calcineurin, 994
Calcitriol, 795
Calcium ion channels, 382
Calcium ion pump, 372–374, 372f
Calcium ions
  calmodulin activation, 407
  coordination to multiple ligands, 406, 406f
  imaging, 406, 406f
  in phosphorylase activation, 626, 627f
  pump structure, **371**
  pumping, 372, 372f
  as second messenger, 398, **399,** 405–406
  in signal transduction, 405–407
  in vision, 972–973
Calmodulin
  defined, 626
  in mitochondrial biogenesis, 813
  in signal transduction, 407, 407f
Calmodulin-dependent protein kinases (CaM kinases), 407, 407f
Calnexin, 335
Caloric homeostasis, 802–807
  in body weight regulation, 802–804
  brain role in, 804–807
  defined, 801
  in diabetes, 807–812
  dieting and, 807
  evolution and, 802–804
  insulin in, 805–806
  leptin in, 805–807
  obesity and, 801–812
  satiation signals in, 804–805, 804f
  signaling in, 804–807
  suppressors of cytokine signaling (SOCS) in, 806–807, 807f
Calreticulin, 335
Calvin, Melvin, 589
Calvin cycle, 589–601
  ATP (adenosine triphosphate) in, 597
  C_4 pathway and, 599–601, 600f
  carbon dioxide in, 591–598, 599–601
  defined, 566, 589
  five-carbon sugar formation in, 595, 596f
  glycolate in, 593–594, 593f
  hexose sugar formation in, 594–596, 595f
  illustrated, 590f
  light regulation of, 598, 598f
  magnesium ion and, 592, 592f, 598–599
  NADPH in, 589–590, 597
  overview of, 589–590
  oxygenase reaction in, 593–594, 593f
  pentose phosphate pathway and, 610
  3-phosphoglycerate formation in, 591–592, 592f
  photorespiration in, 594, 594f
  reactions in, 590–597, 597f
  regulation of, 598–601
  ribulose 1,5-biphosphate in, 591–592, 591f, 592f, **592**
  rubisco in, 591–594, 591f, 592f, 593f, 598–599
  salvage pathway in, 593–594
  stages, 590–591, 590f

  thioredoxin in, 599, 599t, **599**
cAMP. *See* Cyclic AMP
cAMP response element binding (CREB) protein, 403
Camptothecin, 839
Cancer
  aerobic glycolysis in, 474–476
  breast, 793
  citric acid cycle defects in, 513–514
  colorectal, 851, 851f, 1006
  defective DNA repair in, 850–852
  drug resistance in, 1053–1054
  fatty acid metabolism in, 667–668
  hypoxia inducible factor 1 (HIF-1) in, 513
  immune system in, 1005–1006
  in Li-Fraumeni syndrome, 851
  ovarian, 793
  pyruvate dehydrogenase kinase (PDK) in, 513
  signal transduction abnormalities in, 416–417, 416f, 417f
  skin, in xeroderma pigmentosum, 851, 851f
  tumor hypoxia in, 475–476, 476t
  tumor suppressor genes and, 851
  tumor visualization, 474, 475f
  Warburg effect in, 474
Cancer therapy, 759–760
Capillary electrophoresis, 139
Capsaicin, 977–978
Capsaicin receptor, 977–978, 977f, 978f
Captopril, 263
Carbamate
  in Calvin cycle, 592
  formation of, 204, 204f
Carbamate groups, 204f
Carbamoyl phosphate
  formation of, 693–694
  in pyrimidine synthesis, 745
  reaction, 694–695
  in urea cycle, 693–695
Carbamoyl phosphate synthetase I, 693–694
Carbamoyl phosphate synthetase II, 745
  in pyrimidine synthesis, 745
  structure of, 745, **745**
Carbanion, 606
Carbanion intermediates, 607, 607f
Carbohydrate-asparagine adduct, **57**
Carbohydrates, 315–338
  as building block, 20
  disaccharides, 323–324
  glucose generation from, 450
  isomeric forms of, 317f
  lectins and, 333–336, 334f
  monosaccharide, 316–323
  N-linked, 326, 326f
  oligosaccharides, 323, 331, 331f
  O-linked, 326
  overview of, 315–316
  polysaccharides, 324, 325f
Carbon dioxide
  binding site, 266, 266f
  in Calvin cycle, 591–598, 599–601
  defined, 203
  hydration acceleration, 264
  hydration of, 268, 268f
  oxygen release and, 202–204
  pH and, 203, 203f, 204
  transport from tissue to lungs, 204, 204f
Carbon fuels
  free energy of, 432–435, 432f
  prominent, 432, 432f
Carbon monoxide
  defined, 201
  in oxygen transport disruption, 201–202
Carbonic acid, 203
Carbonic anhydrases, 204
  bound zinc in, 265
  in carbon dioxide hydration acceleration, 264
  catalytic strategies of, 251
  defined, 264
  evolution of, 268
  mechanism of, 266, 266f
  pH effect on, 265, 265f
  proton shuttle, 267–268, 268f
  structure of, 265, **265**
  synthetic analog model system for, 266–267, 267f
Carbonium ion intermediate, 621
Carbon-nitrogen bond, 253
Carboxamides, 33
γ-carboxyglutamate, 57–58, 306–307, 306f
Carboxyhemoglobin, 201
Carboxylation, of pyruvate, 479–480, 514
Carboxyl-terminal domain (CTD)
  in coupling transcription to pre-mRNA, 884f
  phosphorylation of, 875
  serine residues of, 872
Carcinoembryonic antigen (CEA), 1006
Carcinogens, tests for, 852, 852f
Cardiotonic steroids, 373
Cargo receptor, 919
Carnitine, 649–650, 650f
Carnitine acyltransferase I, 650
Carnitine acyltransferase II, 650
Carotenoids, 581–582
Carriers, 367
Cartilage, 328–329, 329f
Caspases, 558
Cassette mutagenesis, 151, 151f
Catabolism
  ATP generation by, 432
  defined, 424, 714b
  energy from, 432–435
  free energy of, 431, 432–435, 435f
  stages of, 434–435, 434f
Catabolite activator protein (CAP), 931–932, 931f, 932f
Catabolite repression, 931–932
Catalysis
  by approximation, 252
  by ATCase, 285
  Circe effect in, 231, 231b
  covalent, 252, 253–255, 254f, 255f
  efficiency of, 230–231, 231f
  enzyme-substrate binding in, 225
  enzyme-substrate complex formation in, 222–223, 222f
  general acid-base, 252
  maximal rate, 228–229, 230
  metal ion, 252–253
  as selective binding of transition state, 241
  specificity constant, 230–231, 231f
  transition state formation and, 222
  velocity of, 231
  zinc activation of water molecule, 265–267, 266f
Catalytic antibodies, production of, 241
Catalytic strategies, 251–283
  of carbonic anhydrases, 251, 264–269
  in chymotrypsin, 253–255, 254f, 255f
  of myosins, 251–252, 275–281
  overview of, 251–252
  of restriction endonucleases, 251, 269–275
  of serine proteases, 251, 255–258
Catalytic triads
  in chymotrypsin, 255–258, 256f
  in elastase, 258, 259f
  in hydrolytic enzymes, 258–260, 258f, 259f
  serine in, 255–258
  site-directed mutagenesis and, 260, 260f
  of subtilisin, 259, 259f
  in trypsin, 258, 258f, 259f
Cataract formation, 469, 469f
Cataracts, 469, 469f
CD3, 999, 999f
CD4, 1001, 1001f, 1004–1005
CD8, 998–1000, 999f, 1004–1005
CD28, 1000
CD45, 1000
cDNA library, 149
CDP-ethanolamine, 770, **770**
Cech, Thomas, 859
Celecoxib (Celebrex), 1048, **1048**
Cell-mediated immunity, 995
Cells
  defined, 2
  hybridoma, 81–82
  motion within, 1011, 1012f
Cell-to-cell channels, 389–390, 389f, 390f
Cellular immune response, 984
Cellular respiration
  citric acid cycle in, 496–497, 496f
  enzymes in, 217
  in oxidative phosphorylation, 552–558
Cellulose, 324–325
Cell-wall biosynthesis, 1042, 1042f
Central dogma, 105
Centrifugation
  differential, 68, 68f
  sedimentation coefficients in, 76–77, 76t, 77f
  ultracentrifugation, 76–78, 77f, 287, 288f
  zonal, 77, 77f
Cephalopods, 329
Ceramidase, 775

Ceramide
  as precursor, 774
  synthesis of, 772, 772f
  in tumor growth, 774–775
Cerebroside, 346, **346,** 772
cGMP phosphodiesterase, 972
cGMP-gated ion channels, 972, 973
Chain, Ernest, 1041
Chair form, 320–321, 321f
Chanarin-Dorfman syndrome, 648
Changeux, Jean-Pierre, 198
Chaperones, 50
Charcot, Jean-Martin, 136
Charcot-Marie-Tooth disease, 1022
Chargaff, Erwin, 110
Charged tRNA, 898
Chemical shifts, 98
Chemiosmotic hypothesis, 542–543, 542f, 543f
Chemoattractants, 1028, 1029
Chemokines, 55
Chemorepellant, 1028
Chemotaxis, 1028–1029, 1029f
Cheng, Yung-Chi, 1035
Cheng-Prusoff equation, 1036
CheY, 1028
CheZ, 1028
Chirality
  of amino acids, 721, 721f
  establishment of, 717, 718f
Chitin, 329, 329f
Chlamydomonas, 887
Chloramphenicol, 914, 914t
Chlorobium thiosulfatophilum, 584
Chlorophyll *a*, 569, 569f, 582f
Chlorophyll *b*, 581–582, 582f
Chlorophylls
  defined, 568
  in photosynthesis, 568–572
  phytol, 569
  structure of, 568–569, 568f
Chlorophylls, light absorption by, 569, 569f
Chloroplasts
  ATP synthase, 578–580
  defined, 567
  electron micrograph of, 567f
  evolution of, 568
  genome of, 568
  in photosynthesis, 567–568
  reaction center, 569–570, 570f
  redox conditions, 579–580
  structure of, 567, 567f
Chlorpromazine, 1042, **1042**
Cholecystitis, 788
Cholecystokinin (CKK), 804–805
Cholera, 417–418
Choleragen, 417
Cholesterol
  "bad," 787
  carbon numbering, 790, 790f
  discovery of, 1043–1044
  excess, effects of, 785, 785f
  fatty acid chains and, 358, 358f
  formation of, 779f
  "good," 787
  levels, clinical management of, 788
  lipid rafts, 358
  as membrane fluidity regulator, 358
  in membrane lipid, 346
  as precursor for vitamin D, 794–795
  structure of, 346
Cholesterol synthesis, 776–788
  blocking of, 788
  condensation mechanism of, 778, 778f
  defined, 776, 776b
  isopentenyl pyrophosphate in, 776–777, 777f
  labeling of, 776f
  liver in, 779
  metabolism, 784
  mevalonate in, 776–777, 777f
  rate of, 779–781
  regulation of, 779–788
  site of, 782, 782f, 784
  squalene in, 777–779, 778f, 779f
  stages of, 776
  sterol regulatory element binding protein (SREBP) in, 779–781, 780f, 781f
Choline, 771
Chorismate, in amino acid synthesis, 727–729, 727f
Chromatin, 943–944, 948–954
  defined, 943
  in gene expression, 943, 948–954
  higher-order, structure of, 944, 944f
  remodeling of, 948–954, 953f
  structure of, 941, 942t
Chromatin immunoprecipitation (ChIP), 948, 948f
Chromatin-remodeling complexes, 953
Chromatography
  affinity, 70–71, 70f
  gel-filtration, 69, 69f
  high-performance liquid (HPLC), 71, 71f
  ion-exchange, 69–70, 70f
Chromogenic substrate, 254, 255f
Chromophore, 971
Chromosomes
  bacterial artificial, 147
  defined, 109
  Indian muntjac, 109, 109f
  yeast, 941, 942t
  yeast artificial, 147, 147f
Chronic myelogenous leukemia (CML), 417
Chronic obstructive pulmonary disease (COPD), 303
Chylomicron remnants, 782
Chylomicrons, 646–647, 646f, 782, 782t, 783
Chymotrypsin, 181, **182**
  active site, 255–256, 256f
  catalysis kinetics, 254–255, 255f
  catalytic mechanism, 254, 254f
  catalytic triad in, 255–258, 256f
  conformations of, 301, 301f
  covalent catalysis in, 253–255, 254f, 255f
  diisopropylphosphofluoridate (DIPF) and, 254, 254f
  elastase and, 258, 259f
  natural substrate for, **237**
  oxyanion hole, 257, 257f
  peptide hydrolysis by, 256, 257f
  S_1 pockets of, 259f
  serine residue, 253–254
  specificity of, 254f
  specificity pocket of, 258, 258f
  structure of, 255–256
  substrate preferences of, 230–231, 231t
  trypsin and, 258, 258f, 259f
Chymotrypsinogen, 255
  conformations of, 301, 301f
  defined, 299–300
  proteolytic activation of, 300, 300f
Cilia, microtubules in, 1023
Ciprofloxacin, 839
Circe effects, 231, 231b
Circular DNA, 113, 113f
Cirrhosis, 821
Cis configuration, peptide bonds, 38, 38t, 39t
Citrate
  in fatty acid metabolism, 666, 671, 672f
  in glyoxylate cycle, 517, 517f
  isomerization of, 504, 504f
  phosphofructokinase inhibition by, 472
  in polymerization, 671
  synthesis of, 513
  transport to cytoplasm, 512
Citrate synthase
  conformational changes on binding, 502, 503f
  defined, 502
  mechanism of, 502–503, 503f
Citric acid cycle, 495–518, 819
  acetyl CoA (acetyl coenzyme A) in, 495, 498–500, 501–503, 503f, 515
  aconitase in, 504, 504f
  ADP in, 406f, 506
  ATP in, 496–497, 508–510, 513, 514
  biosynthetic roles of, 514–516, 514f
  in cancer, 513–514
  carbon oxidation in, 501–510
  in cellular respiration, 496–497, 496f
  citrate isomerization in, 504, 504f
  citrate synthase in, 502–503, 503f
  citryl CoA in, 502, 503, 503f
  components of, 509t
  control sites of, 512–513, 512f
  defects in, 513–514
  entry to, 510–514
  evolution of, 516
  in exercise, 514, 514f
  glycolysis and, 497–501, 497f
  high-energy electron harvesting in, 496–497
  illustrated, 509f
  intermediates in, 514
  isocitrate dehydrogenase in, 504, 512–513, 512f
  isocitrate in, 504–505

  α-ketoglutarate in, 504–505, 505f
  α-ketoglutarate dehydrogenase complex in, 505, 512–513, 512f
  ketone bodies in, 819, 819f
  lipoamide in, 500–501, 501f
  in mitochondria, 496, 496f
  overview of, 495–497, 496f
  oxaloacetate in, 496, 502, 507–508
  pathway integration, 514, 514f
  pattern of, 496, 496f
  in photosynthesis. *See* dark reactions
  pyruvate dehydrogenase in, 511–512
  pyruvate dehydrogenase complex in, 497–501, 497f, 497t, 501f, 511–512, 511f
  pyruvate dehydrogenase phosphatase (PDP) in, 511
  rate of travel, 512, 512f
  reactions of, 508
  regulation of, 511–513
  replenishment, 514–515
  substrate channeling in, 510
  succinate dehydrogenase in, 507–508
  succinyl CoA in, 505–507, 506f
  succinyl CoA synthetase in, 506–507, 507f
  thiamine pyrophosphate (TPP) in, 499, 499f
Citrulline, 694–695
Citrullinemia, 705t
Citryl CoA (citryl coenzyme A), 502, 503, 503f
Cladribine, 760
Clamp loaders, 840, 841f
Class I MHC proteins, 996–997, 996f, 998, 1002–1003, 1003f
Class II MHC proteins, 1000–1003, 1001f
Class switching, 994–995
Clathrin, 360, 784
Clathrin-coated pit, 360
Cleavage
  DNA. *See* DNA, cleavage of
  protein, 88–89
Cleland, W. Wallace, 232
Clinical trials, 1051–1052, 1052f
Clofarabine, 760
Cloning
  of cDNA, 380
  expression, 149
  plasmid vectors in, 144–146
  in recombinant DNA technology, 147–148
Cloning vectors, 145
Closed promoter complex, 865–866, 866f
Clostridium perfringens, 464
Clostridium tetani, 1006
Clotting. *See* Blood clotting
Cluster of differentiation, 998
Coactivators, 950–951
Coat proteins (COPs), 919
Coated pits, 784
Cobalamin, 654–655, 655f. *See also* Vitamin B_{12}
Cobalt atom, 654–655
Codon-anticodon interactions, 898
Codons
  deciphered, 125, 125t
  defined, 21, 106, 123
  maximizing number of, 898
  of mitochondria, 126, 126t
  stop, 910–911, 911f
  as synonyms, 125
  in translation, 897–898, 898f
Coenzyme A, 437, **437**
Coenzyme B_{12}, 654–655, 655f, 656
Coenzyme Q, 530–531
Coenzymes
  in amino acid degradation, 682
  defined, 217
  prosthetic groups, 217
  types of, 217t
  vitamin, 438–440, 438t
Cognate DNA, 269, 272–274, 273f, **273, 274**
Cohesive ends, DNA, 144, 144f
Coiled-coil proteins, 44–45, 44f, **44,** 45f
Collagen
  amino acid sequence of, 45, 45f
  ascorbate and, 822
  in cartilage, 328
  defined, 45
  structure of, 45f
  triple helix, 45
Collagenase, 300
Color blindness, 974–975, 974f
Color vision
  in animals, 974, 974f
  cone receptors, 973–974
  defective, 974–975
  evolution of, 974, 974f
Combinational association, antibody diversity and, 992–993
Combinatorial chemistry, 185, 1045
Combinatorial control, 946
Committed step, 730
Comparative genomics, 19
Compartmentalization, 444
Compartments, drug target, 1037, 1038f
Competitive inhibition. *See also* Enzyme inhibition
  defined, 234
  dissociation constant, 235
  double-reciprocal plot, 236, 236f
  kinetics of, 235, 235f
  use of, 235
Complement cascade, 985
Complementarity-determining regions (CDRs), 988–990, 989f
Complementary DNA (cDNA)
  cloning and sequencing of, 380
  formation of, 149, 149f
  hybridization with, 135
  screening of, 149–150, 150f
Concerted model
  allosteric enzymes, 290
  defined, 198, 290
  formulation of, 211–212
  modeling oxygen binding with, 212f
  T and R states, 199f
  tetramers, 199
Condensing enzyme, 663
Cones, 970, 973–974
Conformation selection, 224
Congenital disorders of glycosylation, 332
Congenital erythropoietic porphyria, 737
Congestive heart failure, 373
Conjugation, in drug metabolism, 1037, 1038, 1039f
Connexin, 390
Connexons, 390
Conservative substitutions, 174, 175f, 176f
Controlled termination of replication, 138–139
Convergent evolution, 179, 181–182, 181f
Cooley anemia, 207
Cooperative binding
  concerted model, 198–199, 199f
  defined, 196
  oxygen delivery and, 196–197, 196f
  sequential model, 199, 199f
  substrates, 233
Copper ions, in cytochrome *c* oxidase, 536
Coproporphyrinogen III, 736, 737f
Corepressors, 931
Cori, Carl and Gerty, 637, 638
Cori cycle, 486, 486f, 493
Cori disease, 637t
Corrin ring, 654–655
Corticosteroids, 792
Cosmids, 146
Cotransporters. *See* Secondary transporters
Coulomb energy, 7
Covalent bonds
  in biological molecules, 6–7
  defined, 5
  multiple, 7
  as strongest bonds, 6–7
Covalent catalysis
  chymotrypsin as example, 253–255, 254f, 255f
  defined, 252
Covalent enzyme-bound intermediate, 458
Covalent modifications
  acetylation, 293–294, 294t
  common, 294t
  dephosphorylation, 293
  in enzyme regulation, 293–298
  irreversible, 294
  phosphorylation, 293, 294t
COX2 inhibitors, 1047–1048, 1048f
Crassulacea, 601, 601f
Crassulacean acid metabolism (CAM), 601
Creatine, **232**
Creatine kinase, 431f
Creatine phosphate, 813–814, 814t
Creutzfeldt-Jakob disease (CJD), 56
Crick, Francis, 17, 105, 109, 123, 124, 827
Critical concentration, 1018
Cro, in genetic circuit formation, 933, 933f
Cross talk, 398–399

Cross-links, 36–37, 37f
Cross-peaks, 99
CTP. *See* Cytidine triphosphate
CTP-phosphocholine cytidylyltransferase (CCT), 770
C-type lectins, 334–335, 334f
Cumulative feedback inhibition, 732
Cyanobacteria, 568, 568f
Cyanocobalamin, 655
Cyclic AMP (cAMP)
  binding to regulatory subunit, 297
  defined, 743
  effects in eukaryotic cells, 297
  in eukaryotic cells, 403
  generation by adenylate cyclase, 402–403
  in glycogen metabolism, 628–629
  phosphorylation stimulation, 403
  as second messenger, 398, **399,** 415
  in signal transduction, 402–403
  structure of, **297**
Cyclic GMP (cGMP)
  defined, 743
  as second messenger, 398, **399**
Cyclic nucleotides, 743
Cyclic photophosphorylation, 580, 580f
Cyclin-dependent protein kinases, 844
Cycloheximide, 914, 914t
Cyclooxygenase inhibitors, development of, 1047–1048
Cyclosporin, 994, **994**
Cystathionase, 726
Cystathionine, 726
Cystathionine β-synthase, 726
Cysteine
  linked, 36
  residue modification, 287f
  structure of, 32f, 33
  synthesis of, 722–723, 726
Cysteine proteases, 261–262, 261f, **261**
Cysteine thiyl radical, 754
Cystine, 36
Cytidine, 107
Cytidine diphosphodiacylglycerol (CDP-diacylglycerol), 769, **769**
Cytidine monophosphate (CMP), 769, **769**
Cytidine triphosphate (CTP), 291–292, 291f, 292f
  ATCase inhibition by, 287, 287f, 291, 758
  defined, 287
  effect on ATCase kinetics, 292, 292f
  in pyrimidine synthesis, 747–748
  T state stabilization, 291, 291f
Cytidine triphosphate synthetase, 747
Cytidylate, 108
Cytochrome
  defined, 534
  in photosynthetic reaction center, 570, 570f
Cytochrome b_5, 668, 668f
Cytochrome *bf* complex, 572, 575, 575f
Cytochrome *c*
  conformation of, 541, 541f
  evolution of, 541, 541f
  in oxidative phosphorylation, 530f, 533–534
Cytochrome *c* oxidase
  defined, 535
  electron flow in, 556
  heme, 536–537
  mechanism, 537–538, 537f
  peroxide bridge, 538, 538f
  proton transport by, 538, 538f
  in respiratory chain, 529–531, 530f, 530t, 535–538
  structure of, 536, 536f
  subunits, 536
Cytochrome P450, 1037–1038, 1038f, 1041
  defined, 790–791
  hydroxylation by, 790–791
  mechanism, 791
  protective function, 791–792
Cytoglobin, 208
Cytokines, 1002
Cytoplasm, 601, 666–667, 666f
Cytosine, **4,** 5f, 110, **110,** 850
Cytoskeleton, 1011, 1022
Cytotoxic (killer) T cells
  CD8 on, 998–1000
  defined, 984
  foreign peptide recognition, 1001, 1001f

D amino acids, 29, 29f
D genes, 992
Dalgarno, Lynn, 906
Daltons, 34, 36b
Dark reactions, 566
Darst, Seth, 862
Dawkins, Richard, 53
De novo pathways. *See also* Nucleotide synthesis
  defined, 744
  purine, 748, 748f
  pyrimidine, 744, 744f
Deamination
  in amino acid degradation, 692
  example of, 846, 846f
Death cap, 873f
Debranching enzyme, 638
Decarboxylation
  in citric acid cycle, 498
  in gluconeogenesis, 480
  in pentose phosphate pathway, 601
Decorated actin, 1018
Dedicated protein kinases, 295
Deficiency disorders, 20
Degrons, **684**
Dehydratases, 692
7-dehydrocholesterol (pro-vitamin D_3), 794–795, 794f
Deinococcus radiodurans, 828, 828f
Deleterious reactions, 456
Denisovans, 185, 185f
Density-gradient equilibrium sedimentation, 115, 115f
Deoxyadenosine, 107
5′-deoxyadenosyl radical, 655, 655f
Deoxyadenylate, 107
Deoxycytidine, 107
Deoxycytidylate, 107
Deoxyguanosine, 107
Deoxyguanosine 3′-monophosphate (3′-dGMP), 108, **108**
Deoxyguanylate, 107
Deoxyhemoglobin
  αβ dimers, 195
  carbon dioxide and, 204
  defined, 198
  quaternary structure of, 195f, **195**
Deoxymyoglobin, 192, 193, **193**
Deoxynucleoside 5′-triphosphates, 117
Deoxyribonucleic acid. *See* DNA
Deoxyribonucleoside 3′-phosphoramidites, 139, 140f, **140**
Deoxyribonucleoside triphosphate (dNTP), 829–830
Deoxyribonucleotide synthesis
  control of, 759–760
  deoxyuridylate in, 755–756, 756f
  dihydrofolate reductase in, 756
  overview of, 753
  ribonucleotide reductase in, 753–755, 755f, 756f, 759, 759f
  thymidylate, 757–758
  thymidylate in, 755–756, 756f
Deoxyribose, 4, **106,** 317, 318f, 320f
Deoxyribose phosphodiesterase, 849
Deoxyuridylate (dUMP), 755–756, 756f
Dephosphorylation, 293, 296
Deprotonation
  effect of buffer on, 268, 268f
  water, kinetics of, 267, 267f
Designer genes, 152
Desmolase, 792
Destroying angel, 873
α-Dextrinase, 450
Diabetes mellitus
  defined, 808, 808b
  glucose homeostasis in, 808
  incidence of, 808
  insulin in, 808–812
  insulin resistance and, 808–810, 810f
  ketosis in, 659–660, 660f
  obesity and, 807–812
  oxaloacetate in, 657
  type 1, 808, 812, 812f
  type 2, 808, 809–810
Diacylglycerol (DAG), 398, **399,** 647
  in lipid synthesis, 768
  in signal transduction, 405, 405f, 415
Diacylglycerol kinase, 768
Dialysis, in protein purification, 69, 69f
Diastereoisomers, 317, 317f
Diazotrophic microorganisms, 715
Dicoumarol, 307
Dictyostelium discoideum, 276, 629, 1014
Dicyclohexylcarbodiimide (DCC), 94f, 556
Diels-Alder reaction, 728
2,4-dienoyl CoA, 653, **653**

Diet
  fatty acid metabolism and, 672
  ketogenic, 660
  low-carbohydrate, 807
  low-fat, 807
  obesity and, 807
Differential centrifugation, 68, 68f
Diffusion
  facilitated, 367, 369
  lateral, 356
  lipid, 356
  membrane protein, 357
  simple, 368
  transverse, 357, 357f
Diffusion coefficient, 356, 357
Digestion
  of dietary proteins, 682, 683f
  enzymes in, 299–301, 300f
  of lipids, 645–646, 646f
  proteolytic enzymes in, 299–303
  starved-fed cycle and, 816–817
Digestive enzymes
  chymotrypsinogen, 299–301, 300f
  synthesis of, 299
Digitalis, 373
Digitoxigenin, 373, 373f
Diglyceride acyltransferase, 768
Dihydrofolate reductase, 756
Dihydrolipoyl transacetylase, 499, 500f
Dihydropteridine reductase, 703
Dihydrotestosterone (DHT), 793
Dihydroxyacetone, **316,** 317, 317f
Dihydroxyacetone phosphate (DHAP), 323
  in Calvin cycle, 595
  in glycolysis, 452f, 454–455, 455f, 456, 456f
  in lipid synthesis, 768, 768f
Diisopropylphosphofluoridate (DIPF), 237, 237f, **237,** 254, 254f
Dimerization arm, 412, 412f, 413, 413f
Dimethylallyl pyrophosphate, 777
Dimethylbenzimidazole, 655
2,4-dinitrophenol (DNP), 556–557
Dioxygenases, 704–705, 821
Diphosphatidylglycerol (cardiolipin), 770, **770**
Diphthamide, 915, 915f
Diphtheria toxin, 914–915, 915f
Dipolar ions, 29–30, 30f
Direct DNA repair, 848
Disaccharides
  defined, 323
  structure of, 323–324, 324f
  types of, 323–324, 323f, 324f
Diseases and disorders
  albinism, 705t
  alcaptonuria, 705
  alcohol-related, 821–822
  Alzheimer's disease, 56–57
  amyloidoses, 56–57
  amyotrophic lateral sclerosis (ALS), 143
  Anderson disease, 637t
  anemia, 327
  Angelman syndrome, 685
  anthrax, 839
  argininosuccinase deficiency, 697, 697f
  arsenite poisoning, 516, 516f
  atherosclerosis, 661, 784–785, 787–788
  autoimmune, 1005, 1005f
  beriberi, 515, 515b
  bovine-spongiform encephalopathy, 56
  cancer. *See* cancer
  carbamoyl phosphate synthetase deficiency, 697–698, 698f
  carnitine deficiency, 650
  cataracts, 469, 469f
  Charcot-Marie-Tooth disease, 1022
  cholera, 417–418
  citrullinemia, 705t
  congenital disorders of glycosylation, 332
  congestive heart failure, 373
  Cooley anemia, 207
  Cori disease, 637t
  coronary artery disease, 785
  Creutzfeldt-Jakob disease (CJD), 56
  deficiency disorders, 20
  diabetes. *See* diabetes mellitus
  drug-resistant, 1053–1054
  emphysema, 303
  environmental factors in, 20
  falciparum malaria, 612
  familial hypercholesterolemia, 767
  galactosemia, 468
  glucose 6-phosphate dehydrogenase deficiency, 610–612
  glycogen-storage, 637–638, 637t, 638f
  gout, 761
  Hartnup disease, 682
  heart disease, 788
  hemolytic anemia, 610–612
  hemophilia, 308
  Hers disease, 637t
  HIV infection. *See* human immunodeficiency virus (HIV) infection
  homocystinuria, 705t
  Huntington disease, 56, 683, 850
  Hurler disease, 328f, 332
  hyperammonemia, 697
  hyperlysinemia, 705t
  I-cell disease, 332
  lactose intolerance, 467–468
  Leber hereditary optic neuropathy (LHON), 557
  Lesch-Nyhan syndrome, 761–762
  Li-Fraumeni syndrome, 851
  long QT syndrome (LQTS), 388–389
  Lynch syndrome, 851, 851f
  mad cow disease, 56
  malaria, 206
  maple-syrup urine disease, 705
  McArdle disease, 637t, 638
  mercury poisoning, 515–516
  mitochondrial, 557
  mucopolysaccharidoses, 328
  multidrug resistance in, 374–376
  mutations causing, 143
  neurological, protein misfolding in, 56–57
  ornithine transcarbamoylase deficiency, 697–698, 698f
  osteoarthritis, 328
  osteogenesis imperfecta, 46
  osteomalacia, 795
  Parkinson disease, 56–57, 683, 685
  phenylketonuria, 705
  Pompe disease, 637–638, 637t, 638f
  porphyrias, 737–738
  predisposition to, 18
  prion, 56–57, 57f
  protein aggregates in, 56–57
  respiratory distress syndrome, 774
  retinitis pigmentosa, 884–885
  ricin poisoning, 915
  rickets, 795
  scrapie, 56
  scurvy, 821
  severe combined immunodeficiency (SCID), 164, 760–761
  sickle-cell anemia, 205–206, 205f, 206f
  spina bifida, 762
  Tay-Sachs disease, 774
  thalassemia, 884, 884f
  transmissible spongiform encephalopathies, 56–57
  tuberculosis, 687
  tyrosinemia, 705t
  vanishing white matter (VWM) disease, 913, 913f
  vitamin D deficiency, 795
  von Gierke disease, 637, 637t, 638
  Wernicke-Korsakoff syndrome, 821
  whooping cough, 417–418
  xeroderma pigmentosum, 851, 851t
  Zellweger syndrome, 657
Dismutation, 539b
Displacement loop (D-loop), 853
Dissociation constant (K_d), 229, 235, 1017–1018
Distal histidine, 194
Distribution, drug, 1037, 1037f, 1038f
Disulfide bonds
  formation of, 36–37, 37f
  reduction, 89, 90f
Diuron, 584, **584**
Divergent evolution, 181
DNA
  A-form, 111–112, 111f, 112f, 112t
  ancient, amplification and sequencing of, 185, 185f
  backbone of, 106f
  bases in, 4, **4,** 10, 10f, 108
  B-form, 111–112, 111f, 112t
  building blocks, 4–5
  chemically synthesized linker, 144
  circular, 113, 113f
  coding strand of, 862
  cognate, 269, 272–274, 273f, **273**
  cohesive ends, 144, 144f

DNA—(*continued*)
  complementary (cDNA), 135, 149–150, 149f, 150f, 380
  complementary single-stranded ends, 144
  covalent structure, 4, 4f
  damage to, 828, 845, 847–849
  defined, 105
  denaturation, 14–15, 14f
  directionality of, 108–109
  distortion of, 273–274, 273f
  double helix of, 5, 6, 9–10, 14–15, 105, 109–111
  double-stranded, 121, 152–153
  electroporation and, 163, 164f
  elongation, 118, 118f
  exchange between species, 184, 184f
  fingerprint, 137
  forensics and, 142, 143f
  functions of, 2
  heredity and, 5
  hybridization, 117
  information flow to RNA, 119, 119f
  ionic interactions, 10f
  length of, 108–109
  as linear polymer, 4, 105, 106
  linking number of, 834–836, 834f
  melting temperature of, 116
  methylation, 274–275
  microinjection of, 159–160, 159f
  nucleotides, 107
  promoter sites in, 122, 122b, 122f, 860
  proofreading of, 847, 848f
  properties of, 4–5
  proviral, 159
  recombinant. *See* recombinant DNA technology
  resolution by density-gradient, 115, 115f
  stability of, 142
  stem-loop structure, 113, 113f
  in storage of genetic information, 4, 5
  structure of, **108,** 111f, 113–114, 113f
  sugars, 4
  supercoiled, 113, 113f, 833–839
  synthesis of, 139–141, 140f, 141
  topoisomers of, 835–836, 836f
  transferred (T-DNA), 163
  unwinding of, 833–839, 860, 865–866, 866f
  Watson-Crick model, 111, 116
  winding, 944
  wrapping of, 943–944
  X-ray diffraction of, 109f
  Z-form, 112, 112f, 112t
DNA, cleavage of, 144, 144f
  EcoRV endonuclease, 269
  metal ion catalysis in, 271–272, 272f
  restriction enzymes and, 269–275
  stereochemistry, 271, 271f
DNA fragments
  covalent insertion of, 143–144
  insertion and replication of, 145
  insertional inactivation of, 145, 145f
  joined by DNA ligases, 144
  library of, 147–148, 148f
DNA gyrase, 839
DNA ligase, 135, 849
  defined, 832
  DNA fragments joined by, 144
  in DNA replication, 832, 844
  in forming recombinant DNA molecules, 143–144
  reaction, 832, 832f
DNA microarrays
  defined, 158
  gene-expression analysis with, 159, 159f
  using, 158–159, 158f
DNA photolyase, 848
DNA polymerase α, 843, 844, 844t
DNA polymerase β, 844t
DNA polymerase δ, 844, 844t
DNA polymerase I, 217, 829, **829,** 842, 844t
DNA polymerase II, 844t
DNA polymerase III, 831–832, 840–842, 840f, 844t
DNA polymerase switching, 843–844
DNA polymerases
  common structural features, 829
  in correcting DNA mistakes, 118
  defined, 117, 829
  DNA fragment of, 830
  error-prone, 846
  eukaryotic, 843–844, 844t
  holoenzyme, 840, 841f, 842–843
  mechanism, 829–830, 830f
  phosphodiester-bridge formation and, 117–118
  polymerization reaction catalyzed by, 117, 117f
  primer, 118, 829
  prokaryotic, 844t
  replication by, 117–119
  specificity of, 830
  structure of, 829, **829**
  template, 829
  as template-directed enzymes, 117, 829
  types of, 844t
DNA probes
  amino acid sequences in making, 91
  defined, 138
  generated from protein sequences, 147, 147f
  as primer, 140
  synthesis by automated solid-phase methods, 139–141
DNA recombination
  in cell division, 855
  defined, 852
  functions of, 853
  Holliday junctions in, 854, 854f
  illustrated, 853f
  initiation of, 853
  mechanism, 854, 854f
  overview of, 828
  RecA in, 853
  recombinases in, 854
  strand invasion in, 853, 853f
  V(D)J, 992, 992f
  VJ, 991–992, 991f
DNA recombination synapse, 854
DNA repair
  base-excision, 848, 849f
  direct, 848
  double-stand, 849
  in *E. coli*, 847–849
  enzyme complexes in, 848–849, 848f
  example of, 846, 846f
  illustrated, 828f
  ligase in, 849
  mismatch, 848, 848f
  nonhomologous end joining (NHEJ) in, 849
  overview of, 828, 845
  proofreading in, 847, 848f
  single-strand, 839–841
  thymine in, 850–851
  trinucleotide repeats and, 850
  uracil DNA glycosylase in, 850, 850f
DNA replication, 5f, 115f, 116f, 828–845
  ATP hydrolysis in, 832–833, 833f
  cell cycle and, 844, 844f
  clamp loaders in, 840, 841f
  controlled termination of, 138–139, 139f
  coordinated process in, 839–845
  cross-linking in, 847, 847f
  defective, in cancer, 850–852
  defined, 109
  DNA polymerase III in, 839, 840–842, 840f
  DNA polymerases in, 829–830, 842–843, 844t
  in *E. coli*, 115, 115f, 839–840, 842–843, 842f
  error rate, 118
  errors in, 846
  in eukaryotes, 843–844, 843f, 844f
  in eukaryotic cell cycle, 844, 844t
  helicases in, 832–833, 833f
  illustrated, 828f
  lagging strand in, 831f, 832, 840–842, 841f
  leading strand in, 831f, 832, 840–842, 841f
  licensing factors in, 843
  ligase in, 832, 832f, 844
  minor-groove interactions in, 830, 830f
  Okazaki fragments in, 831–832, 831f, 841
  origin of, 842–843, 842f, 843f
  origin of replication complexes (ORCs), 843–844
  overview of, 827
  polymerase switching in, 843–844
  by polymerases, 117–119
  prepriming complex in, 842, 842f
  primer in, 831, 831f
  processivity in, 839–840, 839f
  replication fork in, 831, 841, 841f
  replicon, 843
  RNA polymerases in, 831, 831f
  semiconservative, 115–116
  shape complementarity in, 830, 830f

  - shape selectivity in, 830, 831f
  - sites of, 842–844
  - sliding DNA clamp in, 839–840, 839f
  - specificity of, 830
  - telomeres in, 844–845, 845f
  - template in, 828–829
  - trombone model in, 841, 841f
  - tumor-suppressor genes in, 851
- DNA sequencing, 89–90
  - amino acid sequences and, 90f
  - amplification by PCR, 141–142
  - ancient DNA, 185, 185f
  - by controlled termination of replication, 138–139, 139f
  - decreasing costs of, 18f
  - defined, 135
  - as gene exploration tool, 136
  - human migrations and, 19f
  - methods for, 18
  - next-generation (NGS), 155–156, 155f
  - pyrosequencing, 155–156
  - reversible terminator method, 155–156
  - semiconductor, 156
- DNA vectors, 143, 144–147
- DnaA, 842, 842f
- DnaB, 840
- DNA-binding domains
  - defined, 945
  - in eukaryotes, 945–946
- DNA-binding proteins
  - basic-leucine zipper (bZip) in, 945, 945f
  - binding to regulatory sites in operons, 927–932
  - in eukaryotes, 945–946
  - helix-turn-helix motif in, 927, 927f
  - homeodomains in, 945, 945f
  - in prokaryotes, 926–932
  - symmetry matching in, 926–927
  - transcription inhibition by, 928–931
  - transcription simulation by, 931–932
  - zinc-finger domains in, 945–946, 946f
- DNA-binding sites, 931, 931f
  - evolution of, 931
  - GAL4, 948, 948f
  - hypersensitive, 948
- Domains
  - acetyllysine-binding, 953, 953f
  - defined, 3
  - DNA-binding, 926–932, 945–946
  - homeodomains, 945, 945f
  - immunoglobulin, 986, 988–989
  - nuclear-hormone receptor, 950, 950f
  - protein, 48, 48f
- Dopamine D2 receptors, 1042
- Double helix, 5, 6
  - acid-base reactions and, 14–15
  - base pairs, 10
  - destabilization, 14–15
  - DNA molecule form, 105
  - as expression of rules of chemistry, 9–10
  - left-handed, 112
  - minor groove, 875
  - reversibly melted, 116–117
  - right-handed, 112, 835
  - sequence of bases, 114
  - stabilization of, 109–111
  - structure, 5, **5**
  - topoisomerases and, 836–839, 837f, 838f
  - in transcription, 875, 875f
  - in transmission of hereditary information, 114–117
  - unwinding of, 836
- Double helix formation
  - from component strands, 6
  - entropy and, 13f
  - heat release in, 12–13
  - illustrated, 6f
  - principles of, 10
- Double-blind studies, 1052
- Double-displacement reactions, 232, 233
- Double-reciprocal plot, 229, 229f
- Double-stranded DNA, 121, 152–153
- Double-stranded RNA, 162, 162f
- Downstream core promoter element (DPE), 874
- Dreyer, William, 991
- *Drosophila melanogaster*
  - bases and genes, 66
  - fluorescence micrograph of, 82f
  - in genetic studies, 847
  - genome of, 154, 982
  - sensory bristles in, 976
  - Toll receptor in, 982
- Drug candidates
  - absorption of, 1036–1037, 1037f
  - ADME properties of, 1036–1040, 1036f
  - administration routes for, 1036–1037
  - characteristics of, 1034–1041
  - distribution of, 1037, 1037f, 1038f
  - effective concentrations of, 1035, 1035f
  - excretion of, 1039–1040
  - ligand binding in, 1035–1036, 1035f
  - metabolism of, 1037–1039
  - number of, 1045–1046
  - oral bioavailability of, 1036, 1037f
  - potency of, 1035–1036
  - side effects of, 1035
  - target compartments of, 1037, 1038f
  - therapeutic index of, 1041
- Drug development, 1033–1055
  - animal testing in, 1044
  - challenges of, 1034–1041
  - clinical trials in, 1051–1052, 1052f
  - combinatorial chemistry in, 1045
  - genetic differences and, 1050–1051
  - genomics in, 1048–1051
  - high-throughput screening in, 1045
  - natural products in, 1043–1044
  - overview of, 1033–1034
  - pharmacogenetics/pharmacogenomics in, 1050
  - phases of, 1051–1052
  - screening libraries in, 1044–1046, 1046f
  - serendipitous observations in, 1041–1043
  - 7TM receptors in, 1048
  - split-pool synthesis in, 1045, 1045f
  - structure-based, 1046–1048, 1047f, 1048f
- Drug targets, 1033, 1034f
  - animal-model testing of, 1049
  - compartments, 1037, 1038f
  - emerging, 1050, 1050f
  - identified in genomes of pathogens, 1050
  - identified in human proteome, 1048–1049
- Drugs
  - absorption of, 1036–1037, 1037f
  - administration routes for, 1036–1037
  - delivery with liposomes, 349
  - discovery approaches, 1033–1034, 1034f
  - distribution of, 1037, 1037f, 1038f
  - excretion of, 1039–1040, 1040f
  - half-life of, 1040, 1040f
  - metabolism of, 1037–1039
  - natural products in, 1043–1044
  - resistance to, 1053–1054
  - response to genetic variation in, 1050–1051
  - side effects of, 1035
  - targets of, 1033, 1034f
  - therapeutic index of, 1041
  - toxicity of, 1040–1041, 1040f
- Dynamic instability, 1023
- Dynein
  - AAA ATPases in, 1012, 1014
  - ATP binding to, 1014–1016
  - structure of, 1014, 1015f

- *E. coli. See Escherichia coli*
- E site, ribosomal, 905, 905f
- Ear, hair cells of, 975–976, 975f, 976f
- EcoRV endonuclease
  - cleavage of DNA, 269, 271–272, 271f
  - magnesium ion-binding site in, 271–272, 272f
  - nonspecific and cognate DNA with, **274**
  - recognition site structure, 272, 272f
  - twofold rotational symmetry, 272, 272f
- Edman degradation, 87, 87f
- Effector functions, 895
- EF-hand protein family, 407, 407f
- Eicosanoids, 669, 669f, 670f, **670**
- Elastase
  - blocking of, 303
  - catalytic triad in, 258, 259f
  - S_1 pockets of, 259f
- Electrochemical potential. *See* Membrane potential
- Electron transfer
  - half-reactions in, 528–529
  - inhibitors, 556–557, 556f
  - in oxidative phosphorylation, 526–529, 540–541, 540f
  - in photosynthesis, 568–572
  - rate of, 540, 540f
  - uncoupling, 556–557
- Electron transport chain, 497
- Electron-density maps, 96–97, 96f, 97f
- Electron-proton transfer reactions, 533, 533f
- Electron-transferring flavoprotein (ETF), 651

Electron-transport chain
  components of, 530f, 530t
  in desaturation of fatty acids, 668–669, 668f
  electron flow through, 538, 539f
  FAD (flavin adenine dinucleotide) and, 497, 510
  $FADH_2$ (flavin adenine dinucleotide reduced) and, 526, 527
  inhibition of, 556
  iron-sulfur clusters in, 531–532, 532f
  NADH (nicotinamide adenine dinucleotide reduced) and, 497, 510, 526, 528–529
  in oxidative phosphorylation, 523, 529–541
Electron-transport potential, 526
Electrophilic catalyst, 691
Electrophoresis
  capillary, 139
  gel, 71–73, 72f, 73f, 137–138, 138f, 350–351
  SDS, 72–73, 73f
  two-dimensional, 74–75, 74f
Electroporation, 163, 164f
Electrospray ionization (ESI), 85
Electrostatic repulsion, 429
Elongation factors
  bacterial versus eukaryotic, 913
  G (EF-G), 909–910, 910f
  Ts (EF-Ts), 907–908
  Tu (EF-Tu), 907, 907f, 908
Embden-Meyerhof pathway, 450
Emphysema, 303
Enantiomers, 317, 317f
Encoding of amino acids, 124–127
Endocytosis, 784
Endoplasmic reticulum (ER), 360
  protein glycosylation in, 330, 330f
  protein synthesis in, 915–919
  protein targeting from, 915–919
  ribosome binding to, 915–919, 916f
  rough, 916
  smooth, 916
Endoplasmic reticulum (ER) stress, 811
Endoplasmic reticulum membrane, 668
Endosomes
  defined, 361, 784
  LDL release in, 786, 786f
Endosymbiosis
  mitochondria evolution from, 360
  receptor-mediated, 360–361, 360f
Endosymbiotic event, 525–526
Enediol intermediate, in glycolysis, 455, 456f
Energy. *See also* Thermodynamics
  activation, 221–222
  binding, 225, 252
  free. *See* free energy
  kinetic, 11
  light, 584–585, 970
  potential, 11
  resting human being requirement, 548b
  status, 444
  total, 11
  units of, 219b
Energy charge, 444, 444f, 482–483
  intracellular, 625
  in regulation, 554, 554f
Energy coupling agent, 428
Energy homeostasis. *See* Caloric homeostasis
Energy transfer
  from accessory pigments to reaction centers, 583, 583f
  resonance, 582–583, 582f
Enhancers
  binding sites for, 947f
  defined, 876, 946–947
  experimental demonstration of, 947f
  in gene expression, 946–947
  in transcription, 876
Enol CoA hydratase, 651–652, 652f
Enol intermediates, 502
Enol phosphate, 461
Enolase, 461
Enoyl reductase, 664
Ensemble studies, 242
Enterohepatic cycling, 1040, 1040f
Enthalpy, 11
Entropy
  change during chemical reaction, 11, 12
  double helix formation and, 13f
  overall, 12
  total, 11
Envelope form, 321, 321f
Enzymatic cascades, 303–304, 303f
Enzymatic velocity, 230
Enzyme inhibition
  affinity labels, 237–238, 237f, 238f
  competitive, 234
  by diisopropylphosphofluoridate (DIPF), 237, 237f
  illustrated, 234f
  irreversible, 234, 237–238
  mechanism-based (suicide), 238, 238f
  noncompetitive, 234–235
  reversible, 234, 234f
  by specific molecules, 234
  by transition-state analogs, 240–241, 241f
  transition-state analogs in, 234
  uncompetitive, 234
Enzyme kinetics
  for allosteric enzyme, 233, 233f
  chymotrypsin, 254–255, 255f
  of competitive inhibitors, 235, 235f
  defined, 225
  in first-order reactions, 225–226
  Lineweaver-Burk plot, 229, 229f
  maximal rate, 228–229, 230
  Michaelis constant in, 227, 228–230, 229t
  Michaelis-Menten, 229, 233, 235, 254
  Michaelis-Menten model for, 225–233
  of noncompetitive inhibitors, 235, 235f
  in pseudo-first-order reactions, 226
  in second-order reactions, 226
  sigmoidal, 287, 287f
  specificity constant, 230–231, 231f
  steady-state assumption and, 226–228, 226f
  of uncompetitive inhibitors, 235, 235f
  of water deprotonation, 267, 267f
Enzyme multiplicity, 732, 732f
Enzyme regulation
  by covalent modification, 293–298
  of protein kinase A (PKA), 297, 297f
  strategies, 285–286
Enzyme-linked immunosorbent assay (ELISA)
  defined, 82
  indirect, 82, 83f
  sandwich, 82–83, 83f
Enzyme-pyridoxamine phosphate complex (E-PMP), 690
Enzymes, 215–245
  acceleration of reactions, 221–225
  activation energy and, 221, 221f, 222
  active sites, 216, 223–224, 223f, 230, 252
  allosteric, 233, 233f, 287
  amount control, 286
  assay measurement of, 67
  ATP hydrolysis and, 276
  branching, 631–632, 632f
  catalytic activity, control of, 443–444
  catalytic efficiency, 230–231, 231f
  catalytic power, 215, 216–218
  catalytic reaction, 222–223, 222f
  in cellular respiration, 217
  classes of, 245, 245t
  cofactors for, 217, 217t
  debranching, 638f
  defined, 450b
  digestive, 299
  energy-transducing, 217–218
  ensemble studies, 242f
  homologous, 696f
  isozymes, 285–286, 292–293, 293f
  kinetic properties of, 225–233
  kinetically perfect, 456
  metabolism control of, 443
  multiple forms of, 285–286
  overview of, 215–218
  peptide-cleaving, 260–262
  in photosynthesis, 217
  P-loop structures, 280–281
  processive, 840b
  as proteins, 215
  proteolytic, 216, 286, 299–308
  of purine nucleotide synthesis, 752
  pyridoxal phosphate, 691–692, 691f, 692f
  rate enhancement by, 216, 216t
  reaction rate and, 220–221, 220f
  restriction, 137, 269–275
  reversible covalent modification, 286
  single molecule studies of, 242–243, 242f
  specificity, 215, 216–218, 217f
  spectroscopic characteristics of, 223
  substituted intermediate, 233
  substrate interaction, 223

  ternary complex of, 232
  turnover number of, 230, 230f
  urea cycle, 696–697
Enzyme-substrate binding
  in catalysis, 225
  conformation selection, 224
  induced-fit model of, 224, 224f, 252, 453
  lock-and-key model of, 224, 224f
  multiple weak attractions, 224
Enzyme-substrate complex
  defined, 222
  diffusion-controlled encounter, 231
  dissociation constant for, 229
  evidence of existence, 222–223
  fates, 226
  formation, in catalysis, 222–223, 222f
  hydrogen bonds in, 224, 224f
  reformed, 226
  structure of, 223, **223**
Epidermal growth factor (EGF)
  defined, 411
  Ras activation and, 413–414, 413f
  in signal transduction, 397, 411–414
  signaling pathway, 414, 414f
  structure of, 411–412, 411f
Epidermal growth factor receptor (EGFR)
  defined, 411–412
  dimerization of, 412, 412f, 413
  modulator structure of, 412, 412f
  overexpression of, 416–417
  phosphorylation of carboxyl-terminal tail, 413
  unactivated, structure of, 412–413, 413f
Epigenome, 942
Epimers, 317f, 318
Epinephrine
  defined, 399
  in fatty acid metabolism, 671–672
  in glycogen metabolism, 627–629, 628f, 633
  in signal transduction, 399–407
  synthesis of, 734, 734f
Epitopes, 79
Equatorial bonds, 320–321, 321f
Equilibrium constant
  defined, 219
  dissociation of water, 13–14
  between enzyme-bound reactants and products, 279
  metabolism and, 428
  rate constants, 221
  of reactions, 219–220
Equilibrium potential, 387–388, 387f
Equilibrium reaction, 220–221
Error-prone polymerases, 846
Erythropoietin (EPO), 327, 327f
Erythrose 4-phosphate, 604, 604f
Escherichia coli (*E. coli*)
  amino-terminal protein residues, 905–906
  DNA polymerase I, 829, **829**
  DNA recombination in, 853
  DNA repair in, 847–849
  DNA replication in, 115, 115f, 839–840, 842–843, 842f
  enterotoxigenic, 773
  fatty acid synthesis in, 664
  flagella, 1012, 1026–1029
  gene expression in, 925–932
  genome of, 109, 109f
  lac operon of, 929–932, 929f, 930f
  membranes, 359
  methionine repressor, 927, 927f
  promoter sequences, 865
  pyruvate dehydrogenase complex of, 497f, 497t
  RecA protein, 933
  recombinant systems and, 78
  restriction enzymes in, 269
  ribonucleotide reductase of, 753
  RNA in, 119, 119t
  RNA polymerases in, 123, 123f, 861–862, 862t
  two-dimensional electrophoresis and, 74
Essential amino acids
  defined, 682, 719
  pathway steps, 719–720, 720f
  table of, 682t
Estradiol, 793, 951
Estrogen response elements (EREs), 950
Estrogens
  defined, 789
  DNA-binding receptors and, 949
  pathways for formation of, 794f
  synthesis of, 792–793, **794**
Estrone, 793
Ethanol
  fermentation of, 462–463, 463f
  in glycolysis, 449
  metabolism, 819–822
Ethylene, 726, 726f
Eukarya, 3f
Eukarya domain, 3
Eukaryotes
  defining characteristics, 3
  DNA replication in, 843–844, 843f, 844f
  fatty acid synthesis in, 664
  glycolysis in, 451
  membranes, 359–362
  nuclear envelope, 360, 360f
  protein synthesis inhibition in, 914–915
  transcription factors in, 874
  transcription in, 871–886
  translation in, 871–872, 871f
  translation initiation in, 911–912, 912f
  tubulins in, 1023
Eukaryotic cell cycle, 844, 844f
Eukaryotic genes
  as discontinuous, 127
  mosaic nature of, 127
  organization of, 942
  quantitation and manipulation of, 157–159
Eukaryotic RNA polymerases, 860, **860**
Evolution
  of active sites, 252
  of amino acid sequences, 37
  of aminoacyl-tRNA synthetases, 902
  of blood types, 331–332
  caloric homeostasis and, 802–803
  of carbonic anhydrases, 268
  of chloroplasts, 568
  of citric acid cycle, 516
  convergent, 181–182, 181f
  of cytochrome *c*, 541, 541f
  divergent, 181
  of DNA-binding sites, 931
  of drug resistance, 1053–1054
  experimental studies of ancient DNA amplification and sequencing in, 185, 185f
  of globins, 183–184
  of glycogen metabolism, 629
  of glycogen phosphorylase, 629
  of immune system, 981–982
  of introns and exons, 128
  in the laboratory, 186, 186f
  of metabolism, 444–445
  molecular, 185–187
  obesity and, 802–803
  of oxygen, 574b
  of photoreceptors, 973–974, 974f
  of proteasomes, 686, 686f
  of proteins, 128
  of ribosomes, 903
  of signal transduction pathways, 415
  split genes in, 128
  of vitamins, 438–439
Evolutionary trees, 183–184, 183f
Excinuclease, 849
Excretion, drug, 1039–1040, 1040f
Exemestane, 793
Exercise
  ATP in, 431, 431f, 476, 813–815, 814t
  citric acid cycle in, 514, 514f
  creatine phosphate in, 813–814, 814t
  diabetes and, 811–812
  fatty acid metabolism in, 813, 813f
  fuel sources for, 813–815, 814t, 815f
  glycolysis during, 476
  mitochondrial biogenesis and, 813, 813f
  oxidative phosphorylation in, 814–815
  super compensation (carbo-loading) and, 815
Exons
  defined, 106
  in encoding protein domains, 128–129
  shuffling, 128, 128f, 129f
Expression cloning, 149
Expression vectors, 146
Extracellular signal-regulated kinases (ERKs), 414
Extrinsic pathway, clotting, 304

2-^{18}F-2-D-deoxyglucose (FDG), 474, 475f
F$_{ab}$ fragments, 985–987
Facilitated diffusion, 367, 369
F-actin, 1017
Facultative anaerobes, 464

FAD (flavin adenine dinucleotide)
  as catalytic cofactor, 498
  defined, 435
  electron transfer potential of, 500
  structure of oxidized form, 435, 436f
  structure of reactive components of, 436, 436f
$FADH_2$ (flavin adenine dinucleotide reduced), 650–652
  defined, 436
  electron-transport chain and, 497, 510, 526, 527
  in oxidation-reduction reactions, 440, 440f
  structure of reactive components of, 436, 436f
Falciparum malaria, 612
Familial hypercholesterolemia, 767, 784–785
Faraday constant, 369, 528
Farnesyl pyrophosphate, 778, **779**
Fast switch, 464
Fasting, 817
Fat
  in adipose tissue, 815
  body, energy storage in, 645
  brown, 555
  as building block, 20
  neutral. *See* triacylglycerols
Fat cells, 645
Fatty acid chains
  melting temperature, 357, 357t
  packing of, 358, 358f
Fatty acid metabolism, 643–672
  acetyl carnitine in, 649–650
  acetyl CoA carboxylase in, 670–672, 671f
  acetyl CoA in, 512, 648–649, 650–652, 666–667, 666f
  acetyl CoA synthase in, 649
  activation in, 648–649
  acyl carrier protein (ACP) in, 661–662, 662f, **662,** 664–665, 665f
  β-oxidation pathway in, 650–651
  chylomicrons in, 646–647, 646f
  citrate in, 666, 671, 672f
  coenzyme B_{12} in, 654–655, 655f
  degradation in, 644, 644f, 651–661, 651f, 657f, 661–662
  diet and, 672
  enoyl CoA hydratase in, 651–652, 652f
  epinephrine in, 671–672
  in exercise, 813, 813f
  $FADH_2$ in, 650–652
  glucagon in, 671–672
  insulin in, 671–672
  ketone bodies in, 657–660
  lipases in, 647–648
  lipid mobilization and transport in, 645–647, 646f
  lipolysis in, 648, 648f
  malonyl CoA in, 662, 671
  methylmalonyl CoA in, 655–656, 655f, **656**
  NADH in, 650–652
  NADPH sources for, 667
  overview of, 643–645
  oxidation in, 648–649, 650–652, 651t, 656–657
  palmitoyl CoA in, 652, 652f, 653, 671
  pancreatic lipases in, 645–646, 646f
  pathway integration, 667, 667f
  peroxisomes in, 656–657, 657f
  steps in, 644–645, 644f
  triacylglycerols in, 645–648, 647f
  in tumor cells, 667–668
Fatty acid synthase
  catalytic cycle of, 664, 665f
  defined, 661, 662–663
  structure of, 664, 665f
Fatty acid synthesis
  in animals, 664–666
  in cytoplasm, 666–667, 666f
  defined, 644–645
  degradation versus, 661–662
  by fatty acid synthase, 661–668
  intermediates in, 662
  malonyl CoA in, 662
  maximal, 670–671
  reactions in, 662–664
  steps in, 644f, 662–664, 664f
Fatty acid thiokinase, 649
Fatty acids
  animals and, 660
  β oxidation of, 818
  chain length in, 343–344, 664
  cholesterol and, 358, 358f
  covalent attachment of, 643
  defined, 342
  degree of unsaturation, 343–344, 358
  derivatives, 643
  desaturation of, 668–669, 668f
  as fuel, 643, 647–652
  generation by lipolysis, 648, 648f
  in lipids, 342–344, 343f
  in muscle, 810, 815
  naturally occurring, 343t
  in obesity, 810
  odd-chain, 654, 654f
  physiological roles of, 643
  polyunsaturated, 661, 669
  saturated, 661
  structures of, 343, 343f
  unsaturated, 652–654, 652f, 653f, 661, 668–670
Fatty liver, 820
Favism, 611
F_c fragment, 985, 986
Feed forward stimulation, 472
Feedback inhibition, 285, 287, 443
  in amino acid synthesis, 731–732
  cumulative, 732
  enzyme multiplicity and, 732, 732f
  in purine synthesis control, 758–759, 758f
FeMo cofactor, 716, 716f
Fermentation
  to alcohol, 449, 462–463, 463f
  as anaerobic process, 464–465
  defined, 462
  in glycolysis, 462–464
  to lactic acid, 449, 463–464, 464f
  start and end points of, 465t
Ferredoxin, 580, 716
Ferredoxin-$NADP^+$, 576–577, 577f
Ferredoxin-thioredoxin reductase, 599
Ferritin, 736, 954–955, 954f
Ferrochelatase, 241, 736
Fetal hemoglobin, 201
Fiber types, muscle, 625, 626t
Fibrils, 325
Fibrin, 305, 305f, 308
Fibrin clots, 305–306, 305f
Fibrin monomer, 305
Fibrinogen
  conversion by thrombin, 304–306
  structure of, 304, 305f
Fibrinopeptides, 304–305
Fibrous proteins, 44–46
50S subunit, of ribosomes, 902–903, 903f, 908, 910
Fight-or-flight response, 399
Fingerprint, DNA, 137
First Law of Thermodynamics, 11
First-order reactions, 225
First-pass metabolism, 1039
Fischer, Emil, 224, 1046
Fischer projections, 22
5′ cap, 878–879, 879f
Flagella
  microtubules in, 1023
  rotary movement of, 1026–1029
  structure of, 1026, 1026f
Flagellar motor
  chemotaxis and, 1028–1029, 1029f
  components of, 1027, 1027f
  rotation of, 1026–1029
  schematic view of, 1027f
Flagellin, 1026, 1026f
Flavin adenine dinucleotide (FAD), 848
Flavin mononucleotide (FMN), 436, 436f, 532, 867, 867f
Flavoproteins, 500
Fleming, Alexander, 1041
FliG, 1027
FliM, 1027
FliN, 1027
Flip-flop, 357, 357f
Florey, Howard, 1041
Fluconazole, 1038f
Fluorescence microscopy, 82f, 84, 84f
Fluorescence recovery after photobleaching (FRAP), 356, 356f
Fluorodeoxyuridylate (F-dUMP), 757
Fluorouracil, 757
Folding funnel, 54, 54f
Foodstuffs, energy extraction from, 434–435, 434f
Formylmethionyl-tRNA, 906, 906f, 907
N-formylmethionine (fMet), 906, 907
Formyltetrahydrofolate, 749, 750, 750f

43S preinitiation complex (PIC), 912
Fourier transform, 96
Foxglove, 373, 373f
Fractional saturation, 195
François, Jacob, 928
Franklin, Rosalind, 109
Free energy
  of activation, 218
  ATP and, 426–431
  change during chemical reaction, 218–220
  defined, 12
  Gibbs, 12, 218
  in membrane transport, 369, 369f
  negative, 12
  of oxidation of single-carbon compounds, 432, 432f
  in oxidation-reduction reactions, 528
  of phosphorylated compounds, 431t
  of phosphorylation, 296
  standard change, 219–220
  thermodynamics of metabolism and, 425–426
Free radicals. *See* Reactive oxygen species
Friedreich's ataxia, 531–532
Fructofuranose, 320, 320f
Fructokinase, 465–466
Fructopyranose, 320, 320f
Fructose, 318, 318f
  activation of phosphofructokinase by, 472, 472f
  excessive consumption of, 466
  in glycolysis, 465–466, 466f
  metabolism, 466, 466f
  regulation of phosphofructokinase by, 472, 472f
  ring form, 320f
  ring structures, 320, 320f
Fructose 1,6-biphosphate
  in gluconeogenesis, 477f
  in glycolysis, 452f, 453–454, 454f
Fructose 1-phosphate, in glycolysis, 466
Fructose 2,6-biphosphate (F-2,6-BP)
  in gluconeogenesis, 483–485, 484f
  in glycolysis, 472, 472f
Fructose 6-phosphate
  in Calvin cycle, 594, 595f, 598, 598f
  in gluconeogenesis, 477f
  in glycolysis, 452f, 453, 454f, 472
  in pentose phosphate pathway, 604, 604f
  phosphorylation of, 454
Fructose biphosphatase 2 (FBPase2), 484
FtsZ, 1023
Fuel sources for, 816–817
Fumarase, 508
Fumarate
  from phenylalamine, 704, 704f
  in purine synthesis, 751
  in urea cycle, 695, 695f
4-fumarylacetoacetate, 704, **704**
Functional groups, of proteins, 28
Functional magnetic resonance imaging (fMRI), 193–194, 194f
Furan, 319
Furanose, 319, 319f, 320–321
Futile cycles, 485, 486

G elongation factor (EF-G), 909–910, 910f
G proteins
  activation of, 400–401, 401f
  ATP synthase and, 548–549
  defined, 400
  in glycogen metabolism, 627–629
  heterotrimeric, 400–402, 401f
  resetting of, 403–404, 403f
  role in signaling pathways, 401
  small, 413
  subunits, 401
G-actin, 1017
GAL4 binding sites, 948, 948f
Galactitol, 469
Galactokinase, 466
Galactolipids, 567
Galactose, 317, 318f
  defined, 466
  in glycolysis, 466–467, 466f
  missing transferase and, 468–469
  ring form, 320f
Galactose 1-phosphate uridyl transferase, 467
Galactosemia, 468
β-galactosidase, 332–333, 928, 928f
β-galactosides, 930
Galdieria sulphuraria, 184, 184f
Gangliosides, 346
  disorders of, 774
  structure of, 773, 773f
  synthesis of, 772–773, 773f
Gap junctions
  closing of, 390
  defined, 368, 389
  illustrated, 389f
  in intercellular communication, 389
  structure of, 390, 390f
Gas-phase ions, 85
Gastrointestinal peptides, 804–805, 805t
GC box, 874, 874f
GDP (guanosine diphosphate)
  in citric acid cycle, 506
  hydrolysis of, 427
  in olfaction, 964
  in signal transduction, 401–402, 413, 413f, 414
  in translation, 907–908
  in tubulin, 1023
  in vision, 972
Gel electrophoresis
  defined, 71
  isoelectric focusing and, 73, 73f
  polyacrylamide, 72, 72f
  protein separation by, 71–75
  SDS, 72–73, 73f
  SDS-PAGE, 73, 73f, 74
  two-dimensional electrophoresis and, 74–75, 74f
Gel-filtration chromatography, 69, 69f
Gellert, Martin, 836
Gene disruption, 160–162
  consequences of, 160–161, 161f
  defined, 160f
  by homologous recombination, 160, 160f
Gene expression
  analysis with microarrays, 159, 159f
  bacterial, 910
  constitutive, 925
  control of, 925–926
  as DNA information transformation, 119–124
  levels of, 157–158
  regulated, 925
  RNA in, 119–120
  transcriptional, 910, 925–926
  transcriptional, in eukaryotes, 954–957
  transcriptional, in prokaryotes, 935–937
  translational, 910, 954–956
Gene expression (eukaryotes), 941–958
  activation domains in, 945, 946
  basic-leucine zipper (bZip) in, 945, 945f
  chromatin in, 943–944, 952–953
  coactivators in, 950–951
  combinatorial control in, 946
  DNA methylation and, 949
  DNA-binding structures in, 945–946
  enhancers in, 946–947
  histones in, 943–944
  homeodomain in, 945, 945f
  hypomethylation in, 949
  in liver, 942, 942t
  mediator in, 946, 946f
  nuclear hormone receptors in, 949–951, 950f
  nucleosomes in, 943–944, 943f
  overview of, 941–943
  in pancreas, 942, 942t
  posttranscriptional, 954–957
  versus in prokaryotes, 941–943
  steroid-hormone receptors in, 951–952, 952f
  tissue-specific, 942t
  transcription factors in, 945–947
  zinc-finger domains in, 945–946, 946f
Gene expression (prokaryotes), 925–938
  attenuation in, 935–937, 936f
  autoinducers in, 934, 934f
  biofilms and, 934–935
  catabolite activator protein (CAP) in, 931–932, 931f, 932f
  catabolite repression in, 931–932
  chromatin remodeling in, 948–954, 953f
  corepressors in, 931
  DNA-binding proteins in, 926–932
  DNA-binding sites in, 931, 931f
  versus in eukaryotes, 941–943
  helix-turn-helix motif, 927, 927f
  lac operon in, 929–932, 929f, 930f
  lac repressor in, 927, 929–930, 929f, 930f
  λ repressor in, 932–933, 933f, 934f
  ligand binding in, 930
  operon model, 928–932
  overview of, 925–926

Gene expression (prokaryotes)—(*continued*)
  posttranscriptional, 935–937
  pur repressor in, 931, 931f
  quorum sensing in, 934, 934f
  regulatory sites in, 926–927
  signaling in, 933–934
  social interactions in, 934
  symmetry matching in, 927–928
  transcriptional, 925–932
"Gene guns," 163
Gene knockdown, 163
Gene knockout, 160–162, 160f, 161f
Gene therapy, 164
Gene transfer, horizontal, 184, 184f
General acid-base catalysis, 252
Genes. *See also specific genes*
  comparative analysis of, 156–157
  defined, 21
  designer, 152
  horizontal transfer, 184, 184f, 275
  number of, in human genome, 154
  regulator, 928
  reporter, 145
  RNA and, 118–119
  split, 128
  structural, 928
  synthesis by automated solid-phase methods, 139–141
  tumor suppressor, 851
Genetic code
  amino acids, 125, 125t
  aminoacyl-tRNA synthetases and, 898–902
  defined, 21, 124
  as degenerate, 125
  directionality of, 124
  features of, 125
  as nonoverlapping, 124
  universality of, 126–127
Genetically modified organisms (GMOs), 164
Genomes
  analysis of, 155–157
  of *Arabidopsis thaliana*, 154
  of *Caenorhabditis elegans*, 153
  of chloroplasts, 568
  comparative, 19, 156–157, 156f
  complete, 153f
  defined, 66
  of *Drosophila melanogaster*, 154, 982
  of *E. coli*, 109, 109f
  editing, 161–162, 162f
  of *Haemophilus influenzae*, 153, 177
  human, 154, 154f, 156, 156f
  of Indian muntjac, 109, 109f
  long interspersed elements, 154
  of mitochondria, 525–526, 525f, 526f
  next-generation sequencing, 155–156, 155f
  noncoding DNA in, 154
  number of genes in, 154
  proteome as functional representation, 66
  of puffer fish, 157, 157f
  of *Reclinomonas americana*, 526
  of *Rickettsia prowazekii*, 525–526
  of *Saccharomyces cerevisiae*, 153, 941
  sequencing of, 17–20, 152–156
  size of, 109
Genomic library
  creation of, 146–147, 147f
  defined, 147, 148
  screening of, 148, 148f
Genomic variation, 18
Genomics
  comparison, 19
  in drug discovery, 1048–1051
  revolution, 17–22
Geranyl pyrophosphate, 778, 778f
Geranyl transferase, 778, **779**
Ghrelin, 805, 805t
Gibbs free energy, 12, 218, 221
Gigaseal, 379
Gla domain, in prothrombin, 304
GlcNAcase, 327
Gleevec (imatinib mesylate), 1048, 1054
Globins. *See also* Hemoglobin; Myoglobin
  defined, 171
  evolution of, 183–184
  in human genome, 208
  sequence alignment in, 171–177
Glomeruli, 1039
Glucagon
  in essential enzyme regulation, 485
  excess in type 1 diabetes, 812
  in fatty acid metabolism, 671–672
Glucagon-like peptide 1 (GLP-1), 805, 805t
Glucocorticoids, 789
Glucogenic, amino acids, 698–703
Glucokinase, 473, 816
Gluconeogenesis, 476–487
  defined, 449, 476
  energy charge and, 478, 482–483
  fasting and, 817
  fructose 1,6-biphosphate in, 477f
  fructose 2,6-biphosphate in, 483–485, 484f
  fructose 6-phosphate in, 477f
  glucose 6-phosphate in, 477f, 481, 481f
  glucose generation and, 481
  glycolysis and, 478, 482–487
  historical perspective on, 450
  in kidney, 478
  in liver, 478, 483–485, 818
  in muscle contraction, 485–487, 486f
  overview of, 449, 476–478
  oxaloacetate in, 477f, 478–480, 819
  pathway integration, 486, 486f
  pathway of, 476–478, 477f
  phosphoenolpyruvate (PEP) in, 477f
  pyruvate conversion in, 478–480, 479f
  reactions of, 482t
  reciprocal regulation in, 482–487
  regulation of, 482–487, 812, 812f
  stoichiometry of, 481
  substrate cycles in, 485, 485f
  urea cycle in, 696, 696f
Glucose, 317–318, 318f
  in adipose tissue, 816
  as cellular fuel, 451
  characteristics of, 451
  complete oxidation of, 552–553, 553t
  conversion into pyruvate, 461–462
  in diabetes, 808
  as essential energy source, 317
  formation of, 451
  generation from glucose 6-phosphate, 481, 481f
  generation of, 450
  in glycogen, 324, 324f, 617, 618–619
  historical perspective on, 450
  homopolymers of, 324–325
  in liver-glycogen metabolism, 635–636
  metabolism, 424f
  as reducing sugar, 321–322
  ring form, 320f
  storage forms of, 324, 324f
  synthesis from noncarbohydrate precursors, 476–482
Glucose 1-phosphate, in glycogen metabolism, 619–620, 622–623
Glucose 6-phosphate (G-6P), 323
  galactose conversion into, 466–467, 467f
  in gluconeogenesis, 477f, 481, 481f, 623
  in glycolysis, 452f
  homeostasis, 816
  isomerization of, 453–454, 454f
  in liver, 622–623, 637
  metabolism of, 607–610, 618, 618f
  in pentose phosphate pathway, 602, 603f, 607–610
  transporter, 637
Glucose 6-phosphate dehydrogenase (G6PD)
  deficiency, 610–612
  in pentose phosphate pathway, 602, 610–612
  in reactive oxygen species protection, 610–612
Glucose homeostasis
  in diabetes, 807–812
  in starvation, 818–819
  starved-fed cycle in, 816–817
Glucose transporters (GLUTs), 368
  families, 473, 474t
  in glycolysis, 473–474, 474t
Glucose-alanine cycle, 692–693
Glucose-stimulated insulin secretion (GSIS), 810–812
α-1,6-glucosidase, 638
Glutamate, **233,** 700
  chirality of, 717, 718f
  formation of, 687, 692, 720–721
  in nitrogen fixation, 717–718
  oxidative deamination of, 687–689
  structure of, 33, 34f
  synthesis of, 722, 722f
Glutamate dehydrogenase, 688–689, 717, 718
Glutamate synthase, 718

Glutamine, 717–718
  degradation, 701
  in nitrogen transport, 693
  in pyrimidine synthesis, 745
  structure of, 32f, 33
  synthesis of, 722
Glutamine phosphoribosyl amidotransferase, 749
Glutamine synthetase, 717, 718, 732–733
  regulation of, 732–733, 733f
  structure of, 732–733
Glutathione, 610, 611
  conjugation reaction, 1038, **1039**
  defined, 734
  structure of, **734**
Glutathione peroxidase, 611, 735, 735f, **735**
Glutathione reductase, 611, 734
Glycan-binding proteins, 334
Glyceraldehyde, 316, **316,** 317, 317f
Glyceraldehyde 3-phosphate (GAP), 323
  in Calvin cycle, 595
  catalytic mechanism of, 458, 459f
  free-energy profiles for, 458, 458f
  in glycolysis, 452f, 454–455, 455f, 456, 456f, 457–460, 458f, 459f
  oxidation of, 432–433, 458–459, 459f
  in pentose phosphate pathway, 603, 604, 604f
  structure of, 458f, **458**
Glycerol
  generation by lipolysis, 648, 648f
  in gluconeogenesis, 476–478
  in liver, 648
  in phosphoglycerides, 344
Glycerol 3-phosphate
  in lipid synthesis, 768
  reoxidation of, 549
Glycerol 3-phosphate shuttle, 549–550, 549f
Glycerol phosphate acyltransferase, 768
Glycine
  in Calvin cycle, 593
  conversion into serine, 700
  defined, 30
  in liposomes, 349, 349f
  porphyrins from, 736–737, 737f
  structure of, 31f
  synthesis of, 722–723, 723f
Glycine synthase, 724
Glycine-glycine-glutamine (GGQ) sequence, 911
Glycoaminoglycans, 326
Glycocholate, 646f
Glycogen, 333
  branch point in, 324, 324f
  defined, 324, 617
  glucose storage in, 617, 618–619
  in glycogen metabolism, 627–629, 628f, 633
  in liver, 618, 618f, 627
  molecules, 617, 618f, 632f
  in muscle, 618, 618f
  phosphorolytic cleavage of, 620–621
  remodeling, 622, 622f
  storage efficiency, 632
  storage sites of, 618, 618f
  structure of, 618f
Glycogen lakes, 638f
Glycogen metabolism
  branching enzyme in, 631–632, 632f
  cAMP in, 628–629
  coordinate control of, 632–633, 633f
  degradation of, 618–629
  enzyme breakdown, 619–623
  epinephrine in, 627–629, 628f, 633
  evolution of, 629
  G proteins in, 627–629
  glycogen in, 627–629, 628f, 633
  glycogen phosphorylase in, 619–626
  glycogen synthase in, 630–632, 631f
  glycogen synthase kinase (GSK) in, 632, 633, 633f
  glycogenin in, 631
  α-1,6-glucosidase in, 621–622
  hormones in, 627–629, 628f
  insulin in, 635, 635f
  in liver, 635–637, 636f
  overview of, 617–619
  pathway integration, 628f
  phosphoglucomutase in, 622, 623f
  phosphoglycerate mutase in, 622
  phosphorolysis in, 619–623
  phosphorylase in, 619–627, 621f, 636, 636f
  protein kinase A (PKA) in, 629, 633, 633f
  protein phosphatase 1 (PP1) in, 629, 633–635, 634f, 636
  pyridoxal phosphate (PLP) in, 621, 621f
  regulation of, 618–619, 632–638
  regulatory cascade for, 627–629, 628f
  7TM receptors in, 627–629, 628f
  termination of, 629
  transferase in, 622, 622f
  UDP-glucose and, 630–631
Glycogen phosphorylase
  a, 623–624, 624f, 626, 627f
  allosteric regulation of, 624, 624f, 625, 625t
  amino-terminal domain of, 620–621, 620f
  b, 623, 624f, 625, 626, 627f
  carboxyl-terminal domain of, 620–621, 620f
  defined, 623
  evolution of, 629
  in glycogen metabolism, 619–626
  glycogen-binding site of, 620–621, 620f
  in liver, 623–624, 634f
  in muscle, 625, 625f
  regulation of, 623–627, 624f, 625t, 629
  structure of, 620
Glycogen synthase
  α-1,6 linkages, 631–632, 631f
  defined, 630
  in glycogen synthesis, 632
  isozymes of, 630–631
Glycogen synthase kinase (GSK)
  defined, 632
  in glycogen metabolism, 633, 633f
Glycogenin, 631
Glycogen-storage diseases, 637–638, 637t, 638f
Glycolate, 593–594, 593f
Glycolipids, 344, 345–346, 348–350
N-glycolylneuraminate, 772
Glycolysis
  aerobic, 474–476, 510
  aldehyde oxidation in, 457–458
  anaerobic mode, 510, 814
  ATP formation in, 459–462
  1,3-bisphosphoglycerate (1,3-BPG) in, 433, 457–460, 459f
  in cancer, 474–476
  citric acid cycle and, 497–501, 497f
  covalent enzyme-bound intermediate in, 458
  defined, 449
  dihydroxyacetone phosphate (DHAP) in, 452f, 454–455, 455f, 456, 456f
  as Embden-Meyerhof pathway, 450
  enediol intermediate in, 455, 456f
  energy charge and, 482–483
  as energy-conversion pathway, 451–469
  in eukaryotic cells, 451
  fermentation in, 462–464
  first stage of, 451, 451f, 452f
  fructose 1,6-bisphosphate in, 452f, 453–454, 454f
  fructose 1-phosphate in, 466
  fructose 2,6-bisphosphate in, 472, 472f
  fructose 6-phosphate in, 452f, 453, 454f, 472
  fructose in, 465–466, 466f
  galactose in, 466–467, 466f
  gluconeogenesis and, 478, 482–487
  glucose 6-phosphate (G-6P) in, 452f
  glucose transporters in, 473–474, 474t
  glucose trapping in, 451–453
  glyceraldehyde 3-phosphate (GAP) in, 452f, 454–455, 455f, 456, 456f, 457–460, 458f, 459f
  hexokinase in, 451–453, 453f, 470–471, 473
  historical perspective on, 450
  insulin in, 816
  isomerization of carbon sugars in, 453–454, 454f
  in liver, 472–473, 483–485
  in muscle, 469–471, 471f
  NAD^+ in, 458, 459f, 462–464, 465
  NADH in, 458, 462–464
  overview of, 449, 451
  pathway integration, 486, 486f
  pentose phosphate pathway and, 602–610
  phosphofructokinase (PFK) in, 469–470, 470f, 472, 472f
  phosphoglycerate kinase in, 459
  phosphoglycerate mutase in, 460
  2-phosphoglycerate in, 460–461, 460f
  3-phosphoglycerate in, 460–461, 460f
  pyruvate in, 452f, 459–464

- Glycolysis—(*continued*)
  - pyruvate kinase in, 471, 473, 473f
  - reactions of, 462t–463t
  - reciprocal regulation in, 482–487
  - regulation of, 812, 812f
  - second stage of, 451, 452f, 457f
  - stages of, 451, 451f, 452f, 457f
  - thioester intermediate in, 457–458, 458f
  - triose phosphate isomerase (TPI) in, 455–456, 455f, 456f
- Glycolytic intermediates, 610
- Glycolytic pathway
  - glucokinase in, 473
  - hexokinase in, 470–471, 473
  - phosphofructokinase (PFK) in, 469–470, 470f, 472, 472f
  - pyruvate kinase in, 471, 473, 473f
  - role of, 469
- Glycopeptide transpeptidase, 239
- Glycophorin, 336, 355, 355f
- Glycoproteins, 325–329
- Glycosaminoglycans, 327–328, 328f
- α-1,6-glucosidase, in glycogen metabolism, 621–622
- Glycosidic bonds, 322, 322f, 325, 325f, 326f
- Glycosylation, 330, 331, 331f
  - congenital disorders of, 332
  - errors in, 332
  - in nutrient sensing, 327, 327f
- Glycosyltransferases, 331, 331f
- Glyoxylate, 517, 517f, 593
- Glyoxylate cycle, 516–517, 517f
- Glyoxysomes, 517
- GMP (guanosine monophosphate)
  - in purine synthesis, 751–752, 751f
  - synthesis of, 758–759, 758f
- GMP synthetase, 752
- Goldstein, Joseph, 784
- Golgi complex, 330, 330f, 332, 918
- Gout, 761
- G-protein receptor kinase 2 (GRK2), 404
- G-protein-coupled receptors (GPCRs), 402
- Gradient centrifugation, 77–78, 77f
- Granzymes, 1000
- Grb2, 413, 413f
- Green fluorescent protein (GFP), 58–59, 58f, 84f
- Greider, Carol, 1, 845
- Group-specific reagents, 237
- Group-transfer reactions, 441, 441f
- GTP (guanosine triphosphate)
  - as energy source, 743
  - hydrolysis, 403–404
  - in olfaction, 964
  - in resetting G proteins, 403–404
  - in signal transduction, 401–402
  - in translation, 907–908
  - in tubulin, 1023
  - in vision, 972
- GTPases
  - defined, 414
  - Ras family of, 414, 414t
  - in signal transduction, 414, 414t
- Guanidinium chloride, 49
- Guanine, **4,** 5f, 110, **110**
- Guanine-nucleotide-exchange factor (GEF), 413
- Guanosine, 107
- Guanylate, 108, 752
- Guanylate cyclase, 973
- Guide strand, 162–163
- Gustation. *See* Taste
- Gustducin, 967, 967f

- H zone, 1020, 1020f
- *Haemophilus influenzae*, 153, 177
- Hair cells, 975–976, 975f, 976f
- Hairpin turns. *See* Reverse turns
- Half-life
  - of drugs, 1040, 1040f
  - of proteins, 683, 684, 685f
- Half-reactions
  - defined, 527
  - in electron transport, 528–529
- Haptenic determinants, 994
- Haptens, 994
- Hartnup disease, 682
- Hatch, Marshall Davidson, 599
- Haworth projections, 319
- Hearing, 975–977
  - hair cells in, 975–976, 975f, 976f
  - ion channels in, 976–977
  - mechanism of action, 975
- Heart disease, 788
- Heat
  - defined, 11
  - oxidative phosphorylation uncoupling in generation of, 554
  - release in double helix formation, 12–13
  - thermodynamics and, 11
- Heat shock protein 70 (Hsp70), 179, **179**
- Heat-shock response element, 875–876, 876f
- Heat-shock transcription factor (HSTF), 875–876
- Heavy (H) chains
  - in antibody diversity, 992–993
  - antigen-binding and, 991–992
  - defined, 985–986
  - in immunoglobulin classes, 987t
- Heavy meromyosin (HMM), 1013
- Heinz bodies, 612, 612f
- Helicases
  - defined, 832
  - in DNA replication, 832–833
  - mechanism, 833, 833f
  - structure of, 832, **832**
  - symmetry, 833, 833f
- Helix-turn-helix motif, 48, 48f, 927, 927f
- Helper T cells
  - action, 1002, 1002f
  - in cytokine secretion, 1002
  - defined, 984, 1000
  - in HIV infection, 1003–1004
  - peptide recognition, 1001, 1001f
  - T-cell receptors (TCRs) and, 1000–1002
- Hemagglutinin, 335–336, 335f
- Heme
  - biosynthetic pathway, 737f
  - in cytochrome *bf* complex, 575
  - in cytochrome *c* oxidase, 536–537
  - defined, 46
  - intrinsic reactivity of, 194–195
  - labeling of, 735b, 736, 736f
  - in oxygen-binding, 192, 193–194, 194f
- Heme prosthetic group, 534
- Hemichannels, 390
- Hemoglobin, 191–212
  - $\alpha_2\beta_2$ tetramer of, 49f
  - alignment comparison, 173–174, 173f
  - alignment with gap insertion, 173, 173f
  - αβ dimers, 195
  - α chains, 195, 207–208
  - amino acid sequences of, 171–172, 171f, 172f
  - β chains, 191, 195, 205, 205f
  - conformational changes in, 200, 200f
  - cooperativity, 198–199
  - defined, 171, 191
  - fetal, 201
  - globin curve, 195
  - Hill plot, 210f
  - myoglobin comparison, 191–192
  - oxygen delivery by, 196, 196f
  - oxygen-binding, 192–202, 196f
  - oxygen-binding curve, 196, 196f
  - polypeptide chains, 192, 195
  - purified, 200, 200f
  - quaternary structure of, 195, **195,** 197–198, 198f
  - R state, 198, 199f, 200, 211–212
  - sequence alignment of, 176, 176f
  - sickle-cell, 205, 205f
  - space-filling model, 195f
  - T state, 198, 199f, 200, 203, 211–212
  - tertiary structure of, 178–179
  - thalassemia and, 207
- Hemoglobin A (HbA), 195
- Hemoglobin H (HbH), 207
- Hemoglobin S (HbS), 205–206, 206f
- Hemolytic anemia, G6PD deficiency and, 610–612
- Hemophilia, 308
- Hemorrhagic disposition, 307b
- Hemostasis, 303
- Henderson-Hasselbalch equation, 16
- Heparin, 307
- Heptoses, 316
- HER2 receptor, 413, 417
- Herbicides, photosynthesis and, 584
- Hereditary nonpolyposis colorectal cancer (HNPCC), 851, 851f
- Hers disease, 637t
- Heterodimeric sweet receptor, 968–969, 968f
- Heterotrimeric G proteins, 400–402, 401f
- Heterotrophs, 566, 590
- Heterotropic effects, 292
- Hexokinase
  - defined, 451
  - in glycolysis, 451–453, 453f

  inhibition of, 471
  liver and glycolysis and, 473
  metal ion requirement, 453
  muscle and glycolysis and, 470–471
Hexose monophosphate pathway. *See* Pentose phosphate pathway
Hexose monophosphate pool, 595
Hexose sugars, formation in Calvin cycle, 594–596, 595f
Hexoses, 316, 453, 596f
High-density lipoproteins (HDLs), 782, 782t
  defined, 783
  properties of, 787
  protective effects and, 787–788
  reverse cholesterol transport in, 787
High-performance liquid chromatography (HPLC), 71, 71f
High-throughput screening, 1045
Hill, Archibald, 210
Hill coefficient, 210, 211f
Hill plot, 210–211, 210f, 211f
Histamine, 734, 734f
Histidine
  degradation, 700, 700f
  distal, 194
  ionization of, 33
  proton shuttle, 268, 268f
  proximal, 193, 200
  structure of, 33, 33f
Histidine operon, 936–937, 936f
Histone acetyltransferases (HATs), 952, **952**
Histone code, 954
Histone deacetylases, 953–954
Histone octamer, 943–944
Histones
  acetylation of, 952–953
  amino-terminal tails of, 952–953
  defined, 943
  in gene regulation, 943–944, 944f, 952–954, 954t
  homologous, 944, 944f
  modifications, 954, 954t
HIV. *See* Human immunodeficiency virus (HIV) infection
HMG-CoA reductase, 1044
HMG-CoA reductase inhibitor, 1044–1045
Hodgkin, Alan, 378
Hoffman, Felix, 1043
Hogness box, 122
Holliday, Robin, 854f
Holliday junctions, 854, 854f
Homeodomain, 945, 945f
Homeostasis, 442, 443f. *See also* Caloric homeostasis; Glucose homeostasis
Homocysteine
  in activated methyl cycle, 725, 725f
  in amino acid synthesis, 725–726
  in cysteine synthesis, 726
  levels, reducing, 726
  in vascular disease, 726
Homocysteine methyltransferase, 725
Homocystinuria, 705t
Homogenization, in protein purification, 67
Homogentisate, 704, **704,** 705
Homogentisate oxidase, 704
Homologies
  databases for, 177, 178f
  defined, 170
  detection of, 171–177
  evolutionary trees and, 183–184, 183f
  repeated motifs and, 180–181
  sequence alignment in, 173–177, 173f, 179–180
  shuffling in, 173–174, 173f
  statistical analysis in, 173–174
  substitution matrices in, 174–177
  three-dimensional structures and, 179–180
Homologous recombination, 160, 160f
Homologous sequences, 177
Homologs, 170, 171f
Homolytic cleavage reaction, 655, 655f
Homopolymers, 324
Homotropic effects, 290
Hood, Leroy, 991
Horizontal gene transfer, 184, 184f, 275
Hormone receptors, 950–952, 951f
Hormone-receptor complex, 402
Hormones
  in acetyl CoA carboxylase regulation, 671–672
  eicosanoid, 669, 669f, 670f, **670**
  in fatty acid metabolism, 670–672
  in gene expression, 950–952
  in glucose metabolism, 485
  in glycogen metabolism, 627–629, 628f
  local, 669
  metabolic functions of, 443–444
  in gluconeogenesis, 485
  in signal transduction, 400–402
  steroid, 789–791, 789f
Human genome, 154, 154f, 156, 156f
Human immunodeficiency virus (HIV) infection
  classes of, 1003
  drug development effects, 1047, 1047f
  helper T cells in, 1003–1004
  host cell for, 1003
  immune system and, 1003–1004
  protease, 262, 263f
  protease inhibitors, 263, 263f, 792, 1046, 1046f, 1053
  receptor, 1003f
  schematic representation, 1003f
  vaccine for, 1007
Humoral immune response, 984
Huntington disease, 56, 683, 850
Hurler disease, 328f, 332
Huxley, Andrew, 378
Hybridoma cells, 81–82
Hydrogen bonds, 8f
  acceptors, 15
  in base pairs, 5
  breaking with membranes, 354
  in enzyme-substrate complex, 224, 224f
  interaction, 8
  as noncovalent bond, 7
  strength of, 8
  water, 9, 10
Hydrogen ions
  in acid-base reactions, 13
  concentration in solutions, 13
  oxygen release and, 202–204
Hydrogen-bond donors, 8
Hydrolases, 245t
Hydrolysis. *See also* ATP hydrolysis
  GTP (guanosine triphosphate), 403–404
  of lipids, 647–648
  in metabolism, 427–429, 441–442, 442f
  of peptide bonds, 253, 256, 257f
  of phosphodiester bond, 269–270, 269f
Hydronium ions, 13
Hydropathy plots, 355, 356f
Hydrophilic amino acids, 33, 47
Hydrophilic moiety, 347, 347f
Hydrophobic amino acids, 30–32
  structures of, 31f
  types of, 30–32
Hydrophobic effect, 9, 9f, 10, 32
Hydrophobic interactions
  defined, 9
  as noncovalent bond, 7
Hydrophobic moiety, 347, 347f
3-hydroxy-3-methylglutaryl CoA, 702
3-hydroxyanthranilate, 704, **704**
25-hydroxycholesterol, 781
2-hydroxyglutarate, 513
Hydroxyl groups, 32–33, 57
Hydroxylation
  cytochrome P450 in, 791–792, 791f
  steroid hormones, 790–791
3-hydroxy-3-methylglutaryl CoA reductase (HMG-CoA reductase), 776–777, 777f, 779, 781f, 788, 788f
P-hydroxyphenylpyruvate, 704, **704,** 728
P-hydroxyphenylpyruvate hydroxylase, 704
Hydroxyproline, **57**
Hyperammonemia, 697
Hyperbaric oxygen therapy, 202
Hyperlysinemia, 705t
Hypersensitive sites, 948
Hypervariable loops, 988–990, 989f
Hypochromism, 116, 116f
Hypomethylation, 949
Hypoxanthine, 761
Hypoxanthine-guanine phosphoribosyltransferase (HGPRT), 752, 761
Hypoxia
  defined, 475
  tumor, 475–476, 476t
Hypoxia-inducible factor 1 (HIF-1), 476, 476f, 513

I band, 1020, 1020f
Ibuprofen, 1038, 1038f
Ice, 9, 9f
I-cell disease, 332, 332f
Imatinib mesylate (Gleevec), 1048, 1054

Immune response
  basis of, 985
  cellular, 984
  development of, critics of, 985
  humoral, 984
Immune system, 981–1009
  adaptive, 984–985
  in autoimmune diseases, 1005, 1005f
  B cells in, 984, 993–994, 1006
  in cancer, 1005–1006
  in disease, 1004–1007
  evolution of, 981–982
  innate, 982–983
  MHC proteins in, 995–1004
  overview of, 981–982
  T cells. *See* T cells
  T-cell receptors. *See* T-cell receptors (TCRs)
Immunity, cell-mediated, 995
Immunizations, 1006–1007
Immunoelectron microscopy, 84, 84f
Immunoglobulin A (IgA), 987, 987t
Immunoglobulin D (IgD), 987, 987t
Immunoglobulin domains. *See also* Immunoglobulin fold
  constant, 988, 988f
  defined, 986
  variable, 988, 988f, 989f
Immunoglobulin E (IgE), 987–988, 987t
Immunoglobulin fold
  complementarity-determining regions (CDRs), 988–990, 989f
  defined, 988
  elements of, 988–989
  structure of, **989**
Immunoglobulin G (IgG)
  antigen cross-linking, 986, 986f
  cleavage of, 986, 986f
  defined, 985
  properties of, 987t
  structure of, 985–986, 986f
Immunoglobulin M (IgM)
  defined, 987
  properties of, 987t
Immunoglobulins. *See also* Antibodies
  classes of, 986–988, 987f, 987t
  defined, 79, 984
  heavy chains, 985–987, 987t, 991–993
  light chains, 985–987, 987t, 991–993, 991f, 992f
  production of, 984, 984f
  segmental flexibility of, 987, 987f
  sequence diversity in, 988f
  structure of, 79f
Immunologic techniques
  enzyme-linked immunosorbent assay (ELISA), 82–83, 83f
  fluorescence microscopy, 84, 84f
  hybridoma cells in, 81–82
  monoclonal antibodies in, 80–82, 80f, 81f
  polyclonal antibodies in, 80, 80f
  in protein studies, 79–84
  western blotting, 83–84, 83f
Immunological memory, 1006
Immunoreceptor tyrosine-based activation motif (ITAM), 993, 993f
Immunosuppression, 994
Immunotoxins, 152
Indian muntjac, 109, 109f
Indinavir (Crixivan), 263, 263f
Indinavir complex, 263–264, 263f
Indirect ELISA, 82, 83f
Induced pluripotent stem (iPS) cells, 947, 947f
Induced-fit model, 224, 224f, 252
Influenza virus, 335–336, 335f
Inhibition
  competitive, 235, 235f, 236f
  noncompetitive, 235–236, 235f, 236f
  reversible, 235–236, 235f, 236f
  uncompetitive, 235, 235f, 236f
Inhibition constant (K_i), 1036
Inhibitory factor 1 (IF1), 554
Innate immune system, 982–983
Inosinate, 759
Inosine, 760, 761, 898
Inositol 1,4,5-trisphosphate (IP_3), 398, **399,** 404, 405f, 415
Insertional inactivation, 145, 145f
Insulin
  amino acid sequence of, 37f
  binding of, 408–409, 409f
  defined, 27
  in diabetes, 808–812
  in essential enzyme regulation, 485
  in fatty acid metabolism, 671–672
  in glycogen metabolism, 635, 635f
  in glycolysis, 816
  MALDI-TOF mass spectrum of, 86f
  in obesity, 805–806
  pancreatic failure and, 810–812
  in protein synthesis, 816
  release of, 810, 811f
  secretion of, 805
  in signal transduction, 407–411
  signal transduction, 808–809, 808f
Insulin receptor
  activation of, 408–409, 409f
  binding sites for, 808
  defined, 408
  structure of, 408, 408f
  subunits, 408, 408f
Insulin resistance
  biochemical basis of, 808–809
  in muscle, 810–812
  in pancreatic failure, 810–812, 811f
Insulin signaling
  illustrated, 409f
  lipid kinase in, 410, 410f
  pathway, 411, 411f
  termination of, 411
Insulin-receptor substrates (IRS), 409–411, 410f, 635
Integral membrane proteins, 351, 351f
Interatomic distances, 7b
Intercalation, 870
Intermediary metabolism. *See* Metabolism
Internal guide sequence (IGS), 887
Internal ribosome entry sites (IRES), 912
Intracellular pathogen, 995, 995f
Intramolecular hemiacetal, 318
Intramolecular hemiketal, 318–319
Intramolecular rearrangements, 654, 655f
Intrinsic pathway, clotting, 304
Intrinsically unstructured proteins, 55–56
Introns
  defined, 106
  detection of, 127, 127f
  self-splicing, 887, 887f
Inverted repeats, 272, 272f
Ion channels, 378–389
  acetylcholine receptor, 385–387, 386f, 387f
  action potentials and, 378, 378f, 387–388
  ball-and-chain model for inactivation, 384–385, 385f
  calcium, 382
  cell-to-cell, 389–390, 389f, 390f
  cGMP-gated, 972, 973
  defined, 368, 378
  disruption of, 388–389
  energetic basis of selectivity, 382, 382f
  equilibrium potential and, 387–388, 387f
  gap junction, 389–390, 389f, 390f
  in hearing, 976–977
  inactivation of, 384–385, 385f
  ligand-gated, 386
  membrane permeability and, 390–391
  nerve impulses and, 378
  patch-clamp technique, 379, 379f
  potassium, 378, 379–385, 381f, **381,** 384f, 385f
  selectivity filter, 381, 381f, 382, 382f
  sequence relations of, 380, 380f
  shaker, 380
  sodium, 378, 382–385, 382f, 383f
  in taste, 969, 969f
  transient receptor potential (TRP), 977
  voltage-gated, 383–384, 384f
Ion gradients, 433–434, 433f
Ion semiconductor sequencing, 156
Ion-exchange chromatography
  defined, 69–70
  illustrated, 70f
Ionic interactions, 7
IRE-binding protein (IRP), 955–956, 956f
Iron
  metabolism of, 954–956
  oxygen-binding to, 192–195, 194f
  structural transition in subunit, 200
Iron center, of ribonucleotide reductase, 753, 753f
Iron-response element (IRE), 955, 956
Iron-sulfur clusters, 531–532, 532f
Iron-sulfur proteins
  defined, 531
  in nitrogen fixation, 715–716, 716f
  in oxidative phosphorylation, 531–532
  structure of, **715**

Irreversible inhibition. *See also* Enzyme inhibition
  defined, 234
  in mapping active site, 237–238
  mechanism-based (suicide), 238, 238f
Isocitrate
  in citric acid cycle, 504–505
  in glyoxylate cycle, 517, 517f
Isocitrate dehydrogenase
  in citric acid cycle, 504, 512–513, 512f
  mutations in, 513
Isocitrate lyase, 517
Isoelectric focusing, 73, 73f
Isoform, 292
Isoleucine, 31f, 32
Isomerases, 245t
Isomerization reactions, in metabolism, 441, 441f
Isomers
  constitutional, 317, 317f
  diastereoisomers, 317, 317f
  stereoisomers, 317, 317f
Isopentenyl pyrophosphate, 776–777, 777f, **777**
Isopeptide bonds, 683
Isopropylthiogalactoside (IPTG), 930
Isotope labeling studies, 510, 736
Isovaleryl CoA, 702
Isovaleryl CoA dehydrogenase, 702
Isozymes
  in blood, 293
  defined, 292
  distinguishing, 292
  expression of, 286
  as homologous, 285
  of lactate dehydrogenase (LDH), 292, 293f
  in varying regulation, 285–286

J genes, 991–992
Jagendorf's demonstration, 578, 578f
Jenner, Edward, 1006

K^+ ions. *See* Potassium ions
k_{cat} (rate constant), 230
$k_{\text{cat}}/K_{\text{M}}$ (specificity constant), 230–231, 231f
K_{d} (dissociation constant), 229, 235, 1017–1018
Kendrew, John, 192
Ketimine, **690**
α-ketoacids, 701–702, 720–721
β-ketoacyl synthase, 663
α-ketobutyrate, 701
Ketogenic diets, 660
Ketoglutarate, **233**
α-ketoglutarate
  in amino acid degradation, 698, 700–701, 700f
  in amino acid synthesis, 717–718, 720
  in citric acid cycle, 504–505, 505f
  in double-displacement reactions, 233
  in glutamate synthesis, 717, 718
  in nitrogen fixation, 717
  oxidative decarboxylation of, 505
α-ketoglutarate dehydrogenase complex
  in citric acid cycle, 512–513, 512f
  defined, 505
α-ketoisocaproate, 701
Ketone bodies
  acetyl CoA formation from, 657–658
  in citric acid cycle, 819, 819f
  defined, 657
  in diabetes, 659–660, 660f
  in fatty acid metabolism, 657–660
  formation of, 657–658, 658f
  as fuel source, 658–660
  high levels of, 659–660
  in liver, 659, 659f, 819, 819f
  as water soluble, 659
Ketoses
  aldoses conversion to, 454
  defined, 316
3-ketosphinganine, 772
β-ketothiolase, 651
Keyhole limpet hemocyanin (KLH), 994
Khorana, Har Gobind, 124
K_{i} (inhibition constant), 1036
Kidney
  drug excretion in, 1039
  gluconeogenesis in, 478
Killed (inactivated) vaccines, 1006
Killer T cells. *See* Cytotoxic (killer) T cells
Kilobase (kb), 120b
Kilocalories (kcal), 219
Kilodaltons (kDa), 34, 36b
Kilojoules (kJ), 219
Kinase fold, 298
Kinases, 453, 453f. *See also specific kinases*
Kinesin
  ADP in, 1025, 1025f
  ATP binding to, 1014–1016, 1016f
  ATP hydrolysis in, 1024–1026, 1025f
  defined, 1012
  gene mutations, 1022
  monitoring movements mediated by, 1024f
  motion processivity, 1024–1026
  movement along microtubules, 1022, 1024–1026, 1025f
  neck linker, 1016, 1016f
  P-loop NTPase, 1012
  relay helix, 1016, 1016f
  structure of, 1014, 1014f
  walk, 1025
Kinetic energy, 11
Kinetics
  defined, 225
  enzyme. *See* enzyme kinetics
  as study of reaction rates, 225–226
  of water deprotonation, 267, 267f
Klenow fragment, 829
Klug, Aaron, 943
K_{M}. *See* Michaelis constant
Kornberg, Roger, 862
Krebs, Hans, 434, 516b
Krebs cycle. *See* Citric acid cycle
Kringle domain, 304
Kühne, Friedrich Wilhelm, 450b

L amino acids, 29, 29f
Laborit, Henri, 1042
Lac operon, 929–932, 929f, 930f
Lac regulatory site, 926f
Lac repressor
  binding of, 929
  components of, 929
  defined, 927
  effects of IPTG on, 930f
  inhibition relief, 931–932
  structure of, 929, 929f, 930
Lac repressor-DNA complex, 926–927, 926f
Lactase, 324
  deficiency of, 467–468
  defined, 450
Lactate, **232**
  in Cori cycle, 486, 486f
  formation from pyruvate, 463–464
  formation of, 485–486, 486f
  in gluconeogenesis, 476
  in glycolysis, 449
  in muscle contraction, 485–486, 486f
Lactate dehydrogenase (LDH), 292, 293f, 487
Lactic acid fermentation, 449, 463–464
Lactobacillus, 468f
β-lactoglobulin, 86f
Lactonases, 602
Lactose
  defined, 323–324
  structure of, 323–324, 324f
Lactose intolerance, 467–468
Lactose operon. *See Lac* operon; *Lac* repressor
Lactose permease, 377, 377f, **377**
Lagging strand
  defined, 832
  synthesis of, 831f, 840–842
  template, 841
γ chains, 987, 987f
λ phages
  alternative infection modes for, 146, 146f
  for DNA cloning, 144–147
  mutant, as cloning vector, 146, 147f
λ repressor
  defined, 933
  in gene expression, 932–933
  in genetic circuit formation, 933, 933f
  structure of, 933f
  synthesis control, 934, 934f
Lamprey, 183, 183f
Lanosterol, 778, **779,** 781
Lansoprazole, 1049, **1049**
Lateral diffusion, 356, 357, 357f
Lavoisier, Antoine, 714
Laws of thermodynamics, 10–12
Leader peptide sequences, 936, 936f
Leader sequences, 935–936, 935f

Leading strand
  defined, 832
  synthesis of, 831f, 840–842
Leber hereditary optic neuropathy (LHON), 557
Lectins
  as carbohydrate-binding proteins, 334–336
  classes, 334–335
  C-type, 334–335, 334f
  defined, 334
  in interactions between cells, 334
Leder, Philip, 991
Leghemoglobin
  sequence alignment of, 176, 176f
  tertiary structure of, 178–179
Leptin
  in caloric homeostasis, 805–807
  defined, 805
  effects in brain, 806–807, 806f
  obesity and, 806–807, 806f
  secretion of, 805, 806
Leptin resistance, 806–807, 807f
Lesch-Nyhan syndrome, 761–762
Leucine, 31f, 32
Leucine-rich repeats (LRRs), 982
Leukemia, 474–475
Leukocyte antigen A2 (HLA-A2), 996–997, 997f
Lever arm, 1015, 1015f, 1022, 1022f
Levinthal, Cyrus, 53
Levinthal's paradox, 53
Licensing factors, 843
Li-Fraumeni syndrome, 851
Ligand binding
  concerted model, 198–199, 199f
  in gene expression, 930
  sequential model, 199, 199f
Ligand-gated channels, 386
Ligands, 950
Ligases, 245t
Ligation reactions, in metabolism, 440–441
Light
  absorption, 971–972
  electromagnetic spectrum of, 970, 970f
  in lowering calcium level, 972–973
Light (L) chains, 985–987, 987t, 991–992, 991f, 992f
Light absorption, 569, 569f
Light energy, 584–585, 970
Light meromyosin (LMM), 1013
Light reactions. *See also* Photosynthesis
  in Calvin cycle, 598, 598f
  defined, 566
  herbicides and, 584
  illustrated, 566f
  stoichiometry for, 581
Light-harvesting complexes, 583
Light-independent reactions. *See* Dark reactions
Limit dextrin, 450
Lineweaver-Burk plot, 229, 229f
α-1,6 linkages, 631–632, 631f
Linking number, 834–836, 834f
Linoleoyl CoA, 653, 653f
Lipases, 645–646, 646f
Lipid bilayers. *See also* Membrane lipids
  as cooperative structures, 348
  defined, 342, 348
  diagram, 348f
  formation of, 348
  as permeability barrier, 349–350, 350f
  self-assembly process, 348
  as self-sealing, 348
  stabilization of, 348
Lipid droplet, 645
Lipid rafts, 358
Lipid vesicles, 348–349, 349f
Lipids
  digestion of, 645–646, 646f
  energy storage in, 645
  fatty acids in, 342–344, 343f, 343t
  hydrolysis of, 647–648
  membrane. *See* membrane lipids
  metabolism of. *See* fatty acid metabolism
  transport of, 646–647, 646f
Lipinski's rules, 1036–1037, 1037f
Lipoamide, in citric acid cycle, 500–501, 501f
Lipoic acid, 499, 499f
Lipolysis, 648, 648f
Lipopolysaccharide (LPS), 982–983
Lipoprotein particles, 782
Lipoproteins, 781, 782f
  chylomicrons, 782, 782t, 783
  components of, 782
  high-density (HDLs), 782, 782t, 783, 787–788
  intermediate-density (IDLs), 782, 782t, 783
  low-density (LDLs), 782, 782t, 783–787, 783f, 786f
  metabolism, 783f
  very-low-density (VLDLs), 782, 782t
Liposomes
  defined, 348
  formation of, 348–349, 349f
  therapeutic applications of, 349
Lipoxygenase, 669, 669f
Live attenuated vaccines, 1006
Liver
  alcoholic injury of, 820–821
  in amino acid degradation, 687, 692–693
  in cholesterol synthesis, 779
  cirrhosis of, 821
  drug metabolism in, 1039
  ethanol metabolism in, 819–822
  fasting and, 817
  fatty, 820
  gene expression in, 942, 942t
  gluconeogenesis in, 478, 483–485, 818
  glucose 6-phosphate (G-6P) in, 622–623, 637
  glucose levels and, 622–623
  glucose sensor in, 636
  glycerol in, 648
  glycogen in, 618, 618f, 627
  glycogen metabolism in, 635–637, 636f
  glycogen phosphorylase in, 623–624, 624f
  glycolysis in, 472–473, 472f, 473f, 483–485
  ketone bodies in, 659, 659f
  ketone body synthesis in, 819, 819f
  peroxisomes in, 657f
  in starvation, 818–819
  in starved-fed cycle, 816–817
  in triacylglycerol synthesis, 769
L-lectins, 335
Local hormones, 669f
Lock-and-key model, 224, 224f
Long interspersed elements, 154
Long QT syndrome (LQTS), 388–389
Loops, 44, 44f
Lou Gehrig's Disease, 136
Lovastatin, 788, 788f, 1044, **1044**
Low-density lipoprotein receptor
  absence of, 784–785
  destruction of, 785–786
  LDL release, 785–786, 786f
  mutations in, 785–786
Low-density lipoproteins (LDLs), 782, 782t
  in cholesterol metabolism, 784
  cycling of, 787
  defined, 783
  in familial hypercholesterolemia, 784–785
  metabolism of, 783f
  receptor-mediated endocytosis of, 784, 784f
  schematic model of, 783f
LuxR, 934
Lyases
  defined, 666b
  reaction type, 245t
Lymphotactin, 55, 55f
Lynch syndrome, 851, 851f
Lysine
  acetylated, 952–953
  structure of, 33, 33f
Lysogenic pathway, 146
Lysosomes
  defined, 332
  function of, 332
  in I-cell disease, 332
  with lipids, 774, 774f
Lysozyme
  antibodies against, 990, 990f
  backbone model, 62f
  ball-and-stick model, 61f
  ribbon diagram, 62f
  space-filling model, 61f
Lytic pathway, 146

MacKinnon, Roderick, 380, 384
Mad cow disease, 56
Magnesium ions
  in ATP hydrolysis, 276–277
  in Calvin cycle, 592, 592f, 598–599
  in DNA cleavage, 269–271

Major histocompatible complex (MHC), 984–985, 996
Major histocompatible complex proteins, 995–1004
  anchor residues, 997–998, 997f
  class I, 996–997, 996f, 998, 1002–1003, 1003f
  class II, 1000–1003, 1001f
  diversity of, 1002–1003
  peptide presentation by, 996–998, 996f
  in plasma membrane, 996
  structure of, 996–998
  T-cell receptors and, 998–1003, 998f
  in transplant rejection, 1002–1003
Malaria, 206, 206f
Malate, 517, 517f
  in Calvin cycle, 600f
  in citric acid cycle, 508
  in gluconeogenesis, 480
Malate dehydrogenase, 508, 667
Malate synthase, 517
Malate-aspartate shuttle, 550, 550f
MALDI-TOF mass spectroscopy, 86, 86f
4-maleylacetoacetate, 704, **704**
Malic enzyme, 667
Malonyl ACP, 661, 663
Malonyl CoA, 662, 671
Malonyl transacylase, 663, 663t
Malonyl/acetyl transacylase (MAT), 664, 665f
Maltase, 324, 450
Maltose, 324, 324f
Mammalian liver homogenate, 852
Manganese, 574, 574f
Manganese center, 574, 574f
Mannose, 317–318, 318f, 320f
Mannose 6-phosphate, 332, 332f
Mannose 6-phosphate receptor, 334
Maple-syrup urine disease, 705
Mass spectroscopy
  MALDI-TOF, 86, 86f
  peptide sequencing by, 87–88, 88f
  in protein and peptide identification, 85–92
  proteomic analysis by, 91–92, 92f
  tandem, 87–88, 88f
Mass-to-charge ratio, 85
Mast cells, 307, 307f
Matrix-assisted laser desorption/ionization (MALDI), 85, 332
Maximal rate, 228–229, 230
McArdle disease, 637t, 638
Mechanism-based (suicide) inhibition, 238, 238f
Mediator, 946, 946f
Megasynthases, 670
Melanin, synthesis of, 734, 734f
Melanocyte-stimulating hormone (MSH), 805–806, 806f
Melting temperature
  of DNA, 116
  of fatty acid chains, 357, 357t
  of phospholipid membrane, 357, 357f
Membrane anchors, 354, 354f
Membrane channels
  gap junction, 368
  ion, 368, 378–389
  membrane permeability to, 390–391, 391f
  water, 390–391, 391f
Membrane diffusion
  facilitated, 367, 369
  lateral, 356, 357, 357f
  lipid, 356
  protein, 357
  simple, 368
Membrane lipids. *See also* Lipid bilayers
  as amphipathic molecule, 347
  archaeal, 346–347, 346f
  carbohydrate moieties, 345–346
  cholesterol, 346, 776–788
  defined, 342
  diffusion coefficient, 356
  fatting acids in, 342–344, 343f, 343t
  glycolipids, 344, 345–346
  hydrophilicity of, 347, 347f
  hydrophobicity of, 347, 347f, 348
  lateral diffusion, 356, 356f, 357, 357f
  metabolism, 775–776
  movement in membranes, 357, 357f
  permeability barrier, 350
  phospholipids, 344–345
  phospholipids, synthesis of, 768–776
  rate of travel, 356
  representations of, 347f
  sphingolipids, synthesis of, 772–774
  synthesis of, 767–797, 775f
  triacylglycerols, synthesis of, 768–776
  as two-dimensional solutions, 342
Membrane potential, 369
Membrane proteins
  α helix of, 351–352, 355–356, 355f, 355t
  ATP hydrolysis, 370–376
  β strands of, 352, 352f
  carriers, 367
  channels. *See* membrane channels
  content variation, 350
  defined, 342
  diffusion, 357
  function of, 350
  gel patterns of, 350, 350f
  hydropathy plots for, 355, 356f
  hydrophobicity of, 354, 354f
  integral, 351, 351f
  linking to membrane surface, 353
  membrane interaction, 351–354
  peripheral, 351, 351f
  pumps. *See* pumps
  as two-dimensional solutions, 342
Membrane transport
  ABC transporters in, 367, 374–376, 374f, 375f
  active, 367, 369
  free energy in, 369, 369f
  passive, 369
  potassium ion channels and, 383, 383f
  primary active, 367
  secondary active, 367
  transporters. *See* transporters
Membranes, 341–363
  archaeal, 346–347, 346f
  as asymmetric, 342, 357–358, 359f
  common features of, 342
  defined, 341
  as electrically polarized, 342
  endoplasmic reticulum (ER), 668
  enzymatic activities, 358–359
  fluidity of, 357–359
  ion gradients across, 433–434, 433f
  lipid bilayer, 342, 348–350
  mitochondria, 524–525
  as noncovalent assemblies, 342
  overview of, 341–342
  permeability of, 341, 349–350, 350f, 367
  planar bilayer, 349, 349f
  polarity scale for transmembrane helices, 355, 355t
  processes of, 350–356
  protein interaction, 351–354
  as sheetlike structures, 342
  synthesis of, 359
Membrane-spanning α helices, 351–352, 355, 355f
Memory B cells, 1006
Memory T cells, 1006
Menten, Maud, 226
6-mercaptopurine, 1051, **1051**
β-mercaptoethanol, 49, 49f, 50f
Mercury poisoning, 515–516
Merrifield, R. Bruce, 94
Meselson, Matthew, 115, 116
Metabolic pathways. *See also specific pathways*
  amphibolic, 425
  biosynthetic, 425
  classes of, 424
  defined, 424
  degradative, 425
  formation of, 426
  illustrated, 425f
  motifs, 435–445
  regulation of, 424
  thermodynamically favorable, 425, 426
  thermodynamically unfavorable, 426
Metabolic syndrome, 809–810, 810f
Metabolism, 423–446
  activated carriers in, 435–440
  anabolic reactions in, 428–429
  carbon bonds cleavage, 442, 442f
  catabolic reactions in, 428
  catalytic activity control and, 443–444
  cholesterol synthesis, 784
  common motifs in, 423–424, 435–445
  defined, 423
  drug, 1037–1039
  enzyme control and, 443
  evolution of, 444–445
  first-pass, 1039
  free energy in, 426–427
  fructose, 466, 466f

Metabolism—(*continued*)
  glucose, 424f
  of glucose 6-phosphate, 607–610
  group-transfer reactions in, 441, 441f
  hormones and, 443–444
  hydrolytic reactions in, 441–442, 442f
  integration of, 801–822
  interconnected interactions in, 424–426, 424f
  iron, 954–956
  isomerization reactions in, 441, 441f
  ligation reactions in, 440–441, 440f
  lipid, 775–776
  lipoproteins, 783f
  overview of, 423–424
  oxidation-reduction reactions in, 440, 440f
  of pyruvate, 462–464
  regulation of, 442–444
  in starvation, 818–819, 819t
  substrate accessibility control and, 444
  substrate cycles in, 485, 485f
  thermodynamics of, 425–426
  types of reactions in, 440t
Metabolites, 2, 650
Metal ion catalysis
  in ATP hydrolysis, 276–277
  in carbon dioxide hydrolysis, 265–267
  defined, 252–253
  in DNA cleavage, 271–272, 272f
Metal ions, **829**
Metalloproteases, 261f, **261,** 262
Metals, cofactor, 217, 217t
Metamorphic proteins, 55–56
Metarhodopsin, 972
Methionine
  degradation, 701
  from homocysteine, 725
  metabolism, 701, 702f
  oxidation of, 303, 303f
  structure of, 31f, 32
  in translation, 906, 906f
Methionine sulfoxide, 303, 303f
Methionine synthase, 725
Methotrexate, 757
Methylases, 274
Methylation
  of adenine, 274–275, 275f
  in amino acid synthesis, 724–726
  DNA protection by, 274–275, 274f
  in gene expression, 949
  of phospholipids, 726
  reaction, 654
Methylcobalamin, 725
β-methylcrotonyl CoA, 702
β-methylglutaconyl CoA, 702
Methylmalonyl CoA, 655–656, 655f, **656**
N-methylmesoporphyrin, 241, 241f
Metmyoglobin, 194
Metoprolol, 1050
Mevalonate, 776–777, 777f
Micelles, 348, 348f
Michaelis, Leonor, 226
Michaelis constant (K_M)
  in Cheng-Prusoff equation, 1036
  defined, 227
  determination of, 228–229
  as enzyme characteristic, 229–230
  physiological consequences of variations, 228
  values of enzymes, 229t
Michaelis-Menten equation, 229, 233
Michaelis-Menten kinetics, 225–233, 227f, 235, 254, 287
Microbiomes, 19, 19f
Microbodies, 593
MicroRNAs, 879, 879f, 956–957, 956f
Microsomal ethanol-oxidizing system (MEOS), 820
Microtubules
  arrangement of, 1023, 1023f
  in cilia, 1023
  defined, 1022
  dynamic instability of, 1023
  in flagella, 1023
  function of, 1023
  kinesin movement along, 1022, 1024–1026, 1025f
  structure of, 1022–1023, 1022f
  tubulins in, 1023, 1023f
Mineralocorticoids, 789
Minoxidil, 1038
Mismatch DNA repair, 848, 848f
Mitchell, Peter, 542, 542b, 558, 578
Mitochondria
  in apoptosis, 557–558
  ATP synthase in, 550–552
  brown fat, 555
  in citric acid cycle, 496, 496f
  codons of, 126, 126t
  electron entry via shuttles, 549–550
  electron micrograph and diagram of, 525f
  endosymbiotic origin of, 525–526
  genome of, 525–526, 525f, 526f
  matrix, 524
  membrane, 524
  overlapping gene complements of, 526, 526f
  oxidative phosphorylation in, 524–526
  properties of, 524–526
  structure of, 524–525, 525f
Mitochondrial ATP-ADP translocase, 550–551, 551f, 557
Mitochondrial ATPase. *See* ATP synthase
Mitochondrial biogenesis, 813, 813f
Mitochondrial diseases, 557
Mitochondrial mutants, 557
Mitochondrial outer membrane permeabilization (MOMP), 558
Mitochondrial porin, 524
Mitochondrial transporters, 551–552, 551f, 552f
  defined, 552f
  illustrated, 552f
  for metabolites, 551–552
  structure of, 551, 551f
Mixed-function oxygenase, 703, 790–791
Molecular evolution, 185–187
Molecular heterogeneity, 242–243, 242f
Molecular imaging agents, 406
Molecular models
  backbone, 61–62, 62f
  ball-and-stick, 22–23, 23f, 61, 61f
  proteins, 61–62
  small molecules, 22–23
  space-filling, 22, 23f, 61, 61f
Molecular motors, 1011–1031
  ATP binding to, 1014–1016, 1015f, 1016f
  dynein, 1012, 1014, 1015f, 1022–1026
  flagella, 1012, 1023, 1026–1029
  kinesin, 1012, 1014, 1022–1026
  myosin, 1012, 1013–1014, 1013f, 1014f, 1018–1022
  operation of, 1011–1012
  overview of, 1011–1012
  P-loop NTPase superfamily, 1012–1016
  structures of, 1012–1016, 1013f, 1014f, 1015f
Molecular oxygen, toxic derivatives of, 538–540
Molecules
  amphipathic nature of, 348
  Fischer projections, 22
  homologous, 170
  permeability of, 350, 350f
  stereochemical renderings, 22
  three-dimensional structure of, 22–23
Moloney murine leukemia virus, 159
Monoclonal antibodies
  defined, 80
  generation for proteins, 80–82
  illustrated, 80f
  preparation of, 81f
  in signal transduction inhibition, 416–417
Monod, Jacques, 198, 928
Monomers, 107
Monooxygenase, 703, 790–791
Monosaccharides. *See also* Carbohydrates
  alcohols and, 322
  aldoses, 316
  amines and, 322
  boat form of, 320–321, 321f
  chair form of, 320–321, 321f
  defined, 316
  diastereoisomers, 317, 317f
  envelope form of, 321, 321f
  glycosidic bonds, 322, 322f
  isomers of, 317, 317f
  ketoses, 316
  linkage of, 323–325
  modified, 322–323, 322f
  reducing sugars, 321–322
  ring forms of, 319–321, 319f, 320f
  stereoisomers, 317, 317f
  structure of, 316–318
Morphine, 1037
MotA-MotB pairs, 1027, 1028f
Motifs
  defined, 48
  helix-turn-helix, 48

  metabolism, 423–424
  repeating, 91, 91f
mRNA
  cDNA prepared from, 149–150
  complementarity with DNA, 122, 122f
  defined, 105, 120
  5′ cap of, 878–879, 879f
  FMN and, 867
  modification of, 123, 123f
  poly(A) tail of, 878–879
  precursors, 876, 880–881, 882–883, 882t
  in protein synthesis, 126
  RNA editing and, 879–880, 879f
  structure of, 912, 912f
  transcription and, 883–884, 884f
  transferrin-receptor, 955, 955f
Mucins
  defined, 326, 329
  overexpression of, 329
  structure of, 329, 329f
Mucolipidosis, 332
Mucopolysaccharidoses, 328
Mucus, 329
Muller, Hermann, 847
Multidrug resistance, 374
Multidrug resistance protein, 374
Multifunctional protein kinases, 295
Multiple myeloma, 81
Multiple-substrate reactions
  classes of, 232
  defined, 231–232
  double-displacement, 232, 233
  sequential, 232
Muscle
  ATP in contraction, 469–470
  excess fatty acids in, 810
  fatty acids in, 810, 815
  fiber types, 625, 625t
  glycogen in, 618
  glycogen phosphorylase in, 625, 625f
  glycolysis in, 469–471
  insulin resistance in, 810–812
  myofibrils in, 1020
  PP1 regulation in, 634, 634f
  sarcomere in, 1020, 1020f
Muscle contraction
  actin in, 1019–1021
  alanine in, 486, 486f
  ATP formation in, 813–815
  ATP hydrolysis in, 1019–1022, 1020f
  fuel sources for, 813–815, 814t, 815f
  gluconeogenesis in, 485–487, 486f
  lactate in, 485–486
  myosin in, 1019–1021
  sliding-filament model of, 1020–1021, 1021f
Muscle-relaxation pathway, 1042–1043, 1043f
Mutagenesis
  cassette, 151, 151f
  oligonucleotide-directed, 150, 151f
  by PCR, 151–152, 151f
  site-directed, 150–151, 151f, 260, 260f
Mutagens, 846–847
Mutase, 460
Mutations
  deletion, 150, 151–152, 151f
  disease-causing, functional effects of, 152
  in genes encoding hemoglobin subunits, 204
  insertion, 150, 151
  at level of function, 177–178
  at level of sequence, 177
  point, 150
  in recombinant DNA technology, 150–152
  substitution, 150
MWC model, 198–199, 199f
Mycobacterium tuberculosis, 142, 687
Myofibrils, 1020
Myogenin, 160, 161f
Myoglobin
  alignment comparison, 173–174, 173f
  alignment with gap insertion, 173, 173f
  amino acid sequences of, 171–172, 171f, 172f
  as compact molecule, 46
  defined, 46, 171, 191
  distribution of amino acids in, 47f
  hemoglobin comparison, 191–192
  Hill plot, 210f
  oxygen-binding, 192–195, 196f
  oxygen-binding curve, 196, 196f
  as single polypeptide, 192
  structure of, 192, **192,** 194–195
  tertiary structure of, 178–179
  three-dimensional structure of, 46f
Myosin
  active site, 279, 279f
  altered conformation persistence, 278–279
  ATP binding to, 1014–1016, 1015f, 1016f
  ATP complex structure, 276, 276f
  ATP hydrolysis and, 276–278
  ATPase transition-state analog, 277, 277f
  binding to actin filaments, 1018, 1018f
  catalytic strategies of, 251–252
  conformational changes, 278, 278f
  defined, 275, 1012
  heavy chains, 1012, 1014, 1014f
  kinetic studies of, 276
  lever arm, 1015, 1015f, 1022, 1022f
  light chains, 1013, 1013f
  motion observation, 1018–1019, 1019f
  movement along actin, 1016–1022, 1020f
  in muscle contraction, 1019–1021
  P-loop NTPase, 1012
  P-loop structures, 280–281
  power stroke release, 1019
  regulatory light chain, 1012
  relay helix, 1016, 1016f
  S1, 1013, 1013f, 1015, 1015f
  S2, 1013–1014, 1013f
  single-molecule motion, 279–280, 280f, 1018–1019, 1019f
  as slow enzymes, 278
  structure of, 1013–1014, 1013f
  switch I and switch II, 1015–1016, 1016f
  in thick filaments, 1020, 1021f
  in thin filaments, 1020
Na$^+$ ions. *See* Sodium ions
Na$^+$-K$^+$ pumps, 370, 373
NAD$^+$ (nicotinamide adenine dinucleotide)
  binding site for, 465, 465f
  in glycolysis, 458, 459f, 462–464, 465
  light absorption and, 67
  from metabolism of pyruvate, 462–464
  reduction potential of, 528
  regeneration of, 464, 464f
  structures of oxidized form of, 435, 435f
  synthesis of, 734, 734f
NADH (nicotinamide adenine dinucleotide reduced)
  in ATP generation, 436
  electrons from, 549–550
  electron-transport chain and, 497, 510, 526, 528–529
  ethanol metabolism in, 820–821
  in fatty acid oxidation, 650–652
  in glycolysis, 458, 462–464
  light absorption, 67
  pyruvate reduction by, 464
  in respiratory chain, 532–533, 533f
  structures of oxidized form of, 435, 435f
  transport of, 549–550
NADH-cytochrome b_5 reductase, 668, 668f
NADH-Q oxidoreductase, 529–531, 530f, 530t, 532–533, 533f
NADP$^+$ (nicotinamide adenine dinucleotide phosphate), 602, 607
NADPH (nicotinamide adenine dinucleotide phosphate reduced)
  in Calvin cycle, 589–590, 597
  dihydrofolate reductase and, 756
  in fatty acid synthesis, 667
  formation by photosystem I, 579
  in glucose 6-phosphate conversion, 602
  pathways requiring, 601f
  in pentose phosphate pathway, 608–610
  in reductive biosynthesis, 436
Nalidixic acid, 839
Neanderthals, 185, 185f
Neck linker, 1016
Negatively charged amino acids, 33–34, 34f
Neher, Erwin, 379
Nernst equation, 387
Nerve impulses, 378, 385
Neural-tube defects, 762
Neuroglobin, 208
Neurological diseases. *See* Diseases and disorders
Neuropeptide Y (NPY), 805–806, 806f
Neurotransmitter release, 360, 361f
Neurotransmitters, 385
Next-generation sequencing (NGS)
  defined, 155
  detection methods in, 155, 155f
  as highly parallel, 155
  ion semiconductor, 156
  pyrosequencing, 155–156
  reversible terminator method, 155
NF-κB, 687
$9 + 2$ array, 1023

Nirenberg, Marshall, 124
Nitric oxide (NO), synthesis of, 735, 735f
Nitric oxide synthase, 735
Nitrogen
  in amino acids, 714
  excess, disposal of, 693–698
  metabolism, 696f, 733
  peripheral tissue transport of, 692–693
Nitrogen fixation
  in amino acid synthesis, 714–718
  ATP in, 715–718
  defined, 714
  FeMo cofactor in, 716, 716f
  glutamate in, 717–718
  glutamine in, 717–718
  iron-sulfur proteins in, 715–716, 715f
  P clusters in, 716, 716f
Nitrogenase, 715, 716, 716f, **716**
Nitrogenase complex, 715
^{15}N labeling, 735b
N-linkage, 326, 326f
N-linked oligosaccharides, 326, 326f, 332
Nociceptors, 977
NompC, 976
Noncompetitive inhibition. *See also* Enzyme inhibition
  defined, 234
  double-reciprocal plot, 236, 236f
  example of, 236
  inhibitor binding, 236
  kinetics of, 235–236, 235f
Nonconservative substitutions, 174, 175f
Noncovalent bonds
  in biological molecules, 7–8
  hydrogen bonds, 5, 7, 8, 8f, 9, 10
  hydrophobic effect and, 9–10, 9f
  types of, 7
  van der Waals interactions, 7, 8, 8f, 10
Nonessential amino acids
  defined, 719
  synthesis of, 719, 720
Nonheme iron proteins, 531
Nonhomologous end joining (NHEJ), 849
Nonribosomal peptides, 670
Nonshivering thermogenesis, 555f, 556, 558
Northern blotting, 138
Novobiocin, 839
N-terminal rule, **684**
NTPases, P-loop. *See* P-loop NTPases
Nuclear envelope, 360, 360f
Nuclear hormone receptors
  defined, 949
  domain structures, 950, 950f
  drug-binding to, 951–952
  in gene expression, 949–951
  ligand-binding to, 950, 951f
Nuclear magnetic resonance (NMR) spectroscopy, 65, 97–100
  basis of, 98, 98f
  chemical shifts, 98
  defined, 97
  NOESY and, 99–100, 99f, 100f
  one-dimensional, 98, 98f
  RNA structure, 187, 187f
  signals, 98f
Nuclear Overhauser effect (NOE), 99
Nuclear Overhauser enhancement spectroscopy (NOESY), 99–100, 99f, 100f
Nuclear pores, 360
Nucleation-condensation model, 53
Nucleic acids. *See also* DNA; RNA
  backbones in, 106–107, 106f
  bases, 106–109
  complementary sequences, 109–114
  complex structures, 113–114, 113f, 114f
  defined, 105
  melting of, 116
  nucleotides as monomeric units of, 107–108
  polymeric structure, 106f
  solid-phase synthesis of, 136
Nucleoside 5′-phosphate, 108
Nucleoside diphosphate, 245
Nucleoside diphosphate kinase, 427, 747
Nucleoside diphosphokinase, 506
Nucleoside monophosphate, 427
Nucleoside monophosphate kinases, 245, 427, 747
Nucleoside phosphorylases, 760, 761
Nucleosides
  defined, 107, 744
  nomenclature of, 744
  units, 107–108
Nucleosome core particle, 943, 943f
Nucleosomes, 943–944
Nucleotidases, 760
Nucleotide synthesis, 743–763
  de novo pathways in, 744–752, 744f
  deoxyribonucleotide, 753–758, 759–760, 759f
  disorders of, 760–762
  inosinate in, 759
  overview of, 743–744
  of purine, 748–752, 748f, 758–759, 758f
  of pyrimidine, 744–748, 744f, 758
  regulation of, 758–760
  salvage pathways in, 744–752, 744f
  substrate channeling in, 745–746, 746f
Nucleotide triphosphates, 107
Nucleotides
  cyclic, 743
  defined, 106, 743, 744
  DNA, 107
  in encoding amino acids, 124
  ester linkage, 107
  metabolism disruptions, 760–762
  as monomeric units of nucleic acids, 107–108
  nomenclature of, 744
  RNA, 107–108
  sequences in DNA, 135–136
  in signal transduction pathways, 743
Nutrition, 20, 20f

Obesity, 801–812
  causes of, 803–804
  diabetes and, 807–812
  dieting and, 807
  evolution and, 802–804
  health consequences of, 803t
  insulin in, 805–806
  insulin resistance and, 809–810, 810f
  leptin resistance in, 806–807, 806f
  overview of, 801–802
  prevalence of, 803–804
Obligate anaerobes, 464, 465t
Octadecanoic acid, 342
Odd-chain fatty acids, 654, 654f
Odorant receptors (ORs), 964f
  activation of, 965f
  conserved and variant regions, 963–964, 964f
  evolution of, 963–964, 963f
  in olfaction, 963–965
Off-diagonal peaks, 99
Okazaki, Reiji, 831
Okazaki fragments, 831–832, 831f, 841
Olfaction, 962–966. *See also* Sensory systems
  anosmias, 962
  combinatorial mechanisms in, 964–966
  electronic nose in, 965–966, 966f
  evolution of, 963–964, 963f
  impaired, 962
  main olfactory epithelium in, 962, 963f
  molecule shape and, 962
  odorant receptors (ORs) in, 963–965, 963f, 964f
  7TM receptors in, 963
  signal transduction in, 964, 964f
Olfactory neurons, 964, 965f
Oligomeric 7TM receptors, 969
Oligomerization, in B-cell activation, 993–994
Oligomycin, 556
Oligonucleotide-directed mutagenesis, 150, 151f
Oligopeptides. *See* Peptides
Oligosaccharide chain, 772
Oligosaccharides, 332f
  antigen structures, 331, 331f
  attached to erythropoietin, 327, 327f
  defined, 323
  enzymes responsible for assembly, 331
  N-linked, 326, 326f, 332
  O-linked, 326
  sequencing of, 332–333, 333f
O-linkage, 326
Omeprazole (Prilosec), 1049, **1049**
Oncogenes, 416
One-dimensional NMR, 98, 98f
Open promoter complex, 866, 866f
Open reading frames (ORFs), 177
Operator site, 928
Operons, 929f, 930f
  defined, 928–929
  histidine, 936–937, 936f

  lac, 929–932, 929f, 930f
  structure of, 928, 929f
  threonine, 936, 936f
  trp, 936
Opsin, 970, 971
Optical traps, 1019f
Oral bioavailability, 1036, 1037f
Origin of replication complexes, 843
Origin of replication (oriC locus), 842
Ornithine, 694–695
Ornithine transcarbamoylase, 694, 696
Ornithine transcarbamoylase deficiency, 697–698, 698f
Orotate, 746–747, 746f, 747f
Orotate phosphoribosyltransferase, 747
Orthologs, 170, 171f
Orthophosphate, 619
Osteoarthritis, 328
Osteogenesis imperfecta, 46
Osteomalacia, 795
Otto, John, 307b
Overlap peptides, 89, 89f
Oxaloacetate, **233**
  in amino acid degradation, 698, 700
  in Calvin cycle, 600, 600f
  in citric acid cycle, 496, 502, 507–508
  conversion into phosphoenolpyruvate, 480
  in fasting or diabetes, 657
  formation of, 480
  in gluconeogenesis, 477f, 478–480, 480f, 819
  in glyoxylate cycle, 517f
  synthesis of, 440–441, 441f
Oxidation
  activated carriers of electrons for, 435
  of aldehydes, 457
  carbon, 432–433
  in drug metabolism, 1037, 1039
  energy, 433
  in fatty acid metabolism, 648–649, 650–652, 651t
  of glyceraldehyde 3-phosphate (GAP), 458–459, 459f
  of membrane proteins, 652f
  phase I transformations in, 1039
  pyruvate dehydrogenase complex and, 498–499
  of succinate, 507–508
Oxidation-reduction potential. *See* Reduction potential
Oxidation-reduction reactions
  free-energy change in, 528
  in metabolism, 440, 440f
Oxidative phosphorylation, 523–560
  ADP in, 550–551, 551f, 553–554, 554f
  ATP yield in, 552–553, 553t
  ATP-ADP translocase in, 550–551, 551f, 557
  cellular respiration in, 552–558
  chemiosmotic hypothesis in, 542–543, 542f, 543f
  defined, 433, 523
  electron transfer in, 526–529
  electron-transport chain in, 548f
  in exercise, 814–815
  inhibition of, 556
  iron sulfur clusters in, 531–532, 532f
  in mitochondria, 524–526, 525f, 526f
  mitochondrial transporters in, 551–552, 551f, 552f
  NADH in, 526, 528–529
  overview of, 523–524, 524f, 548f
  photosynthesis comparison, 579f
  proton gradients in, 433, 433f, 524, 529, 541–549
  proton-motive force in, 523, 542–543, 542f, 544–545, 545f
  rate of, 553–554, 554f
  reduction potential in, 526–528, 526f
  respiratory chain in, 433, 529–541
  respiratory control in, 553–554, 554f
  shuttles in, 549–552, 549f, 550f
  transporters in, 549–552, 551f, 552f
  uncoupling of, 554–556, 555f
Oxidized lipoamide, 499–500
Oxidoreductases, 245t
Oxidosqualene cyclase, 778
Oxoguanine-adenine base pair, 846f
Oxyanion hole
  of chymotrypsin, 257, 257f
  defined, 257
  of subtilisin, 259, 259f
Oxygen
  affinity in red blood cells, 200–201, 201f
  bound, stabilizing, 194f
  carbon monoxide and, 201–202
  concentration in tissues, 197, 197f
  cooperative release of, 197
  evolution of, 574b
  in hydroxylation function, 790–791
  partial pressure, 194–195
  photons for generation of, 574, 574f
  reactive, 194
  toxic derivatives of, 538–540
Oxygen binding
  with concerted model, 212f
  cooperative, 196–197
  heme in, 193–194
  hemoglobin, 192–195, 196f
  hemoglobin quaternary structure and, 197–198, 198f
  myoglobin, 192–195, 196f
  pure hemoglobin, 200, 200f
  sites, 197
Oxygen therapy, hyperbaric, 202
Oxygenase reaction, 593–594, 593f
Oxygenases
  in aromatic amino acid degradation, 703–705
  mixed-function, 703
Oxygen-binding curve
  defined, 195
  fractional saturation, 195
  for hemoglobin, 196, 196f
  for Hill coefficients, 210–211, 211f
  for myoglobin, 196, 196f
  sigmoid, 196
  T-to-R transition, 199, 199f
Oxyhemoglobin, 198
Oxymyoglobin, 192, **193**

P clusters, 716, 716f
P site, ribosomal, 905, 905f
p53, 851
p160 family, 951
P680, 572, 573
P700, 572, 576, 576f
P960, 571–572
PALA, 289–290, 289f, **289,** 290f
Palindromes, 137, 137b
Palmitate, 652, 652f, 666
Palmitoleate, 652–653, 652f
Palmitoyl CoA, 652, 652f, 671, 772
Pamaquine, 611
Pancreas
  α cells, 802
  β cells, 804
  gene expression in, 942, 942t
Pancreatic failure, 810–812
Pancreatic lipases, 645–646, 646f
Pancreatic trypsin inhibitor, 302–303, 302f
Pancreatic zymogens, 301–303, 301f
Papain, 216–217
Paracoccus denitrificans, 541
Paralogs, 170, 171f
Paraquat, 584
Park, James, 1042
Parkinson disease, 56–57, 683, 685
Partial pressure, oxygen, 194–195
Passenger strand, 162
Passive membrane transport, 369
Pasteur, Louis, 450, 1006
Patch-clamp technique, 379, 379f
Pathogen-associated molecular patterns (PAMPs), 982–983, 983t, 984f
Pauling, Linus, 193, 204–205, 222b, 240
PCSK9 (proprotein convertase subtilisin/kexin type), 787, 788
Penicillin, 1041–1042, 1041f, **1041**
  conformations of, 240, 240f, **240**
  mechanism of action, 239–240, 240f
  reactive site of, 239, 239f
  thiazolidine ring, 239
Penicillium citrinum, 1044
Penicilloyl-enzyme derivative, 240, 240f
Pentose phosphate pathway, 601–612
  Calvin cycle and, 610
  in cell growth, 610
  defined, 589, 601
  erythrose 4-phosphate in, 604, 604f
  fructose 6-phosphate in, 604, 604f
  glucose 6-phosphate in, 602, 607–610
  glucose 6-phosphate dehydrogenase in, 610–612
  glyceraldehyde 3-phosphate (GAP) in, 603, 604, 604f
  glycolysis and, 602–610
  illustrated, 602f
  modes, 608–609

Pentose phosphate pathway—(*continued*)
  $NADP^+$ in, 607
  NADPH in, 608–610
  nonoxidative phase of, 602–607, 605t
  overview of, 589–590
  oxidative phase of, 602, 603f, 605t
  rate of, 607
  reactions, 605–607, 605f, 606f
  ribulose 5-phosphate in, 602, 603, 603f, 604, 608–609
  sedoheptulose 7-phosphate in, 603, 603f, 604f
  tissues with, 609t
  transaldolase in, 602–605, 606–607, 606f
  transketolase in, 602–606, 605f
Pentose shunt. *See* Pentose phosphate pathway
Pentoses, 316
Peptide bonds
  chemical nature of, 253
  cis configuration, 38, 38t, 39t
  cleavage of, 59, 258
  defined, 35
  formation in translation, 908–909, 908f
  formation of, 35f
  hydrolysis of, 253
  lengths, 38, 38t
  as planar, 38, 38t
  rigidity of, 39
  rotation of, 38–39, 39t
  stability of, 35
  torsion angles, 39, 39b
  trans configuration, 38, 38t, 39t
  X-Pro linkages, 38, 39t
Peptide mass fingerprinting, 91
Peptide sequences, 52f
Peptide-ligation methods, 95
Peptides
  gastrointestinal, 804–805, 805t
  mass spectroscopy for sequencing, 87–88, 88f
  nonribosomal, 670
  overlap, 89, 89f
  presentation by internalized proteins, 1000
  presentation by MHC proteins, 996–998, 996f
  synthesis of, 92–95, 94f
Peptidoglycan, 239, 239f
Peptidyl transferase center, 908
Perforin, 1000
Peripheral membrane proteins, 351, 351f
Periplasm, 359
Periplasmic side, 570
Permeability
  lipid bilayers, 349–350, 350f
  membrane, 341, 367, 390–391
  of potassium ion channels, 382
  selective, 341
Permeability coefficients, 350, 350f
Perovskite, 585
Peroxide bridge, in cytochrome *c* oxidase, 538, 538f
Peroxisomes
  in Calvin cycle, 593
  defined, 657
  electron micrograph of, 594f, 657f
  in fatty acid oxidation, 656–657, 657f
Perutz, Max, 195
PEST sequences, 684
P-glycoprotein, 374
pH
  buffers and, 15–17
  carbon dioxide and, 203, 204
  defined, 13
  effect on carbonic anhydrase activity, 265, 265f
  ionization state as function of, 30f
Pharmacogenetics/pharmacogenomics, in drug development, 1050
Pharmacology, 1034b. *See also* Drug development
Phase I transformations, in oxidation, 1039
Phase II transformations, in conjugation, 1039
Phenotype-genotype correlation, 1050–1051, 1050f
Phenyl isothiocyanate, 87
Phenylalanine
  degradation of, 703, **703,** 704f
  structure of, 31f, 32
  synthesis of, 727–728, 728f
Phenylalanine hydroxylase, 703
Phenylketonuria, 705
Phenylpyruvate, 728
Phosphatases
  deficiency, 512
  defined, 295
  in phosphorylation, 294–296, 295t
  PP2A, 296
Phosphate carrier, 552
Phosphate esters, 434
Phosphates, 16, 434
Phosphatidate, **344,** 769, **769**
Phosphatidic acid phosphatase (PAP), 768, 775–776, 775f
Phosphatidylcholine, synthesis of, 770–771, 771f
Phosphatidylethanolamine, 770, **770**
Phosphatidylethanolamine methyltransferase, 771
Phosphatidylinositol, 769, **769**
Phosphatidylinositol 3,4,5-trisphosphate (PIP_3), 410, 410f, 808–809
Phosphatidylinositol 4,5-bisphosphate (PIP_2), 404, 405f, 410, 410f, 770, 808
Phosphatidylinositol-dependent protein kinase (PDK), 809
Phosphatidylserine, 771
Phosphocreatine, **232**
Phosphoenolpyruvate (PEP)
  formation of, 461
  in gluconeogenesis, 477f
  in glycolysis, 461
  NAD^+ regeneration in, 462–464
  phosphoryl-transfer potential, 430, 461
Phosphoenolpyruvate carboxykinase, 480
Phosphoenolpyruvate carboxylase, 600
Phosphofructokinase (PFK), 454
  activation of, 472, 472f
  in liver, 472, 472f
  in muscle, 469–470, 470f
  regulation of, 472, 472f
Phosphofructokinase 2 (PFK2), 483–484, 484f
Phosphoglucomutase, 623f
Phosphogluconate pathway. *See* Pentose phosphate pathway
6-phosphogluconate dehydrogenase, 602
6-phosphoglucono-δ-lactone, 602, 603f
Phosphoglucose isomerase, 454
2-phosphoglycerate, in glycolysis, 460–461, 460f
3-phosphoglycerate
  in Calvin cycle, 591–592, 592f
  in cysteine synthesis, 722–723
  in glycine synthesis, 722–723, 723f
  in glycolysis, 460–461, 460f
  in oxygenase reaction, 593, 593f
  in serine synthesis, 722–723, 722f
3-phosphoglycerate dehydrogenase, 730–731
Phosphoglycerate kinase, 459
Phosphoglycerate mutase, 460, 622
Phosphoglycerides, 344
Phosphoglycolate, 593, 593f, 594f
Phosphoinositide cascade, 629
  activation of, 404–405
  defined, 404
  illustrated, 405f
  reaction, 405, 405f
Phospholipase C, 404
Phospholipid synthesis
  from activated alcohol, 770
  activated intermediate, 769–770
  phosphatidylcholine, 770–771, 771f
  sources of intermediates in, 768–776, 768f
Phospholipids
  base-exchange reactions in generation of, 771
  in bimolecular sheet formation, 348–350
  flip-flop, 357, 357f
  lipid vesicles formed from, 348–349
  melting temperature, 357, 357f
  membrane, 344–345
  platform for, 344
Phosphopantetheine, 662f
Phosphopentose epimerase, 595
Phosphopentose isomerase, 595
Phosphoribomutase, 760
5-phosphoribosyl-1-pyrophosphate (PRPP)
  in purine synthesis, 749, 759
  in pyrimidine synthesis, 728, 746–747, 747f
Phosphorolysis, in glycogen metabolism, 619–623
Phosphorothioates, 270–271, 271f

Phosphoryl group, 296
Phosphorylase. *See* Glycogen phosphorylase
Phosphorylase *a*, 623–624, 624f, 626, 627f, 636, 636f
Phosphorylase *b*, 623, 624f, 625, 626, 627f
Phosphorylase kinase
  activation of, 626, 627f
  defined, 626
  subunits, 626, 627f
Phosphorylation
  amplified effects of, 296
  ATP formation by, 580, 580f, 581
  cAMP stimulation of, 403
  of carboxyl-terminal domain (CTD), 875
  of carboxyl-terminal tail, 413
  in citric acid cycle, 511–512
  control of, 294–296
  in covalent modification, 293, 294t
  dephosphorylation and, 296
  EGF receptor, 413
  in enzyme regulation, 293–298, 294t
  free energy of, 296
  of fructose 6-phosphate, 454
  in gluconeogenesis, 480, 484
  in glycogen metabolism, 619–620
  in glycolysis, 451–453, 454
  in metabolism, 427, 433
  of nucleoside monophosphates, 427
  oxidative. *See* oxidative phosphorylation
  in phosphorylase activation, 626, 627f
  in phosphorylase conversion, 626
  in purine nucleotide synthesis, 749–751, 749t, 750f
  of pyruvate dehydrogenase, 511
  reactive intermediates, 323
  of serine residue, 484
  substrate-level, 460
  sugars, 323
Phosphorylethanolamine, 770, **770**
Phosphoryl-transfer potential, 429, 430–431, 430f, 432–433
Phosphoserine, **57,** 58
Phosphothreonine, 58
Phosphotriesters, 139, 140f, **140**
Photoinduced charge separation, 569–572, 569f
Photophosphorylation, cyclic, 580, 580f, 581
Photoreceptors, 970, 973–974, 973f
Photorespiration
  in C_4 pathway, 599–601
  in Calvin cycle, 594, 594f
Photosynthesis, 565–586
  accessory pigments in, 581–584
  artificial photosynthetic systems and, 585
  in autotrophs, 566
  bacterial reaction center, 569–572, 570f, 571f
  basic equation of, 565
  chlorophylls in, 568–572
  in chloroplasts, 567–568, 567f
  components of, location of, 583–584, 584f
  cyclic photophoshorylation in, 580, 580f, 581
  dark reactions, 566, 589
  defined, 565
  electron transfer in, 568–572
  energy conversion in, 566–567
  enzymes in, 217
  herbicide inhibition of, 584, **584**
  in heterotrophs, 566
  light absorption in, 569, 569f
  light energy conversion in, 566–567
  light reactions in, 566, 566f, 581, 584, 589
  light-harvesting complexes in, 583, 583f
  overview of, 565–567
  oxidative phosphorylation comparison, 579f
  photo charge separation in, 569–572, 569f
  photosystem I. *See* photosystem I
  photosystem II. *See* photosystem II
  proton-motive force in, 578
  reaction centers in, 569–572, 570f, 571, 572f, 576, 576f, 581–584
  resonance energy transfer in, 582–583, 582f
  in thylakoid membranes, 567–568
  yield in, 566b
  Z scheme of photosynthesis, 577, 577f
Photosynthetic catastrophe, 567b
Photosynthetic systems, 584–585, 584t
Photosystem I. *See also* Photosynthesis
  defined, 567, 572
  electron flow through, 580
  ferredoxin generated by, 576–577
  illustrated, 572f
  inhibitors of, 584
  link to photosystem II, 575, 575f
  NADPH formation by, 579
  reaction center, 572, 576, 576f
  structure of, 575–576, 575f
  Z scheme of photosynthesis, 577, 577f
Photosystem II. *See also* Photosynthesis
  defined, 567
  electron flow through, 573b
  electron source, 573–574
  illustrated, 572f
  inhibitors of, 584
  link to photosystem I, 575, 575f
  location of, 574–575
  photochemistry of, 573
  reaction center, 572, 573
  structure of, 573, 573f
  Z scheme of photosynthesis, 577, 577f
Phytol, 569
Pichia pastoris, 78
Ping-pong reactions, 233
Pinopsin, 974
pK_a values, 34t
Placebo effect, 1052
Planar bilayer membrane, 349, 349f
Planck's constant, 222
Plants
  C_3, 601
  C_4, 600–601
  genetically engineered, 163–164, 163f
  glyoxylate cycle in, 516–517, 517f
  oxaloacetate synthesis, 660
  photosynthesis in. *See* photosynthesis
  starch in, 597
  sucrose synthesis in, 597–598, 598f
  thylakoid membranes of, 583
Plaques, in genomic library screening, 148, 148f
Plasma-membrane proteins, 916, 916f
Plasmids
  defined, 144
  engineered, 145
  expression vectors, 146
  genes, 144
  microinjection of, 159f, 160
  polylinker region, 145, 145f
  Ti, 163–164, 163f
  as vectors for DNA cloning, 144–146
Plasmin, 308
Plasminogen, 308
Plasmodium falciparum, 206, 336, 525
Plastocyanin, 583
Plastoquinone, 572–573, 583
Pleckstrin homology domain, 410
P-loop NTPases
  in helicases, 832
  molecular motors, 1012–1016
  proteins containing, 280–281
P-loop structures, 280–281
PLP-Schiff-base linkage, 621
Pluripotent stem cells, 947
Point mutation, 150
Poisoning
  arsenite, 516, 516f
  mercury, 515–516
  ricin, 915
Polar amino acids
  structure of, 33
  types of, 32–33
Poly(A) tail-binding protein I (PABPI), 912, 912f
Polyacrylamide gel electrophoresis (PAGE), 72, 72f
Polyampholytes, 73
Polyclonal antibodies, 80, 80f
Polygalacturonase, 164
Polyketides, 670
Polylinker region, plasmid, 145, 145f
Polymerase chain reaction (PCR)
  cycle steps, 141f, 142, 142f
  defined, 141
  DNA sequence amplification by, 141–142, 141f, 142f
  first cycle of, 141f
  as gene exploration tool, 136
  inverse, 151, 151f
  multiple cycles of, 142f
  mutagenesis by, 151–152, 151f
  quantitative (qPCR), 157–158, 158f
  uses of, 142–143
Polymerase switching, 843–844
Polymerization reactions, 1018
Polymorphisms, 1002–1003, 1003f

Polypeptide chains
  backbone, 36, 36f
  bond rotation in, 38–39, 39t
  cleavage of, 88, 89t
  components of, 36f
  cross-linked, 36–37, 37f
  directionality of, 35–36
  disulfide bonds of, 36–37, 37f
  flexibility of, 38–39
  formation of, 35
  loops, 44, 44f
  random-coil conformation, 50
  residue, 35
  reverse turns, 44, 44f
  side chains, 36, 36f, 47
  subunit structures, 48–49
Polypyrimidine tract, 880
Polysaccharides
  defined, 324
  glycosidic bonds, 325, 325f
Polysomes, 910, 910f
Polyunsaturated fatty acids, 661, 669
Pompe disease, 637–638, 637t, 638f
Porin
  amino acid distribution in, 47f
  amino acid sequence of, 352, 352f
  defined, 352
  hydropathy plot for, 355, 356f
  structure of, **352**
Porphobilinogen, 736, 737, 737f
Porphobilinogen deaminase, 736
Porphyrias, 737–738
Porphyrins, 241
  disorders of, 737–738
  synthesis of, 736–737, 737f
Porter, Rodney, 985
Positively charged amino acids, 33, 33f
Posttranscriptional gene expression
  in eukaryotes, 954–957
  in prokaryotes, 935–937
Posttranslational modifications, 90
Potassium ion channels
  as archetypical structure, 379–380
  hERG, 389
  inactivation of, 384–385, 385f
  path through, 381, 381f
  permeability of, 382
  purification of, 380
  selectivity filter, 381, 381f, 382, 382f
  structure of, 380–382, 381f, 382
  transport model, 383, 383f
  voltage-gated, 383–384, 384f
Potassium ions
  action potentials and, 378
  dehydration of, 382, 382f
  hydration of, 383f
Potential energy, 11
Power stroke, 1019
PP2A, 296
Precursor ions, 87
Pregnenolone
  androgen synthesis by, 792–793
  corticosteroids from, 792
  defined, 792
  estrogen synthesis by, 792–793
  progesterone from, 792
  structure of, **793**
  synthesis of, 792–793
Pre-mRNA processing, 877, 877t, 878–879, 878f, 884–885, 884f
Prephenate branch, 728
Prilosec (omeprazole), 1049, **1049**
Primaquine, 611
Primary active transport, 367
Primary antibody, 83–84
Primary messenger, 398
Primary protein structure, 27, 35–40, 48, 78–79
Primase, 831
Primers
  defined, 829b
  DNA probes as, 140
  in DNA replication, 831, 831f
  match stringency, 142
  in polymerase chain reaction (PCR), 141–142, 141f
  RNA, 841
Prion diseases, 56–57, 57f
Prions, 56, 56f
Probes. *See* DNA probes
Procaspases, 299
Processivity
  defined, 621, 839, 840b
  in DNA replication, 839–840, 839f
  kinesin motion, 1024–1026
Procollagen, 300
Product ions, 87
Progesterone, 789, 792, **793**
Progestogen, 789
Programmed cell death. *See* Apoptosis
Proinsulin, synthesis of, 150, 150f
Prokaryotes. *See* Bacteria
Prokaryotic RNA polymerases, 860, **860**
Proliferating cell nuclear antigen (PCNA), 832
Proline
  degradation, 701, 701f
  structure of, 31f, 32
  synthesis of, 722–723
Prolyl hydroxylase, 821
Prolyl hydroxylase 2, 513
Promoter sites
  base sequences, 122b
  defined, 122
  for transcription, 122, 122f
Promoters
  alternative sequences, 865, 865f
  bacterial, 864, 864f
  closed complex, 865–866, 866f
  core, 864
  defined, 864
  open complex, 866, 866f
  strong, 864
  upstream of, 864
  weak, 864
Pro-N-terminal degrons, 684
Proofreading
  in DNA repair, 847, 848f
  in transcription, 863
  in translation, 900–901
Propionyl CoA, 654, 654f, 701–702
6-*n*-propyl-2-thiouracil, 967, **967**
Prostacyclin, 669
Prostacyclin synthase, 669, 669f
Prostaglandin, 669
Prostaglandin H_2
  attachment of, **353**
  defined, 353
  formation of, 353, 353f
  synthase-1, 353f, 354f
Prostaglandin H_2 synthase-1, 353–354, 353f
Prosthetic groups, 46, 217
Protease inhibitors
  α_1-antiproteinase, 303
  drugs, 263–264, 263f
  in HIV infection treatment, 263, 263f, 792, 1046, 1046f, 1053
  initial design of, 1046, 1046f
  pancreatic trypsin inhibitor, 302–303, 302f
  serine, 302
Proteases, 333
  active sites, 261f
  applied to glycoproteins, 333
  aspartyl, 261f, **261,** 262, 262f
  catalytic triad in, 258–260
  cysteine, 261–262, 261f, **261**
  metalloproteases, 261f, **261,** 262
  reaction facilitation, 253–264
  serine, 251
Protease-substrate interactions, 258, 258f
Proteasomes. *See also* Amino acid degradation
  19S regulatory unit, 685, 685f
  20S, 685, 685f
  26S, 685, 685f
  in amino acid degradation, 685–686
  defined, 681
  evolution of, 686, 686f
  free amino acid generation, 686f
  prokaryotic, 686, 686f
Protein colipase, 646
Protein Data Bank, 100
Protein domains, 48, 48f
Protein folding, 904f
  essence of, 53
  funnel, 54, 54f
  as highly cooperative process, 52–53
  illustrated, 21f
  Levinthal's paradox in, 53
  misfolding and, 811
  nucleation-condensation model, 53
  pathway of chymotrypsin inhibitor, 54f
  by progressive stabilization, 53–54
  transition from folded to unfolded, 52f
  typing-monkey analogy, 53, 53f
Protein identification
  cleavage in, 88–89, 89f
  genomic and proteomic methods as complementary, 89–90

  MALDI-TOF mass spectroscopy in, 86, 86f
  mass spectroscopy in, 85–92, 86f, 88f, 92f
  peptide mass fingerprinting, 91
  in protein studies, 65
Protein kinase A (PKA)
  bound to inhibitor, 298, **298**
  cAMP activation of, 297, 297f
  catalytic subunit, 298, 298f
  chains, 403
  consensus sequence, 295
  defined, 286
  gene stimulation, 403
  in glycogen metabolism, 633, 633f
  pseudosubstrate binding to, 298, 298f
  regulation of, 297, 297f
  in signal transduction, 415
Protein kinase B (PKB), 809
Protein kinase C (PKC), 810
Protein kinase inhibitors, as anticancer drugs, 417
Protein kinases
  catalysis, 286
  dedicated, 295
  defined, 294
  kinase fold, 298
  multifunctional, 295
  in phosphorylation, 294–296, 295t
  serine, 294–295, 295t
  in signal transduction, 415
  specificity, 295
  threonine, 294–295, 295t
Protein phosphatase 1 (PP1)
  functions of, 629, 633–635
  in glycogen metabolism, 629, 633–635, 634f, 636
  phosphorylase *a* and *b* and, 636
  regulation in muscle, 634, 634f
  regulation of glycogen synthesis by, 633–634, 634f
  substrate for, 636
  subunits, 634
Protein purification, 78
  affinity chromatography in, 70–71, 70f
  assays in, 67
  binding affinity and, 68–71
  cell release and, 67–68
  charge and, 68–71
  dialysis in, 69, 69f
  electrophoretic analysis of, 75f
  gel electrophoresis in, 71–73, 72f, 73f
  gel-filtration chromatography in, 69, 69f
  high-performance liquid chromatography (HPLC) in, 71, 71f
  homogenization in, 67
  ion-exchange chromatography in, 69–70, 70f
  isoelectric focusing in, 73, 73f
  in protein studies, 65
  quantitative evaluation of, 75–76, 75f
  recombinant DNA technology in, 78–79
  salting out in, 68
  SDS-PAGE in, 73, 73f, 74
  sedimentation coefficient and, 76, 77f
  sedimentation-equilibrium technique in, 78
  separation of proteins in, 71–75
  size and, 68–71
  solubility and, 68–71
  two-dimensional electrophoresis in, 74–75, 74f
  ultracentrifugation and, 76–78, 77f
  zonal centrifugation in, 77, 77f
Protein sorting
  defined, 915
  pathways, 918, 918f
Protein structures, 2f, 3
  amino acid sequence as determinant, 49–59
  amino acid sequences and, 37, 37f
  complex assembly, 28, 28f
  dictating function, 28f
  elucidation of, 100
  family of, 100, 100f
  models of, 22–23, 23f, 61–62
  primary, 27, 35–40, 48, 78–79, 178–179
  quaternary, 27, 48–49
  secondary, 27, 40–46, 48
  synthetic peptides and, 93
  tertiary, 27, 46–48, 178–179
  three-dimensional prediction from sequence, 54
Protein studies
  enzyme-linked immunosorbent assay (ELISA) in, 82–83, 83f
  fluorescence microscopy in, 84, 84f
  immunology in, 79–84
  mass spectroscopy in, 85–92, 86f, 88f, 92f
  peptide synthesis, 92–95
  purification methods for, 66–79
  steps in, 65–66
  western blotting in, 83–84, 83f
  x-ray crystallography in, 95–97
Protein synthesis, 893–921. *See also* Translation
  accuracy of, 894–895, 894t
  adaptors in, 123, 123f
  antibiotic inhibitors of, 913–915, 914f, 914t, 915f
  endoplasmic reticulum (ER) in, 915–919
  eukaryotic versus bacterial, 911–913
  insulin in, 816
  mRNA in, 126
  peptide-ligation methods, 95
  polypeptide-chain growth in, 894, 894f
  ribosomes as site of, 893, 902–911
Protein targeting, 915–919
Protein turnover. *See also* Amino acid degradation
  defined, 682
  regulation of, 683–687
Proteins, 27–63
  acetylation of, 293–294
  adaptor, 410
  affinity tags and, 78
  aggregated, in neurological diseases, 56–57, 56f
  aggregation of, 683
  allosteric, 285, 286–292
  alpha helix of, 40–41
  amino acids. *See* amino acids
  antibody generation to, 79–80
  β pleated sheets of, 44–45, 44f, 45f
  as building block, 20
  building blocks, 2
  carbohydrate units of, 58
  cargo, 918–919
  cellular, degradation of, 682–683
  chaperone, 50
  cleavage of, 57–59, 88–89, 89f
  coat (COPs), 919
  coiled-coil, 44–45, 44f, **44,** 45f
  covalent modification of, 293–298, 294t
  crystallization of, 95
  defined, 2, 36
  degradation of. *See* amino acid degradation
  denatured, 52, 52f
  dietary, digestion and absorption of, 682, 683f
  disulfide bonds, 36–37
  DNA-binding, 926–932
  enzymes as, 215
  evolution of, 128
  fibrous, 44–46
  flexibility of, 29, 29f
  functional groups of, 27–28
  functions of, 27–29
  genetically engineered, 152
  glycan-binding, 334
  glycosylation of, 327–332
  half-life of, 683, 684, 685t
  hemoglobin as model of, 191–212
  interaction of, 28
  intrinsically unstructured, 55–56
  as linear polymers, 27–28, 35
  loops, 44, 44f
  membrane. *See* membrane proteins
  metamorphic, 55–56
  misfolding of, 56–57
  molecular weights of, 76t
  overview of, 65–66
  plasma-membrane, 916, 916f
  properties of, 27–29
  pure, 66
  refolding of, 50, 50f
  regulatory, 930
  release factors, 126
  repressor, 928
  reverse turns, 44, 44f
  ribosomal. *See* ribosomes
  rigidity of, 29
  S values of, 76t
  secretory, 916, 916f
  secretory pathway, 915–916
  separation of, 65, 71–75
  subunits of, 48–49
  tagging for destruction, 683–685
  translocation of, 915–919
  unfolding of, 52, 52f
  unstructured, 55–56

Proteoglycans
  in cartilage, 328–329, 329f
  defined, 326
  properties of, 327–328
  structural roles, 327–328
Proteolysis, 216, 819
Proteolytic activation, 286, 299–308
  apoptosis by, 299
  of chymotrypsinogen, 299–300, 300f
  zymogens, 301, 301f
Proteolytic enzymes
  activation of, 299–308
  in blood clotting, 303–304
  chymotrypsinogen as, 299–301, 300f
  in digestion, 299–303
  function of, 216
  inhibitors of, 302–303
Proteomes, 66
Prothrombin, 304, 304f
Proton abstraction, 268
Proton gradients
  across thylakoid membrane, 578–581
  in ATP synthesis, 541–549
  cytochrome *bf* contribution to, 575, 575f
  directionality of, 575, 575f
  in oxidative phosphorylation, 433, 433f, 523, 524, 529, 541–549
  power transmission by, 558, 558f
Proton shuttle, 267–268, 268f
Proton transport, 538, 538f
Proton-motive force
  ATP forms without, 544–545, 545f
  in oxidative phosphorylation, 523, 542–543, 542f
  in photosynthesis, 578
Proto-oncogenes, 416
Protoporphyrin, 192
Protoporphyrin IX, 736, 737f
Proviral DNA, 159
Proximal histidine, 193, 200
PrP, 56
Prusoff, William, 1035
Pseudo-first-order reactions, 226
Pseudogenes, 154
Pseudosubstrate sequence, 297
Psoralens, 847, 883
P-type ATPases
  defined, 367, 370
  as evolutionarily conserved, 374
  SERCA, 370–373
Puffer fish, genome of, 157, 157f
Pumps
  action, 371, 371f
  ATP-driven, 367
  calcium ion, 371, 371f, 372–374, 372f
  defined, 367
  ion gradients, 368
  MDR, 374
  Na^+-K^+, 370, 373
  purification of, 370
Pur repressor, 931, 931f
Purine biosynthetic pathway, 696
Purine catabolism, 760f
Purine nucleotide synthesis, 24, 34, 724
  AMP in, 751–752
  control of, 758–759, 758f
  de novo pathway for, 450f, 748, 748f, 749t
  enzymes of, 752
  GMP in, 751–752
  phosphorylation in, 749–751, 749t, 750f
  ribose phosphate in, 749
  salvage pathway for, 748, 752
Purine nucleotides, **107,** 748
Purinosomes, 752, 752f
Puromycin, 914, 914t, **914**
Pyran, 318
Pyranose, 318, 319f, 320–321
Pyridoxal phosphate enzymes
  bond cleavage in, 691, 691f
  reaction choice, 691–692, 692f
  stereoelectronic effects, 691, 691f
Pyridoxal phosphate (PLP), 621, 621f
  in amino acid degradation, 682, 691–692
  in Schiff-base intermediates formation, 689–690
  in Schiff-base linkage, 720
Pyridoxamine phosphate (PMP), 690, 720, 720f
Pyridoxine (vitamin B_6), 689
Pyrimidine biosynthetic pathway, 696
Pyrimidine nucleotide synthesis, 734
  carbamoyl phosphate in, 745, **745**
  control of, 758
  cytidine triphosphate (CTP) in, 747–748
  de novo pathway for, 744, 744f
  glutamine in, 745
  mono-, di-, and triphosphates in, 747
  orotate in, 746–747, 746f
  substrate channeling in, 745–746, 746f
Pyrimidine nucleotides
  defined, 744
  recycling of, 748
Pyrimidines, **107**
Pyrosequencing, 155–156
Pyrrolidine rings, 45, 45f
Pyruvate, **232**
  in amino acid degradation, 692–693, 698, 699–700, 699f
  in ATP formation, 460–461
  carboxylation of, 479–480, 514
  conversion into phosphoenolpyruvate, 478–480, 479f
  fates of, 462, 462f
  glucose conversion into, 461–462
  in glycolysis, 452f
  metabolism disruption, 515–516
  oxaloacetate synthesis from, 440–441, 440f
  reduction of, 464, 464f
Pyruvate carboxylase
  in citric acid cycle, 514–515
  in gluconeogenesis, 478–480, 479f
Pyruvate decarboxylase, 462–463, 513
Pyruvate dehydrogenase, in citric acid cycle, 511–512
Pyruvate dehydrogenase complex
  carbon dioxide production, 498–500
  in citric acid cycle, 497–501, 497f, 497t, 501f, 511–512, 511f
  components of, 498–500, 499f
  of *E. coli*, 497f, 497t
  mechanism, 498–500, 499f
  reactions of, 500–501, 501f
  regulation of, 511–512, 511f
  response to energy change, 511, 511f
Pyruvate dehydrogenase kinase (PDK), in cancer, 513
Pyruvate dehydrogenase phosphatase, 511
Pyruvate kinase
  liver and glycolysis and, 473, 473f
  muscle and glycolysis and, 471
Pyruvate kinase M, 475

Q cycle
  defined, 535
  in respiratory chain, 535, 535f
Q-cytochrome *c* oxidoreductase
  defined, 533–534
  in respiratory chain, 529–531, 530f, 530t, 533–534
  structure of, 534, 534f
Quantitative PCR (qPCR), 157–158, 158f
Quaternary protein structure, 27, 48f
  complex, 49f
  defined, 48
Quinones
  oxidative states of, 531, 531f
  ubiquitous, 530
Quinonoid intermediate, 690
Quorum sensing, 934, 934f

R groups. *See* Amino acid side chains
R state, of hemoglobin, 198, 199f, 200, 211–212
Racker, Efraim, 542b
Raf, 414
Raloxifene, **952**
Ramachandran plot
  for angles of rotation, 40f
  β stands, 42f
  defined, 39
  for helices, 40f
Random-coil conformation, 50
Ranitidine (Zantac), 1049, **1049**
Ras
  activation of, 413, 413f
  affixation to cytoplasmic face, 294
  GTPase activity of, 414, 414t
  in protein kinase cascade initiation, 414
Rate constants, 225–226
RBP4, 806
Reactants, 219
Reaction centers
  accessory pigments and, 581–584, 583f
  bacterial, 569–572, 570f, 571f
  cyclic electron flow in, 572, 572f
  defined, 569

  photosystem I, 572, 576, 576f
  photosystem II, 572, 573
Reaction rates
  enzymes and, 220–221, 220f
  free-energy difference and, 218
  kinetics as study of, 225–226
  rate constants, 225–226
Reactions
  acid-base, 13–15
  ATP hydrolysis, 279, 279f
  bimolecular, 226
  in Calvin cycle, 590–597, 597f
  carbonic anhydrases and, 264–268
  of citric acid cycle, 508
  deleterious, 456
  DNA ligase, 832, 832f
  double-displacement, 232, 233
  enzyme acceleration of, 221–225
  equilibrium, 220–221
  equilibrium constant of, 220
  in fatty acid oxidation, 651t
  in fatty acid synthesis, 662–664
  first-order, 225
  free-energy difference of, 218, 219
  of gluconeogenesis, 482t
  group-transfer, 441, 441f
  hydrolytic, 441–442, 442f
  isomerization, 441, 441f
  ligation, 440–441, 440f
  multiple-substrate, 231–233
  oxidation-reduction, 440, 440f
  oxygenase, 593–594, 593f
  pentose phosphate pathway, 605–607, 605f, 606f
  polymerization, 1018
  pseudo-first-order, 226
  of pyruvate dehydrogenase complex, 500–501, 501f
  reduction potentials of, 527t, 528–529
  second-order, 226
  sequential, 232
  standard reduction potentials of, 527
  transaldolase, 606–607, 606f
  transketolase, 605–606, 605f
  velocity versus substrate concentration, 222, 222f
Reactive oxygen species (ROS)
  defined, 539
  glucose 6-phosphate dehydrogenase in protection against, 610–612
  pathological conditions that may entail injury, 539t
  release prevention, 194–195
  source of, 656
Reactive substrate analogs, 237–238, 237f, 238f
RecA, 853, 933
Receptor-mediated endocytosis, 360–361, 360f, 784, 784f
Reclinomonas americana, 526
Recognition helix, 927
Recognition sites (sequences), 269
  in cognate and noncognate DNA, 272–274, 273f, 274f
  defined, 269
  distortion of, 273–274, 273f
  EcoRV endonuclease, 272, 272f
  structure of, 272, 272t
  tRNA template, 123
Recombinant DNA
  formation of, 143–144
  manipulation of, 143
Recombinant DNA technology, 135–166
  amino acid sequence information, 89–90
  bacterial artificial chromosomes in, 147
  in biology, 143–152
  blotting techniques in, 136, 138, 138f
  cloning in, 147–148
  cohesive-end method in, 144, 144f
  complementary DNA (cDNA) in, 149–150, 149f, 150f
  defined, 135
  in disease-causing mutations identification, 143
  DNA probes in, 138, 139–141
  DNA sequencing in, 136, 138–139
  DNA synthesis in, 139–141, 140f, 141
  electroporation in, 163, 164f
  functional effects of disease-causing mutations and, 152
  λ phase in, 144–146, 147f
  gel electrophoresis in, 137–138, 138f
  gene disruption in, 160–163, 160f, 161f
  gene expression analysis in, 157–159, 158f, 159f
  gene therapy in, 164
  genomic libraries in, 147–148, 148f
  mutation creation, 150–152
  in mutation identification, 143, 143f
  overview of, 135–136
  in plants, 163–164, 163f
  plasmids in, 144–146
  polymerase chain reaction (PCR) in, 136, 141–143, 141f, 142
  in protein purification, 78–79
  requirement, 136
  restriction-enzyme analysis in, 136, 137
  RNA interference in, 162–163, 162f
  solid-phase approach in, 139–141, 140f
  tools of, 136–143
  transgenic animals in, 159f, 160
  vectors in, 145–146
  yeast artificial chromosomes (YACs) in, 147, 147f
Recombinases, 854
Recombination
  in antibodies, 991–995, 991f, 992f
  in color blindness, 974–975, 974f
  DNA. *See* DNA recombination
  homologous, 974b
Recombination signal sequences (RSSs), 992
Recombination synapse, 854
Redox balance, 463, 463f
Redox couples, 527
Redox potential. *See* Reduction potential
Reducing sugars, 321–322
Reductase mRNA, in cholesterol regulation, 781
5α-reductase, 793
Reduction potential
  measurement of, 526, 526f
  of NAD$^+$, 528
  in oxidative phosphorylation, 526–528, 526f
  of reactions, 527t, 528–529
Reed, Randall, 963
Regulator genes, 928
Regulatory domains
  in amino acid synthesis, 731–732
  recurring, 731f
  structures of, 732f
Regulatory light chain, 1012
Regulatory protein P$_{II}$, 733, 733f
Regulatory proteins, 930
Regulatory sites, 287
Relay helix, 1016, 1016f
Release factors
  defined, 126
  ribosome (RRF), 911
  translation termination by, 910–911, 911f
Repeating motifs, 91, 91f, 180–181, 180f
Replication factor C (RFC), 844
Replication fork. *See also* DNA replication
  defined, 831
  schematic view of, 840f
Replication protein A, 843
Replicon, 843
Reporter genes, 145
Repressors
  corepressors, 931
  λ, 932–934, 933f
  lac, 928–930, 929f, 930f
  protein, 928
  pur, 931, 931f
Resistin, 806
Resonance energy transfer, 582–583, 582f
Resonance structures
  ATP (adenosine triphosphate), 429
  defined, 7
  depiction of, 7
  improbable, 429f
Respirasome, 529
Respiration, 524b
Respiratory chain
  coenzyme Q in, 530–531
  components of, 530f, 530t
  cytochrome *c* oxidase in, 529, 530f, 530t, 535–538
  defined, 523
  electron transfer in, 540–541, 540f
  NADH-Q oxidoreductase in, 529–531, 530f, 530t, 532–533, 533f
  in oxidative phosphorylation, 529–541
  Q cycle in, 535, 535f
  Q-cytochrome *c* oxidoreductase in, 529, 530f, 530t, 533–534
  succinate-Q reductase in, 529, 530f, 530t, 533

Respiratory control, 553–554, 554f
Respiratory distress syndrome, 774
Respiratory quotient (RQ), 815
Restriction enzymes (endonucleases), 251
  analysis, 137
  defined, 137b, 269
  in DNA cleavage, 137, 269–275
  in *E. coli*, 269
  in forming recombinant DNA molecules, 143–144
  hydrolysis of phosphodiester bond, 269–270, 269f
  inverted repeats, 272, 272f
  recognition sites, 272, 272f, 273–274, 273f
  restriction-modification systems, 274
  specificity, 137, 137f, 272, 274
  type II, 275
Restriction fragments
  separation by gel electrophoresis, 137–138, 138f
  in Southern blotting, 138
Restriction-modification systems, 274
11-*cis*-retinal, 970, 971–972, 972f
Retinitis pigmentosa, 884–885
Retrovir, 263
Retroviruses
  defined, 118
  in drug resistance evolution, 1053
  flow of information in, 119, 119f
  in gene introduction, 159
Reverse cholesterol transport, 787
Reverse transcriptase, 119, 119f
Reverse turns
  amino acid residues in, 51–52
  defined, 44
Reversible covalent modification, 286, 443, 732–733, 733f
Reversible inhibition, 234, 234f. *See also* Enzyme inhibition
Reversible terminator method, 155
Rhizobium bacteria, 714
Rho, 868, 868f
Rhodopseudomonas viridis, 569, 570f, 584
Rhodopsin, 400, 400f, 970–971, 971f
Rhodopsin kinase, 972
Rhodospirillum rubrum, 541
Ribbon diagrams, 62, 62f
Ribonuclease
  amino acid sequences in, 49–50, 49f
  denatured, 50
  reduction and denaturation of, 50f
  sequence comparison of, 169, **170**
  structure of, 49–51, 49f
Ribonuclease III (RNase III), 870
Ribonuclease P (RNase P), 870
Ribonucleic acid. *See* RNA
Ribonucleotide reductase
  as cancer therapy target, 759–760
  defined, 753
  in deoxyribonucleotide synthesis, 753–755
  elements of, 753, 753f
  mechanism, 754, 754f
  regulation of, 759, 759f
  stable radicals, 755
  structure of, **753**
  tyrosyl radicals, 753, 753f
Ribose, 106, **106,** 317, 318f, 320f
Ribosomal initiator element (rInr), 873
Ribosome release factor (RRF), 911
Ribosomes
  bacterial, 911
  catalysis by proximity and orientation, 908
  defined, 126, 893
  endoplasmic reticulum bound, 915–919, 916f
  eukaryotic, 911
  50S subunit of, 902–903, 903f, 908, 910
  polysomal, 910, 910f
  in protein synthesis, 893, 902–911
  schematic representation, 905f
  70S subunit of, 903, 903f
  sites of, 905, 905f
  structure of, 903, 903f
  subunits of, 902–903, 903f
  30S subunit of, 902–903, 903f, 907, 907f
  in translation, 898–911
  tRNA-binding sites, 905, 905f
Riboswitches, 867, 867f
Ribulose 1,5-bisphosphate, 591–592, 591f, 592f, **592,** 595–597, 596f, 597f
Ribulose 5-phosphate
  in Calvin cycle, 602, 603f
  in pentose phosphate pathway, 603, 604, 608–609
Ricin, 915, 915b
Ricinus communis, 915, 915f
Rickets, 795
Rickettsia prowazekii, 525–526
Rieske center, 534
Rifampicin, 869, 869f
Ritonavir, 792
RNA. *See also* Transcription
  ATP binding of, 186–187, 186f, 187f
  backbone of, 106, 106f
  base composition of, 121, 121t
  defined, 107
  double-stranded, 162, 162f
  in *E. coli*, 119, 119t
  flow of information from DNA to, 119, 119f
  in gene expression, 119–120
  guide strand, 162–163
  hybridization with, 135
  as linear polymer, 105, 106
  messenger. *See* mRNA
  micro, 879, 879f, 956–957, 956f
  nucleotides, 107–108
  passenger strand, 162
  primer, 841
  ribosomal. *See* rRNA
  small interference (siRNA), 162, 162f
  small nuclear (snRNA), 882–883
  small regulatory, 879, 879f
  splicing of, 880–883, 880f, 881f, 882t
  stem-loop structure, 113, 113f
  structure of, 113–114, 113f, 114f, 187, 187f
  synthesis of, 120–121
  transfer. *See* tRNA
RNA editing, 879–880, 879f
RNA interference, 162–163, 162f
RNA polymerase holoenzyme complex, 865, **865**
RNA polymerase I
  in RNA synthesis, 872, 873, 873f
  rRNA production, 877
RNA polymerase II
  promoter region, 874
  in RNA synthesis, 872, 873, 873f
RNA polymerase III, 873–874, 873f, 877, 878f
RNA polymerases, 120–121, 873f
  activated precursors, 121
  active site of, 861
  backtracking and, 863–864, 863f
  catalytic action of, 861–871
  components of, 121
  defined, 859, 860
  divalent metal ion, 121
  in DNA replication, 831, 831f
  DNA templates and, 121–122, 121t, 861
  in *E. coli*, 123, 123f, 861–862, 862t
  eukaryotic, 860, **860,** 872–874, 872t, 873f
  eukaryotic promoter elements, 873, 873f
  functions of, 860–861
  illustrated, 120f
  prokaryotic, 860, **860**
  promoter sites in, 864–865
  in proofreading, 863
  RNA-directed, 118
  structures of, 860, **860**
  subunits of, 862, 862t, 865
  synthesis of, 121f
  in transcription, 861–871
  transcription mechanism, 121, 121f
RNA processing
  eukaryotic pre-rRNA, 877, 877f
  of pre-mRNA, 877f, 878–879, 878f
  in transcription of eukaryotes, 872, 883–884, 884f
  tRNA, 877, 878t
RNA sequences, comparison of, 182–183, 182f
RNA splicing. *See* Splicing
RNA-DNA hybrid
  backtracking, 863–864, 863f
  during elongation, 869
  lengths of, 863
  separation, 863, 863f
  translocation, 863, 863f
RNA-induced silencing complex (RISC), 162–163, 162f, 956
Rods, 970–971, 970f
Rofecoxib (Vioxx), 1048, **1048,** 1052
Rossmann, Michael, 465
Rossmann fold, 465
Rosuvastatin, 1044, **1044**

Rotational catalysis, in ATP synthase, 546, 546f
Rotenone, 556
rRNA
  in base pairing, 903
  defined, 120
  folding of, 903, 904f
  in structural scaffolding, 903
  transcription of, 870–871, 870f, 877, 877f
  in translation, 903–905, 904f
  types of, 120
Rubisco
  in Calvin cycle, 591–594, 591f, 592f, 593f, 598–599
  defined, 591
  magnesium ion in, 592, 592f
  oxygenase reaction, 593–594, 593f
  structure of, 591, 591f
Rubisco activase, 593

S_1 pockets, 258, 259f
Saccharomyces cerevisiae, 153, 941
Sakmann, Bert, 379
Salicin, 1043
Salicylic acid, 1043, **1043**
Salmonella test, 852, 852f
Salt bridges, 203, 203f
Salting out, 68
Salty taste, 966, 969
Salvage pathways. *See also* Nucleotide synthesis
  defined, 744
  for IMP and GMP synthesis, 762
  purine, 748, 752
  pyrimidine, 748
Sample half-cell, 526–527
Sandwich ELISA, 82–83, 83f
Sanger, Frederick, 37, 138, 152
Sanger dideoxy method, 138–139, 139f
Sarcomere, 1020, 1020f
Sarcoplasmic reticulum Ca^{2+} ATPase. *See* SERCA
Saturated fatty acids, 661
Schiff bases, 451, 606, 621
  in amino acid degradation, 689–690
  in amino acid synthesis, 717
  in aminoacrylate, 729, **729**
  defined, 621b
  in retinal, 971, 971f
Scrapie, 56
Screening libraries, 1044–1046, 1046f
Screw sense, 40–41, 40b, 40f
Scurvy, 821
SDS (sodium dodecyl sulfate), 72
SDS-PAGE, 73, 73f, 74
SDS-polyacrylamide gel electrophoresis, 350, 351
Second Law of Thermodynamics, 11–12, 13
Second messengers, 398, **399,** 406, 415
Secondary active transport, 367
Secondary antibody, 84
Secondary protein structure, 27, 40–46, 48, 51t
Secondary transporters, 376, 376f, 377
Second-order reactions, 226
Secretory pathway, 915–916
Secretory proteins, 916, 916f
Sedimentation coefficients, 76, 77f
Sedimentation equilibrium, 78
Sedoheptulose 7-phosphate, 603, 603f, 604f
Segmental flexibility, 987, 987f
Selectins, 335
Selective estrogen receptor modulators (SERMs), 952
Selectivity filter, 381, 381f, 382, 382f
Self-splicing
  defined, 886
  example of, 886, 886f
  intron structure, 887f
  mechanism, 887, 887f
Self-tolerance, 1005
Sensory systems, 961–979
  brain connection, 962, 962f
  hearing, 975–977
  olfaction, 962–966
  overview of, 961–962
  taste, 966–970
  touch, 977–978
  vision, 970–975
Sequence alignment
  with conservative substitution, 176f
  with gap insertion, 172–173, 173f
  of hemoglobin, 176f
  of identities only versus Blosum-62, 176f
  of leghemoglobin, 176f
  of repeated motifs, 180, 180f
  scoring system, 176, 176f
  shuffling and, 173–174, 173f
  statistical analysis of, 171–177
  statistical comparison of, 173, 173f
Sequence comparison methods, 169–170
Sequence identities, 172
Sequence template, 180
Sequential model
  allosteric enzymes, 290–291
  of hemoglobin-oxygen binding, 199, 199f
Sequential reactions, 232
SERCA
  defined, 370
  P-type ATPase, 370–373
  pumping by, 372, 372f
  structure of, 372
Serine
  in catalytic triads, 255–258
  in chymotrypsin, 253–254, 254f
  in cysteine synthesis, 722–723, 726
  defined, 32–33
  from glycine, 700
  in glycine synthesis, 722–723
  pyruvate formation from, 699f, 700
  in sphingolipid synthesis, 772, **772**
  sphingosine from, 734
  structure of, 32f
  synthesis of, 722, 722f, 726
Serine dehydratase, 692
Serine hydroxymethyltransferase, 723
Serine kinases, 294–295, 295t
Serine protease inhibitors, 302
Serine proteases
  catalytic strategies of, 251
  convergent evolution and, 181–182
Serotonin, synthesis of, 734, 734f
Serpins, 302
7TM (seven-transmembrane-helix) receptors
  biological functions mediated by, 400t
  defined, 399
  in drug development, 1048
  in glycogen metabolism, 627–629, 628f
  ligand binding to, 400–402
  in olfaction, 963
  oligomeric, 969
  phosphoinositide cascade activation, 404–405, 405f
  in signal termination, 404f
  in taste, 967–969, 967f
  in vision, 970–974
70S initiation complex, 907, 907f
70S subunit, of ribosomes, 903, 903f, 907
Severe acute respiratory syndrome (SARS), 1050
Severe combined immunodeficiency (SCID), 164, 760–761
Shaker channel, 380, 384
Shaker gene, 380
Shape complementarity, 830, 830f, 831f
Shemin, David, 735b, 736
Shikimate, in amino acid synthesis, 727–729
Shine, John, 906
Shine-Dalgarno sequences, 126, 906
Shuffled sequences, 173–174, 173f
Sialic acids, 772
Sickle-cell anemia, 17–18, 205–206, 205f, 206f
Side chains
  amino acid. *See* amino acid side chains
  hydrophilic, 47
  hydrophobic, 47
  polypeptide chains, 36, 36f, 47
Sigmoid oxygen-binding curve, 196
Sigmoidal curve, 291, 291f
Sigmoidal kinetics, 287, 287f
Signal transduction, 397–420
  abnormalities in cancer, 416–417, 416f, 417f
  abnormalities in cholera, 417–418
  abnormalities in whooping cough, 417–418
  adaptor proteins in, 410
  β-adrenergic receptor in, 399–400, 400f
  calcium ions in, 405–407, 406f, 415
  calmodulin in, 407, 407f
  cAMP in, 402–403
  cross talk, 398–399
  defects, 415–418
  defined, 397
  element recurrence in, 415
  epidermal growth factor in, 397, 411–414
  epinephrine in, 399–407

Signal transduction—(*continued*)
  evolution of, 415
  function of, 397, 398f
  G proteins in, 400–403, 401f, 402f
  GTPases and, 414, 414t
  insulin in, 407–411
  molecular circuits, 398–399
  monoclonal antibodies as inhibitors, 416–417
  nucleotides in, 743
  in olfaction, 964, 964f
  overview of, 397–399
  primary messenger, 398
  principles of, 398–399, 398f
  protein kinases in, 415
  protein kinase A in, 403, 415
  Ras in, 413–414, 413f
  second messengers, 398, 406, 415
  secondary messengers, **399**
  7TM receptors, 399–402, 400t, 404f
  Src homology domains in, 410, 410f, 413, 415, 416, 416f
  in vision, 972–973, 972f
Signal-recognition-particle (SRP), 916–918, 917f
Sildenafil, 1042–1043
Simple diffusion, 368
Single-molecule studies, enzyme, 242–243, 242f
Single-stranded-binding protein (SSB), 840, 840f
Singulo method, 242
Site-directed mutagenesis, 150–151, 151f
Slack, C. Roger, 599
Sliding DNA clamp, 839–840, 839f
Sliding-filament model, 1020–1021, 1021f
Small G proteins, 413
Small interference RNA (siRNA), 162, 162f
Small nuclear ribonucleoprotein particles (snRNPs), 882–883, 882t
Smell. *See* Olfaction
SNARE proteins, 361, 362f
Social interactions, in gene expression, 934
SOD1 gene, 159
Sodium dodecyl sulfate (SDS)
  in gel electrophoresis, 72–73, 73f
  PAGE, 73, 73f
Sodium ion channels
  amiloride-sensitive, 969, 969f
  inactivation of, 384–385
  paddles, 388
  purification of, 379–380
  in taste, 969
Sodium ions, 378
Solid-phase DNA synthesis, 139–141, 140f
Solid-phase peptide synthesis, 93–94, 94f
Somatic mutation, antibody diversity and, 992–993
Sonicating, 349
Sos, 413, 413f
Sour taste, 966, 969–970
Southern, Edwin, 138
Southern blotting, 138, 138f, 160
Space-filling models, 22, 23f, 61, 61f, 195f
Special pair, 570–571
Specificity constant, 230–231, 231f
Sphingolipids
  ceramide and, 772, 772f
  defined, 772
  diversity and, 773–774
  gangliosides, 772–773, 774
  synthesis of, 772–774, 773f
Sphingomyelin
  defined, 345, 772
  structure of, **345**
Sphingosine, 344
  defined, 345
  structure of, **345**
  synthesis of, 734, 734f
Spina bifida, 762
Spleen tyrosine kinase (Syk), 993
Spliceosomes
  assembly and action, 882–883, 882f
  catalytic center, 883, 883f
  defined, 128, 881
Splicing
  alternative, 128, 129f, 877, 885–886, 885f, 885t
  branch points in, 880, 881f
  catalytic center, 883, 883f
  defined, 128, 880
  group I, 887, 888f
  group II, 887–888, 888f
  mechanism, 881, 881f
  mutations affecting, 880–881, 884–885, 884f
  pathways comparison, 888f
  self-splicing and, 886–888, 886f, 887f
  sites of, 880–881, 880f
  snRNPs in, 882–883, 882t
  spliceosomes in, 881, 882–883, 882f
  transesterification in, 881–882, 882f
Splicing factors, 882
Split genes, 128
Split-pool synthesis, 1045, 1045f
Spudich, James, 1019
Squalene
  cyclization of, 778–779, 779f
  synthesis of, 777–779, 778f
Squalene synthase, 778
Src
  affixation to cytoplasmic face, 294
  in cancer, 416
Src homology 2 (SH2) domain, 410, 410f, 415, 416, 416f
Src homology 3 (SH3) domain, 413, 415, 416, 416f
SREBP (sterol regulatory element binding protein), 779–781, 780f, 781f, 784
SREBP cleavage activating protein (SCAP), 780–781, 781f
SRP receptor, 917, 917f
Stacking forces, 111
Stahl, Franklin, 115, 116
Standard free-energy change, 219–220
Standard reference half-cell, 526, 527
Staphylococcus aureus, 239, 239f
Starch, 324, 597
Starvation, metabolic adaptations in, 818–819, 819t
Starved-fed cycle, 816–817
Statins, 788
Steady-state assumption
  defined, 227
  in enzyme kinetics, 226
Stearoyl CoA desaturase, 668, 668f
Steatorrhea, 646
Steitz, Tom, 829
Stem-loop structure, 113, 113f
Stereochemical renderings, 22
Stereochemistry
  of cleaved DNA, 270–271, 271f
  observation of, 270
  of proton addition, 721, 721f
Stereocilia, 975–976
Stereoelectronic control, 691f, 692
Stereoisomers
  carbohydrate, 317, 317f
  notation for, 29b
Steric exclusion, 39
Steroid hormones
  anabolic, 951
  binding and activation, 789–790
  classes of, 789
  defined, 789
  hydroxylation of, 790–791
  identification of, 790
  synthesis of, 789–791, 789f
Sterol regulatory element binding protein (SREBP), 779–781, 780f, 781f, 784
Sterol regulatory element (SRE), 779
Sticky ends, DNA, 144, 144f
Stoichiometry
  of gluconeogenesis, 481
  for light reactions, 581
  of palmitate synthesis, 666
Strand invasion, 853, 853f
Strand separation, 141, 141f
Streptomyces coelicolor, 865
Streptomyces lividans, 380
Streptomycin, 914, 914t, **914**
Stroma, 567
Stroma lamellae, 567–568
Strominger, Jack, 1042
Structural genes, 928
Structure-activity relationship (SAR), 1046
Structure-based drug development, 1046–1048, 1047f, 1048f
Substituted enzyme intermediates, 233
Substitution matrix, 174–176, 175f, 176f
Substitutions
  in amino acid sequences, 174–177, 175f, 176f
  conservative, 174, 175f, 176f
  nonconservative, 174, 175f
Substrate binding
  in catalysis, 225
  conformation selection, 224
  cooperative, 233